STATE-OF-THE-SCIENCE REVIEW

Management of Contaminants Stored in Low Permeability Zones

SERDP Project ER-1740

October 2013

T. Sale
Colorado State University

B.L. Parker
University of Guelph

C.J. Newell
GSI Environmental Inc.

J.F. Devlin
University of Kansas

Distribution Statement A
This document has been cleared for public release

SERDP
DOD ▪ EPA ▪ DOE

Management of Contaminants Stored in Low Permeability Zones

A State-of-the-Science Review

STRATEGIC ENVIRONMENTAL RESEARCH AND DEVELOPMENT PROGRAM

ER-1740

Principal Investigators:

T. Sale (Colorado State University, Fort Collins, Colorado)
B.L. Parker (University of Guelph, Guelph, Ontario, Canada)
C.J. Newell (GSI Environmental Inc., Houston, Texas)
J.F. Devlin (University of Kansas, Lawrence, Kansas)

Draft Report October 2013

REPORT DOCUMENTATION PAGE

Form Approved
OMB No. 0704-0188

The public reporting burden for this collection of information is estimated to average 1 hour per response, including the time for reviewing instructions, searching existing data sources, gathering and maintaining the data needed, and completing and reviewing the collection of information. Send comments regarding this burden estimate or any other aspect of this collection of information, including suggestions for reducing the burden, to the Department of Defense, Executive Services and Communications Directorate (0704-0188). Respondents should be aware that notwithstanding any other provision of law, no person shall be subject to any penalty for failing to comply with a collection of information if it does not display a currently valid OMB control number.

PLEASE DO NOT RETURN YOUR FORM TO THE ABOVE ORGANIZATION.

1. REPORT DATE *(DD-MM-YYYY)*	2. REPORT TYPE	3. DATES COVERED *(From - To)*
10-2013	Technical Report	11-2009-10-2013

4. TITLE AND SUBTITLE

Management of Contaminants Stored in Low Permeability Zones - A State of the Science Review

5a. CONTRACT NUMBER

5b. GRANT NUMBER

5c. PROGRAM ELEMENT NUMBER

6. AUTHOR(S)

T.Sale
B.L. Parker
C.J. Newell
J.F. Devlin

5d. PROJECT NUMBER

ER-1740

5e. TASK NUMBER

5f. WORK UNIT NUMBER

7. PERFORMING ORGANIZATION NAME(S) AND ADDRESS(ES)

Colorado State University
1320 Campus Delivery, Dept. of Civil and Environmental Engineering
Fort Collins, CO 80523-1320

8. PERFORMING ORGANIZATION REPORT NUMBER

ER-1740

9. SPONSORING/MONITORING AGENCY NAME(S) AND ADDRESS(ES)

SERDP/ESTCP
4800 Mark Center Drive, Suite 17D08
Alexandria, VA 22350-3605

10. SPONSOR/MONITOR'S ACRONYM(S)

SERDP/ESTCP

11. SPONSOR/MONITOR'S REPORT NUMBER(S)

12. DISTRIBUTION/AVAILABILITY STATEMENT

Unlimited

13. SUPPLEMENTARY NOTES

14. ABSTRACT

The following is a state-of-the-science review of management of contaminant in "low k" (low permeability) zones in aquifers. This work was funded by SERDP under project ER-1740 as one of five 2010 SERDP project addressing contaminants in low k zones. The authors of this report include leading academic and industry researchers in the field of contaminant hydrology. The foundation for this effort is more than three decades of groundbreaking research conducted by Drs. John Cherry and Beth Parker. Supporting authors of this document wish to explicitly recognize Drs. Cherry's and Parker's contributions to this effort.

15. SUBJECT TERMS

16. SECURITY CLASSIFICATION OF:			17. LIMITATION OF ABSTRACT	18. NUMBER OF PAGES	19a. NAME OF RESPONSIBLE PERSON
a. REPORT	b. ABSTRACT	c. THIS PAGE		346	Tom Sale
					19b. TELEPHONE NUMBER *(Include area code)* 970-491-8224

Reset

Management of Contaminants Stored in Low Permeability Zones:

A State-of-the-Science Review

STRATEGIC ENVIRONMENTAL RESEARCH AND DEVELOPMENT PROGRAM

Section **Page No.**

Table of Contents

Abbreviations vi

PROJECT FACT SHEET 1

EXECUTIVE SUMMARY 2

OVERVIEW OF CHAPTER 1: *LOW k Zones* 1

1.0 INTRODUCTION 2
1.1 THE PROBLEM 2
1.2 OBJECTIVES 4
1.3 AUTHORIZATION 5
1.4 CONTENT AND ORGANIZATION 6

OVERVIEW OF CHAPTER 2: *LOW k ZONES* 8

2.0 LOW PERMEABILTY ZONES 9
2.1 HISTORICAL PERSPECTIVES 9
2.2 ARCHITECTURE OF TRANSMISSIVE AND LOW k ZONES 10
2.2.1 Terminology and Concepts 11
2.2.2 Key Features of Low k Zones 13

OVERVIEW OF CHAPTER 3: *CHARACTERIZING LOW k ZONES* 16

3.0 CHARACTERIZING LOW k ZONES 17
3.1 "FIRST GENERATION" CHARACTERIZATION APPROACHES 17
3.1.1. The Problem with Conventional Groundwater Wells for Site Characterization 18
3.1.2. The Problem with Traditional (1G) Soil Sampling and Analysis 20
3.1.3 Goals of Low k Zone Characterization 22
3.2 2G CHARACTERIZATION APPROACHES 24
3.2.1 Key Themes for Characterization 24
3.2.2 Methods 38
3.3 EMERGING NEEDS AND OPPORTUNITIES ("3G" CHARACTERIZATION APPROACHES) 46
3.4 CHAPTER 3 CHARACTERIZING LOW k ZONES – KEY RESEARCH PRODUCTS 49

OVERVIEW OF CHAPTER 4: *TRANSPORT IN HETEROGENEOUS MEDIA* 50

4.0 TRANSPORT IN HETEROGENEOUS MEDIA 51
4.1 OVERVIEW 52
4.2 DIFFUSION IN PERMEABLE POROUS MEDIA 52
4.2.1 Darcy's Law and Fick's First Law: Functional Brothers 52
4.2.2 The Effect of Sediment Texture on D* 53
4.2.3 Modeling to Show the Effects of Heterogeneity on Diffusion Coefficients 55
4.2.4 Factors Controlling Effective Diffusion Coefficients 57
4.2.5 Methods for Estimating D_o and D* 59
4.2.6 SERDP Diffusion Experiments: The Dead-End Column ("DEC") 61
4.2.7 Measurement of D* in F.E. Warren AFB Sediments 62
4.2.8 Measurement of D*: Conclusions 64
4.3 CONTAMINANT DEGRADATION IN LOW k ZONES 66
4.3.1 Introduction 66
4.3.2 Microbial Presence and Contaminant Biodegradation in Low k Units 67
4.3.3 Methodologies for Assessing Degradation in Low k Zones 70
4.3.4 Application of Compound-Specific Isotope Analyses (CSIA) 71
4.3.5 Example Datasets from Field Sites 72
4.4 CHAPTER 4 TRANSPORT – KEY RESEARCH PROGRAMS 78

OVERVIEW OF CHAPTER 5: *TYPE SITE SIMULATIONS* 79

5.0 TYPE SITE SIMULATIONS 80
5.1 OVERVIEW 80
5.2 TWO-LAYER ANALYTICAL SOLUTION FOR POROUS MEDIA 81
5.3 FRACTURED MEDIA TYPE SITE MODELING 91
5.3.1 Parallel Fracture Type Site Scenarios 91
5.3.2 Fracture Network Type Site Scenario 103
5.4 POROUS MEDIA TYPE SITE SIMULATIONS 108
5.4.1 Two-Layer Sand/Clay Type Site 109
5.4.2 Multi-layer Scenarios 123
5.4.3 Random Clay Layer Type Site 134
5.5 MODEL BENCHMARKING WITH LABORATORY EXPERIMENTAL DATASETS 139
5.5.1 Sand Tank Visualization Tracer Experiment 140
5.5.2 Numerical Simulation of Sand Tank Visualization Tracer Experiment 143
5.5.3 MultiLayer Tank Experiments 157
5.6 CONCLUSIONS 173
5.7 TEXT BOX 5-1: ADDITIONAL MODELING 174
5.8 CHAPTER 5 TYPE SITE SIMULATIONS – KEY RESEARCH PRODUCTS 177

OVERVIEW OF CHAPTER 6: *TREATING LOW k ZONES* **178**

6.0 TREATMENT OF CONTAMINANTS IN LOW PERMEABILTY ZONES **179**

6.1 STRATEGIES AND GOALS 180
6.1.1 Strategies 180
6.1.2 Goals 181
6.2 TECHNOLOGIES FOR CONTAMINANTS IN LOW K ZONES 182
6.3 DEMONSTRATIVE LABORATORY STUDIES - METHODS 185
6.3.1 Setup 185
6.3.2 Analytical Methods 190
6.4 DEMONSTRATIVE LABORATORY STUDIES: RESULTS 190
6.4.1 Tank 1: Control 190
6.4.2 Tank 2: Enhanced Flushing 192
6.4.3 Tank 3: Permanganate 193
6.4.4 Tank 4: Lactate and KB1 196
6.4.5 Tank 5: Lactate, KB1, and Xanthan Gum 198
6.4.6 Tank 6: Lactate, Sulfate Reducing Bacteria (SRB), and Magnesium Sulfate 200
6.5 COMPARISON BETWEEN TREATMENTS 202
6.6 COMPARISION TO FIELD OBSERVATIONS 205
6.6.1 Order of Magnitude Rule of Thumb 205
6.6.2 Sustained Treatment Observations 205
6.6 OPPORTUNITIES 207
6.7 CHAPT. 6 - TREATMENT IN LOW k ZONES – KEY RESEARCH PRODUCTS 208

OVERVIEW OF CHAPTER 7: *IMPLICATIONS* **209**

7.0 IMPLICATIONS FOR SELECTING SITE REMEDIES **210**

7.1 OVERVIEW 210
7.2 KEY IMPLICATIONS FOR REMEDIATION 211
7.2.1 Implication 1: Amendments are More Difficult to Apply in Low k Units 211
7.2.2 Implication 2: Thermal Processes Have a Theoretical Advantage, But… 212
7.2.3 Implication 3: Destroying the Heterogeneity Works 213
7.2.4 Implication 4: Interfaces and Targeted Treatment 213
7.2.5 Implication 5: These are Nonpoint Sources 214
7.2.6 Implication 6: Containment, Perhaps in Different Forms, Makes a Comeback 215
7.2.7 Implication 7: It is Important to Know if Your Site is In Its Early, Middle, or Late Stage 216
7.2.8 Implication 8: This is a Management and Regulatory Problem Too 217
7.2.9 Implication 9: What is the Objective? 218
7.2.10 Implication 10: Don't Underestimate Human Ingenuity 219

8.0 GUIDE TO CONTRACTED TASKS **220**

9.0 REFERENCES **223**

APPENDICES

Appendix A. Supporting Information for Section 3: Characterizing Low k Zones: F.E. Warren Field Work

Appendix B. Supporting Information for Section 3: Characterizing Low k Zones: NAS Jacksonville Field Work

Appendix C. Supporting Information for Section 4: Transport in Heterogeneous Media

Appendix D. Screening Method To Estimate if a Chlorinated Solvent Site is in its *Early, Middle or Late Stage*

ABBREVIATIONS

1G, 2G, 3G	First, Second, and Third Generation
14C	14 Compartment
AFCEE	Air Force Center for Engineering and the Environment
CDPHE	Colorado Department of Public Health and Environment
CF	Confidence Factor
cis-DCE	cis-Dichloroethene
COV	Coefficient of Variation
CRWQCB	California Regional Water Quality Control Boards
CSM	Conceptual Site Model
DNAPL	Dense Non-Aqueous Phase Liquid
ESTCP	Environmental Security Technology Certification Program
ITRC	Interstate Technology and Regulatory Council
GSI	GSI Environmental Inc.
GTS	Geostatistical Temporal/Spatial
k	Permeability
LNAPL	Light Non-Aqueous Phase Liquid
LoRSC	Low-Risk Site Closure
LTMO	Long-Term Monitoring Optimization
LUFT	Leaking Underground Fuel Tank
MAROS	Monitoring and Remediation Optimization System
MCL	Maximum Contaminant Level
MNA	Monitored Natural Attenuation
NAPL	Non-Aqueous Phase Liquid
NRC	National Research Council
NSZD	Natural Source Zone Depletion
OoM	Orders of Magnitude
PBC	Performance Based Contracting
POE	Point of Exposure
PV	Pore Volume
PWS	Public Water Supply
SERDP	Strategic Environmental Research and Development Program
SRT	Sustainable Remediation Toolkit
TCE	Trichloroethene
TCEQ	Texas Commission on Environmental Quality
TDS	Total Dissolved Solids
PCE	Tetrachloroethene
POE	Point of Exposure
USAF	U.S. Air Force
USEPA	U.S. Environmental Protection Agency
UST	Underground Storage Tank
WQP	Water Quality Protection

PROJECT FACT SHEET

This is a state-of-the-science review of management of contaminant in "low k" (low permeability) zones in aquifers. Funded by the Dept. of Defense SERDP Program.

Four research teams collaborated to write this review: Colorado State (CSU), University of Guelph (UG), GSI Environmental (GSI), University of Kansas (KU). Dr. Tom Sale of CSU was the Prime Contractor for the project.

The foundation for this effort is more than three decades of groundbreaking research conducted by Drs. John Cherry and Beth Parker of the University of Guelph.

Chapter 1 - Introduction. Contaminants in low permeability (what we call "**low k**") units requires rethinking our conceptualization of contaminant transport in heterogeneous porous media.

Chapter 2 - Site Characterization. We need to recognize the limitations of long screen monitoring wells for site characterization (the first generation approach, or "1G site characterization"). More recently second generation (2G) tools have revealed previously missed "stylistic" understanding of contaminants in low k zones, and 3G tools increase these capabilities.

Chapter 3 – Transport. Understanding contaminant transport in low k zones, and related implications for transmissive zones, requires a detailed understanding of diffusion processes and diffusion variables. Careful laboratory column experiments show that diffusion coefficients in sediments with textures between sand and silt may vary by as much as an order of magnitude. Understanding how and where degradation in low k zones is beginning to be revealed.

Chapter 4 - Modeling. We used novel modeling techniques that showed: 1) matrix diffusion can be a larger contributor to overall source lifetime than DNAPL source; 2) simulations of idealized "Type Settings" show that low k zones can cause tailing for decades or longer, but that even slow degradation rates in low k zones can be very important to site management. Even thin clay layers can prevent attainment of drinking water standards for decades.

Chapter 5 – Remediation Experiments. Detailed experiments of remediation in controlled research tanks show that under ideal laboratory conditions that **2.6 to 3.8 OoMs** (order of magnitude) reductions in transmissive zone concentrations were achieved by active treatment at the end of the experiments compared to a **2.6 OoM** reduction in a flushing only control. Chemical oxidation seemed to show immediate partial rebound, but biological remediation technologies showed up to 20 pore volumes (many years) worth of "sustained treatment." None of the five technologies tested were able to achieve drinking water standards in the research tanks, even after 50 pore volumes of flushing.

Chapter 6 - Implications. The remediation field may be at the cusp of a new generation of thinking on how to manage sites with contaminants in low k zones. A key question is what is an appropriate cleanup standard (if any) for low k zones? Ten Implications are presented.

Key Words: low k zone, matrix diffusion, 1G 2G 3G site characterization, numerical modeling, Type Site, tank studies, remediation, OoM. Cleanup standards, sustained treatment implications.

EXECUTIVE SUMMARY

Lead Author for This Chapter

Tom Sale, Colorado State University

The following is a state-of-the-science review of management of contaminant in "**low k**" (low permeability) zones in aquifers. This work was funded by SERDP under project ER-1740 as one of five 2010 SERDP project addressing contaminants in low k zones. The authors of this report include leading academic and industry researchers in the field of contaminant hydrology. The foundation for this effort is more than three decades of groundbreaking research conducted by Drs. John Cherry and Beth Parker. Supporting authors of this document wish to explicitly recognize Drs. Cherry's and Parker's contributions to this effort.

The motivation for this effort is a conviction that managing contaminants in low k zones is central to developing sound solutions at sites where releases of chlorinated solvents and other persistent contaminants have occurred. The corollary to this is that failing to consider contaminants in low k zones will, in many instances, lead to remedies that fall short of expectations. Perhaps the most problematic aspect of failing to recognize low k zones is that they can sustain contaminant concentrations in transmissive zones for decades or even centuries after the primary sources have been addressed (Chapman and Parker 2005). An early adopter of the paradigm of contaminants in low k zones made the thoughtful observation "…there is no going back".

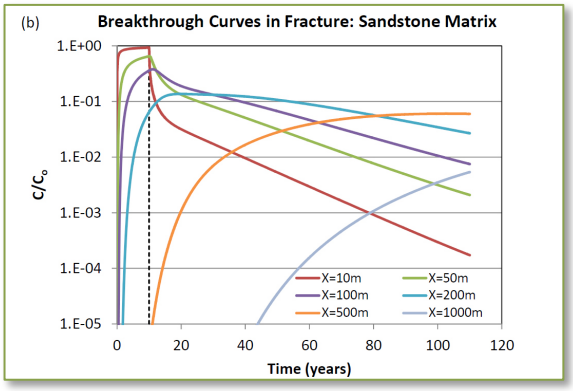

Unfortunately, the path to embracing the importance of contaminants in low k zones is not simple. First it requires rethinking our conceptualization of contaminant transport in heterogeneous porous media. This includes:

- Recognizing that the long-standing principle of homogeneous–isotropic aquifers employed in groundwater supply hydraulics are inappropriate for contaminant transport,
- Embracing diffusion and slow advection as fundamental governing processes at contaminated sites,
- Abandoning dispersion as a basis for accounting for local heterogeneities in aquifers and as an explanation for dilute concentrations in wells,
- Recognizing that sorption and reactions in low k zones are critical fate and transport processes,

- Developing dynamic site conceptual models that evolve with time (e.g. the problem begins with nonaqueous phase liquids and ends with contaminants in low k zones),

- Employing contaminant transport models that can address governing processes that occur at a small scale (centimeters to millimeters) over large domains (kilometers)

Secondly, we need to recognize the limitations of long screen monitoring wells for site characterization (the first generation approach, or "1G site characterization"). Conventional monitoring wells leave us largely ignorant of contaminant in nonaqueous, sorbed phases in transmissive zones and are blind with respect to all contaminant phases in low k zones. Herein lies a root of our frequent lack of success with remediation; far too often we only see "the tip of the iceberg", through the lens of a conventional groundwater monitoring network based on long-screened wells, while the bulk of the problem remains unseen.

Reflecting the limitation of conventional wells for site characterization, a second generation (2G) of site characterization tools has been developed over the past three decades. These include:

- Multiple level sampling systems,
- High resolution of subsamples from core for total contaminant concentrations
- The Membrane Interface Probe (MIP)
- The Waterloo Advance Profiling System™

These tools have revealed previously missed "stylistic" understanding of subsurface contaminant occurrence including:

- The existence of contaminants that have diffused into low k zones

- Diffusion/sorption controlled transport of contaminants, into and out of, low k zones

- A nascent introduction to reactions in low k zones

- Weak transverse mixing in plumes leading to:

  - Local variations in aqueous contaminant concentrations as large three orders of magnitude (OoMs) over distances of a meter or less.

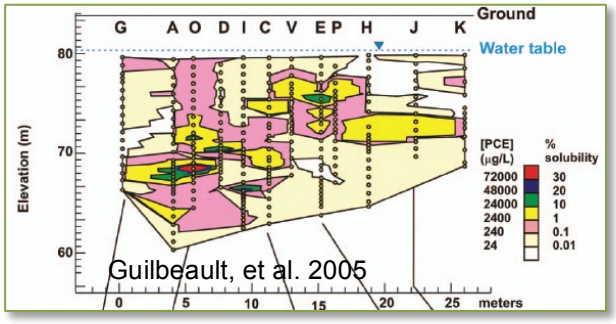

- Tight plume cores at large distances leading to the observations that much of what we perceive as large and dilute plumes is actually largely unaffected media.

- Illumination of the opportunity to take a "surgical" approach to remediation.

Side-by-side application of these tools provides insights regarding the niches for existing 2G site characterization tools. Unfortunately, given limitations of 2G tools, the current state-of-the-art is to apply combinations of 2G tools in the hope that collectively the information will provide the data needed to build site conceptual models and design site remedies. This is perceived by many as being impractical from the perspective of the level of effort. The counter argument to this is that proceeding with remedies, with flawed understandings of the problem, is even more impractical. A critical question that emerges from all of this is whether a third generation of site characterization tools (3G) can be developed that addresses limitations of 2G tools and better enables the pursuit of "surgical" site remedies. This issue is the focus of a 2013 2-year extension of this project (ER-1740).

Building on the above, novel analytical and numerical modeling techniques have been developed to address transport and fate of contaminants in heterogeneous media. Analytical models suggest that matrix diffusion sources are likely a larger contributor to overall source lifetime than DNAPL sources. Decision frameworks can help site managers determine if their site is dominated more by DNAPL vs. matrix diffusion sources. Benchmarking of numerical transport models against data from laboratory sand tank studies and analytical solutions reveals the need for high resolution spatial discretization (i.e. 10,000 nodes per square meter of cross-section) and small-scale temporal discretization to accurate capture storage and release of contaminants in low k zones. Fortunately, modern computers and efficient computational schemes allow high resolution analysis of idealized geologic architectures at plume-scales. Unfortunately, only a few individuals are familiar with modeling techniques needed to capture storage and release of contaminants in low k zones in large domains.

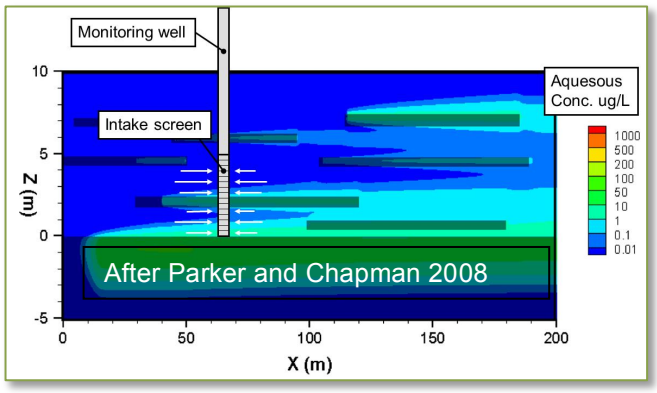

To advance insights from high resolution models, this document provides results from idealized hydrogeologic systems. Settings include "2-layer systems", "multilayer systems", "random low k inclusions" and fractured media with high and low matrix porosity. Results from detailed research-based model simulations of these Type Site Settings include cross-sectional depictions of contaminants concentrations and evaluations of contaminant concentrations in downgradient wells as a function of position and hydrogeologic conditions. Type site simulation provide:

- Insight regarding parameters governing contaminant storage and release from low k zones including:
    - Even very slow rates of degradation in low k zones can substantially impact aqueous concentrations in transmissive portions of plumes.
    - Thin clay layers can cause appreciable tailing for decades, while the thicker aquitard, or a thicker clay layer(s), can cause tailing for much longer periods.
- A basis for developing site conceptual models that address contaminant storage and release from low k zones as a function of settings

Lastly, the challenge of treating contaminants in low k zones is large. Herein, treatment of contaminants in low k zones is explored via laboratory sand tanks studies involving layers of transmissive sand and low k silts (charged with TCE) from F.E. Warren AFB. Treatment options explored include steady water flushing (control), enhance water flushing, flushing permanganate, a dechlorinating culture (KB1) and lactate, KB1 lactate and guar gum, and lacate, sulfate, and sulfate reducing bacteria (SRBs).

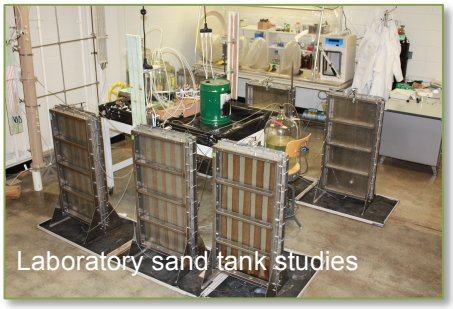
Laboratory sand tank studies

Concentration Reduction in Remediation Tank Experiments
(OoM: Order of Magnitude. PV: Pore Volume)

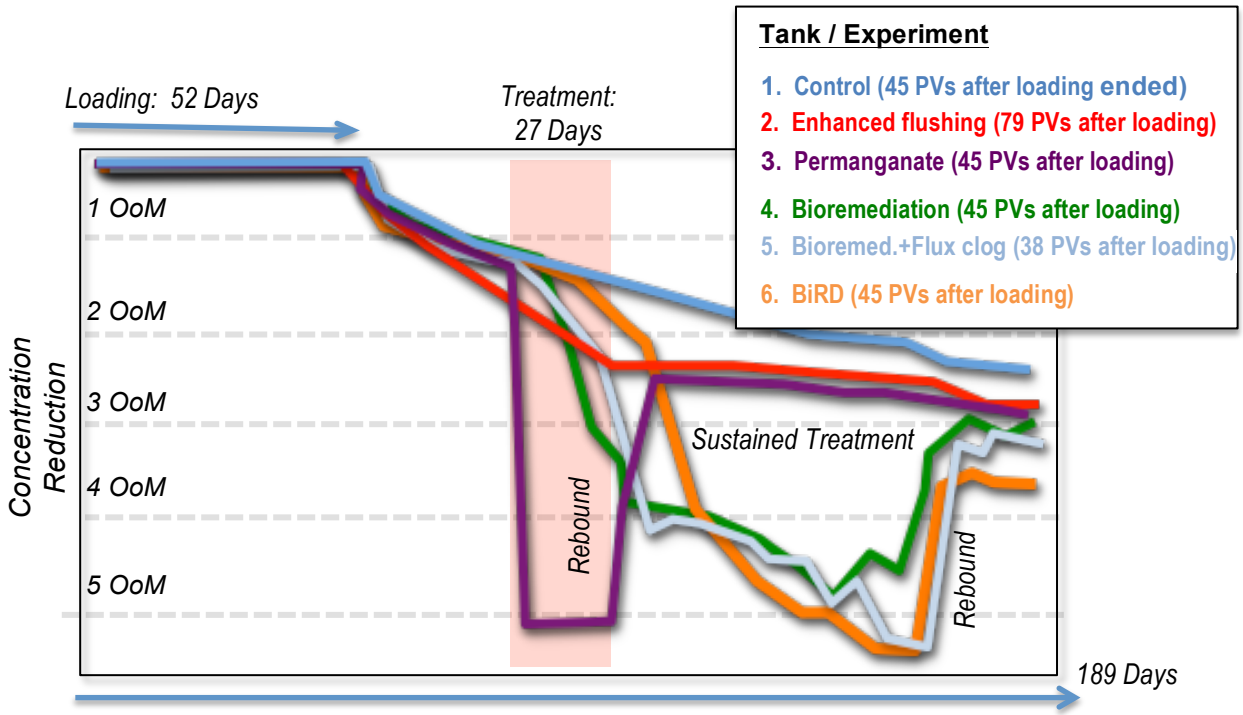

Results indicate that active treatments under ideal laboratory conditions can achieve ½ to 1 OoM (Order of Magnitude) reductions in aqueous phase contaminants in transmissive zones relative to the steady flushing control. Furthermore, results provide insight as to the factor limiting the efficacy of each of the studied site remediation approaches.

Modeling and sand tank studies raise critical questions about appropriate cleanup standards for low k zones. Specifically, what level of cleanup is needed in low k zones to protect receptors exposed to water from transmissive zones? Resolving the debate on the quantitative goal for contaminant concentrations in low k zones is beyond the scope of this document. Nevertheless, it is central to developing strategies for managing contaminants in low k zones.

Significant rethinking about remediation objectives in a low k world is now emerging, as shown by recent guides from ESTCP, the Interstate Technology and Regulatory Council, and the National Research Council. The remediation field may be at the cusp of a new generation of thinking on how to manage sites with contaminants in low k zones.

OVERVIEW OF CHAPTER 1: *LOW K ZONES*

- We have come a long way and had many successes.
- Reflecting on the past three decades, our goal has been to restore contaminated groundwater to its original condition, the result at many sites has been only partial cleanup leading to a need for chronic site management
- 1G (first generation) site characterization tools provide a limited, and sometimes misleading, picture of the subsurface.
- Much of the contaminants we are trying to cleanup have been hidden from sight in low k zones analogous to an **iceberg**.
- We have to deal with multiple phases and compartments. The **14-compartment model** acknowledges contaminants present in vapor, DNAPL, sorbed, and aqueous phases, on both transmissive and low k compartments.

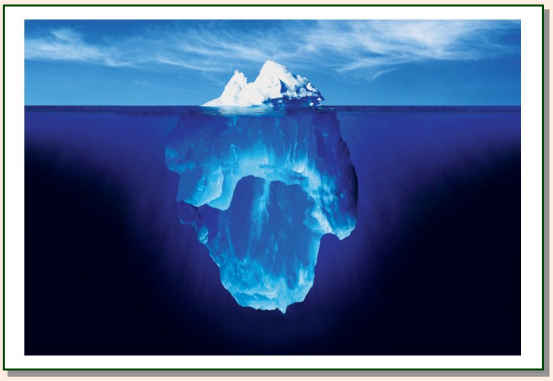

- One of the greatest challenges to embracing the paradigm of contaminants in low k zones is that it is perceived to be inconsequential, intractable or just inconvenient.
- This document explores the current scientific thinking, practical experience, and knowledge about how to manage contaminants in low k zones. Through this, a knowledge base is advanced that can facilitates better decisions and outcomes from our actions. We stress that site managers need to:
  - "**Pull back the curtain**" – evaluate all processes and compartments
  - Understand heterogeneity and its impacts by investigating at appropriate scale to answer questions
  - Use integrated approach with complimentary datasets
  - Increase **stylistic understanding** to build better conceptual site model

---

Key Words: 14 compartment model, 1G site characterization, heterogeneity

1.0 INTRODUCTION

1.1 THE PROBLEM

Lead Author for This Chapter

Tom Sale, Colorado State University

Given Freeze and Cherry's 1979 classic textbook Groundwater as a starting point, the field of groundwater contamination can now be said to be entering its fourth decade. Reflecting back in time we can claim a number of impressive achievements, such as:

- Recognizing that subsurface contamination is a widespread problem
- Eliminating many environmentally harmful practices that let to groundwater contamination
- Protecting human health via elimination of dangerous exposure pathways
- Developing clever site characterization and innovative remediation technologies
- Partial depletion of historical groundwater contaminant sources through active and passive measures
- On occasion, near complete cleanup of historical contamination at a small number of sites.

Given the youth of the field of contaminant transport, we can be proud of our progress. At the same time, despite our achievements and best efforts, many sites that have been the focus of our attention and resources for decades, remain as chronic liabilities to current and future generations (NRC 2012). Reflecting on the past three decades, our goal has been to restore contaminated groundwater to its original condition, the result at many sites has been only partial cleanup leading to a need for chronic site management.

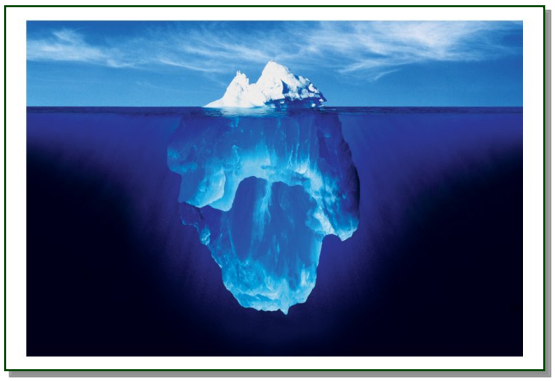

Outcomes falling short of expectations can be attributed to many things including only seeing part(s) of the problem that needs to be address. Much of our investments to date have been analogous to chipping away at the top of an iceberg while thinking we only need to deal with what we can see. In fact, what we have seen and have dealt with at many sites, has only been the tip of the iceberg. Carrying this analogy forward, much of what lies below our current view is contaminant stored in low permeability (k) zones

More comprehensively a key constraint to success with cleanup of chlorinated solvent releases has been our inability to take a holistic view of groundwater contamination problem. Historically we have characterized groundwater contamination by using "First Generation" (1G) monitoring strategies that rely on conventional groundwater monitoring wells. It is now becoming clear that the 1G approach provides a limited and many ways

misleading picture of subsurface contamination, In retrospect, 1G site characterization approaches often have the following shortcomings:

- They only informs us (directly) of aqueous phase contamination. Unfortunately, this often led us to give far too little consideration to nonaqueous, sorbed, and vapor contaminant phases.
- Water produced from wells comes from the most transmissive layers (transmissive zones) adjacent to wells. Unfortunately, this often led many to miss equally if not more important contaminants in less transmissive zone (low k zones).
- At best, reported concentrations from conventional monitoring wells are average values weighted to the most transmissive layers encountered by the well. This averaging has led many to see plumes as large and dilute bodies when in fact laminar flow in porous media often yield plumes composed of local high concentration cores and multiple order of magnitude variations in concentrations over distances of a meter or less (Guilbeault et al. 2005).

In contrast, a holistic vision of subsurface releases is advanced in A Guide for Selecting Remedies for Subsurface Releases of Chlorinated Solvents - SERDP ER-0530 (Sale and Newell 2009). The cornerstone of the Guide is the 14 Compartment Model (14C Model). The 14C Model explicitly recognizes:

- Contaminants occurring in vapor, nonaqueous, aqueous, and sorbed phases
- Contaminants occurring in transmissive and low permeability zones (low k zones) in source zones and plumes
- A network of contaminant fluxes linking compartments

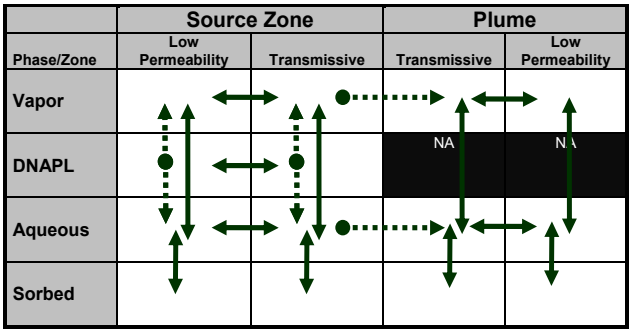

Contemplating the adjacent illustration of 14C model, one can ask:

- If one only knows about the aqueous phase in the transmissive zones will one able to make the right decisions? (Probably Not!)
- Given ignorance of low k zones is it possible to succeed? (Only in rare cases for certain containment technologies)

Interactive 14-Compartment Model

As a companion task to this project, SERDP funded Colorado State, GSI Environmental, and Geosyntec to build an interactive, web-based version of the 14-C model:
www.gsi-net.com

1.2 OBJECTIVES

This document explores the current scientific thinking, practical experience, and knowledge about how to manage contaminants in low k zones. Through this, a knowledge base is advanced that can facilitates better decisions and outcomes from our actions.

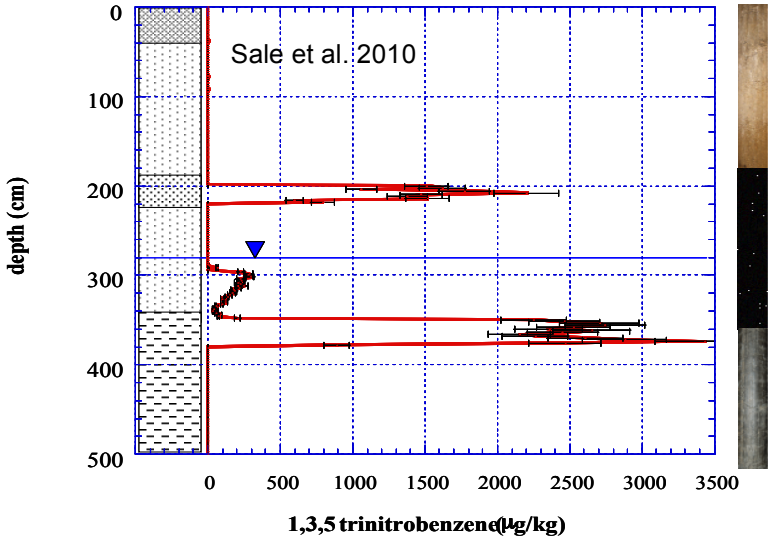

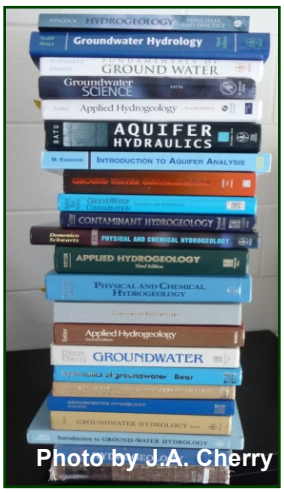

Interestingly, scientific research focusing on contaminants in Low k zones extends back to the 1960s, but the importance of these zones to remediation and site management was not fully appreciated until recently. For example, the key textbooks used by universities to educate contaminant hydrology students are largely silent on the critical topics of contaminants transport via diffusion and low k zones. Two notable exceptions are Groundwater by Freeze and Cherry (1979) and Remediation Hydraulics by Payne et al. (2007). In 1979 Groundwater provided a limited introduction to contaminants in low k zones that is now more than three decades old. More recently, Remediation Hydraulics advanced the hypothesis that embracing the existence of contaminants in low k zones is central to successful remediation. Unfortunately, far too few are familiar with Remediation Hydraulics.

Fortunately, research on contaminants in low k zones has been ongoing for more than five decades (for example, see Foster 1967). Correspondingly, a rich body of knowledge is available in peer reviewed scientific literature. Furthermore, research on the topic of contaminants in low k zones has grown dramatically in recent years. As an example, since 2005 the US Department of Defense ESTCP/SERDP programs have invested in excess $10 million of funding for related research. In addition, since 2005 industry has invested in excess of $20 million of funding for low k zone research though The University Consortium[1].

[1] 1987-2005 University Consortium for Solvents-in-Groundwater, 2005-2012 University Consortium for Field-Focused Groundwater Contamination Research.

One of the greatest challenges to embracing the paradigm of contaminants in low k zones is that it is perceived to be inconsequential, intractable or just inconvenient. Challenges to embracing advective-diffusion transport in heterogeneous media and the principles behind the 14C Model include:

- The concepts advanced in the 14C Model are complicated. A verbal comment from a regulator was… "I can't handle two compartments much less fourteen".
- Historically our attention has been drawn to theme of DNAPLs to the exclusion of other relevant phases
- Finding plume cores in transmissive zones and corresponding contaminants in low k zones requires collection of data on a spatial scale that is perceived by many as being impractical.
- Capturing diffusion controlled transport process in models requires small-scale spatial and temporal discretization that is perceived by many as being impractical.
- Treatment of contaminants in low k zones that are diffusion controlled is difficult and not well understood.

Despite these challenges, an early adopter of the paradigm of contaminants in low k zones made the thoughtful observation "…there is no going back". It seems given the alternatives comprehensive and incomplete understandings of subsurface releases, there is but one path.

1.3 AUTHORIZATION

Funding for this project was provided by the Strategic Environmental Research Development Program (SERDP) in August of 2010 under the project title *Basic Research Addressing Contaminants in Low Permeability Zones* (Project No. ER-1740). Funded institutions and investigators are presented in the following table.

Institution	Principle Investigator	Technical Contributors	Students
University of Guelph (UG), Ontario	Dr. Beth Parker	Steve Chapman	Glaucia Lima (PhD)
Colorado State University[2] (CSU), Colorado	Dr. Tom Sale	Dr. Julio Zimbron	Kevin Saller (PhD) Azadeh Bolhari (PhD)
GSI Environmental Inc. (GSI), Texas	Dr. Chuck Newell	Dr. David Adamson Nick Mahler	
Kansas University (KU), Kansas	Dr. J.F. Devlin		Angela Eichler (MS)

[2] Prime contractor for project

The *Basic Research* project is organized into eight different activities. This documents results from all activities. The body of the report covers Activity 8 as shown in the adjacent activity chart. Our goals are to:

- "Pull back the curtain" – evaluate processes and compartments
- Understand heterogeneity and its impacts by investigating at appropriate scale to answer questions
- Use integrated approach with complimentary datasets
- Increase stylistic understanding to build better conceptual site model

Concurrent to this project, SERDP funded three complementary low k zone projects. These include:

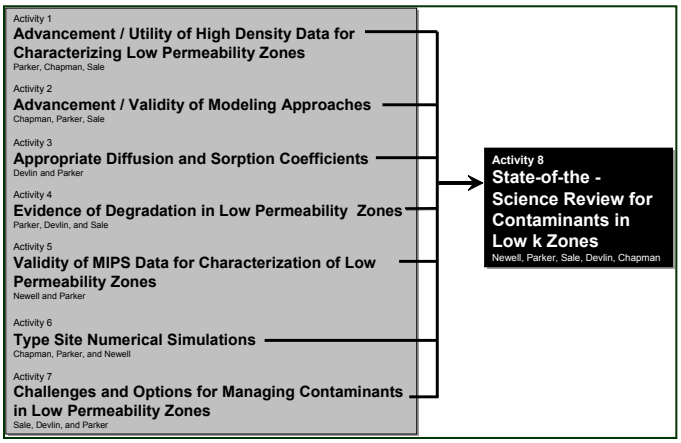

- **ER-1737:** Impact of Clay-DNAPL Interactions on Transport and Storage of Chlorinated Solvents in Low Permeability Zones (SERDP), Lead Principal Investigator: Avery Demond, University of Michigan.

- **ER-1738:** The Importance of Sorption in Low-permeability Zones on Chlorinated Solvent Plume Longevity in Sedimentary Aquifers (SERDP), Lead Principal Investigator: Richelle Allen-King, University at Buffalo.

- **ER-1739:** The Behavior of Compound Specific Isotopes during the Storage of Chlorinated Solvents in Low-Permeability Zones through Diffusion and Sorption (SERDP), Lead Principal Investigator: Orfan Shouakar-Stash, University of Waterloo.

1.4 CONTENT AND ORGANIZATION

This report is organized into seven chapters with supporting Appendices. The goal of the body of the report is to provide review of processes governing storage and release of contaminants in low k zones can be read in a few hours. Appendices provide more lengthy documentation of results from project activities. Content of this report includes:

Chapter 2 Overview of Low k Zones: As a point of embarkation, a brief introduction to low k zones is provided. This provides foundational terminology and concepts that are used in the subsequent chapter.

Chapter 3 Characterization of Low k Zones: This chapter describes methods used to characterize low k zones including their advantages and limitations. Field data are included to illustrate common "styles" of contaminant occurrences in low k zones.

Chapter 4 Transport in Heterogeneous Porous Media: The paradigm of contaminants in low k zones requires an appreciation of contaminant transport via advection, diffusion, and reaction in heterogeneous porous media. Initially, three widely used contaminant transport codes are tested using data from a sand tanks study. Results show that high resolution spatial and temporal discretization is needed to capture critical process. Next, factors controlling diffusive transport are addressed. Lastly, the nascent topic of reactions in low k is addressed.

Chapter 5 Type Site Simulations: A set of numerical simulations of contaminant transport in heterogeneous media via advection-diffusion-reactions are presented in the chapter. Bound geologic "Type Sites" are considered. The simulations provide insight regarding governing process and a basis for conceptualization of governing processes at similar sites.

Chapter 6 Treatment of Contaminants in Low k Zones: This chapter explores the topic of what can be done to manage contaminant in low K zones. Common remedies are introduced and demonstrated using sand tank studies.

Chapter 7 Implications for Selecting Site Remedies: Lastly, results from the study are summarized in the format of implications for selecting site remedies.

Chapter 8 contains the references and ***Chapter 9*** provides a map showing how the contracted research tasks were fulfilled and a list of key research products.

OVERVIEW OF CHAPTER 2: *LOW K ZONES*

- Plume maps are often flawed in two ways that are consequential: 1) they fail to recognize vapor, nonaqueous and sorbed phases; and 2) diverse and time variant geologic processes create subsurface bodies that are (with rare exceptions) highly heterogeneous with respect to their capacity to conduct fluids (permeability).

- Common spatially variations in permeability of 3-6 OoM (Orders of Magnitude) leads to transmissive zones where advective transport dominates, and low k zones where diffusive transport dominates. Low k zones store and release contaminants via diffusion and slow advection.

- Perhaps the most problematic aspect of failing to recognize low k zones is that they can sustain contaminant concentrations in transmissive zones for decades or even centuries after the primary sources have been addressed (Chapman and Parker 2005).

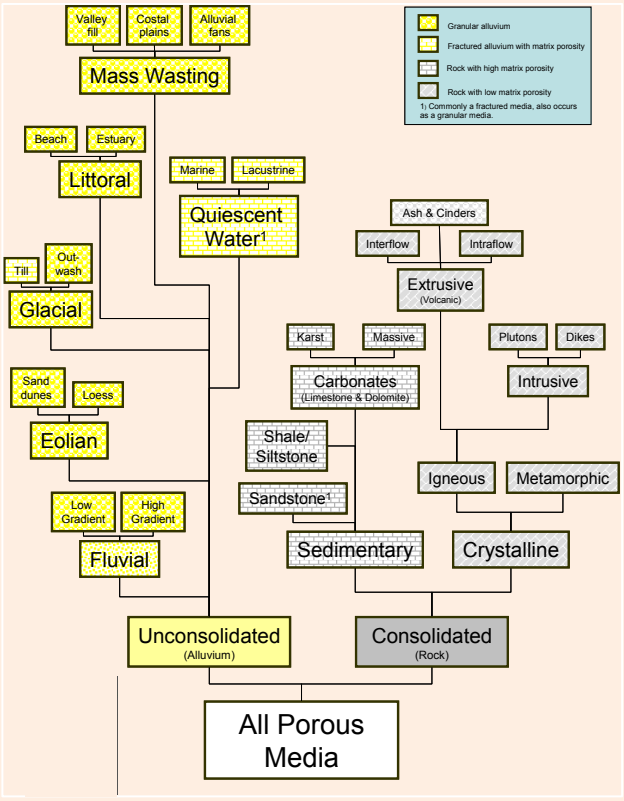

- Our need to embrace transport in heterogeneous media leads to the question; what do systems of transmissive and low k zones look like? The answer to this lies in understanding depositional and post deposition geologic processes.

- The terms **transmissive** and **low k** describe contrasts in permeability as opposed to absolute values of permeability. Two examples: 1) A fine-sand can be a transmissive zone given that the remainder of the domain is silt and/or clay; or 2) a fine-sand can be a low k zone given that the remainder of the media is a well-sorted coarse sand or gravel.

- Two general idealized types of porous media are described. The first type is: **granular porous media** and **fractured porous media**. Noteworthy aspects of low k zones include: **High potential to sorb contaminants; Reducing conditions, Size, DNAPL in Transmissive Zones at Contacts**

- Site conceptual models should embrace the idea of relevant sub meter-scale geologic heterogeneity.

Key Words: heterogeneity, spatial variation, OoM, advection, diffusion, depositional processes, permeability contrast, granular porous media, fractured porous media, DNAPL, contacts.

2.0 LOW PERMEABILTY ZONES

2.1 HISTORICAL PERSPECTIVES

Lead Author for this Chapter

Tom Sale, Colorado State University

Conventional reports describing subsurface releases commonly include plan view contour maps of contaminants in groundwater based on analysis of water samples collected from wells with well screens that are 10 or more feet in length. These images are referred to as plume maps. Plume maps portray largely homogeneous geologic bodies with contaminant concentrations that smoothly grade through multiple Orders of Magnitude (OoMs) over distances of 100s to 1000s of meters. Furthermore, conventional plume maps depict systems that are vertically uniform.

In many ways, principles underlying conventional plume maps follow those employed in the Theis (1935) solution for drawdown about a pumping well. For example, conditions commonly depicted in plume maps are consistent with aquifers that are homogeneous and isotropic, have a constant thickness, and have no variations in parameters of concern in the vertical direction. Given the outgrowth of contaminant hydrology from the field of well field hydraulics, similar visions of aquifers in the fields of hydraulics and transport are not surprising.

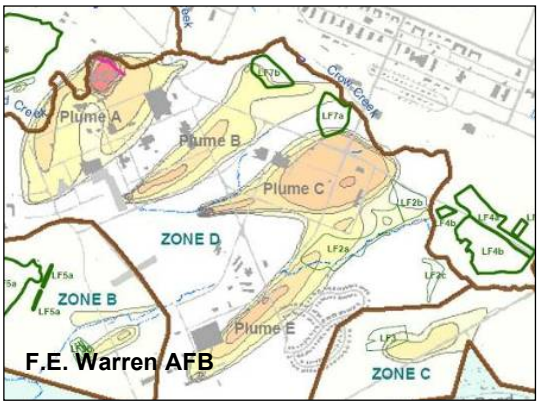

Unfortunately, with respect to contaminant transport, idealizations associated with plume maps are often flawed in two ways that are consequential. First, plume maps fail to recognize vapor, nonaqueous and sorbed phases. Missing these phases is a primary reason many contaminated sites proceeded with the implementation of pump-and-treat systems under the belief that this would lead to near-term restoration of groundwater.

> *"The type of aquifer study in which our homogeneous model of groundwater flow is most grossly inadequate is that of dealing transport phenomena… the simple and useful model for problems of well field development will mislead us if we apply it to problems of transport…. "*
>
> *Theis, C. V., 1967*

Secondly, diverse and time variant geologic processes create subsurface bodies that are (with rare exceptions) highly heterogeneous with respect to their capacity to conduct fluids (permeability). Common spatially variations in permeability of 3-6 OoM (Orders of Magnitude) leads to transmissive zones where advective transport dominates, and low k zones where diffusive transport dominates. Low k zones store and release contaminants via diffusion and slow advection. Diffusion is driven by gradients in contaminant concentration per principles embodied in Fick's first law (Shackelford 1989).

Initial uptake of contaminant by low k zones leads to dilute concentrations in transmissive zones. Dilute concentrations in transmissive zones have widely been attributed to hydrodynamic mixing of waters in aquifer. This is despite the conflicting fact that groundwater flow in porous media is almost always laminar and, consequently, transverse mixing should be a weak process. In fact, early time dilution of plumes (attenuation) can be due (in large part) to contaminant attenuation in low k zones.

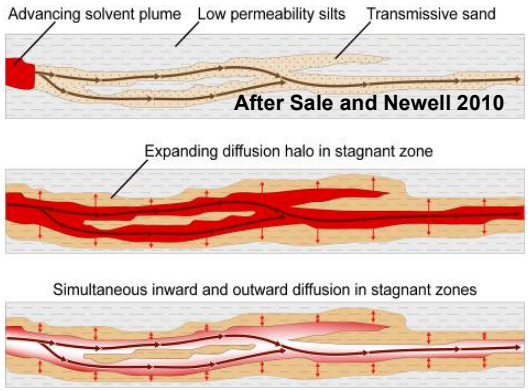

Perhaps the most problematic aspect of failing to recognize low k zones is that they can sustain contaminant concentrations in transmissive zones for decades or even centuries after the primary sources have been addressed (Chapman and Parker 2005). This is in contrast to the historical paradigm that eliminating and/or reducing contaminant discharge from source zones would lead to near-term attainment of targeted contaminant concentrations in plumes. As an analogy, we thought that addressing sources would be like shutting off a smoke stack; once the smoke stack is off, the skies will clear. Experience in groundwater remediation has shown us otherwise. Far too often, plumes persist long after primary sources have been addressed. This observation is central to the realization that storage and release of contaminant from low k zones is paramount to managing subsurface releases.

Embracing the paradigm of advective-diffusive transport of contaminants in heterogeneous media (transmissive and low k zones) holds great promise. First, it explains the limitations of historical First Generation (1G) approaches to site characterization. Secondly, it explains why many site remedies have failed to achieve the anticipated outcomes. Thirdly, it provides a basis to make better decisions based on a complete understanding of the governing processes. Per the adjacent note, C.V. Theis recognized both the need and opportunity of embracing heterogeneity in our analysis of transport in groundwater forty five years ago. It seems it is time to take his advice.

> *"…a new conceptual model containing the know heterogeneities of the natural aquifer, to explain the phenomena of transport in groundwater"*
>
> *Theis, C. V., 1967*

2.2 ARCHITECTURE OF TRANSMISSIVE AND LOW k ZONES

Our need to embrace transport in heterogeneous media leads to the question; what do systems of transmissive and low k zones look like? The answer to this lies in understanding depositional and post deposition geologic processes. Interestingly, the topic of architecture of transmissive and low k zones has seen only sporadic attention in groundwater text books and peer reviewed literature. Notable exceptions include Davis and De Weist 1966, Back et al 1988, Ritter et al. 1995, NRC 2005, and Sale and Newell 2011.

2.2.1 Terminology and Concepts

First, it is important to note that the terms **transmissive** and **low k** describe contrasts in permeability as opposed to absolute values of permeability. As examples:

- A fine-sand can be a transmissive zone given that the remainder of the domain is silt and/or clay.

- A fine-sand can be a low k zone given that the remainder of the media is a well-sorted coarse sand or gravel.


Photo Steve Chapman

Two general idealized types of porous media are envisioned. The first type is **granular porous media** wherein transmissive granular media is typically present as a continuum through the domain of interest. Granular porous media are typically the product of erosion, transport, and deposition.

The second type is **fractured porous media**. Fractures are typically the product of post deposition geologic processes including: desiccation, consolidation, release of overburden pressure, and tectonic activity. Fractures are ubiquitous in most geologic media, and can be open or closed. Herein, discussions of fractured media focus on the scenario of open fractures. Clays, silts, and rock are commonly classified as fractured porous media. Note bioturbation introduces another set of processes that can introduce transmissive features.

The portion of fractured media that is not fractured is referred to as **matrix blocks**. Typically, matrix blocks are low k zones. In the case of sedimentary deposits (alluvium, sandstones, carbonate, and shales) matrix block are typically porous. Sedimentary matrix blocks typically have sufficient interconnected pore space to store and release contaminants via diffusion and/or slow advection. In contrast, matrix blocks found in crystalline rock (granite, schist, niece, and basalt) often have little if any interconnected pore space. Absent this interconnected pore space, these matrix blocks in crystalline rock generally have a limited potential to store and release contaminants.

Subsurface settings reflect a continuum of conditions that are bounded by the idealized scenarios of granular and fractured porous media

In an attempt to move beyond the vision of homogeneous-isotropic porous media, NRC (2005) identifies 5 general "**Type Sites**" (see following figure). An update to the NRC (2005) Type Sites is presented in Sale and Newel (2011). Type I and II settings are considered rare. Types III, IV and V setting are the most common. Relative to this report, Type III and Type V are the most important due to the presences of low k zones that can store and release contaminants. It is important to note that some sites are composed of combinations of these Type Settings. Examples include:

- Canadian Force Base Borden, Ontario (Great Lakes) - A Type III a shoreline sands (littoral) underlain by a Type V fractured silt lake bottom (lacustrine).

- Air Force Plant 6, Marietta, Georgia (Piedmont of Southern US) - A Type III layered silts (saprolite) underlain by a Type V fractured crystalline schist (metamorphic rock).

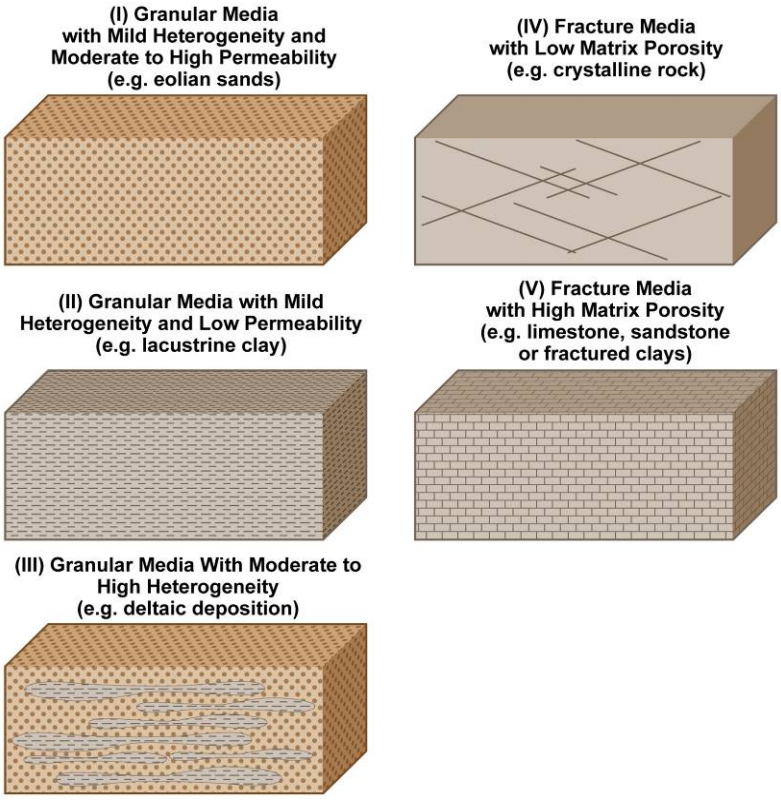

NRC (2005) Type Sites

2.2.2 Key Features of Low k Zones

High potential to sorb contaminants - Low k zone are commonly deposited in low energy environments with the associated properties of small grain sizes and large fractions of organic carbon (relative to transmissive zones). These properties can lead to a greater potential for sorption of contaminants. Sorption of contaminants in both transmissive and low k zones is a focus of SERDP project ER-1738.

Reducing conditions - Given high organic carbon and limited groundwater flow, geochemical conditions in low k zones are likely to reducing. Reducing conditions in low k zones can sustain natural degradation of oxidized compounds (i.e. chlorinated solvents) via biotic and/or abiotic processes. This topic is expanded upon in Section 4.4 of this report.

Size - The sizes of low k zones varies widely. Thick (10s of m) aerially extensive (km) low k zones are referred to as aquitards. Aquitards help protect potable water in aquifers from natural and anthropogenic contaminants. The Eau Claire Formation in Wisconsin, Alpine Formation in Utah, Hawthorn Formation in Florida and Bellflower Formation in Southern California are

examples of important aquitards. A comprehensive review of aquitards is presented in Cherry et al. 2006. Moving to smaller scales, low k zones come in a wide variety of shape and sizes. Smaller low k zones are also potentially important. Parker and Chapman (2007) describe centimeter thick low k layers that provide persistent releases of contaminant after reducing upgradient contaminant discharge.

DNAPL in Transmissive Zones at Contacts - Following Feenstra et al. (1996) and Kueper and McWhorter (1991), DNAPL entry into unfractured low k zones is typically precluded by large pressures (displacement pressure) needed to displace water from fine grained media. Instead, DNAPL tends to occur (initially) in transmissive zones above low k layers (acting as capillary barriers) and/or in secondary permeability features (e.g. fractures and root holes) in low k zones. With time, these DNAPL pools are depleted via dissolution (Parker 1994). The relevance of DNAPL at transmissive, low-k zone contacts is that large aqueous phase concentration gradients can drive large amounts of dissolved and sorbed phase contaminants into low k zones.

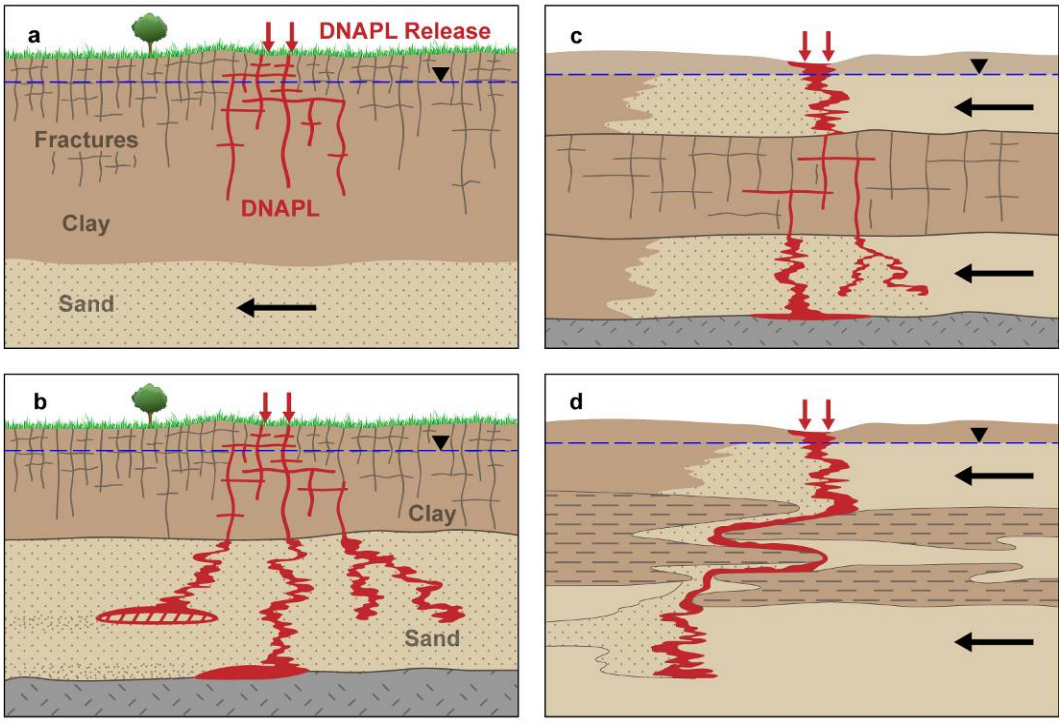

DNAPL Site Conceptual Models (after Feenstra et al. 1996)

Most site conceptual models begin with an assumption of uniform-isotropic geologic media at the meter-scale. At most sites, conceptual models consider macro-scale layers that are themselves uniform. The authors of this document wish to argue that instead of this, site conceptual models should embrace the idea of relevant sub meter-scale geologic heterogeneity. Unfortunately, knowing where every sub-meter layer is impractical. The alternative is to develop a stylistic understanding of the architecture of transmissive and low k zones based on:

- An understanding of depositional and post depositional history
- Rigorous characterization of a representative element of the impacted media

The following figure identifies common depositional environments for media impacted by releases. Supporting references on depositional environments include Davis and De Weist 1966, and Back et al 1988.

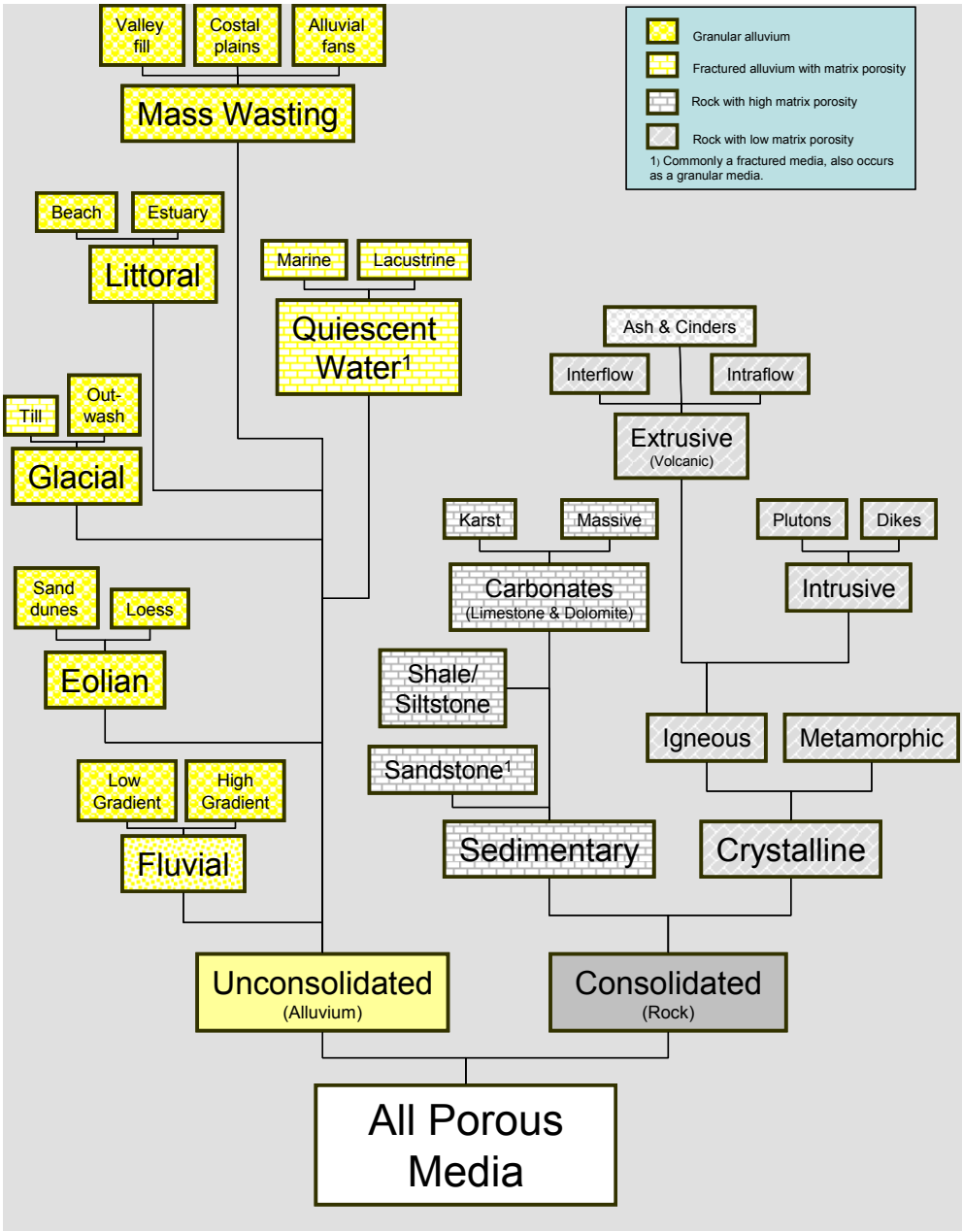

OVERVIEW OF CHAPTER 3:
CHARACTERIZING LOW K ZONES

- 1G site characterization provides limited information that often constrains or ability to efficient address impacts of subsurface releases. 2G site characterization techniques have limitations that are difficult to fully appreciate before they are applied

- Address limitations of current 2G methods by applying multiple 2G methods with the vision that the sum of the data will provide the information needed to select and/or design remedies. There is a clear need, for even better 3G, site characterization tools.

- All compartments and all processes should be considered during site characterization. Heterogeneity is an important governing factor for contaminant fate and transport.

- High-resolution characterization is key to understanding heterogeneity—the scale must be appropriate for the site conditions.

- Focus on the right metrics for understanding the site. Site characterization must be dynamic and adaptive.

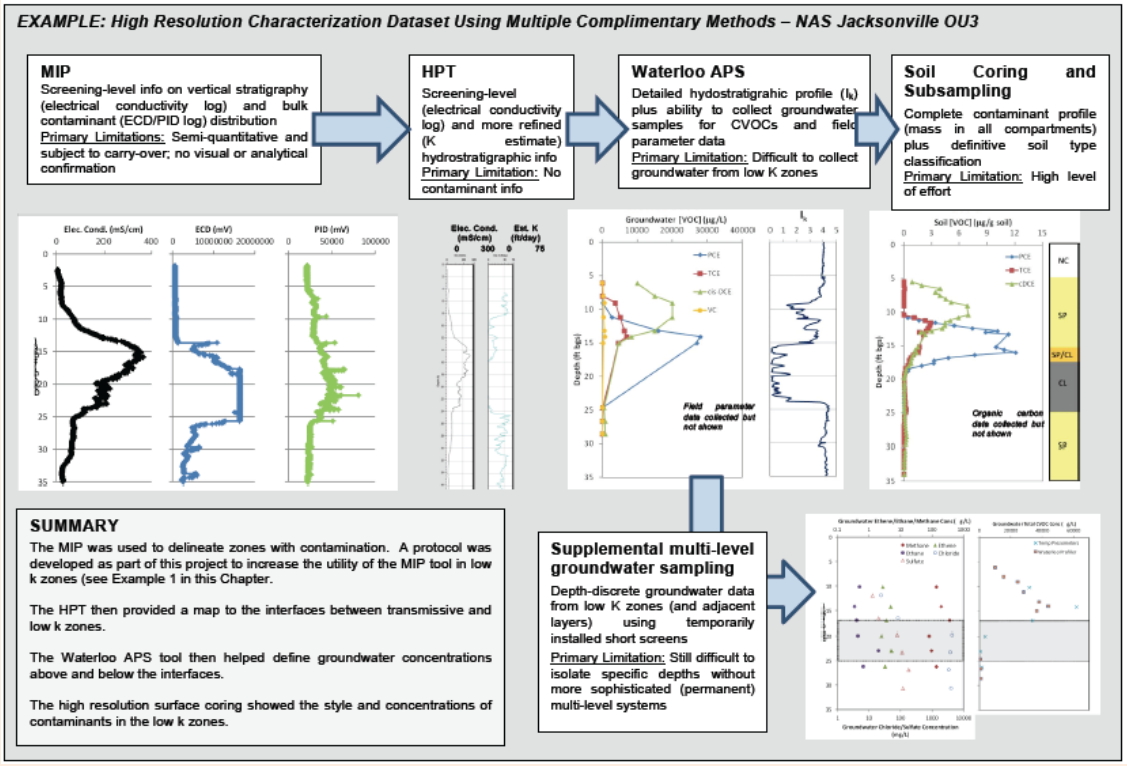

Key Words: Soil Sampling, high-resolution, multi-level groundwater monitoring, hydraulic profiling, membrane interface probe (MIP), laser-induced fluorescence (LIF), borehole, geophysics, rock coring, borehole liners/packers, tracer tests, dynamic site investigation, adaptive site investigation, Triad approach, discrete fracture network analysis, 2G site characterization, 3G site characterization.

3.0 CHARACTERIZING LOW K ZONES

The following chapter describes "high resolution" or "second generation" (2G) techniques for characterizing contaminants in low k zones. Content includes a review of the limitations of 1G site characterization practices, an introduction to 2G site characterization techniques, results from project specific applications of 2G methods to low k zones (Activities 3 and 7), and a summary of key results. Complementary information is included in Appendices.

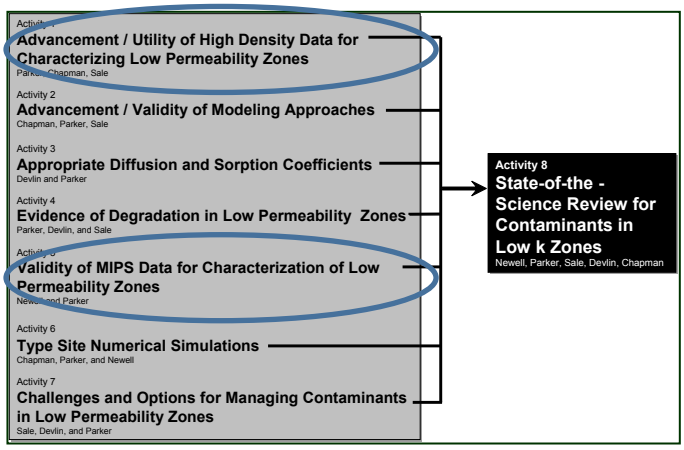

Lead Authors for This Chapter

Dave Adamson, GSI Environmental and Steve Chapman, U. of Guelph

3.1 "FIRST GENERATION" CHARACTERIZATION APPROACHES

Traditional approaches to site characterization have relied heavily on conventional (long-screened) groundwater monitoring wells within aquifers, and sparse soil samples within the focused on sources zones (**Figure 3.1**). Following NRC 2005, a source zone is a body in which NAPL are or were present. "First-generation" methods dates back to the early 1980's (Einarson, 2006). They are generally based on the assumption that all subsurface releases fit into a conceptual model where there is source material in the vadose zone, the water table (LNAPL), or the base of the aquifer (DNAPL) that supplies contaminant mass to the saturated zone for subsequent plume development. Soil sampling is focused on identifying source material, which is assumed to be NAPL. Monitoring wells are used to delineate the

Figure 3.1. Key elements of first-generation approaches to site characterization.

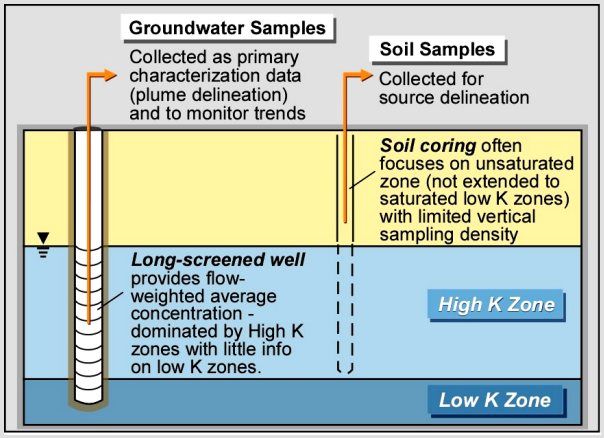

extent of the plume based on a (probably faulty) assumption that transverse dispersion leads to plume with ever growing plan view widths with distance.

Hydrostratigraphic information is typically inferred and/estimated based on geologic cross sections and localized hydraulic testing (e.g., pump test at limited number of long-screened monitoring wells). This follows the classical application of Darcy's equation, where characterization is done with relatively large volumes of pore space where the aquifer characteristics become uniform (i.e., the representative elementary volume), and smaller-scale heterogeneities are ignored. As a result of these assumptions, the aquifer system essentially becomes isotropic and all parameters can be represented as scalar quantities (Payne et al., 2008).

As described below (and summarized in **Table 3.1**), first-generation approaches have considerable limitations at all sites, but these limitations are particularly noticeable at sites where low k soils are present.

3.1.1. The Problem with Conventional Groundwater Wells for Site Characterization

Groundwater monitoring wells are the most widely-used tool for environmental site investigations (Einarson, 2006), but their role—particularly as part of the site characterization process—is often out of proportion to the information that they provide. This is related to two factors: 1) Wells are constructed with little attention to identifying and characterizing small-scale heterogeneities; 2) Sampling groundwater (in the absence of soil sampling) provides an incomplete picture of contaminant concentrations and the influence of hydrostratigraphy on contaminant distribution. Because of these limitations, wells are more appropriately categorized as a monitoring tool, not a characterization tool.

Typically, monitoring wells are designed and installed with a 10-ft (or longer) screened interval to cover the most transmissive zones of a groundwater-bearing unit. As a result, they yield information on the bulk contaminant concentration in transmissive zones (i.e., the mobile porosity) in the screened interval. This can be useful because it mimics the concentration that would be measured within a water supply well (which necessarily use longer screens to maximize yield). This also means that a conventional monitoring well generates information that is easy to convey to regulators because the measured concentration can be directly compared to a risk-based drinking water standard. Wells also function nicely when transitioning into a long-term monitoring phase because they are designed to document temporal trends in concentration.

However, the historical consequence of this practice within the environmental field is that groundwater data from monitoring wells ended up being used not only to satisfy the needs of the regulatory community but also became the primary means to characterize a site. This failure to appreciate the differences between characterization and monitoring can hinder the development of an appropriate conceptual site model.

The primary problem is that conventional long-screened monitoring do not provide depth-discrete information, and thus do not provide information at a scale that is relevant to understanding important fate and transport processes at a site (Puls and Paul, 1997). As noted above, the concentration obtained from these monitoring wells is a flow-

weighted average that preferentially draws from the most transmissive zones within the screened interval (Martin-Hayden and Robins, 1997). If those transmissive zones are lower in concentration than adjacent finer-grained soils, then the well will not identify the peaks or the overall distribution. **Figure 3.2** shows a hypothetical example of how the data from a long-screened well can lead to poor assessment of the actual concentration distribution. The lack of information provided by conventional monitoring wells can contribute to a false confidence that conditions at the site are well-understood. Or, even worse, a sense of large dilute plumes where, in fact, contaminants occur in tight plume cores (e.g. Guilbeault et al., 2005)

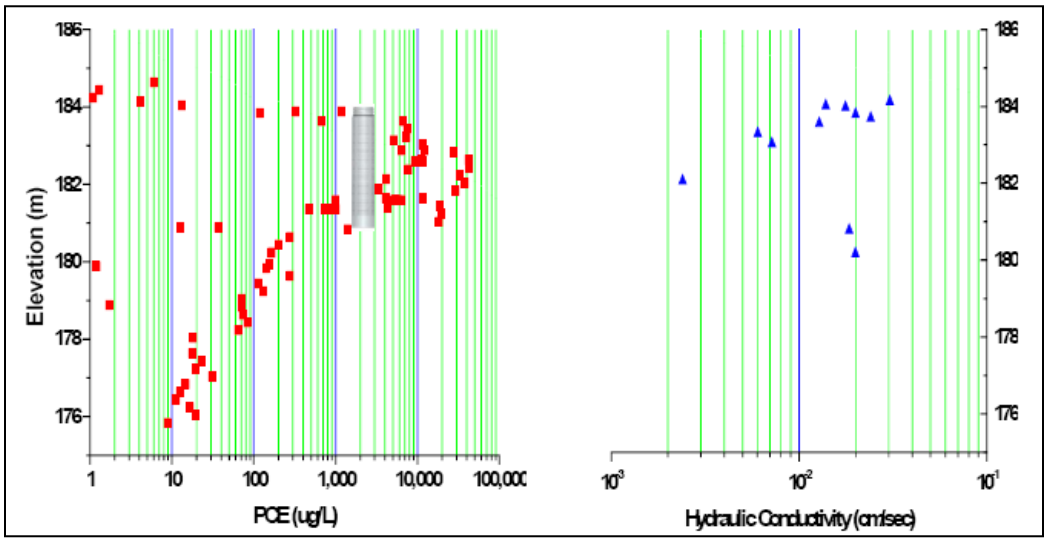

Figure 3.2. Example of how long-screened monitoring wells can misrepresent groundwater concentrations. The left-panel shows that the actual PCE concentration varies several orders of magnitude over short vertical distances, including the 3-m (10-ft) screened interval for the hypothetical monitoring well (shown as gray box). The hydraulic conductivity also varies widely over the same interval, but groundwater samples collected from the well will be dominated by the highest permeability intervals that are associated with concentrations of approximately 5000 μg/L. This flow-weighted average concentration is much lower than the peak concentration of approximately 50,000 μg/L that is associated with less permeable intervals. Diagram courtesy of Stone Environmental Inc.

As a result, a long-screened well is particularly poorly-suited for low k zone investigations. Even if the screen covers the lower permeability interval of interest, groundwater will be sampled from soil layers that represent a distribution of hydraulic conductivities, and the most transmissive layers will be over-represented in the measured groundwater concentration. This is problematic at late stage sites (discussed in Chapter 7) where the more transmissive zones might be cleaner (due to extended advective flushing) than the less transmissive zones (where inward diffusion may have led to significant mass storage).

Further, there is considerable evidence that conditions within a long-screened monitoring well are not necessarily representative of formation conditions. This is due to the

potential for ambient (vertical) flows within the open borehole that develop in response to temperature or solute-derived density gradients (Ecli et al., 2001, McDonald et al., 2009). These gradients cause in-well groundwater mixing (McHugh et al., 2012) and thus can limit the utility of depth-discrete groundwater sampling approaches (i.e., no purge and/or passive diffusive samplers) within these wells. To overcome this limitation, specific intervals of interest have to be isolated using careful packer and filter pack design.

Collectively, these factors mean that it is very difficult to characterize groundwater with long-screened monitoring wells unless there is basically negligible heterogeneity at a site—a condition that may not actually exist in nature. More effective groundwater characterization should focus on shorter screens installed at multiple levels that provide depth-discrete data for evaluating contaminant distribution (Einarson, 2006).

However, even if properly constructed, groundwater wells still have significant limitations as a primary site characterization tool. Specifically, they provide information on aqueous-phase concentration but do not address contaminant mass present in other aquifer compartments. This includes sorbed-phase, non-aqueous phase, and vapor-phase mass, none of which can be quantified via groundwater well sampling. The contaminant mass present in these compartments can be considerable at many sites, and their persistence may be a major contributor to the time required to achieve cleanup objectives.

Groundwater wells also provide no stratigraphic information unless cores were logged and sampled when the well was installed. In some cases, groundwater is being sampled "blindly", with only limited knowledge of the specific intervals that may be contributing most to the measured concentration. It is a much different situation than soil sampling, where the contaminant concentration can be tied directly to the soil type being sampled.

Within fractured rock settings, groundwater sampling is used extensively as a characterization tool because of the belief that these formations are too challenging to warrant core collection. This practice is basically a concession that the complexity of fractured rock cannot be characterized, and that the only useful information that can be obtained is through collecting groundwater from hydraulically active fractures. However, this approach generally yields compromised data because it relies on sampling intervals that are not appropriate to the scale of the problem and boreholes that promote cross connection between fractures (Parker, 2007). Just like in unconsolidated formations, these groundwater-based methods ignore mass stored in the soil matrix (in this case, within the rock itself) and provide potentially misleading information on the distribution of contaminants.

3.1.2. The Problem with Traditional (1G) Soil Sampling and Analysis

Soil sampling is typically undertaken during the initial stages of the site characterization process. Therefore, it does not suffer from the same inherent problem as groundwater sampling, where monitoring methods have been misapplied as characterization methods. In soil sampling, the primary investigative method—the collection of material from the locations and intervals of interest—remains the same regardless of whether standard or "high-resolution" characterization principles are being considered. The primary differences lie in the way these various methods are applied, particularly the

scale and level of detail associated with the investigative approaches. Simply, soil sampling has traditionally not been used to generate sufficiently detailed data for the purposes of characterizing low k zones.

Soil sampling has frequently focused on the unsaturated zone during traditional site characterization. This is a largely a function of the overreliance on groundwater monitoring wells as the primary method for measuring contaminants within saturated zones. Under this conceptual model, soils are collected from the vadose zone to identify contaminant sources and potential migration routes, but the investigation is often not extended to the underlying aquifer. Clean-up objectives for a site may be based solely on concentrations from groundwater wells, such that there is little interest from regulators or stakeholders in collecting soil data from this zone. There is also the general perception that soil coring and analysis within the saturated zone is technically challenging, and that collecting groundwater data provides a more comfortable route for everyone involved.

The problem is further compounded at sites where lower k zones make up a significant portion of the soil matrix. There is little reason to expect that low k soils will be adequately characterized if groundwater monitoring data is the primary method being used to investigate the saturated zone.

When soil sampling and analysis *is* attempted within the saturated zone, the efforts may not be rigorous enough to provide information at the appropriate scale for characterizing heterogeneity. This can occur both at the coring and the sampling steps of the process:

- Collection of cores must maintain the integrity of the soil structure and retain as high a percentage of the drilled interval as possible. This requirement has led to a shift to direct push hollow-stem auger, and sonic methods as the preferred options for soil collection within the environmental profession. It is still not uncommon to see geologic logs constructed using cuttings from standard auger-based drilling methods. This approach does not allow soils to be assigned to a particular depth and are particularly susceptible to missing thin low k lenses as well as interfaces between low and high permeability zones.
- Soil sampling methodologies may purposely ignore heterogeneity and its impact on contaminant distribution. This occurs by sampling at relatively wide intervals (e.g., every 5 ft) that are not sufficient for identifying contaminant distributions or even hotspots with any level of confidence. Similarly, the practice of compositing across locations is still frequently used to generate an average soil concentration that is perceived as more representative and less subject to bias/error (ITRC, 2012). While this approach has value in certain applications, it should be recognized that it limits insights on the small-scale heterogeneity present at a site that is provided by more discrete sampling methods.
- Characterization often focuses on soil classifications based on visual inspection that may not representative of the true lithology. A geologic log generated without the use of information from supporting physical property analyses or stratigraphic logging methods may miss subtle changes. Similarly, soil analyses may include contaminant concentrations, but ignore parameters such as the organic carbon fraction which greatly influence transport of these contaminants.

In particular, the lack of attention to scale can cause problems when interpreting soil data collected using more traditional methodologies. For example, it can be difficult to evaluate remedy performance using soil data when there is little understanding of the level of heterogeneity. A limited pre-treatment dataset can lead to a lot of anxiety when it comes time to demonstrate post-treatment success.

Collectively, conventional approaches for collecting and analyzing soil samples represent a missed opportunity for characterizing sites, particularly for those with low k zones. The authors of this document view soil coring as a cornerstone of the high-resolution ("second-generation") characterization approaches described in the next section.

3.1.3 Goals of Low k Zone Characterization

- "Pull back the curtain" – evaluate all processes and compartments
- Understand heterogeneity and its impacts by investigating at appropriate scale to answer questions
- Use integrated approach with complimentary datasets
- Increase stylistic understanding to build better conceptual site model

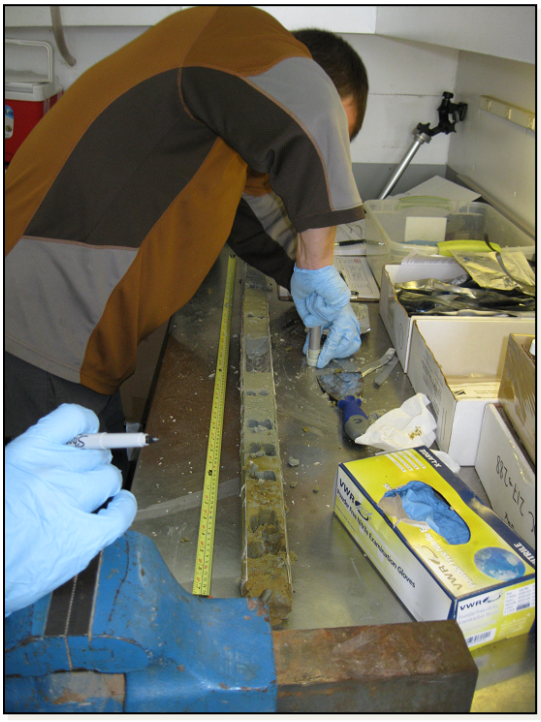

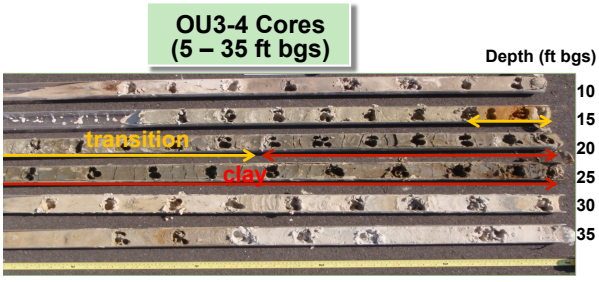

Table 3.1. Summary of Key "First-Generation" Tools for Site Characterization

Tool/Method	Description	Primary Data Generated	Advantages	Limitations
Groundwater Monitoring Wells	Monitoring wells with 10-ft (or longer) screened intervals placed in transmissive zone	Groundwater contaminant concentration and geochemical parameters	• Provides data for assessing temporal trends • Concentration data are generally acceptable for regulatory purposes	• Not a true characterization method because wells are a poor indicator of heterogeneity (concentrations are flow-weighted averages) • Overemphasizes contaminants in higher k subintervals – low k zones rarely considered in well design • No vertical gradient data generated • Data quality can be impacted by in-well effects (mixing, volatilization, degradation) • Not suitable for assessing small-scale processes contributing to contaminant fate and transport (e.g., diffusion
Soil Sampling	Soil or cores collected in interval(s) of interest (typically unsaturated zone only) using variety of standard methods (split spoon, Shelby tubes, drill cuttings)	Soil contaminant concentration physical properties; hydrostratigrapy	• Quantifies mass present in all compartments • Provides method for identifying low k units and understanding heterogeneity • Can provide more complete vertical contaminant profile (assuming sampling frequency is consistent with scale of heterogeneity)	• Soil lithology may be lost depending on drilling method that is selected (particularly those where only cuttings are generated) • Many practitioners focus only on unsaturated soils (and assume groundwater is sufficient for characterizing saturated zone) • Many drilling methods are poorly suited for tight soils and fractured rock • Samples are frequently composited such that small-scale heterogeneity is lost

3.2 2G CHARACTERIZATION APPROACHES

There has been an increased recognition of the importance of a process-driven approach to site characterization that more accurately reflects site conditions than the more conventional methods described above. This shift has helped spur the development and technical maturation of second Generation (2G) tools and methods for site characterization. Many of these are now considered valuable and even indispensable elements of site characterization. In general, these are methods that provide data at a smaller and more appropriate scale than conventional characterization data. Often this type of data is referred to as high-resolution or high definition. The objective is to obtain a better understanding of contaminant distribution in the context of the hydrogeologic conditions that define the site. More specifically, 2G site characterization approaches can:

- Provide a "stylistic" understanding of the occurrence of all contaminant phases in transmissive zones and low k zones
- Define the target for focused remedial measures

3.2.1 Key Themes for Characterization

The logic for utilizing 2G characterization methods is built around several important themes, all of which relate to our field's greater appreciation of the complexity of contaminant fate and transport in heterogeneous media.

All compartments and all processes should be considered during site characterization.

The overall goal of site characterization is support the development of an accurate and defensible conceptual site model. This model is an invaluable component of the site management process because it integrates all available site information, but it is critical that it be based on sound science and reflect all potentially-relevant processes. As noted above, conventional characterization has often ignored lower permeability zones based on the long-held assumption that groundwater and contaminant flow within the higher permeability elements largely define the magnitude of the problem at most contaminated sites. However, over timescales that are relevant to the long-term site management (decades or less), relatively "slow" processes such as diffusion and advection within low k strata can result in considerable mass storage within these compartments (see Chapters 4 and 5).

A useful element of the site conceptual model can be the 14 Compartment Model (14 C Model) developed by Sale et al. (2008). The model provides a framework for documenting where the mass and mass fluxes are located at (including the low permeability compartments) and in what phase (i.e., vapor, NAPL, aqueous, and sorbed). The 14 C Model should be considered a complimentary tool for building a conceptual site model and not an absolute requirement. However, a site characterization problem that did not provide *sufficient* information to complete the 14 C Model would likely be *insufficient* for constructing a representative conceptual site model.

Consequently, *no* processes or compartments should be ignored during the characterization phase(s), and data collection efforts should always be focused on strengthening the conceptual site model and addressing any perceived knowledge gaps. Characterization should focus on establishing the site hydrostratigraphy (e.g., soil type, hydraulic properties) and the distribution of relevant parameters (e.g., contaminant mass/concentration, organic carbon) to permit a comprehensive understanding of all processes.

Heterogeneity is an important governing factor for contaminant fate and transport.

Geological formations are—by nature—heterogeneous because they result from a combination of complex depositional processes that vary over time and space. These processes, which are described in detail in Chapter 2 of this report, can result in hydrogeologic settings with complexities that are often not well understood. Interpretations of site lithology typically rely on cross sections generated from geologic logging of soil cores. These interpretations are often not refined enough to differentiate between relatively similar soil types, and thus can omit subtle transitions that might actually be associated with relevant differences in permeability (**Figure 3.3**). Several of the most well-known hydrogeologic test sites, such as the Borden Aquifer and the Massachusetts Military Reservation, are generally labeled as homogeneous, but exhaustive characterization studies have proven that even these sites contain relatively complex hydraulic conductivity fields (e.g., Sudicky, 1986; LeBlanc et al., 1991; Hess et al., 1992; Rivett et al. 2001).

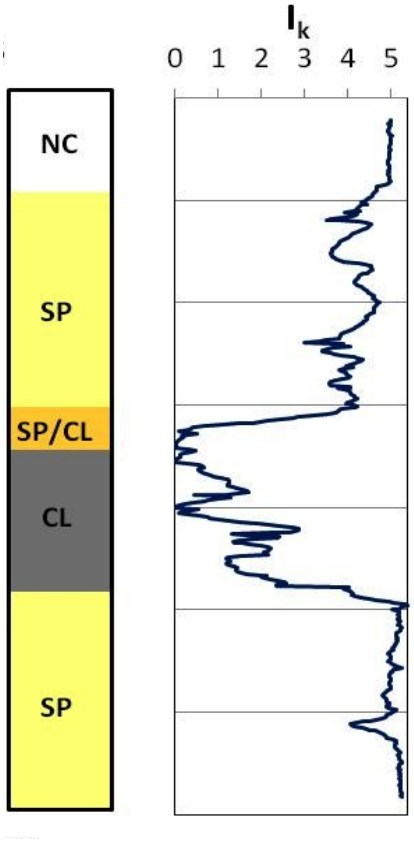

Figure 3.3. Example of small-scale variability in hydraulic conductivity. The right panel shows that the index of hydraulic hydraulic conductivity (I_k - log-scale estimate of hydraulic conductivity generated using the Waterloo APS) varies significantly over short vertical distances. The high resolution of these direct sensing data allow this heterogeneity to be captured even within intervals that are considered a uniform soil type based on classification. Data collected at NAS Jacksonville OU3 (Building 106 source area) as part of SERDP ER-1740 and ESTCP ER-201032.

It is this heterogeneity and anisotropy that largely dictates where contaminants will reside following release, how plumes will develop over time, and the response following remediation (Haggerty and Gorelick, 1995). Within a heterogeneous groundwater-bearing unit, contaminant transport and storage within those facies that contain mobile porosity are greatly influenced by advective processes. The presence of this mobile pore space—which may constitute a relatively small percentage of the total porosity of the aquifer—can lead to contaminant spreading far beyond what is assumed using bulk

values or erroneously assigned to dispersivity (Payne et al., 2008). Similarly, the immobile porosity associated with finer-grained unconsolidated soils or rock matrices can contribute to diffusive-driven storage of contaminants. This can limit the advance of a contaminant front, such as when contaminant migration through a hydraulically-active fracture is retarded by diffusion into the adjacent lower permeability rock (Parker et al., 1994; AWWA, 2007). Therefore, it is critical that any site characterization program be designed to address the site heterogeneity, specifically by identifying the distribution of mobile pore space and the immobile pore space. This includes the identification of fracture networks and other preferential pathways.

High-resolution characterization is key to understanding heterogeneity—the scale must be appropriate for the site conditions.

The hydrostratigraphy and contaminant distribution at a site must be mapped at a scale that matches the level of heterogeneity that is anticipated or known. The use of high-resolution characterization methods ensures that the transport and storage of contaminants within higher and lower permeability regions can be understood because the distribution of each of these facies is established. The focus of initial efforts should be gathering information on the extent of heterogeneity and its potential impacts (e.g., by identifying interfaces between high and low k units) to help establish the appropriate scale for subsequent efforts.

For example, mapping the location of hydraulically-active fractures within fractured bedrock is virtually impossible without using high-resolution techniques. The presence of a fracture with an aperture of 5 μm or even 50 μm requires the application of a sampling collection methodology that is consistent with this scale, particularly within dense networks. This means that continuous coring with methods that preserve the existing fracture network, followed by rock sampling at intervals of 0.5 m or less, are essential. A protocol for conducting fractured rock investigations, known as the Discrete Fracture Network (DFN), has been developed by Parker et al., (2007) and has successfully resolved fracture-contaminant relationships at fine spatial scales at multiple sites (Figure 3.4). The borehole can then be temporarily sealed by employing everting liners or packers to allow for further high-resolution characterization approaches while minimizing cross-connection (Keller et al., 2013). This can include geophysical logging as well as vertical profiling of the head and/or hydraulic conductivity within the fracture network (Meyer et al., 2009; Pehme et al., 2010; Pehme et al., 2013). These boreholes are also well-suited for collecting temporal data on depth-discrete contaminant concentrations by installing multi-level groundwater systems (Cherry et al., 2007).

Similar resolution is required within unfractured formations that contain significant lower permeability zones. Stratigraphic heterogeneity within these units can lead to complex vertical contaminant distributions that can be documented only if suitably granular characterization approaches are employed. This can include several commercially-available tools (e.g., the Membrane Interface Probe) that are designed to capture data on various parameters at intervals of 2 cm or less. If soil cores are collected, then the recommended procedure for sampling of these cores should involve as closely-spaced samples as practical (every 15 - 30 cm or less within intervals of interest).

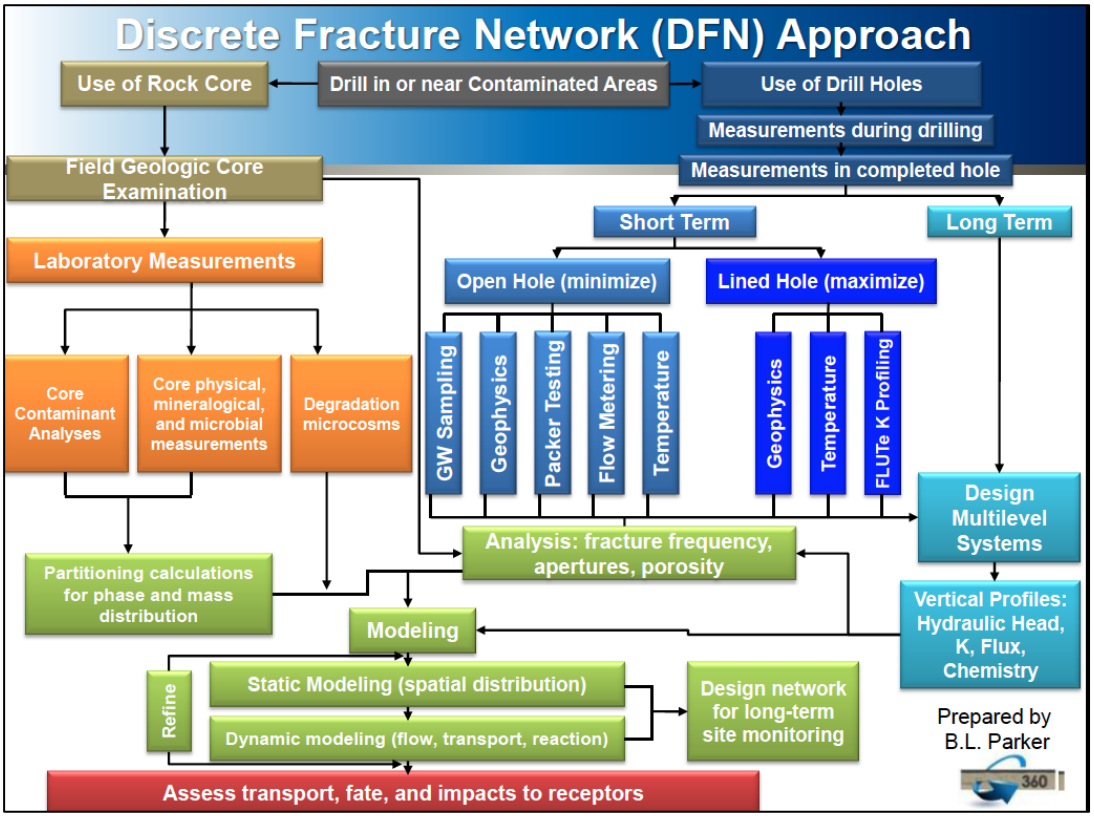

Figure 3.4. Discrete Fracture Network (DFN) (Prepared by B.L. Parker)

The utility of this soil sampling approaches illustrated in Figure 3.5 using data from OU3 at Naval Air Station Jacksonville obtained jointly as part of SERDP ER-1740 and ESTCP ER-201032. Concentrations in cores collected at several locations were characterized by sharp concentration gradients, particularly within and near the interfaces of lower permeability zones. Sampling at intervals of 15 cm within the lower permeability clays (present between approximately 19 and 25 ft bgs) established that CVOC concentrations changed by approximately an order of magnitude within intervals of less than 30 cm. Thus, the high-resolution soil subsampling increased confidence that the intervals where elevated concentrations are present were accurately defined, along with the depths where the maximum concentration of each constituent were encountered. These are important in establishing the overall shape—or ***style***—of the contaminant profile. At this location at OU3 (near the Building 780 source area), the highest concentrations are within the lowest permeability soils and then decrease moving up into the shallow soils. This shape is consistent with back diffusion from the lower permeability unit because the source strength in the more transmissive sands has weakened over time.

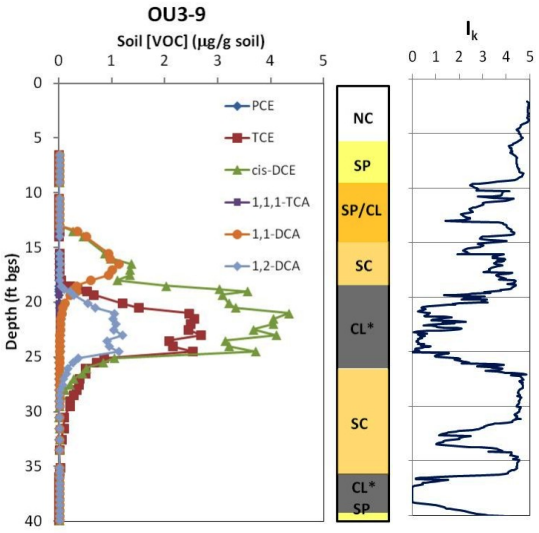

Figure 3.5. Example of sharp concentration gradients obtained with high-resolution soil subsampling. Left panel shows detailed concentration distribution, with soil concentrations that varied significantly within short vertical distances of the interface between lower and higher permeability soils. Right panel shows stratigraphic data obtained using a combination of geologic logging of soil cores and the Waterloo APS for vertical profiling of the index of hydraulic conductivity (I_k – log-scale estimate of hydraulic conductivity). Data collected at NAS Jacksonville OU3 (Building 780 source area) as part of SERDP ER-1740 and ESTCP ER-201032.

At most sites, initial characterization efforts should focus on sampling discrete depths at a small scale in order to establish if the selected scale is appropriate and providing valuable information. During subsequent characterization efforts, the scale can be expanded if data from these initial efforts have been successful at defining site conditions and identifying relevant compartments, distributions, and processes.

Several rapid data acquisition tools and methods can provide valuable data as part of an integrated characterization approach.

As noted above, the level of characterization data obtained at a site is inherently tied to the scale that is selected, and defining the initial scale can be difficult. To aid the process, there are several tools that have been developed with the goal of provding characterization data both rapidly and at a relatively fine scale. Several of the most widely-used methods for low k zone investigations are summarized in Section 3.2.2. These include commerically-available subsubsurface profiling systems such as the Membrane Interface Probe (MIP), Geprobe's Hydraulic Profiling Tool (HPT™), the Waterloo APS™, and various optical screening tools (OSTs). Other examples include mobile analytical labs that can be brought on-site to significantly reduce turnaround time. In addition, there are a number of geophysical logging techniques that generate real-time data. These tools and methods can be a valuable part of an integrated site management approach, where the data generated from an initial screening-level characterization is used to optimize subsequent characterization efforts.

These tools generate a large amount of data and at a unit cost that can often be justified based on the objectives of the investigation (Profiling systems typically cost between $2000 to $6000 per day for unconsolidated soils, plus the rate for rig to push the tooling). Data is collected using high-performance sensors at intervals of 2 cm (or less) during advancement of the tools at a rate of 1 to 4 ft per minute, such that profiling of several hundred feet per day is not uncommon. Most of the profiling methods provide detailed vertical stratigraphic data, including estimates of relative hydraulic conductivity and/or electrical conductivity logs that can be used to interpret soil type. Others, such as the MIP, can be used to generate semi-quantiative data on contaminant distribution.

Currently, soil cores remain the most effective and comprehensive characterization method because they can be used to both define lithology and quantify total contaminant mass (including sorbed phases) at whatever scale is desired. Consequently, it is highly recommended that soil coring be included in any rigorous characterization of a site with low permeabilty matrices, particularly when building a conceptual site model that will be used to guide remedy selection. However, the direct sensing tools can play a role in reducing the intensity of subsequent coring and sampling efforts, and there is considerable interest in developing better quantiative relationships between these two types of data. This was the motivation for a MIP optimization study that was part of the SERDP ER-1740 scope of work (see **Example 1**). This study, which was performed at OU3 at NAS Jacksonville with partial funding support from ESTCP ER-201032, demonstrated that the MIP can be a useful component of low k zone investigations and that mariginal benefits can be gained by slightly modifying operating parameters.

A further example is that the practicality of installing depth-discrete (multi-level) groundwater systems is greatly enhanced if the units to be targeted are well-defined in advance. Because the goal of these systems is to confirm that plume development is consistent with the hydrostratigraphic and mass profiles, they are typically designed to sample key intervals where contaminant storage and transport processes are being elucidated. Consequently, a multi-level system for groundwater is naturally installed only after one or more initial characterization steps has been completed in advance (e.g., stratigraphic mapping or sore core analysis). These initial data provide a technical basis for designing and installing a system and can help to optimize costs.

Note that the rapid data acquistion tools are almost exclusively driven by direct push platforms, and thus are primarily applicable to characterization of unlithified deposits where the low k zones consist of clayey and/or silty soils. Regardless, the integration of several characterization and monitoring methods is highly recommended regardless of the type of low permeabilty zone that is being investigated. Descriptions of possible integrated approaches for characterizing unlithified and lithified geologic settings are presented in Section 3.2.2, along with examples of complimentary datasets.

EXAMPLE 1: Developing a MIP Protocol for Characterizing Low Permeability Zones

The objective of this SERDP-sponsored study was to develop and test a protocol for the Membrane Interface Probe (MIP) as a lower-cost rapid data acquisition tool for characterizing lower permeability zones (Adamson et al., 2013). At the demonstration site (OU3 at NAS Jacksonville, Florida), MIP operating parameters were varied systematically at several locations to quantitatively evaluate the impact of these changes on data quality relative to i) conventional MIP operation; and ii) concentrations in co-located soil samples (i.e., a baseline high-resolution dataset for contaminant distribution). The goal was to test modifications that would improve signal resolution and reduce carryover at high concentration areas, and then test a different set of modifications to increase sensitivity at areas with less mass present.

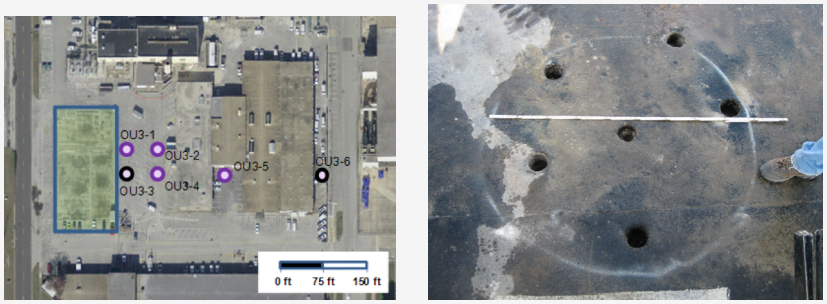

Sampling Locations at NAS Jacksonville OU3. Black symbols represent locations where MIP optimization study was conducted. Purple symbols represent where only baseline MIP was conducted. Blue outline is former location of Building 106 (source area). Right-hand panel shows surface view of various MIP runs at location OU3-3.

The following modifications to standard MIP operating parameters were tested:

Run No.	Parameter	Operating Condition Tested at OU3-3 (High Concentration Location)	Operating Condition Tested at OU3-6 (Low Concentration Location)
1	(Baseline)	Heated	Heated
2	Trunk Line	Unheated PEEK	Unheated PEEK
3	Drive Rate	Fast – 2 ft/min	Slow – 0.5 ft/min
4	Gas Flow Rate	Fast – 80 mL/min	Slow – 20 mL/min
5	Probe Temperature	Low – 100ºC	High – 140ºC
6	Data Collection	"Up-logged"	"Up-logged"

Notes: (1) For all runs, only a single operating condition was changed at a time; (2) The baseline run used a standard flow rate (1 mL/min), drive rate (1 ft/min), probe temperature (120ºC), and "down-logged" data collection direction; (3) "Up-logged" refers to collection of MIP data from the deepest point up to the surface.

Soil coring demonstrated that the majority of the contaminant mass (consisting of PCE and TCE with some cis-1,2-DCE) resides near the interface between lower and higher permeability soils at location OU3-3. At downgradient location OU3-6, most of the mass was found in the more transmissive zone (primarily as cis-1,2-DCE). At all locations, the MIP was able to identify the depth intervals coinciding with lower permeability soils (via electrical conductivity logging) and typically was successful at locating the top of contaminated intervals. Overall, the PID datasets provided more accurate representations of contaminant distributions for regions where contaminant levels are high (generally greater than 1 mg/kg). In areas where soil CVOC concentrations are lower (down to 100 of μg/kg), the ECD was more useful because of its greater sensitivity and lower detection limits.

However, carry-over of elevated MIP signals to deeper intervals than those suggested by soil concentration data was a persistent problem.

EXAMPLE 1: Developing a MIP Protocol for Characterizing Low Permeability Zones (Continued)

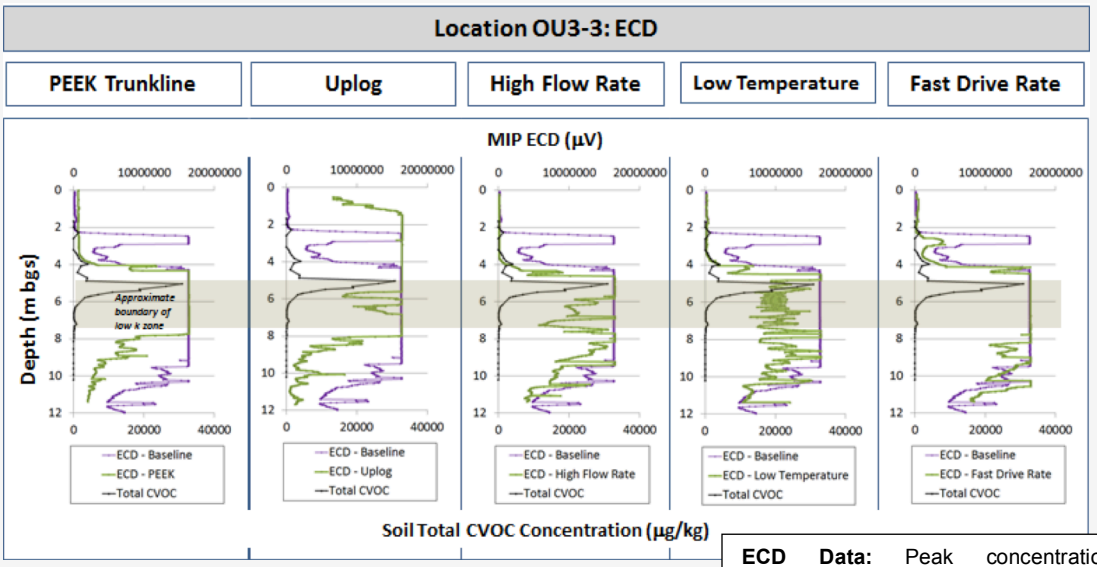

ECD Data: Peak concentration identified but significant carry-over limits delineation of bottom of contaminated zone.

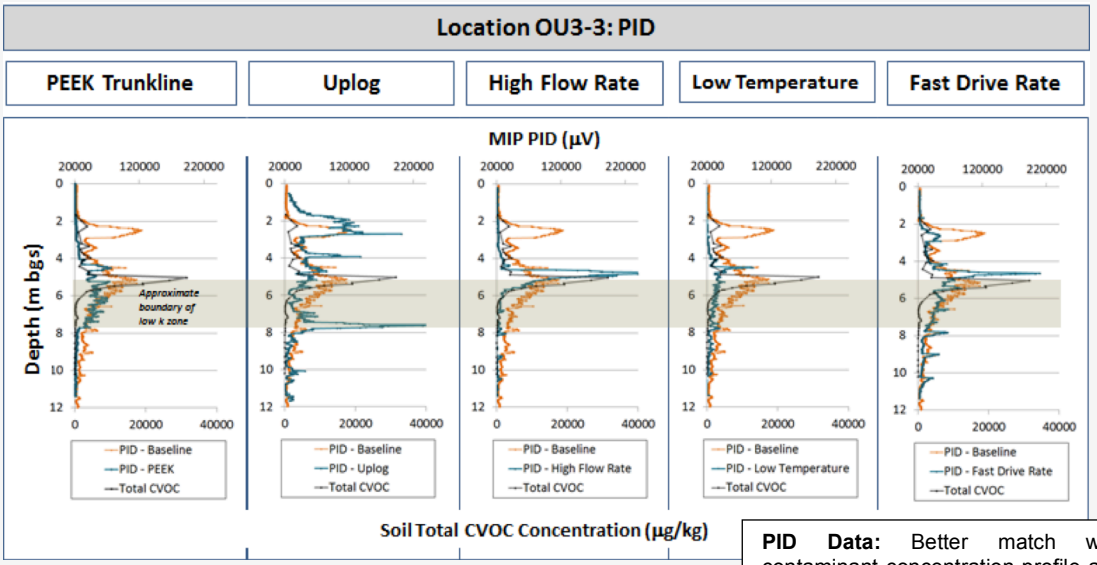

PID Data: Better match with contaminant concentration profile and peak; minor improvements achieved by modifying MIP operation

MIP Characterization Data for All Runs vs. Soil CVOC Concentration Data (log scale) at High Concentration Location OU3-3. ECD comparison made to soil CVOC concentration without cis-1,2-DCE because of poor detector response. Data from low concentration location (OU3-6) included in Appendix B.

EXAMPLE 1: Developing a MIP Protocol for Characterizing Low Permeability Zones (Continued)

Carry-over of contaminant mass is a particular concern at locations with higher concentrations, where more sensitive detectors may get overloaded (in this case, the ECD) and the amount of time required to flush mass from the MIP trunk line may have been inadequate. It is also problematic within low permeability zone investigations because mass present in these zones may be confined to a relatively narrow depth interval (near a permeability interface).

To overcome this carryover issue, completing an "up-logged" MIP run is recommended at all locations to complement the baseline characterization and better identify the base of contamination. Most changes in other MIP operating parameters resulted in little or marginal improvements in data quality and signal resolution. A high carrier gas flow rate is recommended as part of an optimized MIP protocol for low permeability zone investigations in high concentration areas (to dilute contaminant mass that crossed the membrane and reached the detector and to promote more rapid flushing through the entire MIP system), as well proper detector selection and uplogging for data correction at all locations.

The result of this study was a recommended standard operating protocol (SOP) for using the MIP during low k zone investigations (see next page). These procedures resulted in corrected MIP profiles more representative of contamination throughout the entire vertical extent of the interval being characterized.

Rigorous statistical analyses were conducted to evaluate the impact of the various modifications to MIP operation. Linear regression indicated scatter in all MIP-to-Soil comparisons, including R^2 values using the SOP of 0.32 in the low concentration boring and 0.49 in the high concentration boring. In contrast, a control dataset with Soil-to-Soil correlations from borings 1-m apart exhibited an R^2 of ≥0.88, highlighting the uncertainty in predicting soil concentrations using MIP data. However, the MIP performed similarly or better in identifying contamination in lower k soils compared to high k soils.

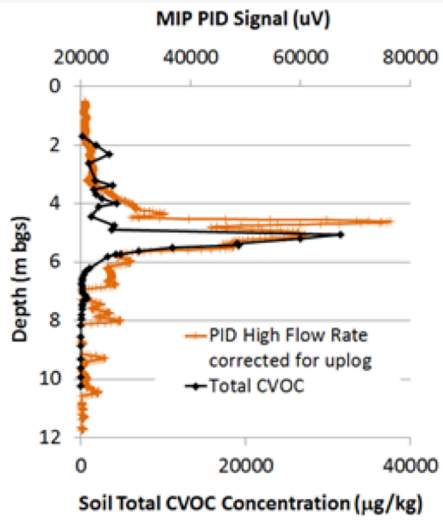

MIP PID data collected using SOP, showing improved correlation to soil CVOC concentration data at OU3-3

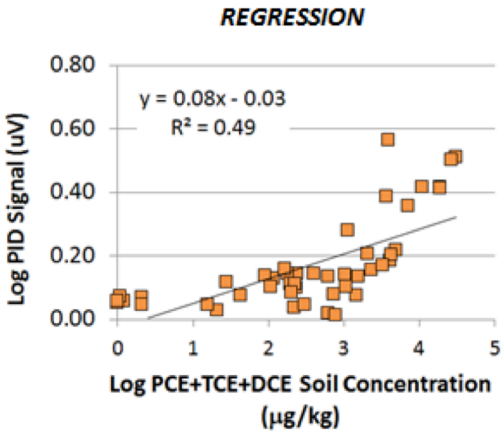

Linear regression of MIP PID data collected using SOP with soil CVOC concentration data at OU3-3.

EXAMPLE 1: Developing a MIP Protocol for Characterizing Low Permeability Zones (Continued)

Recommended Standard Operating Protocol for MIP in Low k Zone Investigations.

Option	Recommendation	
	Higher Concentration Areas	Lower Concentration Areas
Detector Utility	PID unless dominated by poorly-detected CVOCs (e.g., 1,1,1-TCA)	ECD if no DCE is present; PID if DCE is present
Heated Trunk Line	Utilize if available	Utilize if available
Drive Rate	Standard	Standard
Flow Rate	High	Standard
Temperature	Standard	Standard for ECD applications: High for PID applications
Uplogging	Use with baseline characterization to establish base of contaminated interval and for data correction	Use with baseline characterization to establish base of contaminated interval and for data correction

The results of this study demonstrate that the utility of the MIP as a tool for characterizing low k zones is similar to that for sites dominated by higher permeability soils, The MIP can help in locating contamination in low-k zones, determining the extent to which relative magnitude relationships can (or should) be established quantitatively, and weighing the cost-benefit of the MIP data relative to other characterization methods. At a minimum, the MIP helps reveal the presence and relative distribution of contamination within lower-k intervals that are too often ignored in conventional site characterization efforts. The MIP is capable of resolving contamination in low-k zones as well as it does in high-k zones, and its overall efficacy is not limited to specific soil types. The capability of the MIP to collect a large amount of depth-discrete data is valuable in demonstrating the general horizontal and vertical distribution of contamination at a site in both transmissive and low-k compartments.

However, it is clear that it may not accurately reflect contaminant distribution and heterogeneity relative to more intensive high-resolution characterization methods such as soil coring. It is best used as a screening tool for rapidly establishing if contaminants are present within lower permeability zones, then followed up with confirmatory soil coring. Ultimately, the choice to use MIP as part of a dynamic site characterization program depends on site-specific factors that weigh data objectives and costs. The use of the protocol generated as part of this study enhances the utility of MIP as a complementary investigative tool for identifying the location and magnitude of contamination within all impacted zones, including critical low-k zones. (Source: Adamson et al., 2013).

Site characterization must be dynamic and adaptive.

A site investigation program that integrates data collected in phases using multiple different, complementary characterization methods should lend itself to a dynamic, adaptive, and ultimately more representative site conceptual model. This is because information collected in one phase of investigation better informs decisions made during the next phase. However, these need not be discrete phases. If data are being generated in near real-time (e.g., using one of the direct-sensing tools mentioned above), then decision-making shifts to the field level, and the characterization process essentially becomes dynamic.

The goal should be continuing refinement of the conceptual site model, based on an understanding that the site model is never really "finished". Any hypotheses that are part of the site model should be tested to the extent practical through the characterization process, and the model should be adapted to reflect the available information. Payne et al. (2008) summarized the results of performance survey that identified reasons why some projects were more successful than others, concluding that: "One characteristic of successful projects stood out: all of the high-performance projects followed a pattern of interpretation, analysis, review, and revision, at all stages of project development and operation".

The USEPA developed a framework for this type of dynamic and adaptive site investigation and characterization process called the Triad approach. It includes several features that USEPA has identified as necessary for successful investigation and remediation programs.

Among the potential benefits of this approach are a reduction in the level of data uncertainty, more successful remedial outcomes, and lower life-cycle costs. ITRC has published technical and regulatory guidance for the Triad process (2003), along with a framework for implementing the approach at a site (2007). While these documents do not explicitly address sites with significant low k zones, the approach is wholly consistent with recommended methods for these zones because they typically utilize high-resolution stratigraphic data generated in near real-time.

Key Features of the Triad Approach (ITRC, 2007)

1. Systematic Planning. Develop a conceptual site model and determine any data gaps in this model that need to be addressed. Identify all key personnel and stakeholders to ensure that they are involved in a well-defined decision-making framework throughout the project lifetime.
2. Real-Time Measurements: Employ techniques that generate data that permit real-time and near real time decision-making.
3. Dynamic Work Strategies. Use on-going data collection efforts as an opportunity to update the conceptual site model.

Focus on the right metrics for understanding the site.

Groundwater concentration is the typical metric for site monitoring, but mass-based metrics provide a broader and more complete understanding of site conditions. The most direct approach is to quantify the total mass present (at a particular depth, location, or site-wide) using high-resolution soil sampling and analysis. Within the saturated zone, this establishes the amount of mass in all compartments (dissolved, sorbed, and

non-aqueous phase) and is independent of groundwater flow conditions. Comparisons between pre-treatment and post-treatment contaminant mass are a more accurate method for evaluating remedial performance than groundwater concentrations because the latter is influenced by phase re-equilibration of contaminants following treatment. Because of advection-driven limitations in collecting groundwater samples from finer-grained soils, quantifying mass instead of aqueous-phase concentration is also well-suited for investigation of lower permeability zones.

Characterizing a site based on contaminant mass flux or mass discharge is another powerful approach that places concentration data in context with groundwater flow within the region being characterized (ITRC, 2010; Newell et al., 2011). Mass discharge (in units of mass per time) represents the total mass transported across a plane located transverse to groundwater flow, meaning that in the simplest terms, it can be calculated by multiplying the Darcy velocity by the concentration. However, a heterogeneous aquifer contains soil layers with permeabilities that may span several orders of magnitude, resulting in concentration of the groundwater flow within the highest permeability channels. Therefore, all distinguishable zones should be included in the calculation to reduce uncertainty in mass discharge estimates. This is accomplished by high-resolution, multi-level groundwater sampling across a transect, combining the measured concentration with a known or estimated Darcy velocity for each of the sampled depths. Sampling across multiple transects in the direction of groundwater flow provides can help document attenuation processes and rates within the system, such as contaminant mass degraded or stored in lower permeability units.

While there are multiple methods for estimating mass discharge, collecting data across a transect is an effective tool for quantifying source strength, investigating plume boundaries, and documenting remediation performance because it is consistent with our current understanding of contaminant transport in heterogeneous porous media. Specifically, most plumes are characterized by laminar groundwater flow within preferential flow channels represented by mobile porosity and do not expand significantly in the transverse direction (Payne et al., 2008). This allows plumes to maintain a high concentration core structure that can decrease significantly when moving relatively short distances in the transverse and vertical directions. Because of this, it is possible to miss the plume core if high-resolution transects are not included in the investigation.

There are several studies that have documented complex two-dimensional plume geometries using high-resolution transect data (e.g., Einarson and Mackay, 2001; Guilbeault et al., 2005; Basu et al., 2006; Parker et al., 2008). Guilbeault et al. (2005) used this approach at several DNAPL sites to demonstrate that 5 to 10% of the plume cross sectional area accounted for approximately 75% of the mass discharge, even if a relatively homogeneous system and uniform flow field is assumed (**Figure 3.6**). Subsequent research by Li and Abriola (2009) provided valuable insight on optimizing sampling densities for mass discharge estimates. The Mass Flux Toolkit is a free software package that can be used to calculate rates using a variety of methods (Farhat et al., 2006).

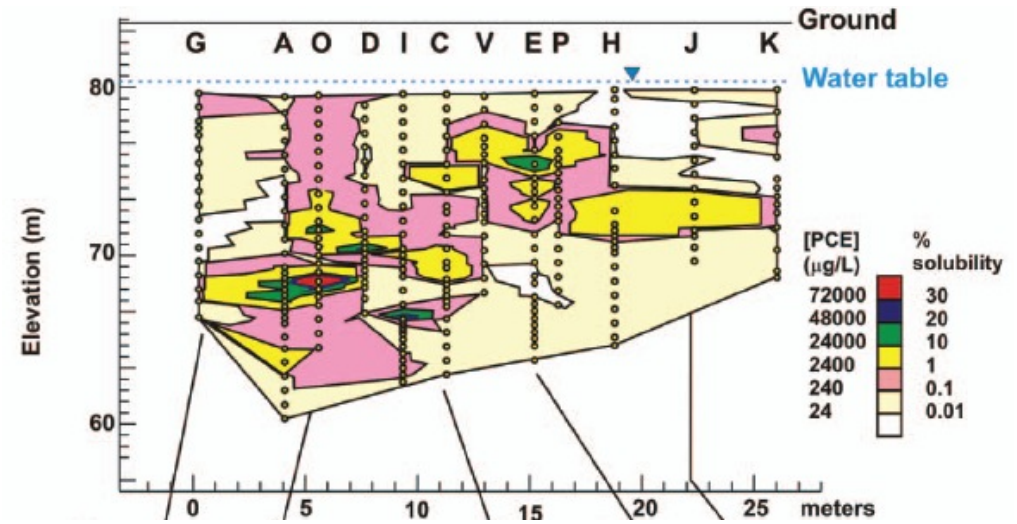

Figure 3.6. Example of high-resolution transect approach. Cross section perpendicular to flow direction at site in New Hampshire, with PCE groundwater concentrations presented as percent of pure-phase solubility. Data illustrate the highly localized nature of mass discharge. Reprinted from Guilbeault et al., 2005.

Sample collection, handling, and analysis methods must ensure maximum possible data quality.

Measuring contaminants and other properties in environmental media can be challenging because obtaining data is a multi-step process. It involves identifying the location(s) to be sampled, collecting the sample, transferring the sample to a media and method-specific container, shipping the container. There are opportunities for the data quality to be compromised during any of these steps. To address these challenges, soil and groundwater sampling and analysis procedures adhere to rigorous protocols that are typically based on agency specifications. However, there is still potential for significant reduction in data quality even if these procedures are followed. A typical example is the loss of chlorinated solvent mass from soil samples due to volatilization during the sample handling steps. Core data collected from the Building 106 source area at OU3 at NAS Jacksonville demonstrate these losses can be significant even when following generally-accepted procedures (**Figure 3.7**).

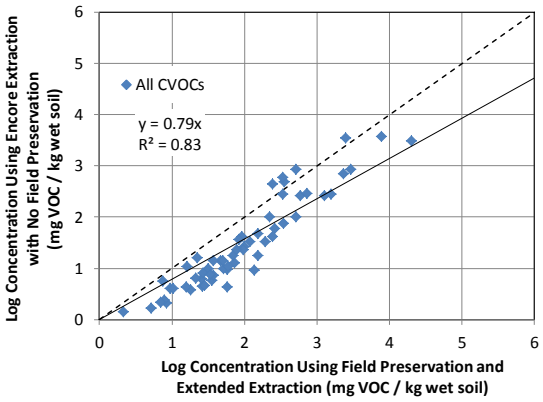

Figure 3.7. Correlation between soil data collected using Encore samplers without field preservation vs. data collected using field preservation and extended extraction. Linear regression (log scale) using aggregate data for all detected constituents and all soil types. Solid line is best-fit regression and dashed line is slope = 1. Data collected at NAS Jacksonville OU3 (Building 106 source area) as part of ESTCP ER-201032.

A goal of second-generation characterization approaches is to look for opportunities to improve data quality whenever possible. This ensures that high-resolution characterization data—i.e., that intend to reflect information at very fine scales—are not further compromised by the variability that is frequently associated with sampling and analysis.

Given that soil coring is an integral component of most low k zone investigations, it is important to highlight several advances in generating high-quality data from these cores:

- *Soil cores must be collected properly.* For unconsolidated soils, this means that disruption of the cores should be minimized. Direct push and rotosonic drilling can generally provide high integrity cores, and there are several piston methods that can be used to improve core retention (e.g., Aqualok™ sampler).
- *Soil samples must be preserved in field.* The use of methanol or other preservatives are essential to minimizing volatile losses. This step must be done in the field. Data from the NAS Jacksonville study demonstrate that delaying the methanol preservation step until the sample was received at the lab biased the sample results (Slope = 0.93 log-scale) and introduced significant variability (R^2 = 0.87) (ESTCP ER-201032, unpublished data).
- *Improved sample preparation methods can greatly shorten turnaround time, with field extraction as an achievable goal.* Commercial laboratory extraction procedures are relatively time-consuming and may be not be rigorous enough to ensure that complete mass recovery is achieved. Dincutoiu et al. (2008) provided evidence that microwave energy could be used to improve solvent extraction kinetics, with identical recoveries of mass obtained within 10 minutes. This study was performed on clay samples, demonstrating the utility of this method for low k zone investigations, and further research has demonstrated its applicability to rock samples. Data from the NAS Jacksonville study obtained using a field method for rapidly extracting contaminants from the soil matrix (**Figure 3.8**) demonstrated a very strong correlation (R^2 = 0.99, Slope = 0.99) with data obtained using standard lab extraction (ESTCP ER-201032, unpublished data). The majority of the comparative dataset was finer-grained soils (clays and silts), and the results were particularly strong

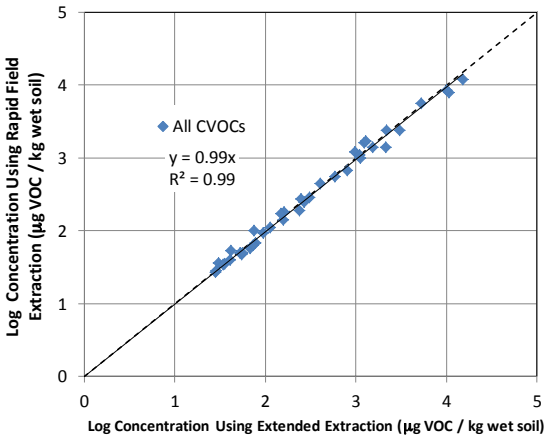

Figure 3.8. Correlation between soil data collected using standard (extended) extraction vs. rapid field extraction. Linear regression (log scale) using aggregate data for all detected constituents and all soil types. Solid line is best-fit regression and dashed line is slope = 1. Data collected at NAS Jacksonville OU3 (Building 106 source area) as part of ESTCP ER-201032.

with less hydrophobic constituents (e.g., DCE). When used in combination with a mobile laboratory that can be brought on-site, these techniques can provide near-real time data as part of a highly dynamic characterization program.

Similar methodology exists for ensuring high data quality in rock samples from fractured media, as embodied in the DFN approach (Parker, 2007). Investigations based on this approach emphasize techniques that minimize volatile losses of contaminants during the rock crushing process. A commercialized version of DFN (CORE $^{DFN\ TM}$) includes an enclosed, stainless steel crushing cell capable of withstanding high pressures used during the crushing process. Crushed samples are directly extruded from this cell into a 40-mL sampling vial with preservative for analysis.

3.2.2 Methods

For low k zone investigations, there are a number of methods that can be considered "second-generation" in nature. All are designed to provide high-resolution characterization data on contaminant concentration and/or site hydrostratigraphy.

They include distinct tools (like MIP) or systematic approaches (like multi-level groundwater sampling systems). Each can be used singly to provide screening-level data or address a well-defined question, or in combination as part of a process-driven, integrated approach to site characterization. They include methods that are highly quantitative, as well as methods that enhance our stylistic understanding of site conditions. What these methods have in common—and what gives them inherent value—is that each can reveal information that was missing or poorly represented in conceptual site models using first-generation methods.

Table 3.2 summarizes a number of second-generation characterization methods for sites with low k zones. This is not all-inclusive list—there are certainly others that are being implemented—but it includes those that are widely and successfully applied for low k zone investigations.

There is no single tool that serves as a magic bullet for investigating sites with low k zones. As noted previously, these second-generation methods provide complimentary information that can be used in an integrated approach to enhance understanding of site conditions. A typical scenario in unconsolidated media involves the use a direct-sensing tool as a first step to provide screening-level data, followed by detailed subsampling of soil cores for confirmation and to establish relationships between the observed stratigraphy and concentrations of key parameters measured in the soil samples. Boreholes can then be instrumented with multi-level systems for groundwater sampling, or used for geophysical logging or hydraulic testing.

There are numerous cases where this integrated approach has been successfully applied at sites with low k zones (e.g., Parker et al., 2003; Chapman and Parker, 2005; Adamson et al., 2013). Recent work completed as part of ESTCP ER-201032 (with partial support from SERDP ER-1740) was focused on generating a high-resolution dataset from locations at the Building 106 source area at OU3 at NAS Jacksonville (see **Example 2**). Several investigative techniques were used, and the study demonstrates the complimentary nature of the various data. Various direct-sensing and

profiling tools were used to establish the vertical permeability distribution, providing relatively similar data regardless of the method. Coring data proved the best method for confirming that at locations close to the source zone, most of the contaminant mass was found just above and below the interface between higher and lower permeability layers.

Figure 3.8 displays potential investigative protocols for sites where the low k zones are located in unconsolidated (unlithified) (**Figure 3.8a**) and lithified (rock) (**Figure 3.8b**) formations. These are multi-step protocols that are consistent with the scientific method. A site-specific investigative approach should aim to address gaps in the conceptual site model, and it is understood that it may not be practical or necessary to include all of these steps.

Regardless, data should be collected at an adequate scale to establish the level of heterogeneity and the style of contaminant distribution, with the understanding that this may lead to the selection of a coarser scale for later phases of investigation. In most cases, an increased upfront effort should reduce uncertainty and therefore long-term costs. It should be appreciated that the insights that these second-generation methods provide on fate and transport within low k zones mean that there is really no going back to more conventional site characterization approaches.

Table 3.2. Summary of Key "Second-Generation" Tools for Site Characterization

Tool/Method	Description	Primary Data Generated	Advantages	Limitations
Soil Sampling (high-resolution)	Collect continuous cores throughout entire interval(s) of interest focusing on drilling/sampling methods that preserve intact cores (e.g., rotosonic, direct-push)	Soil contaminant concentration, physical properties; hydrostratigrapy	• Quantifies mass present in all compartments • Provides method for identifying low k units (definitive soil classification) and understanding heterogeneity • Provides complete vertical contaminant profile if sampling frequency is consistent with scale of heterogeneity • Field preservation and enhanced extraction techniques greatly improves mass retention/recovery	• Core recovery can be challenging in loose soils • Some drilling methods are poorly suited for tight soils and fractured rock
Multi-Level Groundwater Monitoring	Systems designed to isolate and sample multiple discrete depths at a location; several multi-port systems commercially available (e.g., Westbay, Solinst Waterloo/CMT, FLUTe)	Groundwater contaminant concentration and geochemical parameters; hydraulic head	• Better able to isolate and characterize specific depths, including low k zones, relative to conventional monitoring wells • Provides data for assessing temporal trends • Well-suited for collecting transect data • Uses single borehole so typically faster and easier to install than piezometer network • Highly customizable • Applicable to fractured rock	• Efficient design of MLS requires some knowledge of site hydrostratigraphy (through initial site characterization) • Number of sampling depths is limited by instrumentation that can fit within boreholes – typically less than 12 discrete depths per location • Only provides data on mass in aqueous-phase compartments
On-Site Analytical Laboratory	Accredited mobile lab analyzes samples on-site using truck/trailer as support platform	Contaminant concentration of matrices of interest (soil, groundwater, vapor), potentially other geochemical properties	• Rapid data acquisition (minutes to hours) • Dynamic and expedited site characterization, particularly integrated with other 2G methods • Generates defensible data • Most can handle many different sample matrices	• Additional cost considerations • May not be feasible for sites where QAPP has strict guidelines on lab selection • Limited capabilities to perform analyses that generate hydrostratigraphic data

Table 3.2. Summary of Key "Second-Generation" Tools for Site Characterization *(continued)*

Tool/Method	Description	Primary Data Generated	Advantages	Limitations
Waterloo$^{APS\ TM}$ (Stone Environmental)	Vertical profiling tool equipped with downhole sensor and ports to collect continuous hydrostratigraphic data with depth along with groundwater samples at discrete depths; driven using direct-push rig	Groundwater contaminant concentration and geochemical parameters; hydrostratigraphy (index of hydraulic conductivity); hydraulic head	• Better able to isolate and characterize specific depths, including low k zones, relative to conventional monitoring wells • Provides method for identifying low k units and understanding heterogeneity • Real-time data • Well-suited for 3-D site characterization for developing/improving site conceptual model	• Not well-suited for collecting water from lower K zones (volume constraints) • Hydrostratigraphic data provided by tool is comparable to hydraulic conductivity but site-specific benchmarking should be completed • Not as well-suited for assessing trends (i.e., groundwater data not collected from permanent well with fixed location) • Groundwater sampling involves some purging and purged during collection
Hydraulic Profiling Tool (HPT) (GeoProbe)	Vertical profiling tool equipped with downhole sensor and ports to collect continuous hydrostratigraphic data with depth; option for groundwater sampling (using new HPT-GWS sampler); driven using direct push rig	Hydrostratigraphy (electrical conductivity log, estimate of hydraulic conductivity (I_k) using vertical pressure and flow data); groundwater concentrations (only if HPT-GWS option is employed)	• Provides method for identifying low k units and understanding heterogeneity • Real-time data • Well-suited for 3-D site characterization for developing/improving site conceptual model • Tool can be combined into a single MIP-HPT probe	• Hydrostratigraphic data provided by tool is comparable to hydraulic conductivity but site-specific benchmarking should be completed
Membrane Interface Probe (MIP)	Vertical profiling tool equipped with downhole membrane and sensor to collect continuous data on contaminant vapor concentration and soil stratigraphy with depth; driven using direct push rig	Hydrostratigraphy (electrical conductivity log); bulk contaminant vapor concentration	• Provides vertical contaminant profile to better identify depths where contamination is present • Provides method for identifying low k units and understanding contaminant distribution • Functions equally well in all soil types • Contains various detectors that are responsive to multiple different contaminant types • Real-time data that is well-suited for 3-D site characterization for developing/improving site conceptual model	• Semi-quantitative with limited ability to correlate to actual soil concentrations (not a replacement for core data) • MIP response is subject to carry-over that can cause depth misidentification • MIP provides a bulk response that does not differentiate between individual compounds • May not provide accurate representation of heterogeneity

Table 3.2. Summary of Key "Second-Generation" Tools for Site Characterization *(continued)*

Tool/Method	Description	Primary Data Generated	Advantages	Limitations
Optical Screening Tools/Laser-Induced Fluorescence	Downhole optical screening tool that measures light or laser induced fluorescence (LIF) of NAPL constituents with depth; driven by direct push rig	NAPL presence and magnitude	• Identifies where NAPL is present along with implied heterogeneity • Real time data • Functions well in low k zones • Applicable to multiple NAPL types (assuming PAH present as co-contaminant) • Dye co-injection should improve detection of chlorinated solvent DNAPL	• Primary function is NAPL detection so applicability to "late-stage" sites (i.e., NAPL depleted, loading dominated by back diffusion from low K zones) may be limited
Surface Geophysical Methods	Survey using electrical resistivity measurement methods or ground-penetrating radar to document subsurface formation characteristics	Soil type; anomalies may indicate presence of contaminants	• Non-invasive method for identifying depth and extent low k zones • Relatively inexpensive when compared to coring • Rapid data acquisition	• Data are highly subject to interpretation • Subject to interferences, such as naturally-occurring radiation (gamma logging) or highly salinity groundwater (resistivity logging) • Difficult to distinguish the presence of multiple low k layers • Data collection at deeper intervals can be challenging • Difficult to categorize anomalies as contaminants vs. soil type heterogeneity • Requires benchmarking with core data
Borehole Geophysical Methods	Vertical profile of interval of interest within open boreholes using a variety of geophysical methods such as gamma, temperature, and resistivity logging	Soil type; anomalies may indicate presence of contaminants	• Provides method for identifying low k units and understanding stratigraphic heterogeneity • Rapid data acquisition • Well-suited for fractured rock settings	• Data is quantitative but subject to interpretation • Subject to interferences, such as naturally-occurring radiation (gamma logging) or highly salinity groundwater (resistivity logging) • Difficult to categorize anomalies as contaminants vs. soil type heterogeneity • Requirement for open boreholes is difficult at sites with collapsible sands • Benchmarking with core data is recommended

Table 3.2. Summary of Key "Second-Generation" Tools for Site Characterization *(continued)*

Tool/Method	Description	Primary Data Generated	Advantages	Limitations
Rock Coring	Collect continuous rock cores throughout entire interval(s) of interest focusing on drilling/sampling methods that maintain discrete fracture network within cores	Soil contaminant concentration, physical properties; hydrostratigrapy	• Quantifies mass present in all compartments, including rock matrix • Provides vertical contaminant profile to better identify depths where contamination is present • Maps fracture network to identify pathways for contaminant transport • Not subject to borehole cross-contamination	• Limited number of companies offer rock coring services • Cost is generally higher (per linear foot) than in unfractured media • Care must be taken to not induce fractures during drilling
Borehole Liners/Packers	Variety of methods designed to temporarily seal selected borehole intervals (using packers) or entire borehole (using liners) to allow for additional downhole testing; several types commercially available (e.g., Solinst, FLUTe)	No direct information, but provides opportunity to generate data through additional sampling/testing	• Can be used to isolate intervals of interest for further groundwater sampling (including installation of permanent multi-level systems) or hydraulic testing (e.g., slug/pump tests to estimate k) • Can be used to maintain borehole integrity for geophysical and/or temperature logging	• Requires open boreholes during installation, which may be difficult in some soil types
Tracer Tests	Breakthrough of injected tracer or heat is monitored at downgradient wells (or alternatively, washout in injection well)	Range of actual groundwater velocities in heterogeneous media	• Provide detailed information on travel time of groundwater and contaminants that reflects heterogeneity (without having to measure that heterogeneity) • Breakthrough data can be used to estimate the mobile porosity • Breakthrough data can indicate if diffusive exchange between mobile and immobile porosity is occurring along flow path (log-normal breakthrough curve)	• Requires design and installation of an injection-monitoring network

EXAMPLE 2: High Resolution Characterization Dataset Using Multiple Complimentary Methods – NAS Jacksonville OU3

MIP
Screening-level info on vertical stratigraphy (electrical conductivity log) and bulk contaminant (ECD/PID log) distribution
Primary Limitations: Semi-quantitative and subject to carry-over; no visual or analytical confirmation

HPT
Screening-level (electrical conductivity log) and more refined (k estimate) hydrostratigraphic info
Primary Limitation: No contaminant info

Waterloo APS
Detailed hydostratigrahic profile (I_k) plus ability to collect groundwater samples for CVOCs and field parameter data
Primary Limitation: Difficult to collect groundwater from low k zones

Soil Coring and Subsampling
Complete contaminant profile (mass in all compartments) plus definitive soil type classification
Primary Limitation: High level of effort

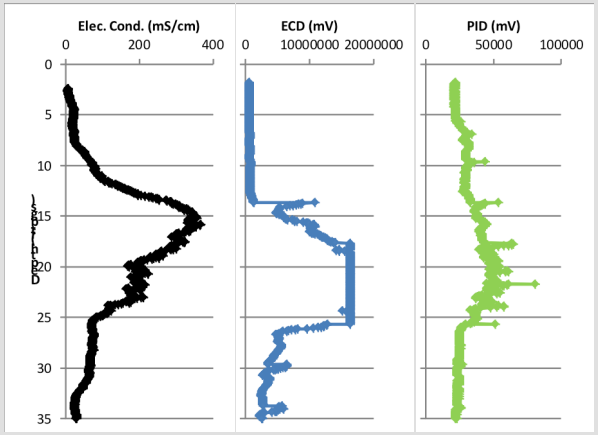

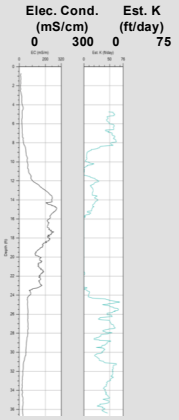

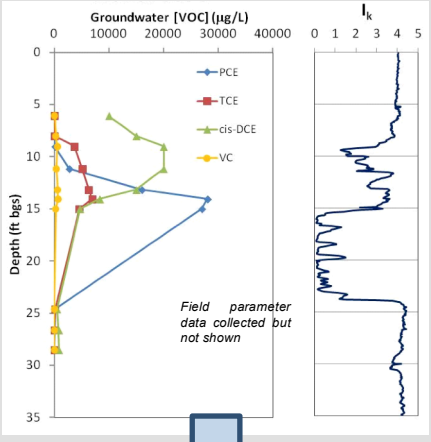

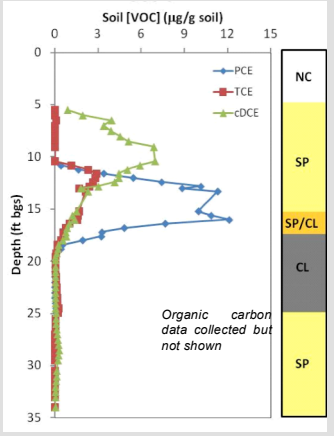

SUMMARY

The MIP was used to delineate zones with contamination. A protocol was developed as part of this project to increase the utility of the MIP tool in low k zones (see Example 1 in this Chapter.

The HPT then provided a map to the interfaces between transmissive and low k zones.

The Waterloo APS tool then helped define groundwater concentrations above and below the interfaces.

The high resolution surface coring showed the style and concentrations of contaminants in the low k zones.

Supplemental multi-level groundwater sampling
Depth-discrete groundwater data from low k zones (and adjacent layers) using temporarily installed short screens
Primary Limitation: Still difficult to isolate specific depths without more sophisticated (permanent) multi-level systems

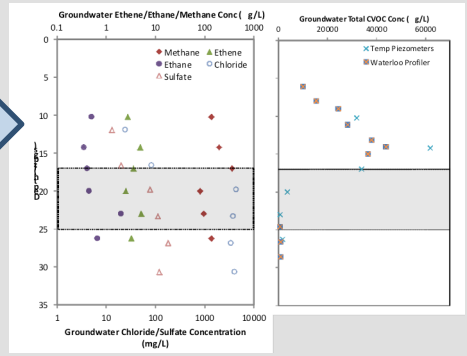

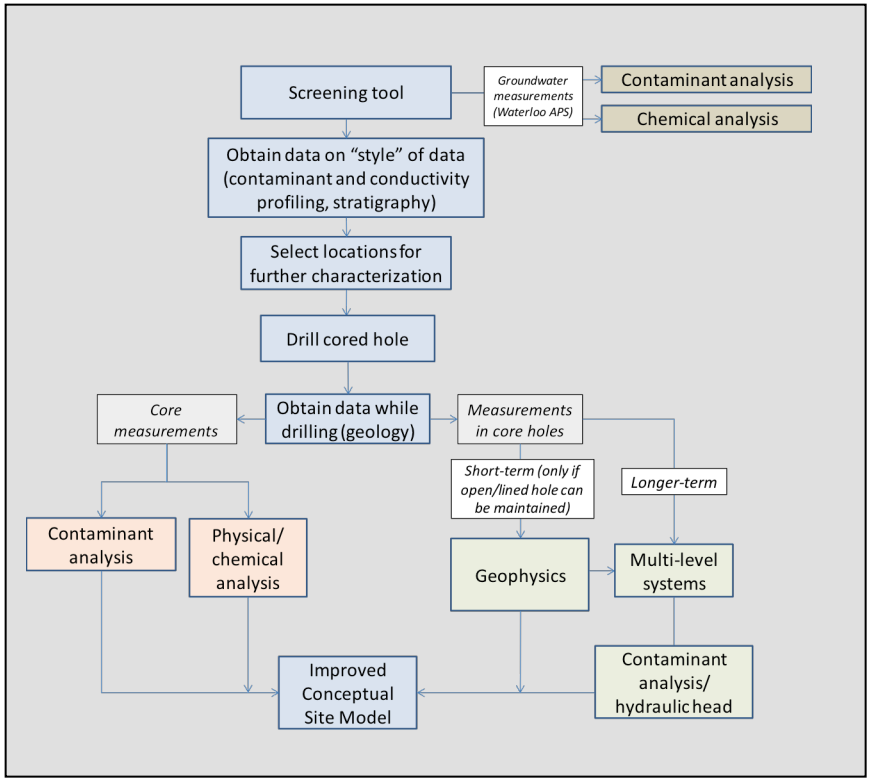

Figure 3.8a. Integrated field approach for characterizing low permeability zones in unconsolidated (lithified) setings. Screening-level tools are relatively easy to use in these formations because they are driven by direct push rigs, but open borehole tests (e.g., geophysics) are typically not practical. The objective of the integrated approach is to improve conceptual site model by generating high-resolution data at appropriate scale to understand all relevant processes and compartments. The chart is not intended to be inclusive of all potential steps that could be part of an actual site investigation, and does not include modeling or other data evaluation steps.

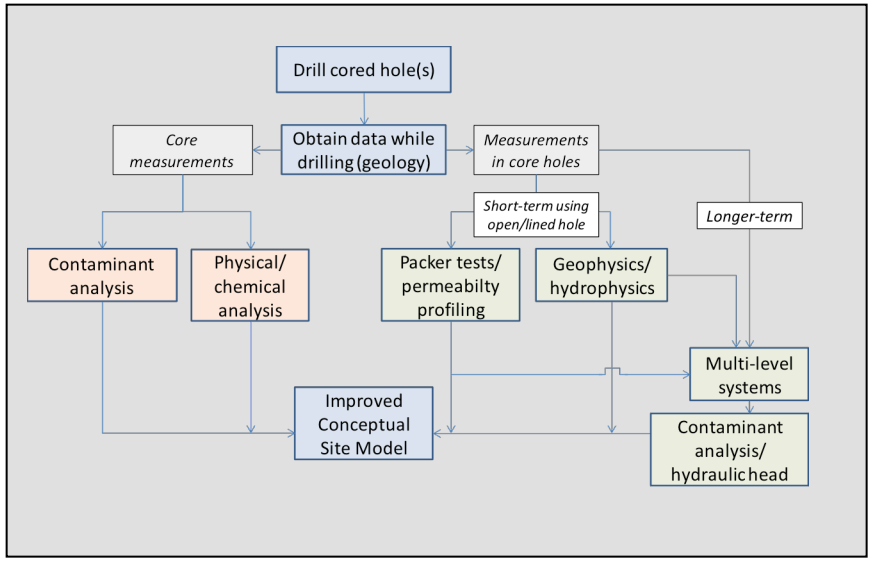

Figure 3.8b. Integrated field approach for characterizing low permeability zones in unlithified (rock) settings. Coring is the initial step in the characterization process due to the lack of appropriate screening-level tools. Formations are well-suited for completing borehole tests, particularly using liners that temporarily seal the hole and minimize cross connections between fractures. The objective of the integrated approach is to improve conceptual site model by generating high-resolution data at appropriate scale to understand all relevant processes and compartments. The chart is a condensed version of the Discrete Fracture Network approach developed by Parker (2007). It does not describe all potential steps that could be part of an actual site investigation, and does not include modeling or other data evaluation steps. For a more detailed description, see Parker, 2007.

3.3 EMERGING NEEDS AND OPPORTUNITIES ("3G" CHARACTERIZATION APPROACHES)

The growing use and acceptance of the second-generation methods described in the previous section has increased our appreciation for the importance of high-resolution characterization for evaluating contaminant storage in low k zones. However, many of the second-generation methods have characteristics that may limit their applicability or the usefulness of the information they generate. Consequently, the opportunity remains to develop better characterization methods as part of a "third-generation" of approaches for low k zone investigations.

The following list includes a number of investigative methods that could fall into this third-generation category. It includes techniques that improve data collection and quality, as well as tools that help with interpreting those data. Some of these are already in development, while others would be available in a "perfect world".

- ***MIP with constituent-specific detection capabilities.*** As an investigative tool, MIP provides a tremendous amount of data in a short period of time, but a major limitation is that it generates bulk detector responses that do not differentiate between the individual compounds that might be present. This hampers interpretation when the contaminants are poorly detected and/or generate widely different responses. A promising solution is a modified MIP approach—known as the Enhanced In Situ Soil Analysis (EnISSA)—that uses a GC/MS system connected to the MIP so that individual constituents within the vapor stream can be identified and their relative contributions quantified (at a frequency of 30 cm). EnISSA has been developed by a multi-partner team and, following rigorous field testing, has recently become commercially available for use in high-resolution site characterization.
- ***Better optical screening tools:*** At sites with low k zones, optical screening tools can be effective in determining if DNAPL remains and needs to be incorporated into the site model. An improved tool, DYE-LIF, is being developed and demonstrated under ESTCP ER-201121. By co-injecting a dye that partitions into DNAPL and fluoresces, this technology is compatible with the available optical screening tools while overcoming their primary limitation (naturally-fluorescing aromatic hydrocarbons must be present as co-contaminants to identify DNAPL).
- ***More robust tooling for direct-push driven systems.*** Direct push-driven profiling tools may encounter difficulties when advancing through tight or cobbled soils, resulting in refusal and/or damage to tooling due to excessive hammering. More robust systems are needed to minimize any problems in profiling through these soil types, and service providers should ensure that these next-generation tools are compatible with increasingly-powerful direct push rigs.
- ***Refined geophysical methods:*** Existing geophysical methods continue to be improved, with low k zone investigations (particularly for fractured rock) driving these developments. An example is the use of fiber optic distributed temperature sensing (DTS) for improved borehole temperature logging within fractured rock (e.g., Leaf et al., 2012; Read et al., 2013). Relative to standard techniques for temperature logging (wireline trolling), fiber optic DTS provides data much more

rapidly at sufficient resolution for defining flow characteristics within fractured rock formations.

- ***Rapid field extraction.*** As noted in Section 3.2.1, advancements in sample preparation procedures mean that soil sample extraction can effectively be done in the field. When combined with an on-site mobile laboratory capable of analyzing these extracts as soon as they are ready, this means that same-day results can be obtained for a truly dynamic field investigation. Because all of the mass is extracted and analyzed, it provides a more representative data than other rapid analysis approaches for soils (e.g., direct sampling ion trap mass spectrometry (DSITMS)). The commercial availability of these capabilities will increase over the next several years, greatly improving the utility of high-resolution soil sampling as an investigative tool.
- ***Core collection techniques.*** Obtaining high quality cores is an important component of investigating sites with low k zones, but remains challenging in adjacent intervals that are less cohesive and have a tendency to flow. Problems can be encountered both during advancement of the core barrel or tube (excessive disturbance, poor clearing of cuttings, flushing to maintain pressure head) and during retrieval (gravity drainage, drop out of material). Several techniques to improve collection have been envisioned, including better liners and catchers, as well as in situ freezing of cores during collection to improve cohesiveness. It is anticipated that further development of these and other methods will be a priority within the next several years.
- ***Visualization tools.*** High-resolution site characterization data should be collected and communicated in a way that is easily interpretable, and visualization tools are one of the best methods for accomplishing this. An example of an already well-developed approach is borehole imaging using analog, digital optical, or digital acoustic methods, where the image can be viewed above-ground in real-time while the camera is being lowered down the hole. Other examples include various software packages which are specifically designed for 3-dimensional data presentation (e.g., Environmental Visualization System). The development of effective visualization tools remains a continuing objective for sites or settings with low k zones.
- ***Better tools to measure and understand attenuation rates***. Current strategies for assessing concentration trends and degradation patterns focus on collecting groundwater over time, a process which is time-consuming and not necessarily well-suited for low k zones. The continuing maturation of molecular biological tools and compound-specific isotope analyses has benefitted these evaluations (**see Chapter 4**), but the data generated from these approaches are not always conclusive. Further, they may not be sufficiently quantitative to estimate rates, let alone differentiate between various attenuation processes. Consequently, there is an opportunity to develop in situ methods for measuring and understanding rates at sites with low k soils.
- ***Tools and/or methods to assess contaminant/amendment accessibility.*** Current high-resolution characterization methods show promise in providing quantitative knowledge of how *accessible* contaminants are to different remediation processes and how *accessible* a treatment zone is to amendment delivery. The next generation of tools should focus on expanding this knowledge

base because these are the important questions to answer to ensure that the selected remedy is appropriate and effective.

- ***Passive flux meters for measuring mass release rates.*** Passive flux meters (PFMs) have been successfully used to document the vertical distribution of contaminants and groundwater flow within relatively permeable zones (Annable et al., 2005). Newer versions are being developed to deploy at the interfaces between high and low k zones to measure the mass discharge rates attributable to diffusion-based release from the low k zones (Brown et al., 2012). Field trials of these interface PFMs are on-going. In addition, passive flux meters for fractured rock investigations have been developed and successfully tested (Acar et al., 2013).
- ***Simple modeling tools to aid data interpretation.*** Interpreting the data generated from high-resolution site characterization can be challenging, and there are several free software tools currently in development to provide guidance for the environmental professionals. The first—termed "Source History"— takes soil coring data from a low k zone to make predictions about the concentration vs. time pattern in an adjacent high permeability zone (i.e., the "source history"). It is based on a simple 1-D diffusion model and is being funded as part of ESTCP ER-201032 (Newell et al., 2013; Farhat et al., 2013). The second—the Matrix Diffusion Toolkit—contains several modules that predict mass discharge and concentrations over time (in the simple module) or even distance (in the more complex module) (Farhat et al., 2012). These predictions can be used for planning-level purposes, with comparisons to high-resolution field data helping to calibrate input values. This toolkit was funded as part of ESTCP Project ER-201126.

3.4 CHAPTER 3 CHARACTERIZING LOW k ZONES – KEY RESEARCH PRODUCTS

2G Site Characterization Programs

- F.E. Warren AFB Wyoming (MIP, HPT, Waterloo^{APS} System, High Resolution Soil Coring) (Appendix A)
- Naval Air Station Jacksonville (MIP, HPT, Waterloo^{APS} System, High Resolution Soil Coring) (Appendix B)

Procedures/Protocols

- Membrane Interface Probe Protocol for Contaminants in Low-Permeability Zones (Adamson et al., 2013)

Journal Articles

Adamson, D. T., Chapman, S., Mahler, N., Newell, C., Parker, B., Pitkin, S., Rossi, M. and Singletary, M. (2013), Membrane Interface Probe Protocol for Contaminants in Low-Permeability Zones. Ground Water. doi: 10.1111/gwat.12085

OVERVIEW OF CHAPTER 4:
TRANSPORT IN HETEROGENEOUS MEDIA

- The conventional approach to contaminant transport in groundwater has been "advection-dispersion" but this approach has serious limitations with regard to the impact of low k zones.
- We propose an alternative "advection-diffusion" approach where
  - Advection and diffusion are the primary transport process
  - Transverse dispersion is a weak process
  - Longitudinal spreading is dominated by storage and release of contaminates in low k zones
  - Reactions (sorption and degradations) in low k zones are central to understanding aqueous phase concentrations in transmissive zones
  - Local heterogeneity is addressed by considering idealized architecture of transmissive and low k zones. One of the key parameters in the advection diffusion model is the effective diffusion coefficient, D^*. There are three main ways to measure effective diffusion coefficients in porous media: 1) dual reservoir techniques, 2) capillary tube methods, and 3) closed column methods.

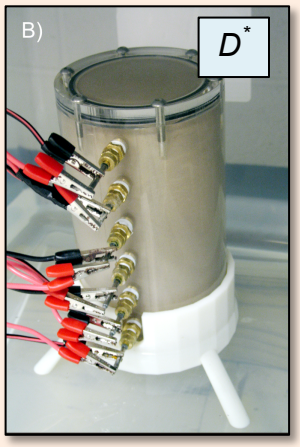

- A variant of the closed column method using a **Dead-End Column (DEC)** was used to do research on how the type of porous media (sand vs. silt vs. clay) affects effective diffusion coefficients.
- Key result diffusion research: diffusion coefficients in sediments with textures between sand and silt may vary by as much as an order of magnitude, much more than simple planning level relationships based on literature values of porosity and tortuosity. This is a need to develop better measurement techniques and predictive methods for effective diffusion coefficients in order to use to better understand and model low k units at contaminated sites.
- Degradation in low k zones is an important process. Unfortunately, we don't much about the prevalence, rates, and sustainability of both abiotic and biotic degradation processes in low k zones.

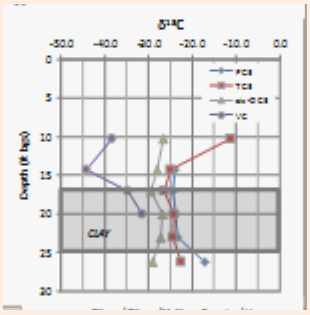

- For the SERDP research study, eight studies that focused on degradation in low k zones were reviewed. These studies showed a wide range of results, from no likely degradation, potential presence of native indigenous population of paleoenvironments; microbes at interfaces, to apparent degradation in a clay aquitard
- Degradation studies performed by this research team, including one SERDP project field site, are highlighted: one with limited evidence for degradation and one with no evidence.

Key Words: diffusion, effective diffusion coefficient, storage, release, Fick's Law, tortuosity, texture, Crank, Dual reservoir, capillary tube, closed column, endogenous decay, biogeochemical, organo-clays, reactive minerals, iron reduction, pore throats, interfaces, paleoenvironments, Dehalococcoides, KB-1, reductase, compound specific isotope analysis (CSIA), redox, cis-DCE).

4.0 TRANSPORT IN HETEROGENEOUS MEDIA

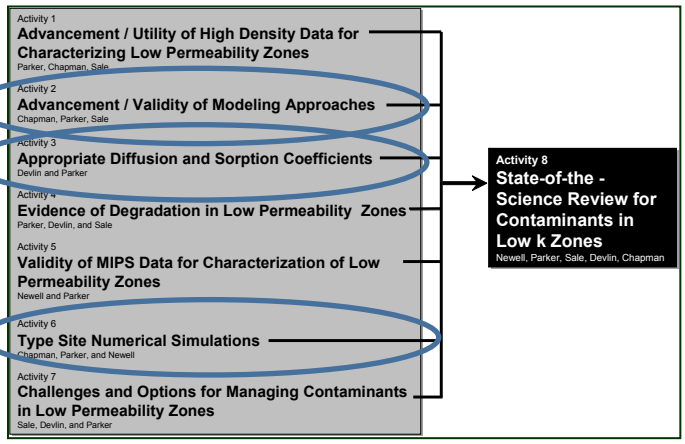

Historically, our primary approach to describing contaminant transport has been to 1) envision subsurface systems as combination of large-scale homogeneous-isotropic aquifers and aquitards and 2) to use dispersion as a "fudge factor" to address local heterogeneities that are ubiquitous in almost all geologic systems. Unfortunately, this approach has numerous limitations including the failure to recognize that low k zones can sustain contaminant concentrations in transmissive zones for decades or even centuries after the primary sources have been addressed (Chapman and Parker 2005).

The following chapter advances an alternative approach to describing contaminant transport wherein:

- Advection and diffusion are the primary transport process
- Transverse dispersion is a weak process
- Longitudinal spreading is dominated by storage and release of contaminates in relatively low k zones
- Reactions (sorption and degradations) in low k zones are central to understanding aqueous phase concentrations in transmissive zones
- Local heterogeneity is addressed by considering idealized architecture of transmissive and low k zones

Content of this chapter includes an introduction to diffusive transport, from SERDP-funded laboratory experiments of effective diffusion coefficients in different geologic media, and an overview of degradation in low k geologic media for chlorinated solvents.

Lead Authors for This Chapter

Diffusion Studies: J.F Devlin, University of Kansas
Degradation Studies: Glaucia Lima, Beth Parker and Steve Chapman, University of Guelph; David Adamson, GSI Environmental

4.1 OVERVIEW

In an advection-diffusion world, there are two key processes that will control the fate and transport of contaminants in the plume. First, diffusion of contaminants in and out of the low k zones becomes a controlling process, and knowledge of what **effective diffusion** coefficient to use becomes an issue of primary importance. Second, degradation of contaminants in the low k zones can become a critical factor in understanding how sites will age and on how to manage sites in general over long time periods. While the degradation processes of concern are generally the same as in transmissive zones (abiotic degradation, reductive dechlorination, etc.), the low k environment in which this degradation may or may not occur is very different, and efforts must be made to better understand the effects of this different environment on the **degradation processes**.

Therefore, this Chapter is concerned with the transport of solutes in heterogeneous media and is divided into two primary parts:

- Diffusion In Permeable Porous Media
- Contaminant Degradation in Low k Zones

4.2 DIFFUSION IN PERMEABLE POROUS MEDIA

The study of contaminant transport in aquifers has tended to be dominated by consideration of advection, modified by processes such as sorption and transformation. However, there is a growing awareness that conventional models over-predict the rates of contaminant flushing from many aquifers. Typically, plumes are quickly flushed at first and then linger, exhibiting long tails and longer than expected times to flush contaminants through the system. This has implications for both risk assessment and remediation designs.

The concept of 'back-diffusion' has been proposed as an explanation for the plume tailing phenomenon in aquifers. Back-diffusion refers to the delivery of contaminants to the most permeable parts of the aquifer from relatively low k geologic features (layers, strata, lenses) due to diffusion limited mass transport. The accurate prediction of mass transport rates by diffusion depends upon accurate knowledge of diffusion coefficients.

4.2.1 Darcy's Law and Fick's First Law: Functional Brothers

Diffusion has been studied for many decades and much is known about it. Nevertheless, it has not been at the forefront of hydrogeological training and therefore is not a process most hydrogeologists can think about intuitively. A useful first step to enable hydrogeologists to acquire intuition about diffusion is to compare Fick's First Law and Darcy's Law; the two mathematical functions might be described as brothers.

Darcy's Law: (1)

$$q = -K\frac{\Delta H}{\Delta x}$$

Fick's First Law (2)

$$J = -D\frac{\Delta C}{\Delta x}$$

Hydrogeologists are well acquainted with Darcy's Law, which relates the water flux to a constant of proportionality called the hydraulic conductivity, K, and the hydraulic gradient, $\Delta H/\Delta x$. The flux can be increased either by modifying the porous medium or the fluid to increase hydraulic conductivity (e.g. by inducing fracturing or supplying additives that change fluid viscosity), or by increasing the driving force for flow by raising the hydraulic gradient (e.g. by pumping). Fick's First Law suggests that diffusion rates can be similarly manipulated. The flux of contaminant moving in a system depends on a constant of proportionality, the diffusion coefficient, *D*, and a gradient – in this case a spatial concentration gradient, $\Delta C/\Delta x$. Rates of diffusion increase with increasing *D* and with increasing concentration gradient. In natural media, the measured diffusion coefficient may actually be a function of sorption, chemical species, tortuosity, temperature, and other factors discussed later on. For this reason, *D* estimated from fitting data with models is sometimes referred to as the *effective diffusion coefficient, D^**.

Hydrogeologists are well aware of the importance of determining hydraulic conductivity as accurately as possible in the assessment of water movement in aquifers. An enormous literature has developed over the years addressing the problem of measuring hydraulic conductivity at various scales with the greatest representativeness for the purposes of contaminant transport modeling. In particular, *hydraulic conductivity* presents challenges because it can vary so greatly within a single geologic deposit, and between strata of different textures. It should therefore be easy for hydrogeologists to appreciate that accurate determinations of D^* in varying geologic materials is also important. The present knowledge of diffusion in natural porous media indicates that the range of *D* is much less than that of hydraulic conductivity. Nevertheless, where back-diffusion is concerned, variations in *D* by as little as a factor of two might be important to know. Therefore, a review of the literature to gain an appreciation of how D^* varies with sediment texture was performed, as described below.

4.2.2 The Effect of Sediment Texture on D*

There is a large literature concerned with diffusion in general, including consideration of many diffusing substances. In this chapter, attention will be limited to simple cases of non-reactive, non-sorbing diffusion, as exemplified by a NaCl solution and tritiated water. A review of 70 individually measured values of D^* for chloride (as $Cl^-_{(aq)}$ and $^{36}Cl^-_{(aq)}$) in clayey sediments yielded a range from unquantifiable to 0.92 cm^2day^{-1} (**Figure 4-1A**). A similar review of 81 sodium (as $Na^+_{(aq)}$ and $^{22}Na^+_{(aq)}$) D^* values yielded a range from unquantifiable to 0.64 $cm^2\ day^{-1}$ for clayey sediments (**Figure 4-1B**).

A)

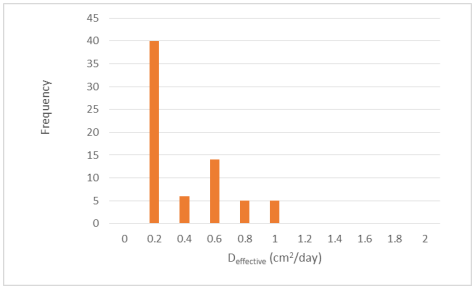

B)

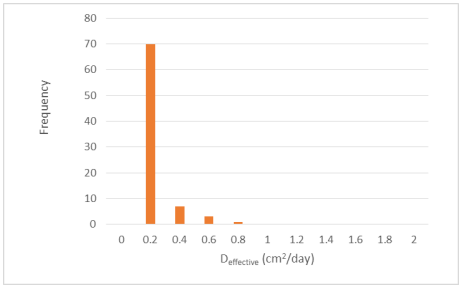

Figure 4-1. Distributions of measured D^* for A) chloride and B) sodium in sediments of various textures (data given in Appendix C).

According to Robinson and Stokes (1959) and Shackleford and Daniels, (1991) diffusion coefficients measured for solutions containing both Na^+ and Cl^- will exhibit D^* values different from the ideal coefficients for each ion due to factors including electrical gradients, water content (all water saturations considered here approach 90% or greater), solute-solute interactions and solute solvent interactions. Also, D^* values are not always reported consistently or at identical temperatures, so direct comparisons can sometimes be difficult. These issues account in part the variations displayed in Figure 1.

It is noteworthy that most of the studies found for review in **Figure 4-1** were conducted with porous media that included substantial clay fractions, explaining the high frequencies of $D_{effective} < 0.2$ cm^2 day^{-1}. This is not surprising since clayey sediments represent an environment that severely restricts transport by advection, and strongly favors diffusion. Nevertheless, a few studies in which diffusion was measured in permeable material have been reported. A study by Dytynyshyn *et al*. (1984) reported a D^* of 0.86 cm^{2}day^{-1} for $^{36}Cl^-$ in sand. The addition of 5% to 50% bentonite to the sediment reduced the D^* to < 0.7 cm^{2}day^{-1} with no clear trend downward with additional addition of bentonite. Apparently, in some cases a small amount of clay is sufficient to modify D^* and additional clay makes little difference. Sulfate was found to diffuse with a D^* of 1.21 cm^2 day^{-1} in sand by Berner *et al*. (1969). These limited data suggest that D^* may vary with sediment texture, with higher values associated with coarser material. To assess this possibility further, studies on the diffusion of tritiated water (HTO) were examined, making use of literature that considered a broader range of sediment textures (**Figure 4-2**).

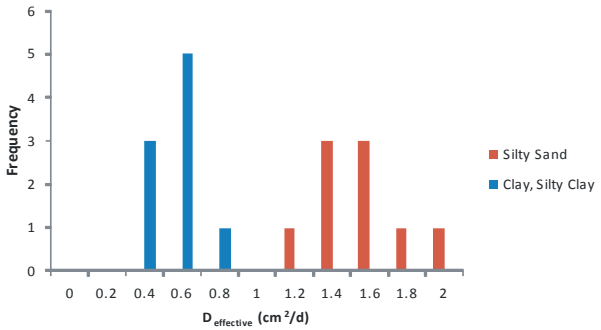

Figure 4-2. Distribution of D^* for ^3H_2O in clay, silty clay and silty sand (Appendix C).

The data presented in **Figure 4-2** comprise 25 individual diffusion coefficient measurements in a variety of sediment types. The distributions indicate a clear difference between the D^* values in clay-rich sediments compared to sandy sediments. The clay-rich samples were associated with D^* values as much as an order of magnitude less than those obtained from experiments with silty sand.

Comparison of **Figures 4-1 and 4-2 reveals** that the range of magnitudes of D^* are similar for ^3H_2O and the ions Na^+ and Cl^- where diffusion in clayey material is concerned. The D^* for tritiated water in sandy material is notably greater and it is hypothesized that a similar increase might apply to the ionic species, Na^+ and Cl^- in sand. The hypothesis is generally consistent with the $^{36}Cl^-$ and $SO_4^=$ data mentioned above, but further experimentation is needed to test this hypothesis more quantitatively.

If D^* varies by up to an order of magnitude in natural porous media, a question remains as to the significance of this variation. To address this question in a preliminary fashion, a stylized modeling exercise was undertaken, as described below.

4.2.3 Modeling to Show the Effects of Heterogeneity on Diffusion Coefficients

To assess the possible importance of texture dependent diffusion coefficients, a one dimensional numerical model was constructed and simulations were performed for 4 cases of 27.5 cm thick sediment columns: 1) a homogeneous sandy column, D^* = 2.0 $cm^2\ day^{-1}$; 2) a homogeneous clayey silt column, D^* = 1.0 $cm^2\ day^{-1}$; 3) a heterogeneous column containing a 7 cm thick layer of clayey material within sandy material; 4) the result of a 1000 realization Monte Carlo simulation in which the D^* value of the 7 cm layer is permitted to vary randomly from D^* = , 0.04 $cm^2\ day^{-1}$. In all simulations, at time 0 C_o = 10 (arbitrary concentration units) within the lens and 0 without. The C_o at the boundaries (x = 0 and 27.5 cm) was 0 at all times.

In all simulations the solute approaches but does not fully reach the domain boundaries (**Figure 4-3).** The final contaminant distribution is more restricted in the homogeneous silt case, with solute mass moving slowly from the lens (**Figure 4-3B**). This is a direct result of a lower D^* throughout the domain. The effect of a lens of clayey silt in an otherwise sandy matrix (**Figure 4-3C**) is a concentration profile that exhibits a hump within the lens, reflecting the relatively slow release of solute from the feature. The

hump is slightly different in the realization shown in **Figure 4-3D** because the effective diffusion coefficients at each location in the lens were variable in that simulation.

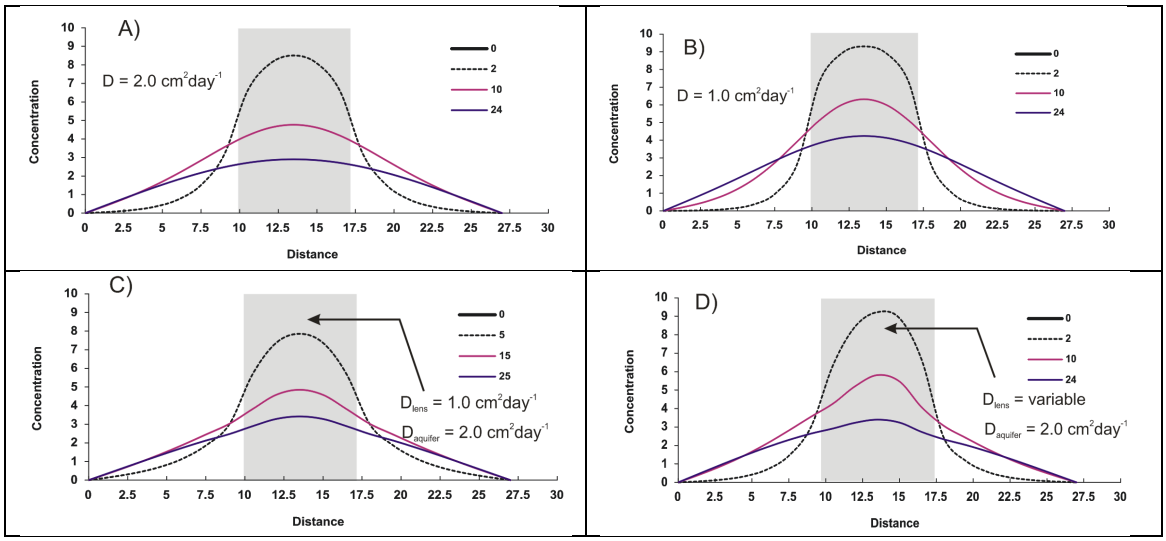

Figure 4-3. Comparison of concentration profiles for a hypothetical solute diffusing from a 7 cm clay lens (grey) into the surrounding sand material. Numbers in legends represents times of the simulations in days. A) D^* of the lens and matrix are 2.0 cm^2day^{-1}. B) D^* of the lens and matrix are 1.0 cm^2day^{-1}. C) D^* of the lens is 1.0 cm^2day^{-1} and matrix 2.0 cm^2day^{-1}. D) One of 1000 realizations in which D^* of the lens was varied randomly from 1.0 to 2.0 cm^2day^{-1} across the lens.

The simulations in **Figure 4-3** demonstrate that relevant variations in D^* within a diffusion limited porous medium exerts a notable effect on solute concentration distributions. However the significance of these data is more readily apparent when solute fluxes across the lens boundaries are considered (**Figure 4-4**).

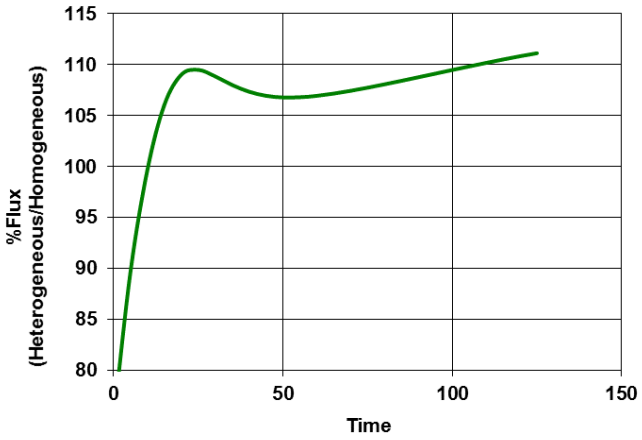

Figure 4-4. Comparison of fluxes across lens boundaries expressed as % of flux from heterogeneous case (clayey silt lens in sandy material) compared to homogeneous case (sandy source 'lens' in sandy matrix).

Initially, flux across the lens boundary is greater when the sediment column is homogeneous because the source 'lens' transmits solute to the matrix as quickly as the matrix can accept it; both have identical values of D^*; the heterogeneous case flux is initially 75% of the homogeneous case flux (**Figure 4-4**). However, with increasing time, as the source 'lens' is depleted in solute, the diffusive flux in the homogeneous case diminishes faster than that in the heterogeneous case. This results in an increase in %Flux in **Figure 4-4**. Ultimately, the solute mass in the clayey silt lens remains higher than that of the homogeneous case, retaining a higher concentration gradient across the source lens boundaries. The result is a rising %Flux; by about day 10 in **Figure 4-4** the homogeneous and heterogeneous cases have about equal fluxes (ratio of 100%), and the heterogeneous case has the higher flux after that. The magnitude of the effect might be more or less pronounced depending on the specific conditions simulated. It is sufficient for the purposes here to show that the effect is not negligible. In terms of long-term plume behavior, this phenomenon is a manifestation of back diffusion and suggests that variations in D^* due to sediment texture are worth more detailed study.

4.2.4 Factors Controlling Effective Diffusion Coefficients

The review and analysis presented above focuses on the effective diffusion coefficient, D^*. For the purposes of contaminant transport modeling, D^* is the parameter of greatest significance. However, diffusion research has explored many factors, that can be represented numerically, that contribute to D^*. In some cases the quantification of these factors is not easily accomplished leaving considerable uncertainty in the fundamental physical and chemical processes that determine diffusion rates. For this reason, practical applications depend primarily on empirical measurements of D^* (or estimates from empirical equations) rather than *ab initio* estimates.

Despite the present limitations on our understanding of diffusion coefficients in aquifers, a brief review of factors thought to influence diffusion coefficients in general is instructive. A clear and lucid overview was given by Shackleford and Daniels (1998) and an augmented summary is given here.

Crank (1956) described diffusion as the outcome of a "random walk" of atoms, molecules, or ions – collectively referred to here as particles. There is no preferred direction of movement for any particle. A net transfer of mass from regions of high concentration to those of low concentrations occurs simply because there are more particles in the higher concentration regions and therefore a higher probability that some will move toward a more dilute region. Fick's First Law (eq.2) relates the concentration gradient to the net mass flux through the constant of proportionality, *D*. Under ideal conditions, such as in the case of an ideal gas, the particles do not interact with one another and at a fixed temperature and pressure *D* can be expected to be a true constant. However, in the case of diffusion in aqueous solutions, particles can interact with each other (at sufficiently high concentrations) and with the solvent. It is immediately seen that the diffusion coefficient for a substance such as Cl^- might vary with changing solvent conditions, the presence of other solutes, or even the concentration of Cl^- itself. In the simplest case, Cl^- is infinitely dilute and these complicating interactions are negligible. The diffusion coefficient under these circumstances is at its maximum, and was expressed by Robinson and Stokes (1959) as D_o,

$$D_o = \frac{RT(v_1 + v_2)}{F^2 v_1 |z_1|} \frac{\lambda_1^0 \lambda_2^0}{(\lambda_1^0 + \lambda_2^0)} \tag{3}$$

where *R* is the ideal gas constant, *T* is temperature, v_i refers to the number of moles of ion 'i' formed from one mole of electrolyte, z_i is the charge on ion 'i', λ^o_i is the limiting equivalent conductivity of ion 'i', F is the Faraday constant. For an infinitely dilute solution of NaCl, D_o was reported to be 1.39 $cm^2\ day^{-1}$. This value becomes 1.30 for a 0.05 molar solution (~ 3 g/L).

An equivalent expression based on consideration of Stokes Law was given by Shackelford and Daniels (1991),

$$D_o = \frac{RT}{6\pi N \eta r} \tag{4}$$

where *N* is Avagadro's number, η is the absolute viscosity of the solution and *r* is the molecular or hydrated ionic radius.

In porous media, the area over which diffusion (in water) can occur is restricted by the sediment grains and the presence of other, immiscible fluids – typically air . Thus a correction for porosity and saturation is required. A dilute solution of NaCl (or other solute) diffuses with a diffusion coefficient of D^*, which is related to D_o as follows

$$D^* = D_o n S_r \tag{5}$$

where *n* is porosity and S_r is the fraction of saturation of the porous medium. In saturated porous media S_r = 1.0. Typically, tortuosity is accounted for with an effective tortuosity factor, τ, that can be defined as an actual path length distance traveled by a particle divided by the linear distance travelled. Accordingly, τ values are typically <1.

However, it is convenient to define an effective tortuosity factor, τ_a, that includes tortuosity and all other factors that might affect diffusion, such as solute-solute interactions and solute-solvent interactions and porosity. Volumetric water content is not lumped with the other effects since it can be measured independently (Shackleford and Daniels, 1991). Values of τ_a range from 0.064 to 0.31 in clay-rich material, and from 0.025 to 0.35 in sand (see Table 3 in Shackleford and Daniels, 1991). The lack of a broad, consistent trend in τ_a with sediment type highlights the need for more a detailed assessment of the relationship.

$$D^* = D_o \tau_a S_r \tag{6}$$

In this work, attention is paid to the experimental determination of D^* in saturated, granular porous media (i.e., S_r = 1.0).

4.2.5 Methods for Estimating D_o and D*

To gain perspective on methods likely to succeed in measuring *D** in porous media, it turns out to be helpful to review the challenges that were encountered in measuring diffusion coefficients in open solution, D_o. Robinson and Stokes (1959) describe several methods of determining these diffusion coefficients:

1) **Dual reservoir techniques** in which solution reservoirs separated by fritted glass (15 μm pores) are prepared with different solution concentrations and allowed to equilibrate while concentrations in the two reservoirs are tracked in time.
2) A **capillary tube technique** involves placement of one end of the tube containing an isotopically tagged tracer into a large, stirred reservoir containing an equal concentration of untagged tracer. After a measured time the total amount of solute to leave the capillary tube is determined and fitted with a theoretical prediction by adjusting the diffusion coefficient.
3) **Closed column methods** in which a solute is introduced at one end of the column and monitored as it moves toward the other. The column may be closed at both ends for most of the duration of the experiment. Solute detection techniques were typically optical (spectrophotometric), interferometric, or based on detection of changes in electrical conductance. They found that the single most notable problem in conducting the experiments was preventing unintended flow. Vibrations, temperature fluctuations, or physical disturbances of the water volumes (e.g. due to stirring) could cause small but significant circulation of the solutions, biasing the D_o measurements.

Efforts to measure diffusion coefficients in porous media have most commonly been focused on clay-rich sediments in which water flow is severely impeded. For this reason, the problem of unwanted flow causing measurement bias has been less problematic. In other respects, the history of the efforts bears strong similarities. Both **dual reservoir** and **column style tests** have been employed. An important difference between the porous media and open solution experiments lies in the steps to characterize the progress of diffusion over time, and to subsequently obtain the diffusion coefficient by curve fitting. Open water experiments depend on modeling the changes in

the average concentrations of solutes over time, i.e., *dC/dt*. Porous media studies can take the same approach, or they can examine solution concentration distributions in space at a particular time, i.e., *dC/dx* at time *t*. The latter method (*dC/dx* at time *t* method) has been widely used and involves stopping an experiment after a predetermined time, sectioning the porous medium through which diffusion has been occurring, and analyzing the solution concentration in the sections. An advantage of this approach is that sampling for chemical analysis is possible with adequate sample sizes, and the systems are not subject to biases due to imposed circulation when the medium is one of low k. Disadvantages include problems in achieving complete hydraulic contact between reservoirs, and the difficulty in ensuring full saturation in the clayey material connecting the reservoirs. If studies are performed with complex ionic solutions, problems of counter-diffusion of ions may complicate interpretations.

Hendry *et al*., (2009) used the **double reservoir technique** to show that laboratory measured diffusion coefficients of deuterium in clay-rich aquitard material were comparable to values determined in *in situ* samples. They found values of D^*/n from *in situ* testing (between 0.22 and 0.30 $cm^2\ day^{-1}$) to be similar but consistently smaller in magnitude to the laboratory derived values (0.35 $cm^2\ day^{-1}$) and attributed the difference to porosity changes during or after core recovery.

Van Rees *et al*. (1991) compared results of tritium diffusion coefficients estimated from 3 variations of **column style tests**. Spiked reservoirs causing diffusion into unspiked sediment columns, spiked columns diffusing tracer into unspiked reservoirs, and sediment to sediment diffusion were examined. Samples were gathered from the reservoirs repeatedly in time, and from sectioned columns at the end of the experiments. All three methods were found to yield similar results, with D^* values ranging from 0.92 to 1.82 $cm^2\ day^{-1}$. The lowest values tended to come from the sediment to sediment tests. This was interpreted as a negative bias caused by difficulties of extrusion and sectioning. In the final analysis, the spiked reservoir technique was preferred due to ease of use and favorable performance.

A third technique for estimating diffusion coefficients, called the **radial diffusion method**, was proposed by Novakowsi and van der Kamp (1996). They advocated the boring of a cylindrical reservoir into a larger cylindrical sediment sample contained in a rigid plastic tube or sediment core tube. Monitoring changing concentrations of a tracer in the reservoir is the basis for model fitting and D^* estimation. Experiments involving the diffusion of a conservative organic dye tracer (Lissamine FF) in an Ordovician shale yielded D^* estimates of 0.10 to 0.15 $cm^2\ day^{-1}$. Sulfate was found to have a D^* of 0.08 to 0.11 $cm^2\ day^{-1}$.

In order to measure diffusion coefficients in sediments other than clay, i.e., with permeabilities that permit flow at rates that compete or exceed diffusion rates, the previous experience shows clearly that methods are needed that eliminate as much as possible any factors that could promote fluid circulation. Double reservoir cells are susceptible to flow imposed by slight head differences between the reservoirs. The radial diffusion method is subject to unwanted flow in establishing the central reservoir, and spiking it with the tracer. This leaves a variation on one of the column methods, in particular the **spiked reservoir column method**, as the preferred alternative for investigating diffusion in permeable porous media.

4.2.6 SERDP Diffusion Experiments: The Dead-End Column ("DEC")

The apparatus constructed to conduct the diffusion experiments in sand and silt from the Warren Air Force Base (AFB) consisted of a 7.6 diameter, 15 cm long, Plexiglas column equipped with 6 conductivity probes (**Figure 4-5A**). One end of the column was sealed with a Plexiglas end cap, and the other was closed with a permeable stainless steel screen to prevent the packed media from falling out. The columns were packed in lifts, maintaining about a centimeter of standing water above the sediment at all times. This measure ensured that packing was achieved with virtually no entrapped air. The conductivity probes were installed during packing.

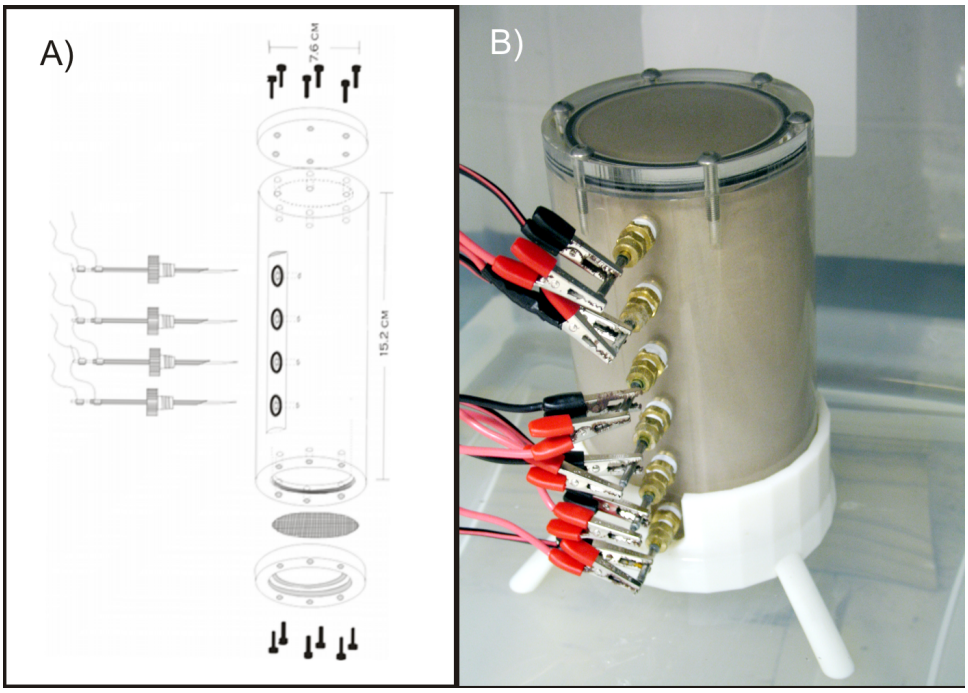

Figure 4-5: Dead End Column Experiment Setup. **A) Exploded diagram of the DEC. Four sampling ports are shown in this diagram, but the columns used in the project were equipped with six ports. B) The DEC packed with Warren Air Force Base silt and held upright in a stand. Six probes are connected with alligator clips to a datalogger (not visible).**

Once a column was packed, it was placed into a stand that supported it in an upright position (**Figure 4-5B**), and was then lowered into a plastic storage bin filled with water. The water level was maintained just below the bottom conductivity probe, a few centimeters above the screen. The water in the bin was stirred with the column in place for several days and the system allowed to equilibrate. The column was removed from the bin while the bin water was spiked to a concentration of about 1g/L of NaCl and mixed. The column was then replaced into the bin with no stirring and data collection was begun.

The probes were constructed from 5.08 cm long, 0.37 cm inner diameter, insulated stainless steel needles inserted into 15 gauge 0.146 cm outer diameter needles and

fixed in place with silicone to prevent short-circuiting and leakage of water (Figure A6-3). The inner needles protruded from the outer needles at both ends. One end was used as the sensor inside the column, and the other was connected to a Campbell Scientific CR1000 data logger with alligator clips (Figure 5B) and commercially available insulated wire. The chief advantage of this system is that nearly continuous sampling could be conducted without any disturbance of the solution. The D^* determinations could be based on conductivity-time curves fit to a solution of Fick's Second Law. The D^* values would represent a combined diffusion coefficient for Na^+ and Cl^- ions. Additional details are provided in **Appendix C.**

4.2.7 Measurement of D* in F.E. Warren AFB Sediments

Prior to conducting the experiments to estimate D^* for the F.E. Warren AFB Sediments, several experiments were conducted with a commercial sand to verify that the DEC was functioning as required. The first experiments were conducted with the DEC laying horizontal in the bin. These experiments resulted in salt breakthrough at all probes in the column within 6 days (blue line in **Figure 4-6**), and fitted D^* values that declined at each probe as distance from the screen increased. Data from the first probe exhibited more noise than the others, and breakthrough was not well described by a calculated diffusion curve. It was hypothesized that the density difference between the solution in the bin (~1 g/L NaCl) and the column (deionized water equilibrated with the sediment) was sufficient to cause density driven flow. The introduction of the stand to hold the column vertical was made at this time.

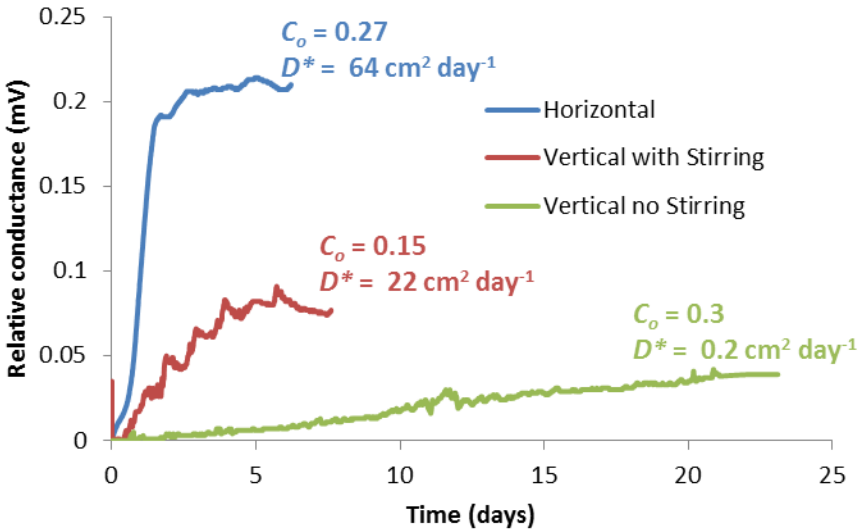

Figure 4-6. Breakthrough curves at the second probe, and the associated best fit D^* values for 3 experiments in commercial sand. "Horizontal" and "vertical" refer to the orientation of the DEC in the reservoir.

Experiments conducted with the DEC oriented vertically also showed higher than expected diffusion rates initially, with an estimated D^* of 22 cm^2 day^{-1} at the second probe (brown line in **Figure 4-6**). It was hypothesized that the stirring of the solution in

the bin was contributing to water circulation in the column. This idea was supported by the results of an idealized numerical simulation of the system (**Appendix C).** Once stirring was discontinued, the diffusion rates declined substantially (green line in **Figure 4-6**).

Two sediment types from the Warren AFB were analyzed: a silt and a sand. Both were examined in sequential replicates, and the first of the replicates is reproduced here (**Figure 4-7**). Over the course of the DEC development, and in the Warren AFB samples presented here, the tests were usually about 30 to 80 days in duration. Where diffusion in sand was being tested, this was sufficient time for responses to be detected at the first four probes (x = 2.5, 5, 7.5 cm from inlet). C_o values were first estimated from averages of probe measurements in the bin water, as shown in **Appendix C**. The data collected by the data logger were in the form of resistances (lower mV readings in more conductive solutions). Therefore, for convenience, a conversion to conductances was performed before fitting the data to arrive at D^* estimates. The conversion was accomplished by a background subtraction and a sign change (see **Appendix C**), so initial relative conductances averaged zero. The linear response of the detectors to the salt concentration in the applicable range of observed responses justified the conversion to conductances (**Appendix C**).

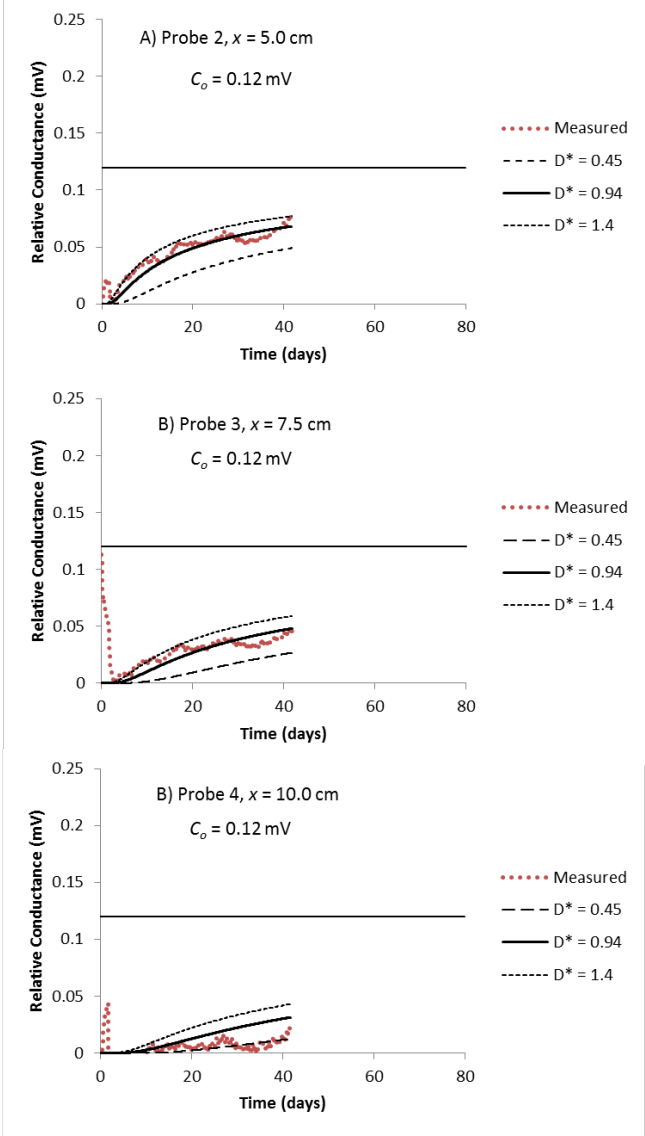

Figure 4-7. Diffusive breakthrough of NaCl solution in the FEW sand-packed column at A) the second probe (x = 5 cm) and B) the third probe (x = 7.5 cm) and C) the fourth probe (x = 10.0 cm).

The signals from the second third and fourth probes in the sand column were found to be well behaved with clear detections above background. The first probe signals were found to be unusable. The cause of the problem may be related to the probe itself, or to the proximity of the location to the column boundary. Further work is needed to resolve this issue.

Examination of the Warren sand using the second third and fourth probe data set yielded a D^* of 0.94 cm^2 day^{-1} (**Figure 4-7**). However, a C_o lower than expected had to be used to achieve a reasonable fit to the data (0.12 mV vs. 0.6 mV). It is hypothesized that the tracer concentration became depleted at the column inlet during the experiment effectively changing C_o downward. The addition of a probe to the reservoir side of the inlet screen would permit an assessment of this phenomenon in future tests.

Breakthrough of the tracer in the Warren silt sample was only discernible at probe 1 (x = 2.5 cm) during the experiment, but the breakthrough appeared generally well behaved after approximately day 10 (**Figure 4-8**). The best fit D^* was found to be 0.04 cm^2 day^{-1}, over an order of magnitude smaller than the value estimated for sand.

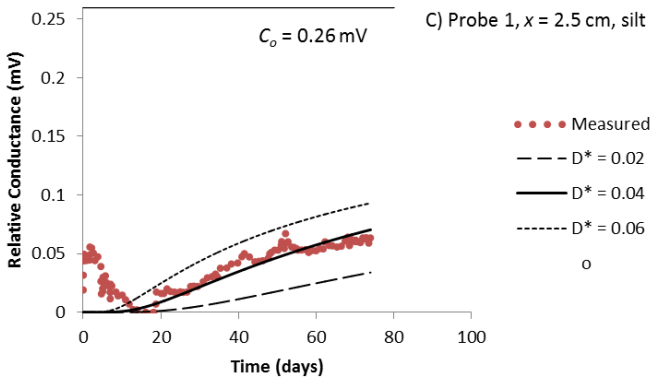

Figure 4-8. Diffusive breakthrough of NaCl solution in the FEW silt-packed column at the first probe (x = 2.5 cm). There was no meaningful signal from the second probe (x = 5.0 cm) over the time of this experiment.

4.2.8 Measurement of D*: Conclusions

Although further work is recommended to verify the preliminary estimates presented here, these data suggest that diffusion coefficients in sediments with textures between sand and silt may vary by as much as an order of magnitude:

- The **sand** sample from F.E. Warren AFB had a measured effective diffusion coefficient value for an NACL solution of **0.94 cm^2 day^{-1} ($1.1x10^{-5}$ cm^2/sec),**
- The **silt** sample from F.E. Warren AFB had a measured effective diffusion coefficient of **0.04 cm^2 day^{-1}** for an NaCl solution of **($4.7x10^{-7}$ cm^2/sec).**

Ratio of D* between sand and silt = $\frac{0.94}{0.04}$**=24.**

These findings are reasonably consistent with expectations based on previously reported diffusion coefficients for NaCl and ^3H_2O, and justify further work to examine the effects of heterogeneous diffusion on plume longevity.

By comparison, a commonly used empirical relationship to estimate effective diffusion coefficients is the Millington-Quirk relationship:

$$D^* = D_o\tau = D_o\theta^p$$

Where

- D^* = Effective diffusion coefficient (L^2/t)
- D_o = Free molecular diffusion coefficient (L^2/t)
- τ = Tortuosity (-)
- θ = Porosity (-)
- p = Apparent tortuosity factor exponent (-)

Generic planning-level values for θ and p of a sand and silt media are

- Sand: θ=0.40 and p=0.33 gives a tortuosity τ of 0.74.
- Silt: θ=0.47 and p=1.1 gives a tortuosity τ of 0.44.

Using these planning-level literature values and the tortuosity relationship indicates the sand and silt **effective diffusion coefficients are within a factor of two.**

However, the Dead End Column experiments show the **effective diffusion coefficient in the silt was 24 times smaller than the sand.**

The lack of a broad, consistent trend in τ with sediment type highlights the need for more a detailed assessment of simple planning-level relationships for tortuosity and the estimation of effective diffusion coefficients.

A further result of this work was to extend the conclusion of Robinson and Stokes, pertaining to their measurements of D_o in water-filled closed columns, to porous media packed closed columns. Specifically, Robinson and Stokes noted how difficult it was to prevent unwanted flow that would bias the estimation of D_o. In this work, similar unwanted flow was demonstrated in a sand column by *gently* stirring a reservoir containing the open end of a closed column. The unwanted flow was indicated by an estimated D^* from the experiment that was an order of magnitude higher than could reasonably be expected to be true. This was a striking demonstration of the ease with which advective flow can be initiated. A similar, though perhaps less pronounced, effect might be expected in some silts, since the range of hydraulic conductivity for silt overlaps that of sand.

The implications of this latter finding are potentially important for the proper interpretation of back-diffusion in field situations. Since advection is so easily caused to occur in permeable sediments, some occurrences of plume tailing that appear to be diffusion controlled may actually be manifestations of *slow advection*. This possibility could be welcome news for remedial systems designers, since it offers the possibility for enhanced advection with an appropriately designed injection-extraction system; strict diffusion controlled mass transport, with its associated long time scale, would not apply in such cases.

4.3 CONTAMINANT DEGRADATION IN LOW k ZONES

4.3.1 Introduction

Low k zones pose a significant challenge to groundwater remediation because contaminant transport is diffusion and sorption controlled, and as a consequence, timeframes for significant removal of contaminant mass and reduction of mass discharge from these zones into adjacent higher permeability zones can be as long as decades, or possibly centuries (Liu and Ball 2002; Chapman and Parker 2005; Sale et al., 2008; Parker et al. 2008; Parker et al., 2010; Damgaard *et al.* 2012). In this context, contaminant degradation, both abiotic and biologically mediated, within these low k zones should be investigated in order to evaluate potential for contaminant break down and reduction of the total mass stored there, which can significantly affect long term contaminant behavior.

Contaminant degradation in low k zones, even at relatively slow rates, has the potential to: 1) reduce the extent of contaminant penetration compared to that expected from diffusion and sorption processes alone. This could render thin, unfractured aquitards more effective barriers to contaminant transport than would otherwise be expected (e.g. Lima et al., 2012a); and 2) reduce the rate of back diffusion from low permeability zones, and the time over which it occurs, shortening the time a dissolved contaminant plume will be sustained in the adjacent higher permeability zones (e.g. Sale et al., 2008).

Table 4.1 summarizes general characteristics of low k zones that either favor or limit degradation capacity. These represent a combination of hydrogeologic, biological, and chemical factors.

Table 4.1. Low k Zone Characteristics that Influence Degradation

Factors FAVORING Low k Degradation	Factors LIMITING Low k Degradation
Long retention times (little advection/flushing) and slow endogenous decay	Pore throat size is small and thus restricts migration of microbes, influx of nutrients and carbon sources, and growth density
Reducing conditions are common (little recharge to introduce of competing electron acceptors) and favorable for biological and biogeochemical reductive dechlorination	Salinity can be high and potentially limit microbial activity
Potentially large reservoir of organic carbon (silts/organo-clays)	Bioavailability of organic carbon may be low (e.g., slow dissolution)
Potentially large reservoir of reactive mineral species	Reactivity of mineral species may be limited due to general dependence on microbial activity (e.g., iron reduction)
Depositional processes often result in heterogeneous settings. In these cases, low k zones may be thin/discontinuous or adjacent to highly transmissive, thin sand lenses. This could result in short migration distances within the low permeability features.	

To-date, research on degradation in lower permeability matrices has been relatively limited with much effort focused on biotic processes. Even though evidence of microbial activity in connection with contaminant degradation within low k zones can be found in the scientific literature (Chambon *et al.* 2010; Fredrickson *et al.* 1997; McMahon 2001; Takeuchi *et al.* 2011; Van Stempvoort *et al.* 2009), there is still a significant knowledge gap involving the characterization of microbial communities and how they contribute to overall plume attenuation and cleanup time frames within these zones.

Restrictions to microbial growth and propagation into low k zones are primarily related to size exclusion. Pore throats in unconsolidated aquitards can be smaller than 2 nm (Reszat and Hendry 2009), which exclude migration of most microbial cells (which are on the order of 1 μm in diameter) beyond a few centimeters from the interface with the aquifer (Chambon *et al.* 2010; Lima and Sleep 2007). Early studies indicated absence of microbial activity in low k zones with pore diameters < 0.2 μm, such as shales (Fredrickson et al. 1997).

The small pore throat sizes associated with lower permeability zones represent a significant impediment to microbial migration and growth. Diffusion of contaminants is less affected by this matrix characteristic, such that contaminants may migrate farther into unfractured low permeability formations than microbes..

As a consequence, in most published reports involving field sites in which low k units are present, the characterization of microbial communities and degradation processes is only performed for groundwater and sediment samples obtained from high permeability zones, i.e., sand and gravel (Van Stempvoort et al. 2009), and fracture spaces. However, many low k units have geological features, such as micro-fractures and sand lenses, which may enable cell growth and migration to distances greater than a few cm (Chambon *et al.* 2010).

4.3.2 Microbial Presence and Contaminant Biodegradation in Low k Units

In general, groundwater samples should not be expected to be representative of conditions within low k units because the water is almost certainly drawn from neighboring or internal permeable features, such as sand lenses or fractures (Cherry et al. 2006). Special effort is needed to acquire water from low permeability media, such as the completion of small vertical interval samplers (e.g. piezoemeters) directly within the lower k units. In addition, shallow low k units typically are assumed to contain fractures or other preferential pathways unless proven otherwise because features such as fractures and sand stringers are difficult to discern (Cherry et al. 2006). Consequently, in order to obtain an accurate characterization of microbial populations in unfractured sections of these units, cores must be used. For this reason, only studies where sediment or rock cores were collected are considered in the following discussion.

Investigations using sediment and rock cores have revealed the existence of microorganisms both at contaminated and uncontaminated sites (Colwell et al. 1997; Coolen and Overmann 1988; Lawrence et al. 2000; Lima et al. 2012b; Takeuchi et al. 2009; Takeuchi et al. 2011; Van Stempvoort et al. 2009); **Table 4.1** provides details on sample types, frequency, and analyses performed in these studies. In two cases (Coolen and Overmann 1988; Takeuchi *et al.* 2009), results indicated long-term preserved DNA

Table 4.1. Literature reports of microbial activities in low k matrices from sediment and rock core samples

Site	Samples and frequency	Analyses	Main findings
Western CO, USA (1) no contamination	Sandstone and shale intervals, 5 samples in a 6 m interval	Culture: Fe(III) and Mn(IV) reducers and DNA extraction	Culturable microbes in sandstone matrix at interface with shale
Mahoney Lake, BC, Canada (2) no contamination	Sediment core (6 m long): 10 samples from 0.4 to 4.6 m below lake bottom	DNA extracted, PCR, DGGE	Detected DNA of fossil origin, no microbial activity observed in sediments (sulfide gas production from NOM†)
Cretaceous clay, SK, Canada (3) no contamination	16 depth intervals sampled from ground surface to 122 m depth	Microscopy, FAME‡, microcosms, DNA extraction from cores and from isolates, PCR, cloning, DGGE	Microscopy: no visible cells. Microbial analyses resulted in low bacterial numbers within the clay sediments. Low permeability sediment bacteria survive geologic time periods.
Kanto plain, Japan (4) no contamination	3 sites, w 50 m core each, 1 sample each cored location (muddy sediment intervals)	Cell (live/dead) counts, molecular (DNA) and geochemical analyses	*Chloroflexi* and Crenarchaeotic Group predominant bacterial and archaeal libraries; lack of bioactivity suggests long-term preserved DNA; indigenous population of paleoenvironments.
Denmark (5) cVOC*	Core clay till, at increasing distances (cm scale) from hydrofractures	qPCR, CSIA in sediment samples	Hydrofracture bioaugmentation with KB-1® successful, but *Dehalococcoides* was also found within the clay till matrix
Yonezawa basin, Japan (6) no contamination	2 cores (sediment) ground surface to 3 and 10 m depth (PCE contamination) – 6 silt and/or clay lenses 1 to 2 samples each	qPCR, cVOC, H_2-bacteria, pore sizes, hydraulic conductivity, bacterial and reductive dehalogenase diversities, enrichments	First study to show that dechlorinating bacteria grows in aquitards. *Dehalococcoides* in higher numbers in organic-rich clay and silt layers than in aquifer.
Florence, SC, USA (7) cVOC	2 sediment cores, 1 to 5 cm sampling interval (DNA and cVOC concentration profile)	DNA-based molecular analyses, CSIA in sediment samples, hydrochemistry	16S rRNA fragments of dechlorinating bacteria found in clay aquitard; CSIA showed strong isotope fractionation into the clay aquitard underlying the aquifer.
Cottage Groove, WI, USA (8) cVOC	98 m deep rock core, discrete sampling, 68 samples for DNA, 250 samples cVOC	DNA-based molecular analyses, cVOC profiles, hydrochemistry, pore sizes	16S rRNA gene fragments *Dehalococcoides* and other dechlorinators associated with detected dechlorination in sandstone matrix samples.

Notes:
(1) (Colwell *et al.* 1997)
(2) (Coolen and Overmann 1988) - † NOM – natural organic matter
(3) (Lawrence et al. 2000) ‡ Fatty acids methyl ester profiles
(4) (Takeuchi et al. 2009)
(5) (Chambon et al. 2010; Damgaard et al. 2012; Scheutz et al. 2010) - * cVOC – chlorinated volatile organic chemicals
(6) (Takeuchi et al. 2011)
(7) (Lima et al. 2012b)
(8) (Lima et al. 2012a)

in Holocene lake sediments reflecting indigenous population associated with paleoenvironments, while the other studies revealed modern, active microbial communities associated with the use of naturally occurring nutrients and/or observed contaminant biodegradation. Some indication has also been found that in low k sediments, such as clay aquitards, bacteria may survive for extremely long (i.e. geologic) time periods, in communities that are extremely slow growing and occur in low numbers, likely exerting little geochemical impact (Lawrence *et al.* 2000).

Aquitard-aquifer interfaces are reactive zones in which the aquitard may serve as source of fatty acids, organic matter, electron donors (i.e. H_2), and electron acceptors for growth of microorganisms at either side of the interface (Krumholz et al. 1997; McMahon 2001; McMahon and Chapelle 1991; Van Stempvoort et al. 2009). Ongoing microbial fermentation within organic carbon rich aquitards may supply acetate and formate for microbial growth in aquifers that are generally poor in both dissolved and sedimentary organic carbon (McMahon and Chapelle 1991). This process has been observed in both consolidated and unconsolidated aquitard-aquifer sequences (Krumholz *et al.* 1997; McMahon and Chapelle 1991; Takeuchi *et al.* 2009). However, there is evidence that consolidated aquitards, such as shales, have much more reduced microbial activity compared to unconsolidated clay aquitards (Krumholz *et al.* 1997).

Evidence that microorganisms responsible for contaminant degradation can grow inside the pores of clay units has been found both in laboratory and field studies (Lima *et al.* 2012b; Lima and Sleep 2007; Scheutz *et al.* 2010; Takeuchi *et al.* 2011). Under laboratory conditions, Lima and Sleep (2007) simulated conditions at an aquifer/aquitard interface in two compacted clay-sand columns in which carbon tetrachloride biodegradation was ongoing The two clays were from natural sources, one was a till from the Halton region of Ontario, Canada, and the second from the city of Rio de Janeiro, Brazil. Significant numbers of microbial 16S rDNA gene copies were found only within a restricted region of the clays, 1-3 cm of the interface (with the sand), indicating limited migration of microbial cells from the sand (source of microbial cells) into the low k zones.

However, a few field studies have demonstrated the presence of biodegrading microbial communities deeper within the matrix of low k zones. Most of these studies were in unconsolidated sediments (Chambon *et al.* 2010; Damgaard *et al.* 2012; Scheutz *et al.* 2010; Takeuchi *et al.* 2011; Van Stempvoort *et al.* 2009) while one involved fractured sandstone (Lima *et al.* 2012b). In the first case, sulfate- and iron-reducing bacteria within a fractured clay aquitard were responsible for hydrocarbon biodegradation via utilization of short chain fatty acids that accumulated in the aquitard (Van Stempvoort et al. 2009). In the second study, large populations of *Dehalococcoides* and H_2-producing bacteria were found in an organic-rich clayey aquitard, rather than in the neighboring aquifer (Takeuchi *et al.* 2011). In that work, vinyl chloride reductase genes were detected only in the clay layer, confirming the results of the incubation experiments, which indicated that only the clay sediment could sustain transformations of tetrachloroethene to vinyl chloride. This finding had important implications for the role of natural attenuation at the site, and for the use of the adjacent aquifer as a supply source for carbon or other electron donors (Takeuchi *et al.* 2011). In a third case, successful bioaugmentation of a hydrofractured till contaminated with chlorinated ethenes was achieved through the injection of a consotium of KB-1®, capable of driving dechlorination transformations, into the hydrofractures (Chambon *et al.* 2010). Sediment cores obtained from the treated

area demonstrated that, even though the dechlorinating microbes grew preferentially within the hydraulically fractured spaces, it was also possible to detect *Dehalococcoides* cells, and evidence that they were active, within the unfractured matrix (Damgaard *et al.* 2012). Lastly, in a study of a fractured sedimentary rock site contaminated with a mixture of VOCs, the presence of dechlorinating microorganisms within a low permeability sandstone was reported (Lima *et al.* 2012b). The majority of the contaminant mass occurred in the dissolved and sorbed phases.

In all of the above studies, microorganisms, such as *Dehalococcoides,* were observed not only within the most porous sections of the subsurface, but well inside geological materials with low permeabilities – i.e., 10's of centimeters or more from an interface with a high permeability zone (Lima *et al.* 2012a; Lima *et al.* 2012b; Scheutz *et al.* 2010; Takeuchi *et al.* 2011). Microbial numbers were admittedly relatively low, as were the growth rates. Nevertheless, the impact these microbial communities exerted on the distribution of contaminants may have been considerable. Therefore, these populations are likely to play an important role in contaminant natural attenuation, to control rates of back diffusion, and to influence the longevity of plumes sustained by back-diffusion.

4.3.3 Methodologies for Assessing Degradation in Low k Zones

Several lines of evidence can be used to assess whether degradation (biotic or abiotic) is occurring, but these are generally focused on aquifers, not aquitards. For example, Wiedemeier et al. (1999) discuss general lines of evidence for evaluating natural attenuation, but the challenge remains to adapt these methods for the assessment of degradation in aquitards. Contaminant transport in low k zones is diffusion limited and relevant processes occur over small spatial scales, meaning that it is necessary to apply tools for these assessments at very fine spatial resolution. Since sampling of groundwater in low k zones presents challenges and issues, methods should primarily focus on use of high quality sediment or rock cores collected across the aquifer-aquitard interfaces and into the low k zones, with high-frequency sub-sampling of these cores on the order of 10's of centimeters or less.

Examples of lines of evidence that can be used to support contaminant degradation in low k zones include the following:

1. ***Distribution of parent compounds and degradation products.*** Patterns favoring low k zone degradation include: i) higher ratios of degradation products occurring in low k zones away from the aquitard-aquifer interface, especially relative to those observed in adjacent transmissive zones; and ii) lower penetration of contaminants into low k zones compared to expectations, based on diffusion and sorption processes without transformations. Note that obtaining a representative contaminant distribution requires high resolution sampling across interfaces and into low k zones as well as appropriate extraction and analytical techniques (to ensure that mass is accurately quantified).

2. ***Analytical data showing favorable geochemical and redox conditions.*** Conditions within the low k zone should be conducive to the targeted degradation reaction. Positive indicators for biotransformations include the following:

a. presence of electron donors (e.g., natural organic carbon) or electron acceptors (dissolved oxygen, nitrate, sulfate) that can be used as redox indicators or serve as lines of evidence for microbial degradation;
b. reduced mineral species (e.g., ferrous iron) than may promote abiotic reactions;
c. presence of metabolic by-products indicative of degradation (e.g., methane);
d. elevated H_2 concentrations that would support reductive dechlorination.

Note that establishing geochemical conditions within lower permeability zones can be challenging given that groundwater sampling is problematic in such zones.

3. ***Microbiological data supporting presence of appropriate microbial communities in the low k zones.*** Typically, these efforts involve microbial characterization of core samples using nucleic acid-based tools (e.g., qPCR). Depth-specific subsamples can be analyzed to identify and quantify genetic signatures associated with various dechlorinating microbial species (e.g., *Dehalococcoides*) or functional genes (e.g., vinyl chloride reductase). The presence of these biomarkers within lower permeability zones is taken as a positive indicator of the potential for microbial activity resulting in dechlorination of contaminants. Microcosm studies can also be used to provide supporting evidence of degradation in low k zones, but these are likely to have restricted application due to the time and expense involved in completing them. Further drawbacks to microcosms are that they rarely reproduce the *in situ* conditions (and heterogeneity) of the sediments they contain, and the rates of degradation they produce are either too slow to measure in reasonable time frames or compare poorly to field rates.

4. ***Compound specific isotope analyses (CSIA).*** Greater shifts in isotopic ratios are expected in lower permeability zones and/or across interfaces when degradation is occurring (see Section 4.3.4 for a more detailed discussion).

5. ***Contaminant distributions that match modeled distributions affected by simulated degradation.*** This can include 1-D modeling showing lower contaminant penetration observed in low k zones than expected based on diffusion and sorption processes without transformations, or more detailed 2-D numerical modeling to compare observed and predicted contaminant distributions.

4.3.4 Application of Compound-Specific Isotope Analyses (CSIA)

Compound specific isotope analyses can be a powerful tool for establishing degradation patterns at sites with low k zones. Through CSIA, shifts in isotopic signatures (typically carbon) due to contaminant degradation are determined. These shifts happen during organic contaminant degradation, where bonds with the lighter carbon isotopes (^{12}C) are broken preferentially over bonds with the heavier isotope (^{13}C). As a consequence, parent compounds become ^{13}C-enriched and the reaction products become ^{13}C-

depleted. In theory, CSIA can establish if the degradation processes are biotic or abiotic, assuming that the extent of degradation is sufficient to estimate the isotopic enrichment factor. However, distinguishing between biotic and abiotic degradation mechanisms may be difficult in low k zones where (presumably) slow degradation rates would be a limiting factor. A more practical application is the use of isotopic data in parallel with data generated from molecular biological tools to provide evidence to support either biotic or abiotic degradation as the dominant mechanism.

There are at least two studies that have used CSIA in parallel with nucleic acid-based molecular tools to characterize biodegradation in low k zones:

- At a study site in Denmark, sediment cores were taken 4 years after hydraulic fracturing of clayey till contaminated with TCE with concomitant injection of KB-1 into the fracture spaces was performed (Chambon *et al.* 2010; Damgaard *et al.* 2012; Scheutz *et al.* 2010). In the plume region, it was observed that $\delta^{13}C$ for cis-DCE varied from -3 to -10‰, less than the value for the parent TCE (~-24‰), indicating TCE degradation to cis-DCE likely occurring within the clay matrix (Damgaard *et al.* 2012). Molecular analyses of sediment DNA confirmed the presence of *Dehalococcoides* species from KB-1 and of *vcrA*, a dehalogenase gene responsible for vinyl chloride biodegradation.
- At a study site in Florence, South Carolina, carbon tetrachloride (CT), chloroform (CF), tetrachloroethene (PCE), TCE, dichloromethane (DCM), and cis-DCE were all attenuated within the first several centimeters into the matrix of an aquitard underlying an aquifer impacted by a mixed DNAPL source (Lima *et al.* 2012a). Biodegradation was confirmed as the primary attenuation mechanism by the application of molecular tools that detected a dechlorinating community, which included members of the genus *Dehalococcoides,* and by isotope signatures that showed strong enrichments of all parent compounds relative to potential transformation products within the low permeability matrix (Lima *et al.* 2012a). In that study, biodegradation was further confirmed by accumulation of daughter products and of chloride within the low k unit.

4.3.5 Example Datasets from Field Sites

To illustrate the methodologies of evaluating contaminant degradation in low k zones, the following unpublished case studies are provided, including data from the study at NAS Jacksonville that was funded by ESTCP ER-201032 with partial support from SERDP ER-1740 (i.e., the project that supported the creation of this report). These examples cover cases where degradation in low k zone degradation was strongly supported, cases where degradation in low k zones could not be unequivocally established, and cases where no degradation in low k zones was apparent. Lines of evidence refer to those described in Section 4.3.3.

STRONG Evidence of Degradation in Low Permeability Zones

Site Location: Florence, South Carolina *(Site information to be reported in upcoming journal article).*

LIMITED Evidence of Degradation in Low Permeability Zones

Site Location: Building 106 Source Area, OU3, NAS Jacksonville, Jacksonville, Florida

Conceptual Model: Former dry cleaning operation released primarily PCE to a sandy transmissive zone underlain by a clay-rich aquitard. Source strength remained relatively high in the transmissive zone but significant contaminant mass became stored in low k zone based on high-resolution characterization completed at several locations near and downgradient of the source area.

*Lines of Evidence (**Figure 4-9**)*

Contaminant Profile: Near the source zone, the parent compounds (PCE and TCE) in soil and groundwater samples generally represented > 80% of contaminant mass within the low k zones. The concentration ratio of metabolites (primarily cis-DCE) to parents increased in samples from overlying transmissive zone, particularly at shallow depths. The degree of dechlorination increased significantly moving downgradient, where DCE was the dominant compound and the highest concentrations were present near the interface. At the farthest downgradient location, the ratio of metabolites to parents was relatively similar in both the high and low K zones. Dechlorination beyond DCE was relatively limited based on soil data, although groundwater sampling established that VC, ethene and ethane were produced in significant amounts, particularly at the farthest downgradient location where the VC concentration exceeded that of the parent compounds.

Geochemical Data in Transmissive Zone: Groundwater sampling established that conditions were generally reducing within the downgradient transmissive zone plume, with low DO (< 2 mg/L), negative ORP, and little sulfate, iron, or nitrate. Nearer the source, conditions were more oxidizing (typically 4 to 6 mg/L DO). Groundwater was generally more acidic than desirable, with samples frequently less than pH 6. Based on field parameters, similar conditions were encountered in both the low k and high k zones at most locations. Methane concentrations were generally between 0.1 and 1 mg/L; high k zones consistently had higher levels of methane than were measured in lower k zones. Significant organic carbon (median f_{oc} = 0.002) was measured in the clayey soils.

Microbiological Data: At two locations were molecular analyses were completed, *Dehalococcoides* was detected in 2 of 6 soil samples from transmissive zones and 2 of 12 samples from low k zones. However, inhibition during qPCR analyses occurred due to an unidentified factor in the soil (i.e., DNA was extracted but not amplifiable), meaning that there was a high probability for false positives. In those samples that were positive for *Dehalococcoides*, concentrations were relatively low (on the order of 10^4/gram) with slightly higher levels generally associated with the more transmissive soils. All samples that were positive for *Dehalococcoides* were also positive for the *vcrA* gene, such that complete dechlorination pathway to ethene exists at the site.

LIMITED Evidence of Degradation in Low Permeability Zones (continued)

Site Location: Building 106 Source Area, OU3, NAS Jacksonville, Jacksonville, Florida *(continued)*

CSIA Data: Parent compounds were generally more enriched in ^{13}C in the transmissive zones relative to low k zones, suggesting that degradation was more prevalent in the high k zones. By-products (cis-DCE and VC) were generally more depleted in ^{13}C relative to parent compounds at all depths. For all compounds, a ^{13}C enrichment pattern was observed moving from the source to downgradient locations, confirming that significant degradation was occurring and contributing to the observed decrease in concentration along the flow path.

Complications: Groundwater contaminant concentrations, isotope and geochemical data within (and near) lower permeability intervals were collected using temporary piezometers with 2 to 3.5-ft screens. As a result, data represent most transmissive subzones within those screened intervals and may not be representative of conditions within the lowest permeability soils. As evidence of this representivity problem, groundwater CVOC data collected are slightly different than soil CVOC data at some depths. Chloride was not diagnostic due to high background concentrations within the low K clays.

Conclusions: Several lines of evidence suggest that degradation may be occurring in the low k zones (particularly downgradient), but the activity is almost certainly less than that of the adjacent transmissive zones (based on the Lines of Evidence 4 and 6, isotope and concentration distributions). The detection of significant amounts of by-products in the low k zones (along with geochemical conditions that are generally favorable for dechlorination) is strong evidence supporting degradation, but understanding the relative contribution of degradation within the low k zones vs. diffusion of mass into these low K zones could not be fully assessed with the available data.

Other Sites with Similar Patterns: Cocoa, Florida Site (Parker et al., 2003; Parker et al., 2008); Connecticut Site (Parker et al., 2004; Chapman and Parker, 2005, Chapman et al., 2007)

LIMITED Evidence of Degradation in Low Permeability Zones (continued)

Site Location: Building 106 Source Area, OU3, NAS Jacksonville, Jacksonville, Florida *(continued)*

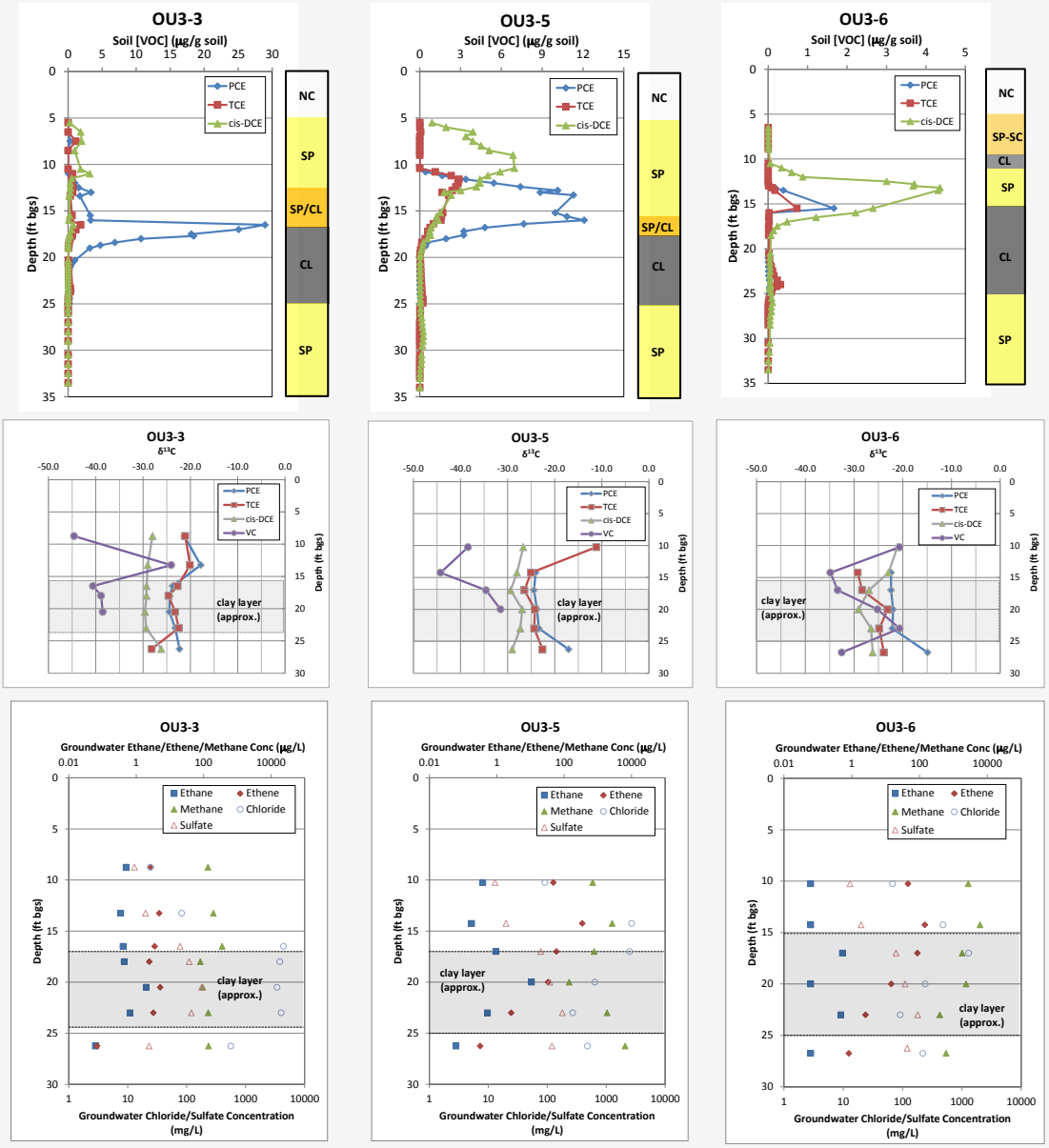

Figure 4.9. Selected data from investigation at Building 106 source area at OU3 at NAS Jacksonville showing limited evidence of degradation in low k zone. Soil concentration, isotope, and geochemical data shown for four locations starting near the source and moving downgradient (left to right panels). Extent of degradation increases at downgradient locations, along with presence of higher concentrations of reductive dechlorination products (including ethene) and methane in low k interval. Isotope data suggest that parent compounds are more enriched in ^{13}C (i.e., less degraded) in low k interval relative to higher k zones. Other soil and groundwater data collected (including geochemical, microbiological, and groundwater CVOC concentration) but not shown.

NO EVIDENCE of Degradation in Low Permeability Zones

Site Location: CS-10 Plume, Massachusetts Military Reservation (MMR), Cape Cod, Massachusetts

Conceptual Model: Several releases of chlorinated solvents (primarily PCE and TCE) have led to a large (> 3 miles) and dilute (typically low 10's of μg/L) plume within a thick sandy transmissive zone containing a discontinuous silt layer(s) at depths starting below approximately 170 ft bgs. High-resolution site characterization established that significant contaminant mass is present in the lower permeability silts, and if these zones are laterally extensive, they may influence the remediation timeframe associated with on-going pump-and-treat operations.

*Lines of Evidence (**Figure 4.10**)*

Contaminant Profile: Parent compounds in soil samples represented greater than 99% of contaminant mass at all depths, including samples from both higher and lower permeability zones. No dechlorination products were detected beyond DCE isomers.

Geochemical Data: Conditions were relatively oxidizing based on groundwater sampling, with significant dissolved oxygen (4 to 6 mg/L) that was similar regardless of the permeability of the sediment. Slightly lower ORP in lower permeability silts (50 mV) relative to overlying sands (100 mv). The fraction of organic carbon was typically below detection limits. There was no evidence for reactive iron species, although mineralogical tests were not completed.

Modeling: 1-D and 2-D numerical modeling without degradation were able to match observed contaminant profiles.

Complications: Depth to lower permeability intervals was significant, resulting in significant cost per datapoint. Collection of cores from transmissive zones was challenging due to flowing sands and gravity drainage at these depths.

Conclusions: No apparent degradation in low k zones could be discerned based on the available data. Patterns within low k zones consistent with lack of degradation observed in site-wide groundwater monitoring data from transmissive zones.

Other Sites with Similar Patterns: F.E. Warren AFB (Appendix A); Kitchener, Ontario).

NO EVIDENCE of Degradation in Low Permeability Zones (continued)

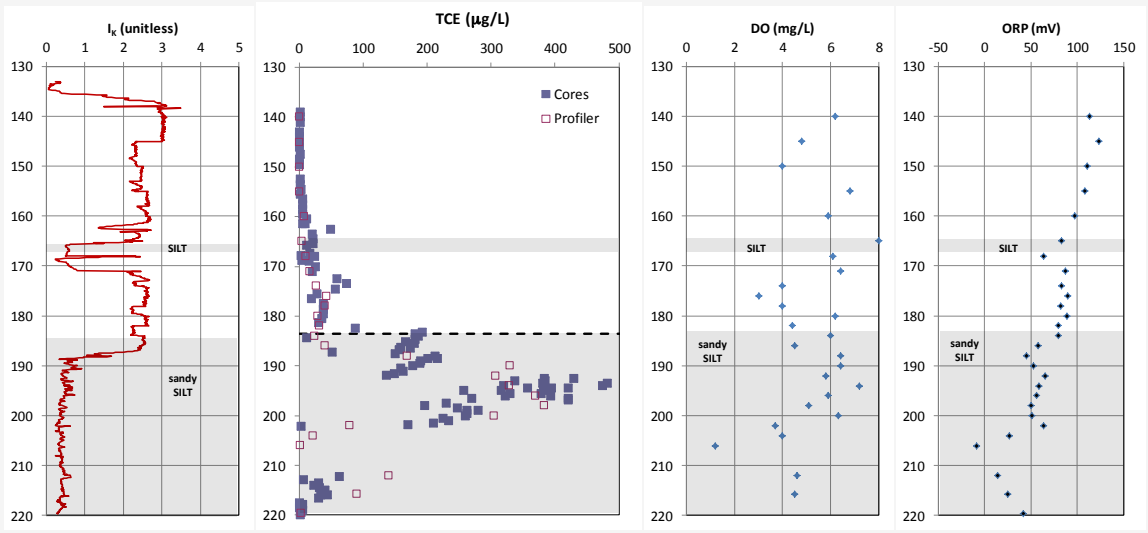

Figure 4.10. Selected data from investigation at CS-10 plume at MMR showing no apparent degradation in low k zone. Only TCE was present in significant amounts, and geochemical conditions are generally unfavorable for biological reductive dechlorination (high DO/ORP).

4.4 CHAPTER 4 TRANSPORT – KEY RESEARCH PROGRAMS

Laboratory Programs

- Diffusion experiments using soil from F.E. Warren AFB Wyoming (Appendix C)

Field Programs:

- Degradation analysis of chlorinated solvents in Low k units, Naval Air Station Jacksonville

Literature Survey

- Studies of degradation in Low k Units

Datasets

- Diffusion data using soil from F.E. Warren AFB Wyoming and Dead End Column Method

Procedures/Protocols

- Improved method for measuring effective diffusion coefficients in porous media using Dead End Column Method
- Example of high resolution field program to evaluate degradation in low k units

OVERVIEW OF CHAPTER 5:
TYPE SITE SIMULATIONS

- Three different numerical groundwater transport models (HydroGeoSphere, FEFLOW, and MODFLOW) were able to match exact analytical solutions and matrix diffusion research tank experiments.
- But the temporal and spatial discretization must be very fine. Simulating a 1.1 by 0.84 meter tank experiment, required ~10,000 grid cells in MODFLOW/MT3D. A complex random layer scenario with a 500 by 10 meter domain required ~3,000,000 nodes in HydroGeoSphere.
- Therefore our conventional approach of modeling an entire site may not be possible if we wish to accurately simulate matrix diffusion processes with conventional transport models. To circumvent this problem, we developed the following "**Type Site"** simulations that illustrate in the "style" of a site, the general concentration vs. time pattern over the life of site, which is presented in a series of figures:
- **Parallel Fractures Type Site** (Figures 5-9 through 5-12). Key observation: Sandstone and siltstone shale Type Sites had more matrix diffusion tailing than granite Type Sites. Degradation in matrix is very important both for longevity of the plume and for the distance the plume travels.

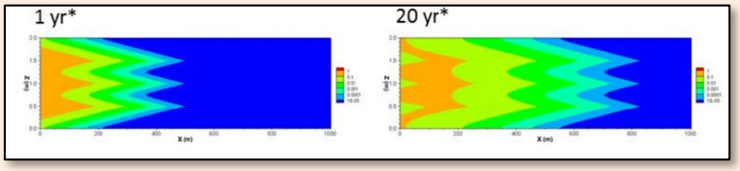

- **Fracture Network Type Site** (Figures 5-14 through 5-15). Key observation: Long-term persistence of the plume occurs after the source is completely removed, due to slow back diffusion of mass stored in the rock matrix. Degradation in matrix is very important.

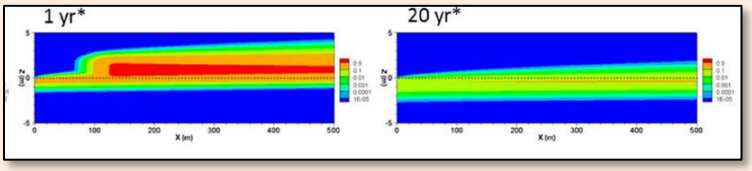

- **Two Layer Sand/Clay Type Site** (Figures 5-14 through 5-22). Key observation: Long-term persistence for many decades at consequential concentration levels following source removal for no degradation case. Higher clay layer sorption increases the storage capacity and leads to longer-term tailing at higher concentration levels and for longer durations. Degradation in the clay reduces the total mass stored in the low K zone and hence can significantly reduce back diffusion effects.
- **Multi-Layer Sand/Clay Type Site** (Figures 5-27 through 5-32). Key observation: Similar trends as the two-layer case but with stronger tailing effects due to the greater sand-clay contact surface area.
- **Random Clay Layer Type Site** (Figures 5-27 through 5-32). Key observation: even thin clay layers can cause appreciable tailing for decades, while the thicker aquitard, or a thicker clay layer(s), can cause tailing for much longer periods.

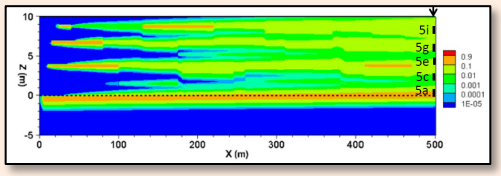

Key Words: Type Site, modeling, HydroGeoSphere, MODFLOW, MT3D, siltstone, granite, sandstone, clay, sand, tailing, diffusion, sorption, degradation.

5.0 TYPE SITE SIMULATIONS

5.1 OVERVIEW

Lead Authors for This Chapter

Steve Chapman and Beth Parker, University of Guelph

Two primary goals of the numerical modeling described in this chapter are:

1. **Test / validate** numerical modeling techniques that can be used to predict the presence and impact of contaminants in low k zones; and
2. Develop a **set of "Type Site" scenarios** representing a range of site conditions that can be used by practitioners and regulators who are managing real sites to help build intuition on low K zone effects and aid in development of site conceptual models.

The first goal, to demonstrate the ability of numerical models to capture diffusion / back diffusion processes, was advanced by comparisons with analytical solutions. This work shows that available numerical models, when adequately discretized spatially and temporally, can accurately solve problems involving diffusive fluxes into and out of lower permeability zones. The comparisons include:

1. **Two-layer analytical solution** of Sale et al. (2008) (results published in supporting information of Chapman et al. (2012) and summarized here);
2. **Analytical solution for parallel fractures** of Sudicky and Frind (1982) (results presented here)

Further testing to show that the governing processes can be incorporated in numerical simulations was advanced by numerical modeling of datasets from well-controlled laboratory experiments:

1. **Sand tank back diffusion / visualization experiment** (CSU Thesis of L. Doner, 2008) (results published in Chapman et al. (2012) and summarized here)
2. **Multilayered tank experiments** conducted at CSU including sorption / degradation reactions (results provided in report "AFCEE source zone initiative" by Sale et al., 2007)

The second goal, to apply modeling tools to demonstrate effects of mass storage and release for "type site" conditions was accomplished via a series of hypothetical simulations conducted for different scenarios expected to be representative of conditions at real sites, including both porous media and fractured rock scenarios. Sensitivity analyses were performed within some of the scenarios to show sensitivity to key parameters, primarily sorption within the lower permeability zones which has the effect of increasing contaminant storage capacity in these zones, and exacerbate back diffusion rates and timeframes, and degradation in the lower permeability zones, which removes contaminant mass from the lower permeability zones, and may reduce the magnitude and longevity of back diffusion.

5.2 TWO-LAYER ANALYTICAL SOLUTION FOR POROUS MEDIA

What was done

- **Why**: Determine if three numerical groundwater models can match an analytical solution?
- **Hydrogeologic Settings**: Unconsolidated setting; transmissive zone overlying a low k zone.
- **Three Numerical Models**: HydroGeoSphere, FEFLOW and MODFLOW/MT3D
- **Analytical Model:** Two-layer solution for matrix diffusion of Sale et al. (2008)
- **Model Domain:** 100 meters in X direction and 2 meters in Z (1 meter thick aquifer overlying 1 meter thick aquitard).
- **Key Processes:** matrix diffusion, sorption, degradation in low k unit.
- **Time Domain:** Case 1: Source loading 500 days; release from low k zone out to 1500 days. Case 2: Source loading 5 years; release from low k zone out to 20 years.
- **What Happened:** Numerical models matched well, but required very fine temporal and spatial discretization.

Thumbnail description of key figures and tables

Figure 5.1: Numerical vs. Analytical solution, Z vs. X plots, three times, two values of R

Figure 5.2: Model domain and grid used

Figure 5.3: Results for Case 2a (no sorption), two layer scenario, Z vs. X plots, 5 times

Figure 5.4: Results of numerical and analytical models, 4 Concentration vs. time plots

Three codes, HydroGeoSphere, FEFLOW and MODFLOW are tested in their ability to simulate results from the two-layer analytical solution of Sale et al. (2008) representing a larger field-scale scenario with a sand aquifer containing an analog DNAPL source perched on an underlying silt layer. Sensitivity analyses on grid spacing are included to provide some guidance for applying these models to accurately capture the governing processes; however an exhaustive evaluation is outside the scope of this paper. This scenario is similar to conditions at the Connecticut site investigated by Chapman and Parker (2005) and simulated using HydroGeoSphere.

The analytical solution assumes uniform media properties within the layers and incorporates advection, transverse dispersion, adsorption and degradation in the transmissive zones; and diffusion, adsorption, and degradation in the underlying low k layer. The analytical solution assumes linear reversible sorption, and degradation via first-order decay allowing different rates in each layer. Simplifying assumptions include:

1) infinite domain in the sand and silt;
2) silt hydraulic conductivity sufficiently low that solute transport occurs solely by diffusion;
3) horizontal transport in sand dominated by advection such that longitudinal dispersion can be neglected; and
4) first-order kinetics for degradation in sand and silt.

The DNAPL source is analogous to a condition with a thin DNAPL layer perched on the aquitard interface at the upgradient boundary, with a concentration representing aqueous solubility at the interface (Co) exponentially decaying with distance above the interface according to $C=C_oe^{-by}$ where b (1/m) is a source distribution coefficient and y is distance above the interface. In numerical simulations this is accommodated using specified concentration nodes generated using this function. The source is active for a specified period of time and then is instantaneously removed to initiate the back diffusion phase (i.e. representing complete source removal, isolation or remediation). Benchmarking numerical models versus results from an analytical solution is an excellent means to test their applicability to simulate such problems and assess whether adequate spatial and temporal discretization is applied, which then allows numerical models to be applied with more confidence to more complex scenarios more representative of actual site conditions.

First the HydroGeoSphere code was used for simulation of the two scenarios shown in Figure 7 of Sale et al. (2008) referred to here as Case 1, which involves a cross-section with a 100 m long domain and source duration of 1000 days. **Table 5-1** summarizes the parameters used and analytical solution results are plotted in the left side of **Figure 5-1.** Longitudinal dispersion is included in the numerical simulations, which slightly affects the comparison since this is process is neglected in the analytical solution.

Two scenarios are examined, the first with no sorption (**Case 1a**: $R_{sand}=R_{silt}=1$) and then with sorption included in both the aquifer and aquitard (**Case 1b**: $R_{sand}=3$, $R_{silt}=15$). No degradation is allowed in either scenario. The grid dimensions were 100 m in X and 2 m in Z (1 m thick aquifer overlying 1 m thick aquitard). The larger Z-domain used for the numerical simulations avoids boundary effects by ensuring the plume does not reach the upper or lower boundary during the simulation period, consistent with infinite domain assumption in the analytical solution, but is truncated for comparison purposes (analytical solution results only plotted for 0.5 m thick aquifer overlying 0.5 m thick aquitard). The finite element grid uses hexahedral blocks with spacing of 0.2 m in X (NX=501) and 0.01 m in Z (NZ=201) with default unit thickness in Y (NY=2) for a total of 100,000 elements and 201,402 nodes. The fine grid discretization in Z was applied to resolve diffusion into and out of the silt and transverse (vertical) dispersion in the aquifer. Adaptive time-stepping was applied with a maximum allowable time step imposed of 1 day.

Table 5-1: Input parameters for simulation of Sale et al. (2008) analytical solution scenarios

Parameter	Symbol	Case 1	Case 2	Units
Flow Properties				
aquifer hydraulic conductivity	$K_{aquifer}$	7.8E-05	1.08E-04	m/s
aquitard hydraulic conductivity	$K_{aquitard}$	1.0E-10	1.0E-10	m/s
aquifer porosity	$\phi_{aquifer}$	0.25	0.30	-
aquitard porosity	$\phi_{aquitard}$	0.40	0.40	-
average horizontal hydraulic gradient	i_h	0.01	0.01	-
Source Conditions				
source concentration at interface	C_o	240	1 (normalized)	mg/L
source distribution coefficient	b	15	10	1/m
source duration	T	1000	1825	days
Contaminant Transport				
free-solution diffusion coefficient	D_o	9.4E-10	9.4E-10	m^2/s
aquifer tortuosity	$\tau_{aquifer}$	0.40	0.25	-
aquitard tortuosity	$\tau_{aquitard}$	0.585	0.16	-
Effective diffusion coefficient (aquitard)	D*	5.5E-10	1.5E-10	m^2/s
aquifer retardation factor	$R_{aquifer}$	1.0 (a), 3.0 (b)	1.0 (a,b,d), 5.0 (c)	-
aquitard retardation factor	$R_{aquitard}$	1.0 (a), 15.0 (b)	1.0 (a,d), 10.0 (b,c)	-
aquifer degradation rate	$\lambda_{aquifer}$	0	0.023 (a,b,c), 0.23 (d)	1/yr
aquitard degradation rate	$\lambda_{aquitard}$	0	0.023 (a,b,c), 0.23 (d)	1/yr
longitudinal dispersivity	α_L	0.20	0.50	m
transverse vertical dispersivity	α_{tv}	0.0014	0.001	m

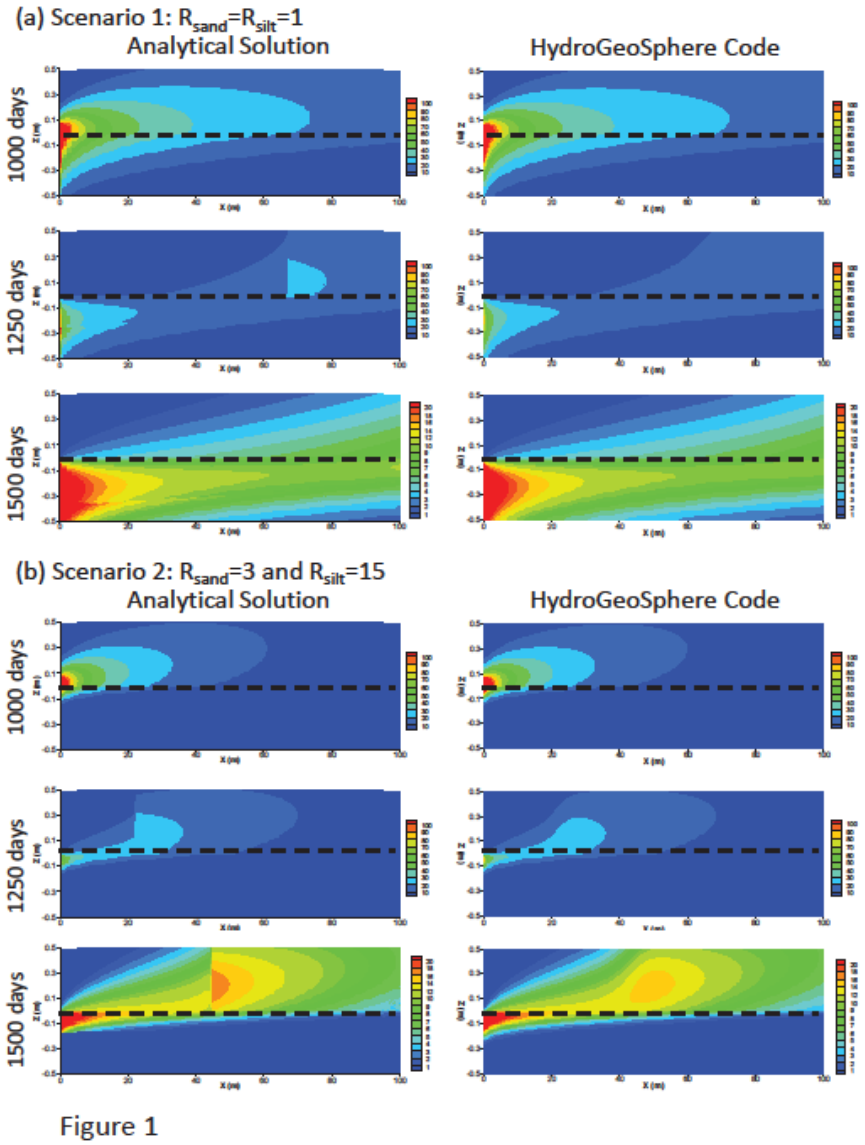

Figure 5-1. Comparison of numerical simulation results using HydroGeoSphere with two-layer analytical solution showing concentration contours at 1000 days when the source is removed and then at 1250 and 1500 days (250 and 500 days after source removal) for (a) Case 1a (R_{sand}=R_{silt}=1), and (b) Case 1b (R_{sand}=3, R_{silt}=15).

Then all three numerical models were used for simulation of selected scenarios in Figure 8 of Sale et al. (2008), referred to as Case 2. The domain (Figure 2a) involves a cross-section with a length of 100 m. For numerical simulations, the aquifer and aquitard thicknesses were 3 m which is large enough to avoid boundary effects (i.e. so plume remains within the aquifer vertical extent and does not diffuse out the base of the

aquitard within the simulation period). **Table 1** summarizes parameters used in the analytical and numerical simulations. The scenarios examined involve differences in sorption and/or degradation rates: the first three scenarios have different sorption (Case 2a: R_{sand}=R_{silt}=1; Case 2b: R_{sand}=1, R_{silt}=10; Case 2c: R_{sand}=5, R_{silt}=10) and slow degradation ($t_{1/2}$=30 yr) in both the aquifer and aquitard, while the fourth scenario has a higher degradation rate ($t_{1/2}$= 3 yr) and no sorption (Case 2d). All four scenarios were simulated using HydroGeoSphere, and Case 2a was also simulated using FEFLOW and MODFLOW/MT3DMS to show these models can produce similar results. The source is on for 5 years, which is still very short compared with source conditions at most contaminated sites where releases occurred decades ago. In numerical simulations the source is applied via specified concentration nodes generated using the exponential decay function with distance above the interface, and at 5 years the source is completely removed allowing clean water (C_o=0) to flush the upgradient boundary.

Results in **Figure 5-2** are presented as concentrations in hypothetical wells with 3 m long screens above the interface at 1, 10 and 100 m downgradient of the source (Figure 2a). Concentrations in numerical simulations represent flux-averaged values based on the simulated nodal concentrations and Darcy flux over the hypothetical well-screen interval. HydroGeoSphere allows direct output of such flux-averaged concentrations for specified well positions at each time step, facilitating generation of breakthrough and elution curves. For FEFLOW and MODFLOW/MT3DMS it was necessary to extract concentrations and flux over the nodes or elements spanning the hypothetical well-screen interval, and then calculate flux averaged concentrations separate within a spreadsheet. For HydroGeoSphere, hexahedral blocks were used for the finite element grid. For the base case a uniform grid spacing of 0.5 m in X (NX=201), variable spacing in Z from 0.02 to 0.10 m (NZ=96) with refinement proximate to the interface (Figure 2b), and default unit thickness in Y (NY=2) were applied, for a total of 19,000 elements. Adaptive time-stepping was applied based on concentration changes with an initial time step of 0.01 days and maximum allowable time step of 1 day. Sensitivity to grid discretization was examined for the no sorption scenario, first using a refined grid with 0.2 m spacing in X and variable spacing from 0.01 to 0.05 m in Z for a total of 102,500 elements, and then for coarser grids, first with a 1.0 m spacing in X and 0.05 to 0.20 m spacing in Z for a total of 5500 elements, and then an even coarser grid with a 2.0 m spacing in X and 0.10 to 0.50 m spacing in Z for a total of 1300 elements (Figure 2b). Finer discretization in the aquitard would likely be required for scenarios with sorption to adequately resolve the smaller diffusive penetration and sharper concentration gradients. For FEFLOW a mesh was generated using the transport mapping option, which allows use of quadrilateral elements, applying a mesh anisotropy ratio of 10 to provide a finer mesh vertically to accurately capture transverse dispersion in the aquifer and diffusion processes in the aquitard. Uniform element sizes were applied of 1.0 m in X and 0.10 m in Z so the grid contained 8000 elements. For MODFLOW/MT3DMS, a grid comprised of 200 columns in X (uniform 0.5 m spacing) and 40 layers in Z (0.1 m spacing within 1 m of the interface in both the aquifer and aquitard and 0.2 m outside this zone). Maximum time steps of 1 day were imposed and the TVD scheme was used for the transport solution in MT3DMS.

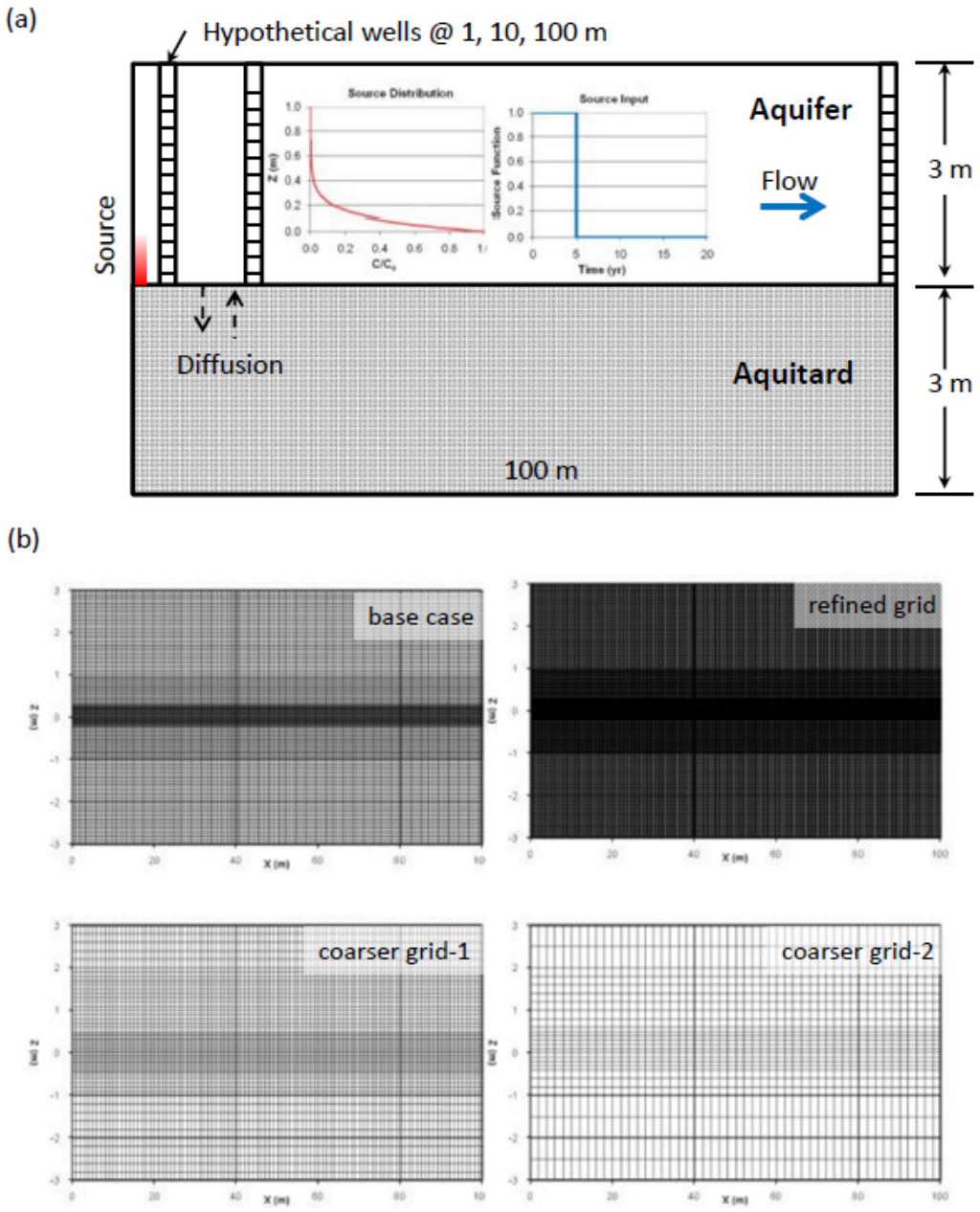

Figure 5-2. Domain and conditions for comparison of numerical and two layer analytical solution (Case 2): (a) source conditions and hypothetical well positions; and (b) grid used in base case HydroGeoSphere simulations along with refined and coarser grids used in sensitivity analyses.

For the scenario with sorption (Case 1b) the plots show aqueous concentrations, while Sale et al. (2008) plot total concentrations, calculated as the product of aqueous concentration, porosity and retardation factor. Additional contour intervals are plotted for comparison purposes. The results are plotted at 1000 days (time of source removal) and then at 1250 and 1500 days (250 and 500 days after source removal, respectively). Minor localized errors are evident in the analytical solution results, which do not affect the overall comparison. In these scenarios the travel time in the aquifer through the 100 m long domain is about 370 days (groundwater velocity of 0.27 m/day) so for the Case 1a scenario with no sorption (**Figure 5-1a**) the plume in the aquifer at 1500 days is sustained entirely from back diffusion from the silt. For the Case 1b scenario with sorption (**Figure 5-1b**) flushing of plume mass from the original analog DNAPL source is still evident at 1500 days. The numerical solution results are nearly identical to the analytical solution, with minor differences attributed to inclusion of longitudinal dispersion in the numerical simulations. This comparison confirms the numerical model, when adequately discretized spatially and temporally, can capture the transport and diffusion processes.

Figure 5-3 shows contour plots for the Case 2a scenario with no sorption and 30-yr half-life using HydroGeoSphere at 2 and 5 years when the source is active, and then at 10, 15 and 20 years (5, 10 and 15 years after source removal). Positions of hypothetical monitoring wells used for the comparison with the analytical solution results are also shown. The aquifer travel time through the 100 m domain is just under one year with a 0.31 m/day groundwater velocity. Simulation results show a persistent plume remains at the base of the aquifer even 15 years after source removal, but with the majority of mass occurring in the aquitard. These conditions are comparable to those examined by Chapman and Parker (2005) where concentrations in an aquifer and underlying aquitard were delineated using high resolution techniques in a plume several years after the DNAPL source zone was isolated.

Numerical and analytical solution results representing concentrations in 3 m long wells are compared in **Figure 5-4** for the four scenarios, as relative concentrations plotted on a log scale over a 6 order of magnitude (OoM) range. Minor differences are expected due to longitudinal dispersion in the numerical simulations, which is not required in the analytical solution. Also in numerical simulations a small value was assumed for vertical transverse dispersivity (α_{tv} =0.001 m); while an even lower value (α_{tv}=1E-6 m) is needed to match the transverse dispersion coefficient (D_t) used in the analytical solution.

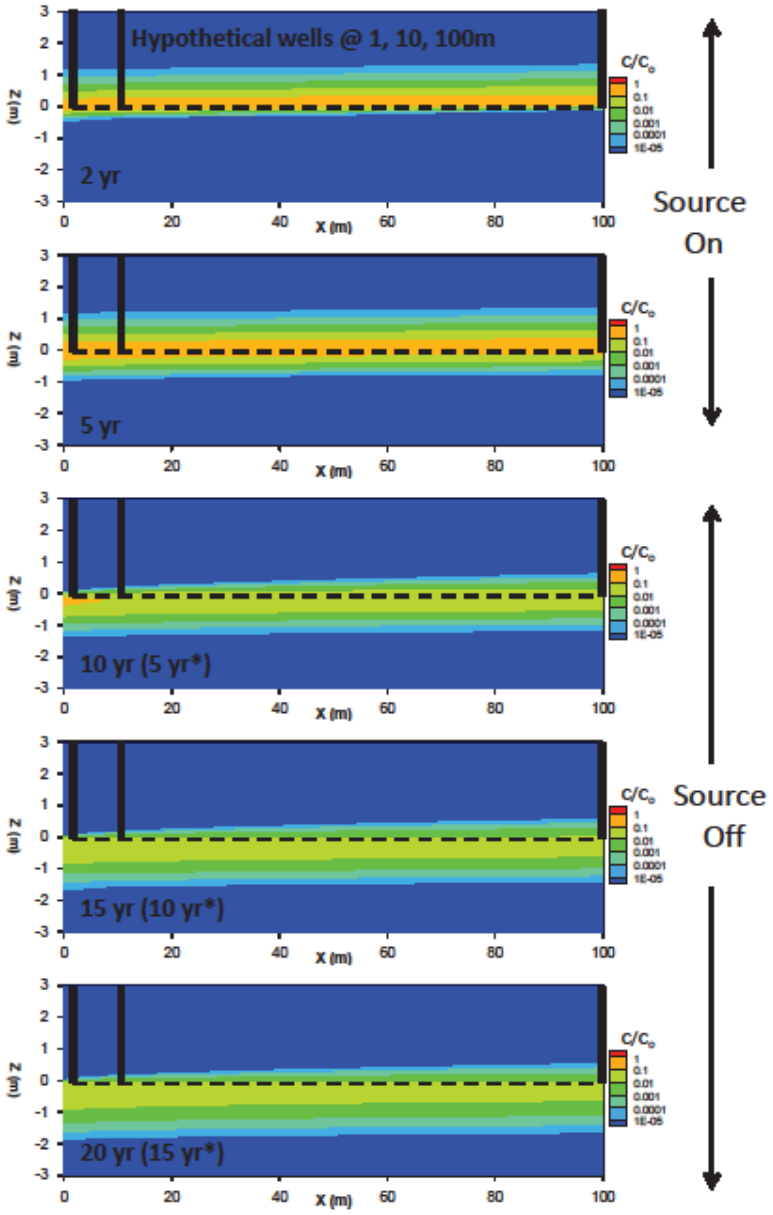

Figure 5-3. Contaminant contours for Case 2a (no sorption) at 2 and 5 years while the source was on, and then at 10, 15 and 20 years (5, 10 and 15 years after source removal). Positions of hypothetical well screens are also shown.

However, testing with HydroGeoSphere showed little difference in the results using such a low value, suggesting the α_{tv} =0.001 m value is sufficiently low to not impact the comparison. Klenk and Grathwohl (2002) provide a summary of laboratory and field-derived values for vertical transverse dispersivity, supporting use of such low values. In general, simulations of back diffusion effects are expected to be sensitive to transverse vertical dispersion, which controls vertical spreading in the aquifer and consequently concentrations at the aquifer-aquitard interface, which in turn controls rates of diffusion

into and out of the aquitard and concentrations that would be encountered in monitoring wells.

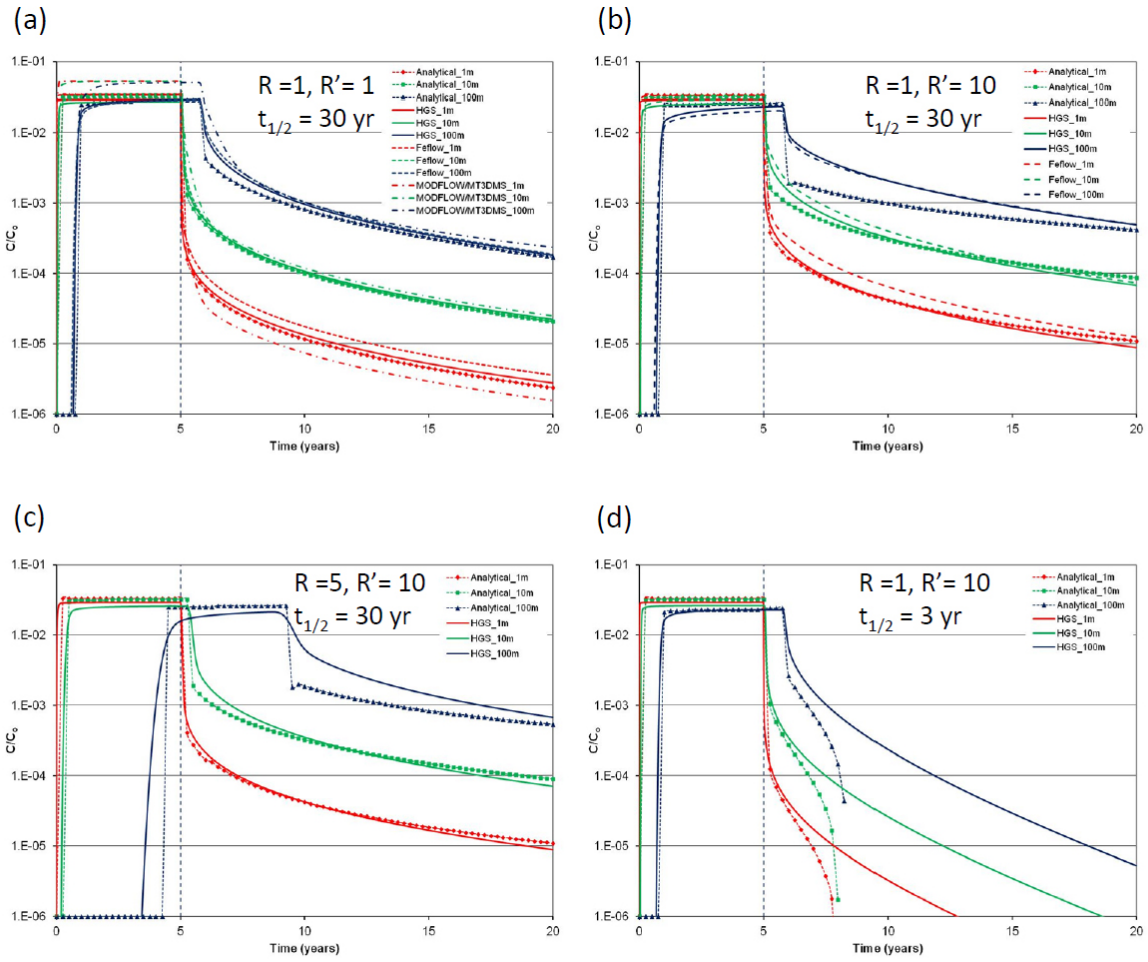

Figure 5-4. Comparison of numerical simulations with two-layer analytical solution showing normalized concentrations in wells 1, 10 and 100 m downgradient with 3 m long screens: (a) Case 2a: no sorption (R_{sand}=R_{silt}=1) and slow degradation (30 year half-life), (b) Case 2b: sorption in silt only (Rs_{and}=1, R_{silt}=10) with same degradation rate, (c) Case 2c: sorption in both sand and silt (R_{sand}=5, R_{silt}=10) with same degradation rate, and (d) Case 2d: sorption in silt only (R_{sand}=1, R_{silt}=10) but with faster degradation (3 year half-life).

Overall HydroGeoSphere results compare well with the analytical solution. For the scenario with no sorption and slow degradation (**Figure 5-4a**) results are very close between the analytical and numerical solutions, with minor differences likely attributed mainly to including dispersion in the numerical simulation. Based on the simulated plume distribution for this scenario (**Figure 5-3**), the concentrations in wells screened over the full 3 m aquifer thickness are expected to be much lower than those at the base of the aquifer. Results for the scenarios with sorption included in the aquitard (**Figure 5-4b**) and in both the aquifer and aquitard (not shown) also compare reasonably well but with minor discrepancy, particularly at the downgradient well, again likely due mainly to dispersion. However the numerical solution still captures the longer-term tailing trends

quite well. For the scenario with more rapid degradation (3-yr half-life) and no sorption (**Figure 5-4d**) the comparison is not as good with the numerical simulation indicating longer-term tailing. Reasons for this discrepancy are not clear, but it appears this is a problem within the analytical solution as it seems unlikely that concentrations would decline so rapidly with what is still a relatively slow degradation rate. Sensitivity to grid discretization was examined using a refined grid and then two coarser grids compared to the base case (**Figure 5-2b**). The HydroGeoSphere simulation using a refined grid provided essentially the same results as the base case, indicating adequate base case discretization was used to capture the diffusion processes. A simulation using a coarser grid also provided similar results, while a simulation with an even coarser grid still compared reasonably well but with minor differences, indicating borderline discretization to accurately capture the diffusion processes. Finer discretization in the aquitard would be required for scenarios including sorption to adequately resolve the smaller diffusive penetration distances and higher concentration gradients. FEFLOW and MODFLOW/MT3DMS produced similar results as HydroGeoSphere (**Figure 5-4a and 5-4b**) confirming ability of these codes to handle this scenario. Refinement of the grids may improve the comparison even more. The larger discrepancy for MODFLOW/MT3DMS may be attributed to the different discretization scheme (block-centered grid) which affects the source distribution and how flux-averaged well concentrations are apportioned.

WHAT HAPPENED: Overall, this exercise confirms that the three numerical models employing different solution schemes can provide a close match with the analytical solution results when adequate spatial and temporal discretization are applied.

5.3 FRACTURED MEDIA TYPE SITE MODELING

5.3.1 Parallel Fracture Type Site Scenarios

What was done

- **Why**: Determine if a numerical groundwater models can match an analytical solution. If so, develop Type Sites for parallel fracture settings.
- **Hydrogeologic Settings**: Fractured rock (sandstone, high sorption siltstone/shale, and granite) with parallel fractures.
- **Numerical Model**: HydroGeoSphere
- **Analytical Model:** CRAFLUSH model (Sudicky and Frind (1982)
- **Model Domain:** 1000 meters in X direction and 2 meters in Z direction. Three parallel fractures along X direction with a uniform 150 micron aperture and fracture spacing of 0.5 m.
- **Key Processes:** Matrix diffusion, sorption, degradation in fractures, degradation in low k unit.
- **Time Domain:** Source loading 10 years; release from low k zone out to 100 years.
- **What Happened:** The HydroGeoSphere model and analytical solutions show good agreement. Three Type Site Plots are provided. For the granite Type Setting there is also much lower tailing following source removal compared to the other matrix types, although still appreciable concentrations occur after several decades. With degradation half-life of 5 years in the sandstone setting, the plume front never reaches the X=1000 m boundary, and by 50 years the plume front is receding and maximum concentrations along the fracture are nearly 4 orders or magnitude below the initial source concentration

Thumbnail description of key figures and tables

Figure 5.5: Model domain and grid used

Figure 5.6: 12 Z vs. X plots for sandstone matrix, no degradation, finite source

Figure 5.7: Concentration vs. time plots for analytical model, curves for various X values

Figure 5.8: Concentration vs. time plots for numerical model, curves for various X values (this is compared to Figure 5-7)

Figure 5-9: *Concentration vs. X Type Site plots for sandstone, siltstone/shale, granite*

Figure 5-10: Concentration vs. time Type Site plots for sandstone, siltstone/shale, granite

Figure 5-11: *Concentration vs. X Type Site plots for sandstone with and without degradation*

Figure 5-12: *Concentration vs. time Type Site plots for sandstone with and without degradation*

This section describes how well a numerical model, HydroGeoSphere, compared to an analytical model for fractured groundwater systems affected by matrix diffusion processes. **Figure 5-5** shows the model domain for comparison of the analytical solution for parallel fractures (CRAFLUSH) of Sudicky and Frind (1982) with numerical simulation results using HydroGeoSphere. For this scenario, parallel fractures with a uniform 150 micron aperture and fracture spacing of 0.5 m was used. Fracture hydraulic conductivity can be estimated using:

$$K_f = \frac{\rho g (2b)^2}{12\mu}$$

where (2b) is the fracture aperture, ρ is water density, μ is water viscosity and g is the gravity constant.

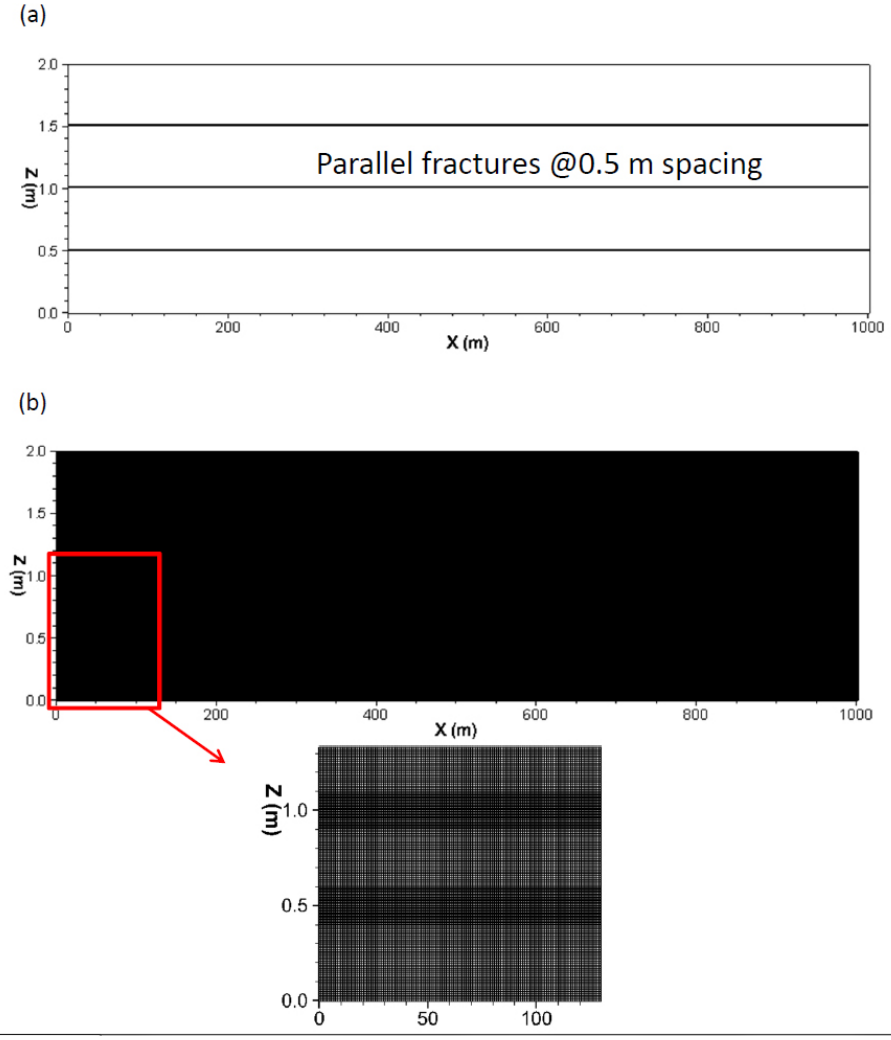

Figure 5-5. (a) Model domain for parallel fracture simulations; and (b) grid discretization for HydroGeoSphere simulations.

Then the groundwater velocity in the fractures can be estimated using:

$$v_f = \frac{K_f\, i}{\phi_f}$$

where i is the hydraulic gradient and ϕ_f is fracture porosity (=1 for open fractures). With hydraulic gradient of 0.5% groundwater velocity in the fractures is about 2900 m/year. So for this scenario, in the absence of matrix transfer and neglecting dispersion in the fracture plane, a solute would travel through the 1000 m domain in about 0.35 years.

First simulations were conducted applying matrix properties typical of a sandstone (ϕ_m=10%, R_m=2.0). No degradation is allowed in either the fractures or matrix. Solute parameters are consistent with TCE as the contaminant. Very fine grid discretization is applied for the numerical solution (**Figure 5-5b**) in HydroGeoSphere to accurately capture diffusion into the matrix. A uniform grid spacing of 0.5 m in the X-direction, and variable spacing of 0.01 m and refined to 0.005 m within 0.10 m of the fractures was used in the Z-direction. Weatherill et al. (2008) provides more guidance on grid discretization for this type of scenario. The domain is unit thickness in the Y-direction. Adaptive time-stepping was applied with an initial time step of 1e-5 years, maximum nodal change of 1% of the source concentration and maximum time step of 0.05 years. Simulations were conducted for two source conditions, first with a constant source and then for a finite source case assuming the source is constant for 10 years and then completely removed.

Figure 5-6 shows concentration contours for the HydroGeoSphere results for the finite source case. With the smaller domain size used, the boundaries are expected to have some effect on the results since contaminants can diffuse out of the top and bottom boundaries but effects on the middle fracture, where comparisons with the analytical solution will be made, should be relatively minor. **Figure 5-7a** shows breakthrough curves using CRAFLUSH along the fracture at different distances for a constant source plotted over a 5 OoM range. Despite the rapid groundwater velocity, matrix diffusion causes strong plume front attenuation, with the plume front (at $C/C_o=10^{-5}$) requiring over 20 years to reach the boundary at 1000 m. Figure **5-7b** shows breakthrough curves for the finite source scenario. This scenario is handled via superposition in the analytical solution (e.g. the solution at 50 years with a 10 year source is solved by subtracting the solution results at 40 years with a constant source from the solution at 50 years with a constant source). Results show the long term tailing effects from back diffusion of mass stored in the matrix to the fractures. Within these timeframes (i.e. 100 years) there is only minor impact of removing the source at X=200 m and negligible effect at the further downgradient locations at X=500 m and 1000 m.

These scenarios were then simulated using HydroGeoSphere to show the numerical model can match the analytical solution. Breakthrough curves for the HydroGeoSphere simulation results are plotted in **Figure 5-8** for comparison with the analytical solution. This shows the numerical model at this level of discretization can accurately match the analytical solution. Minor discrepancy is observed for the further downgradient locations and at later time, particularly at X=1000 m. This is attributed to mass loss in the numerical solution by diffusion out of the top / bottom of the domain and could be easily rectified by extending the domain such that the fractures being targeted are not affected by this mass loss. Otherwise numerical and analytical solutions show good agreement.

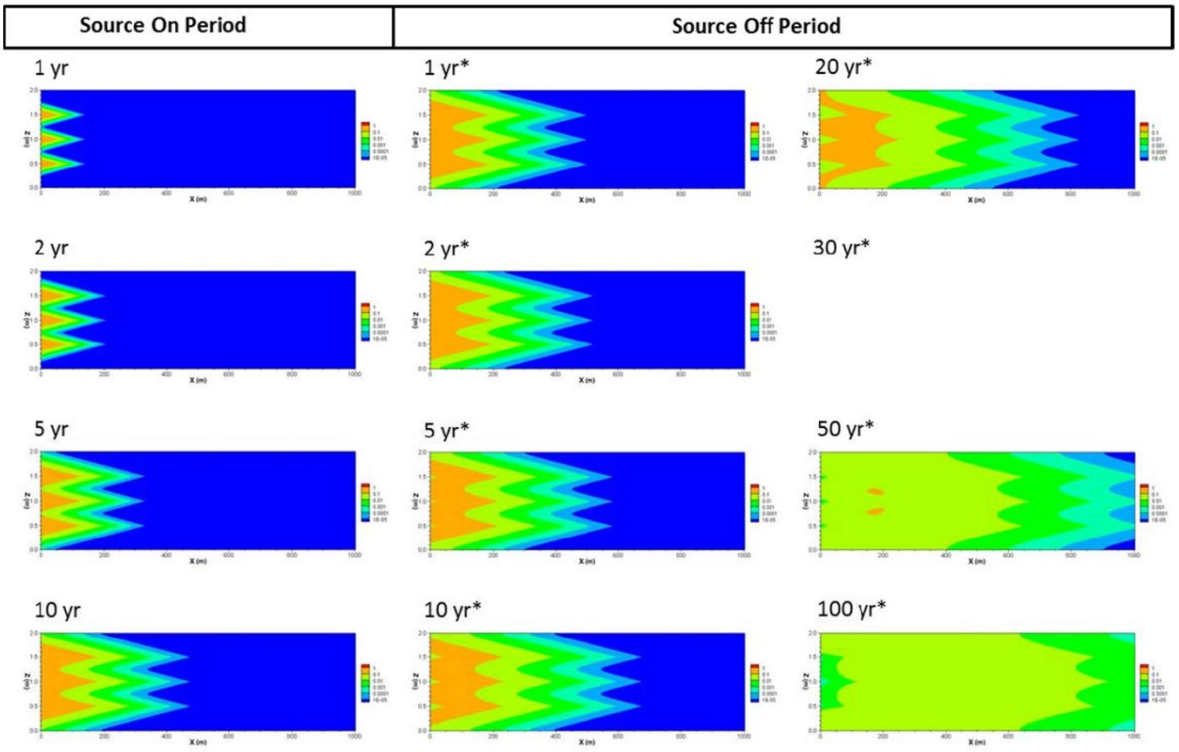

Figure 5-6. HydroGeoSphere simulation results for parallel fractures (150 micron aperture fractures, spacing=0.5 m, sandstone matrix, no degradation): plume distribution for finite source scenario.

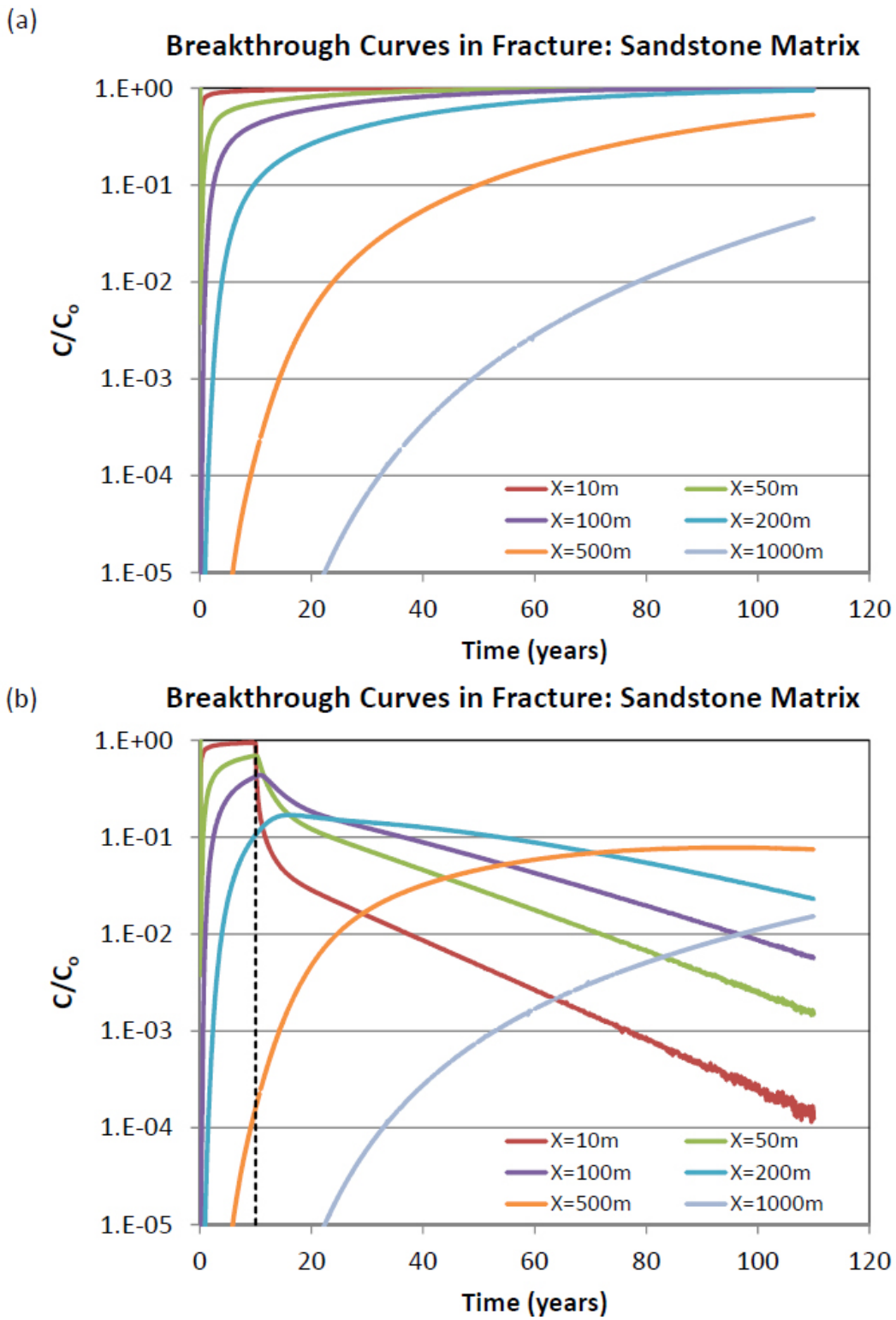

Figure 7. CRAFLUSH BTCs along fracture from (a) constant source, and (b) finite (10-yr) source. The finite source case was solved by superposition. This was compared to Figure 5-8.

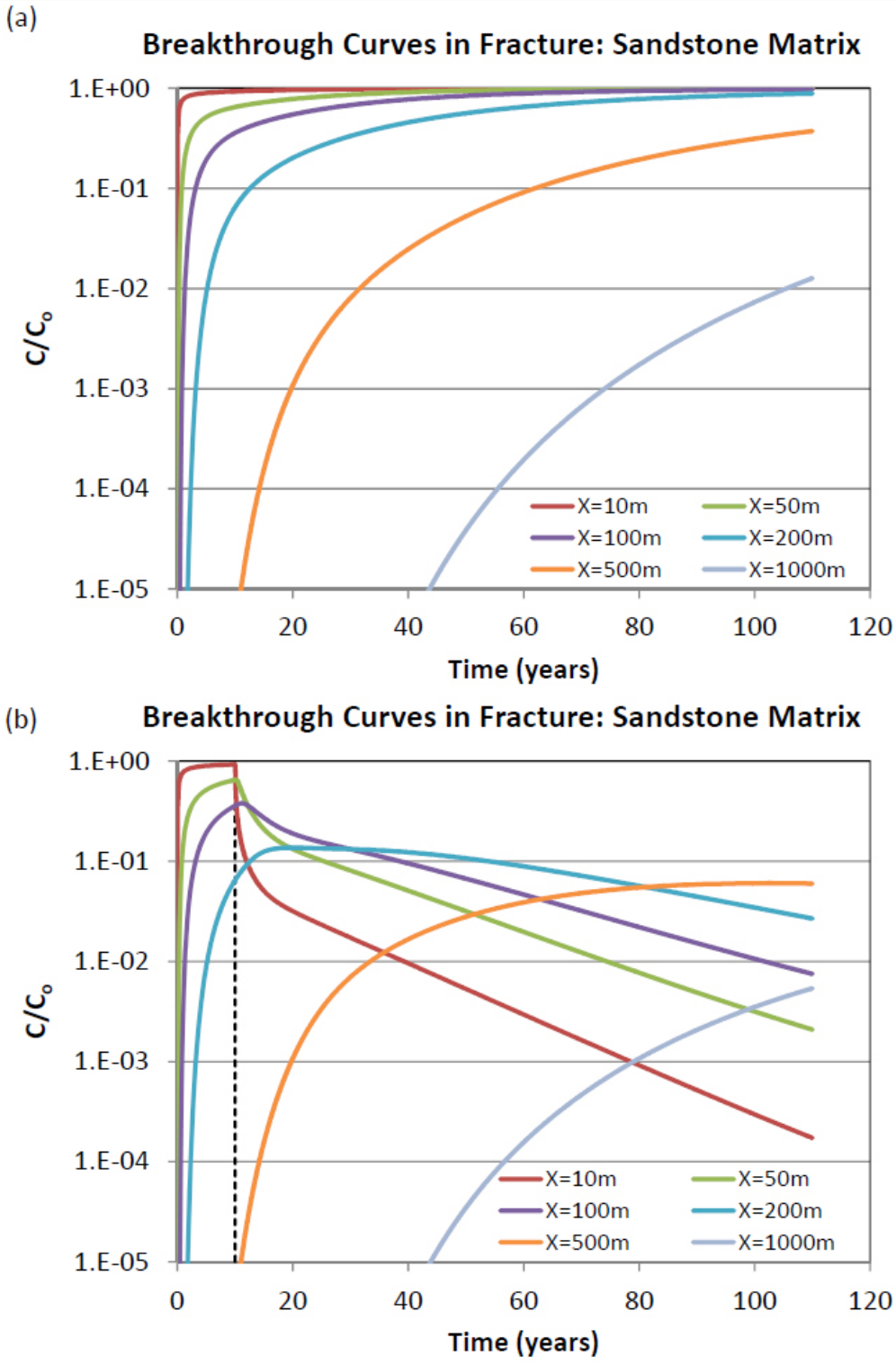

Figure 5-8. HydroGeoSphere BTCs along fracture from (a) constant source, and (b) finite (10-yr) source. This was compared to Figure 5-7.

Sensitivity analyses were performed for two additional matrix types for comparison with the sandstone type matrix (ϕ_m=10%, R_m=2), a high sorption siltstone/shale type matrix (ϕ_m=10%, R_m=10) and a low porosity, low sorption granite type matrix (ϕ_m=1%, R_m=1). For all cases tortuosity is assumed to be the same as porosity. **Figure 5-9** shows a comparison of profiles along the fracture and **Figure 5-10** shows a comparison of breakthrough curves with a 10 year source for all three matrix types. For the siltstone/shale matrix (**Figures 5-9b, 5-10b),** the rate of contaminant migration along the fracture is slower due to higher matrix sorption, which enhances the matrix storage capacity and increases the rate at which TCE diffuses into the matrix. This is evident from the delay in solute arrival (e.g. at X=200 m, the front taken at C/C_o-=10^{-5} arrives at about 10 years for the siltstone/shale case versus 2 years for the sandstone case; at X=500 m the arrival is about 55 years versus 11 years and at X=1000 m the solute does not reach the end of the domain at X=1000 m for the siltstone/shale matrix. Tailing following removal of the source after 10 years is also significantly higher (**Figure 5-10b**) compared to the sandstone case (Figure 10a). For the granite case (**Figures 5-9c, 5-10c)** the opposite is observed. The solute rapidly travels through the domain with little attenuation due to diffusion into the matrix and after 1 year concentrations exceeding C/C_o=0.5 occur throughout the fracture beyond 1000 m (**Figure 5-9c**). There is also much lower tailing following source removal compared to the other matrix types, although still appreciable concentrations occur after several decades.

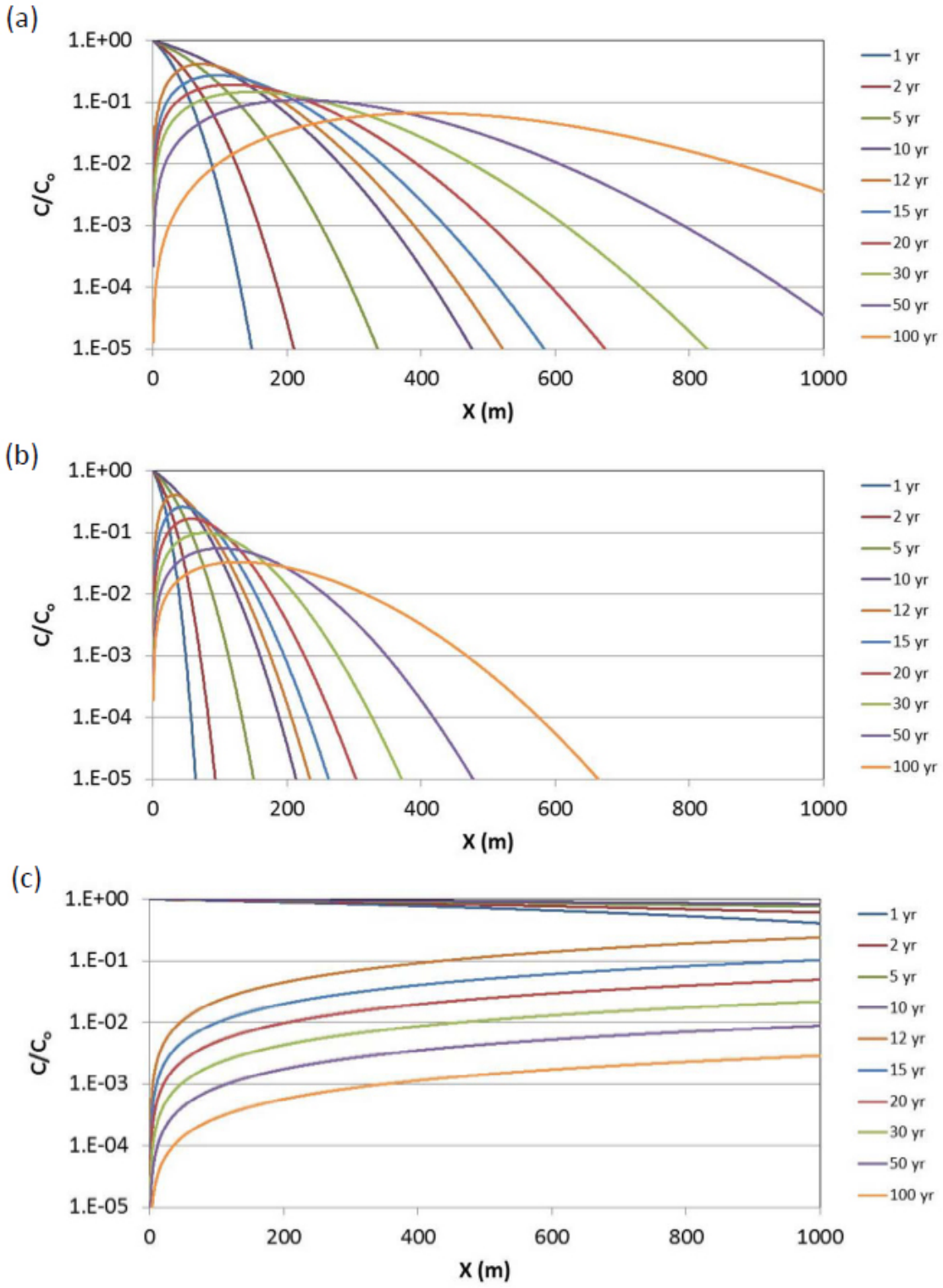

Figure 5-9: HydroGeoSphere profiles along fracture for three different matrix types: (a) sandstone, (b) siltstone/shale, and (c) granite.

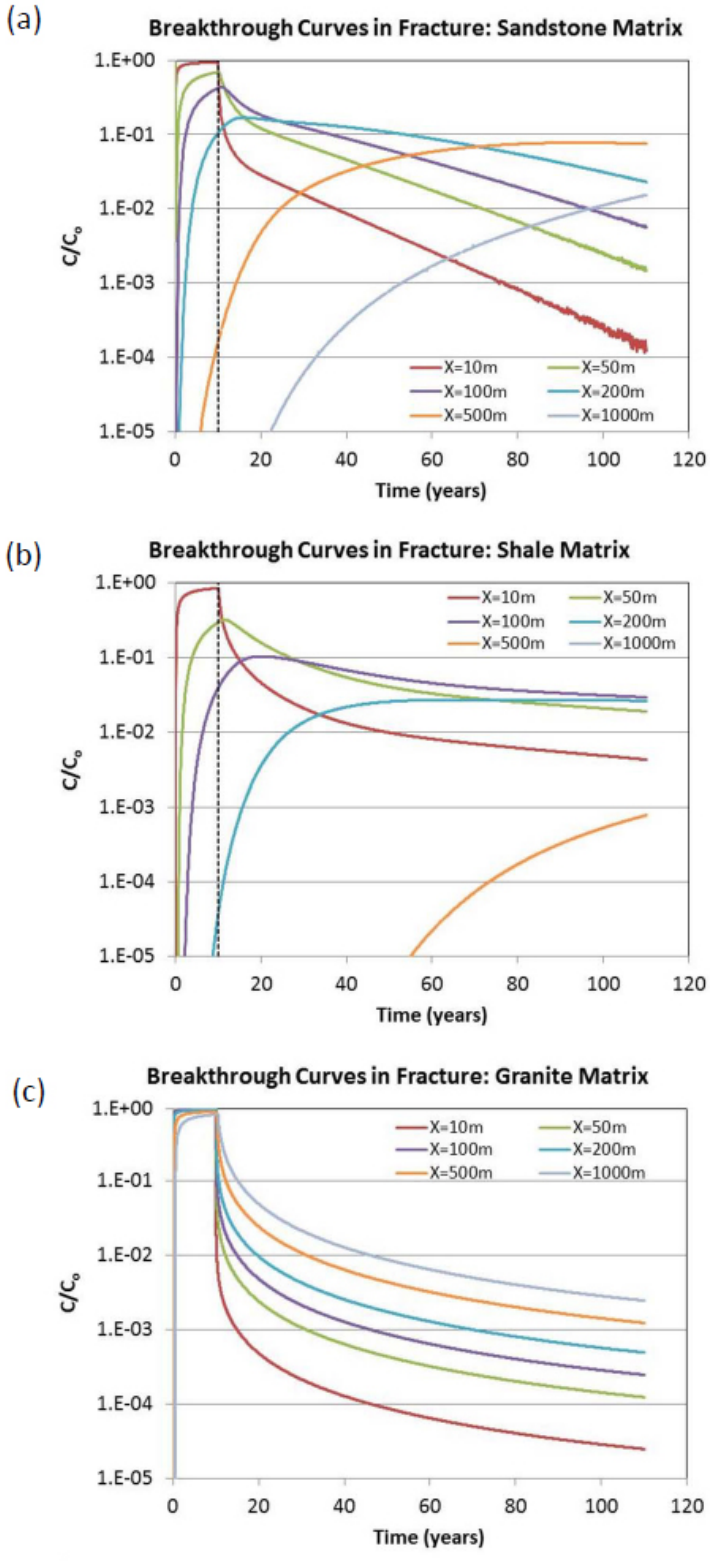

Figure 5-10. HydroGeoSphere BTCs along fracture for three different matrix types: (a) sandstone, (b) siltstone/shale, and (c) granite.

It is also recognized that abiotic and/or abiotic degradation may occur in the rock matrix (Darlington et al., 2009; Lima et al., 2012) which has potential to reduce tailing effects. To examine this, simulations were conducted for the sandstone case applying slow degradation, first allowing degradation only in fractures (half-life of 0.5 years), then allowing degradation in both the fractures (same half-life of 0.5 years) and matrix (slower half-life of 5 years). Figure 11 shows profiles along the fracture and Figure 12 shows breakthrough curves at different positions along the fracture for the three scenarios (no degradation, degradation in fracture only, degradation in both fractures and matrix). Degradation in the fractures only (Figures 11b, 12b) shows negligible difference with the no degradation case (Figures 11a, 12a). Intuitively this makes sense since nearly all of the contamination occurs in the matrix given diffusive transfer combined with the very low bulk fracture porosity (ϕ_f=3x10^{-4} in this case with 150 micron fractures spaced at 0.5 m) versus matrix porosity (0.10). However even slow rates of degradation in the matrix (Figures 11c,12c) has a large impact, producing much lower tailing following source removal. In this case with a half-life of 5 years, the plume front never reaches the X=1000 m boundary, and by 50 years the plume front is receding and maximum concentrations along the fracture are nearly 4 orders or magnitude below the initial source concentration (Figure 12c).

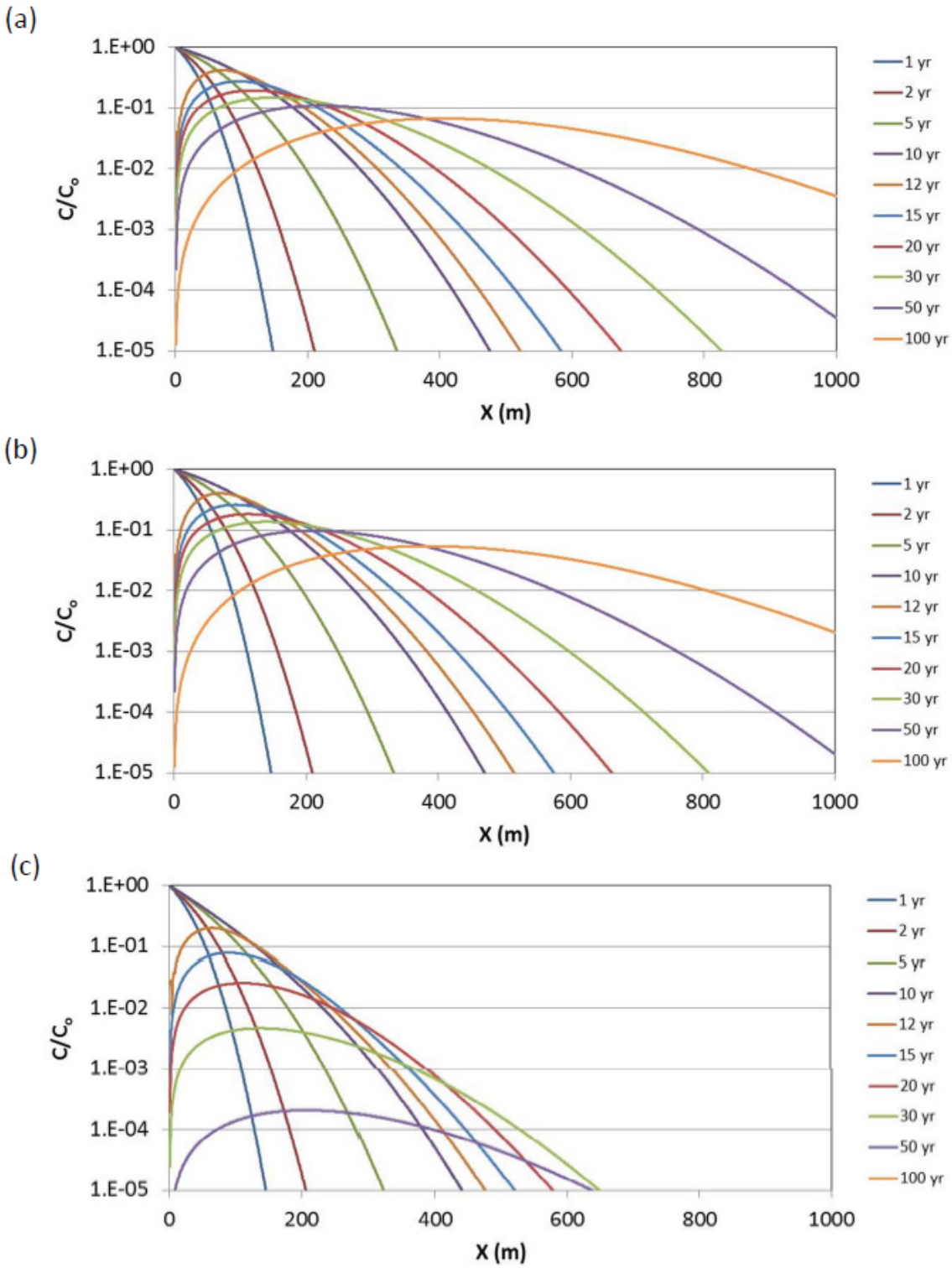

Figure 5-11: HydroGeoSphere profiles along fracture for sandstone case with (a) no degradation, (b) degradation in fractures only (t1/2=0.5 yr), and (c) degradation in fractures ($t_{1/2}$=0.5 yr.) and matrix ($t_{1/2}$=5 yr).

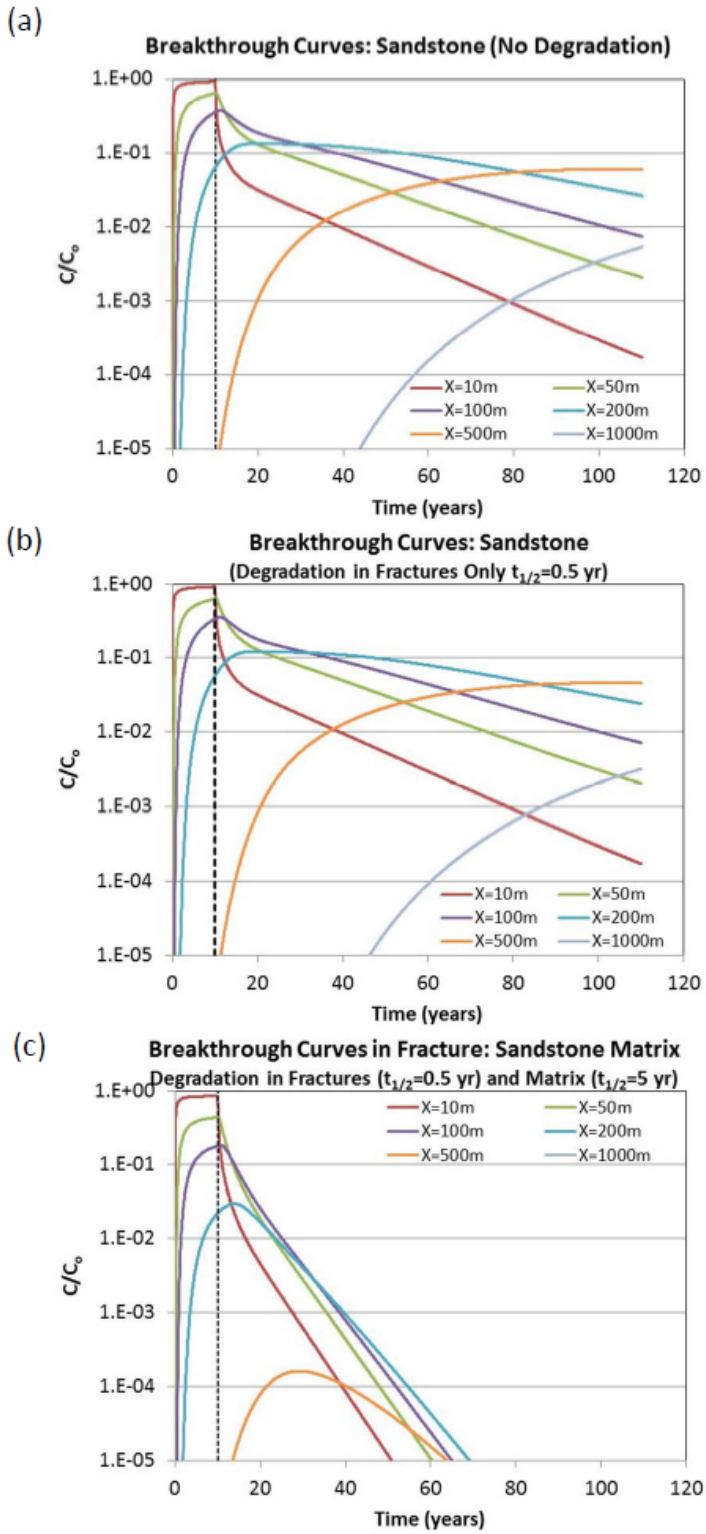

Figure 5-12. HydroGeoSphere BTCs along fracture for sandstone case with (a) no degradation, (b) degradation in fractures only ($t_{1/2}$=0.5 yr), and (c) degradation in fractures ($t_{1/2}$=0.5 yr.) and matrix (t1/2=5 yr).

5.3.2 Fracture Network Type Site Scenario

What was done

- **Why**: Develop type sites for fractured network scenarios.
- **Hydrogeologic Setting**: Complex fractured rock scenarios consisting of sandstone with 13% porosity.
- **Numerical Model**: FRACTRAN
- **Model Domain:** 1000 meters in X direction and 300 meters in Z direction. Fractures with log normal distribution, geomean of 100 microns.
- **Key Processes:** Matrix diffusion, degradation
- **Time Domain:** Source loading 20 years; release from low k zone out to 100 years.
- **What Happened:** Two Type Site plots are provided. Long-term persistence of the plume occurs after the source is completely removed, due to slow back diffusion of mass stored in the rock matrix. Incorporation of even very slow rates of degradation can have a substantial impact on plume attenuation. With the finite source and slow degradation, the plume actually recedes between 50 and 100 years.

Thumbnail description of key figures and tables

Figure 5.13: Model domain and example concentration and flow output

Figure 5.14: X vs. Z Type Site plots for 25, 50, and 100 years, no degradation

*Figure 5.15: X vs. Z Type Site plots for 25, 50, and 100 years, **with degradation***

More complex fracture network scenarios can be handled with numerical models such as FRACTRAN (Sudicky and McLaren, 1992). As an example, **Figure 5-13** shows a more complex fracture network with a statistically generated distribution of orthogonal fractures (adapted from Parker et al., 2012). The matrix is sandstone with 13% porosity. Fracture apertures have a log normal distribution with geometric mean of 100 microns. The source, positioned along the upper portion of the upgradient boundary, is assumed to persist for 20 years and then is removed. The average linear groundwater velocity in the fracture network can be estimated using:

$$\bar{v}_f = \frac{K_b\, i}{\phi_f}$$

where K_b is the bulk hydraulic conductivity (derived from the flow simulation), i is the average hydraulic gradient and ϕ_f is bulk fracture porosity (provided as model output based on the generated fracture network), which assumes all flow occurs through the interconnected fracture network.

With imposed hydraulic gradients of 1% horizontal and 0.5% vertical (downward), the average linear groundwater velocity is about 7 m/day for this scenario. Simulated groundwater velocities in some fractures are much higher than this average value with a maximum of about 30 m/day (**Figure 5-13b**) indicating potential for rapid plume migration in the absence of diffusion and other processes. Simulation results indicate rates of plume migration are much slower even without degradation (**Figure 5-14**), with the plume front about 650 m downgradient after 50 years and not reaching the downgradient boundary at 1000 m by 100 years. Peak concentrations are also significantly attenuated with distance. However, the results also show the long-term persistence of the plume after the source is completely removed, due to slow back diffusion of mass stored in the rock matrix. Figure 15 shows results when degradation is included in the fractures and matrix with a half-life of 10 years. Degradation in the matrix, besides causing direct contaminant loss, also has the effect of enhancing diffusion since higher concentration gradients are maintained driving diffusion into the matrix. This shows that incorporation of even very slow rates of degradation can have a substantial impact on plume attenuation. With the finite source and slow degradation, the plume actually recedes between 50 and 100 years.

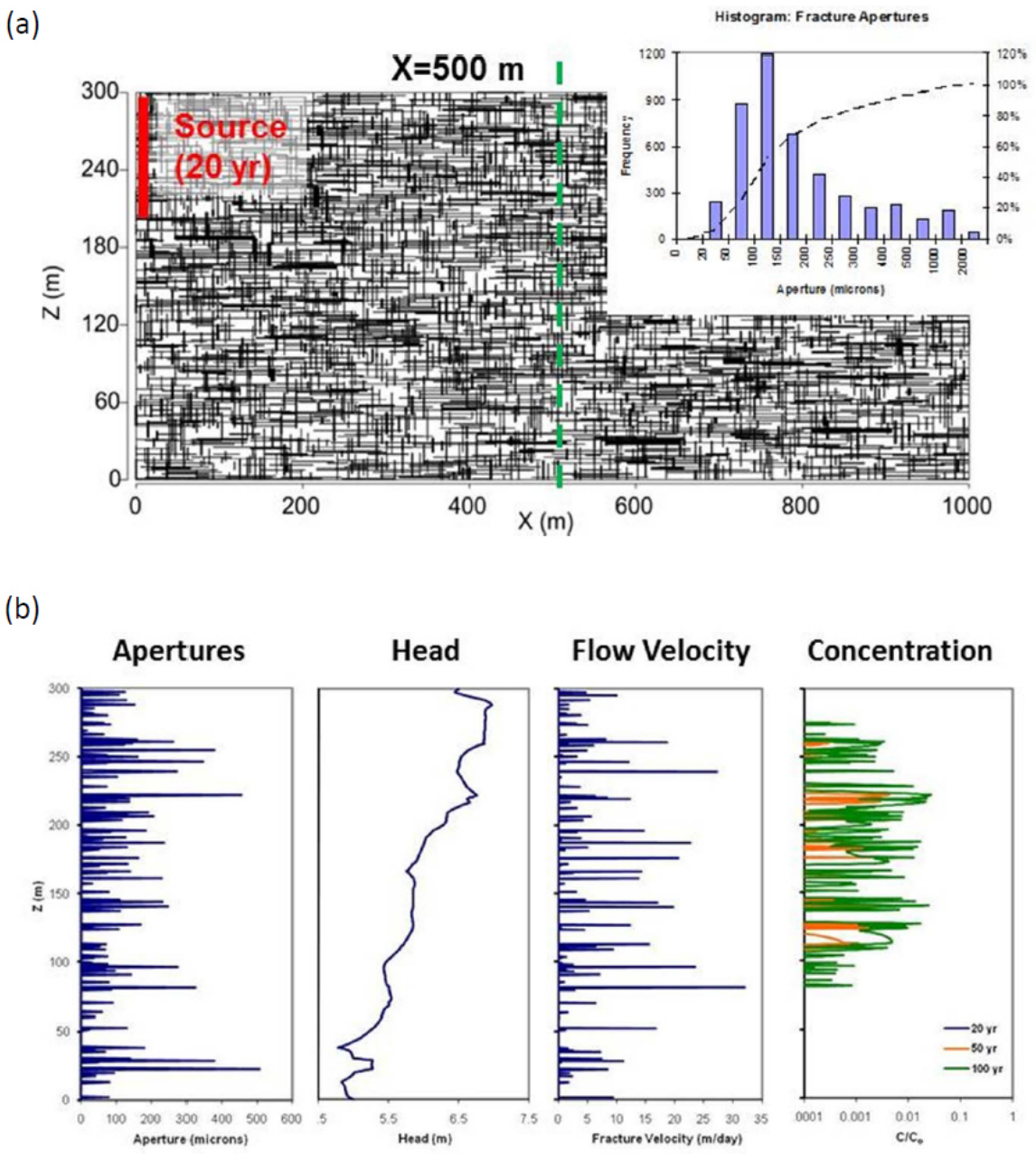

Figure 5-13. FRACTRAN results for fracture network simulation with a sandstone matrix: (a) model domain and fracture network (inset shows aperture distribution), and (b) example profiles at X=500 m of apertures, head, groundwater flow velocity and concentrations at 20, 50 and 100 years (adapted from Parker et al., 2012).

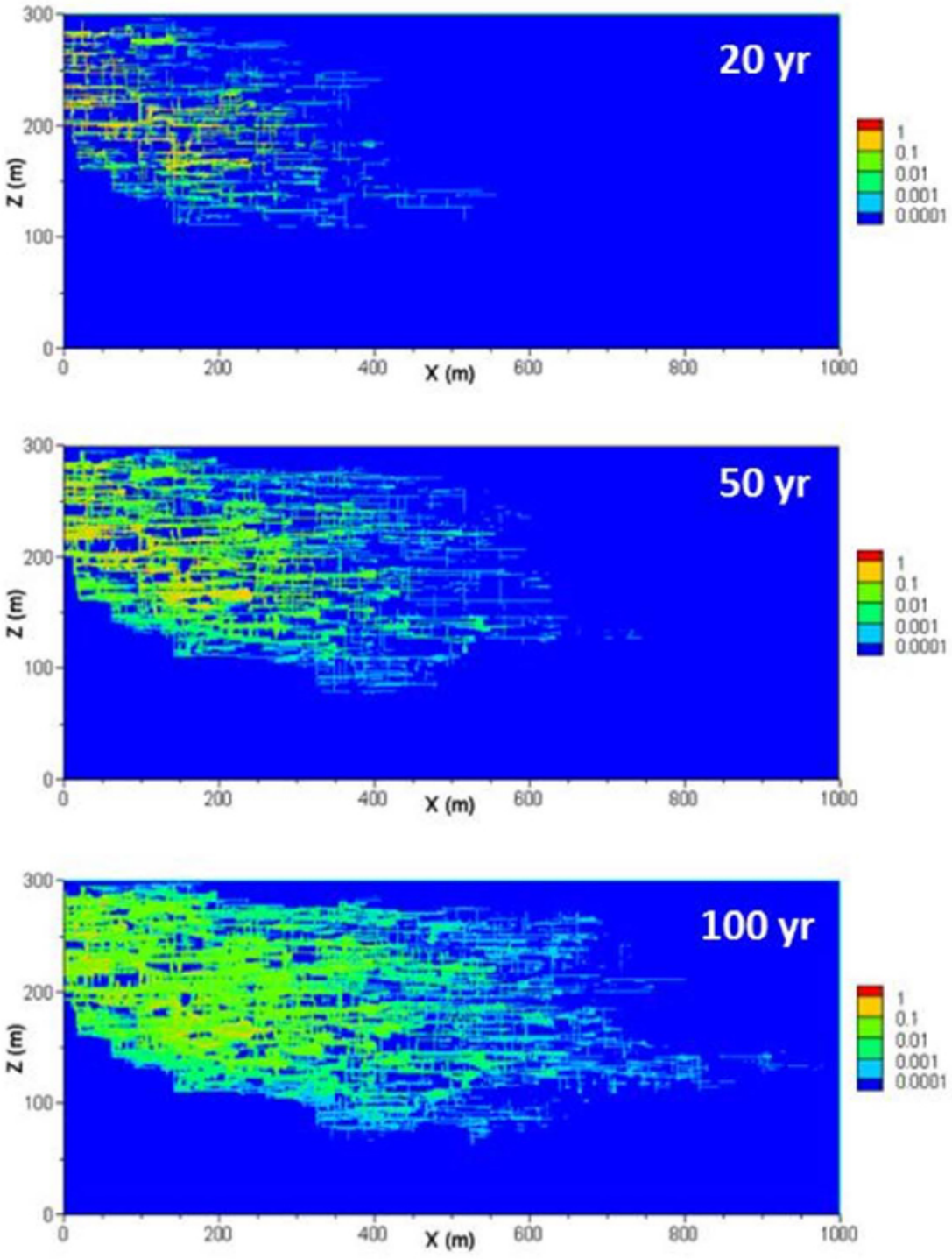

Figure 5-14. FRACTRAN results for fracture network simulation with a sandstone matrix: plume contours at 20, 50 and 100 years with a finite source and no degradation (adapted from Parker et al., 2012).

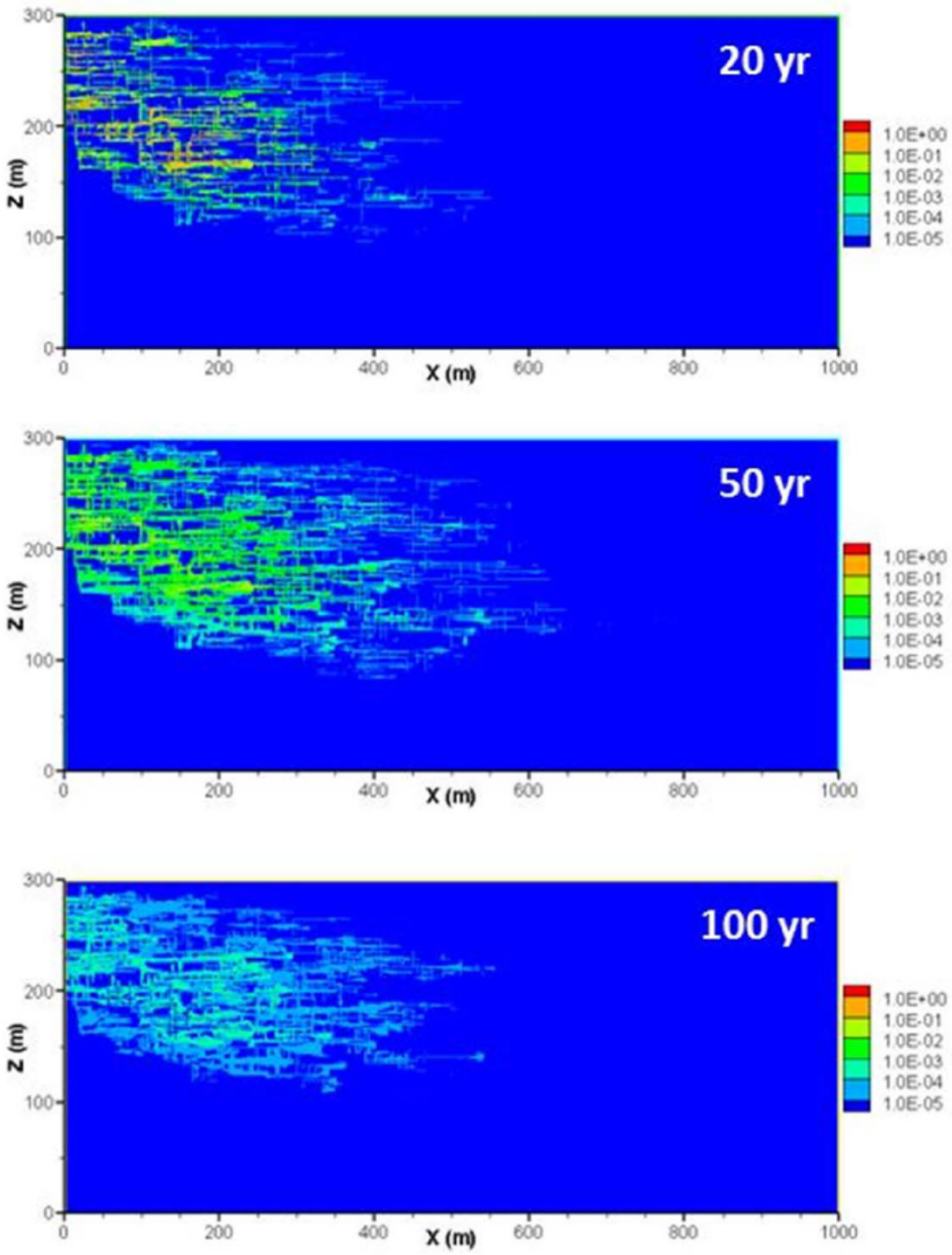

Figure 5-15. FRACTRAN results for fracture network simulation with a sandstone matrix: plume contours at 20, 50 and 100 years with a finite source and degradation in fractures and the matrix with a half-life of 10 years (adapted from Parker et al., 2012).

5.4 POROUS MEDIA TYPE SITE SIMULATIONS

Three different porous media scenarios were examined in type site simulations: 1) two-layer scenario with aquifer and underlying clay layer, 2) multilayer scenario with interbedded sand and clay layers, and 3) random multilayer scenario with random thin clay layers suspended in the aquifer along with an underlying thicker clay layer. **Table 5-2** provides the base case parameters for these simulations, including only minor sorption in the clay layers (R=2) and no degradation. For the first two scenarios, sensitivity analyses were conducted to examine sensitivity to (a) higher sorption in the clay zones (R=10), and (b) inclusion of slow rates of degradation in the clay zones ($t_{1/2}$=5 years).

5.4.1 Two-Layer Sand/Clay Type Site

- **Why**: Develop Type Sites for two-layer porous media settings.
- **Hydrogeologic Setting**: Two layers unconsolidated media: sand over clay. Groundwater seepage velocity: ~110 meters per year.
- **Numerical Model**: HydroGeoSphere
- **Model Domain:** 500 meters in X direction and 5 meter thick sand over 5 meter thick clay.
- **Key Processes:** Matrix diffusion, sorption, degradation
- **Time Domain:** Source loading 10 years; release from low k zone out to 100 years.
- **What Happened:** Several permutations of low sorption, high sorption, and degradation Type Sites generated. Long-term persistence for many decades at consequential concentration levels following source removal for no degradation case. Higher clay layer sorption increases the storage capacity and also increases rates of inward diffusion since higher concentration gradients are maintained. This also leads to longer-term tailing at higher concentration levels and for longer durations. Degradation in the clay reduces the total mass stored in the low K zone and hence can significantly reduce back diffusion effects; all of the mass disappears between 50 and 100 years for one Type Setting with degradation.

Thumbnail description of key figures and tables:

Figure 5-16: Model domain of detailed two layer Type Site settings

*Figure 5-17: **Base Case (low sorption)** Type Site; two layers, R=2, no degradation, 12 Z vs. X plots*

*Figure 5-18: **Base Case (low sorption) Type Site**; two layers, R=2, no degradation, 5 concentration vs. time plots*

*Figure 5-19: **High Sorption Type Site**; two layers, R=10, no degradation, 12 Z vs. X plots*

*Figure 5-20: **High sorption Type Site**; two layers, R=10, no degradation, concentration vs. time plots*

*Figure 5-21: High sorption Type Site; two layers, R=10, **with degradation**, 5 concentration vs. time plots*

*Figure 5-22: **Base Case (low sorption**) Type Site; two layers, R=2, **with degradation**, 5 concentration vs. time plots*

Figure 5-23: Comparison of preceding Type Sites: 12 concentration vs. time plots

Figure 5-24: Mass distribution for preceding Type Sites: 3 mass vs. time plots

Figure 5-25: Mass distribution for preceding Type Site: Base Case, High Sorption, Degradation in Clay, mass percent remaining vs. time

Table 5-3: Mass distribution for preceding Type Sites: 3 mass vs. time plots

For the two-layer Type Site scenarios, the model domain extends 500 m in the flow direction with a 5 m thick sand overlying a 5 m thick clay aquitard (Figure 16a). The source is positioned as a thin layer perched on the clay layer and is assumed to persist for 10 years following which time it is completely removed to examine back diffusion effects. For TCE, assuming initial source concentration at solubility of 1100 mg/L and MCL of 0.005 mg/L, the C/C_o representing the MCL is about $5x10^{-6}$. Tight grid discretization is applied with further nearer the interface to capture the sharp concentration gradients in the aquifer and adequately resolve diffusion processes in the clay (**Figure 5-16b**). **Figure 5-17** shows concentration contours for the "base case" at times of 1, 2, 5 and 10 years while the source is active, and then at times ranging from 1 to 100 years after source removal. The plots at 1, 2 and 5 years following source removal show the advective flushing of the high plume concentrations out of the system. Then following this time long-term plume persistence is attributed solely to back diffusion of mass back out of the aquitard. In the aquifer the plume remains at the base of the aquifer exhibiting sharp concentration gradients, owing to the small vertical transverse dispersivity used in the simulation. The degree of plume tailing is further illustrated with the breakthrough and elution curves in Figure 18 showing concentrations at the sand-clay interface and also depth-averaged concentrations in hypothetical wells with 1.5 m and 3 m long screens. Similar to Sale et al. (2008), these show a few OoM declines in concentration following source removal, particularly nearer the source, but long-term persistence for many decades at consequential concentration levels following source removal.

Table 5-2: Input parameters for porous media simulations (two-layer, multi-layer and random low K zone scenarios).

Parameter	Symbol	Value	Units	Notes
Porous Media Properties				
Sand hydraulic conductivity	K_{sand}	3.0E-04	m/s	
Clay hydraulic conductivity	K_{clay}	1.0E-10	m/s	
Sand porosity	ϕ_{sand}	0.30	-	
Clay porosity	ϕ_{clay}	0.40	-	
Flow System Properties				
horizontal hydraulic gradient	i_h	0.0035	-	
Darcy Flux	q	0.09	m/day	calculated
Groundwater velocity	v	0.30	m/day	calculated
Source Conditions				
source input concentration	C_o	1.0	-	normalized
source duration	T	10	years	
Contaminant Transport Properties				
TCE free-solution diffusion coefficient	D_o	1.0E-9	m^2/s	Literature value (Pankow and Cherry, 1996)
Sand tortuosity	τ_{sand}	0.30	-	assumed same as porosity
Clay tortuosity	τ_{clay}	0.40	-	assumed same as porosity
Sand retardation factor	R_{sand}	1	-	
Clay retardation factor	R_{clay}	2, 10*	-	* sensitivity analysis
Sand half-life	$t_{1/2\ sand}$	0	yr	
Clay half-life	$t_{1/2\ clay}$	no degradation, 5*	yr	* sensitivity analysis
longitudinal dispersivity	α_L	0.50	m	
transverse vertical dispersivity	α_{tv}	0.001	m	

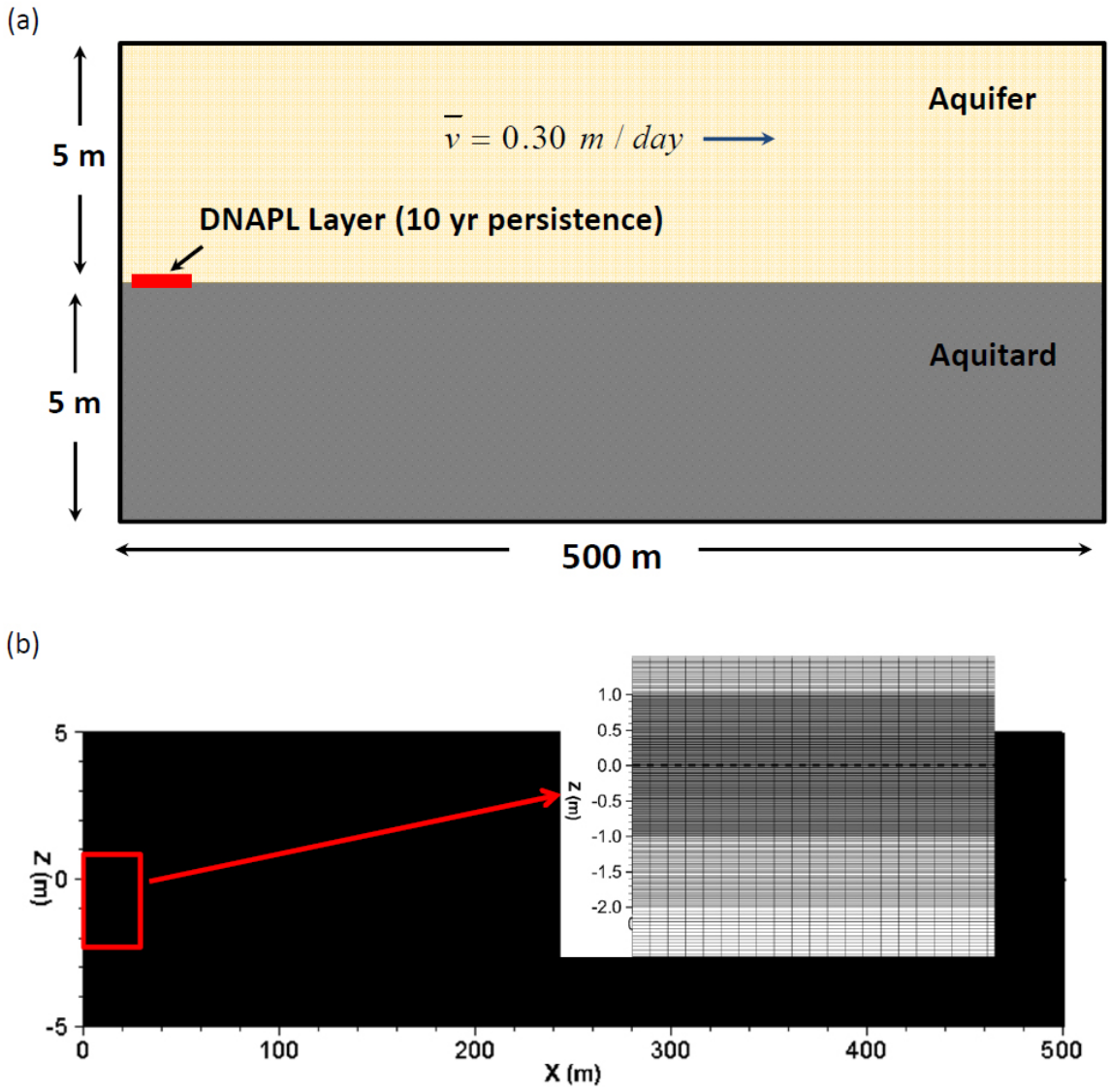

Figure 5-16. (a) model domain, and (b) grid discretization for HydroGeoSphere simulations of two-layer scenario.

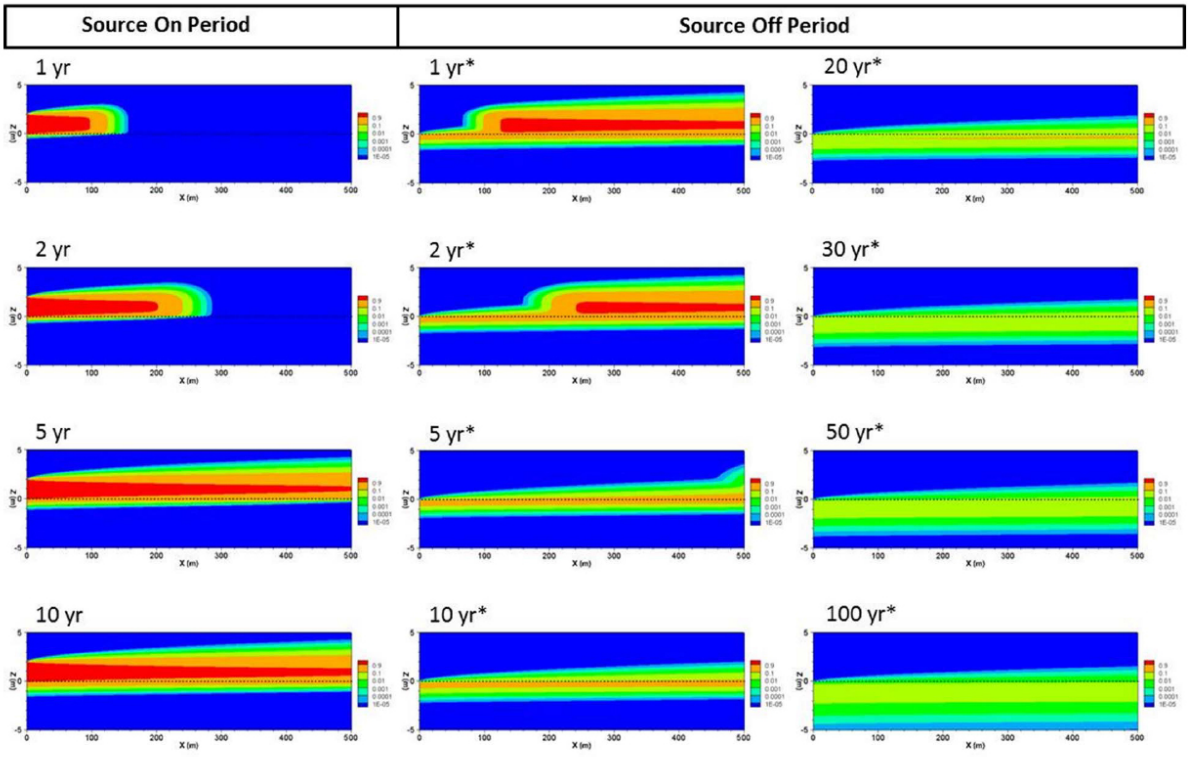

Figure 5-17. Two layer scenario (base case R_{clay}=2, no degradation): plume distribution.

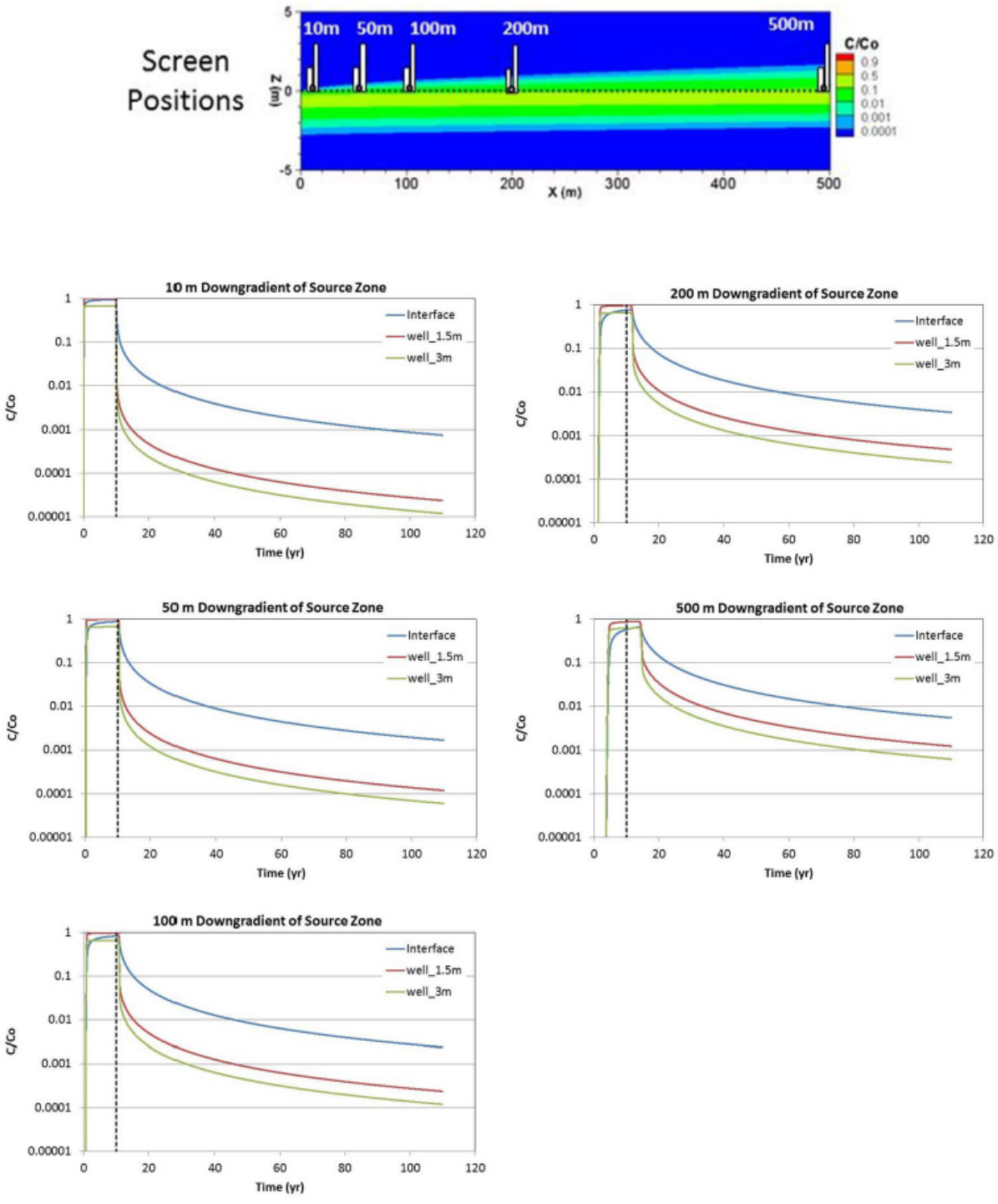

Figure 5-18. Two layer scenario (base case R_{clay}=2, no degradation): downgradient concentrations.

Sensitivity analyses were conducted to examine effects of higher clay sorption and degradation in the clay. **Figure 5-19** shows concentration contours for the scenario with higher sorption in the clay (R_{clay}=10) and **Figure 5-20** shows downgradient concentrations. Higher clay layer sorption increases the storage capacity and also increases rates of inward diffusion since higher concentration gradients are maintained. This also leads to longer-term tailing at higher concentration levels and for longer durations. **Figure 5-21** shows concentration contours for the scenario with degradation included in the clay ($t_{1/2}$=5 years) and **Figure 5-22** shows downgradient concentrations. Degradation in the clay reduces the total mass stored in the low K zone and hence can significantly reduce back diffusion effects. In this case all of the mass disappears between 50 and 100 years. **Figure 5-23** shows graphs of downgradient concentrations for all three scenarios together for comparison. **Figure 5-24** shows a comparison of cumulative mass distribution for the three cases and mass distributions are also summarized in **Table 5-3**. In this case the mass units are nonsensical (since relative concentrations are used) but can be converted to a real mass assuming input at TCE solubility (or other reasonable input concentration). Estimates of mass in the sand and clay layers were made using Tecplot®, based on the contoured output concentrations using integration with value blanking (to separate the sand and clay) and the results were then corrected for differences in porosity and sorption properties between the units. **Figure 5-25** shows remnant mass in the domain for the three scenarios. The mass estimates show the larger persistence of mass in the clay and plume tailing for the scenario with higher sorption, and also lower tailing and mass depletion in the clay when slow rates of degradation are included. Results in **Table 5-3** also show the shift in the total mass proportion in the sand versus clay between when the source is on and large transition while the plume is being flushed out of the domain within the first few years following source removal.

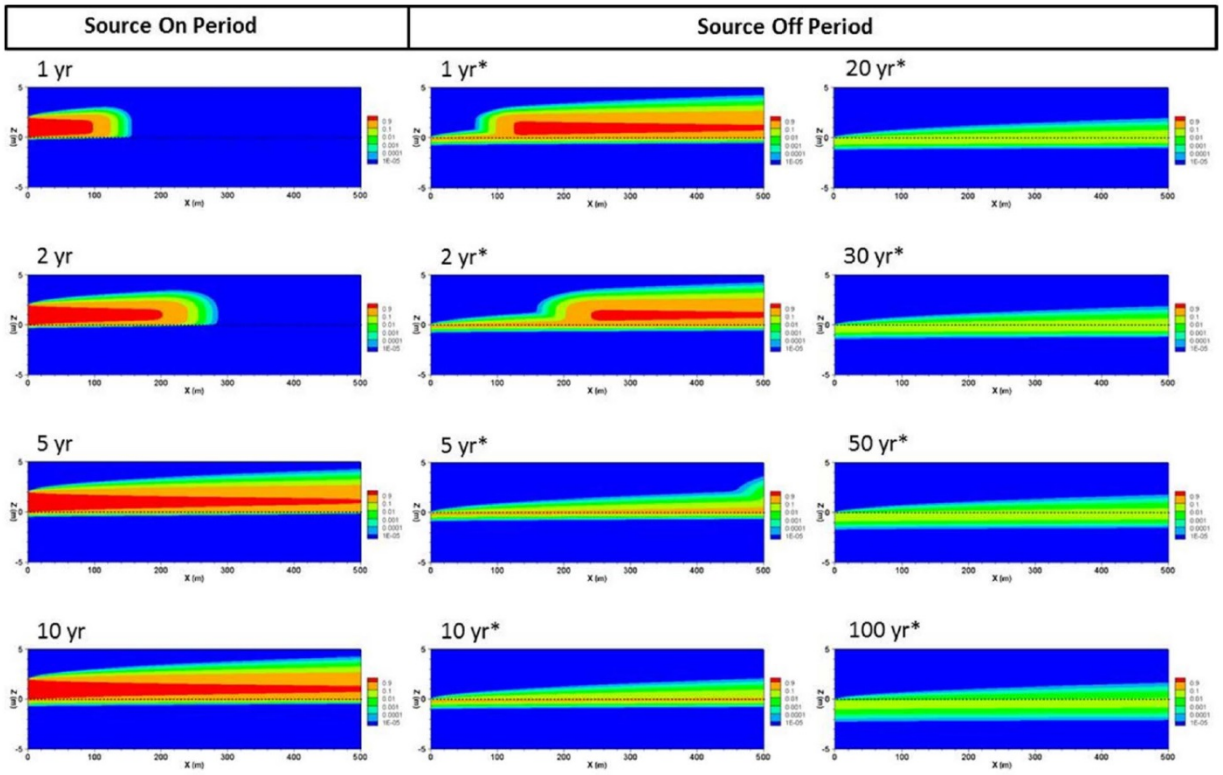

Figure 5-19. Two layer scenario (R_{clay}=10, no degradation): plume distribution.

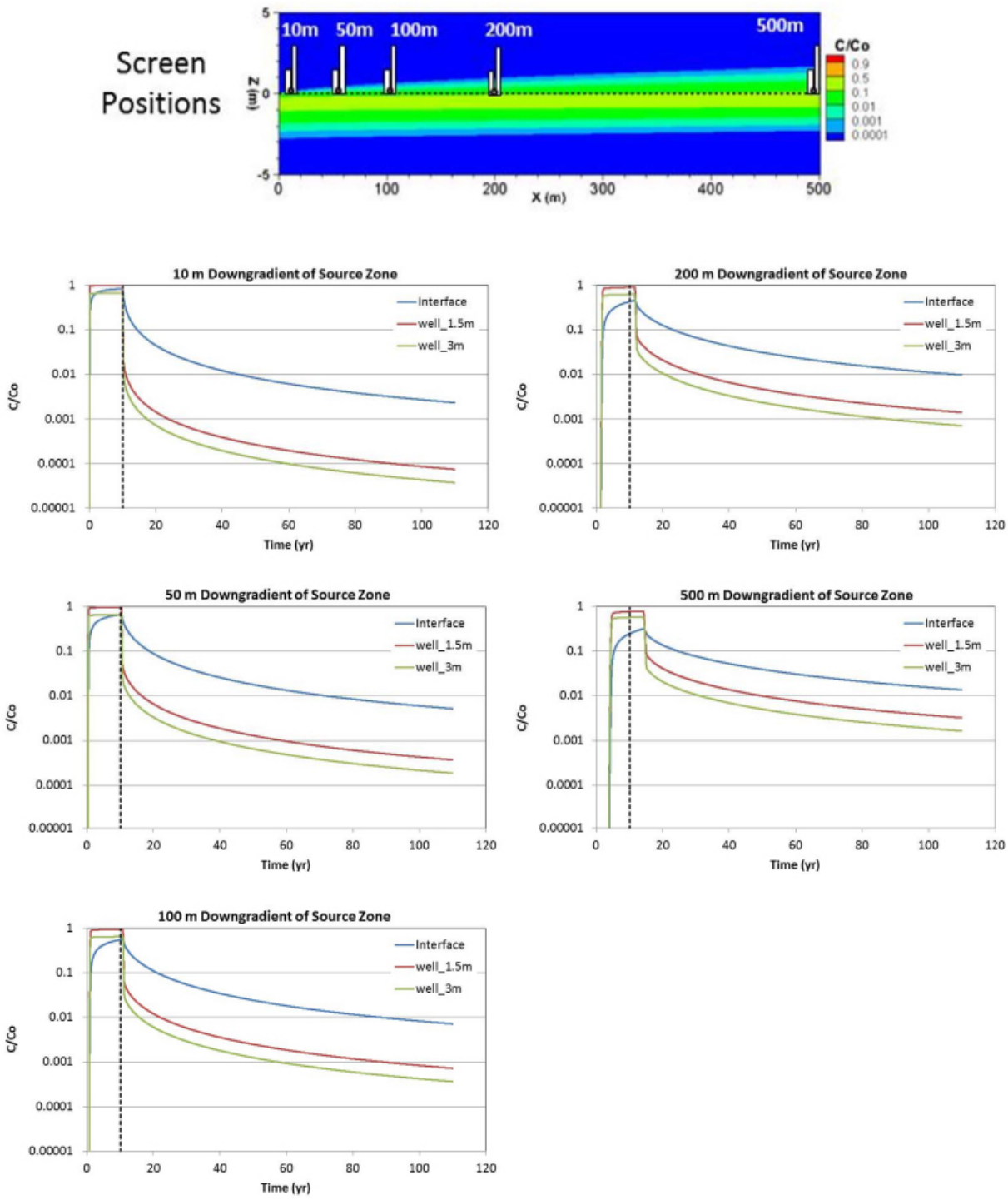

Figure 5-20. Two layer scenario (R_{clay}=10, no degradation): downgradient concentrations.

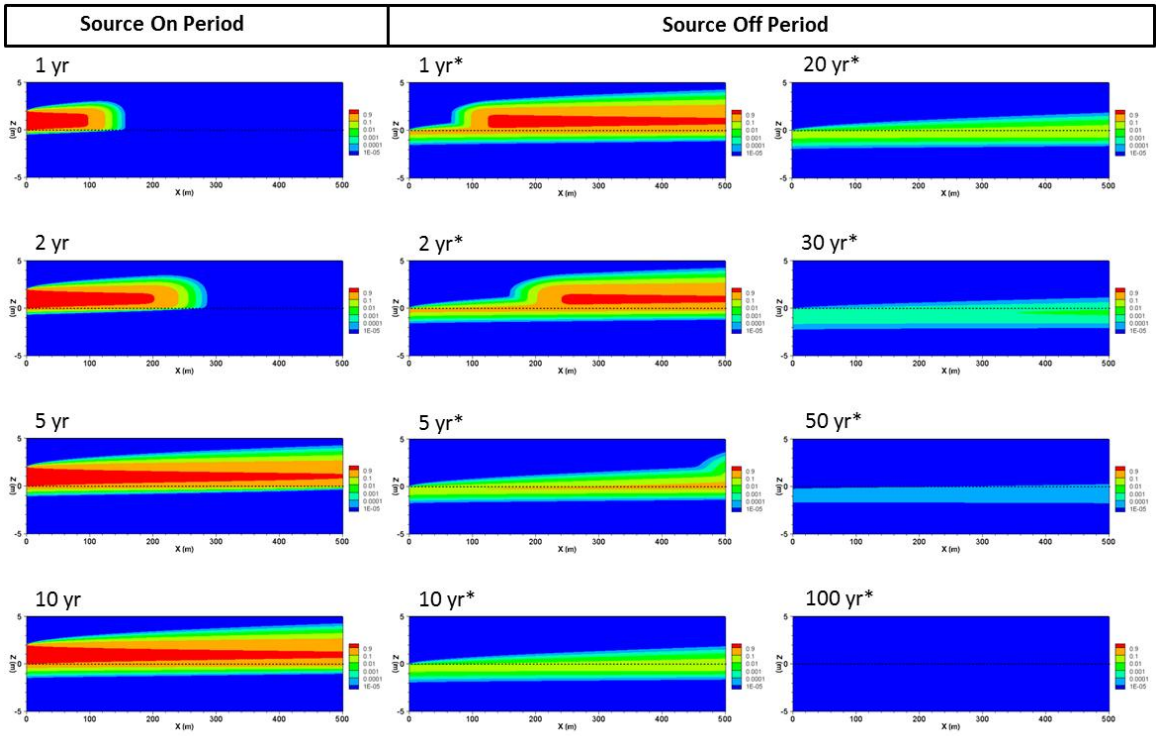

Figure 5-21. Two layer scenario (R_{clay}=2, degradation in clay $t_{1/2}$=5 yr): plume distribution.

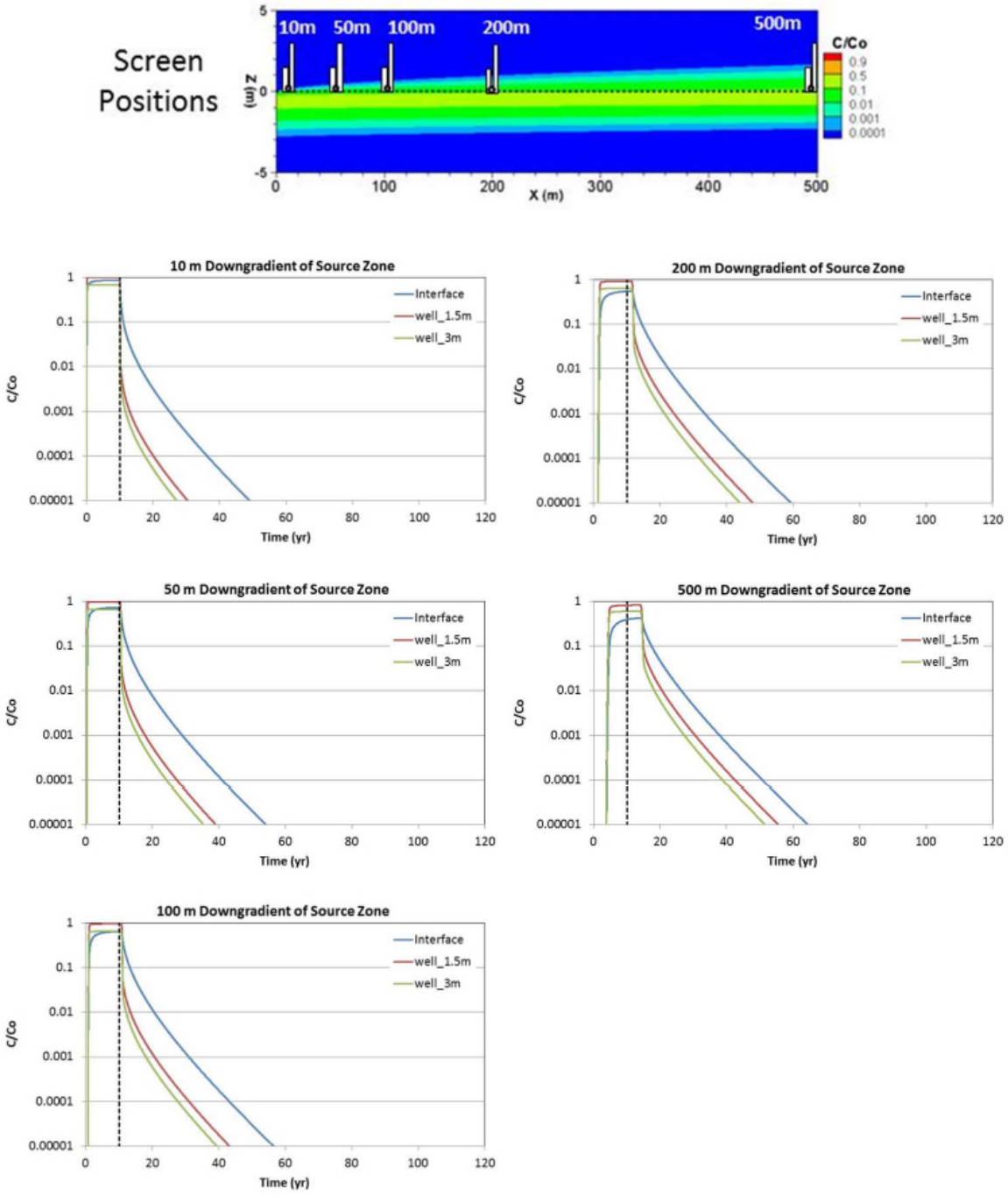

Figure 5-22. Two layer scenario (R_{clay}=2, degradation in clay $t_{1/2}$=5 yr): downgradient concentrations.

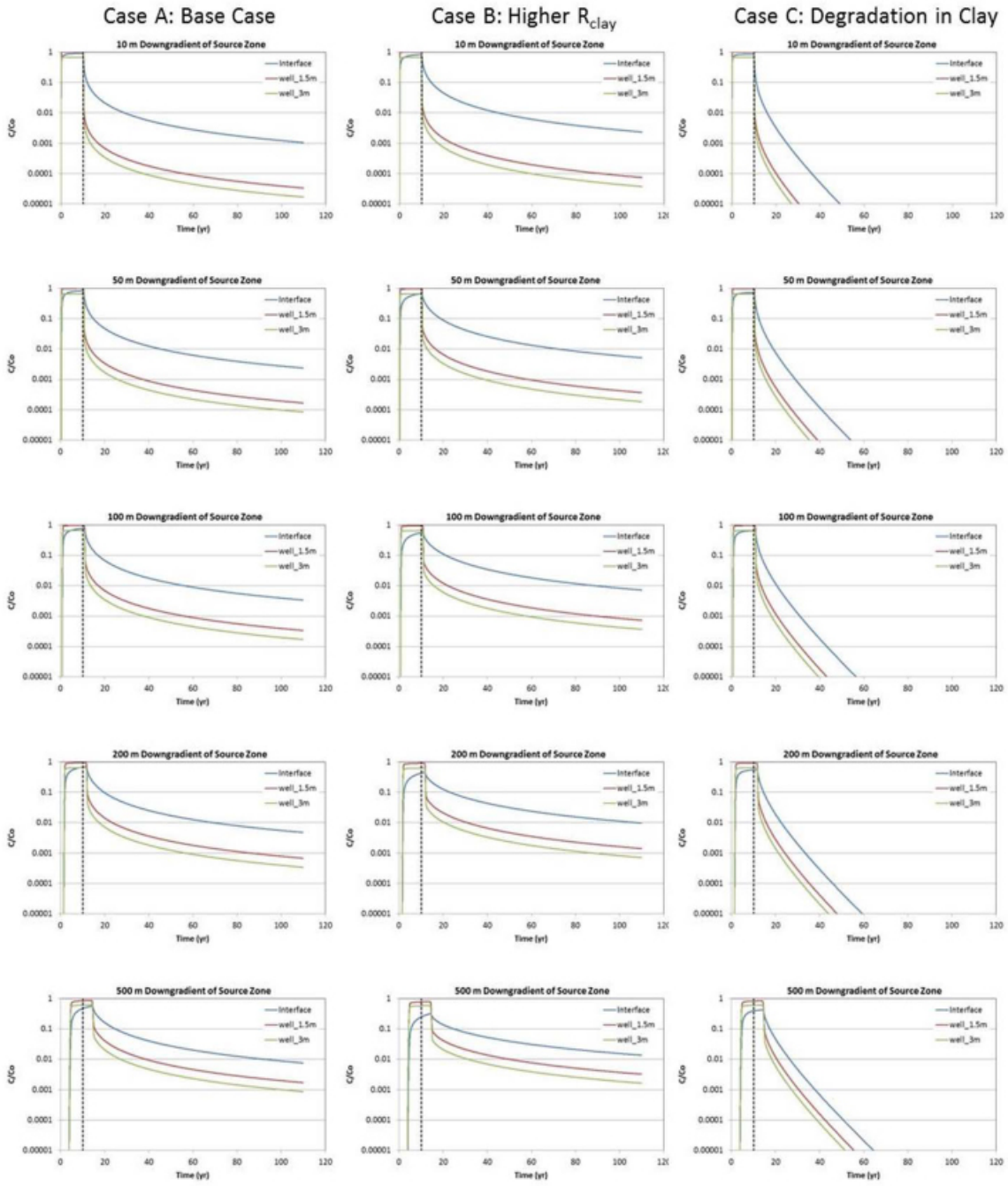

Figure 5-23. Downgradient concentration comparison for two-layer scenarios.

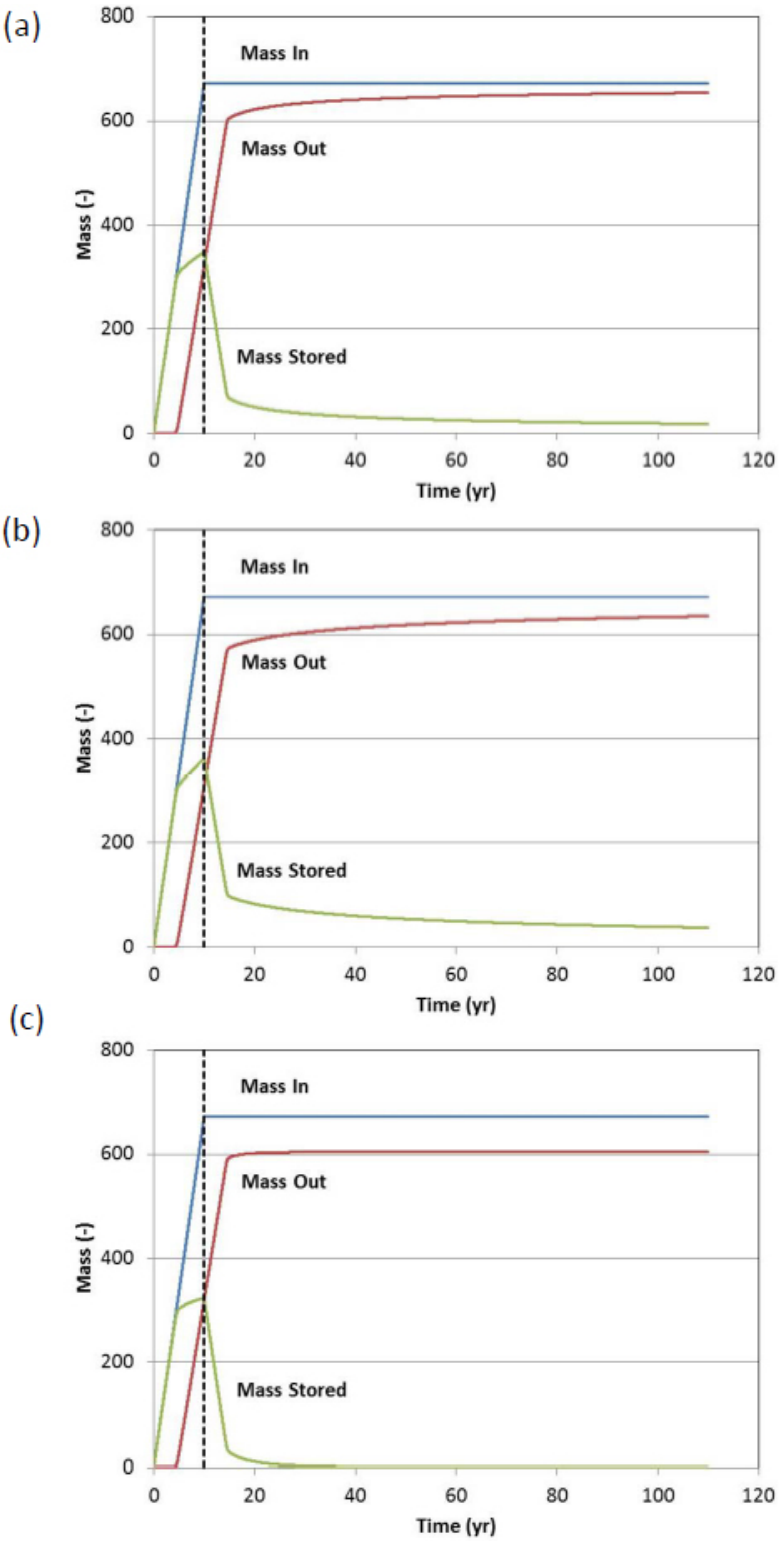

Figure 5-24. Two layer scenario mass distribution: (a) base case R_{clay}=2, no degradation, (b) R_{clay}=10, no degradation, (c) R_{clay}=2, degradation in clay with $t_{1/2}$=5 yr).

Table 5-3: Mass distribution for two-layer scenario.

	Base Case (R_{clay}=2, no degradation)			High Sorption Case (R_{clay}=10, no degradation)			Degradation Case (R_{clay}=2, $t_{1/2}$=5 yr in clay)		
Time (yr)*	Mass in Domain (% of total input)	Aquifer (%)	Aquitard (%)	Mass in Domain (% of total input)	Aquifer (%)	Aquitard (%)	Mass in Domain (% of total input)	Aquifer (%)	Aquitard (%)
0	51.8	83.9	16.1	54.0	79.1	20.9	48.2	88.9	11.1
1	42.7	79.3	20.7	45.4	73.0	27.0	38.4	86.2	13.8
2	33.6	73.2	26.8	36.7	65.3	34.7	28.8	82.7	17.3
5	9.9	15.5	84.5	14.4	10.5	89.5	4.1	20.1	79.9
10	7.4	8.4	91.6	12.3	6.4	93.6	1.5	10.0	90.0
20	5.5	4.6	95.4	10.2	3.9	96.1	0.3	5.4	94.6
30	4.6	3.2	96.8	8.9	2.8	97.2	0.1	3.7	96.3
50	3.6	2.0	98.0	7.4	1.8	98.2	0.003	2.3	97.7
100	2.6	1.0	99.0	5.5	1.0	99.0	0.000	-	-

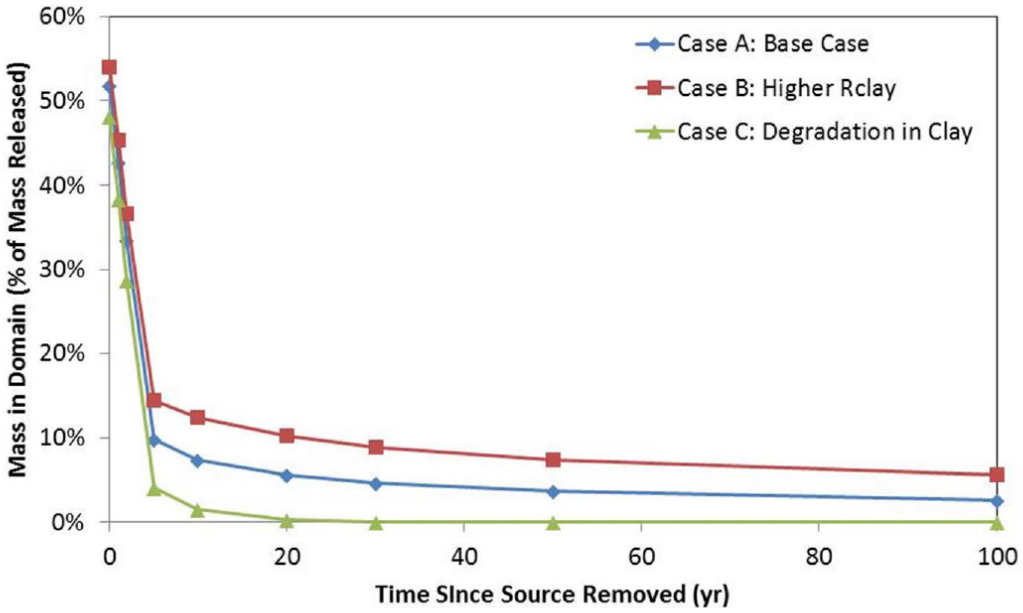

Figure 5-25. Mass distribution comparison for two-layer scenarios showing remnant mass in domain.

5.4.2 Multi-layer Scenarios

What was done

- **Why**: Develop Type Sites for multi-layer porous media settings.
- **Hydrogeologic Setting**: Series of alternating clay and sand layers are alternating each layer 1 meter thick; three sand layers and four clay layers. Groundwater seepage velocity: ~110 meters per year.
- **Numerical Model**: HydroGeoSphere
- **Model Domain:** 500 meters in X direction and 10 meters thick
- **Key Processes:** Matrix diffusion, sorption, degradation
- **Time Domain:** Source loading 10 years; release from low k zone out to 100 years.
- **What Happened:** Similar trends as the two-layer case but with stronger tailing effects due to the greater sand-clay contact surface area.

Thumbnail description of key figures and tables

Figure 5-26. Model domain for multi-layer Type Sites.

*Figure 5-27: **Base Case (low sorption**) Type Site;, R=2, three sand and four clay layers, no degradation, 12 Z vs. X plots*

*Figure 5-28: **Base Case (low sorption)** Type Site; three sand and four clay layers, R=2,, no degradation, 5 concentration vs. time plots*

*Figure 5-29: **High sorption** Type Site; three sand and four clay layers, R=10, no degradation, 12 Z vs. X plots*

*Figure 5-30: **High sorption** Type Site; three sand and four clay layers, R=10, no degradation, concentration vs. time plots*

*Figure 5-31: Base Case (low sorption) Type Site; three sand and four clay layers, R=2, **with degradation**, 12 Z vs. X plots*

*Figure 5-32 : Base Case (low sorption) Type Site; three sand and four clay layers, R=2, **with degradation**, 5 concentration vs. time plots*

Figure 5-33: Comparison of preceding Type Sites: 12 concentration vs. time plots

Figure 5-34: Mass distribution for preceding Type Sites: 3 mass vs. time plots

Figure 5-35: Mass distribution for preceding Type Site: Base Case, High Sorption, Degradation in Clay, mass percent remaining vs. time

Table 5-4: Mass distribution for preceding Type Sites: 3 mass vs. time plots

The multi-layer scenario uses the same properties as the two layer scenario, except in this case the clay and sand layers are alternating each layer 1 m thick (**Figure 5-26a**). This sets up potential for even stronger back diffusion effects due to more surface area for diffusion. Again very tight grid discretization is required to capture the diffusion processes (**Figure 5-26b**). Concentration contours for the three scenarios (base case, higher clay sorption, clay degradation) are shown in **Figures 5-27, 5-29 and 5-31**, respectively; and downgradient contaminant concentrations in **Figures 5-28, 5-30 and 5-32**, respectively. Downgradient concentrations are compared in **Figure 33** and mass distributions are compared in **Figures 5-34** and **5-35** and in **Table 5-4**. As expected the multi-layer scenario results show similar trends as the two-layer case but with stronger tailing effects due to the greater sand-clay contact surface area.

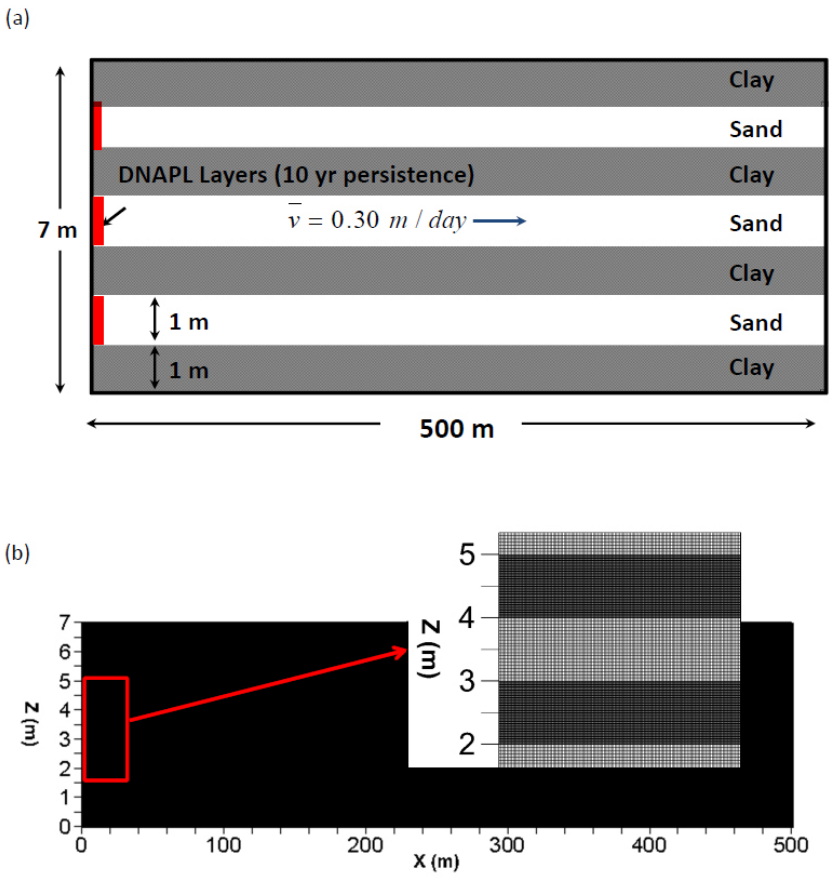

Figure 5-26. (a) model domain, and (b) grid discretization for HydroGeoSphere simulations of multi-layer scenario.

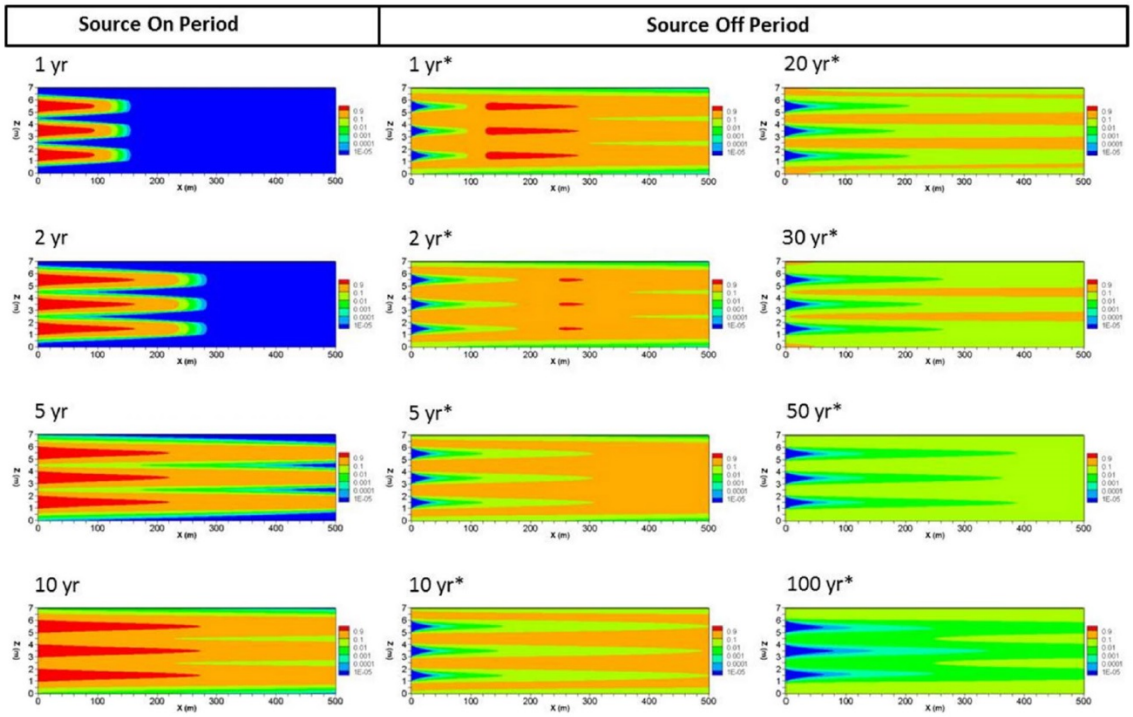

Figure 5-27. Multi-layer scenario (base case R_{clay}=2, no degradation): plume distribution.

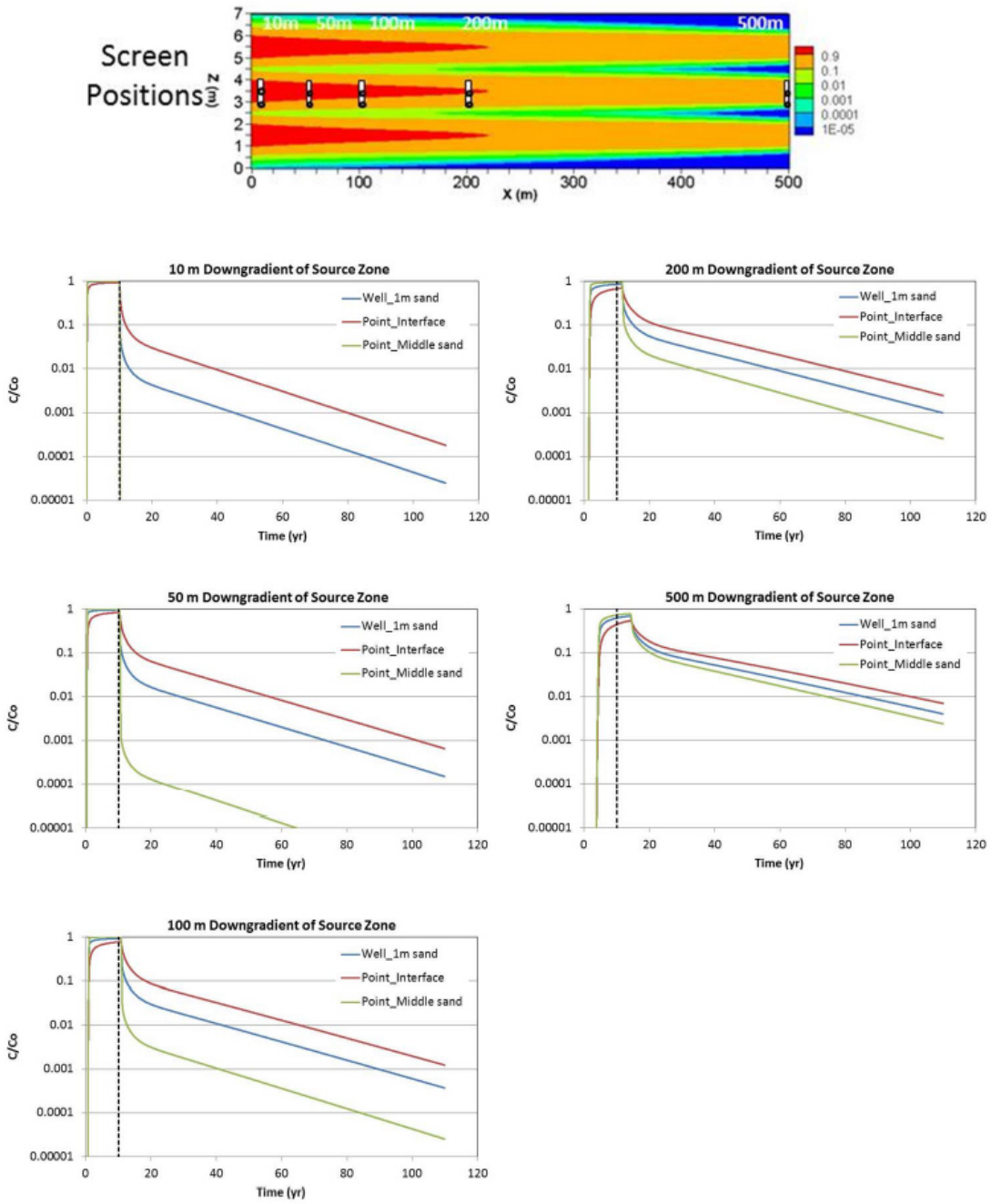

Figure 5-28. Multi-layer scenario (base case R_{clay}=2, no degradation): downgradient concentrations.

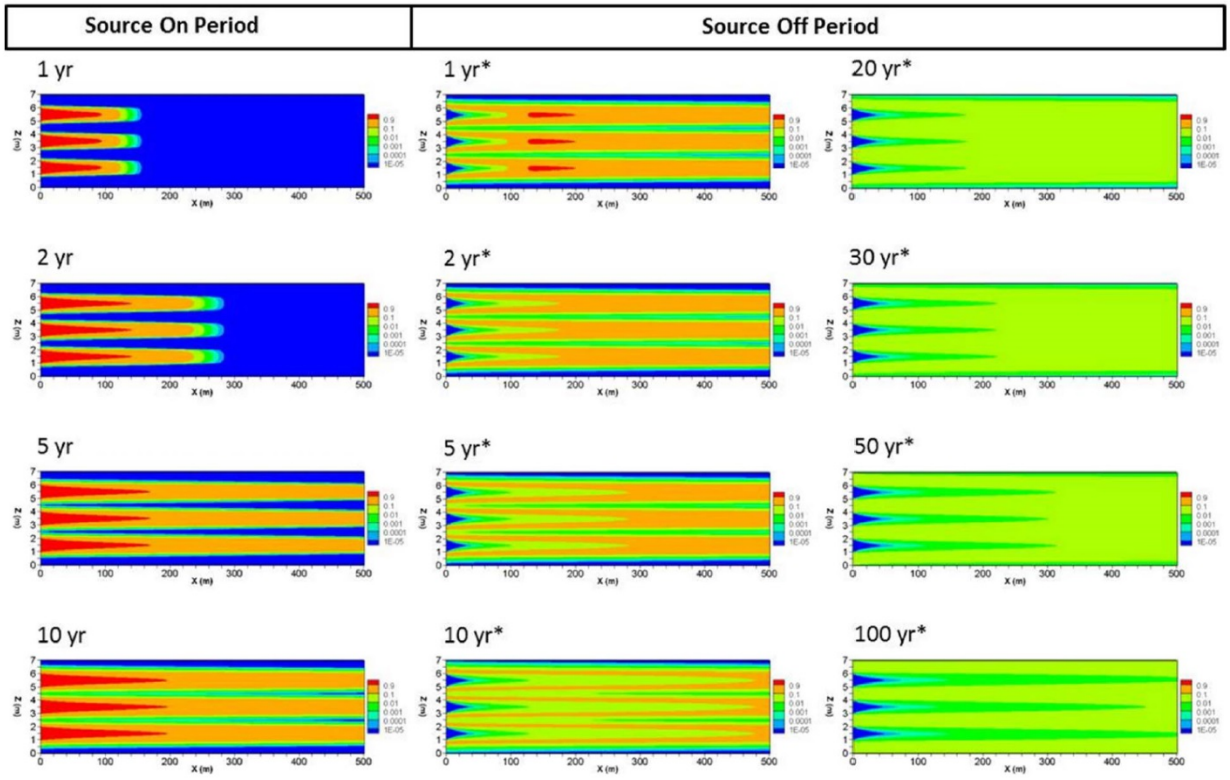

Figure 5-29. Multi-layer scenario (R_{clay}=10, no degradation): plume distribution.

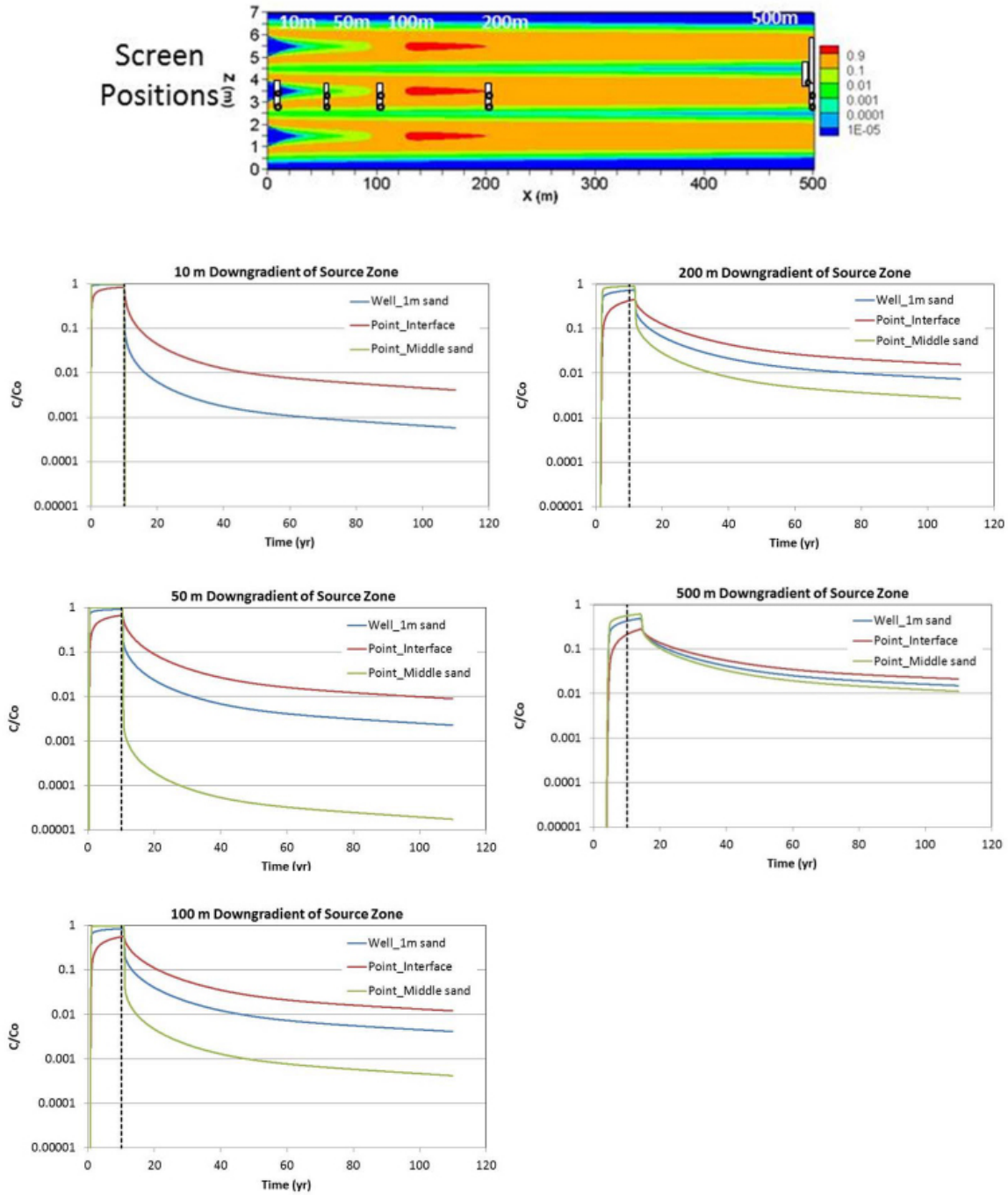

Figure 5-30. Multi-layer scenario (R_{clay}=10, no degradation): downgradient concentrations.

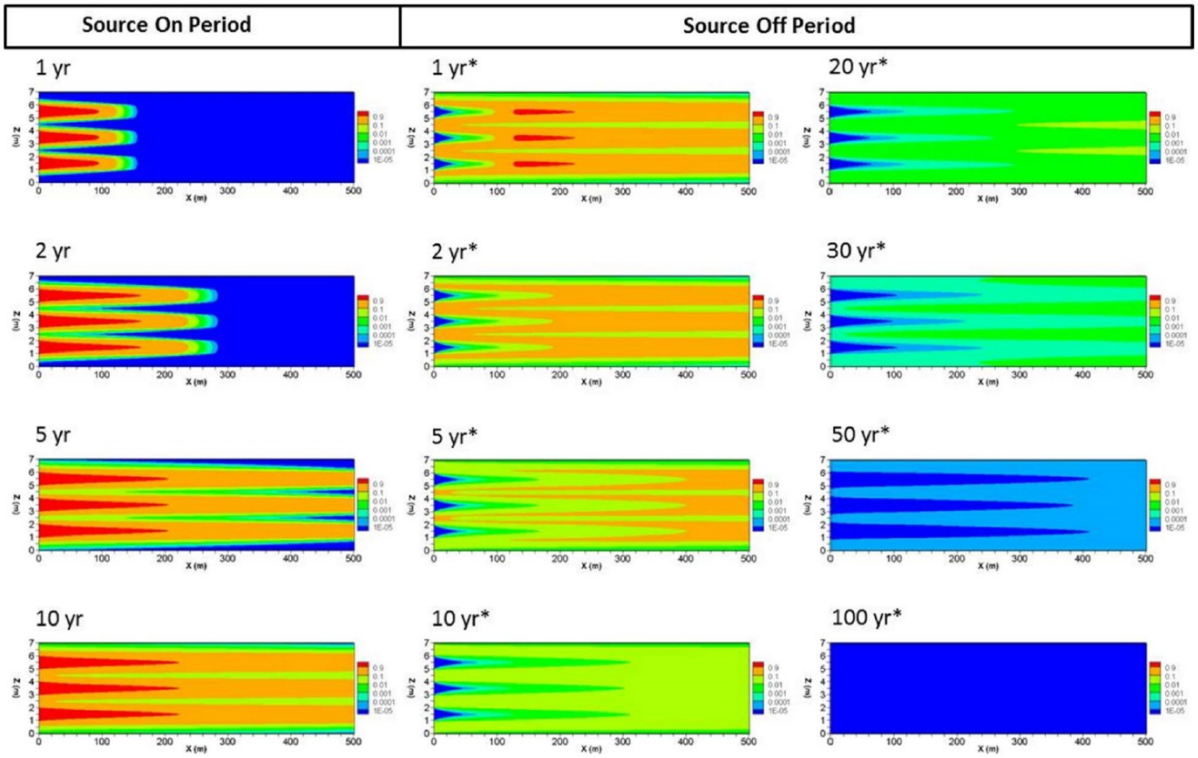

Figure 5-31. Multi-layer scenario (R_{clay}=2, degradation in clay $t_{1/2}$=5 yr): plume distribution.

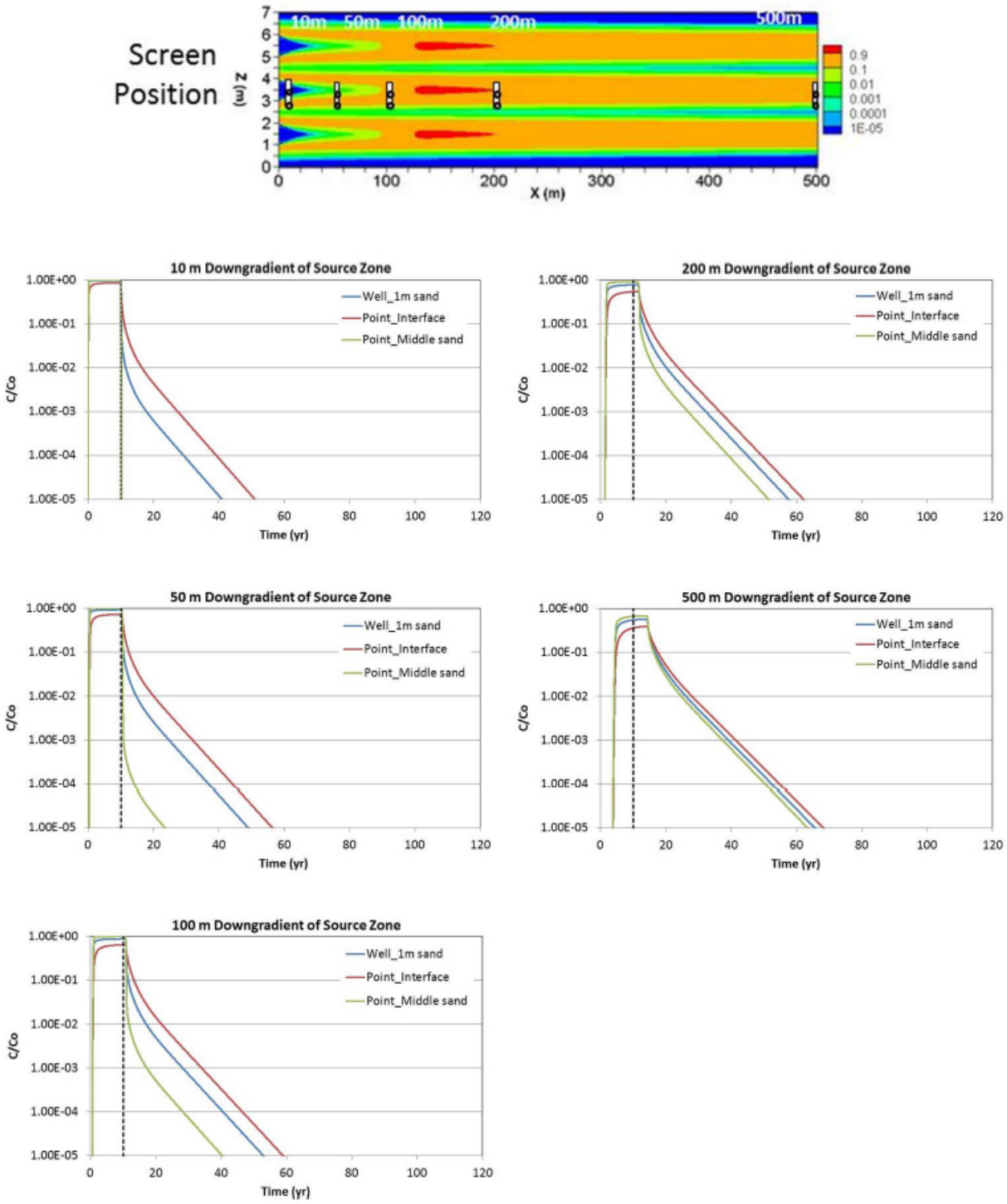

Figure 5-32. Multi-layer scenario (R_{clay}=2, degradation in clay $t_{1/2}$=5 yr): downgradient concentrations.

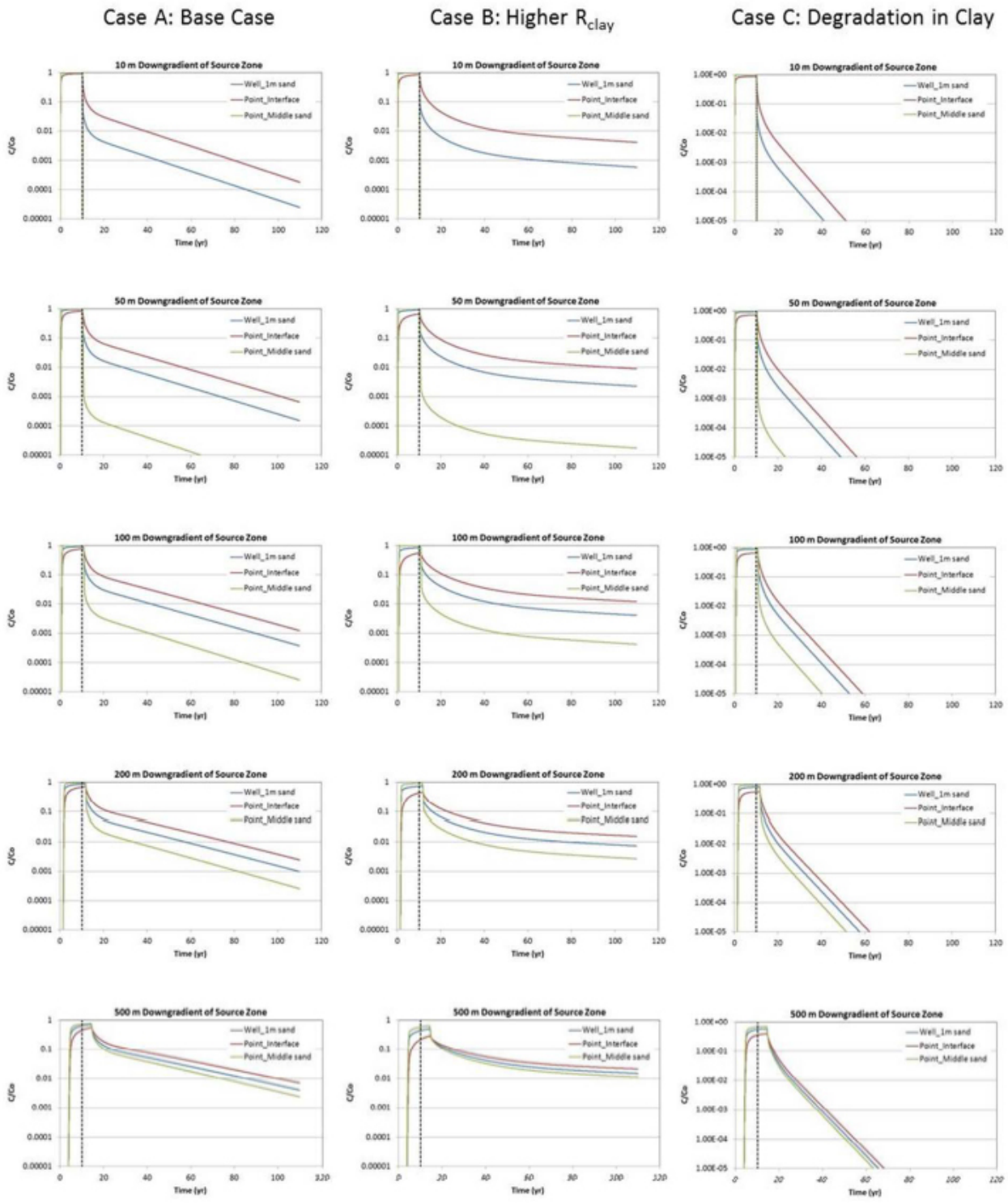

Figure 5-33. Downgradient concentration comparison for multi-layer scenarios.

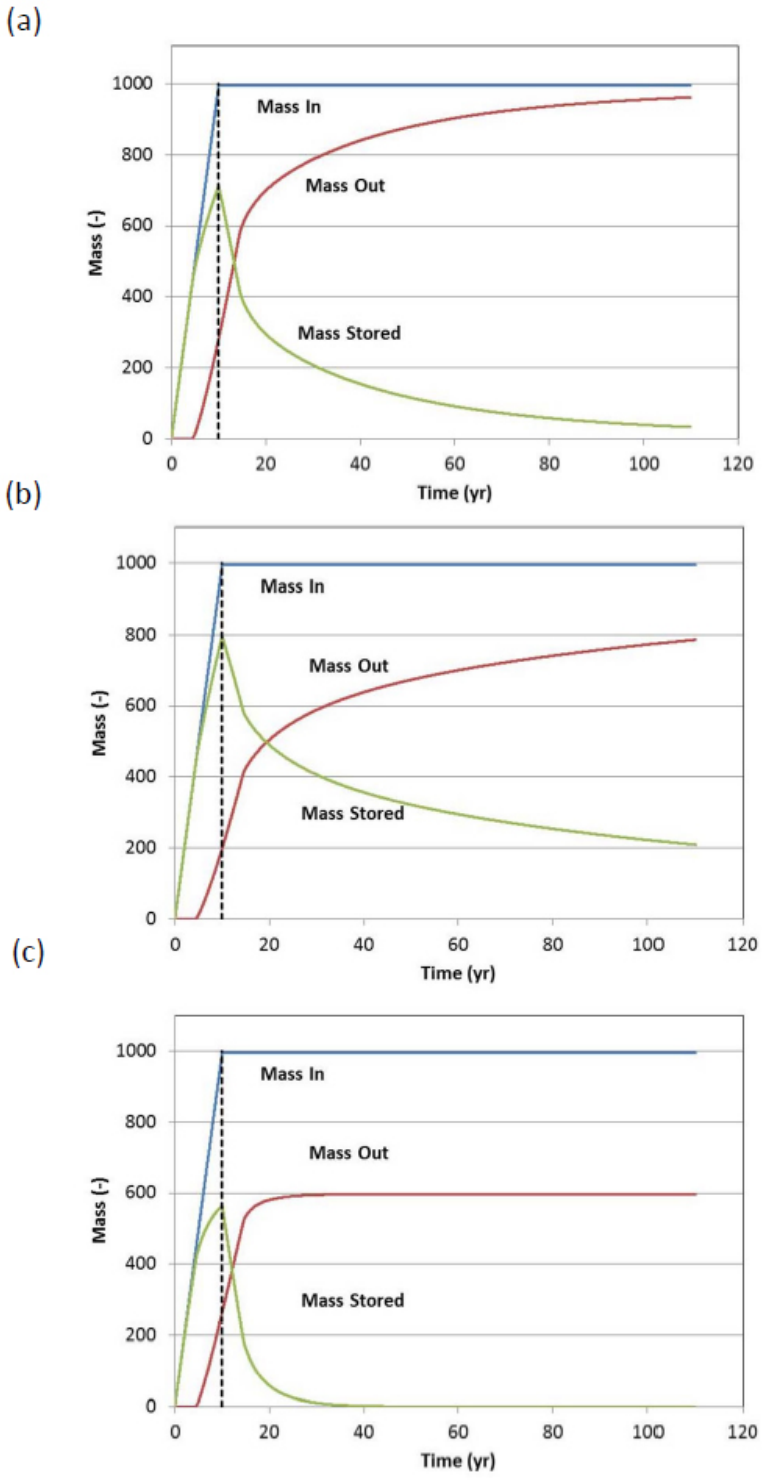

Figure 5-34. Multi-layer scenario mass distribution: (a) base case R_{clay}=2, no degradation, (b) R_{clay}=10, no degradation, (c) R_{clay}=2, degradation in clay with $t_{1/2}$=5 yr).

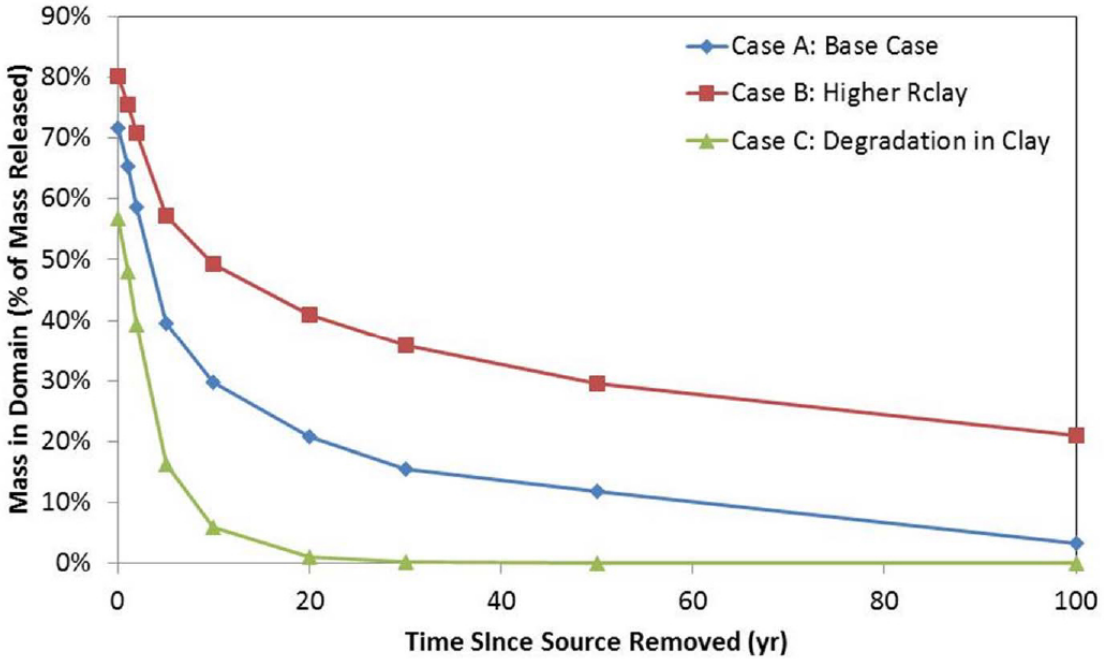

Figure 5-35. Mass distribution comparison for multi-layer scenarios showing remnant mass in domain.

Table 5-4: Mass distribution for multi-layer scenario.

	Base Case (R_{clay}=2, no degradation)			High Sorption Case (R_{clay}=10, no degradation)			Degradation Case (R_{clay}=2, $t_{1/2}$=5 yr in clay)		
Time (yr)*	Mass in Domain (% of total input)	Aquifer (%)	Aquitard (%)	Mass in Domain (% of total input)	Aquifer (%)	Aquitard (%)	Mass in Domain (% of total input)	Aquifer (%)	Aquitard (%)
0	71.7	50.7	49.3	80.1	39.3	60.7	56.9	60.6	39.4
1	65.2	43.0	57.0	75.5	31.6	68.4	48.1	54.2	45.8
2	58.7	35.9	64.1	70.9	25.2	74.8	39.4	48.0	52.0
5	39.5	13.9	86.1	57.3	10.2	89.8	16.4	20.1	79.9
10	29.7	8.1	91.9	49.3	6.4	93.6	5.9	11.1	88.9
20	20.9	6.1	93.9	40.8	3.9	96.1	1.0	8.0	92.0
30	15.5	5.3	94.7	35.8	2.9	97.1	0.2	7.0	93.0
50	11.8	4.3	95.7	29.6	2.0	98.0	0.010	5.7	94.3
100	3.3	2.9	97.1	21.0	1.5	98.5	0.000	-	-

5.4.3 Random Clay Layer Type Site

What was done

- **Why**: Develop Type Sites for multi-layer porous media settings.
- **Hydrogeologic Setting**: Twelve random thin suspended clay layers in sand unit overlying clay aquitard. Groundwater seepage velocity: ~110 meters per year. Retardation factor in clay = 2.
- **Numerical Model**: HydroGeoSphere
- **Model Domain:** 500 meters in X direction and 10 meters thick sand unit with random clay layers, 5 meter thick clay aquitard on bottom.
- **Key Processes:** Matrix diffusion only.
- **Time Domain:** Source loading from four DNAPL pools for 10 years; release from low k zone out to 100 years.
- **What Happened:** Over three million nodes were required to simulate this system, showing the challenges in modeling matrix diffusion with conventional groundwater transport modeling techniques. The Random Clay Layer Type Site showed a range in plume tailing behavior, depending on relative positions of the well screens to the clay zones, but show that even thin clay layers can cause appreciable tailing for decades, while the thicker aquitard, or a thicker clay layer(s), can cause tailing for much longer periods

Thumbnail description of key figures and tables

Figure 5-36. Model domain for random clay layer Type Sites.

Figure 5-37: ***Base Case (random clay layers****) Type Site;, R=2, no degradation, 12 Z vs. X plots*

Figure 5-38: ***Base Case (random clay layers)*** *Type Site, R=2, no degradation, 5 concentration vs. time plots*

As an illustrative example of a more complex scenario, a simulation was conducted for a scenario with suspended thin clay layers (0.4 to 0.8 m thick) in the aquifer along with an underlying clay aquitard (**Figure 5-36a**). This is similar to the scenario provided by Parker et al. (2008) but over a larger domain size and with parameters consistent with the base case values used in the two-layer and multi-layer scenarios (**Table 5-2**). Again very tight grid discretization is required (**Figure 5-36b**), in this case the grid had over 3.3 million nodes (NX=2501, NY=2, NZ=661). Adaptive time-stepping was applied based on concentration changes with an initial time step of 0.01 days , maximum change of 1% of the initial source concentration and maximum allowable time step of 0.5 days. This scenario required a simulation time of about 40 hours on a Workstation with an i7 2.67 GHz CPU and 12GB RAM. All of the simulations in this report are conducted for 2-D vertical cross-section model domains, since the array sizes and simulation times for extending these to fully 3-D simulations would be prohibitive due to computational limitations given the need to use very fine grid discretization and time-stepping to avoid numerical dispersion and accurately capture diffusion processes in the low k zones. However this is not expected to represent a major limitation since the layering /

heterogeneity in sediments is generally dominant in the vertical direction and therefore is well represented in 2-D vertical cross-section simulations.

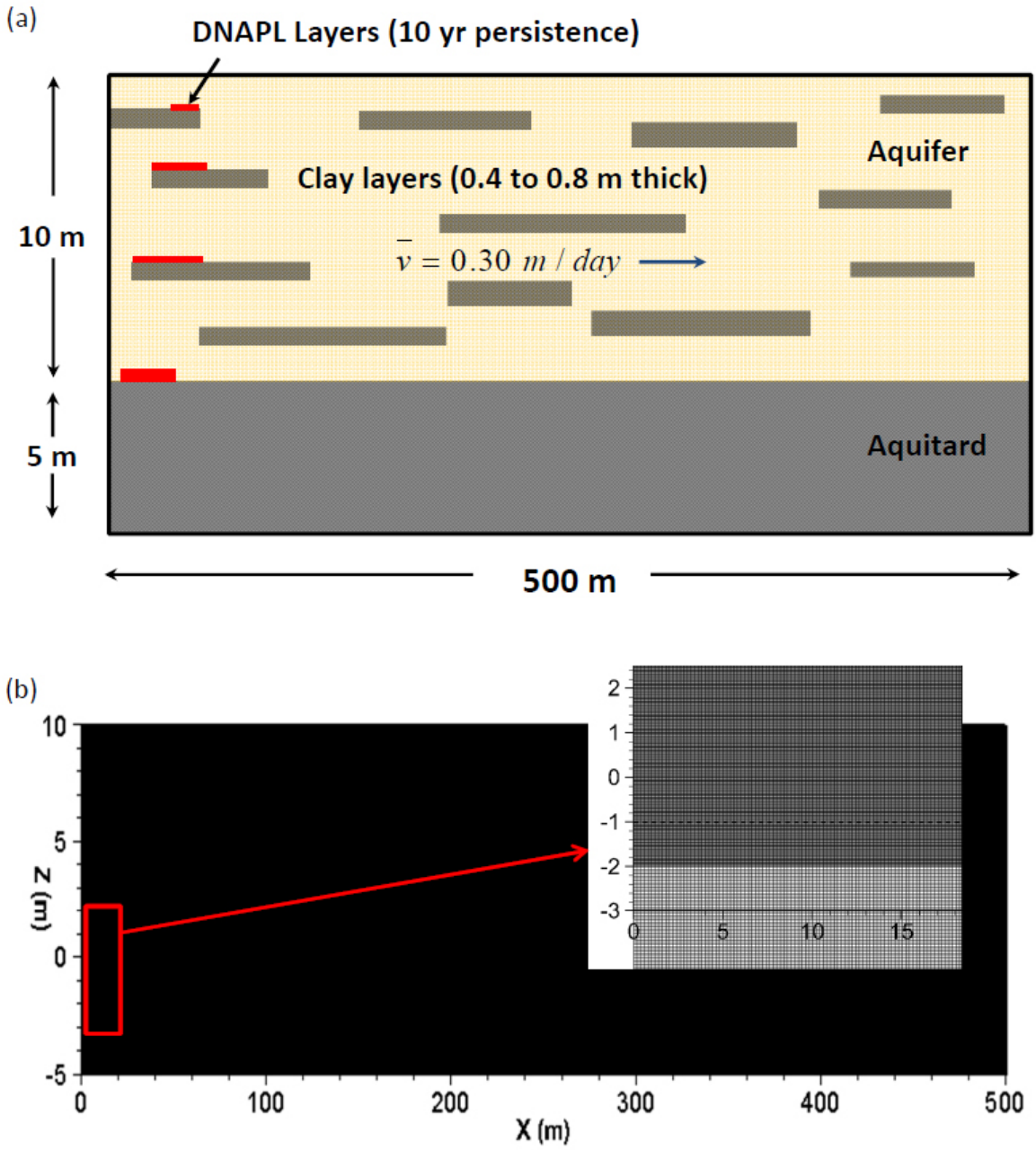

Figure 5-36: (a) model domain, and (b) grid discretization for HydroGeoSphere simulation of random multi-layer scenario with thin suspended clay layers and underlying aquitard.

For this scenario, the source is assumed to consist of thin DNAPL layers perched on several of the clay layers near the upgradient end of the domain, which would be the case for DNAPL released at surface and being impeded by these capillary barriers, with some DNAPL reaching the underlying aquitard. As in the previous simulations the DNAPL source is assumed to be present for 10 years before being completely removed. This timeframe is expected to be on the low end for most sites where DNAPL releases occurred decades ago. With an average groundwater velocity in the aquifer of about 0.3 m/day, the travel time through the 500 m long domain is about 4.5 years.

Figure 5-37 shows simulated contaminant contours at 1, 2, 5 and 10 years (while DNAPL is present) and then at times ranging from 1 to 100 years following removal of the source. At 30 years following source removal, the plume still persists at appreciable concentrations throughout the full vertical extent of the aquifer, while by 50 years some vertical intervals have concentrations below $C/C_o=10^{-5}$ (corresponding to a concentration of about 0.010 mg/L, assuming source concentrations at solubility). By 100 years the plume persistence mainly occurs near the base of the aquifer due to diffusion out of the underlying aquitard, with mass release exhausted from the thin suspended clay layers, which are flushed on both the top and bottom. The thick clayey aquitard releases its stored mass more slowly than the thin suspended layers because only one surface is flushed, and there is much deeper diffused mass below the interface, directly affecting the mass flux across the interface. Plume tailing is also illustrated via breakthrough and elution curves in a hypothetical multilevel well at the downgradient boundary (Figure 38). These show a range in plume tailing behavior, depending on relative positions of the well screens to the clay zones, but show that even thin clay layers can cause appreciable tailing for decades, while the thicker aquitard, or a thicker clay layer(s), can cause tailing for much longer periods.

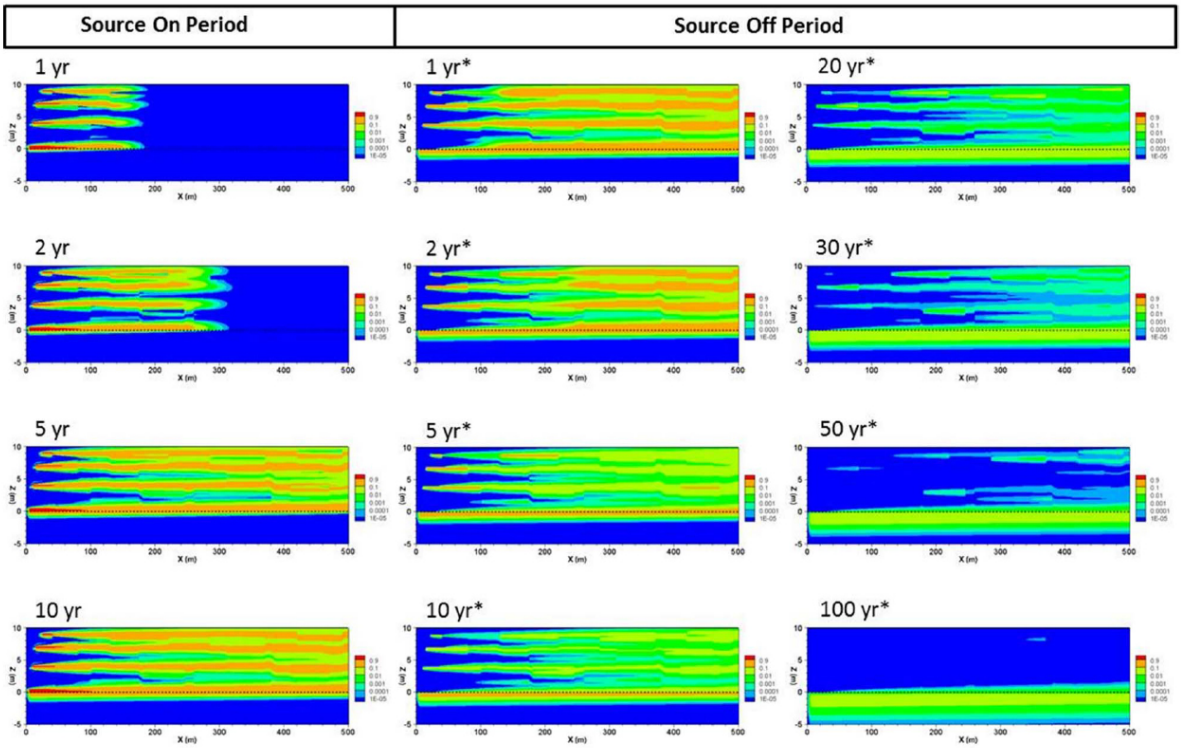

Figure 37

Figure 5-37. Random multi-layer scenario with thin suspended clay layers and underlying aquitard: plume distribution.

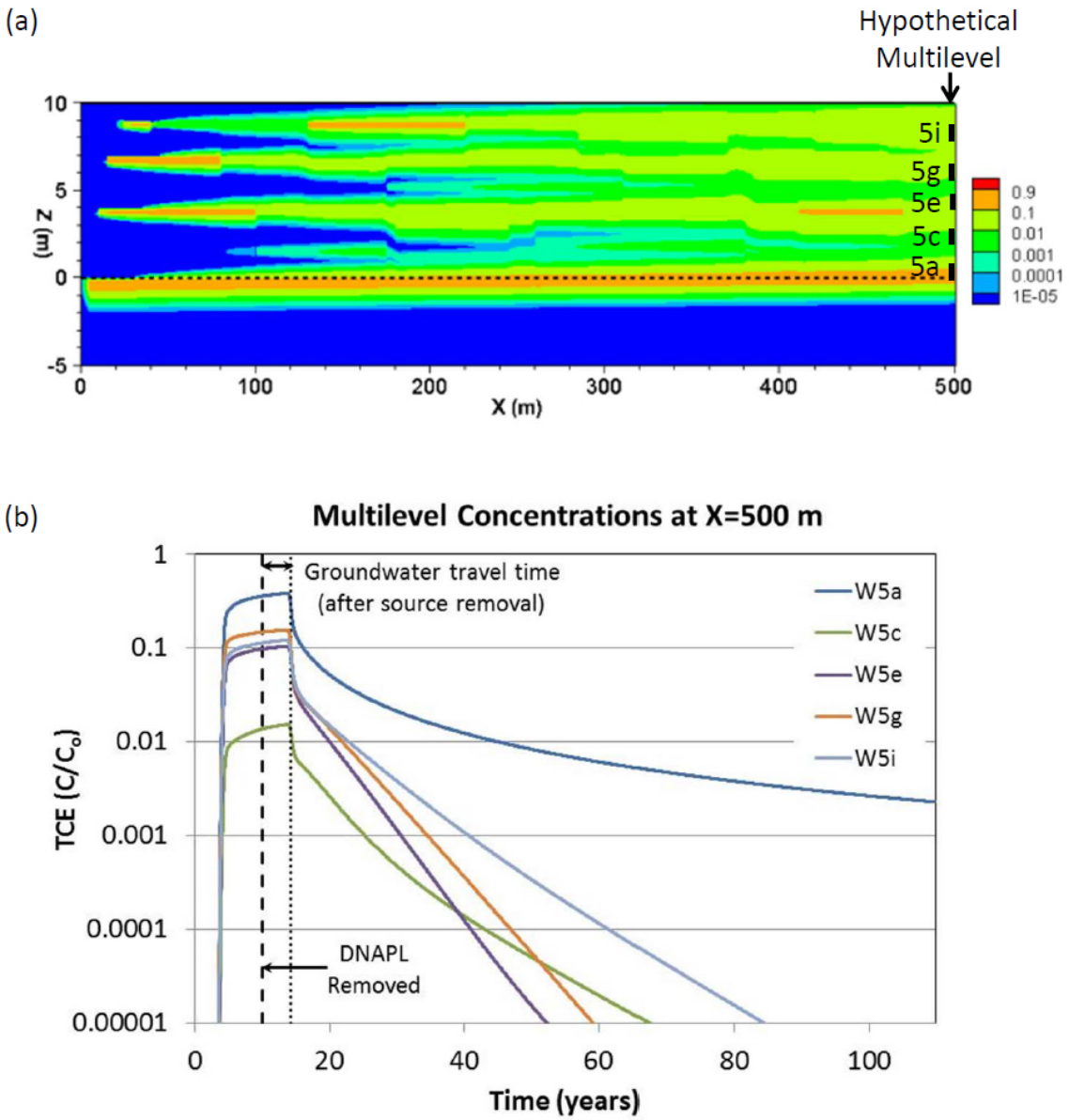

Figure 5-38. Simulated breakthrough and elution curves in hypothetical multilevel well (1 m screens) along the downgradient boundary at X=500 m for random multi-layer scenario with thin suspended clay layers and underlying aquitard.

5.5 MODEL BENCHMARKING WITH LABORATORY EXPERIMENTAL DATASETS

Further testing to show that the governing processes can be incorporated in numerical simulations was done by numerical modeling of datasets from well-controlled laboratory experiments.

The first experiment (CSU Thesis of L. Doner, 2008) involved a large sand tank containing suspended low permeability lenses of varying geometry with injection of fluorescein and bromide tracers for 22 days followed by flushing with clean water for another 100+ days. The fluorescein provided capability to visualize the diffusion and back diffusion processes while the bromide provided more quantitative data for quantifying the processes. Results of modeling of this experimental dataset are provided by Chapman et al. (2012) and briefly outlined below.

5.5.1 Sand Tank Visualization Tracer Experiment

What was done

- **Why**: Compare numerical model to visualization lab experiment
- **Hydrogeologic Setting**: Four thin suspended clay layers in sand unit.
- **Numerical Model**: HydroGeoSphere, FEFLOW, MODFLOW/MT3D
- **Model Domain:** 1.1 meters in X direction and 0.84 meters in Z direction.
- **Key Processes:** Matrix diffusion only.
- **Time Domain:** Source loading for 26 days, experiment and simulations out to 126 days.
- **What Happened:** All three models were able to match the experimental matrix diffusion experiment results, but extremely high spatial and temporal discretization was required. For HydroGeoSphere, for example, ~25,000 nodes were required to simulate this research laboratory experiment.

Thumbnail description of key figures and tables

Figure 5-39. Photograph of sand tank.

Figure 5-40: Experimental results showing (a) bromide and (b) fluorescein breakthrough

Figure 5-41: Photos showing visualization of tank experiment

Figure 5-42: Grid discretization for HydroGeoSphere, FEFLOW, MODFLOW/MT3D

Figure 5-43: Plots showing hydraulic head, flow pathlines from HydroGeoSphere simulation

Figure 5-44: Graphs comparing experimental and simulated bromide and fluorescein tracer arrival and elution

Figure 5-45. Experimental versus simulated bromide mass balance using HydroGeoSphere

Figure 5-46. Simulated concentration contours using HydroGeoSphere

Figure 5-47. Graphs comparing simulated tracer arrival and elution for the three codes (HydroGeoSphere, FEFLOW and MODFLOW/MT3DMS).

Table 5-5: Input parameters for numerical modeling.

The laboratory-scale sand tank used for the back diffusion visualization and tracer experiment was comprised of a metal frame that supports two sheets of plate glass separated by Plexiglas™ spacers (**Figure 5-39**). A continuous rubber gasket with silicon vacuum grease provides a seal between the glass and spacers. The tank was filled with transmissive sand comprised of well sorted quartz sand (US Silica ; F-95 “Ottawa Sand”) with four suspended low permeability clay layers comprised of unamended sodium bentonite (Black Hills Bentonite Company). The upper three layers (A to C) were hydrated before emplacement while the lower layer (D) was placed dry and allowed to hydrate in place. Flow through the tank was controlled with an ISMATEC™ peristaltic pump (influent) and a constant head siphon (effluent). The top of the tank was open to the atmosphere. The flow rate for the first 10 days was about 0.9 mL/min, and then

increased to 1.5 mL/min and held constant thereafter. De-aired tap water containing 400 mg/L fluorescein and 90 mg/L bromide was flushed through the tank for the first 22 days. Subsequently, flushing continued without tracers for an additional 100 days. Throughout the experiment, influent and effluent samples were collected, stored at 4°C, and analyzed for fluorescein and bromide at the conclusion of the experiment. Fluorescein analysis was conducted with an Ocean Optics USB2000 temperature compensating spectrometer with reflectance probe and software supplied by Ocean Optics and 5 mL test tubes. Bromide was analyzed using a Fisher Scientific solid-state bromide ion selective electrode and 10 mL sample vials. Photos were taken with a Nikon D50 SLR digital camera, with fluorescein visualization accomplished using three ultraviolet light bulbs set up at the sides and base of the experiment as well as a suitable flash function on the camera. Doner (2008) provides more details on the sand tank experiment.

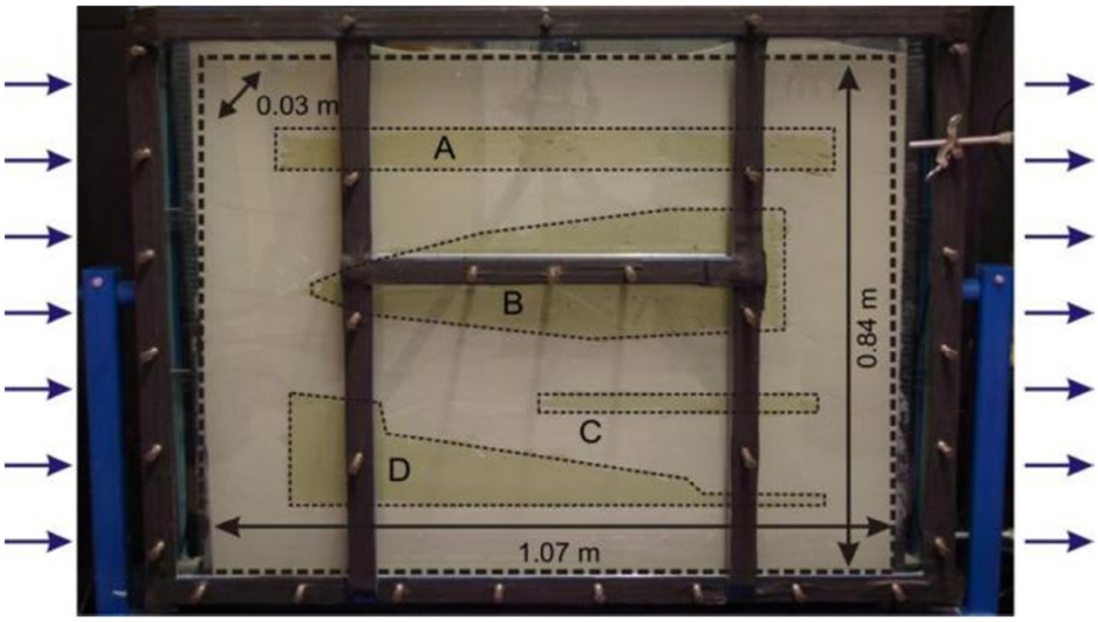

Figure 5-39. Photograph of sand tank for dual tracer study with darker bentonite zones surrounded by lighter sand and assumed geometry of clay layers for incorporation in numerical simulations (from Chapman et al., 2012).

Results of experimental measurements of bromide and fluorescein concentrations on influent and effluent samples are plotted in **Figure 5-40**. Both analytes could be detected over a greater than 3 OoM range. The mean travel time derived from evaluation of the arrival curves at the outflow boundary (i.e. arrival of C/C_o=0.5) is about 7 days, which is the most robust measure of groundwater flow velocity through the tank. However, this is complicated since solute arrival is expected to be delayed due to mass loss via diffusion into the clay zones, and actual flow paths are longer on average due to divergence around the clay zones. **Figure 5-41** shows photos from selected times during the input (day 0-22) and elution (day 22-end) phases, which provide unique visualization of back diffusion processes (a movie clip from the experiment is available at http://www.engr.colostate.edu/CCH/research.html).

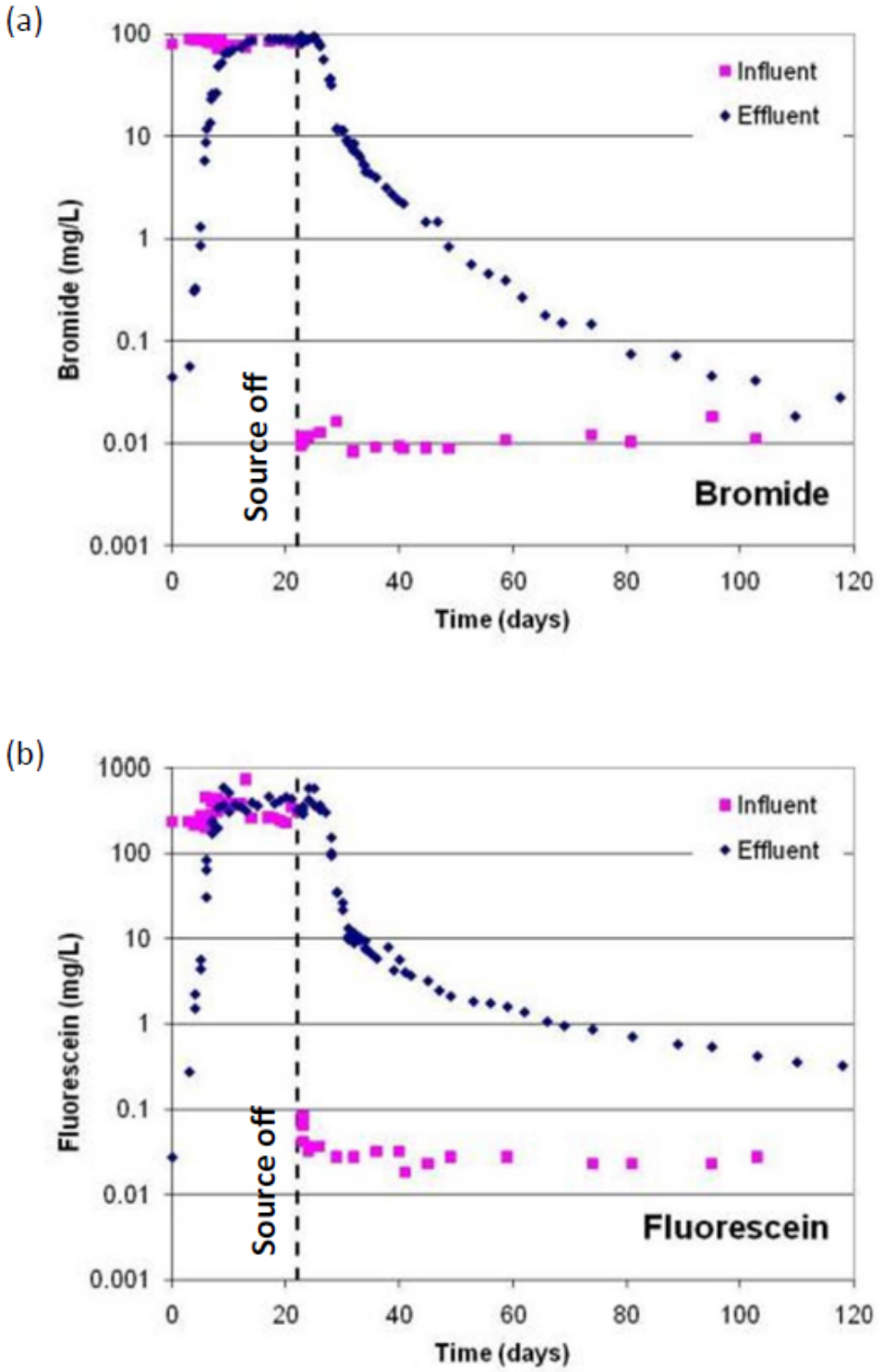

Figure 5-40. Experimental results showing (a) bromide and (b) fluorescein breakthrough and elution curves measured in influent and effluent during the dual tracer sand tank study (from Chapman et al., 2012).

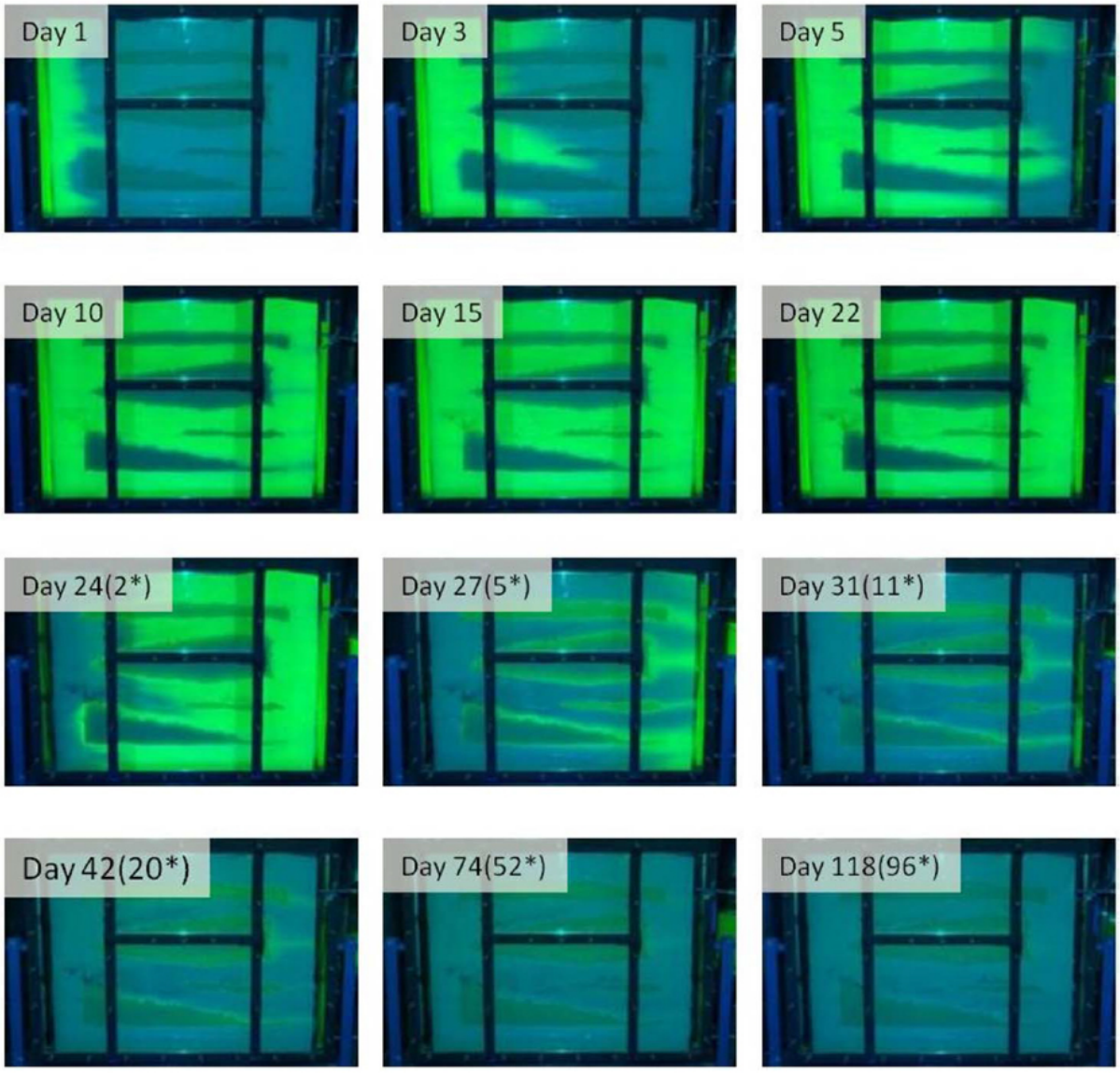

Figure 5-41. Photos showing visualization of the tracer study experiment via fluorescein at selected times during the 22-day loading phase at 1, 3, 5, 10, 15 and 22 days, and during the flushing phase at 2, 5, 11, 20, 52, and 96 days after termination of source input (from Chapman et al., 2012).

5.5.2 Numerical Simulation of Sand Tank Visualization Tracer Experiment

Three numerical models were used to simulate the sand tank experiment: (1) HydroGeoSphere, a finite element model largely used in the research domain (Therrien and Sudicky 1996; Therrien et al. 2010) but also commercially available; (2) FEFLOW v6.0, a powerful finite element model for flow and solute and/or heat transport processes (Trefry and Muffels, 2007), and (3) MODFLOW-2005 and transport code MT3DMS (Zheng and Wang, 1999) (Visual MODFLOW v2009.1 interface), a finite difference

model and probably the most widely used model for groundwater flow and solute transport. The key requirement for simulating contaminant transport in scenarios involving low k zones is use of fine spatial and temporal discretization to capture the system geometry and concentration gradients driving diffusion processes.

For the simulations, clay zone geometry was digitized from experimental photos (**Figure 5-39**). Tight grid discretization was required near interfaces with and within the low k zones to accurately capture diffusion processes. Adequate spatial and temporal discretization must also be applied to ensure solution stability in transmissive zones, including satisfying grid Peclet and Courant criteria (e.g. Daus et al., 1985; Anderson and Woessner, 1992; Zheng and Bennett, 1995) depending on the numerical scheme. Flow was controlled via constant head boundaries at the left and right sides of the domain while the top and bottom boundaries were no-flow. Heads were set for two stages to emulate the experimental flow conditions, using a trial-and-error procedure, which was necessary due to the more complicated geometry which prevented direct calculation. A constant source (C_o=1.0) was applied for a 22-day period along the influent boundary and then the source was instantaneously removed allowing clean water (C_o=0) to flush through the domain for the remainder of the simulation period.

Table 5-5 provides the input parameters used for simulations, which were set to provide as much consistency as possible with experimental conditions or estimated from the literature. For the simulations the only difference between bromide and fluorescein was in the free-solution diffusion coefficients. Fluorescein may also sorb slightly (Sabatini and Austin, 1991) while bromide sorption should be negligible; however for simulation purposes no sorption was applied which produced good fits to the experimental data.

Table 5-5: Input parameters for numerical simulations of laboratory sand tank experiment. Values in brackets were used for the model comparisons (from Chapman et al., 2012).

Parameter	Symbol	Value	Units	Notes
Flow Properties				
sand hydraulic conductivity	K_{sand}	2.4E-04	m/s	calibrated to match experimental flow rate
clay hydraulic conductivity	K_{clay}	1.0E-10	m/s	assumed (negligible flow in clay)
sand porosity	ϕ_{sand}	0.45 (0.40)	-	calibrated to fit tracer arrival curve
clay porosity	ϕ_{clay}	0.60 (0.50)	-	calibrated to fit tracer elution curve
total inflow / outflow (day 0-10)	Q1	0.9	mL/min	experimental (measured day 10)
total inflow / outflow (day 10-end)	Q2	1.5	mL/min	experimental (average day 10-end)
average horizontal hydraulic gradient (day 0-10)	i_1	0.0037	-	calibrated to match experimental flow rate
average horizontal hydraulic gradient (day 10-end)	i_2	0.0063	-	calibrated to match experimental flow rate
Source Conditions				
input concentration	C_o	1.0	-	compare with normalized lab values
source duration	T	22	days	experimental condition
Contaminant Transport				
free-solution diffusion coefficient	D_o	20.1E-10 (bromide) 5.5E-10 (fluorescein) (13.0E-10)	m^2/s	Literature values
sand tortuosity	τ_{sand}	0.45 (0.40)	-	assumed (same as porosity)
clay tortuosity	τ_{clay}	0.60 (0.50)	-	assumed (same as porosity)
sand retardation factor	R_{sand}	1.0	-	assumed (no sorption)
clay retardation factor	R_{clay}	1.0	-	assumed (no sorption)
sand degradation rate	λ_{sand}	0	day^{-1}	assumed (no degradation)
clay degradation rate	λ_{clay}	0	day^{-1}	assumed (no degradation)
longitudinal dispersivity	α_L	0.02	M	assumed
transverse vertical dispersivity	α_{tv}	0.001	m	assumed

The following describes the model conditions specific to each of the three models. HydroGeoSphere was selected as the base case for comparison to the other codes, given it has been rigorously tested for advection and diffusion transport scenarios against analytical solutions (Weatherill et al., 2008; Therrien et al., 2010) and field data (Chapman and Parker, 2005). Mesh generation was performed using Grid Builder (McLaren, 2005) to generate a triangular finite element mesh and define the clay layer geometry. The polygons shown in **Figure 5-39** were used as a guide for assigning clay layer geometry. The mesh was refined within and adjacent to the low k zones to resolve diffusion processes, with the resulting mesh containing about 24,600 elements (**Figure 5-42a**).

For the transport simulation, adaptive time-stepping was applied, with a target maximum allowable concentration change of 0.01 in a time step, and a maximum time step of 0.1 days was imposed to minimize potential for numerical dispersion. For FEFLOW the exact geometry of the polygons representing the clay layers was used by importing these as supermesh boundaries which were incorporated in the mesh generation process, thus the geometry (**Figure 5-42b to 5-42e**) differs slightly from HydroGeoSphere (**Figure 5-42a**) and MODFLOW (**Figure 5-42f).** Sensitivity analyses were conducted to examine effects of grid discretization on accuracy of the numerical solution, since the same geometry of the clay zones could be maintained with different discretization levels. A “base case” mesh was generated using the grid builder option within FEFLOW, using 5000 target elements (proposed number of elements within a non-refined grid) and a relative meshing density of 3 for the clay zones compared to the sand zones to resolve diffusion processes, with the resultant mesh containing about 7260 elements (**Figure 5-42b**).

Three additional cases were examined, one with finer grid discretization containing about 15,250 elements generated assuming 10,000 target elements and relative meshing density of 5 (**Figure 5-42c**) and two with coarser discretization, one with about 1440 elements generated assuming 1000 target elements and relative meshing density of 2 (**Figure 5-42d**) and one with about 720 elements generated assuming 500 target elements and relative meshing density of 2 (**Figure 5-42e**). For transport simulations adaptive time-stepping was used with a maximum time step of 0.1 days. For MODFLOW/MT3DMS, the clay layer geometry **(Figure 5-40f**) differs slightly due to rectangular grid limitations. A downside of the finite difference model used is that local grid refinement extends to the domain boundaries, and thus is not as efficient as with the finite element models. In this scenario a regular grid was used (**Figure 5-42f)** with a spacing of 0.01 m in both directions (84 rows x 107 columns). The layer thickness was set at 0.03 m representing the tank thickness. This orientation was used given the default grid limits of 500 rows x 500 columns x 60 layers. Several computational schemes are available within MT3DMS, all of which have inherent advantages and limitations (Zheng and Wang, 1999). The third-order total-variation-diminishing (TVD) scheme was used for the advective term in the transport simulation, which tends to minimize numerical dispersion and artificial oscillations but is computationally intensive. An initial time-step of 0.01 days, multiplier of 1.1 and maximum time-step of 0.1 days was applied.

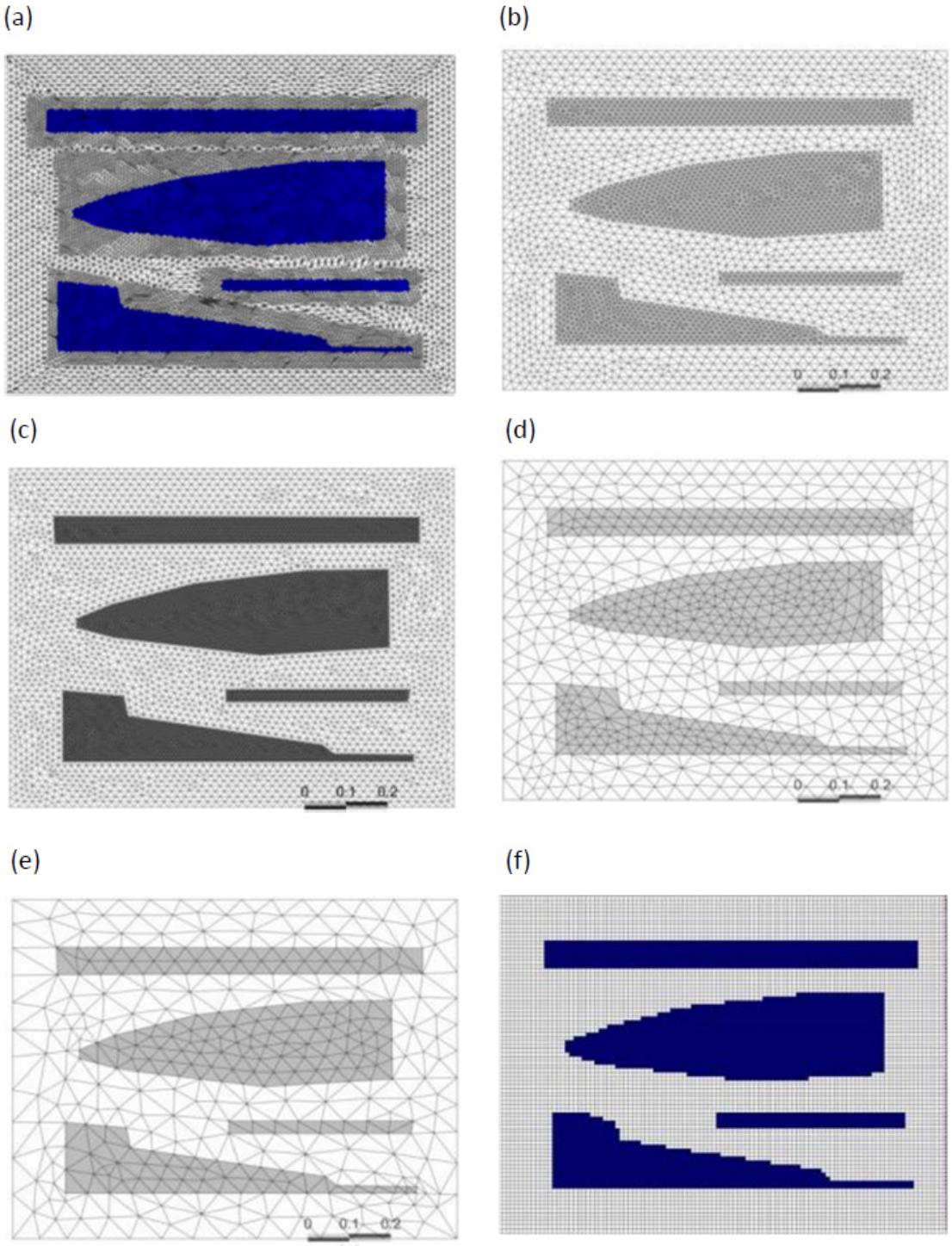

Figure 5-42. Grid discretization used for sand tank simulations: (a) HydroGeoSphere, (b) FEFLOW base case, and sensitivity analyses with (c) refined grid, (d) coarser grid, and (e) even coarser grid, and (f) MODFLOW/MT3DMS. Grid elements representing clay zones are highlighted (from Chapman et al., 2012).

The HydroGeoSphere code was first used in simulations of the sand tank experimental data using the domain and grid shown in **Figure 5-42a**. Experimental flow rates were used to constrain the sand hydraulic conductivity (K_{sand}) and average hydraulic gradients (i) for the two periods of different flow rates (**Table 5-5).** Therefore the flow system and geometry of the low k zones and source input period were highly constrained via the experimental conditions to allow assessment of how well the numerical simulations can capture the mass transfer / diffusion processes. Simulated hydraulic heads and flow pathlines for particles released from the left boundary (**Figure 5-43)** show (as expected) nearly all flow occurs in the sands diverting around the low k clay layers. The experimental bromide and fluorescein effluent results are plotted in **Figure 5-44** as relative concentrations normalized to source concentrations (C/C_o) for comparison with numerical simulation results. Using the parameters provided in Table 5, the simulated arrival and elution curves (**Figure 5-44**) provide an excellent match with experimental data for both tracers, with the difference in free-solution diffusion coefficients appearing to account for the minor differences in behavior. Slightly higher fluorescein tailing at late time in the experiment compared with bromide may be caused by fluorescein sorption effects (Sabatini and Austin, 1991) although these effects appear minor. The simulated effluent concentrations represent flux-averaged values based on the simulated nodal concentrations and Darcy flux along the boundary.

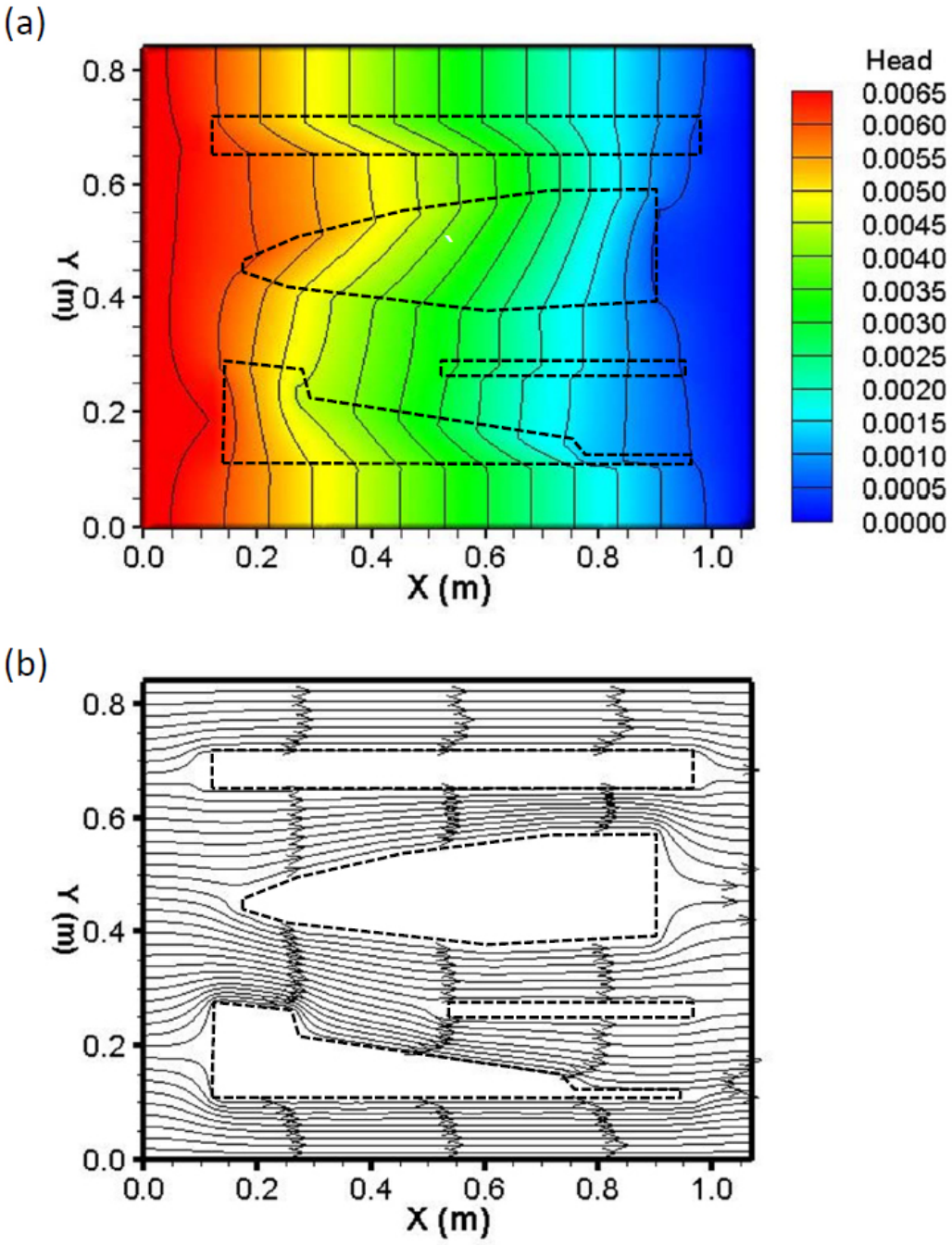

Figure 5-43. Plots showing (a) hydraulic head contours for flow conditions for the second flow stage (after day 10), and (b) flow pathlines from particles released at the upgradient end based on the simulated flow field in HydroGeoSphere (from Chapman et al., 2012).

Average linear groundwater velocity, estimated from the average hydraulic gradients and sand hydraulic conductivity and porosity (**Table 5-**5), was 0.17 and 0.29 m/day for the early (day 0-10) and later (day 10-end) stages, respectively. This indicates a 6.3 day travel time across the tank during early stage, which is slightly faster than the observed mean travel time from the tracer arrival curves of about 7 days, with the difference attributed to mass loss from the sands to the clay lenses. During the later stage following source removal, the travel time is about 3.7 days, which would be the expected time for hydraulic flushing of the tracers through the tank (neglecting dispersion) after source removal. Tracer tailing beyond this time (**Figure 5-44b**) is caused by back diffusion from the clay lenses. The mass balance for bromide (**Figure 5-45**) shows good agreement between experimental and simulation results, showing the slow decline in remnant mass after the flushing phase due to back diffusion from the clay lenses.

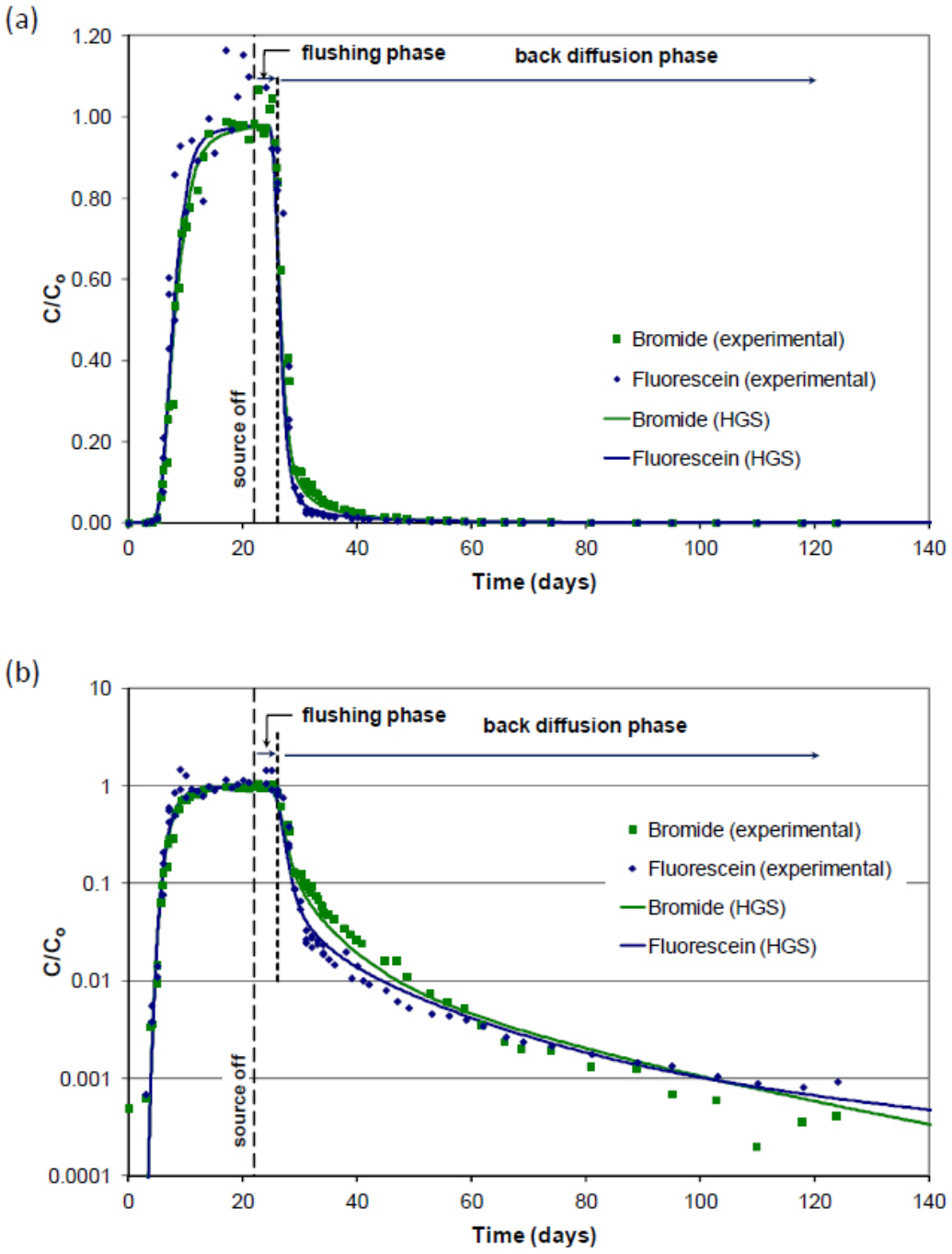

Figure 5-44. Graphs comparing experimental and simulated bromide and fluorescein tracer arrival and elution curves at the effluent end (flux averaged concentrations) using HydroGeoSphere, with normalized concentrations plotted on (a) linear and (b) logarithmic scales (from Chapman et al., 2012).

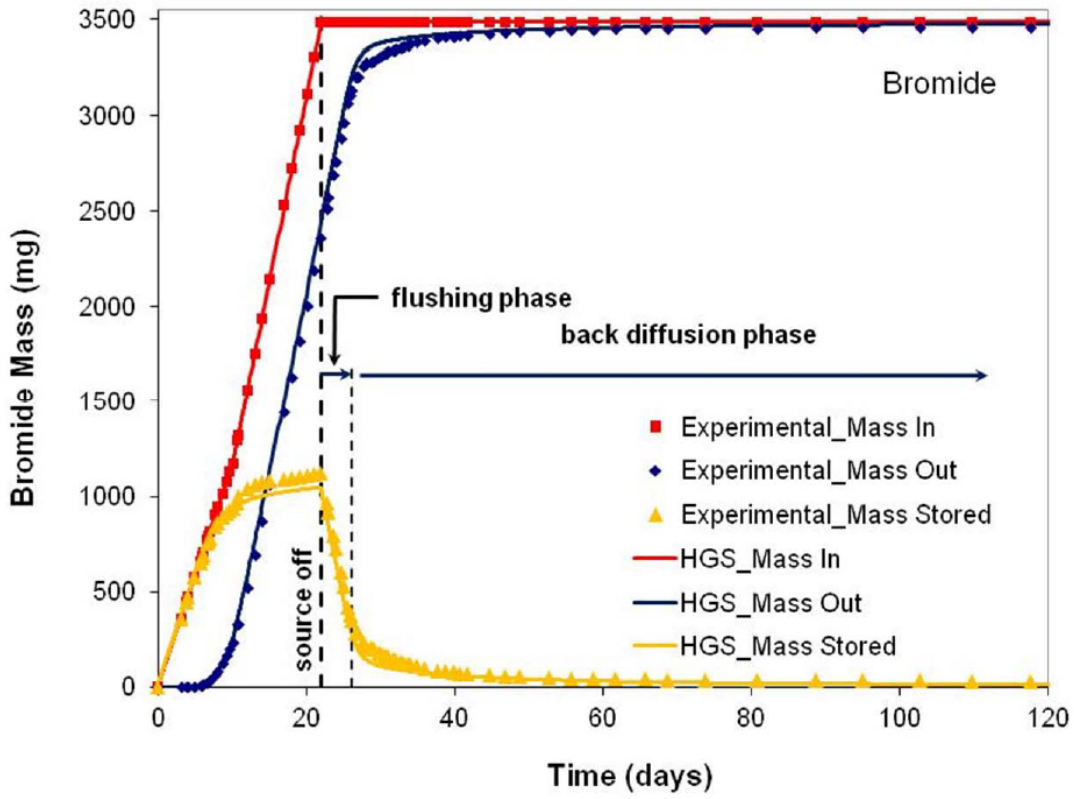

Figure 5-45. Experimental versus simulated bromide mass balance using HydroGeoSphere showing bromide mass in influent and effluent and mass stored in the system (from Chapman et al., 2012).

Figure 5-46 shows simulated concentration contours from HydroGeoSphere plotted at similar times as the experimental photos (**Figure 5-41)** and also at later times beyond the experimental period. Direct comparison is complicated as the range of visual fluorescein detection is not as sensitive as the plotted ranges. However the experimental and simulated concentrations show good general agreement, clearly illustrating diffusive "loading-up" of the low k zones, and subsequent slow release from these zones via back diffusion. The experimental and simulated elution curves clearly demonstrate tailing associated with back diffusion processes, with tailing at nearly 3 OoM of input concentrations for both bromide and fluorescein at 100 days, nearly 80 days after source input was stopped (**Figure 5-44b**), which is nearly 4 times longer than the source duration, even though in this case the low k zones are of limited extent and flushed on all sides (**Figure 5-43b**). Simulations suggest it would take about 200 days for effluent concentrations to decline to 4 OoM below influent concentrations (**Figure 5-47b**), a factor of 10 times longer than the input period. Such low levels would still be consequential for chlorinated solvents such as TCE, which typically exhibit 5 to 6 OoM differences between aqueous solubility and regulatory levels. At most sites, sources have been present for decades indicating the long-term potential for back diffusion to cause consequential plume tailing.

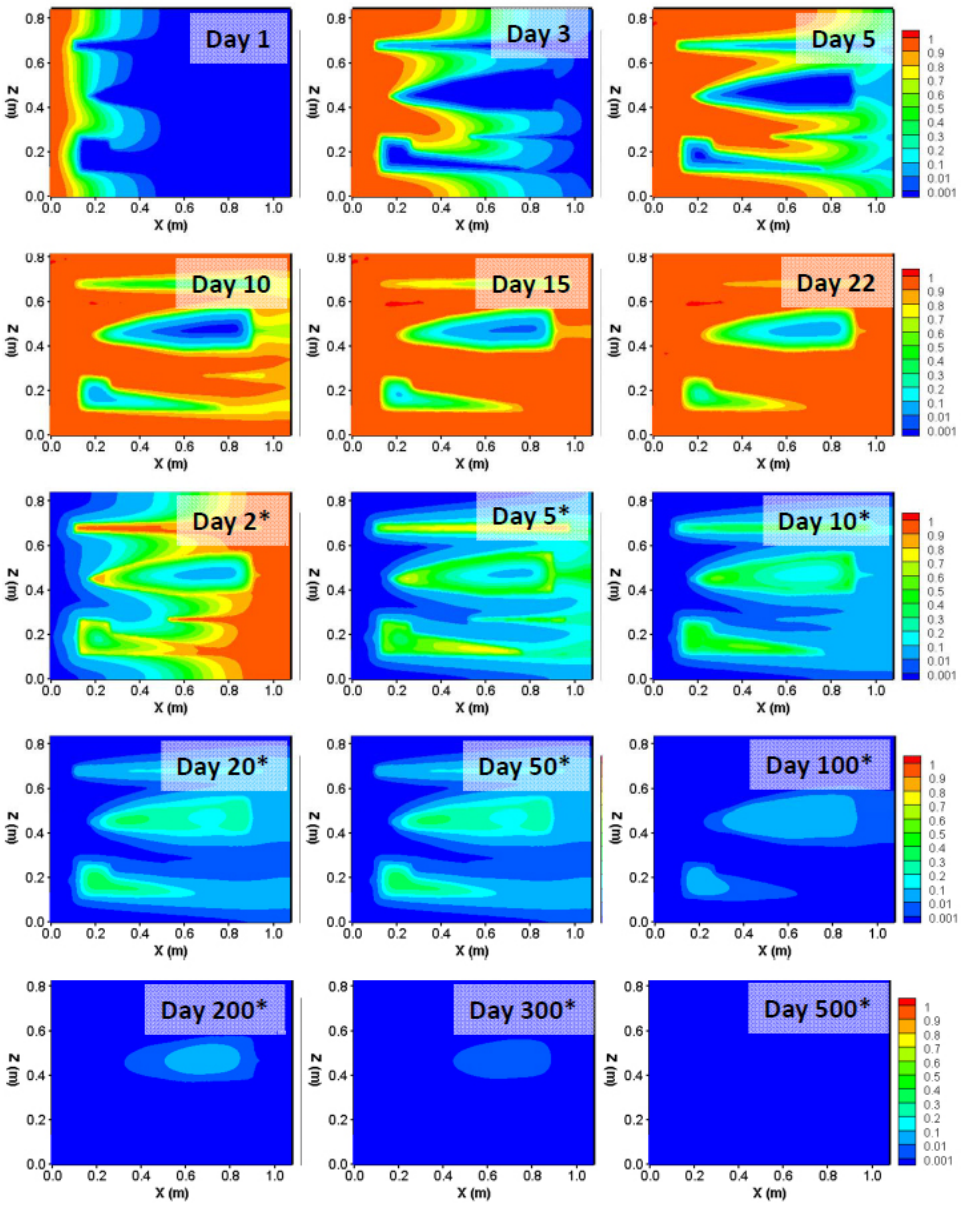

Figure 5-46. Simulated concentration contours using HydroGeoSphere at similar times as the experimental photos during the loading phase at 1, 3, 5, 10, 15 and 22 days and during the flushing phase at 2, 5, 10, 20, 50, and 100 days after termination of source input. Later simulation results at 200, 300 and 500 days are also shown (from Chapman et al., 2012).

Figure 5-47 shows a comparison of simulated tracer arrival and elution curves for all three codes. For this comparison, an average value was used for the free-solution diffusion coefficient and initial estimates of sand and clay porosity and tortuosity were applied (**Table 5-5).** For FEFLOW and MODFLOW/MT3DMS, concentrations and groundwater flux were extracted at individual nodes spanning the effluent boundary by setting these as observation points, and then flux averaged concentrations were calculated in an Excel spreadsheet. Simulation results using FEFLOW with the initial grid (**Figure 5-42b**) were nearly identical to HydroGeoSphere. Run times on a workstation with an Intel i7 CPU at 2.67 GhZ and 12 GB of RAM were about 10 minutes for the HydroGeoSphere and base case FEFLOW simulations. Results for the scenario with a refined grid (**Figure 5-42c**) showed no notable difference indicating the initial grid discretization was adequate to capture the mass transfer / diffusion processes. For the scenario with a coarser grid (**Figure 5-42d**) the simulation results deviated from the base case indicating this discretization was not adequate to accurately capture these processes. With an even coarser grid (**Figure 5-42e**) the results (not plotted) showed much poorer comparison indicating inadequate grid discretization. Such a sensitivity analysis provides an excellent means to assess adequacy of spatial and temporal discretization. It is important to emphasize the scale of this simulation and spatial discretization required to accurately capture the diffusion processes. The sand tank dimensions in cross-section were 1.07 m by 0.84 m, with clay lens dimensions on the order of a few cm up to about 20 cm in thickness. Based on the overall clay (~0.26 m2) and sand (~0.64 m2) areas and base case FEFLOW discretization (**Figure 5-42b**) average element areas were 0.7 cm2 for the clay zones and 1.9 cm2 for the sand zones, which illustrates the high spatial discretization required to adequately capture the concentration gradients driving diffusive mass transfer over the experimental timeframes.

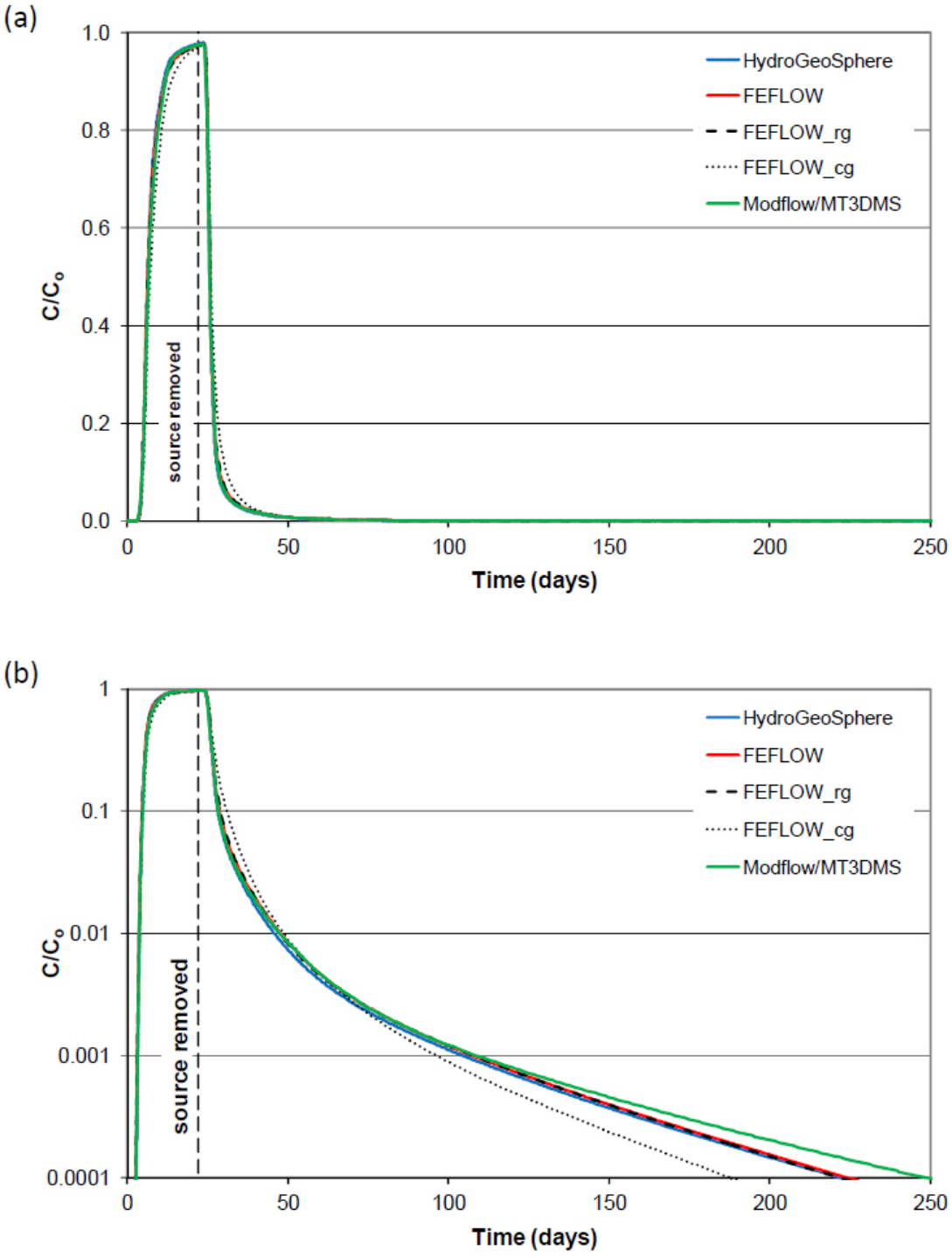

Figure 5-47. Graphs comparing simulated tracer arrival and elution for the three codes (HydroGeoSphere, FEFLOW and MODFLOW/MT3DMS). Results of sensitivity analyses using FEFLOW with a refined grid (rg) and coarser grid (cg) are also shown (from Chapman et al., 2012).

The MODFLOW/MT3DMS code with discretization shown in **Figure 5-42f** also provided a close match with HydroGeoSphere and FEFLOW results, with minor deviation at later times with slightly higher tailing (**Figure 5-47b**). This may be attributed to the slightly different clay layer geometry with the rectangular grid, and further refinement would likely improve the fit, but overall this shows the finite difference model can also accurately solve the governing equations with adequate spatial and temporal discretization. Run times for MODFLOW/MT3DMS were longer than the finite element models, about 25 minutes with the TVD scheme, where time steps remained well below the maximum specified of 0.1 days. It is likely that different numerical schemes and/or adjustment of time stepping parameters and convergence criteria would improve run times.

5.5.3 MultiLayer Tank Experiments

What was done

- **Why**: Compare numerical model to multilayer lab experiments
- **Hydrogeologic Setting**: Five 5-cm thick layers of sand bounded by 5 cm thick layers of silt. Seepage velocity from 0.3 to 0.41 meters per day.
- **Numerical Model**: HydroGeoSphere
- **Model Domain:** 1.0 meters in Z direction and 0.5 meters in X direction.
- **Key Processes:** Matrix diffusion, sorption, degradation.
- **Time Domain:** Source loading for 26 days, then experiments and simulations to 83 days.
- **What Happened:** All three models were able to match the experimental matrix diffusion experiment results, but extremely high spatial and temporal discretization was required. For HydroGeoSphere, for example, ~25,000 nodes were required to simulate this research laboratory experiment.

Thumbnail description of key figures and tables

Figure 5-48. Photograph of one of the multiple layer sand tanks

Figure 5-49. Numerical simulation domain and model

Figure 5-50. Experimental and model assumed influent concentrations for the multiple layer tank experiments

Figure 5-51. Simulated PCE contours for tank 1 (unamended silt layers), 10 Z by X concentration plots for various times.

*Figure 5-53. Experimental and simulated effluent concentrations for **bromide and TCE**, 10 Z by X concentration plots for various times.*

*Figure 5-54. Comparison of **bromide** mass balance for tank 1 (unamended) for (a) experimental, and (b) simulated conditions.*

*Figure 5-55. Comparison of **bromide** mass balance for tank 4 (unamended) for (a) experimental, and (b) simulated conditions.*

Figure 5-56. Comparison of simulated effluent concentrations for bromide and PCE for control tank and activated carbon (AC), and ZVI amended tanks.

Figure 5-57 Comparison of simulated effluent concentrations for bromide and TCE for control tank and AC, and ZVI amended tanks

Figure 5-58. Comparison of simulated PCE mass balances control tank and AC, and ZVI amended tanks

Figure 5-52. Experimental and simulated effluent concentrations for bromide and PCE.

Figure 5-44: Graphs comparing experimental and simulated bromide and fluorescein tracer arrival and elution

Figure 5-45. Experimental versus simulated bromide mass balance using HydroGeoSphere

Figure 5-46. Simulated concentration contours using HydroGeoSphere

Figure 5-47. Graphs comparing simulated tracer arrival and elution for the three codes (HydroGeoSphere, FEFLOW and MODFLOW/MT3DMS).

Table 6: Input parameters for numerical simulations of multilayer tank experiments.

The second set of experimental results simulated in this report consisted of a series of multilayer tank experiments conducted at CSU (Sale et al., 2007). These tank experiments involved layered sand tanks in which bromide (as a conservative tracer) and chlorinated solvents (either PCE or TCE) were injected into tanks that contained 5-cm thick layers of sand bounded by 5 cm thick layers of silt (**Figure 5-48**). A total of six tanks were prepared. In two tanks the silt layers were unamended (tanks 1 and 4), while two tanks had the silt amended with 1% powdered zero valent iron (ZVI) to enhance reaction processes (tanks 2 and 5) while two tanks had the silt amended with 1% powdered activated carbon (AC) to enhance sorption processes (tanks 3 and 6). Bromide was a conservative tracer in all of the tanks. PCE was used as the chlorinated compound in three of the tanks (tanks 1 to 3) while TCE was used in the other three tanks (tanks 4 to 6). Sale et al. (2007) provides more details on the experimental setups.

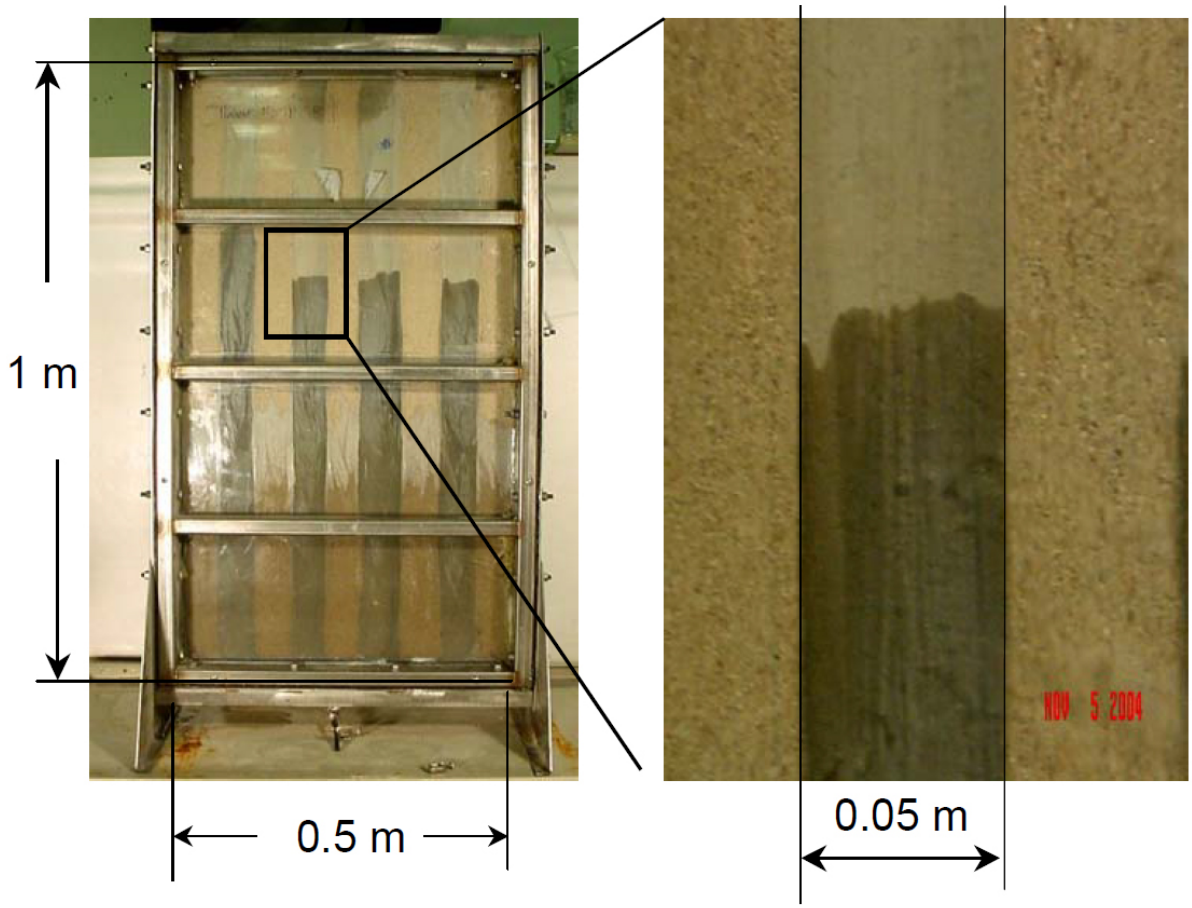

Figure 5-48. Photograph of one of the sand tanks in the multiple layer tank experiments (tanks were run vertically to limit settlement transverse to flow, as shown tanks are filling).

Simulations were done using the HydroGeoSphere code. **Figure 5-49 shows** the numerical model domain used to represent the tank experiments and Table 6 contains the model input parameters. Grid discretization applied was a uniform spacing of 0.01 m

in the Z-direction (flow direction) and 0.005 m in the X-direction (transverse to flow) to adequately discretize the clay layers to capture the diffusion in / out processes. The flow rate varied slightly between tanks so the specified head boundary conditions at the ends of the domain were adjusted for each experiment to capture the variations in flow.

Average linear groundwater velocity ranged from 0.31 to 0.40 m/day for the six tanks. **Figure 5-50** shows the experimental source input concentrations and step functions assigned in the model. Each tank was fed from the same reservoir for the bromide/PCE (tanks 1 to 3) and bromide/TCE (tanks 4 to 6) solutions. The PCE and TCE amended water (with bromide) solutions were driven through the tanks via an influent feed for 28 days. Subsequently, contaminants were removed from influent feed and steady flow was maintained in all of the tanks for an additional 55 days. Influent and effluent contaminant concentrations and flow rates were monitored as a function of time.

In the model, for the tanks amended with ZVI (tanks 2 and 5), PCE and TCE were both assumed to degrade in the silt layers only with a half-life of 10 days. No degradation was assumed to occur in the sand layers. For the tanks amended with AC (tanks 3 and 6), PCE and TCE retardation factors were estimated using the well-known K_{oc}-f_{oc} correlation equation taking the f_{oc} as the natural silt organic carbon content plus 1% to account for the added AC. This provided estimated retardation factors for the silt of R=14.5 for PCE and R=5.7 for TCE, compared to the values of R=4.2 for PCE and R=2.9 for TCE in the tanks that were not amended.

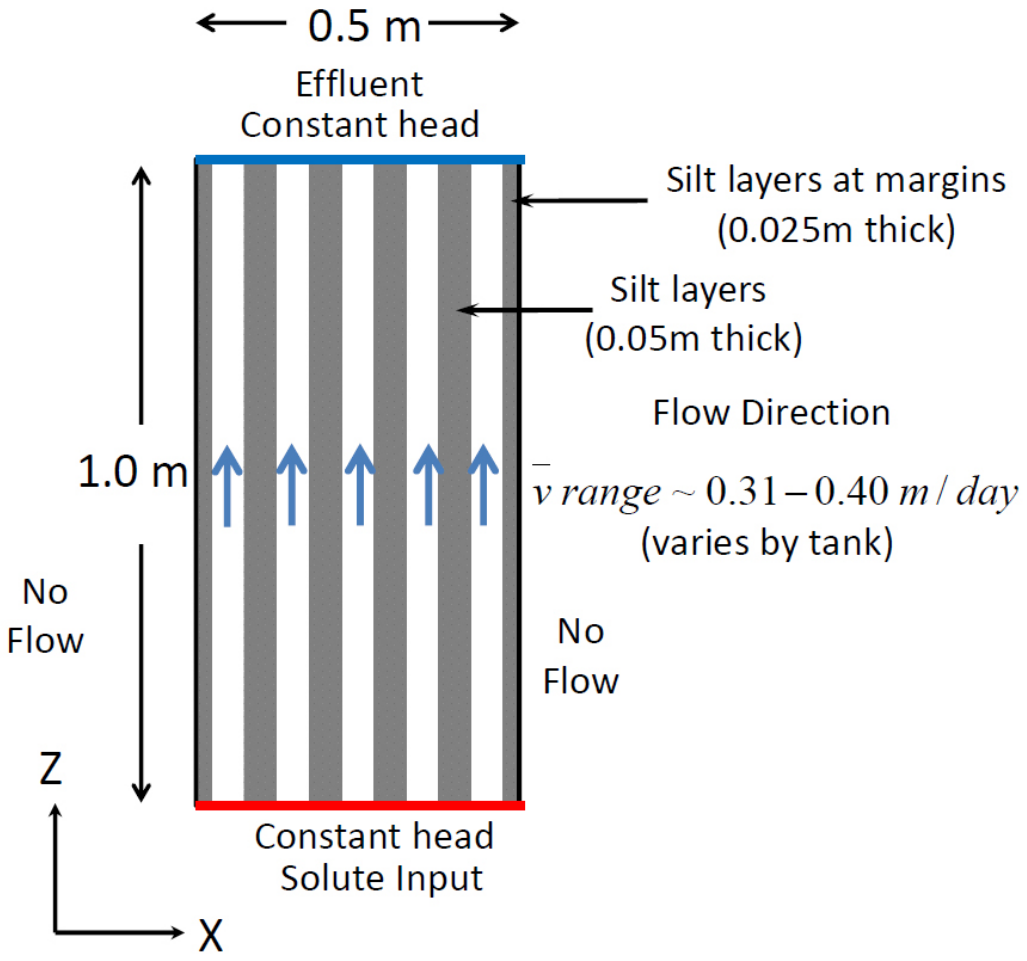

Figure 5-49. Numerical simulation domain and model set up for simulation of the multiple layer tank experiments using HydroGeoSphere

Table 6: Input parameters for numerical simulations of multilayer tank experiments.

Parameter	Symbol	Value	Units	Notes
Flow Properties				
sand hydraulic conductivity	K_{sand}	1.4E-04	m/s	
silt hydraulic conductivity	K_{silt}	1.7E-06	m/s	
sand porosity	ϕ_{sand}	0.36	-	
clay porosity	ϕ_{silt}	0.46	-	
sand bulk density	$\rho_{b\ sand}$	1.70	g/cm^3	
silt bulk density	$\rho_{b\ silt}$	1.60	g/cm^3	
average inflow / outflow	Q	0.48-0.62	mL/min	varies by tank
average hydraulic gradient	i	0.0091 – 0.0118	-	varies by tank
Source Conditions				
input concentration	C_o			See Figure 50
source duration	T	28	days	
Contaminant Transport				
free-solution diffusion coefficient	D_o	13.0E-10 (bromide) 9.4E-10 (PCE) 10.1E-10 (TCE)	m^2/s	Literature values
sand tortuosity	τ_{sand}	0.30	-	assumed
silt tortuosity	τ_{silt}	0.40	-	assumed
sand retardation factors	R_{sand}	1.0 (bromide) 2.1 (PCE) 1.7 (TCE)	-	estimated
silt retardation factors	R_{silt}	1.0 (bromide) 4.2 (PCE) 2.9 (TCE) 14.5 (PCE*) 5.7 (TCE*)	-	estimated * = AC amended tanks
sand degradation rate for PCE, TCE	λ_{sand}	0	day^{-1}	no degradation
silt degradation rate for PCE, TCE	λ_{silt}	0 (unamended, AC) 0.0693 (ZVI amended tanks)	day^{-1}	assumed
longitudinal dispersivity	α_L	0.01	m	assumed
transverse dispersivity	α_T	0.001	m	assumed

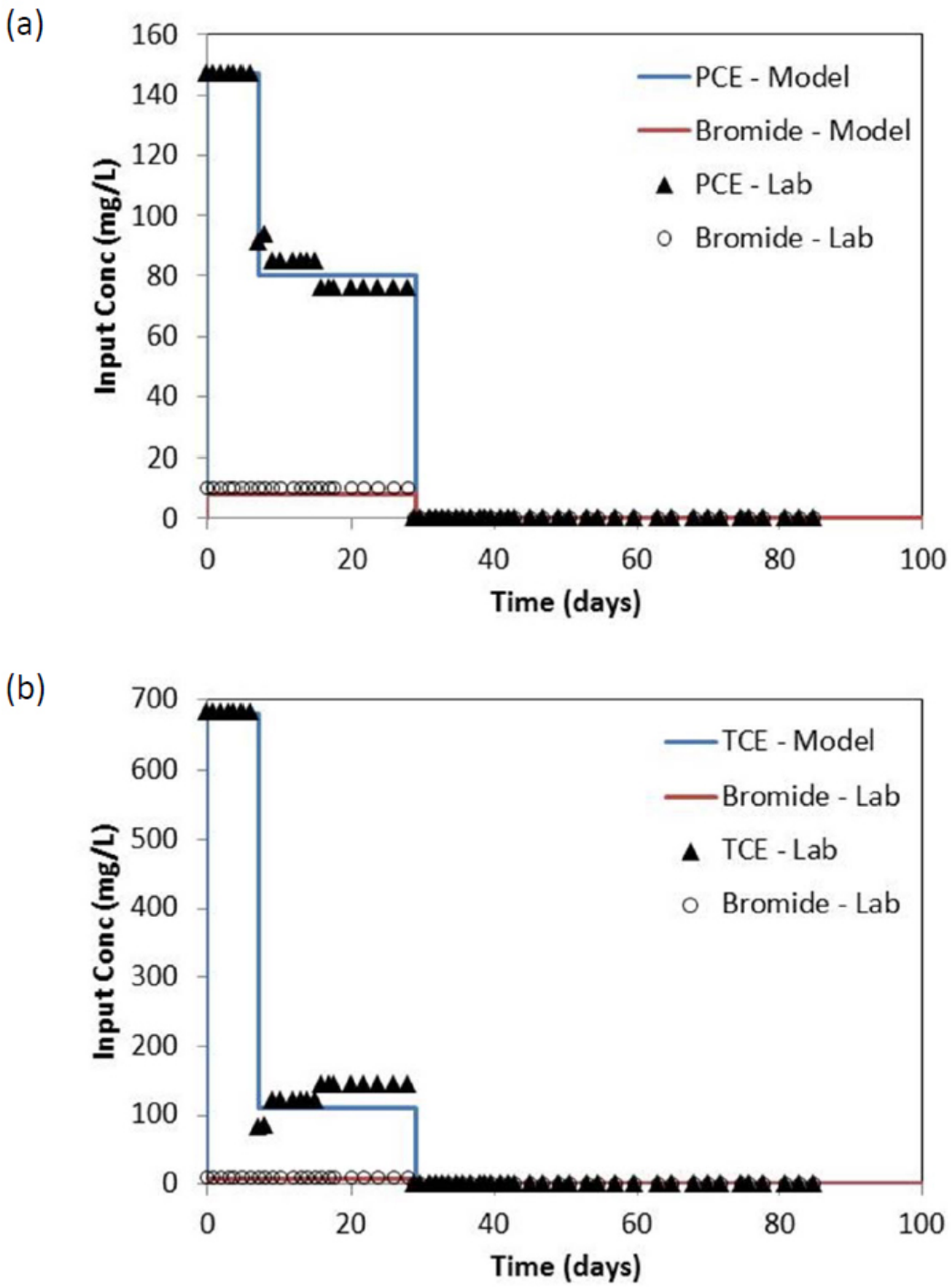

Figure 5-50. Experimental and model assumed influent concentrations for the multiple layer tank experiments.

Figure 5-51 shows an example of the simulation results for PCE in tank 1 (PCE / bromide with no amendments in the silt). These results show the thin silt layers were essentially loaded with PCE (>10 mg/L) by the end of the 28-day loading phase, and

also the expectation of long-term tailing due to slow back diffusion after the source feed was removed, with appreciable mass still present in the domain (PCE > 0.01 mg/L) at day 300 or 272 days after the source was shut off, representing a factor of nearly 10 times longer than the period the source was on. **Figure 5-52** shows the experimental versus simulated effluent concentrations for bromide (**Figure 5-52a**) and PCE (**Figure 5-52b)** for the 3 PCE tanks (unamended, ZVI, AC) and **Figure 5-53** for bromide (**Figure 5-53a**) and TCE (**Figure 5-53b**) for the 3 TCE tanks. Laboratory bromide data for the tanks with AC were erroneously high since the AC had high bromide background levels. **Figures 5-54 and 5-55** show comparisons of the bromide mass balances for the unamended tanks 1 and 4, respectively. Overall the preliminary numerical simulations reasonably match the trends in the experimental data. More analysis and simulations of the datasets is ongoing, particularly for the organics data. **Figures 5-56 and 5-57** show simulated bromide and PCE / TCE effluent concentrations for the six tanks. **Figures 5-58 and 5-59 show** the simulated PCE and TCE mass balances for the six tanks. For the scenarios with ZVI (tank 2, **Figure 5-58b;** and tank 5, **Figure 5-59b**) the total PCE / TCE mass degraded in the silt layers by reaction with ZVI is shown as the difference between the mass in and the mass out and mass stored, or at the longer term is the difference between the mass in and mass out, when the mass stored is negligible.

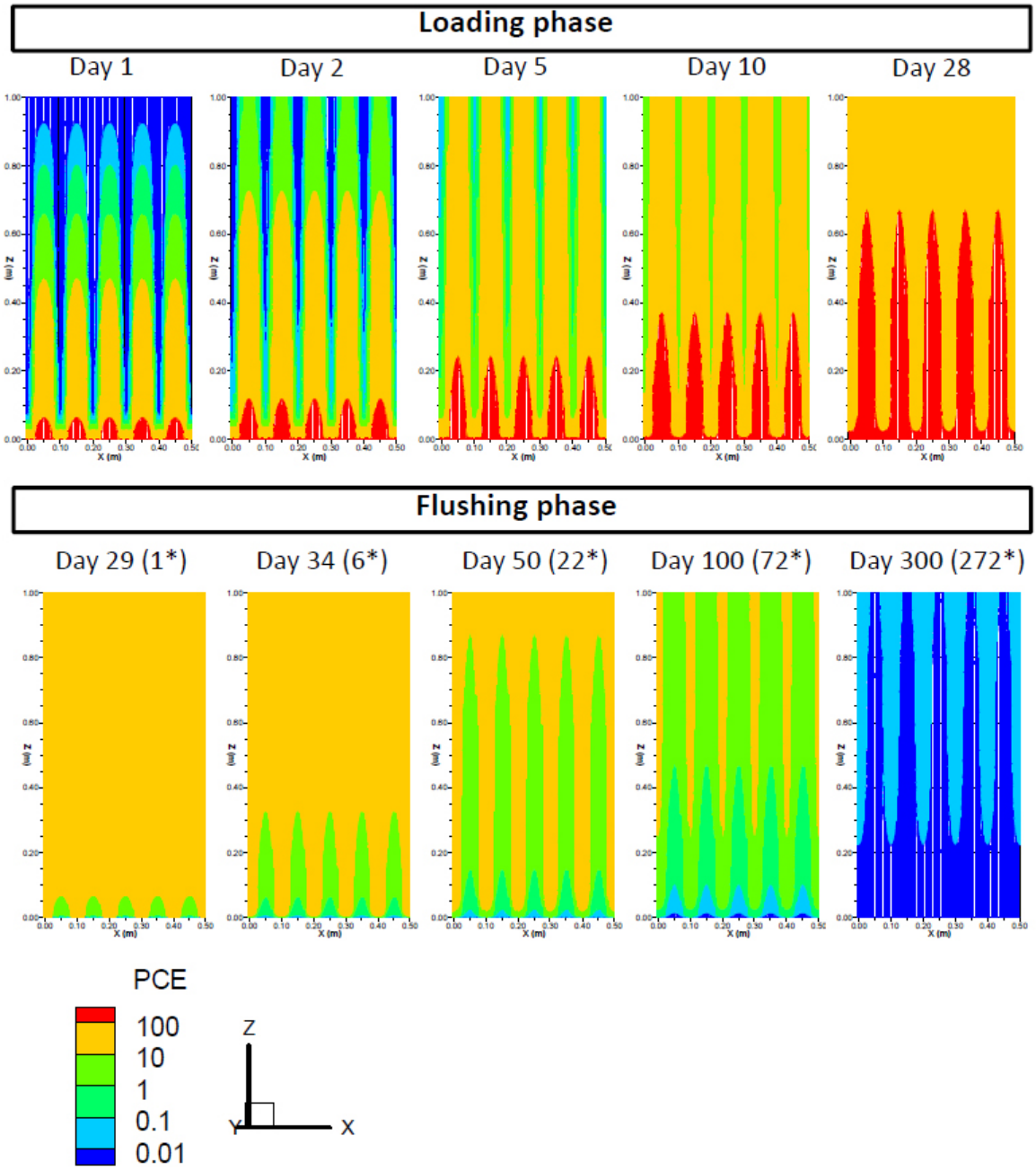

Figure 5-51. Simulated PCE contours for tank 1 (unamended silt layers) during the contaminant loading phase (days 0-28) and elution phase (days 29-300) when the tank was being flushed with clean water.

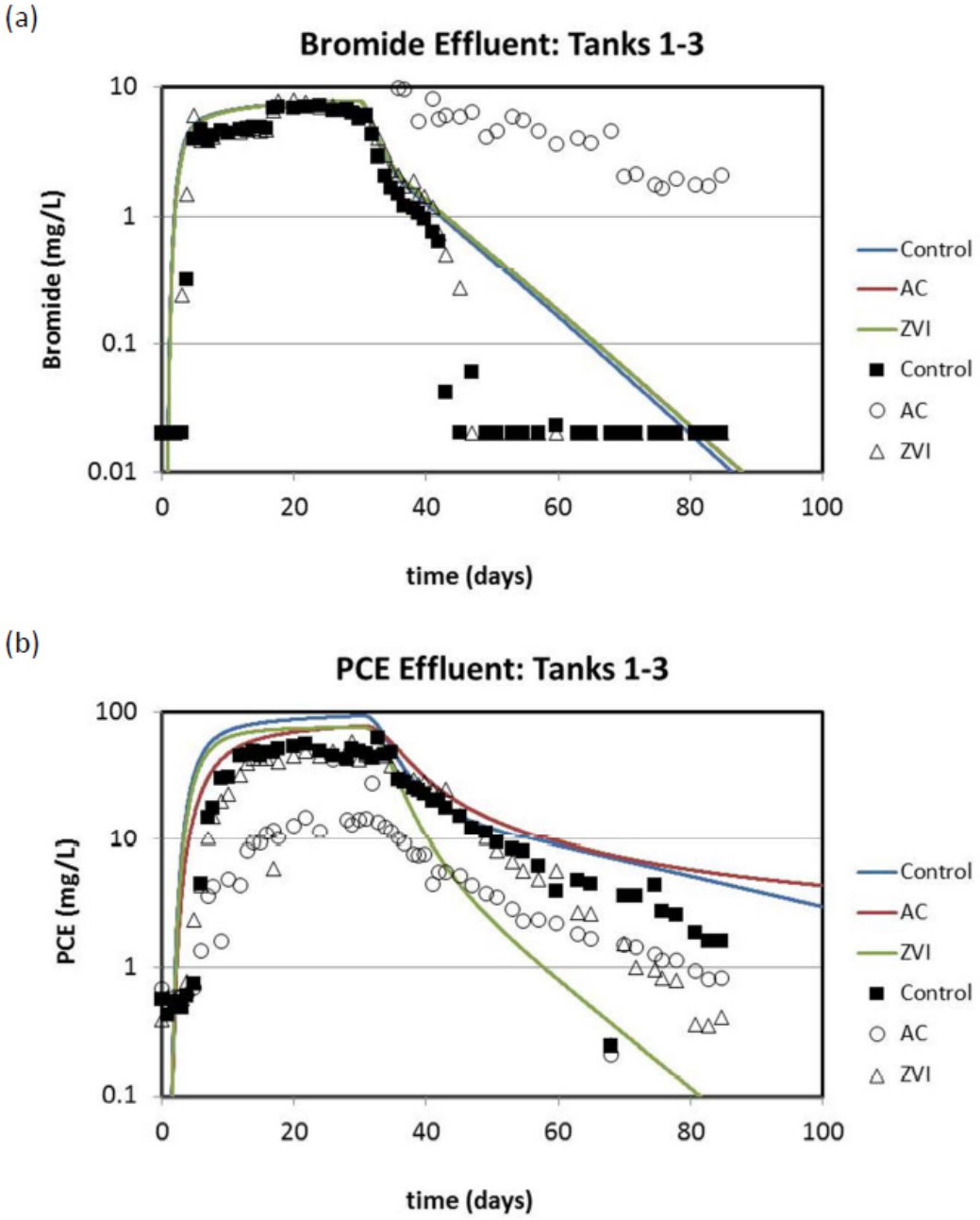

Figure 5-52. Experimental and simulated effluent concentrations for tanks 1 to 3 for (a) bromide, and (b) PCE.

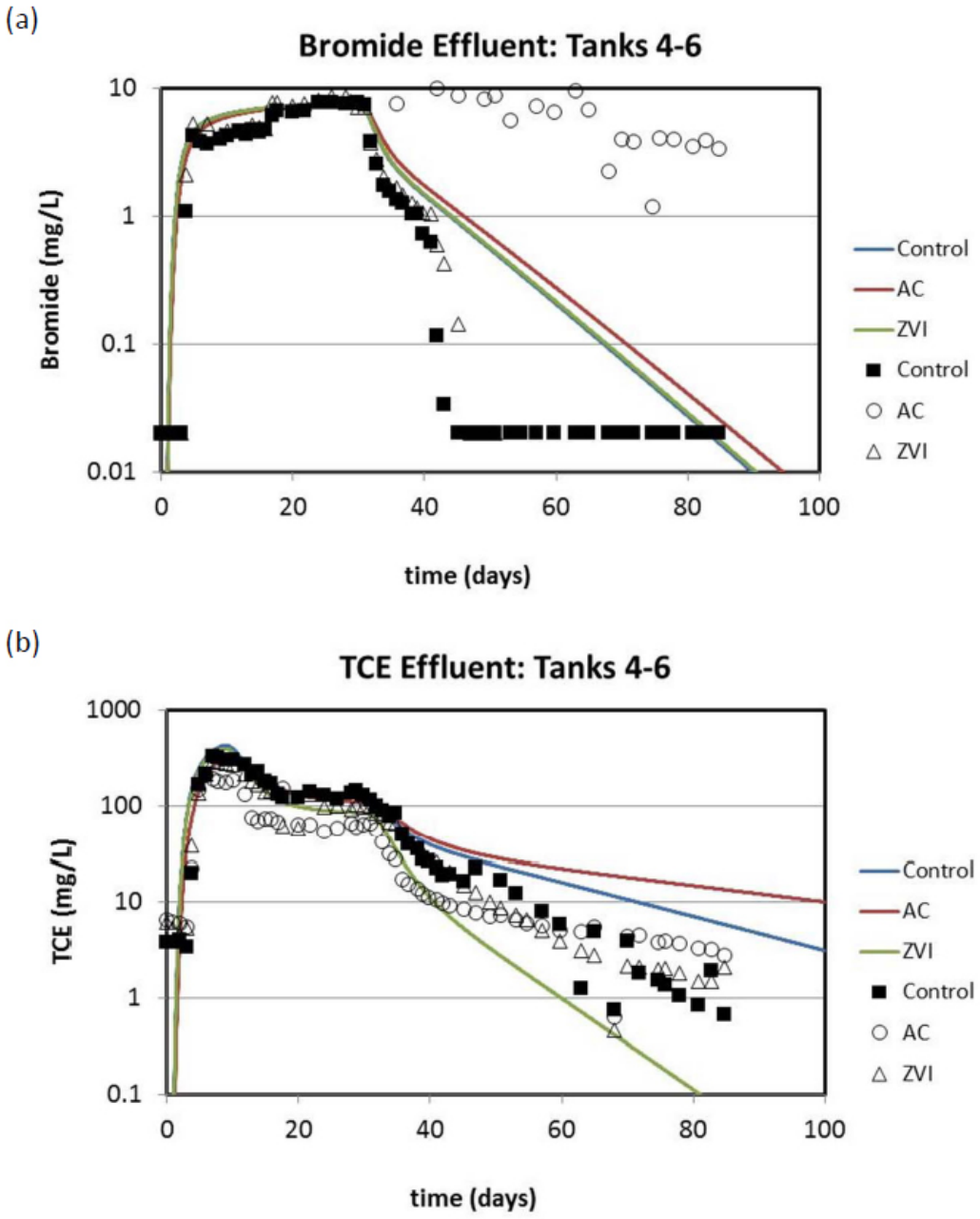

Figure 5-53. Experimental and simulated effluent concentrations for tanks 4 to 6 for (a) bromide, and (b) TCE.

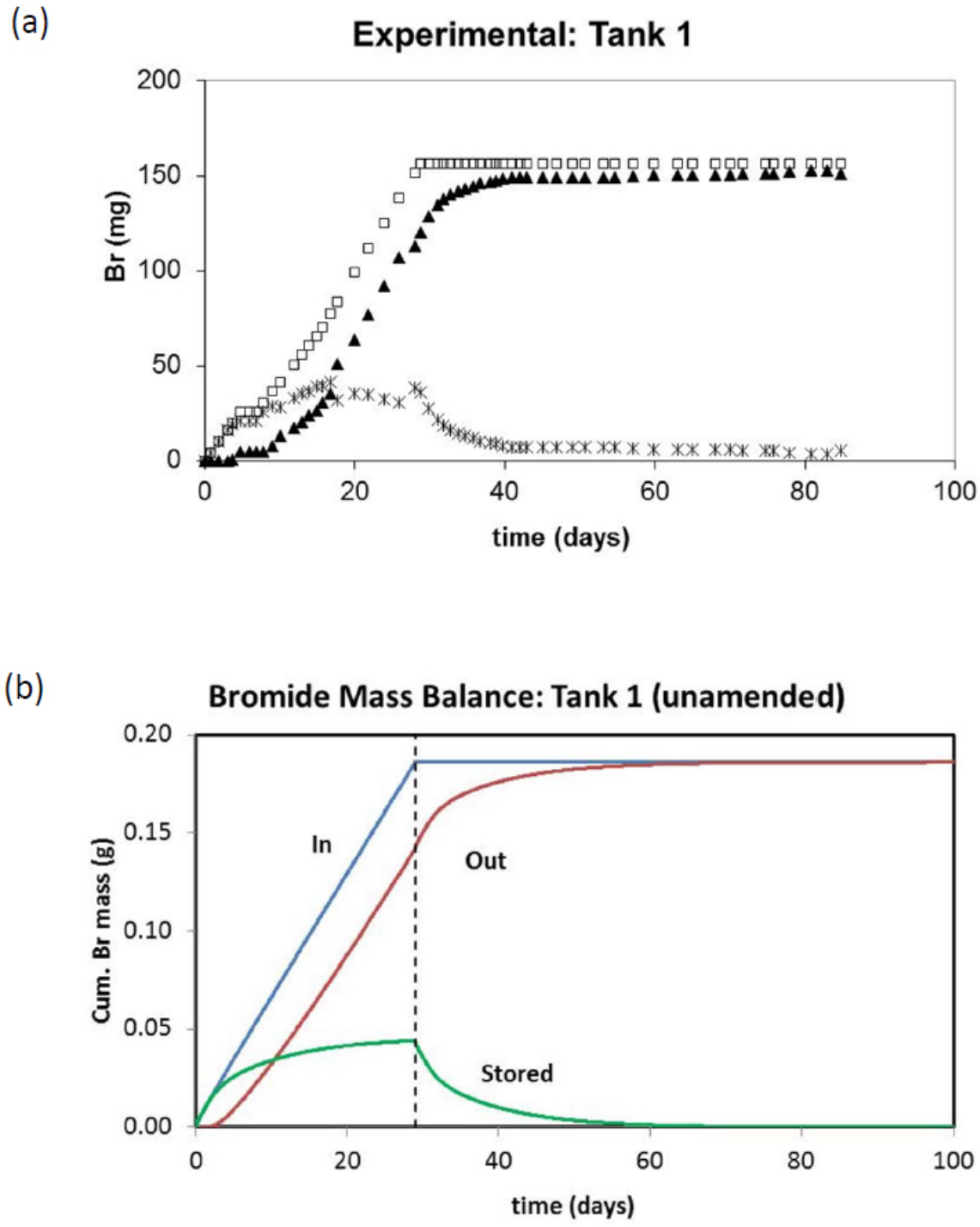

Figure 5-54. Comparison of bromide mass balance for tank 1 (unamended) for (a) experimental, and (b) simulated conditions.

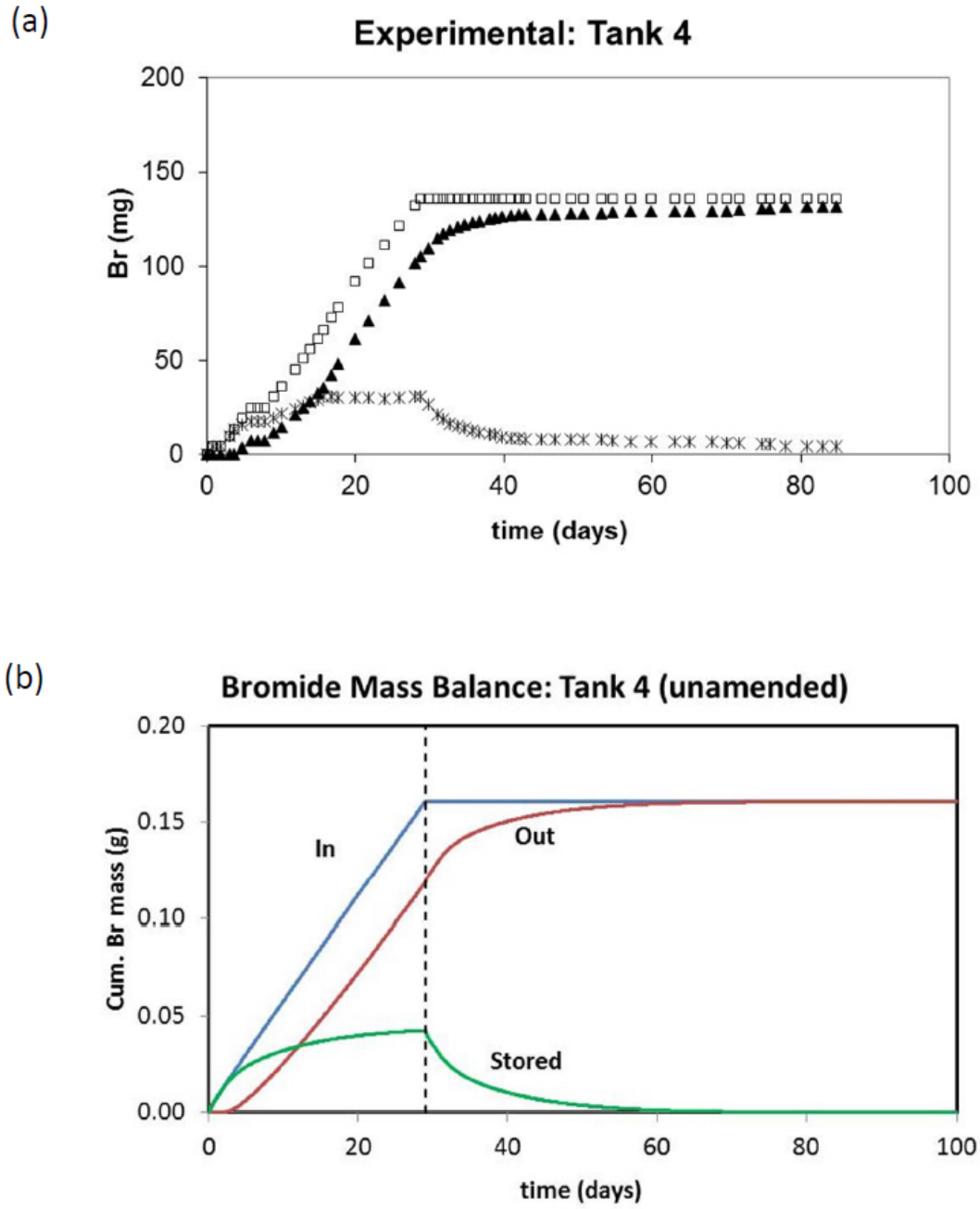

Figure 5-55. Comparison of bromide mass balance for tank 4 (unamended) for (a) experimental, and (b) simulated conditions.

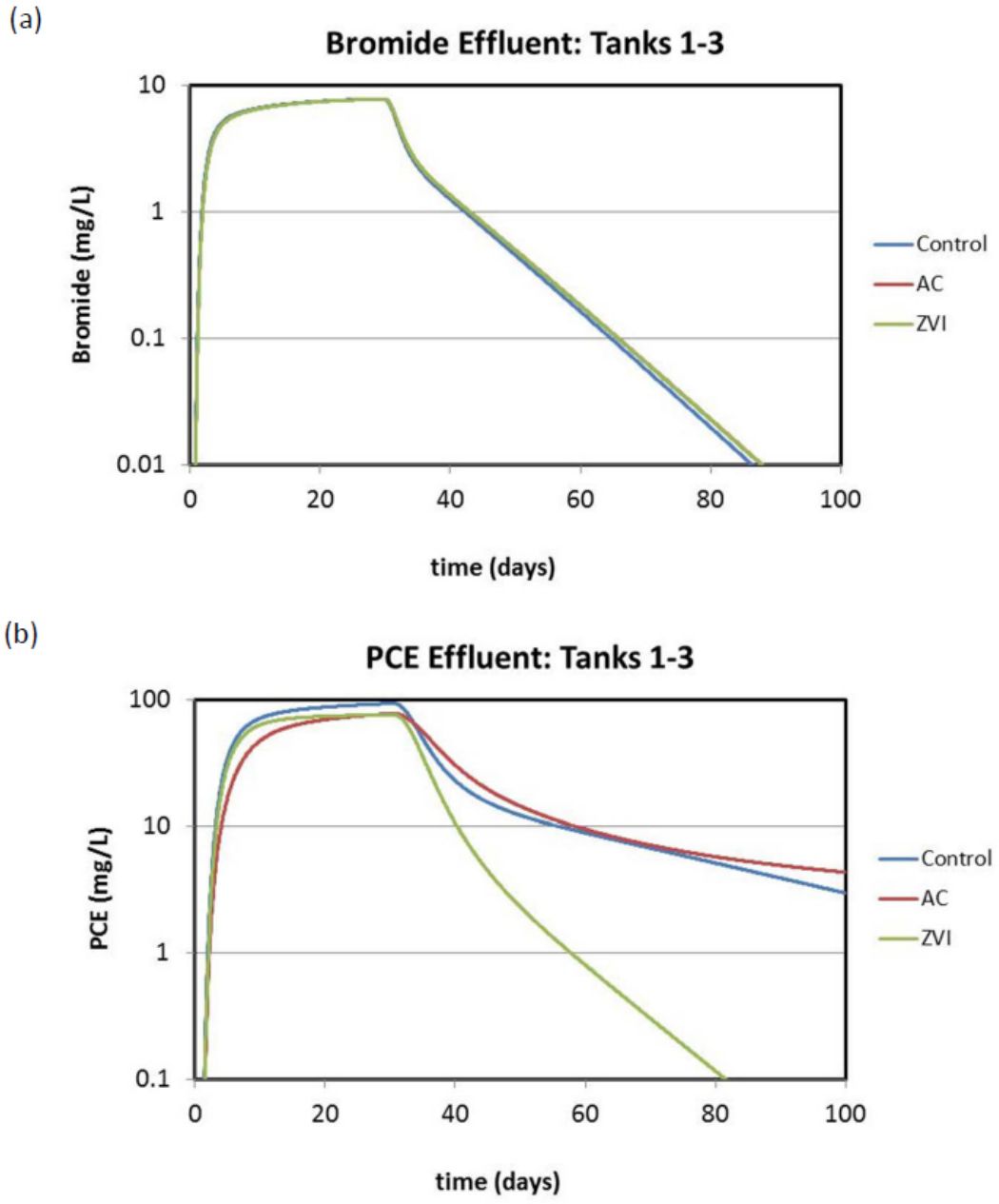

Figure 5-56. Comparison of simulated effluent concentrations for tanks 1 to 3 for (a) bromide, showing only very minor differences related to different flow rates, and (b) PCE, showing different behavior with more tailing for the unamended (control) and AC amended tanks and lower tailing for the ZVI amended tank due to reaction processes.

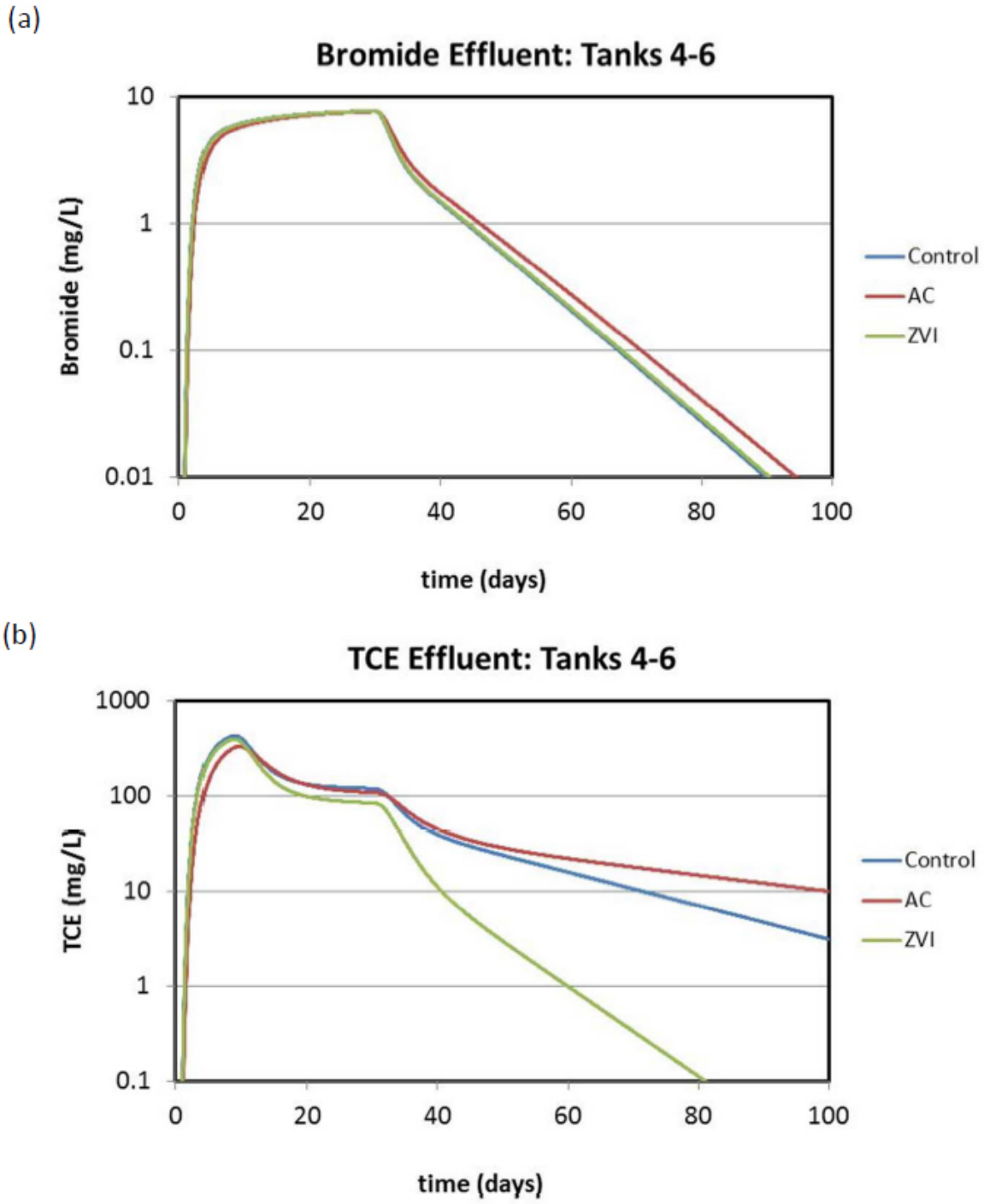

Figure 57. Comparison of simulated effluent concentrations for tanks 4 to 6 for (a) bromide, showing only very minor differences related to different flow rates, and (b) TCE, showing different behavior with more tailing for the unamended (control) and AC amended tanks and lower tailing for the ZVI amended tank due to reaction processes.

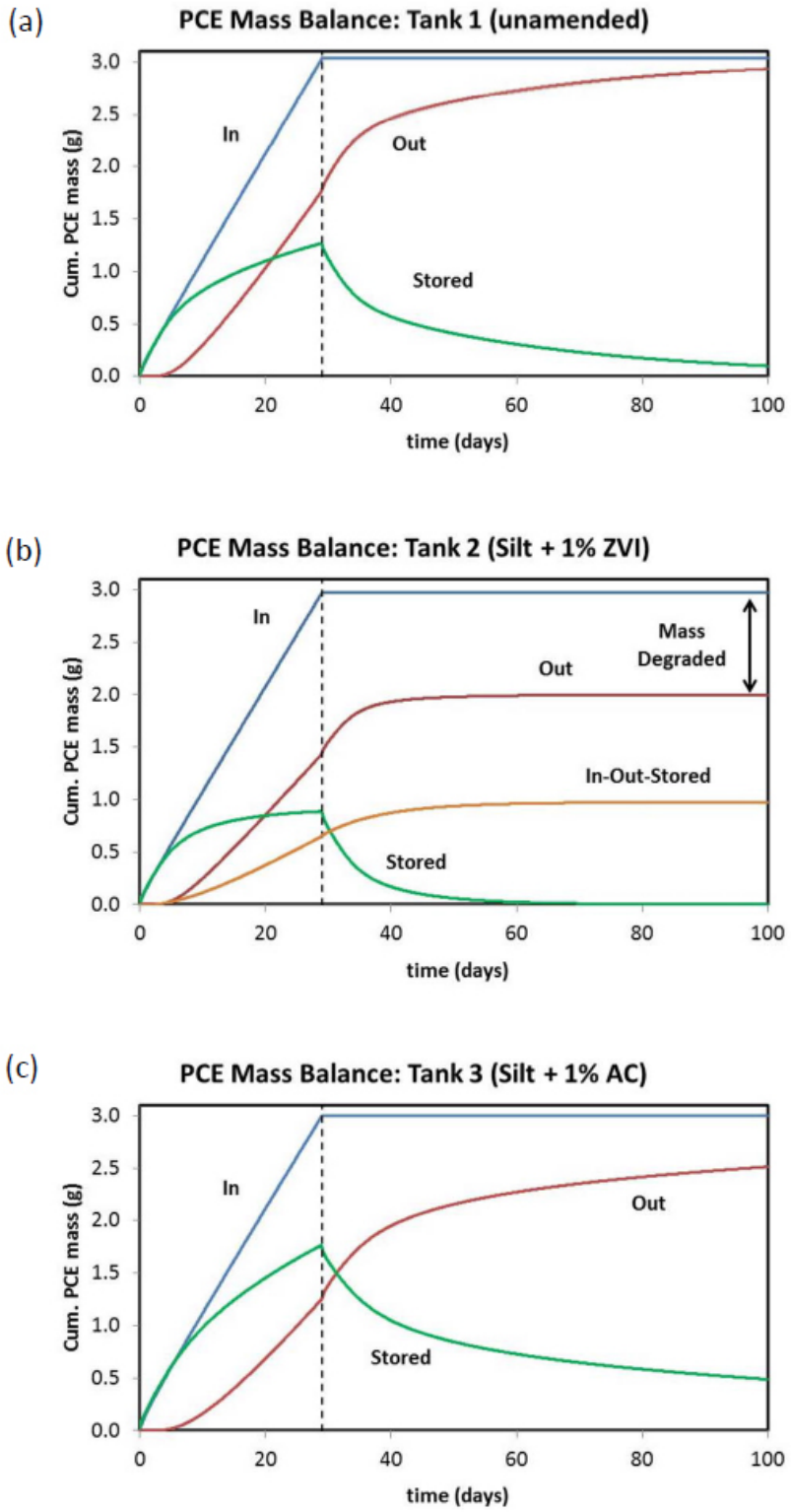

Figure 5-58. Comparison of simulated PCE mass balances for (a) tank 1 (unamended), (b) tank 2 (silt amended with ZVI) and (c) tank 3 (silt amended with AC).

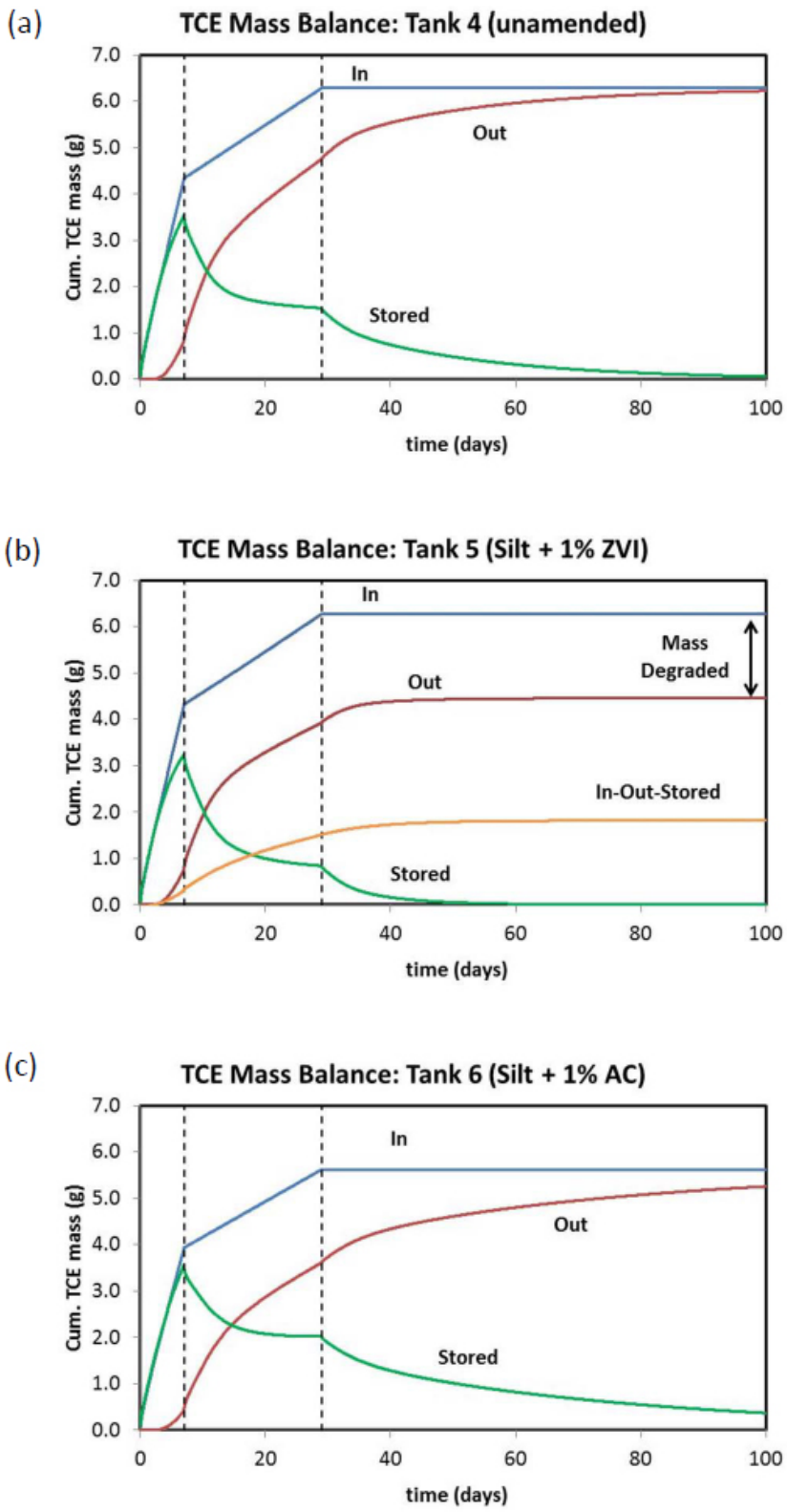

Figure 5-59. Comparison of simulated TCE mass balances for (a) tank 4 (unamended), (b) tank 2 (silt amended with ZVI) and (c) tank 3 (silt amended with AC).

5.6 CONCLUSIONS

Some of the key observations from the experimental data and simulations include: (1) long-term tailing compared to the source input period due to slow back diffusion of mass out of the silt layers, (2) greater tailing of the organics (PCE / TCE) compared to bromide, primarily due to greater sorption in the silt layers, (3) delayed arrival of the organics (PCE / TCE) compared to bromide in the AC amended tanks compared to the unamended tanks, due to increased mass transfer into the silt due to greater sorption, (4) increased tailing in the AC amended tanks compared to the unamended tanks, due to increased mass stored in the silt layers and slower rates of back diffusion, (5) decreased organics (PCE / TCE) tailing in the ZVI amended tanks due to degradation reactions that reduces the mass in the silt layers and therefore reduces the rates and longevity of back diffusion. More tweaking of the simulations is ongoing to better match the experimental datasets and these are planned to be used in a paper to be submitted to a peer reviewed journal.

5.7 TEXT BOX 5-1: ADDITIONAL MODELING

Lead Authors

Ahmad Seyedebbassi and Charles Newell, GSI Environmental Inc.

In a supplemental modeling effort, the relative contribution of dense non-aqueous phase liquid (DNAPL) dissolution versus matrix diffusion processes to the longevity of chlorinated source zones was investigated by Seyedabbasi et al. (2012). In this study, a hypothetical DNAPL source zone architecture consisting of several different sized pools and fingers originally developed by Anderson et al. (1992) was adapted to include defined low k layers (see **Figure 5-59**). The hypothetical DNAPL source zone is located in a 15-m deep aquifer 15 m deep and consisted of 12 pools with different sizes placed at different depths within a cross sectional area of 15 m by 20 m perpendicular to the groundwater flow direction. A coupled dissolution-diffusion model was developed to allow diffusion into these layers while in contact with DNAPL, followed by diffusion out of these same layers after complete DNAPL dissolution of three different compounds, including chlorinated solvents with solubilities ranging from low (tetrachloroethene (PCE)), moderate (trichloroethene (TCE)) to high (dichloromethane (DCM)). Fingers were excluded from the source zone architecture since the fingers had minimal influence on the source longevity (i.e., the mass present in fingers was relatively small (<2% of the mass in pools) and would discharge at high rates due to given spatial dimensions of the fingers).

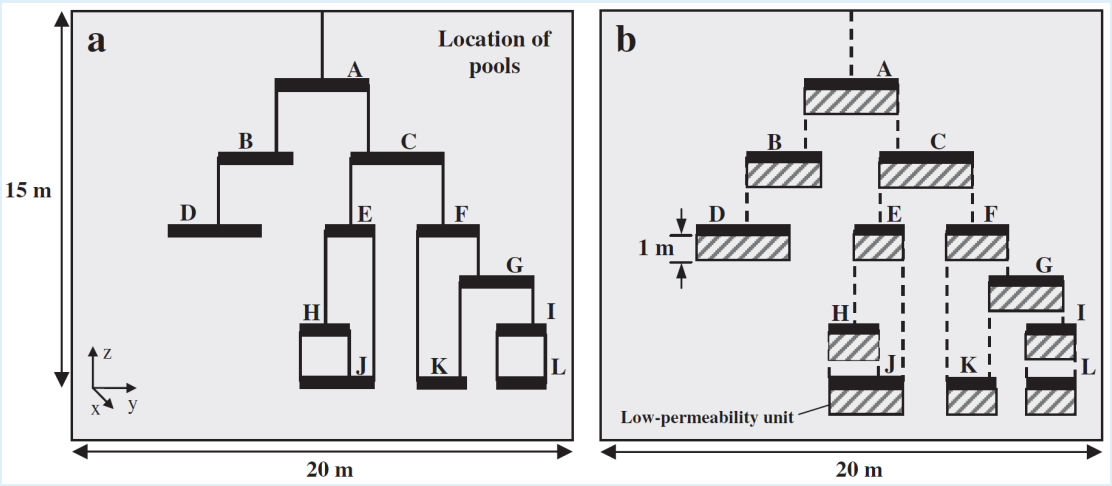

Figure 5-59: Schematic of source geometry with locations of the fingers and pools for (a) Case C of Anderson et al. (1992) (b) 1 m thick low-permeability compartment beneath each pool when considering the matrix diffusion effect. Fingers are also excluded in this study (dashed lines).

TEXT BOX 5-1 CONTINUED

The combined DNAPL dissolution/matrix diffusion model was used to simulate natural attenuation of the chlorinated solvent source zone. The mass discharge rate from the DNAPL source zone is shown in **Figure 5-60** for the three different DNAPL release cases (i.e., PCE, TCE, and DCM). The resulting source attenuation curves show the longevity of each DNAPL source zone, along with the relative contributions of DNAPL dissolution and matrix diffusion from the low k zones. The mass discharge goal of 0.1 g/d is equivalent to the lowest rate that would impact a well pumping approximately 4 gallons per minute using the drinking water standard that is common to the studied compounds (i.e., 5 ug/L). The *y*-axis on the right **in Figure 5-60** shows the average aqueous phase concentration leaving the source for the three different DNAPL types. The average source concentration was calculated right after the source area using the mean groundwater seepage velocity of 54 m/yr and the cross-sectional area of 300 m^2 (i.e., 15 m by 20 m).

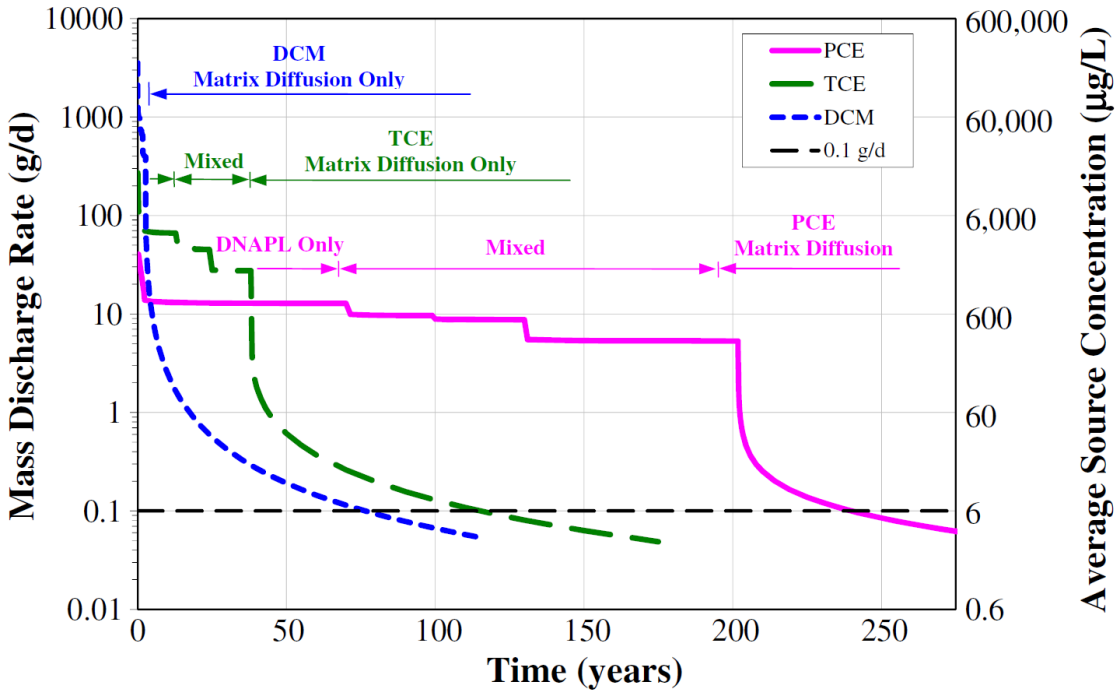

Figure 5-60: Entire source zone attenuation curves for PCE, TCE and DCM. The average source concentration is equal to mass discharge rate divided by the flow rate passing the cross-sectional area in Figure 5-59.

TEXT BOX 5-1 CONTINUED

Starting with an equal DNAPL mass for all three DNAPLs, the total source longevity for PCE, TCE and DCM was determined to be 244, 126, and 78 years, respectively. For the scenario modeled here, the post-DNAPL source longevity (due to matrix diffusion only) was substantial, representing approximately 41 to 87 years for each of the three different DNAPLs (PCE, TCE, and DCM). Matrix diffusion represented approximately 17% in the total source longevity for PCE, while the diffusion-associated contribution to source longevity for TCE and DCM increased to 69% and 97%, respectively. These results show that as the effective solubility of DNAPL constituents increases, matrix diffusion processes play an increasing role in the mass discharge rate and thus the source longevity. For the most soluble of the compounds examined (DCM), complete dissolution occurred within a relatively short period, but its higher solubility generated a large concentration gradient at the permeability interface during this period that promoted diffusion of mass into the low k zone.

The relatively short DNAPL longevities exhibited by the simulated released masses of TCE and DCM (39 and 3 years) suggest that it is possible for many sites with releases in the 1950s, 1960s, 1970s, and even 1980s to be dominated by matrix diffusion processes with only minor contributions from the remaining DNAPL. This agrees with the conceptual model presented by Sale et al. (2008), where their “late stage” chlorinated solvent site has a source zone sustained by back diffusion and with no DNAPL source component. The sensitivity of the TCE DNAPL release to groundwater velocity was evaluated. Lower groundwater velocity resulted in a longer period for complete DNAPL dissolution as well as larger overall source longevity (due to DNAPL dissolution and back diffusion). This allows for longer loading or “charging” period for matrix diffusion into the low k zones. However, while the use of a lower velocity increases the source longevity associated with matrix diffusion only, it actually decreases the relative contribution of diffusion when compared to that of dissolution.

5.8 CHAPTER 5 TYPE SITE SIMULATIONS – KEY RESEARCH PRODUCTS

Numerical Modeling vs. Analytical Solutions vs. Tank Experiments

- Compare numerical model HydroGeoSphere to exact analytical solutions for matrix diffusion for two-layer scenarios and parallel fracture scenarios.
- Compare numerical model HydroGeoSphere to matrix diffusion research tank experiments.

Developed Library of "Type Sites"

- Develop "Type Site" Analysis to show style of matrix diffusion effects for several different type hydrogeologic settings, contaminants, and source types.

Journal Articles

Chapman, S.W., B. L. Parker, T. C. Sale, L. Doner, 2012. Testing high resolution numerical models for analysis of contaminant storage and release from low permeability zones, Journal of Contaminant Hydrology, Volumes 136–137, August 2012, Pages 106-116, ISSN 0169-7722, 10.1016/j.jconhyd.2012.04.006.

Seyedabbasi, M.A., Newell, C.J., Adamson, D.T., Sale, T.C. (2012) Relative Contribution of DNAPL Dissolution and Matrix Diffusion to the Long-Term Persistence of Chlorinated Solvent Source Zones, Journal of Contaminant Hydrology, pp. 69-81 DOI: 10.1016/j.jconhyd.2012.03.010

OVERVIEW OF CHAPTER 6: *TREATING LOW k ZONES*

- There are three general strategies for managing contaminants in low k zones: 1) Low k Zone Degradation; 2) Transmissive Zone Depletion; 3) Containment
- Research tank experiments of these three strategies show how low k units affect remediation performance and concentration vs. time patterns. Typical seepage velocity in tanks: 0.33 m/day.
- The tanks were "loaded" with TCE for 52 days, water flushed for 28 days, treated with a remediation process for 27 days, then the TCE release from the low k zone was measured for 82 days.
- Results are reported in "OoMs", Orders of Magnitude reduction from the starting concentration (1300 mg/L TCE). Chemical oxidation showed an immediate 5+ OoM reduction, but showed partial rebound almost immediately (**0 pore volumes after treatment ended**). Three biological-related technologies show sustained treatment effects that supressed concentrations at 4-5 OoMs before partially rebounding around day 170, or ~60 days (**~20 pore volumes)** after active treatment ended. All five remediation technologies still represented an improvement over the flushing-only scenarios, with the BiRD process showing the most reduction in concentration at the end of the test: 3.8 OoMs.

Tank / Experiment	Analogous field treatments	Drop in effluent TCE (OoM)		
		Day 107	Day 189	C vs. t Pattern
1. Control (loading 52 days, then flushing)	Stop source loading via permeable reactive barriers, containment, and/or source tmt	1.5	2.6	
2. Enhanced flushing	Pump and treat, enhanced clean water flooding	2.3	2.6	
3. Permanganate	Chemical oxidation	4.4	3.1	
4. Lactate and KB1	Bioremediation with bioaugmentation	4.7	3.2	
5. Lactate, KB1, and Xanthan gum	Bioremediation, bioaugmentation + aquifer flux modification ("flux clog")	4.7	3.2	
6. Lactate, Sulfate, Sulfate Red. Bact.	Biogeochemical Reductive Dechlorination (BiRD)	1.7	3.8	

Concentration Reduction in Remediation Tank Experiments

(OoM: Order of Magnitude. PV: Pore Volume)

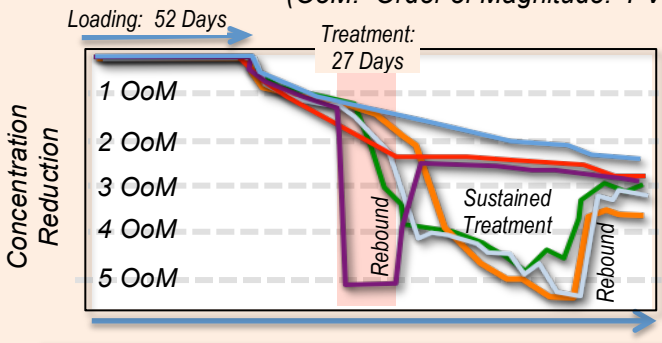

Tank / Experiment
(PVs: Pore Volumes after end of loading)

1. Control (45 PVs)
2. Enhanced flushing (79 PVs)
3. Permanganate (45 PVs)
4. Bioremediation (45 PVs)
5. Bioremed.+Flux-clog (38 PVs)
6. Biogeochemical (45 PVs)

Key Words: Remediation, chemical oxidation, bioremediation, clog, biogeochemical, pore volumes, flushing, sustained treatment, orders of magnitude, OoM, performance.

6.0 TREATMENT OF CONTAMINANTS IN LOW PERMEABILTY ZONES

Lead Authors for This Chapter

Kevin Saller and Tom Sale, Colorado State University

Given contaminants in low k zones, the question arises as to what can and/or should be done to mitigate potential impacts. The following explores answers to this question through:

- A review of general strategies and goals
- An overview of potential remedies for contaminants in low k zones
- Presentation of results from demonstrative laboratory tank studies for six promising approaches.

Per the proposal for SERDP ER-1740, complementary support for development of this chapter was provided by DuPont and GE. Technical support with the biological tank studies was provided by GeoSyntec.

This Chapter reports on our research in Activity 7, Challenges and Options for Managing Contaminants in Low Permeability Zones.

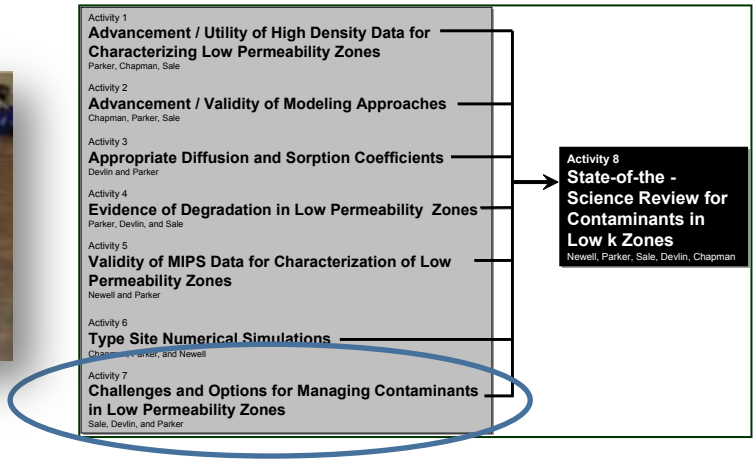

6.1 STRATEGIES AND GOALS

6.1.1 Strategies

Options for degradation of chlorinated solvents

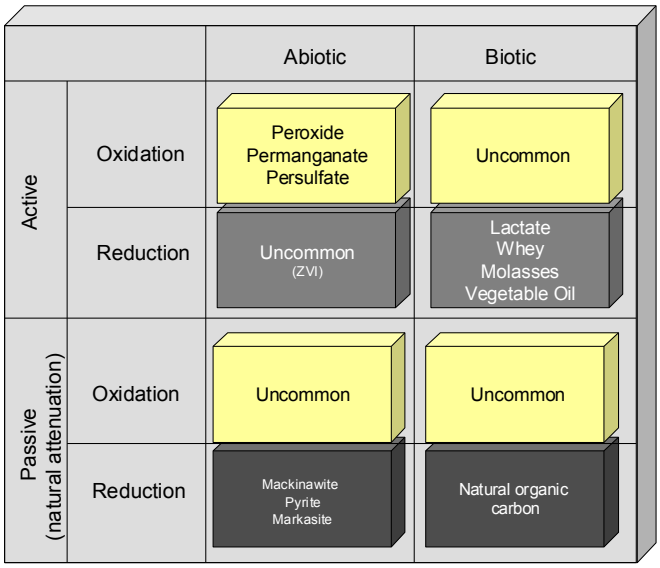

The following describes three general strategies for managing contaminants in low k zones.

Strategy 1: Low k Zone Degradation - The first approach involves degradation of contaminants within the low k zones. This is labeled as low k zone degradation. Contaminants degradation in low k zones can be achieved through oxidation or reduction reactions that are mediated by abiotic and/or biotic processes. *In situ* degradation can be the result of active and/or passive (natural attenuation) processes. Given active approaches, a primary constraint is delivery of oxidants or reductants into the low k zones. Transport of reactants into low k zones is often limited by slow rates of diffusive and /or slow advective transport. Potential benefits of gradation of contaminants in low k zones include:

- Reducing the concentration gradient that driving releases from low k zones (into transmissive zones) with the net benefit of lowering contaminant concentrations in transmissive zones.

- Reducing the longevity of consequential contaminant discharges from low k zones with the net benefit of a reduced period of site management.

Strategy 2: Transmissive Zone Depletion - A second approach is to deplete contaminants in transmissive zones. This can be achieved via enhance flushing of "clean" water, and/or driving degradation of contaminants in transmissive zones. Again, degradation of contaminants can be achieved through oxidation or reduction reactions that are driven by active remedies or passive (natural attenuation) processes. An advantage to transmissive zone depletion (versus low k zone depletion) is that it is comparatively easy to deliver reactants to transmissive zones via advection as opposed to delivering reagents to low k zones via diffusion and/or slow advection. The key disadvantage of transmissive zone depletion is that persistent treatment may be required to address slow releases from low k zones. Potential benefits of depletion of contaminants in transmissive zones include:

- Degradation of contaminants as they are released from low k zones with the net benefit of lower contaminant concentrations in transmissive zones.

- Enhanced concentrations gradients driving diffusion controlled release of contaminants from low k zones with the benefit of reduced the longevity of consequential contaminant discharges from low k zones.

Strategy 3: Containment - A third approach is containment of bodies containing contaminants stored in low k zones. At a source- or plume-scale, physical barrier (i.e. bentonite slurry walls) and soils mixing with stabilizing agent (bentonite) can be used to contain subsurface bodies containing impacted low k zones. At a smaller scale, fluids with high viscosity can be emplaced in transmissive zones about impacted low k zones. This can limit contaminant discharge (via transmissive zones) from bodies containing contaminants in low k zones. Following ER-201328 (GSI project) emplacement of high viscosity solutions for containment (referred to colloquially as a "*Flux Clog*"). Alternatively, precipitation reactions can be driven in transmissive zones and at the contact between transmissive and low k zones. This can limit advective and/or diffusive transport due to the reduced soil void space. An advantage to containment strategies (primarily large-scale) is they are often readily implementable. Disadvantages of containment can include cost, longevity of care, reliability, and limited treatment. The principle benefit of containment would be reduced contaminant loading to downgradient plumes via transmissive zones.

6.1.2 Goals

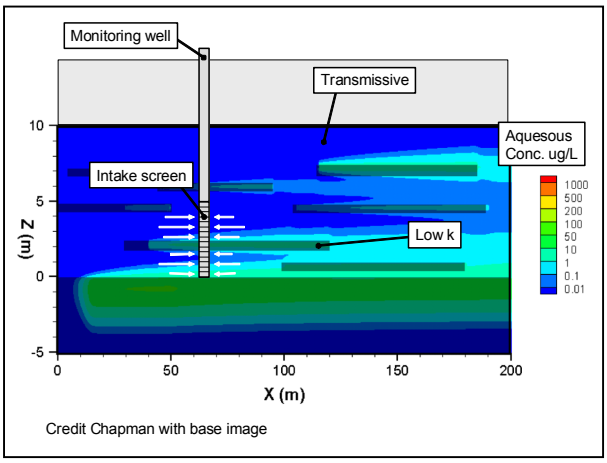

An essential element of any remedy is having specific goals, including an understanding of what constitutes success. Historically, the primary goal for subsurface remedies has been compliance with contaminant specific maximum contaminant levels (MCLs) in groundwater. Typically, MCLs are based on life-time human exposure via drinking water. Typically, groundwater is obtained from monitoring wells with screened intervals of ten feet or more. Following the scenario of a drinking water exposure, monitoring wells are similar in design to domestic water supply wells with the common exception that they are only pumped when sampled.

With the advent of high resolution site characterization (Chapter 2 and high resolution numerical modeling (Chapter 5 new insights have been advanced regarding monitoring wells including:

- Contaminant concentrations through screened intervals can vary by multiple orders of magnitude.

- Water samples are dominated by water quality present in the most transmissive zones.

- At older releases, in dilute plumes, contaminant concentrations in low k zones can be orders of magnitude greater than concentration in transmissive zones.

- Only a small fraction of apparent plumes defined by wells may actually contain consequential contamination.

Two possible paths for managing contaminated sites are open:

1. The first path is that contaminants in low k zones should be depleted sufficiently to prevent exceedances of MCLs in transmissive zones. This is consistent with the goal of preventing unacceptable life-time human exposure to a contaminant via drinking water produced from wells. This leads to scenarios where contaminant concentrations in excess of MCLs could be acceptable in low k zones. The authors of this document are unaware of policy or guidance that explicitly supports this approach.

2. The second path is that all groundwater, independent of being in transmissive or low k zones, should meet MCLs. This is consistent with rigorous interpretations of current regulations and policy. Unfortunately, per the experience of the authors of this report, this is likely to be an unattainable goal at many sites. Furthermore, given the MCL's based on life time exposures to drinking water, MCL's in low k zones would be excessive with respect to the intent of current regulations and policy.

Resolving the debate on which path is more appropriate for dealing with contaminant concentrations in low k zones is beyond the scope of this document. Nevertheless it is central to developing strategies for managing contaminants in low k zones. The authors of this document offer the suggestion that others (the National Research Council, USEPA, and Interstate Regulatory Council) should address the issue of appropriate goals for contaminant concentrations in low k zones.

6.2 TECHNOLOGIES FOR CONTAMINANTS IN LOW K ZONES

Activity Seven of this project involves side-by-side laboratory-scale demonstrations of promising technologies for contaminants in low k zones. The first step was resolving which technologies should be tested. Over the first year of this study a) treatment technology literature (including ESTCP/SERDP reports) was reviewed and b) input was solicited from knowledgeable parties. The later occurred primarily at national meetings including the SERDP/ESTCP Partners meetings and annual Battelle meetings. The review of treatment technologies for contaminants in low k zones provided a basis for selecting technologies for the laboratory studies. Furthermore, it provides a screening level list of technologies that can be used to address contaminants in low k zones.

We then developed the following criteria for testable low k zone treatment technologies:

- The technologies should be proven versus emerging or experimental. Per the definitions provided in Cherry et al. (1996), a proven technology is one where:

- A considerable base of experience and success currently exists;
- Commercial organizations offer the technology in the market place, and;
- The performance (and cost) of the technology is reasonably predictable.

- Low k zone contamination occurs in a wide range of hydrogeologic settings. Selected technologies should provide a range of options and be applicable to the common range of conditions that need to be addressed.

- The primary focus is treating contaminants in low k zones in plumes. Technologies that can address contaminants in low k zones in sources zones (Conductive Heating, Electrical Resistivity Heating, ZVI-Clay soil mixing, and excavation) are generally well-understood and have costs that are prohibitive for plumes.

The **Table 6-1** presents a list of the selected technologies. Inclusive to the table are related tanks studies. The next sections described the tank studies in detail.

Table 6-1. Summary of Remediation Technologies Selected for Tank Testing

Technology	Effect on Low k Zones	Advantages	Limitations	Related Tank
Natural Attenuation				
Abiotic	Low k Zone Depletion - Naturally occurring minerals can drive degradation of chlorinated solvents	Simplicity of implementation and low cost	Reaction kinetics can be slow	Tank 1
Biotic	Low k Zone Depletion - Naturally occurring bacteria can drive degradation of chlorinated solvents	Simplicity of implementation and low cost	Reaction kinetics can be slow	Tank 1
Reduced Upgradient Contaminant Loading				
Permeable Reactive Barrier	Transmissive Zone Depletion - Reduced upgradient contaminant loading to transmissive zones increases concentrations gradient driving releases from low k zone	Technologies implementation is well understood	Available data suggests extended time is required to get to MCL in downgradient water	Tank 1
Source Containment				
Source depletion				
Focused clean water flood	Transmissive Zone Depletion - Aggressive flooding of clean water through transmissive zones increases hydraulic and/or contaminant concentrations driving release of contaminants in low k zones.	Technology is relative simple to implement	Large amounts of clean water may be needed to have a consequential effect on conc. In low k zones	Tank 2

Table 6-1. Summary of Remediation Technologies Selected for Tank Testing (continued)

Technology	Effect on low k zones	Advantages	Limitations	Related Tank
Chemical Oxidation				
Permanganate *(Permanganate was selected over peroxide and sodium persulfate due to greater potential persistence in transmissive zones)*	Low k Zone Depletion and/or Transmissive Zone Depletion - High concentrations of oxidant create large concentration gradients that drive reactants into low k zones and deplete contaminants in transmissive zones	Reaction kinetics can be fast	Oxidant depletion by naturally occurring organics material, Potential for limited persistence. Post treatment rebound is common at field sites.	Tank 3
Biotic Reduction				
Lactate with KB1	Transmissive Zone Depletion - Lactate serves as an electron donor that drive biological reductive dechlorination of chlorinated solvent in transmissive zones and thus enhance rates of release from low k zones	Simplicity and low cost	Reaction kinetics can be slow. Post treatment rebound is possible at field sites once available carbon has been exhausted.	Tank 4
Lactate with KB1 and Xanthan gum	Low k Zone Depletion and/or Transmissive Zone Depletion - Lactate serve as an electron donor that drives biological reductive dechlorination of chlorinated solvents in transmissive zones and enhanced rates of release from low k zones. By slowing groundwater velocities, Xanthan gum could promote diffusion of reagents into low k zones and enhance treatment persistence in transmissive zones.	Simplicity, low cost, and high viscosity solutions in transmissive zones can drive reagents into low k zones	Reaction kinetics can be slow, addition of Xanthan gum can slow delivery of reagents.	Tank 5
Lactate, Sulfate, and Sulfate Reducing Bacteria (BiRD)	Low k Zone Depletion and/or Transmissive Zone Depletion - Lactate and SRB facilitates reduction of sulfate to sulfide and precipitation of potentially reactive metal sulfides in transmissive and low k zones.	Simplicity, low cost, and precipitation of reactive metal sulfides can occur in low k zones	Reaction kinetics can be slow. Not all metal sulfides are reactive.	Tank 6

6.3 DEMONSTRATIVE LABORATORY STUDIES - METHODS

The following describes the methods and results from a six tank laboratory demonstration of existing and promising treatment technologies for managing contaminants in low k zones.

This section addresses the methods involved in the execution of the tank experiments at CSU.

6.3.1 Setup

In order to determine the effectiveness of the treatments outlined earlier, a set of six (6) dual-permeability, 2-dimensional sand tanks were constructed. The tanks themselves are made of a stainless steel backing with a glass front, and are 1-m tall, by 0.5-m wide, and 2.54-cm deep, as shown:

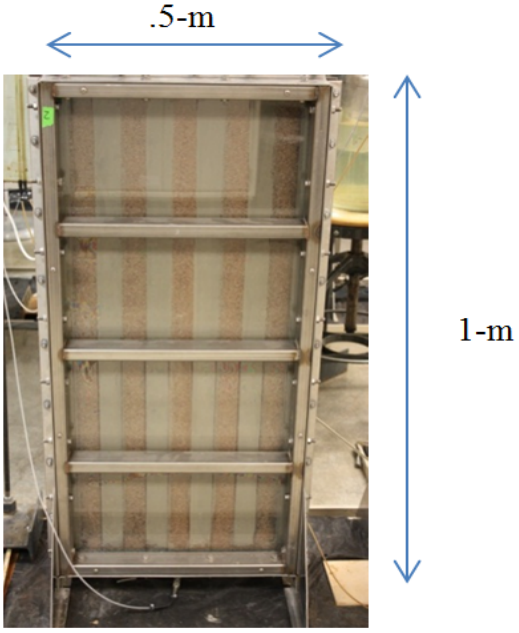

The soils lay within a 1-cm thick, 2.54-cm deep aluminum sidewall that spans each of the 4 sides of the tank. Due to this 1-cm thick sidewall, the total space for the soils was 98-cm x 47.5-cm x 2.54-cm. This sidewall is kept in place by the stainless steel back-plate and the glass front-plate by bolts that connect the two that surround the tank shown in the figure above. A small rubber gasket was affixed between each side of the aluminum sidewall and the back and front plates, and sealed with vacuum grease so that the tank is airtight. Stainless steel T joints were installed at the bottom (inlet) and top (outlet) in order to connect the influent and effluent to piezometers to determine if any plugging was occurring within the tank during the experiment.

Sand and silt samples were acquired from Spill Site 7 at FE Warren AFB in November of 2011 in association with activities described in Chapter 2. The soils used were field soils gathered from F.E. Warren Air Force Base located in Cheyenne, Wyoming, and were sieved in the lab using a #10 and #35 sieve for the sand, and the silts passed a #100

sieve. The sand and silt were tested in column studies using constant flow and falling head setups to have hydraulic conductivities and porosities of:

Soil	K (cm/sec)	Porosity
Silt	2.08E-04	.49
Sand	2.30E-01	.39

This difference in hydraulic conductivity for these soils ensures advective flow in the tanks would be overwhelmingly through the sands, and the silts would be dominated by diffusive processes.

The soils within the tank were arranged in 9 alternating, 5-cm thick layers with 2, 2.5-cm thick silt layers at each end. These layers spanned from the bottom to the top of the tank. The 2, 2.5cm thick silt layers on the sides of the tank were placed as such for diffusive symmetry of the TCE into the low k zones, since these 2 silt layers are only in contact with 1 sand layer each. This soil striping pattern was done in order to maximize the contaminant diffusion into the silts as the contaminant moves through the transmissive sand zones during the loading phase, which will be described shortly. The soil layers were created by sprinkling dry soil from above, with the tank on it's side, so that the layers would be as evenly distributed as possible. The tanks were vigorously tapped throughout the placement of the soils to settle them as much as possible in order to better simulate field conditions. After this, the tanks were placed upright for the duration of the experiment so that the soil layers were vertical. At the top and the bottom of the tank, a reinforced 1-cm tall fine screen was installed to restrict any soil from moving into the inlet and outlet mixing zones of the tanks.

Each tank was given its own separate 1/8 in. molded glass tubing system, along with a unique positive displacement piston pump (Fluid Metering Inc., model #RHSY) to deliver all fluids throughout the experiment.

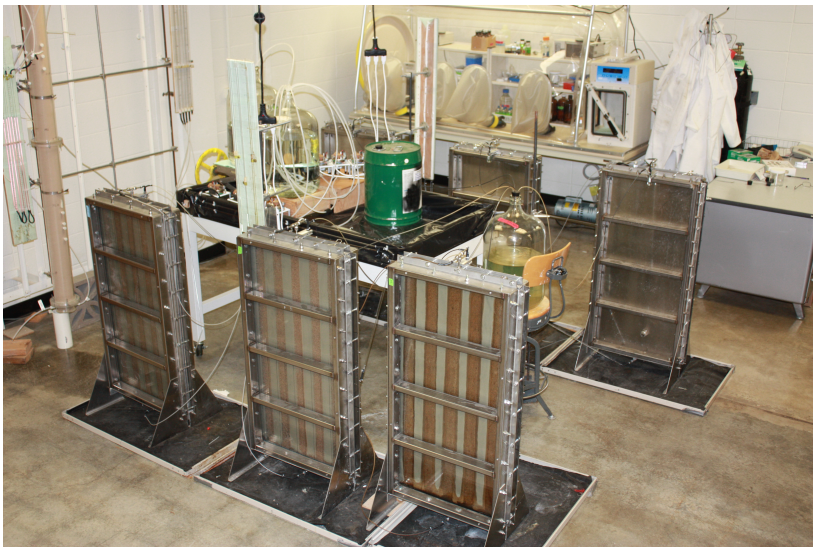

Flushing and Monitoring

After the soil layers were emplaced and the tank sealed, 10 pore volumes of Carbon Dioxide (Airgas, 99%) was flushed into the tank in intervals, in order to remove the majority of the oxygen contained in the pore space of the soils. This was done because Carbon Dioxide dissolves significantly faster in water than oxygen, so that the tanks would be effectively free of any gas pockets during the experiment. Once this gas-flood was complete, de-gassed tap water was then flushed through the tanks from bottom to top for a period of 21 days. The influent de-gassed water contained 3.9 mg/L chloride and 10.9 mg/L sulfate.

The pumps were set at a rate of approximately 0.33 m/day for all tanks throughout the experiment, with the exception of the enhanced flushing treatment, which will be discussed shortly. This flow rate was chosen because it is roughly equivalent to the regional groundwater value. These flow-rates for each pump were tested bimonthly throughout the experiment.

Next, a de-gassed aqueous solution of 1300 mg/L Trichloroethylene (J.T. Baker, A.C.S. Reagent 99.8%, target compound) and 2000 mg/L Potassium Bromide (J.T. Baker, 99.9%, a non-reactive control) was then flushed through the tanks concurrently at the same flow rate of 0.33 m/day for 52 days. This was achieved by using a 1-m tall, 5.2-cm wide hollow glass column that was filled halfway with glass beads (6 mm diameter) and TCE, with the de-gassed water flowing from a bottom port to the top port, where it was distributed to the tanks through their individual glass piping system. The glass beads were added to maximize the surface area of the TCE contacting the water as the water passed through the beads. The system was gas tight, so no TCE losses could be incurred, and the effluent TCE from this exchanger was always at or very near saturation. Since the TCE was constantly dissolving into the aqueous phase as it flushed through, it was replenished every day in the exchanger using a glass syringe inserted into the top plug to keep the tank influent concentrations as constant as possible.

During this contaminant loading, high concentrations in the transmissive layers drove TCE and bromide into the low permeability zones via diffusion. Low contaminant concentrations in the transmissive layers drove the release of stored TCE and bromide stored in low k zones.

Following a 28-day water-only flush, six different strategies were employed to address contaminants stored in the low k zones. The treatments were employed for 27 days. Lastly, the tanks were flushed with water only for an additional 82 days. Over the ~189 day experiment flow rates, head loss, effluent water quality, and endpoint soils concentrations data was collected.

A graphic of the timeline for the experiment is shown on the next page. The number of pore volumes used in five of the six tank experiments is shown (tank experiment 2, enhanced flushing, had five times the pore volumes flushed during each interval). The six, 27-day long treatments employed in this experiment

Pore Volumes (PVs)

A Pore Volume is the amount of water required to replace (flush out) water in a unit volume of porous media. One pore volume is one flush; three pore volumes is three flushes.

The higher the number of pore volumes the more water was flushed through the system.

are listed in the following **Table 6-2.**

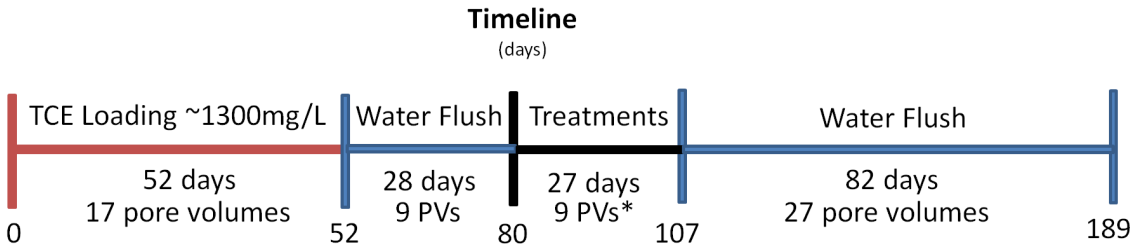

**For all except tanks 2 and 5, the enhanced flushing and Xanthan Gum, which had ~5 and zero times these pore volumes, respectively.*

Table 6-2 Treatment Regime for Tank Studies

Tank	Treatment	Analogous field treatments
1-Control	Flush with water at base transmissive zone seepage rate (0.33 m/day) (about 45 pore volumes flushing after loading)	Eliminating upgradient contaminant loading via permeable reactive barriers, source containment, and or source treatment
2-Enhanced flushing	Enhanced flushing with water at 5 times the base transmissive zone seepage rate (about 81 pore volumes flushing)	Pump and treat an enhanced clean water flooding
3-Permanganate	Flushing 2000 mg/L potassium permanganate at the base seepage rate (about 45 pore volumes flushing)	Chemical oxidation
4-Lactate and KB1	Flushing a 2000 mg/L sodium lactate solution at the base seepage with an initial inoculation of KB1 (about 45 pore volumes flushing)	Biologically enhanced reductive dechlorination with inoculation
5-Lactate, KB1, and Xanthan gum	Delivery of one sand pore volume of 2000 mg/L solution of sodium lactate and 1000 mg/L xanthan gum at the base seepage rate with an initial inoculation of KB1 followed by tank shut in for 24 days.	Biologically enhanced reductive dechlorination with inoculation and "flux clog"
6-Lactate, Sulfate, sulfate reducing bacteria,	Flushing 5370 mg/L sodium lactate and 2880 mg/L magnesium sulfate at base seepage with an initial inoculation of SRB (about 45 pore volumes flushing)	Biogeochemical Reductive Dechlorination (BiRD), where bacteria + donor convert native Fe to reactive FeS minerals

The control tank received no active treatment and the flow-rate through the tank remained unchanged for the entire duration of the 189-day experiment.

The Enhanced Flushing treatment tank was subjected to an increased flow-rate of approximately 5-times, at 2.48 mL/min of the same de-gassed water as the control.

The third tank received a solution of 2000 mg/L Potassium Permanganate (J.T. Baker, 99.5%), dissolved in degassed water, and delivered at the base flow-rate of 0.52 mL/min. Since pore-space plugging from Manganese Dioxide precipitate is usually of

concern when Potassium Permanganate is used as a treatment in soils, 2000 mg/L of Sodium Hexametaphosphate (EMD Chemicals, 99.9%) was added to the Potassium Permanganate solution as a dispersing agent to try and retard the formation of MnO_2 deposits.

The forth tank received an anaerobic injection of KB1 culture (population 5.0E10) grown at SiREM labs (Guelph, Ontario) injected using a syringe pump (Chemvx Inc., model #Fusion 100) into the tank concurrently with a 2000 mg/L de-gassed aqueous solution of Sodium Lactate (Alfa Aesar, Stock #41529) at a 0.52 mL/min flow-rate. A mineral and vitamin cocktail supplied by SiREM for the KB1 culture was added to the injection aqueous solution as well.

The Fifth tank received an anaerobic injection of KB1 culture (population 5.0E10) grown at SiREM labs (Guelph, Ontario) injected using a syringe pump (Chemvx Inc., model #Fusion 100) into the tank concurrently with a de-gassed aqueous solution of 1000 mg/L dissolved Xanthan Gum (Essential Depot, E415 USP FCC Food Grade) and 2000 mg/L Sodium Lactate (Alfa Aesar, Stock #41529) at a 0.52 mL/min flow-rate. A mineral and vitamin cocktail supplied by SiREM for the KB1 culture was added to the injection aqueous solution as well.

The Sixth tank received an anaerobic injection of Sulfate Reducing Bacteria (*Desulfovibrio desulfuricans,* American Type Culture Collection 13541, population 2.0E09) injected using a syringe pump (Chemvx Inc., model #Fusion 100) into the tank concurrently with a de-gassed aqueous solution of 2880 mg/L dissolved Anhydrous Magnesium Sulfate (Fisher Scientific, M65-501 99.9%) and 5.37 gm/L Sodium Lactate (Alfa Aesar, Stock #41529, 60% w/w) at a 0.52 mL/min flow-rate. The SRB was grown using a Modified Baar's Medium for Sulfate Reducers (ATCC #1249), where ferrous chloride was used in lieu of ferrous ammonium sulfate.

Following these 27-day treatments, de-gassed water was once again pumped through the tanks for a period of 82 days, so that the rebound behavior of the effluent TCE concentrations (if any) could be determined. The total sampling period lasted a total of 189 days after the start of the TCE injection into the tanks. Effluent samples from the 10-mL flow-through vials were taken daily during times of large changes in effluent concentrations, such as at the start and end of the treatment period, but were taken less often during periods where effluent concentrations were more stable. These samples were sealed with zero head-space using Teflon lined septa caps, labeled and stored at 36^{o} F until quantitative analysis.

6.3.2 Analytical Methods

Effluent sample concentrations were determined by pipetting 2 mL out of the collected 10 mL aqueous sample vial and using a 1:1 extraction of Methyl-Tert-Butyl-Ether (OmniSolv, MX0826-6, 99.99%). The samples containing the equal volumes of the aqueous sample and the MTBE were then placed in a vortex for 20 minutes (SMI Model #2600 Multi-Tube Vortexer). The MTBE portion of these extractions were then initially analyzed for TCE and DCE with an ECD detector on an HP 5890 GC with a DB-624 column (J\&W Scientific), and then later re-run for detecting DCE concentrations below 350 ug/L as well as all ranges of Vinyl Chloride using an Agilent GCMS 5973 detector on a RTX-624SIL MS column at a 1 mL/min flow rate. The concentrations were determined by using a 16-point calibration curve that range from known values of the chlorinated solvents in MTBE from 100 mg/L to 3 ug/L. The remaining 8 mL of the effluent samples were analyzed for Bromide concentrations using a Metrohm Advanced Compact Ion Chromatograph 861 with an A Supp5 250 column, which used a 5 point calibration curve of values from 100 mg/L to 1 mg/L. The data from both of these analytical methods were stored and analyzed in *Microsoft Excel*.

6.4 DEMONSTRATIVE LABORATORY STUDIES: RESULTS

The following presents tank effluent concentrations as a function of time for each of the sand tanks. The data provides a basis for describing governing processes, benefits of treatment, and limitations of each approach.

6.4.1 Tank 1: Control

During the loading phase (0-52 days) (**17 pore volumes of flushing**) TCE effluent concentrations approach the influent concentration of ~0.01 mol/L (~1300 mg/L) **(Figure 6-1).** Subtracting the total TCE discharge from the tank at 52 days from (0.325 moles – 42.725 g) from total TCE loading to the tank (0.386 moles – 50.75 g), and assuming no consequential losses at this point, 0.061 moles (8.03 g) of TCE remained in the tank at the end of loading. Accounting for aqueous and sorbed phases in the transmissive zones, the total contaminant mass in the low k zones (at 52 days) is 0.038 moles (5.03 gm). This is equivalent to an average low k zones total contaminant concentration of 0.0048 moles/kg dry soils (636 mg/kg).

Following elimination of the influent TCE loading at 52 days, TCE concentrations drop and cDCE appeared in the water samples effluent. Over the first 20 days (**7 pore volumes**) after source removal TCE effluent concentration drop by 1 order of magnitude. It took an additional 70 days (**23 pore volumes**) to see a second order of magnitude drop in effluent TCE concentrations. Persistent TCE concentrations, after elimination of TCE in the influent, are attributed to release of TCE from the low k zones. Declining TCE concentrations over time are attributed to decaying concentration gradients (driving diffusion) within the low k zones.

Observation and increasing concentrations of c-DCE, through time, suggests active biological attenuation of TCE after removing the TCE source. At end of the experiment (after **~ 45 pore volumes** of flushing) effluent cDCE levels rose above those of the TCE with a molar ratio of 0.42 of TCE to cDCE. No other TCE metabolites were observed in

the Tank 1 effluent. Post study analysis of soil from low k zones is inclusive as to the zones in which TCE degradation is occurring.

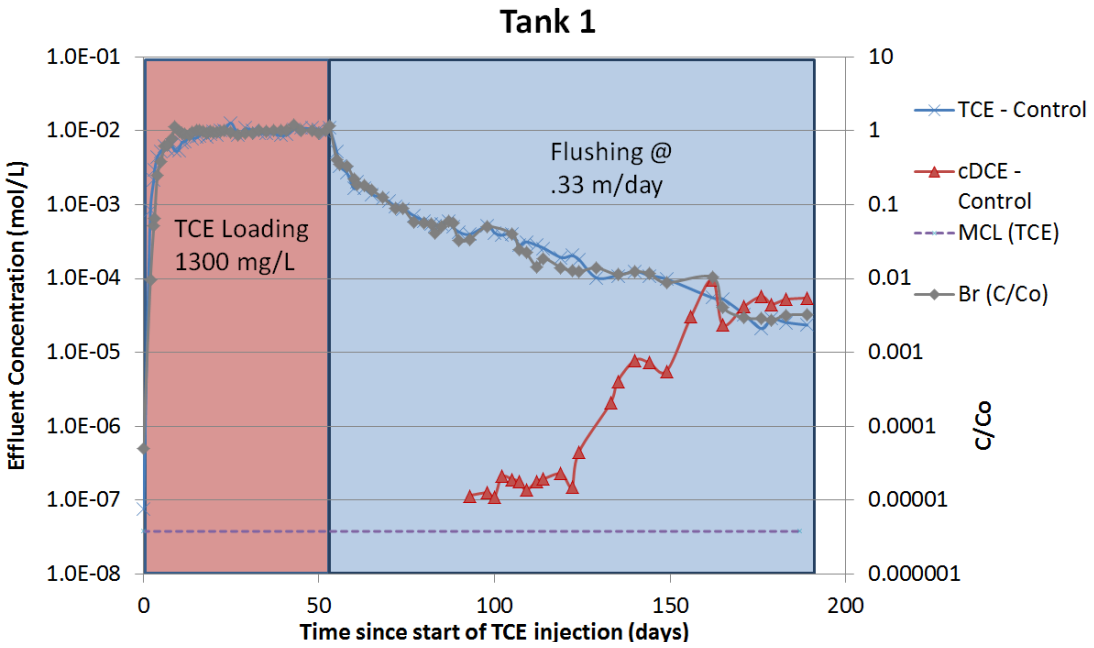

Figure 6-1: Control tank effluent TCE, DCE and Br concentrations

Performance Summary	Order of Magnitude Reduction (% Reduction)	
	TCE	TCE+cDCE
Control *Seepage Velocity 0.33 m/day.* *45 Pore Volumes after loading stopped.*	**2.6** (99.7%)	**2.07**(99.1%)

Two key aspects of the Tank 1 results are 1) after 189 days, total source removal provides a limited (two order of magnitude) reduction in total effluent CVOC's at which TCE tank effluents concentrations are still 3 orders of magnitude above MCL and 2) the Tank 1 breakthrough curve is asymmetrical (also true for all of the tanks).

Key Observations

- Persistent concentration in water after complete source removal, due to releases from low k zones, is consistent with Parker and Chapman (2005), Sale et al. (2008), and Parker and Chapman (2008). Following Sale et al. (2008), observed improvement in downgradient water quality can diminish with large distances (tank length is 1m) due to increasing low k zones surface areas releasing contaminants to transmissive zones.

- Asymmetrical breakthrough curves for heterogeneous media are consequentially different than Gaussian bell-shaped breakthrough curves associated with standard advective-dispersive solutions for transport in uniform porous media (i.e. Hunt 1978, Freeze and Cherry, 1979, Fetter 2008). First the asymmetrical breakthrough curve shows a rapid (convex downward) response to reduced contaminant loading. Secondly, the asymmetrical breakthrough curves show persistent tailing of contaminants concentration after source removal. Others documenting asymmetrical breakthrough curves for transport in heterogeneous media include Rao et al. (1980), Sudicky (1985), Chapman and Parker (2005), Sale et al (2007), and Liu et al. (2007). The above supports an observation that there can be significant flaws to using transport models predicated on homogeneous media for contaminant transport in heterogeneous media.

6.4.2 Tank 2: Enhanced Flushing

Similar to Tank 1 (and all the other tanks) TCE loading results in an average low k zones total contaminant concentration of 0.0064 moles/kg dry soils (850 mg/kg) (**Figure 6-2).** Following TCE loading, flushing with water only at the standard seepage velocity of 0.33 m/day yields a one order of magnitude reduction in effluent concentrations over a period of 20 days (**7 pore volumes**) and the onset of TCE transformation to cDCE. Again, no other TCE metabolites were observed.

Subsequent flushing at five times the standard seepage velocity for 27 days (**45 pore volumes**) yielded a second order of magnitude reduction in TCE effluent concentration. Interestingly, the total contaminant discharge over the period of active flushing (cumulative mass discharge over time) is 1.64 grams of TCE. This is only 1.4 times greater than the total contaminant discharge from Tank 1 over the same period.

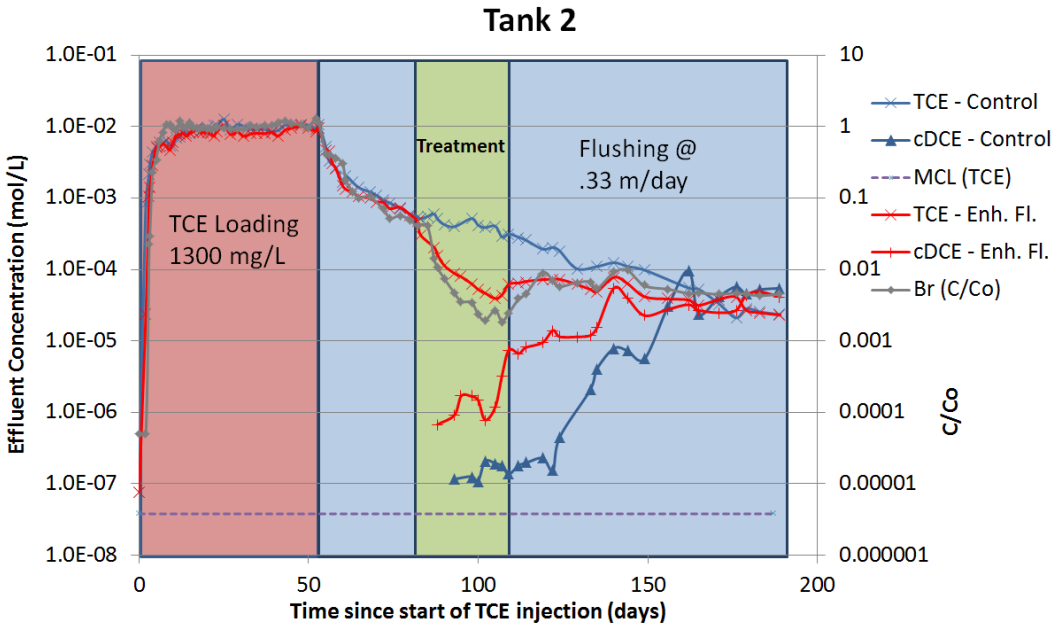

Figure 6-2: TCE levels for the Enhanced Flushing treatment (Red) with Control (Blue). The treatment window is shown in green.

Performance Summary	Order of Magnitude Reduction (% Reduction)	
	TCE	TOTAL CVOCs
Enhanced Flushing treatment *81 Pore Volumes after loading stopped.*	**2.6** (99. 7%)	**2.1** (99.3%)
Control	*2.6 (99.7%)*	*2.07 (99.1%)*

Returning to the seepage velocity of 0.33 m/day and flushing for an additional 82 days (**27 pore volumes**) yielded nearly another order of magnitude reduction in effluent concentrations and TCE and a molar ratio of 0.56 TCE to cDCE. At 189 days the apparent benefit of enhancing flushing by a factor of 5 for 27 days was an 18% reduction in total CVOC in the effluent relative to Tank 1 (control), but only a 2.1% decrease in effluent TCE levels at this time.

Key Observations

- The apparent one order of magnitude reduction in effluent TCE concentration relative to Tank 1 at day 107 decreased to a 18% reduction in total CVOCs relative to Tank 1 at 189 days.
- While the benefits of flushing appear to decline with time, no rebound (increases) in TCE were observed
- Full-scale treatment would likely require far large periods of flushing and could benefit from driving water across low k zones versus along low k zones as done in the Tank 2 study.

6.4.3 Tank 3: Permanganate

Similar to all tanks, TCE loading results in an average low k zones total contaminant concentration of 0.0082 moles/kg dry soils (1079 mg/kg) **(Figure 6-3)**. Following TCE loading, flushing with water only at the standard seepage velocity of 0.33 m/day yielded a one order of magnitude reduction in effluent concentrations over a period of 24 days (**8 pore volumes**) and the onset of TCE transformation to cDCE. Again, no other TCE metabolites were observed.

Addition of 2,000 mg/L of potassium permanganate to the influent at 80 days reduced effluent TCE to level below detection limits (2.28 E-8 moles /L) within 7 days of the onset of treatment. Concurrently, effluent sample were purple due to the presence of permanganate in the effluent. During active treatment, advancement of a brown reaction front into the silt layers was observed along the silt sand contact in all part of the tank. Initially the front moved quickly. With time, advancement of the front slowed and stopped. . Maximum penetration of the front over the 27 day treatment period was 1.3 cm.

Subsequent to permanganate treatment, effluent TCE concentrations rebounded to within levels of one order of magnitude less than Tank 1 concentrations to 4.16E-5 mol/L at day 122 (**5 pore volumes after treatment ended**). Concurrently, cDCE concentrations increase to levels one order of magnitude less than TCE concentrations. Post treatment TCE concentrations peak at 122 days and subsequently decayed slowly. Interestingly, post treatment improvements in water TCE concentrations are slower in the permanganate tank than in the control tank. Furthermore, cDCE levels are lower in the permanganate tank versus the control after day 150. A possible explanation is permanganate was limiting the natural degradation of TCE to cDCE by affecting microbial populations during treatment. At 189 days (35 pore volumes after treatment started) the apparent benefit of the permanganate treatment is a 80% reduction in total CVOC in the effluent relative to Tank 1 (control).

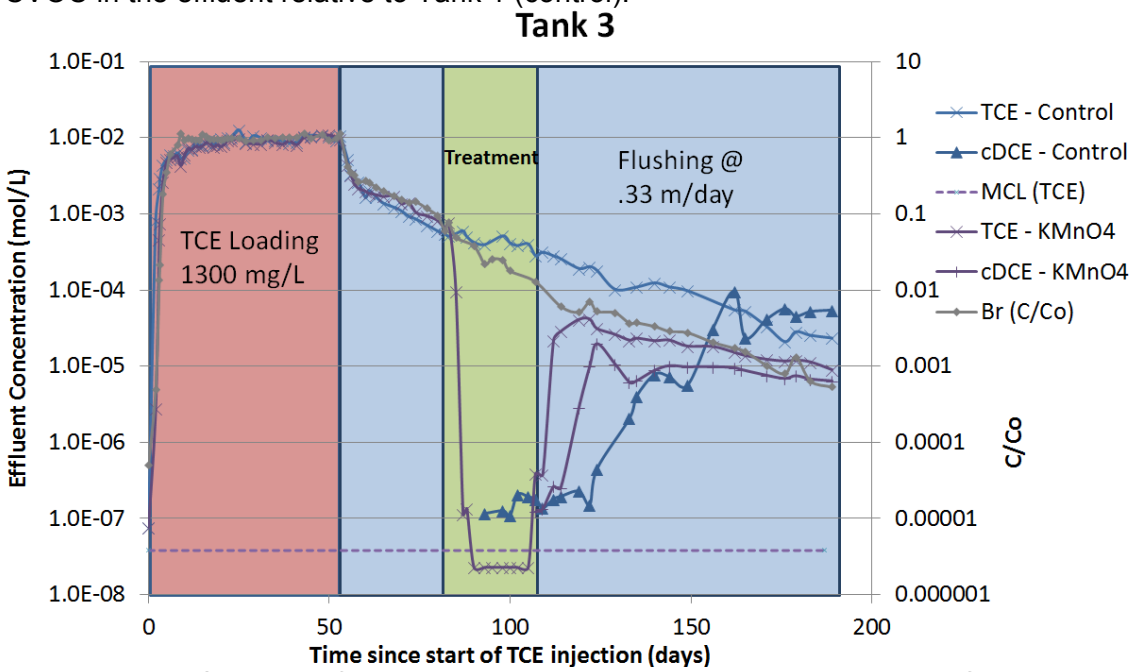

Figure 6-3: TCE levels for the Permanganate treatment (Purple) with Control (Blue)

Performance Summary	Order of Magnitude Reduction (% Reduction)	
	TCE	TOTAL CVOCs
Permanganate Treatment *45 Pore Volumes after loading stopped.*	**3.1** (99.9%)	**2.8** (99.8%)
Control	*2.6 (99.7%)*	*2.07 (99.1%)*

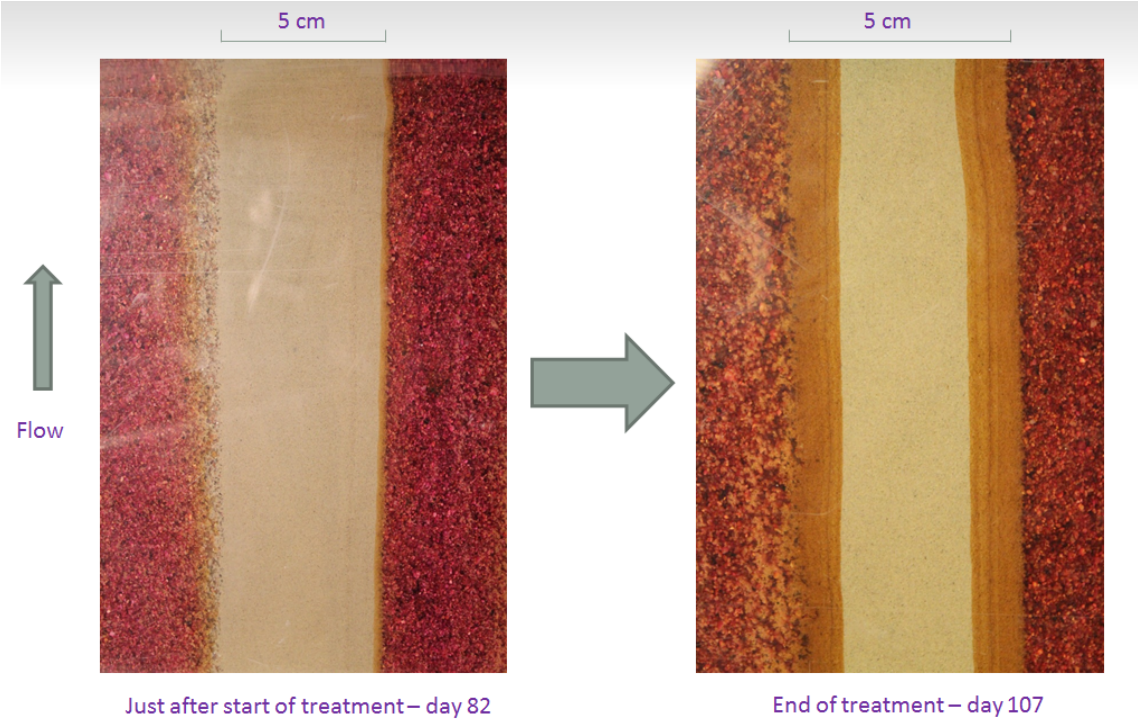

Figure 6-4: Permanganate diffusion into silt zones during the 27-day treatment.

Key observations from the Permanganate treatment tank include:

- Permanganate provided rapid depletion of TCE discharging from transmissive zone while it was present in the transmissive zones.

- Visual penetration of permanganate into the low k zones suggests partial degradation of TCE in the low k zones was achieved (**Figure 6-4)**. With time this may have been limited by plugging of the pore space at the contact by precipitates, or by the NOD of the soil.

- Displacement of the permanganate subsequent to flushing lead to rapid rebound of TCE in the tank effluent. This suggests that longer treatment periods are required in this scenario to achieve more consequential improvements in water quality.

- Late data from the permanganate study and the control suggest that permanganate may have an adverse effect on natural attenuation of TCE via biotic processes.

Figure 6-4 helps explain this rebound behavior illustrated in **Figure 6-3** of the effluent TCE concentrations; incomplete penetrating of the treatment into the low permeability zones. The cause of this is probably due to a number of factors, which include factors such as very slow diffusion rates and the COD within the silt layers (F_{oc} = 0.3%). Again we see increasing levels of cDCE, which could illustrate the presence of biological colonies within the untouched portions of the low permeability zones. No Vinyl Chloride was detected. At the end of the experiment, the effluent TCE concentration was 1.18 mg/L (9.00E-06 mol/L). This tank treatment was able to qualitatively and quantitatively demonstrate the limitations for this remediation technology that field sites must overcome in order to be successful in treating heterogeneous aquifers with TCE stored in the low permeability zones.

6.4.4 Tank 4: Lactate and KB1

Similar to the other tanks, TCE loading results in an average low k zones total contaminant concentration of .0.012 moles/kg dry soils (1572mg/kg) **(Figure 6-5)**. Following TCE loading, flushing with water only at the standard seepage velocity of 0.33 m/day yielded a one order of magnitude reduction in effluent concentrations over a period of 24 days and the onset of TCE transformation to cDCE.

Addition of 2,000 mg/L Sodium Lactate (with an initial KB1 inoculum) from day 80 to 107 leads to:

- An initial spike in effluent TCE concentrations and, at the end of treatment, a three order of magnitude decrease in effluent TCE concentrations.

- Increases in c-DCE and VC concentrations that are proportional to the observed decreases in TCE.

- Production of vinyl chloride.

Following active treatment (at day 107 Sodium Lactate source is removed):

- TCE concentrations are nearing three orders of magnitude lower than Tank 1 levels for 60 days (**20 pore volumes**). Subsequently, TCE concentrations rebound by two orders of magnitude to 7.653E-6 mol/L.

- cDCE concentrations decrease from a factor of 4,518 greater than tank 1 levels at day 98 to a factor of 0.22 of Tank 1 levels at day 189.

- At 189 days the apparent benefit of the lactate plus KB1 is a 73% reduction in total CVOC in the effluent relative to Tank 1 (control).

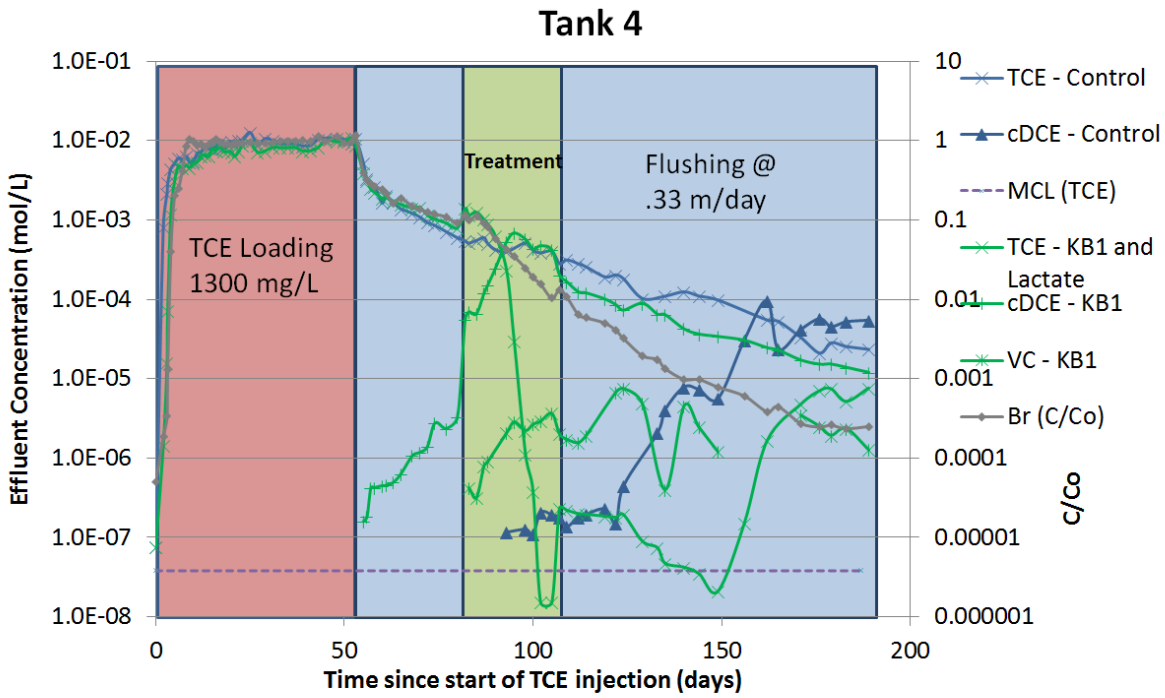

Figure 6-5: TCE levels for the Biodegradation treatment with lactate and KB1 (Green) with Control (Blue)

Performance Summary	Order of Magnitude Reduction (% Reduction)	
	TCE	TOTAL CVOCs
Biodegradation treatment with lactate and KB1 45 Pore Volumes after loading stopped.	**3.2** (99.9%)	**2.71** (99.8%)
Control	*2.6 (99.7%)*	*2.07 (99.1%)*

Key Observations

- During treatment the lactate and KB1 treatment increased total discharge of CVOCs relative to the control. No clear explanation is available for why cDCE and VC were not being effectively dechlorinated during this period.

- After adding KB1 and Sodium Lactate, significant amounts of cDCE and VC were produced.

- Late stage rebound of TCE and decreases in cDCE suggest that the effects of lactate loading persisted for 60 days (**20 pore volumes**) after ending treatment as opposed to an almost instantaneous end of treatment effects seen in the permanganate study.

- Once the tank entered reducing conditions, the bromide tracer could no longer be considered as a conservative tracer. This is shown to be true for each of the biological treatment tanks.

Rebound of TCE near the end of the experiment is evidence that the KB1 did not move into the low permeability zones and degrade the available TCE stored there. Samples were run after the tanks were opened to determine the probable locations of the *Dehalococcoides*; are they populating the sand, the silts or the interface between the two. The following table shows the populations of 3 soil samples tested for *Dehalococcoides*:

Soil	***Dehalococcoides*** **Enumeration/gram**
Middle of Silt	4×10^3 J
Interface Silt/Sand	**3×10^4**
Middle of Sand	3×10^2 J

Note: *J - estimate between detection limit of method and quantitation limit.

Table 6-1: *Dehalococcoides* populations within the KB1 treatment tank.

Table 6-1 shows how the mechanism for treatment occurs within a KB1 treatment; at the interfaces between transmissive and low permeability zones, where the *Dehalococcoides* communities can be found. Further investigation in the literature found similar results about the behavior of these bugs. With this in mind, the mechanism demonstrates the major shortcoming of an inoculation of *Dehalococcoides* into a heterogeneous porous media. Unless the KB1 can penetrate the low permeability zones that are storing and releasing the TCE, the treatment will stall once the available carbon for metabolism is exhausted.

6.4.5 Tank 5: Lactate, KB1, and Xanthan Gum

As with the other tanks, TCE loading results in an average low k zones total contaminant concentration of 0.0093 moles/kg dry soils (1221mg/kg) **(Figure 6-6)**. Following TCE loading, flushing with water only at the standard seepage velocity of 0.33 m/day yielded a one order of magnitude reduction in effluent concentrations over a period of 24 days and the onset of TCE transformation to cDCE.

Key Observations

Addition of 2,000 mg/L Sodium Lactate, 1000 mg/L Xanthan Gum (with an initial KB1 inoculum) from day 80 to 83, followed by a 24-day shut-in period resulted in:

- At the end of treatment, a nearly three order of magnitude decrease in effluent TCE concentrations relative to the control.
- Increases in cDCE concentrations that are proportional to the observed decreases in TCE.
- Production of vinyl chloride.

Following treatment (day 107):

- TCE concentrations are 2-3 orders of magnitude lower than Tank 1 levels for 60 days (i.e., maintained low concentrations for **20 pore volumes** after the 24 day no flow period). Subsequently, TCE concentrations rebound by two orders of magnitude around day 170 to 6.83E-6 mol/L.

- cDCE concentrations decrease from a factor of 4253 greater than tank 1 levels at day 109 to a factor of .132 of Tank 1 levels at day 189.

- At day 189 the apparent benefit of the lactate plus KB1 is a 81% reduction in total CVOC in the effluent relative to Tank 1 (control).

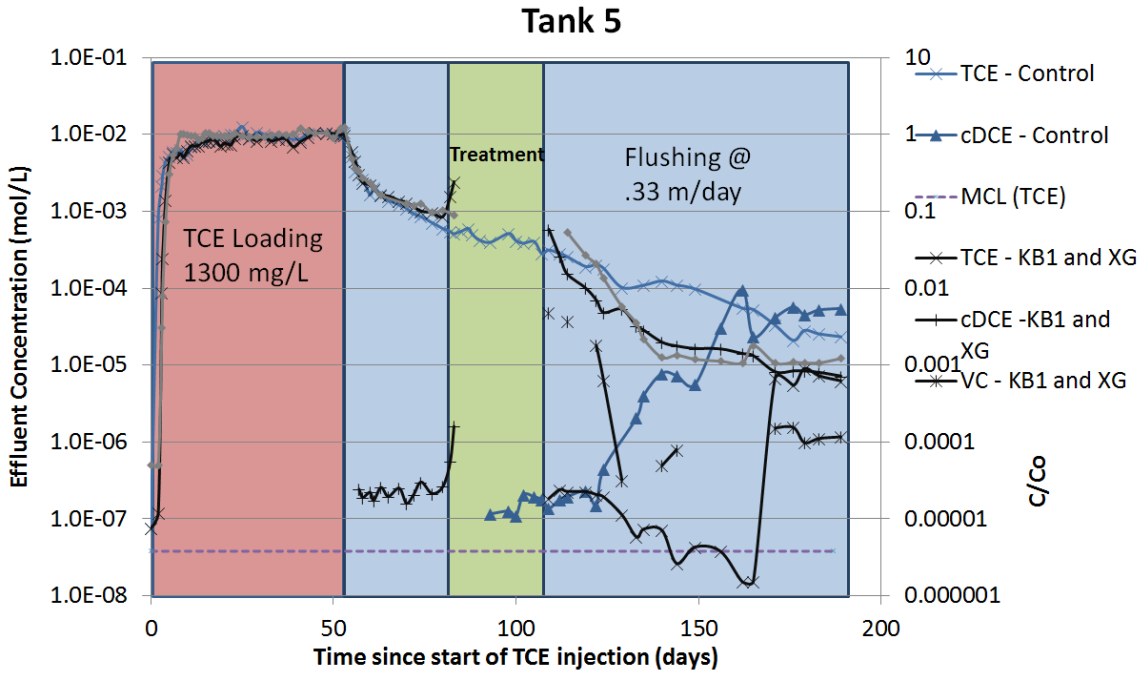

Figure 6-6: TCE levels for the Biodegradation Treatment with KB1 and Xanthan Gum treatment (Black) with Control (Blue)

Performance Summary	Order of Magnitude Reduction (% Reduction)	
	TCE	TOTAL CVOCs
Biodegradation Treatment Lactate, KB1, and Xanthan Gum *38 Pore Volumes after loading stopped.*	**3.2** (99.9%)	**2.8** (99.8%)
Control	*2.6 (99.7%)*	*2.07 (99.1%)*

Again, soil samples were taken from the tanks to determine the population locations of the *Dehalococcoides*; sands, silts or at the interface. The following table shows the populations of 3 soil samples tested for *Dehalococcoides*:

Soil	***Dehalococcoides*** **Enumeration/gram**
Middle of Silt	2×10^3 J
Interface Silt/Sand	**1×10^4**
Middle of Sand	2×10^3 J

Note: *J - estimate between detection limit of method and quantitation limit.

Table 6-2: *Dehalococcoides* populations within the KB1 and Xanthan Gum treatment tank.

As with **Table 6-1,** the population of *Dehalococcoides* is mostly located at the interfaces in the tanks, which means that either the Xanthan Gum was not successful in forcing the treatment media into the low permeability zones, or that the KB1 was indeed forced into the silts but did not survive and/or replicate to a level that would dechlorinate the TCE.

6.4.6 Tank 6: Lactate, Sulfate Reducing Bacteria (SRB), and Magnesium Sulfate

As with the other tanks, TCE loading results in an average low k zones total contaminant concentration of 0.011 moles/kg dry soils (1452 mg/kg) **(Figure 6-7)**. Following TCE loading, flushing with water only at the standard seepage velocity of 0.33 m/day yielded a one order of magnitude reduction in effluent concentrations over a period of 24 days and the onset of TCE transformation to cDCE.

Addition of 5,370 mg/L Sodium Lactate, 2,880 mg/L Magnesium Sulfate (with an initial SRB inoculum) from day 80 to 107 resulted in:

- During treatment, almost no change in effluent TCE concentrations from the control.
- No increase in cDCE concentrations.
- No production of vinyl chloride was observed.

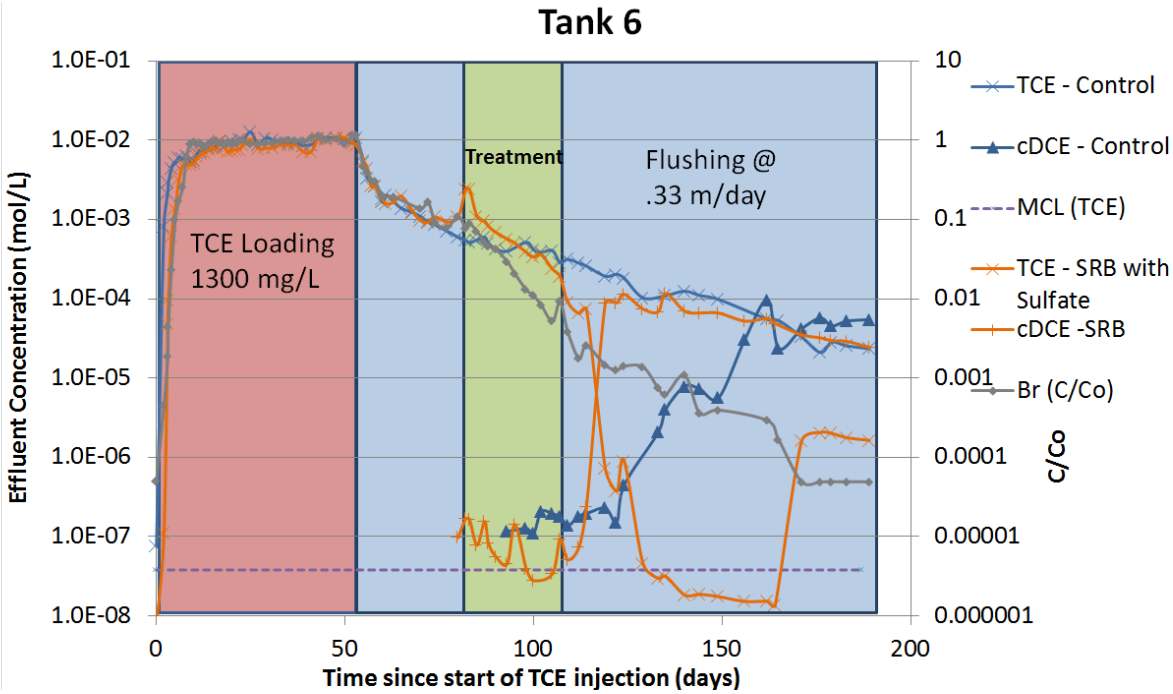

Figure 6-7: TCE levels for the Sulfate Reducing Bacteria and Sulfate treatment (Orange) with Control (Blue)

Performance Summary	Order of Magnitude Reduction (% Reduction)	
	TCE	TOTAL CVOCs
Sulfate Reducing Bacteria and Sulfate treatment *45 Pore Volumes after loading stopped.*	**3.8** (99.98%)	**2.56** (99.7%)
Control	*2.6 (99.7%)*	*2.07 (99.1%)*

Key Observations

Following treatment (day 107):

- TCE concentrations are over 3 orders of magnitude lower than Tank 1 levels for 60 days (**20 pore volumes**), and reach the method detection limits of ~3 ppb around day 140. Subsequently, TCE concentrations rebound by two orders of magnitude around day 170 to 1.599E-6 mol/L, or **21 Pore Volumes** after treatment stopped)

- cDCE concentrations decrease from a factor of 390 greater than tank 1 levels at day 119 to a factor of 0.446 of Tank 1 levels at day 189.

- At day 189 the apparent benefit of the Lactate, $MgSO_4$ plus SRB is a 66.7% reduction in total effluent CVOC relative to Tank 1 (control).

- An obvious color change occurred in the Tank 6 over the course of the experiment **(Figure 6-8).**
- Dechlorination of TCE to cDCE did not occur while sulfate was present in higher concentrations.
-
- Presence of cDCE points to a biological dechlorination pathway instead of a mineralogical.

Figure 6-8: SRB treatment tank at the beginning (left) and end (right) of the 24-day treatment.

6.5 COMPARISON BETWEEN TREATMENTS

A comparison of results from the treatments is shown in in Table 6-3 and Figure 6-9. General observations are:

1. **For flushing alone**, the first 8 pore volumes provided 1 OoM reduction in TCE concentration, while the next 21 pore volumes were required to get to 2 OoMs, and 45 pore volumes to end at 2.6 OoMs. To put the pore volumes in perspective, if one has a source zone or plume 100 meters long in direction of groundwater flow, with groundwater seepage velocity of 30 meters per year, then a 45 pore volume flush would take 152 years.

2. **For enhanced flushing**, a total of 81 pore volumes were required to get a 2.6 OoM reduction.

Table 6.3 Performance of six remediation technologies from tank studies.

	Apparent stored TCE in silts On day 52		Drop in effluent TCE Conc. From loading (OoM)				Total CVOC Effluent Conc. Red. from Control	OoM exceedance of TCE MCL at 189 days	Mol TCE/ Mol DCE day 189
	Moles	mg/kg	Day				%		
			52	80	107	189			
Tank 1 – Control	0.005	637	0	1.2	1.5	2.59	0	2.78	0.43
Tank 2 - Enhanced flushing	0.006	850	0	1.17	2.3	2.58	18	2.78	0.55
Tank 3 - Permanganate	0.008	1079	0	1.1	4.4	3.05	80	2.37	1.4
Tank 4 - Lactate + KB1	0.012	1573	0	1.1	4.66	3.15	73	2.30	0.64
Tank 5 - Lactate+ KB1 + Xanthan gum	0.0093	1221	0	1.0	4.72	3.2	81	2.22	0.86
Tank 6 – Biogeochemical RD	0.011	1452	0	.95	1.7	3.76	66.7	1.63	0.067

Figure 6-9. Concentration Reduction in Remediation Tank Experiments
(OoM: Order of Magnitude. PV: Pore Volume)

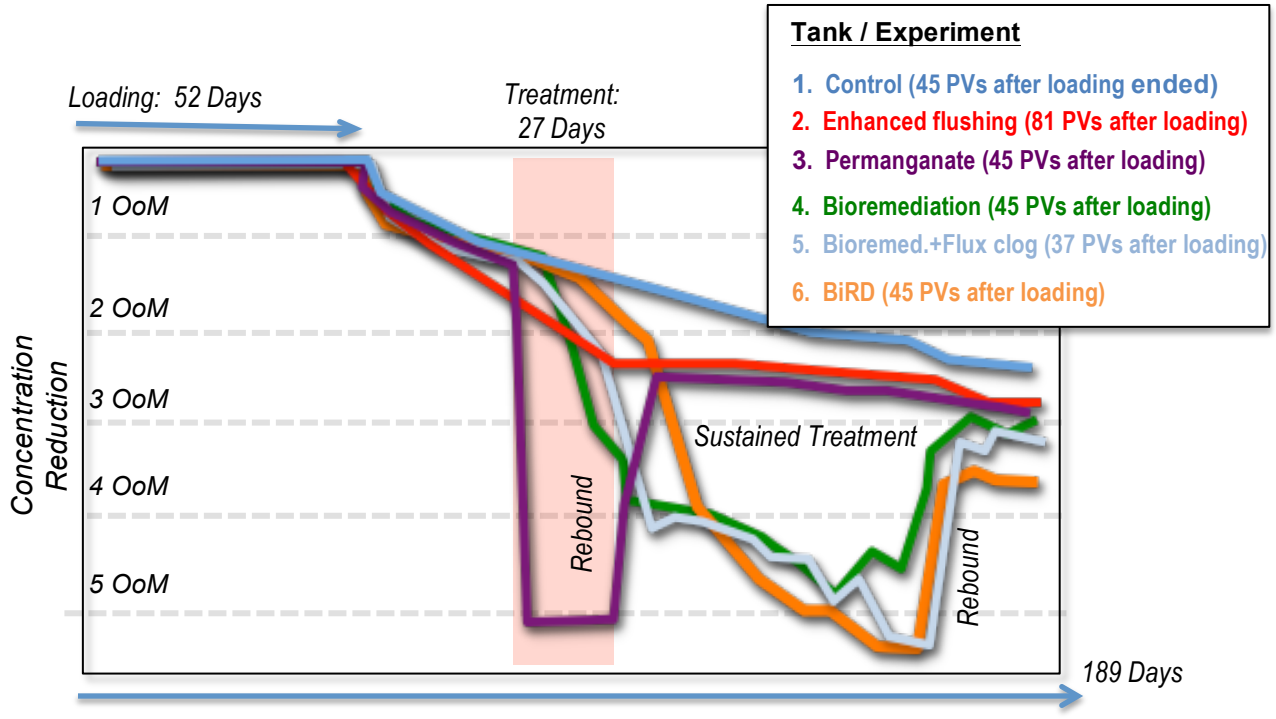

3. **Chemical oxidation** provided some of the lowest concentrations during treatment, but immediately rebounded following treatment to a level about 1 OoM more reduction than the control. At the end, the TCE concentration had been reduced to 3.05 OoMs (compared to 2.6 for the control). The permanganate treatment reduced the total CVOC effluent concentration to about 20% of the control tanks' total CVOC effluent concentrations, indicating significant treatment and removal of TCE by chemical oxidation compared to the flushing scenarios. Chemical oxidation did have the advantage of relatively lower total CVOC concentrations for the period after treatment compared to the three biological treatments in tanks 4, 5, and 6.

4. The **bioremediation/bioaugmentation** scenario had about the same ending performance as the chemical oxidation tank (3.15 vs. 3.05 OoMs), but showed "sustained treatment" (Adamson et al., 2012) for about 60 days or 20 pore volumes after treatment ended. If all other conditions were equal, and if sustained treatment processes are proportional to pore volumes of flushing after treatment, then a sustained treatment process lasting for 20 pore volumes would last 68 years for a source zone 100 meters long with 30 meters per year seepage velocity. At the end of treatment the total CVOC concentrations were similar to the chemical oxidation case: about a 73% reduction in effluent concentrations compared to the control case. Total CVOC concentrations were higher during treatment compared to the control.

5. The **bioremediation + "flux clog"** process was slightly better compared the bioremediation/bioaugmentation results, even though there was about a 20 day period of no flow while the xanthan gum was present. Sustained treatment effects were evident for about 60 days or 20 pore volumes. A permanent clogging agent rather than the temporary guar gum clogging agent would have shown very different results: no effluent mass flux due to the clogging. Total CVOC concentrations were higher during and for about 5 days after treatment compared to the control.

6. The **biogeochemical process** had a different profile than the two previous bioremediation scenarios: no significant reduction in effluent TCE during the sulfate and lactate flushing, then sustained production of cDCE, then a TCE rebound. The ending TCE concentration reduction. 3.76 OoMs, was the best of any technologies at dechlorinating TCE, and the reduction of total CVOC effluent concentrations compared to the control was 66.7%. Cis-DCE concentrations were significantly higher than the control for about half of the post-treatment period (to about day 150).

None of the six tanks achieved effluent concentrations below 0.005 mg/L, the MCL for TCE, at the end of the experiments. Tank 6, the biogeochemical process, came the /closest with effluent concentrations of about 0.236 mg/L at day 189 (45 pore volumes after loading stopped), but the success of this treatment would be up for interpretation as the health risks from exposure and MCLs for cDCE and TCE are different.

6.6 COMPARISION TO FIELD OBSERVATIONS

6.6.1 Order of Magnitude Rule of Thumb

The remediation field has used several "rules of thumb" about remediation performance and behavior of remediation technologies. For example, Sale et al., (2008) suggested that based on multiple site studies of remediation performance that:

> *Based on the results of the studies described above, well-implemented in situ remediation projects are likely to reduce source zone groundwater concentrations by about one to possibly two orders of magnitude (90 - 99% reduction) from pretreatment levels. However, it is difficult to predict the actual performance of an individual remediation project prior to its application in the field.*

In the research tank experiments, which are highly idealized and simplified versions of very heterogeneous systems, reductions in concentrations between 1.7 and 4.2 OoMs were observed immediately after treatment ended at day 107 for the four in-situ tanks, compared to 1.6 OoMs for the control, flushing-only tank. For example, Tank 4 (bioremediation/bioaugmentation) saw a 4.66 OoM reduction at day 107 compared to about 1.5 for the control tanks, or an overall improvement **of 2.6 OoMs.**

By the end of the test (day 189), when back diffusion had reestablished itself, the five remediation processes had improved the quality of the effluent TCE by between **0.02 to 1.16 OoMs** relative to the control**.**

So the "1-2 OoM" rule of thumb from Sale et al., 2008 seemed to underestimate the performance of the research tanks right after treatment ended, but then overestimated performance over the long term as sustained treatment processes faded away and matrix diffusion processes once again controlled contaminant transport at the site.

6.6.2 Sustained Treatment Observations

The sustained treatment aspects of the research tank experiments were very interesting and revealing. Adamson et al., (2011) defined sustained treatment as:

> *Sustained treatment is an emerging concept used to describe enhancements in attenuation capacity after the conclusion of the active treatment period for a given source-depletion technology. The term includes mechanisms that lead to contaminant transformation or destruction over extended periods of time, such as endogenous biomass decay, slow diffusion of remedial amendments from low-permeability zones, and the formation of reactive mineral species. This "value-added" treatment continues after the end of capital expenditures at a site, and it provides additional insight in determining if monitored natural attenuation is a viable long-term option for a site.*

They reported an apparent tendency for sustained treatment for biological processes, such as addition of electron donor, but not chemical oxidation based remediation technologies.

In the tank experiments, this same pattern was observed, but with some nuances between the three different biologically-related processes. Note that in the tanks, all the

flushing was done with de-gassed tap water, making the tanks somewhat different than a field site where aerobic groundwater is the flushing agent before and after remediation.

In the chemical oxidation tank (Tank 3), significant reductions in concentration (> 5 OoMs) was observed during treatment, but almost as soon as the treatment ended the concentrations immediately rebounded. The post-rebound concentrations were still lower then the control tank concentrations at this time (about day 110), and then a slow reduction in concentrations was observed until the end of the test on Day 189.
Key Point: No Observed Sustained Treatment for Chemical Oxidation

In the bioremediation/bioaugmentation tank (Tank 4) there was a 4 OoM drop in concentrations during treatment, which was then slow got lower with some fluctuations over the next ~60 days (about 20 pore volumes after treatment ended).
Key Point: ~ 20 Pore Volumes of Sustained Treatment for Bioremediation

In the bioremediation + "flux clog" tank (Tank 5) there was a 4 OoM drop in concentrations during treatment, which was then slow got lower with some fluctuations over the next ~60 days about 20 pore volumes after treatment ended).
Key Point: ~20 Pore Volumes of Sustained Treatment for Bioremediation/Flux Clog

In the biogeochemical tank (Tank 6) there was a less than a 0.75 OoM drop in concentrations during treatment but the concentrations dropped rapidly over the next 60 days, after which a small rebound in effluent TCE was observed.
Key Point: ~ 20 Pore Volumes of Sustained Treatment for Biogeochemical Process

In summary, unless chemical oxidation can completely penetrate impacted low k zones, this treatment does not appear to provide any sustained treatment benefits, but any type of electron donor addition seems to promote significant sustained treatment: conventional bioremediation, novel processes such as electron donor addition + clogging agents, or for stimulating biogeochemical degradation all seem to promote sustained treatment.

The duration of sustained treatment is difficult to project, but Adamson et al. (2011) suggest that it might last from 1 to 6 years from a combination of biomass decay and biogeochemical decay processes. The 60-day, 20 pore volume duration of sustained treatment in tanks 4, 5, and 6 suggest that under the right conditions, the sustained treatment might (in theory) last longer. If the duration of sustained treatment is proportional to pore volumes flushed, then at a site with 100 meter long source zone (or plume) and groundwater flowing at 30 meters per year, then it would take 68 years to flush 20 pore volumes. No doubt that geochemical conditions of the flushing groundwater is important; for these tank studies anaerobic degassed tap water is used. But these results do suggest that additional field, lab, and modeling work may be fruitful to better understand and predict the effects of sustained treatment.

6.6 OPPORTUNITIES

Key opportunities from this research include:

- More investigation of a “permanent” flux clog type bioremediation process;
- More detailed study of the factors that control the length of the sustained treatment process.
- Better understanding of the key processes, economics, and kinetics of the biogeochemical process, which at the end of the test had the best performance of the different technologies tested.
- Integrating the research tank results into modeling efforts, both for simpler analytical models and for more complex numerical models.
- More research on containment strategies, and how matrix diffusion processes and transmissive zone processes are either improved or hampered by reduction of flow and competing electron acceptors through the treatment zone (e.g., ESTCP project 201328).

6.7 CHAPT. 6 - TREATMENT IN LOW k ZONES – KEY RESEARCH PRODUCTS

Research Tank Studies: Detailed 60-100 Pore Volume Tank Simulations of Six Remediation Technologies

- Concentration vs. time data for six tanks
- Evaluation of mass distribution vs. time
- Degradation of parent to daughter products
- Visualizations of key concepts, like penetration of amendments into silt and production of minerals in low k zones.

OVERVIEW OF CHAPTER 7: *IMPLICATIONS*

The work performed for this SERDP project involved laboratory experiments, fate and transport modeling, work at two field sites, and studies of remediation performance in large research tanks. Some of the key take home points of this work include

- Low permeability zone are a heavily under-sampled compartment at contaminated sites;
- These zones can be "charged" or "loaded" by diffusion processes over the period of decades, and significant mass can accumulate;
- This mass is like "dark matter" that is affecting the outcomes of remediation, but is not part of the DNAPL-centric conceptual model.
- Site characterization has adapted to a second-generation (2G) high resolution approach to find this "dark matter", but third-generation (3G) approaches are still needed.
- We need to better understand how to estimate diffusion coefficients, and if and when degradation in low k units is occurring.
- Matrix diffusion is a key process in every "Type Site" scenario modeled by the research team. Even thin layers of clays can preclude reaching low-ppb cleanup standards for decades because of matrix diffusion.
- Remediation processes are not efficient at removing mass from low k zones. Some technologies provide an apparent period of "sustained treatment" for relatively long periods but even these rebounded so concentrations exceeded low ppb cleanup standards in the research tanks.
- Based on this and other information, nine implications for selecting site remedies were developed:
  - *Implication 1: Amendments are More Difficult to Apply in Low k Units*
  - *Implication 2: Thermal Processes Have a Theoretical Advantage, But…*
  - *Implication 3: Destroying the Heterogeneity Works*
  - *Implication 4: Interfaces and Targeted Treatment*
  - *Implication 5: These are Nonpoint Sources*
  - *Implication 6: Containment, Perhaps in Different Forms, Makes a Comeback*
  - *Implication 7: It is Important to Know if Your Site is In Its Early, Middle, or Late Stage*
  - *Implication 8: This is a Management and Regulatory Problem Too*
  - *Implication 9: What is the Objective?*
  - *Implication 10: Don't Underestimate Human Ingenuity*
- While this is a difficult problem, the authors are **optimistic** about our ability to develop better, more scientifically based solutions to problems caused by matrix diffusion.

Key Words: Objectives, nonpoint, sources, containment, regulatory, site stage, interfaces, amendments, injection.

7.0 IMPLICATIONS FOR SELECTING SITE REMEDIES

7.1 OVERVIEW

Lead Authors for This Chapter

Charles Newell, GSI Environmental
Tom Sale, Colorado State University

Remediation has evolved over time to account for new conceptual models of contaminants in the subsurface. The transition from a pump-and-treat dominated approach in the 1980s and early 1990s to an in-situ focused approach was a response to the overwhelming success of the DNAPL paradigm. Researchers, practitioners, and regulators embraced DNAPL as a new "compartment" that was present at most chlorinated solvent sites that required new ways of characterization, remediation, and thinking about sites. The new compartment had concentrated mass, a different way of moving through the subsurface, and persistence.

The remediation community addressed the new paradigm starting in the early 1990s with vigor, creativity, and an almost single-minded focus. There was an explosion in technology development, with the DNAPL problem being posed to biological, chemical, and physical based processes. The marketplace responded with entire companies built around these processes such as chemical oxidation, bioremediation, zero-valent iron, and thermal remediation. **Figure 7-1** shows the rise of the DNAPL concept as shown in Google Scholar citations: from less than 20 in the entire 1990s, by 2005-2009 there were almost 500 technical citations in the Google universe referring to "DNAPL."

During this period, however, remediation performance studies began to emerge that showed that the new in-situ remediation technologies, while improving site conditions significantly, did not seem to be able to fully restore groundwater to drinking water conditions. This led to a reevaluation of the groundwater conceptual model, and a process that was heavily studied before the full emergence of the DNAPL paradigm was reevaluated: matrix diffusion. Figure 7-1 shows the rise of matrix diffusion as a groundwater transport research topic as indicated by Google Scholar citations.

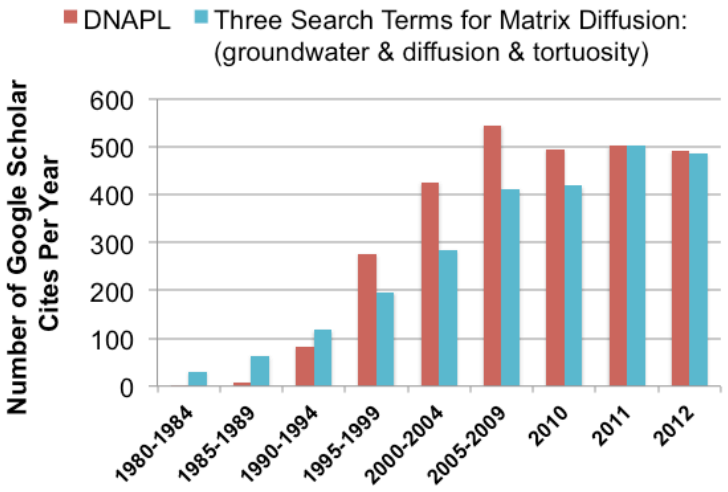

Figure 7-1. Number of Google Scholar citations for term "DNAPL" and three terms designed to identify diffusion studies for groundwater transport studies.

The previous chapters of this report summarize the key features of matrix diffusion paradigm:

- Low permeability zone are a heavily under-sampled compartment at contaminated sites;
- These zones can be “charged” or “loaded” by diffusion and slow advection processes over the period of decades, and significant mass can accumulate;
- This mass is like “dark matter” that is affecting the outcomes of remediation, but is not part of the DNAPL-centric conceptual model.

The emerging matrix diffusion conceptual model has some similarities with emergence of the DNAPL paradigm over the previous pump-and-treat paradigm: there is more mass in the subsurface than thought; it is harder to remove; and persists for a long time. The implications for remediation are significant.

7.2 KEY IMPLICATIONS FOR REMEDIATION

Removal of contaminants from matrix diffusion source zones is a much different problem than removal of DNAPL. Making it more difficult is the low permeability and the large, diffuse volumes that are present at these sites. Making it easier is that there is the potential to target interfaces rather than storage volumes, and the fact that the mass discharge from these areas is sometimes very low and predictable.

7.2.1 Implication 1: Amendments are More Difficult to Apply in Low k Units

Key concept: Several existing remediation technologies used some type of injection to remove DNAPL. The most common examples are the use of surfactants and cosolvents to mobilize or solubilize the DNAPL; chemical oxidants or reductants to chemically destroy the DNAPL; or more recently, addition of electron donors to stimulate dissolved phase remediation, and therefore increase the rate of DNAPL dissolution.
matrix diffusion.

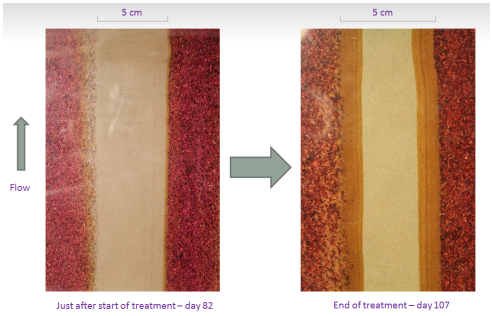

Challenge: Most contaminated zones in unconsolidated hydrogeologic settings have heterogeneity that ranges over several orders of magnitude. This poses extreme problems for injection-based approaches, where amendments such as chemical oxidants or electron donor are injected in an attempt to mix a reaction chemical with the contaminants. In short, getting contaminants into low permeability silts and clays is very difficult over the scale of hundreds or thousands of cubic yards of source zone. Even sources without silts and clays can be problematic, as even a factor of 10 difference in hydraulic conductivity (from a sand to a gravel) means that an injection fluid will flow preferentially in the gravel, leaving the sand almost untreated.

Key implication: It is extremely difficult to distribute amendments uniformly in geologic media, which is almost always non-uniform. To improve remediation efficiency for injection-based approaches, some improvement may be realized by shear thinning type fluids which will reduce the relative permeability difference between two adjacent zones with different hydraulic conductivity. Fracturing technologies will increase in their importance and their applicability.

Example: ESTCP has funded two shear thinning projects, one where shear thinning fluids are mixed with chemical oxidants (ER-200912) and one with a bioremediation chemical (ER-20913). For the chemical oxidation project, the use of polymer resulted in a test plot sweep efficiency of 67%, double that of the control plot (sweep efficiency = 33%). Fracturing technologies using a wide variety of methods are becoming much more common place in the remediation marketplace and have demonstrated an performance advantage and economic value for many remediation projects.

Prognosis: Shear thinning and fracturing will become much more common, but there will still likely be considerable mass in low k zones that remain untreated by injection based technologies. Complete cleanup of contaminated sites will remain elusive.

7.2.2 Implication 2: Thermal Processes Have a Theoretical Advantage, But…

Key concept: A few DNAPL removal technologies don't rely on K (hydraulic conductivity) to make them work. For example, thermal processes rely on thermal conductivity (which only varies by a factor of 2 between sand and clay) compared to hydraulic conductivity (which can vary by a factor of 1000 or more between sand and clay).

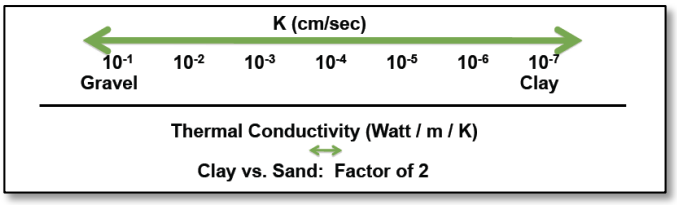

Challenge: While the theoretical case is compelling, actual performance data from thermal remediation sites does not seem to be significantly different than amendment based technologies. This means that the performance data is missing improvements in the low permeability zones, or that the design/implementation thermal projects have been applied have not treated the low permeability zones (e.g., they were not run long enough to heat up the low permeability zones). In addition, thermal remediation is one of the most costly remediation approaches making it difficult to apply to a large diffuse source (see Implication 4 below).

Key Implications: Better data is needed on the actual concentration of contaminants in low permeability zones before-and-after thermal remediation projects to answer this question: is the theoretical advantage of thermal realized at actual field sites?

Example: Data from a detailed study of 14-sites shows a median percent reduction in treatment zone concentration of 1 order of magnitude (90%), which is similar to amendment-based technologies.

Prognosis: This is a proven technology with some very impressive site remediation successes. While having theoretical advantages over amendment based approaches, however, the lack of performance improvement and the high cost of thermal technology make it unclear if it will enjoy widespread use as a method to treat large-scale low-permeability zones.

7.2.3 Implication 3: Destroying the Heterogeneity Works

Key concept: Soil mixing, when combined with reagent addition, is a successful DNAPL treatment technology. The physical disruption of the heterogeneity using large augers, with the simultaneous mixing of chemical oxidants or zero-valent iron, have limited but impressive performance record. The final step in the most common variant of this technology, ZVI-clay, is the addition of a bentonite slurry to almost eliminate groundwater flow through the treatment zone.

Challenges: The soil mixing process is a brute force method to conquer the heterogeneity, with >$100 per cubic yard unit costs and almost unfettered access requirements.

Key Implications: When applicable, the combination of destroying the heterogeneity and flow reduction with the bentonite slurry provides both treatment and contaminant. This combination results in significant reductions in downgradient mass flux. However, matrix diffusion effects are present immediately downgradient of the treatment zone can temper the impressive performance of this belt-and suspender technology.

Example: Olson et al. (2012) report on a deep soil mixing/zero valent iron project where median CVOC concentrations were reduced by >99%, and an estimated 2.5 Order of Magnitude reduction in mass discharge was achieved.

Prognosis: This technology will has significant applicability as a “one-stop-shop: for removing DNAPL and contaminants from matrix source zones at the same time. High unit costs and access issues make this approach less applicable to large, dilute zones with matrix diffusion sources.

7.2.4 Implication 4: Interfaces and Targeted Treatment

Key concept: : The DNAPL paradigm resulted in areal treatments with constant treatment point spacing (often 15 feet) in an attempt to mix amendments or heat to the entire treatment zone. Despite this close spacing, in many cases the amendments did not fully contact the entire treatment zone due to heterogeneity.

Challenges: Treating a large volume low permeability zone is difficult. Methods and approaches are needed to reduce the scale of the problem.

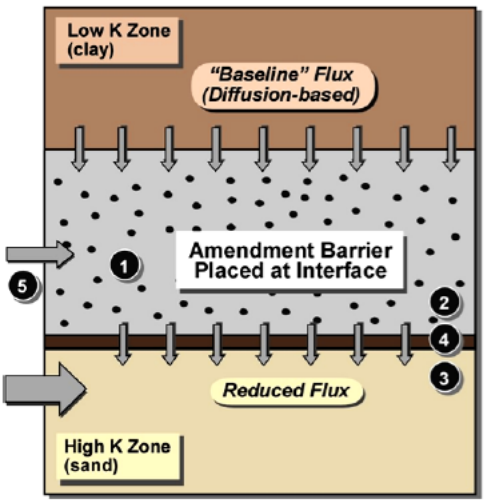

Key Implications: High-resolution sampling may become a required first step to reduce the scale of the problem. By understanding where the low permeability zones are, treatment zones may be able to be placed on the interfaces, or in the high flux zones that are draining matrix diffusion sources. Under this scenario, good (high resolution) site characterization becomes much more important for most remediation projects targeting low permeability zones.

Examples: If one has a high resolution transect of flux that considers both flow and concentration, then there are new possibilities about how to attack low permeability sources. These include "painting" the interfaces with long-lasting amendments (either chemical or biological) to just manage the slow flux coming off the matrix diffusion sources. Other approaches include very focused permeable reactive barriers, wider but smaller area in the high flux zones. The thinking can get way beyond the "treat the box" approach with ideas such as "flux clog" where inexpensive permeation grouting techniques are used to isolate low permeability source zones, making them more anaerobic and enhance natural attenuation processes.

Prognosis: The authors feel high resolution sampling is at the cusp of taking over the remediation industry, and that it will provide a game changer in terms of how sites are remediated.

7.2.5 Implication 5: These are Nonpoint Sources

Key concept: DNAPL remediation projects typically focused on small, highly concentrated areas. For example, a study of 59 remediation projects in 2006 showed a median treatment volume of 2500 cubic feet and treatment area of 0,5 acres. With small treatment sizes, even relatively expensive technologies such as in-situ thermal treatment can be practical at some sites.

Challenge: In the surface water pollution world, the original challenge of controlling point sources (piped discharges) meant building enough wastewater treatment plants. When water quality was still impaired even after the investment of billions of dollars for treatment plants, the emphasis focused on non-point sources. These source were activated by rainfall events where stormwater runoff collected and transport contaminants over vast urban and agricultural areas to receiving streams. The Surface water field is still struggling with managing these sources. The remediation field has a similar issue, where large low permeability zones in both what was considered the small original source, and now in the larger downgradient plume, need to be addressed. Although these data are subjective, multiple plume studies suggest that low permeability

zones may be 10 or 20 times larger than the footprint of the original DNAPL source zone.

Key Implication: In-situ remediation technologies need to have very low unit costs to treat contaminants in large, high-volume low permeability zones at many sites. Because most of the low-permeability zones will have less concentrated mass than DNAPL, the cost per pound of contaminant removed will go up significantly.

Example: A general rule of thumb is that in-situ DNAPL remediation technologies can cost $100 per cubic yard. If the treatment zone for matrix diffusion sources is 10 times larger, than unit costs of $10 per cubic yard are needed to keep the treatment of matrix diffusion sources on the same order of magnitude as treatment of DNAPL sources. This is a very difficult economic and market requirement.

Prognosis: At this time the authors see three potential technology responses: 1) treatment of low permeability zones will only be performed in the DNAPL footprint, either by two-at-once treatment technologies (DNAPL and matrix diffusion treatment at the same time) (see Implication 3 above); and/or 2) extremely low-cost remediation technologies will be developed and applied, even if some of the performance characteristics are not as good; and/or 3) the large low permeability zones will not be treated except in unusual cases, and concepts such as low-risk closure will become much more prevalent.

7.2.6 Implication 6: Containment, Perhaps in Different Forms, Makes a Comeback

Key concept: There is a growing consensus that 1) at most groundwater sites complete cleanup to drinking water standards is difficult to achieve, and 2) at some point a site will transition over to more passive management than continued active remediation. Examples of guidance documents and publications that discuss this philosophy are the ITRC's Integrated DNAPL Site Strategy document (ITRC, 2012; the National Research Council Alternatives for Managing the Nation's Complex Contaminated Sites (NRC, 2012); and the Air Force's Low Risk Manual (Farhat et al., 2012).

Challenge: The remediation/cleanup industry has been focused on a goal of site closure, and changing the focus of cleanup away from "must treat" to "treat until no further benefit" is a significant change.

Implications: The NRC suggests that sites undergoing active treatment should undergo a "transition assessment" to determine if active treatment (either continued treatment or some type of treatment train) is still beneficial, or if a site should go into long-term passive treatment; or long-term active management. Both end states can rely on containment technologies, such as permeable reactive barriers and potentially innovative passive physical/hydraulic containment techniques for long-term passive treatment, and indefinite hydraulic containment using pump and treat for long-term active management.

Key concept: While permeable reactive barriers are perhaps the best example of an commonly used passive containment technique, ESCTP Project 201328, "Contaminated Flux Reduction Barriers for Managing Difficult-to-Treat Source Zones in Unconsolidated Media" is an example of a new approaches for passive containment. This project will test the use of permeation grouting techniques and permeability reduction agents to promote a "flux clog" technology that reduces contaminant flux from contaminated zones and promotes more natural biodegradation by diverting competing electron acceptors. Another examples of innovative passive containment is the use of diversion moats ("Ankany Moats") or geosiphons to bypass water around the contained source zone.

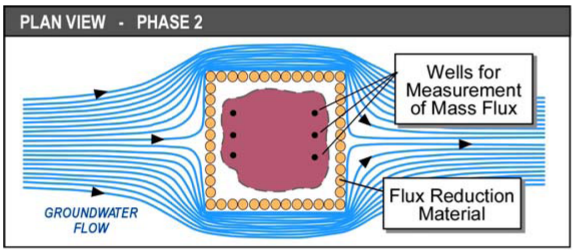

Prognosis: Although difficult to project, we foresee more containment projects as the End State, using conventional vertical barrier walls and hydraulic containment, and innovative technologies such as flux clog and siphon-based diversion systems.

7.2.7 Implication 7: It is Important to Know if Your Site is In Its Early, Middle, or Late Stage

Key concept: The Early, Middle, Late Stage conceptual model, originally proposed by Sale et al., (2008) has these elements:

- An Early stage site is dominated by the DNAPL phase, where most of the mass at the site and most of the mass flux originates from DNAPL pools and ganglia.
- A Middle Stage site still has DNAPL in the source zone, but considerable mass has diffused into low permeability ("low-k") zones in the source zone and in the plume such that if the DNAPL were removed the dissolved plume in the transmissive zone would still be sustained (although potentially at lower concentrations) by back diffusion from the low-k zones.
- A Late Stage site is dominated by back diffusion from low-k units that have been "charged up" during the loading period when the DNAPL was present, and now is the primary source of the mass flux to the dissolved plume in the transmissive zone.

Challenge:
Injection-based approaches work best in Early or Middle stage sites. Transition to passive management my be better suited for Late stage sites. The challenge is: what stage is my site in?

Implications: Current the distinction between Early, Middle, and Late Stage is qualitative. More quantitative, less subjective methods are needed.

Example: As part of this SERDP project, a *Screening Method To Estimate if a Chlorinated Solvent Site is in its Early, Middle or Late Stage* was developed (**see Appendix D**). This method is based on questions about the sufficiency of the DNAPL characterization program, the age and hydrogeologic settings, and simple charts based

on the Matrix Diffusion Toolkit that suggest if these could be enough mass and concentration from low k units to make it a Late Stage site.

Prognosis: The Lines of Evidence methodology in Appendix D is a first generation tool to help people understand where the contaminant mass in their site is located: mostly in the DNAPL phase (Early, Middle stage sites) or in the low k zones (Late Stage sites). With this knowledge, applying the 14-C model will become easier and more reliable.

Screening Method To Estimate if a Chlorinated Solvent Site is in its *Early, Middle or Late Stage*

(C. Newell, T. Sale, D. Adamson)

7.2.8 Implication 8: This is a Management and Regulatory Problem Too

Key concept: Once the DNAPL paradigm was accepted, state and federal regulators began to adapt to the new information with an onslaught of guidance, fact sheets, seminars, and regulations. These regulatory responses were important catalysts to drive the DNAPL remediation business forward.

Challenges: Changing regulatory regimes can be very difficult, as regulators can often say “it's the law” even if the law is in practice impossible to achieve. New thinking about how to reach achievable endpoints, without losing site of the ultimate goal, are needed.

Key Implications: There is a growing realization and acceptance that having flexibility on the remediation timeframe is a key part of a reasonable approach to matrix diffusion sources. These sites can be managed to eliminate risk, not compromise existing or future users of the water, not bankrupt remediation budgets, by applying low-threat or low-risk management approaches.

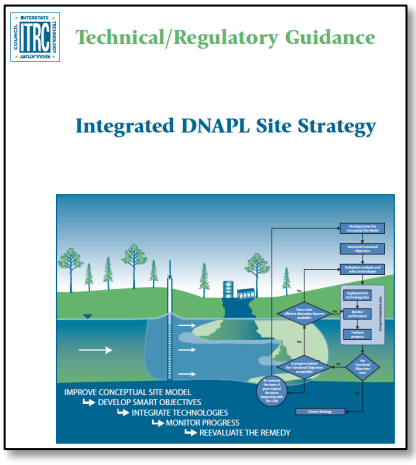

Examples: The Interstate Technology & Regulatory Council’s (ITRC) Integrated DNAPL Site Strategy Document (ITRC 2012), developed by a consortium of regulators, industry, academic and military remediation experts, is a prime example of how sites can be improved when the right Conceptual Model is used and when SMART goals are applied (Specific, Measurable, Attainable, Relevant, and Timebound). More importantly, the IDSS document is one of the first regulatory and decision making documents outside of ESTCP that emphasizes the special and complicated nature of matrix diffusion sources. Two other key examples are the California Regional Water Quality Control Board’s Low-Threat Guidance (CRWQCB, 2009), and the Air Force Center for Environmental

Excellence's Low-Risk Closure Manual (Farhat et al., 2012). The entire source attenuation movement is a final example of this type of new thinking.

Prognosis: The authors feel this is the most promising avenue for managing large, diffuse, hard-to-treat matrix diffusion source zones. The ITRC's Integrated Site Strategy document is an important step by the regulators and regulated community to address low permeability zones.

7.2.9 Implication 9: What is the Objective?

Key concept: With 2G and 3G characterization, and better modeling and lab tools, we can know "look into the box" and understand the distribution of contaminants in low k units.

Challenges: Will the owners of the regulated sites be responsible for achieving cleanup standards in the low k zones? Several regulatory agencies require cleanup of "waters of the state', which in theory would include water in the low k zones (clays, silts, sandstones, etc.).

Key Implications: Some type of practical methods on where to apply cleanup standards in a high-resolution world is needed. We see two potentially useful, and complimentary philosophies: 1) apply mass flux/mass discharge techniques that integrate flow and concentration data; and/or 2) use well screens that approximate the type of well a potential receptor might use (for example, a 20 foot screen for a domestic water well) and apply drinking water standards to this type of monitoring instrument.

Example: The ITRC's Mass Flux Technology Overview document (ITRC, 2010) presents the theory and application of mass flux techniques. Several researchers and practitioners (e.g., Dr. Fred Payne and Dr. Brian Looney) are now advocating specific approaches to the design and use of compliance wells for groundwater plumes.

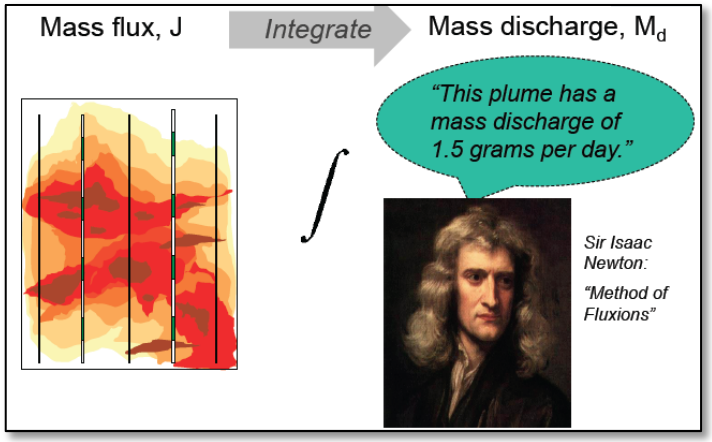

Prognosis: Murky. While these approaches are intuitive and practical, they can be interpreted as being counter to cleanup regulations.

7.2.10 Implication 10: Don't Underestimate Human Ingenuity

Key concept: The DNAPL paradigm sparked a revolution in thinking about the problem, and the focus switched form pump-and-treat to removing DNAPL from a limited in volume source area. Despite not achieving drinking water standards at many sites, these new technologies have made our world better.

Challenges: Developing new technologies or management approaches is difficult. One key challenge is that new ideas will not be accepted by "the regulator across the table" because it cannot meet an impossible collection of requirements: fast, cheap, reliable, predictable, safe.

Key Implications: For matrix diffusion sources, the main question if the winning solutions are more technological ("silver bullet") or regulatory ("declare victory") in nature.

Examples: In the DNAPL world, new technology development was thought to be been retarded by patent issues, lack of venture capital funding, and the partial removal problem, where anything short of achieving drinking water standards would prevent site owners and regulators from pulling the trigger on in-situ treatment. About 10 years and several thousand remediation projects later this has not proved to be the case. There is likely a market need, and regulatory need, to address matrix diffusion sources that will require new thinking.

Prognosis: The authors have been constantly delighted and surprised by the ingenuity of projects coming from SERDP, ESTCP, other technology development groups, and the marketplace. If matrix diffusion becomes the new target (or a companion target along with DNAPL), someone will invent the better mousetrap. We emphasize the better mousetrap may be a new technology, a clever enhancement or twist to an existing technologies, or a new concept in the management/regulatory arena.

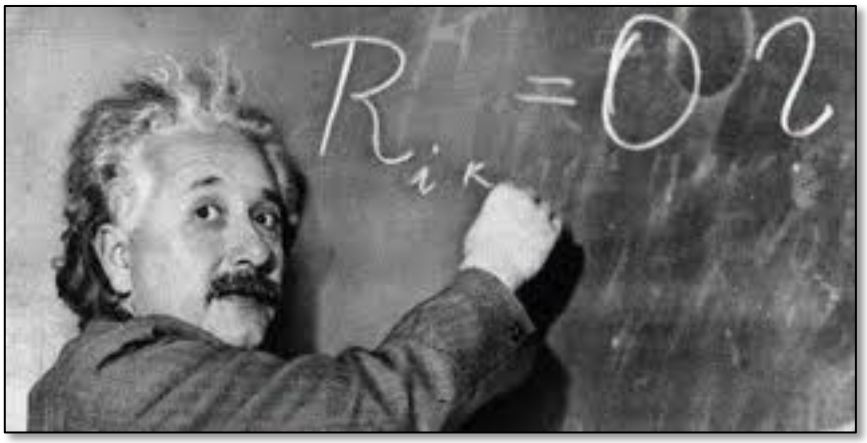

8.0 GUIDE TO CONTRACTED TASKS

Figure 9-1 shows how each contracted task was addressed by a particular chapter number or section numbers of this report. Red indicates chapter numbers in this report, blue are peer-reviewed journal articles published to date reporting on results of this research project. Note that several journal articles are still in review and preparation.

Key research products from this SERDP project are summarized on the following pages.

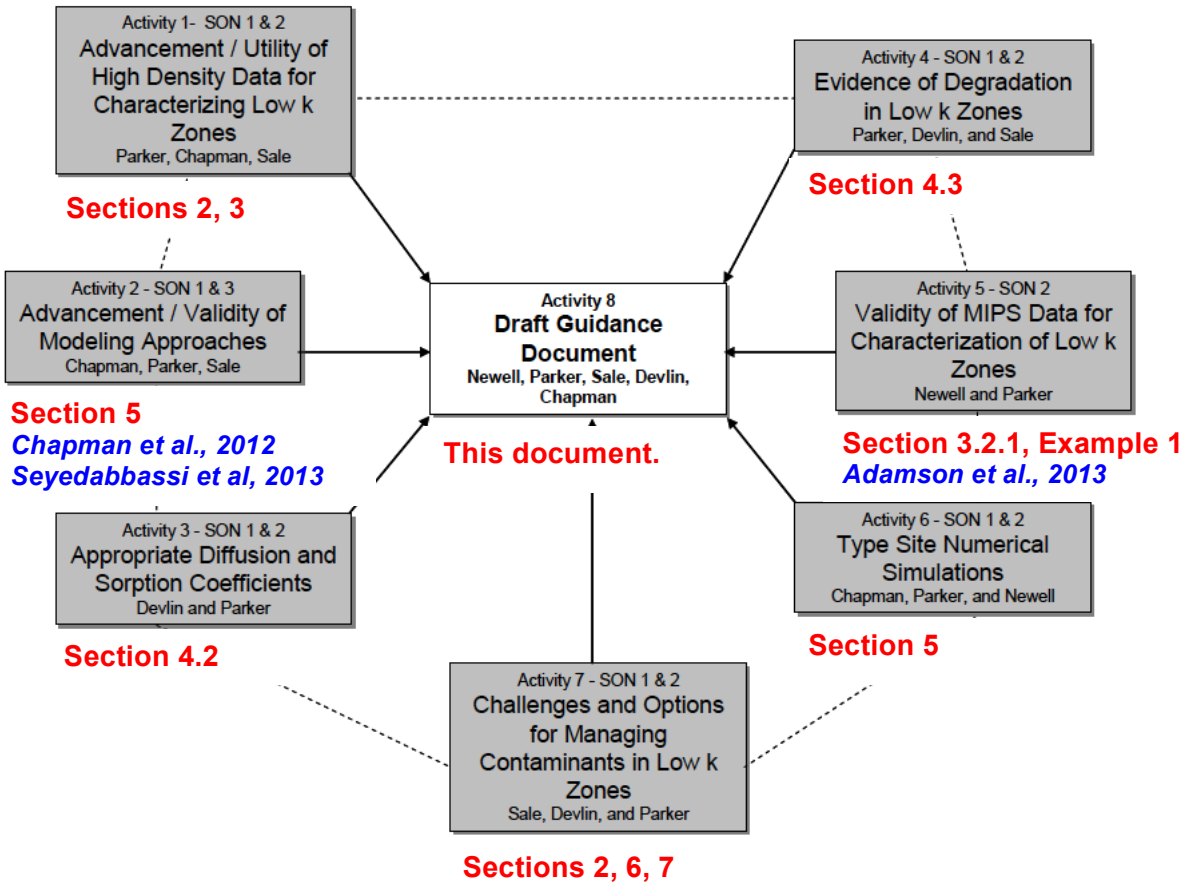

KEY RESEARCH PRODUCTS

CHAPTER 3 CHARACTERIZING LOW k ZONES

2G Site Characterization Programs
F.E. Warren AFB Wyoming (MIP, HPT, Waterloo APS System, High Resolution Soil Coring) (Appendix A)
Naval Air Station Jacksonville (MIP, HPT, Waterloo APS System, High Resolution Soil Coring) (Appendix B)

Procedures/Protocols
Membrane Interface Probe Protocol for Contaminants in Low-Permeability Zones (Adamson et al., 2013)

Journal Articles
Adamson, D. T., Chapman, S., Mahler, N., Newell, C., Parker, B., Pitkin, S., Rossi, M. and Singletary, M. (2013), Membrane Interface Probe Protocol for Contaminants in Low-Permeability Zones. Ground Water. doi: 10.1111/gwat.12085

CHAPTER 4 TRANSPORT IN HETEROGENEOUS MEDIA

Laboratory Programs
Diffusion experiments using soil from F.E. Warren AFB Wyoming (Appendix C)

Field Programs
Degradation analysis of chlorinated solvents in Low k snits, Naval Air Station Jacksonville

Literature Survey
Studies of degradation in Low k Units

Datasets
Diffusion data using soil from F.E. Warren AFB Wyoming and Dead End Column Method

Procedures/Protocols
Improved method for measuring effective diffusion coefficients in porous media using Dead End Column Method
Example of high resolution field program to evaluate degradation in low k units

KEY RESEARCH PRODUCTS (Continued)

CHAPTER 5 TYPE SITE SIMULATIONS

Modeling Studies
Numerical Model vs. Analytical Solutions and Tank Experiments
Compare numerical model HydroGeoSphere to exact analytical solutions for matrix diffusion for two-layer scenarios and parallel fracture scenarios.
Compare numerical model HydroGeoSphere to matrix diffusion research tank experiments.

Developed Library of "Type Sites"
Develop "Type Site" Analysis to show style of matrix diffusion effects for several different type hydrogeologic settings, contaminants, and source types.

Journal Articles
Chapman, S.W., B. L. Parker, T. C. Sale, L. Doner, 2012. Testing high resolution numerical models for analysis of contaminant storage and release from low permeability zones, Journal of Contaminant Hydrology, Volumes 136–137, August 2012, Pages 106-116, ISSN 0169-7722, 10.1016/j.jconhyd.2012.04.006.

Seyedabbasi, M.A., Newell, C.J., Adamson, D.T., Sale, T.C. (2012) Relative Contribution of DNAPL Dissolution and Matrix Diffusion to the Long-Term Persistence of Chlorinated Solvent Source Zones, Journal of Contaminant Hydrology, pp. 69-81 DOI: 10.1016/j.jconhyd.2012.03.010

CHAPTER 6 TREATMENT OF CONTAMINANTS IN LOW k ZONES

Research Tank Studies:
Detailed 60-100 Pore Volume Tank Simulations of Six Remediation Technologies
Concentration vs. time data for six tanks
Evaluation of mass distribution vs. time
Degradation of parent to daughter products
Visualizations of key concepts, like penetration of amendments into clay and production of reactive minerals in low k zones.

CHAPTER 7 IMPLICATIONS FOR SELECTING SITE REMEDIES

Decision Making Guide:

Screening Method To Estimate if a Chlorinated Solvent Site is in its *Early, Middle or Late Stage (*Appendix D)

9.0 REFERENCES

Acar, O, Klammler, H., Hatfield, K., Newman, M.A., Annable, M.A. Cho, J., Parker, B.L., Cherry, J.A., Pehme, P., Quinn, P., and Kroeker, R., 2013. A stochastic model for estimating groundwater and contaminant discharges from fractured rock passive flux meter measurements. Water Resources Research, 49(3), 1277-1291.

Adamski, M., V. Kremesec, R. Kolhatkar, C. Pearson, and B. Rowan, 2005. LNAPL in Fine-Grained Soils: Conceptualization of Saturation, Distribution, Recovery, and Their Modeling, *Ground Water Monitoring and Remediation* 25(1):100-112.

Adamson, D. T., Chapman, S., Mahler, N., Newell, C., Parker, B., Pitkin, S., Rossi, M. and Singletary, M. (2013), Membrane Interface Probe Protocol for Contaminants in Low-Permeability Zones. Ground Water. doi: 10.1111/gwat.12085

Adamson, David T., McGuire, Travis M., Newell, Charles J., and Stroo, H., 2011. "Sustained Treatment: Implications for Treatment Timescales Associated with Source Depletion Technologies", Volume 21, Issue 2, Spring 2011, Pages: 27–50

Adamson, DT and C.J. Newell, 2013. Frequently Asked Questions About Monitored Natural Attenuation in the 21st Century. Environmental Security and Technology Certification Program(ESTCP) Project ER-201211, In Preparation.

AFCEE, 2006. Long-Term Monitoring Optimization Guide. HQ Air Force Center for Environmental Excellence, Brooks City-Base, TX.

AFCEE, 2007. AFCEE Source Zone Initiative. Prepared by T.C. Sale, T.H. Illangasekare, J. Zimbron, D. Rodriguez, B. Wilking, F. Marinelli for AFCEE, Brooks City-Base, San Antonio, TX.

AFCEE, 2010. Sustainable Remediation Tool (SRT), version 2.1, Brooks City-Base, San Antonio, TX.

Anderson, M.P., Woessner, W.W., 1992. Applied Groundwater Modeling: Simulation of Flow and Advective Transport. Academic Press Inc., San Diego, California.

Anderson, M.R., Johnson, R.L., Pankow, J.F., 1992. Dissolution of dense chlorinated solvents into groundwater. 3. Modeling contaminant plumes from fingers and pools of solvent. Environ. Sci. Technol., 26, 901-908

Aziz, J.J.; M. Ling, H.S. Rifai, C.J. Newell, and J.R. Gonzales, 2003. "MAROS: a Decision Support System for Optimizing Monitoring Plans", *Journal of Ground Water*, Vol. 41, No. 3.

Beckett, G. D., and P. Lundegard. 1997. "Practically Impractical—The Limits of LNAPL Recovery and Relationship to Risk," pp. 442–45 in *Proceedings, Petroleum Hydrocarbons and Organic Chemicals in Ground Water: Prevention, Detection, and Remediation Conference*. Houston: Ground Water Publishing Company.

Cameron, K. and P. Hunter, No Date. Optimization of LTM Networks Using GTS: Statistical Approaches to Spatial and Temporal Redundancy, AFCEE. http://www.afcee.af.mil/shared/media/document/AFD-070831-023.pdf. Accessed July 25, 2011.

CDPHE, 2010. Draft Guidance for the Closure of Low-Threat Sites with Residual Ground Water Contamination. Colorado Department of Public Health and Environment, August 13, 2010.

Chambon, J.C., M.M. Broholm, P.J. Binning, and P.L. Bjerg, 2010. Modeling Multi-Component Transport and Enhanced Anaerobic Dechlorination Processes in a Single-Fracture-Clay Matrix System, Journal of Contaminant Hydrology, 112(1-4): 77-90.

Chapelle, F. H., M. A. Widdowson, J.S. Brauner, E. Mendez, and C.C. Casey, 2003. Methodology for Estimating Times of Remediation Associated with Monitored Natural Attenuation. Columbia, S.C., U. S. Geological Survey (USGS): 58.

Chapman, S.W. and B.L. Parker, 2005, Plume Persistence Due to Aquitard Back Diffusion Following Dense Nonaqueous Phase Liquid Removal or Isolation, Water Resource Research, Vol. 41, No. 12, W12411.

Chapman, S.W., B. L. Parker, T. C. Sale, L. Doner, 2012. Testing high resolution numerical models for analysis of contaminant storage and release from low permeability zones, Journal of Contaminant Hydrology, Volumes 136–137, August 2012, Pages 106-116, ISSN 0169-7722, 10.1016/j.jconhyd.2012.04.006.

Chapman, S.W., Parker B.L., 2005. Plume persistence due to aquitard back diffusion following dense nonaqueous phase liquid removal or isolation, Water Resour. Res. 41(12), W12411.

Cherry, J.A., S. Feenstra, and D. Mackay, 1996. Concept for the Remediation of Sites Contaminated with Dense Non-Aqueous Phase Liquids (DNAPLs). In JF Pankow, JA Cherry, eds, Dense Chlorinated Solvents and Other DNAPLs in Groundwater. Waterloo Press, pp. 475-506.

Cherry, J. A., Parker, B. L., Bradbury, K. R., Eaton, T. T., Gotkowitz, M. B., and Hart, D. J., 2006. Contaminant Transport Through Aquitards: A State of the Science Review. AWWA Research Foundation, Denver, CO, USA.

Colwell, F.S., Onstott, T.C., Delwiche, M.E., Chandler, D., Fredrickson, J.K., Yao, Q.-J., McKinley, J.P., Boone, D.R., Griffiths, R., Phelps, T.J., Ringelberg, D., White, D.C., LaFreniere, L., Balkwill, D., Lehman, R.M., Konisky, J. and Long, P.E., 1997, Microorganisms from deep, high temperature sandstones: constraints on microbial colonization. FEMS Microbiology Reviews, 20(3-4): 425-435.

Coolen, M. J. L. and Overmann, J., 1988. Analysis of Subfossil Molecular Remains of Purple Sulfur Bacteria in a Lake Sediment. Applied and Environmental Microbiology, 64(11): 4513-4521.

CRWQCB, 2009. Assessment Tool for Closure of Low-Threat Chlorinated Solvent Sites. California Regional Water Quality Control Board, San Francisco Bay Region, July 31, 2009.

CRWQCB, 2009. “Assessment Tool for Closure of Low-Threat Chlorinated Solvent Sites”. California Regional Water Quality Control Board, San Francisco Bay Region, July 31, 2009.

Darlington, R. L.; Lehmicke, L.; Andrachek, R. G.; Freedman, D.L., 2009. Biotic and abiotic anaerobic transformations of trichloroethene and cis-1,2-dichloroethene in fractured sandstone. Environ. Sci. Technol. 42 (12), 4323−4330.

Damgaard, I., Bjerg, P. L., Jacobsen, C. S., Tsitonaki, A., Kerrn-Jespersen, H. and Broholm, M. M., 2013. Performance of Full-Scale Enhanced Reductive Dechlorination in Clay Till. Groundwater Monitoring & Remediation, 33: 48–61.

Daus, A.D., Frind, E.O., Sudicky, E.A., 1985. Comparative error analysis in finite element formulations of the advection-dispersion equation. Adv. Water Resour. 8, 86-95.

Doner, L.A., 2008. Tools to resolve water quality benefits of upgradient contaminant flux reduction. M.Sc. Thesis, Colorado State University.

Einarson, M.D. and D.M. Mackay. 2001. Predicting the impacts of groundwater contamination, *Environmental Science and Technology* 35, no. 3: 67A-73A.

Falta, R.W., M.B. Stacy, A.N.M. Ahsanuzzaman, M.Wang, and R.C. Earle, 2007. REMChlor Remediation Evaluation Model for Chlorinated Solvents User’s Manual, USEPA, Center for Subsurface Modeling Support, Ada, OK, September 2007.

Falta, R.W., N. Basu and P.S.C. Rao, 2005b. Assessing the impacts of partial mass depletion in DNAPL source zones: II. Coupling source strength functions to plume evolution, *Journal of Contaminant Hydrology* 79(1-2):45-66.

Falta, R.W., P.S. Rao, and N. Basu, 2005a. Assessing the Impacts of partial mass Depletion in DNAPL Source Zones I. Analytical Modeling of Source Strength Functions and Plume Response, *Journal of Contaminant Hydrology* 78(2005): 259-280.

Farhat, S., P. DeBlanc, C. Newell, and D. Adamson, 2013. Source History Toolkit Users Manual, Environmental Security Technology Certification Program (ESTCP) Project ER-201032, ESTCP, Arlington, Virginia. < http://www.serdp.org/Program-Areas/Environmental-Restoration/Contaminated-Groundwater/Persistent-Contamination/ER-201032>

Farhat, S.K., C.J. Newell, T.C. Sale, D.S. Dandy, J.J. Wahlberg, M.A. Seyedabbasi, J.M. McDade, and N.T. Mahler, 2012. Matrix Diffusion Toolkit Users Manual,’ Environmental Security Technology Certification Program (ESTCP) Project ER-201126, ESTCP, Arlington Virginia. < http://www.serdp.org/Program-Areas/Environmental-Restoration/Contaminated-Groundwater/Persistent-Contamination/ER-201126 >

Farhat, S.K., C.J. Newell, M. Vanderford, T.E. McHugh, N.T. Mahler, J.L. Gillespie, P.N. Jurena, and A.A. Bodour, 2012. "Low-Risk Site Closure Guidance Manual to Accelerate Closure of Conventional and Performance Based Contract Sites," developed for the Air Force Center for Engineering and the Environment (AFCEE) by GSI Environmental Inc., Houston, Texas, www.gsi-net.com. July, 2012.

Feenstra, S., J.A. Cherry, and B.L. Parker, 1996. "Conceptual Models for the Behavior of Dense Nonaqueous Phase Liquids (DNAPLs) in the Subsurface". Chapter 23 in Dense Chlorinated Solvents and Other DNAPLs in Groundwater, J.F Pankow and J.A. Cherry, Editors. Waterloo Press, pp. 53-88.

Fetter, C.W., 2008. Contaminant Hydrology, Macmillan Publishing Company, New York.

Fredrickson, J. K., McKinley, J. P., Bjornstad, B. N., Long, P. E., Ringelberg, D. B., White, D. C., Krumholz, L. R., Suflita, J. M., Colwell, F. S., Lehman, R. M., Phelps, T. J., and Onstott, T. C., 1997. Pore-size constraints on the activity and survival of subsurface bacteria in a late cretaceous shale-sandstone sequence, northwestern New Mexico. Geomicrobiol. J., 14(3): 183-202.

GSI, 2002. Groundwater Sensitivity Tool Kit, Software User's Guide, version 1. GSI Environmental Inc., Houston, TX. Developed for the American Petroleum Institute. 2002.

GSI, 2007. RBCA Tool Kit for Chemical Releases, Software Guidance Manual, version 2. GSI Environmental Inc., Houston, TX, 2007.

Guilbeault, M.A., B.L. Parker, and J.A. Cherry, 2005. Mass and flux distributions from DNAPL zones in sandy aquifers. Ground Water, 43(1): 70-86.

Hunt, Bruce, 1978. "Dispersion Sources in Uniform Groundwater Flow". Journal of the Hydraulics Division, American Society of Civil Engineers, Volume 104, No. HY1, pp 75-85, January.

Hunter, P, 2011. Air Force Long-Term Monitoring Optimization Tools, http://www.frtr.gov/pdf/meetings/may11/presentations/hunter-presentation.pdf. Accessed September 14, 2011.

Interstate Technology and Regulatory Council, 2010. Use and Measurement of Mass Flux and Mass Discharge. ITRC Integrated DNAPL Site Strategy Team. < http://www.itrcweb.org/guidancedocument.asp?TID=70 >

Interstate Technology and Regulatory Council, 2012. Integrated DNAPL Site Strategy Technology/Regulatory Guidance ITRC Integrated DNAPL Site Strategy Team. < http://www.itrcweb.org/guidancedocument.asp?TID=82 >

ITRC, 2007. A Decision Flowchart of the Use of Monitored Natural Attenuation and Enhanced Attenuation at Sites with Chlorinated Organic Plumes. T. I. T. R. Council, The Interstate Technology & Regulatory Council: 13.

ITRC, 2009. Evaluating LNAPL Remedial Technologies for Achieving Project Goals. Technical/Regulatory Guidance, the Interstate Technology and Regulatory Council, LNAPLs Team, Washington, DC., December 2009.

ITRC, 2010. Use and Measurement of Mass Flux and Mass Discharge, Interstate Technology Regulatory Council MASSFLUX-1. 154.

Johnson P., P. Dahlen, J. T. Kingston, E. Foote, and S. Williams, 2009. Critical Evaluation of State-of-the-Art In Situ Thermal Treatment Technologies for DNAPL Source Zone Treatment. Developed for the Environmental Security Technology Certification Program, ESTCP Project ER-0314. May 2009.

Kavanaugh, M.C., S.C. Rao, L. Abriola, J. Cherry, G. Destouni, R. Falta, D. Major, J. Mercer, C. Newell, T. Sale, S. Shoemaker, R. Siegrist, G. Teutsch, and K. Udell, 2003. The DNAPL remediation challenge: is there a case for source depletion? National Risk Management Research Laboratory Report EPA/600/R-03/143.

Keller, C.E., Cherry, J.A., & Parker, B. L., 2013. New method for continuous transmissivity profiling in fractured rock. Groundwater, DOI: 10.1111/gwat.12064.

Klenk, I.D., and Grathwohl, P., 2002. Transverse vertical dispersion in groundwater and the capillary fringe. J. Contam. Hydrol. 58, 111-128.

Krembs, F.J., R.L. Siegrist, M. L. Crimi, R.F. Furrer, and B.G. Petri, 2010. Ground Water Monitoring and Remediation, doi: 10.1111/j1745–6592.2010.01312.x.

Krumholz, L. R., McKinley, J. P., Ulrich, G. A., and Suflita, J. M., 1997. Confined subsurface microbial communities in Cretaceous rock. Nature, 386(6620): 64-66.

Kueper, B. and K. Davies, 2009. Assessment and Delineation of DNAPL Source Zones at Hazardous Waste Sites, U.S. EPA, EPA/600/R-09/119.

Kueper, B.H. and McWhorter, D.B., 1991. The behavior of dense, non-aqueous phase liquids in fractured clay and rock. Journal of Ground Water, Vol. 29, No. 5, pp. 716-728.

Lawrence, J. R., Hendry, M. J., Wassenaar, L. I., Germida, J. J., Wofaardt, G. M., Fortin, N., and Greer, C. W., 2000. Distribution and biogeochemical importance of bacterial populations in a thick clay-rich aquitard system. Microbial Ecology, 40(4): 273-291.

Leaf, A.T., Hart, D.J., and Bahr, J.M., 2012. Active thermal tracer tests for improved hydrostratigraphic characterization. Groundwater, 50(5): 726-735.

Lima, G. P. and Sleep, B. E., 2007. The spatial distribution of eubacteria and archaea in sand-clay columns degrading carbon tetrachloride and methanol. Journal of Contaminant Hydrogeology, 94(1-2): 34-48.

Lima, G. P., Gilmore, A., Chapman, S. W., Aravena, R., and Parker, B. L., 2012a. Multiple lines of evidence for aquitard integrity enhanced by biodegradation. Journal of Contaminant Hydrogeology, *In preparation*.

Lima, G. P., Parker, B., & Meyer, J., 2012b. Dechlorinating microorganisms in a sedimentary rock matrix contaminated with a mixture of VOCs. Environmental Science & Technology, 46: 5756-5763.

Liu, G., C. Zheng, and S. Gorelick, 2007. Evaluation of the applicability of the dual-domain mass transfer model in porous media containing connected high-conductivity channels, Water Resource Research, Vol. 43, W12407.

Liu, C., and Ball, W.P., 2002. Back Diffusion of Chorinated Solvent Contaminants from a Natural Aquitard to a Remediated Aquifer Under Well-Controlled Field Conditions: Predictions and Measurements. *Groundwater*, 40(2): 175-184.

Mahler, N., T. Sale, M. Lyverse, 2011. A Mass Balance Approach to Resolving the Stability of LNAPL Bodies. *Groundwater,* 50(6): 861-871.

McGuire, T.M., McDade, J.M., and Newell C.J., 2006. "Performance of DNAPL Source Depletion Technologies at 59 Chlorinated Solvent-Impacted Sites", *Ground Water Monitoring and Remediation*, 26(1): 73-84.

McLaren, R.G., 2005. Grid Builder: A pre-processor for 2-D, triangular element, finite-element programs. Groundwater Simulations Group, Waterloo, Ontario.

McMahon, P. B., 2001. Aquifer/aquitard interfaces: mixing zones that enhance biogeochemical reactions. Hydrogeology Journal, 9(1): 34-43.

McMahon, P. B. and Chapelle, F. H., 1991. Microbial production of organic acids in aquitard sediments and its role in aquifer geochemistry. Nature, 349(6306): 233-235.

National Research Council, 2012. Alternatives for Managing the Nation's Complex Contaminated Groundwater Sites. The National Academies Press, Washington, D.C. Available at www.nap.edu.

Newell, C., D. Adamson, B. Parker, S. Chapman, and T. Sale, 2013. Determining Source Attenuation History to Support Closure by Natural Attenuation, Final Report ESTCP Project ER-201032, ESTCP, Arlington, Virginia. < http://www.serdp.org/Program-Areas/Environmental-Restoration/Contaminated-Groundwater/Persistent-Contamination/ER-201032 >

Newell, C. J., E. Becvar, G. Moore, D. Ruppel, D. Woodward, T.N. Swann, L.M. Beckley, and A. Rahman, 2008. Building Sustainability into the Air Force Remediation Process: Sustainable Remediation Tool. *Proceedings of the Sustainable Remediation Forum 8*, Philadelphia, PA. Oct 2008.

Newell, C. J., Farhat, S. K., Adamson, D. T. and Looney, B. B., 2011. Contaminant Plume Classification System Based on Mass Discharge. *Ground Water*, 49: no. doi: 10.1111/j.1745-6584.2010.00793.x

Newell, C.J., H.S. Rifai, J.T. Wilson, J.A. Connor, and J.J. Aziz, M.P. Suarez, 2002. Calculation and Use of First-Order Rate Constants for Monitored Natural Attenuation Studies, USEPA Remedial Technology Fact Sheet, U.S. Environmental Protection Agency. EPA/540/S-02/500, November 2002. http://www.epa.gov/ada/pubs/issue.html

NRC, 2000. Natural Attenuation for Groundwater Remediation, National Academy Press, Washington, D.C.

Olson, M. R., Sale, T. C., Shackelford, C. D., Bozzini, C. and Skeean, J., 2012. Chlorinated Solvent Source-Zone Remediation via ZVI-Clay Soil Mixing: 1-Year Results. Groundwater Monitoring & Remediation, 32: 63–74. doi: 10.1111/j.1745-6592.2011.01391.x

Parker, B. L., Chapman, S. W., & Cherry, J. A., 2010. Plume persistence in fractured sedimentary rock after source zone removal. Ground Water, 48(6), 799-803.

Parker, B. L., Cherry, J. A., & Chapman, S. W., 2012. Discrete fracture network approach for studying contamination in fractured rock. AQUA mundi 3(2), 101-116.

Parker, B.L., Chapman, S.W., Guilbeault, M.A., 2008. Plume persistence caused by back diffusion from thin clay layers in a sand aquifer following TCE source-zone hydraulic isolation. Journal of Contaminant Hydrology 102, 86–104.

Parker, B.L., R.W. Gillham and J.A. Cherry, 1994. Diffusive disappearance of immiscible phase organic liquids in fractured geologic media. Ground Water, 32(5): 805-820.

Pehme, P.E., Parker, B. L., Cherry, J. A., Greenhouse, J.P., 2010. Improved resolution of ambient flow through fractured rock with temperature logs. Groundwater, 48(2), 191-205.

Pehme, P.E., Parker, B. L., Cherry, J. A., Molson, J.W., Greenhouse, J.P., 2010. Improved resolution of ambient flow through fractured rock with temperature logs. Journal of Hydrology, 484(25), 1-15.

Rao, P.S.C., Rolston, D.E., Jessup, R.E., Davidson, J.M., 1980. Solute transport in aggregated porous media: theoretical and experimental evaluation. Journal of Soil Science of America 44, 1139–1146.

Rasa, E., S. Chapman, B. Bekins, G. Fogg, K. Scow and D. Mackay, 2011. Role of back diffusion and biogeochemical reactions in sustaining an MTBE/TBA plume in alluvial media. J. Contaminant Hydrology: 126: 235-247, 2011.

Read, R., Bour, O., Bense, V., Le Borgne, T., Goderniaux, P., Klepikova, M.V., Hochreutener, R., Lavenant, N., and Boschero, V., 2013. Characterizing groundwater flow and heat transport in fractured rock using fiber-optic distributed temperature sensing. Geophysical Research Letters, 40(10), 2055-2059.

Reszat, T. N. and Hendry, M. J., 2009. Migration of Colloids through Nonfractured Clay-Rich Aquitards. Environmental Science & Technology, 43(15): 5640-5646.

Rice, D.W., R.D. Grose, J.C. Michaelsen, B.P. Dooher, D.H. MacQueen, S.J. Cullen, W.E. Kastenberg, L.G. Everett, and M.A. Marino, 1995a. California Leaking Underground Fuel Tank (LUFT) Historical Case Analyses, Environmental Protection Department.

Sabatini, D. A., Austin, T.A., 1991. Characteristics of rhodamine WT and fluorescein as adsorbing ground-water tracers. Ground Water 29(3), 341–349.

Sale, T. and C. Newell, 2010. The Dependence of Plumes On Source Zones, Chapter 7 *In Situ* Remediation Of Chlorinated Solvent Plumes. Editors H. Ward and H. Stroo. Springer, New York, pp.85-117.

Sale, T**.,** M. Olson, D. Gilbert and M. Petersen, 2010. Cost and Performance Report for Field Demonstration/Validation of Electrolytic Reactive Barriers for Energetic Compounds at Pueblo Chemical Depot, Prepared for the U.S. DoD ESTCP.

Sale, T. and C. Newell, 2011. A Guide for Selecting REMEDIES FOR Subsurface Releases of Chlorinated Solvents. Developed for the Environmental Security Technology Certification Program, ESTCP Project ER-05 30. March 2011.

Sale, T. C., T. H. Illangasekare, J. A. Zimbron, D. R. Rodriguez, B. Wilking, and F. Marinelli, 2007. AFCEE Source Zone Initiative, Unpublished Final Report Submitted to the Air Force Center for Environmental Excellence, May 2007.

Sale, T., C. Newell, H. Stroo, R. Hinchee, and P. Johnson, 2008. Frequently Asked Questions Regarding Management of Chlorinated Solvents in Soil and Groundwater. Developed for the Environmental Security Technology Certification Program (ESTCP), July 2008.

Sale, T.C., Zimbron, J.A., Dandy, D.S., 2008. Effects of reduced contaminant loading on downgradient water quality in an idealized two layer granular porous media. J. Contam. Hydrol. 102, 72-85.

Scheutz, C., Broholm, M. M., Durant, N. D., Weeth, E. B., Jorgensen, T. H., Dennis, P., Jacobsen, C. S., Cox, E. E., Chambon, J. C., and Bjerg, P. L., 2010. Field Evaluation of Biological Enhanced Reductive Dechlorination of Chloroethenes in Clayey Till. Environmental Science & Technology, 44(13): 5134-5141.

Seyedabbasi, M.A., Newell, C.J., Adamson, D.T., Sale, T.C., 2012. Relative Contribution of DNAPL Dissolution and Matrix Diffusion to the Long-Term Persistence of Chlorinated Solvent Source Zones, Journal of Contaminant Hydrology, pp. 69-81 DOI: 10.1016/j.jconhyd.2012.03.010

Sudicky, E., & Frind, E. 1982. Contaminant Transport in Fractured Porous Media: Analytical Solutions for a System of Parallel Fractures. Water Resources Research, 18(6), 1634-1642.

Sudicky, E.A., & McLaren, R.G., 1992. The Laplace transform Galerkin technique for long-scale simulation of mass transport in discretely fractured porous formations. Water Resources Research, 28(2), 499–512.

Sudicky, E.A., Gillham, R.W., Frind, E.O., 1985. Experimental investigation of solute transport in stratified porous media 1. The nonreactive case, Water Resources Research 21, 1035–1041.

Takeuchi, M., Kawabe, Y., Watanabe, E., Oiwa, T., Takahashi, M., Nanba, K., Kamagata, Y., Hanada, S., Ohko, Y., and Komai, T., 2011. Comparative study of microbial dechlorination of chlorinated ethenes in an aquifer and a clayey aquitard. Journal of Contaminant Hydrogeology, 124(1-4): 14-24.

Takeuchi, M., Komai, T., Honada, S., Tamaki, H., Tanabe, S., Miyachi, Y., Uchiyama, M., Nakazawa, T., Kimura, K., and Kamagata, Y., 2009. Bacterial and Archaeal 16S rRNA Genes in Late Pleistocene to Holocene Muddy Sediments from the Kanto Plain of Japan. Geomicrobiology Journal, 26: 104-118.

Theis, C.V., 1967. Aquifers and models, in Symposium on Ground-Water Hydrology, San Francisco, Calif., Proceedings: American Water Resources Association Proceedings Series, no. 4, p. 138-148.

Therrien, R., & Sudicky, E. 1996. Three-dimensional analysis of variably-saturated flow and solute transport in discretely fractured porous media. Journal of Contaminant Hydrology, 23, 1-44.

Therrien, R., McLaren, R.G., Sudicky, E.A., Panday, S.M., 2010. HydroGeoSphere: A three-dimensional numerical model describing fully-integrated subsurface and surface flow and solute transport. Draft User's Manual. Groundwater Simulations Group, Waterloo, Ontario.

TNRCC, 1997. Interim Guidance: Monitoring Natural Attenuation for Verification of Groundwater Plume Stability, Texas Commission on Environmental Quality (formerly Texas Natural Resource Conservation Commission): 5.

Trefry, M.G., Muffels, C., 2007. FEFLOW: a finite-element ground water flow and transport modeling tool. Ground Water 45(5), 525–528.

Truex, M.J., C.J. Newell, B.B. Looney, K.M. Vangelas, 2006. Scenarios Evaluation Tool for Chlorinated Solvent MNA, WSRC-STI-2006-00096, Savannah River National Laboratory, Aiken, South Carolina.

USEPA, 1998. *Technical Protocol for Evaluating Natural Attenuation of Chlorinated Solvents in Ground Water*. US Environmental Protection Agency, Washington DC.

USEPA, 1999. Use of Monitored Natural Attenuation at Superfund, RCRA Corrective Action, and Underground Storage Tank Sites. Washington, D.C., United States Environmental Protection Agency.

USEPA, 2004. Performance Monitoring of MNA Remedies for VOCs in Ground Water. Washington, D.C., USEPA, Cincinnati, OH, EPA/600/R-04/027.

USEPA, 2006. Evaluation of the Role of Dehalococcoides Organisms in the Natural Attenuation of Chlorinated Ethylenes in Ground Water. US Environmental Protection Agency, Washington DC, EPA/600/R-06/029, July 2006.

USEPA, 2008a. A guide for Assessing Biodegradation and Source Identification of Organic and Ground Water Contaminants using Compound Specific Isotope Analysis (CSIA). US Environmental Protection Agency, Washington DC, EPA/600/R-08/148, December 2008.

Vanderford, M., 2010. A Comprehensive Approach to Plume Stability. *Remediation* Winter 2010: 21-37.

Van Stempvoort, D. R., Millar, K., and Lawrence, J. R., 2009. Accumulation of short-chain fatty acids in an aquitard linked to anaerobic biodegradation of petroleum hydrocarbons. Appl.Geochem., 24(1): 77-85.

Weatherill, D., Graf, T., Simmons, C.T., Cook, P.G., Therrien, R., Reynolds, D.A., 2008. Discretizing the fracture-matrix interface to simulate solute transport. Ground Water 46(4), 606-615.

Wiedemeier, T.H., H.S. Rifai, C.J. Newell, and J.T. Wilson, 1999. Natural Attenuation of Fuels and Chlorinated Solvents in the Subsurface. John Wiley and Sons, Inc., New York.

Wiedemeier, T.H., J.T. Wilson, D.H. Kampbell, R.N. Miller, and J.E. Hansen, 1999a. Technical Protocol for Implementing Intrinsic Remediation with Long-Term Monitoring for Natural Attenuation of Fuel Contamination Dissolved in Groundwater, Air Force Center for Environmental Excellence, San Antonio, TX, March 1999.

Wilson, J.T., 2011. An Approach for Evaluating the Progress of Natural Attenuation in Groundwater, USEPA EPA 600/R-11/204, www.epa.gov/ada

Zheng, C, Wang, P.P., 1999. MT3DMS: A modular three-dimensional multispecies transport model for simulation of advection, dispersion, and chemical reactions of contaminants in groundwater systems; documentation and user's guide. Contract Report SERDP-99-1, U.S. Army Engineer Research and Development Center, Vicksburg, MS.

Zheng, C., Bennett, G.D., 1995: Applied Contaminant Transport Modeling: Theory and Practice, Van Nostrand Reinhold, New York, NY.

APPENDICES

Management of Contaminants Stored in Low Permeability Zones

A State-of-the-Science Review

STRATEGIC ENVIRONMENTAL RESEARCH AND DEVELOPMENT PROGRAM
ER-1740

Principal Investigators:
T. Sale (Colorado State University, Fort Collins, Colorado)
B.L. Parker (University of Guelph, Guelph, Ontario, Canada)
C.J. Newell (GSI Environmental Inc., Houston, Texas)
J.F. Devlin (University of Kansas, Lawrence, Kansas)
Draft Report October 2013

Management of Contaminants Stored in Low Permeability Zones:

A State-of-the-Science Review

STRATEGIC ENVIRONMENTAL RESEARCH AND DEVELOPMENT PROGRAM

APPENDICES

Appendix A. Supporting Information for Section 3: Characterizing Low k Zones: F.E. Warren Field Work

Appendix B. Supporting Information for Section 3: Characterizing Low k Zones: NAS Jacksonville Field Work

Appendix C. Supporting Information for Section 4: Transport in Heterogeneous Media

Appendix D. Screening Method To Estimate if a Chlorinated Solvent Site is in its *Early, Middle or Late Stage*

APPENDIX A

SUPPORTING INFORMATION FOR SECTION 3: CHARACTERIZING LOW K ZONES: F.E. WARREN FIELD WORK

D.1 PURPOSE

This following serves a reference for the results of the drilling activities conducted near monitoring wells 38, 173 and 700 at F.E. Warren Air Force Base between the dates of November 1 - 4, 2010 in support of SERDP ER-1740.

D.2 BACKGROUND

The central hypothesis of this project is that release of contaminants stored in low permeability zones can sustain groundwater and vapor plumes for extended periods of time. Our first goal was to test different methods of sampling groundwater known to be contaminated with TCE in order to determine the most effective field method for detecting this compound. The second goal was to install Multilevel Sampling tubes at these well locations for future groundwater sampling and testing.

The first field method employed was the insertion of the Membrane Interface Probe (MIP) followed by the Waterloo Profiler. The MIP is a tool used to provide real-time detection of VOC's in the vadose or saturated zones of the soil by using a VOC permeable membrane in conjunction with a heater that volatilizes VOC's on the tip of the probe. A picture of the membrane is shown below:

These volatilized VOC's transfer through this membrane, where a carrier gas transfers the VOC's up the tubing and into the truck mounted detectors, such as the FID, ECD or PID. The tip also has the ability to simultaneously measure the soil conductivity, which is plotted alongside the VOC measurements. The MIP process is great for quickly identifying high concentration VOC source zones, in multiple areas on-site.

The Waterloo Profiler was next employed at MW's 700 and 38. This groundwater profiler provides hydrostratigraphic and physiochemical graphical data, such as hydraulic conductivity and pH. This data can be useful for better determining sampling intervals. The tip of the Waterloo profiler has 2 unique sampling ports that can detect changes in contaminant concentration with centimeter accuracy. A picture of this tool is shown below:

Upon completion of the MIP insertions, the second field method employed was the use of High-Resolution Sampling from 5 foot continuous core samples. These core samples are collected using a split hollow stem auger with an inserted plastic hollow core that collects the cores. A sample picture of these cores is shown:

Using this core, a small cylindrical sample of soil is removed by a clean stainless steel cylinder and inserted into a sealed vial containing a known amount of methanol to avoid volatilization losses. This is done at any number of desired depths within the cores. A picture of this process is shown:

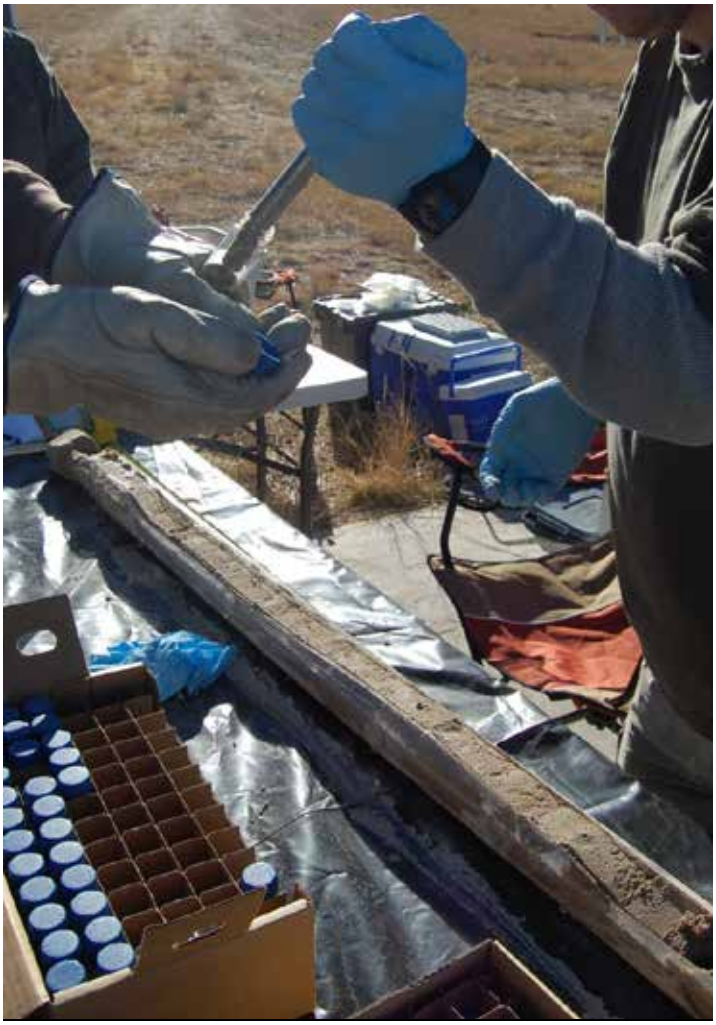

These samples are then analyzed later in the laboratory for the VOC's of concern.

After these activities were completed, the multi-level samplers were installed, which will be discussed later in this report.

D.3 FIELD TESTS – MIP

The drilling company used for the duration of this field test was Drilling Engineers, Inc. based out of Fort Collins, CO. The first drilling activity was the insertion of the MIP device using direct push on November 1st, 2010 near monitoring well 173. A picture depicting this process is shown:

The red tubing shown is what contains the carrier gas that flows between the membrane and the truck mounted field detectors, along with the soil conductivity sensors. The tip of the MIP is designed to fit into any standard direct push rig. The plot of the collected data from a direct push insertion next to MW-173 is reported as Figure 1:

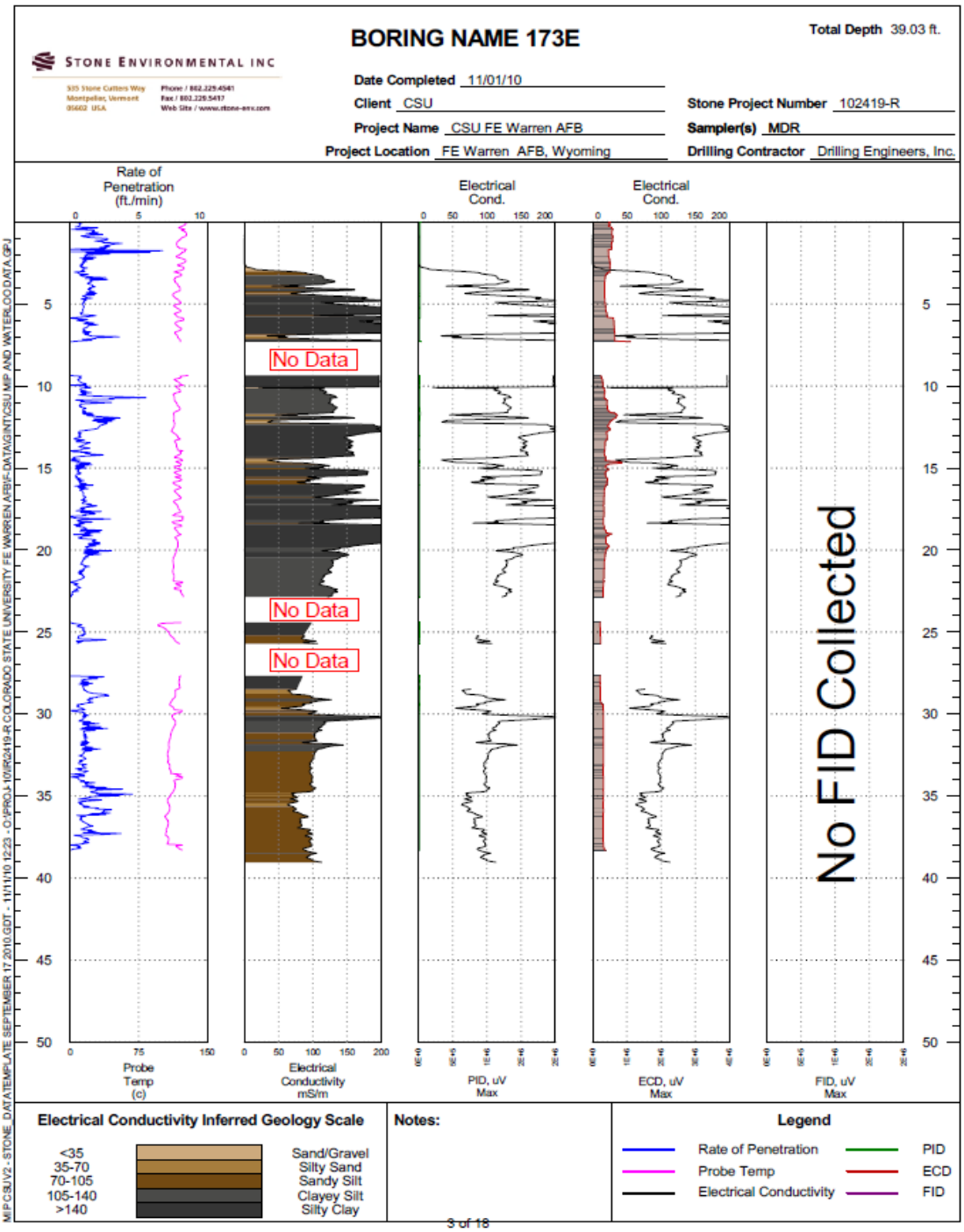

Figure 1. Plot of MIP data acquired from MW 173.

The *No Data* sections shown in the soil were due to the failure of the MIP to penetrate the hard caliche soil layers. These layers required the MIP to be extracted, a small diameter auger to drill the soil zone, and the MIP to be reinserted in order to continue the test.

Figures 2 and 3 are the same tests conducted next to MW's 700 and 38, respectively:

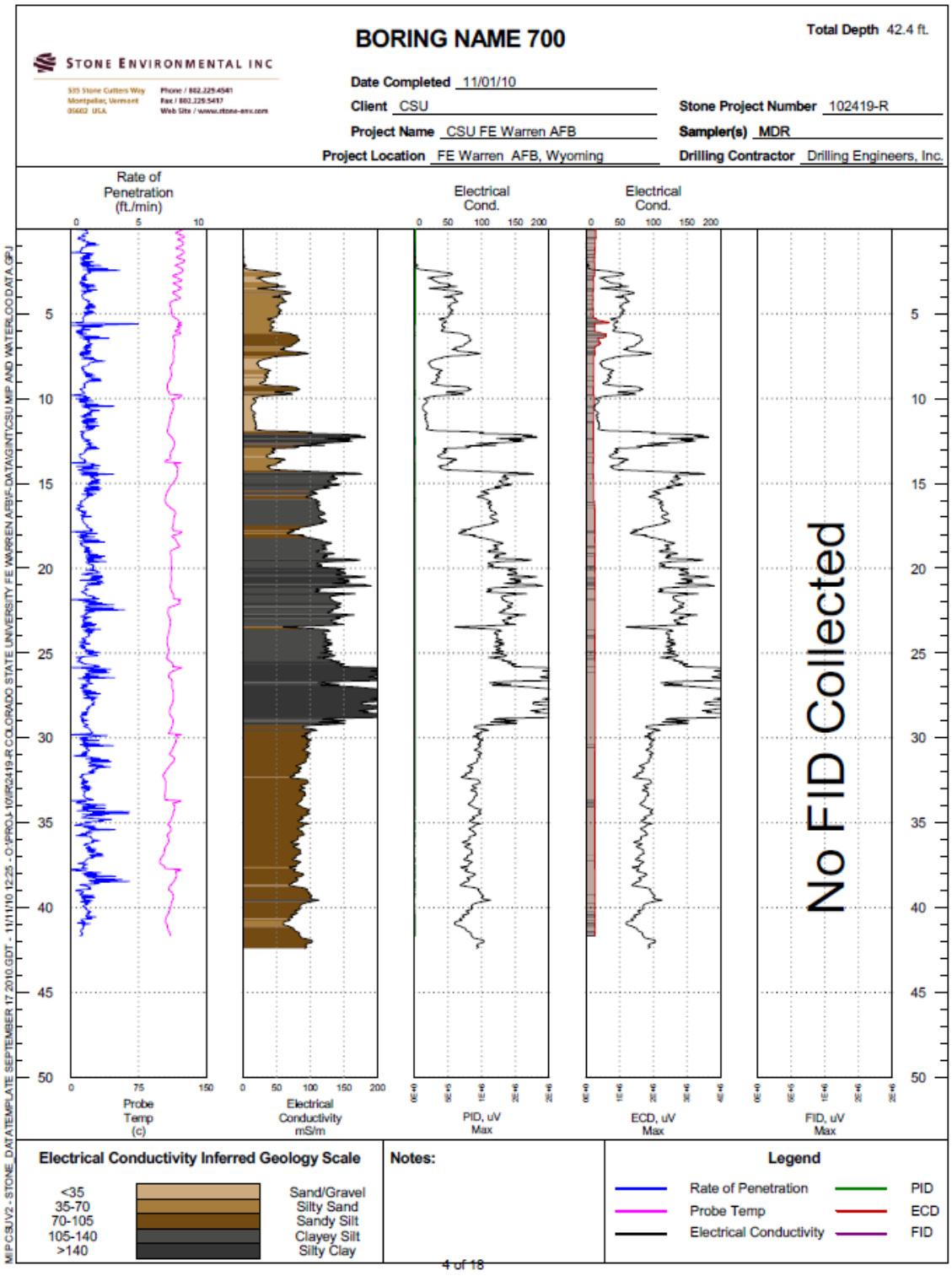

Figure 2. Plot of MIP data acquired from MW 700.

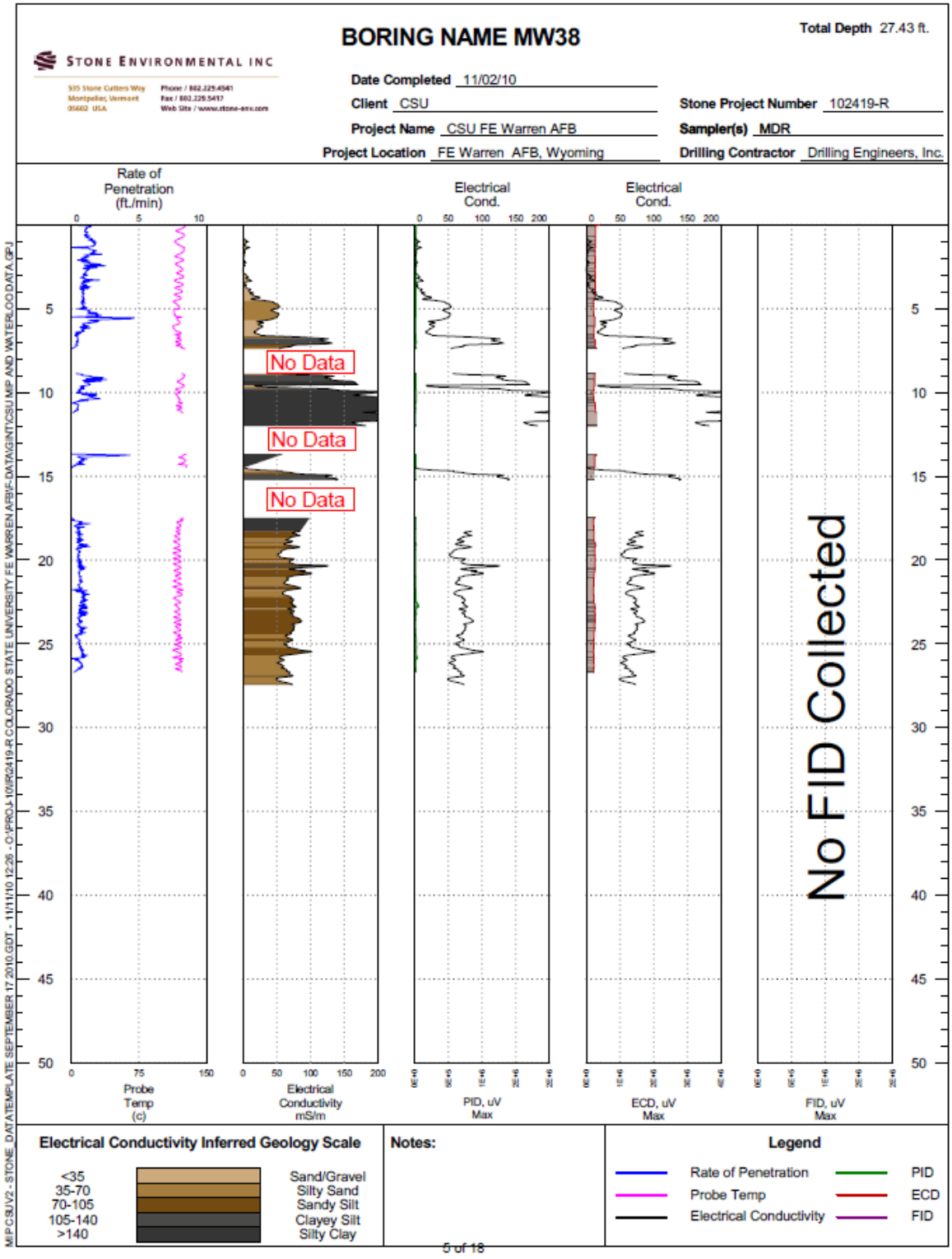

Figure 3. Plot of MIP data acquired from MW 38.

As shown in Figures 1 through 3, the ECD found roughly undetectable levels of VOC's, which should have been detected since the sites do show VOC contamination with the High-Resolution Sampling, which will be discussed later on. The MIP also had difficulty penetrating the lower permeability soil zones, as the drill auger had to be utilized to remove this soil for the test to continue. This suggests that the MIP is better suited for sandy soils.

Following the completion of the MIP test, the Waterloo profiler was employed at the MW 700 and 38 sites. These tests provided the following data:

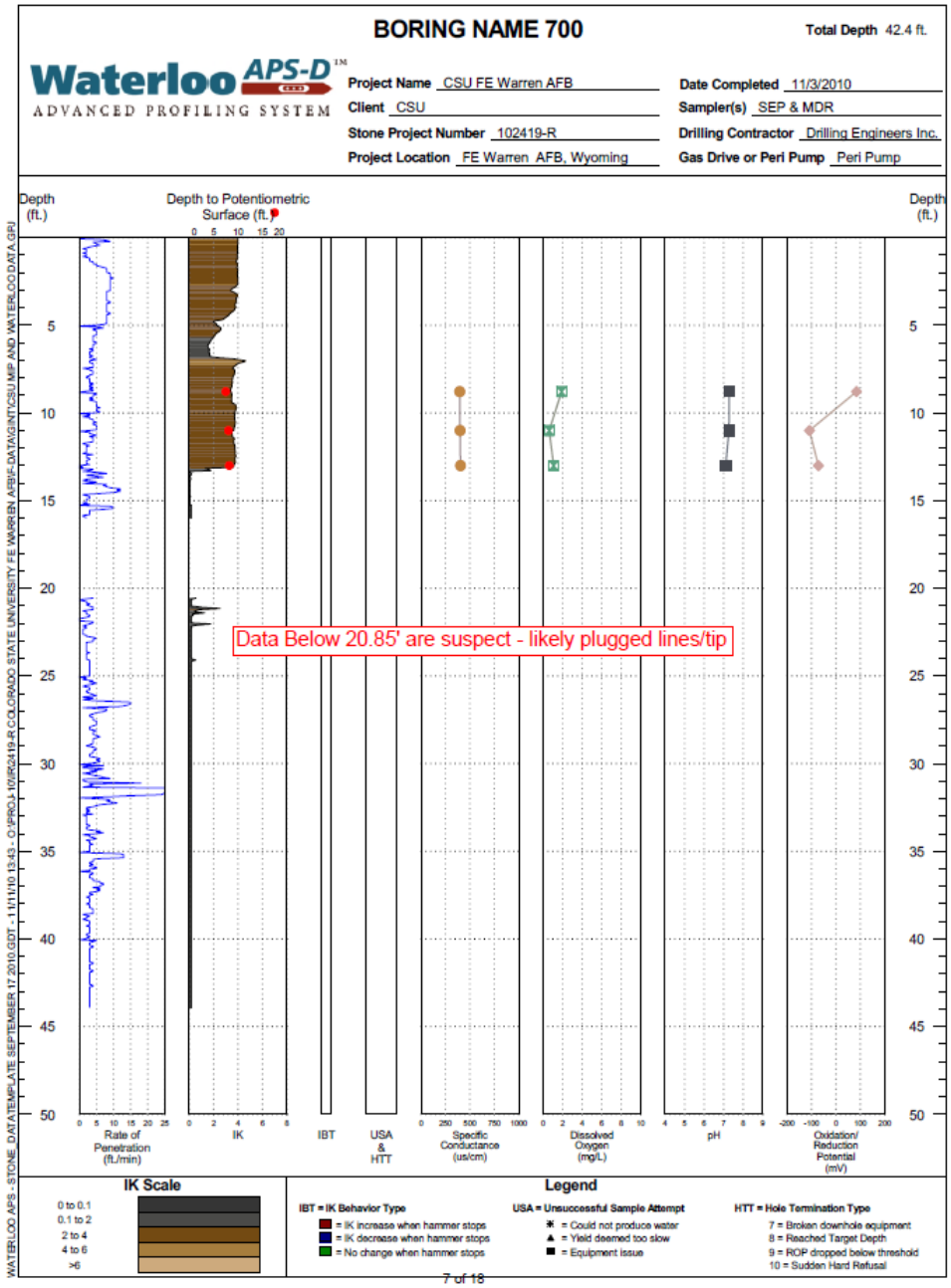

Figure 4. Plot of Waterloo Profiler data acquired from MW 700.

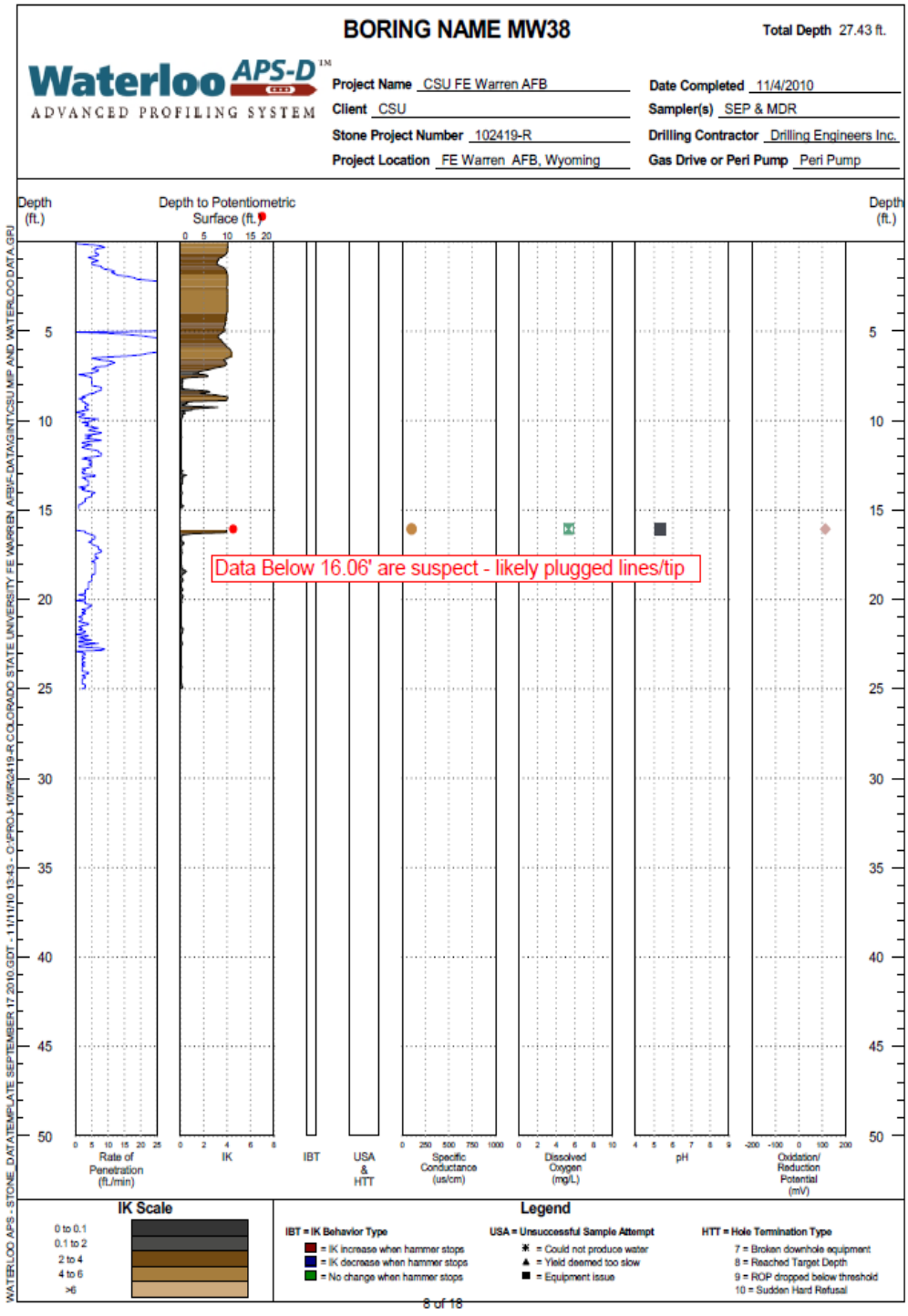

Figure 5. Plot of Waterloo Profiler data acquired from MW 38.

As shown, the Waterloo profiler was plugging with soil at lower depths and was unable to give accurate site data. The cause of this is unknown.

D.4 FIELD TESTS – HIGH RESOLUTION SAMPLING

Following the conclusion of these tests, a hollow stem-auger rig was employed to collect 5-foot long continuous cores at the 3 well locations to generate a high-resolution sample dataset:

A sample of the soil cores that this activity produced is shown below:

With these cores, two sets of 138 soil samples were taken at discrete points. The first set was used to determine the concentration profile of the VOCs of concern, such as PCE, TCE and c-DCE, and the second set (taken at the same points as the first) for the

water content and visual description of the soil. Thirty-three sample points were taken from MW 38, fifty-two from MW 173 and fifty-three from MW 700. Since the theory behind this research is that low permeability zones have been sustaining the VOC concentrations within this sites groundwater, the choice for the locations of the sampling were the clear and distinct changes in the soil between sands, silts and clays.

The following figures display the results of the VOC analyses of soil samples collected during high-resolution sampling at these three locations:

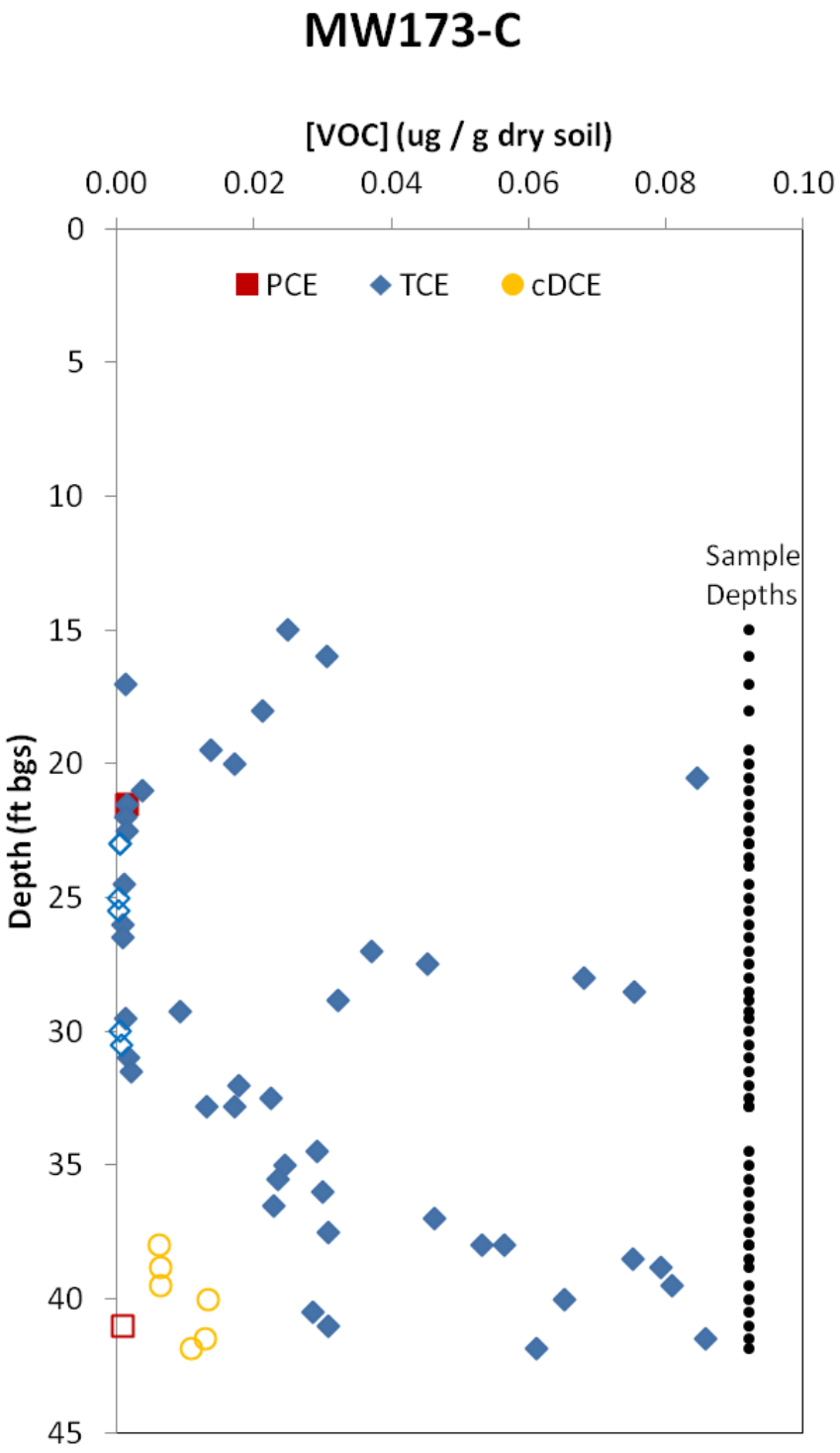

Figure 6. Plot of High Resolution Sampling data acquired from MW 173.

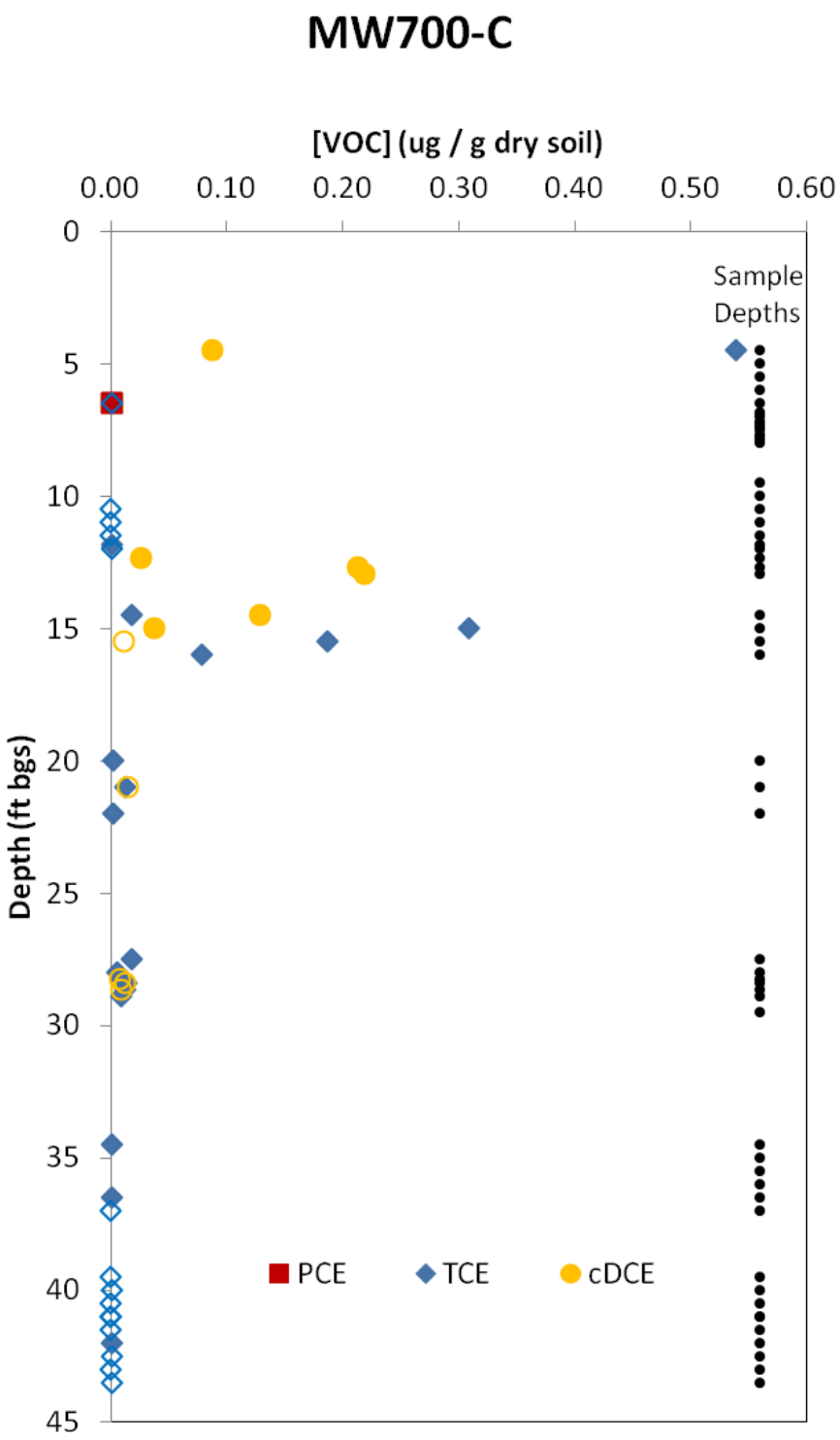

Figure 7. Plot of High Resolution Sampling data acquired from MW 700. cDCE is shown due to the installed PRB that is directly up-gradient of this well, showing incomplete dechlorination of the VOC's within the PRB.

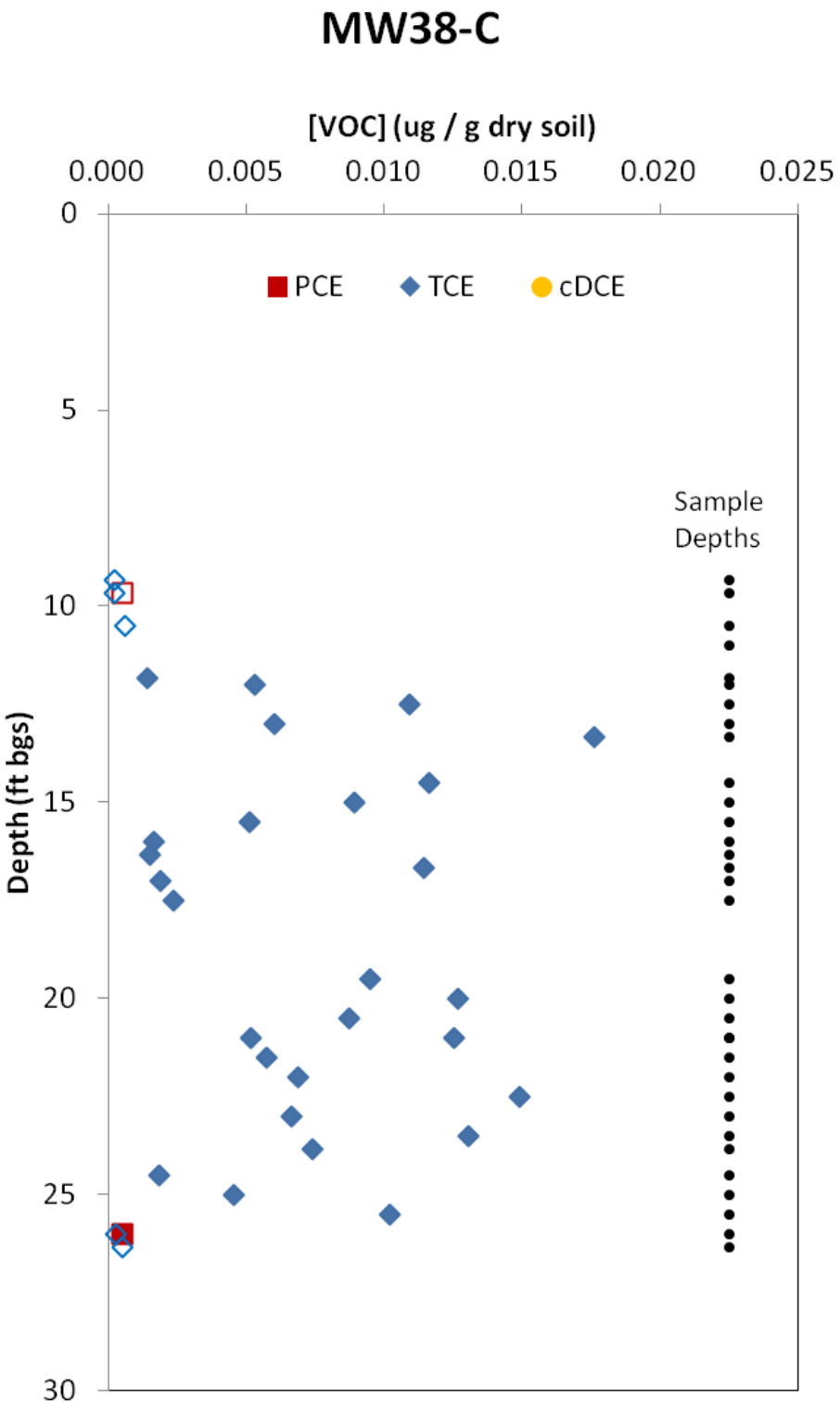

Figure 8. Plot of High Resolution Sampling data acquired from MW 38.

During the course of the High-Resolution Sampling, it became apparent this method worked very well in zones of lower permeability's, like clays and silts, but was less accurate in sands. This is because a sand sample that was removed from the hollow-stem auger likely did not have an accurate VOC distribution due to the migration of the water through the column during removal. This was apparent when flowing sands were documented numerous times in the columns during extraction. That said, the tests worked very well in the silts and clays, as the soil and the water within the soil, were unable to move around during extraction, thus giving more reliable results. As shown, the High-Resolution Sampling event was able to provide VOC data that the MIP did not.

D.5 SEDIMENT ANALYSIS

In the lab, the dried water content samples were used to determine the sediment type, sorting, size and mineralogy at each of the sample locations. This was done visually, and a sample of the soil type is shown:

This was done in order to create a plot of the sediment layers for each drilling location, which can help to quantify the locations of higher VOC concentration with respect to the permeability of the soil the sample was taken from. This layering is shown as:

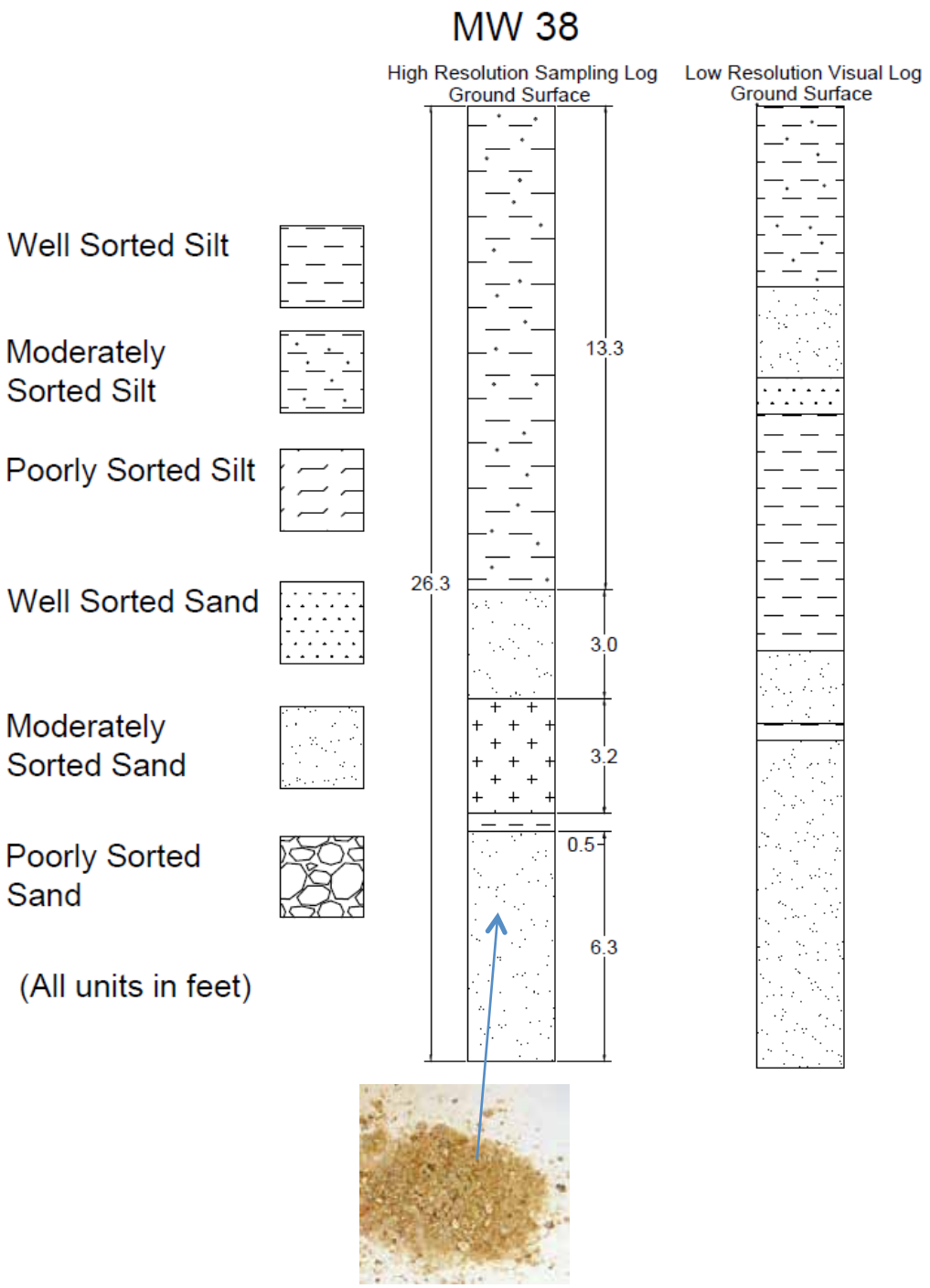

Figure 9. Plot of sediment distribution with depth from MW 38.

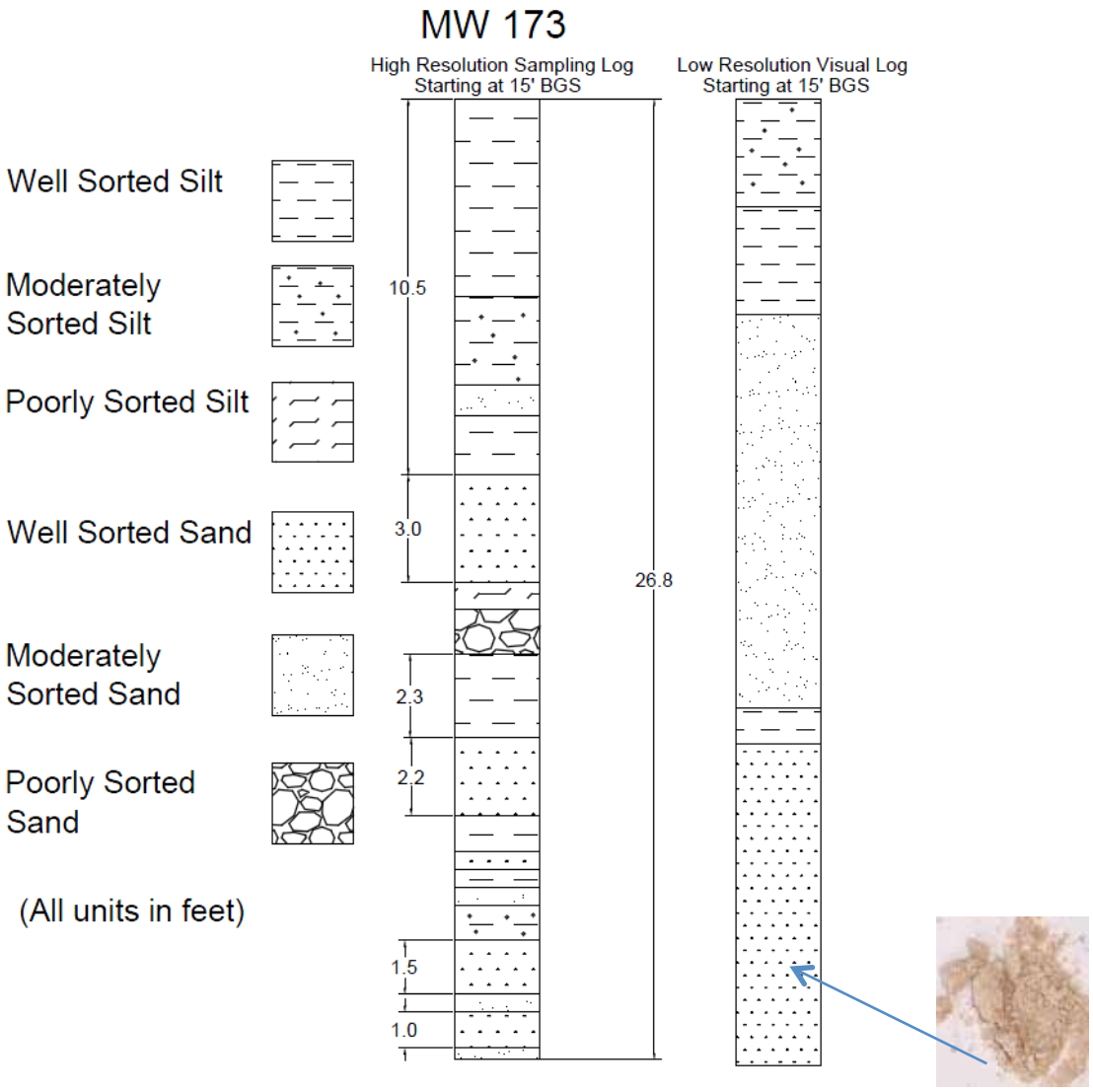

Figure 10. Plot of sediment distribution with depth from MW 173.

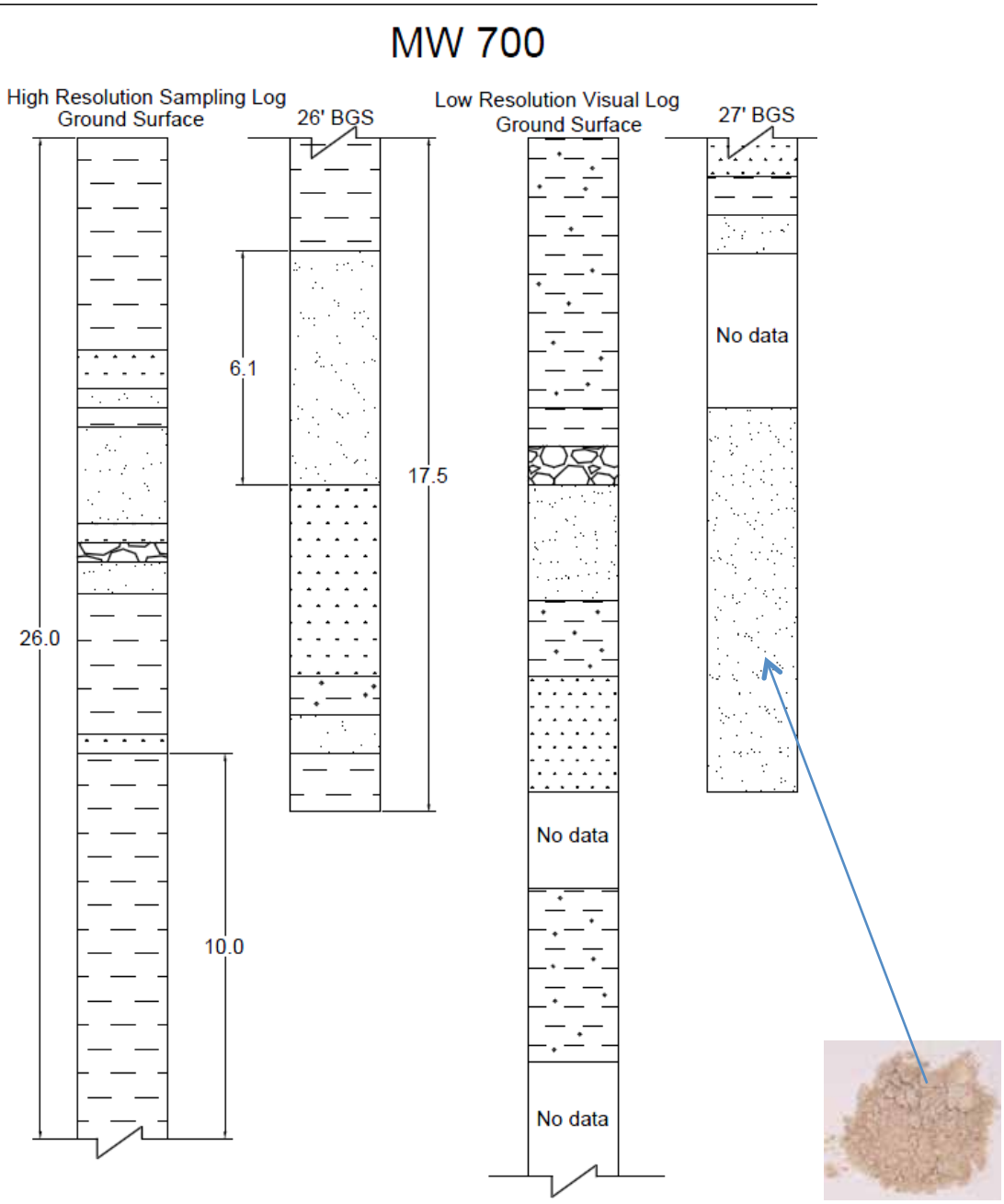

Figure 11: Plot of sediment distribution with depth from MW 700.

The last piece of data obtained from the High-Resolution Sampling event was the fraction of Organic Carbon (F_{oc}) contained within the soil. 17 of the samples used for the water content data were chosen to determine the F_{oc} of the different types of the soils found:

Well	Sample Number	Depth (ft bgs)	Soil Type	F_{oc}
MW 38	FEW 009	13.3	Well Sorted Silt	0
MW 38	FEW 015	16.7	Well Sorted Silt	0.078
MW 38	FEW 016	17	Poorly Sorted Sand	0.075
MW 38	FEW 021	21	Moderately Sorted Sand	0.039
MW 38	FEW 025	22.5	Poorly Sorted Sand	0.083
MW 38	FEW 031	25.5	Moderately Sorted Sand	0.104
MW 173	FEW 040	20.5	Well Sorted Silt	0
MW 173	FEW 055	27.5	Well Sorted Sand	0.11
MW 173	FEW 057	28.5	Poorly Sorted Sand	0.11
MW 173	FEW 076	38	Moderately Sorted Silt	0
MW 173	FEW 078	38.5	Moderately Sorted Silt	0
MW 173	FEW 084	41.5	Well Sorted Sand	0.055
MW 700	FEW 110	15	Well Sorted Silt	0
MW 700	FEW 112	16	Well Sorted Sand	0
MW 700	FEW 116	27.5	Well Sorted Silt	0
MW 700	FEW 123	34.5	Moderately Sorted Sand	0
MW 700	FEW 135	42	Moderately Sorted Sand	0

Table 1. F_{oc} values for the 17 chosen samples

These 17 samples were chosen to describe the rest of the soils within the same soil classifications.

D.6 FIELD TESTS – MULTI-LEVEL SAMPLING

The final stage of the field work was the placement of the Multi-Level Samplers (MLS) that are being used for on-going groundwater monitoring. These are constructed from a piece of medium density polyethylene which has seven (7) open and separate channels that span the length of the tubing, so that the user can sample from the ground surface:

This allows the user of the Multi-Level Sampler to sample from 7 different depth intervals within the groundwater system. This was done in all three monitoring well locations 173, 700 and 38. A picture of a MLS under construction is displayed below:

The screen in the middle of the picture is where a hole was drilled in the outside of the MLS, and a plug was installed inside of the individual tube down-hole. This is done so that the user can sample from ground surface and receive 7 different water samples guaranteed to be uncontaminated from other zones. A screen is then wrapped around the tube at this location to stop sediment from entering the sample space. The locations of these sample ports were chosen after a visual inspection of the soil cores that were drilled in the previous field activity, with the intent of having a good representative sample of the lower and higher permeability zones. The two black spacers shown are just a few of the spacers put onto the MLS, as they are used to keep the tube centered within the drilled hole. The last step is to fill the void area around the MLS and the drilled hole with sand. A 3 foot stickup of the MLS was used for sampling purposes and was

surrounded with a PVC pipe and cemented in place, with a locking well cover. The following are the three as-builts of the MLS's put into the ground at F.E. Warren MW's 173, 700 and 38:

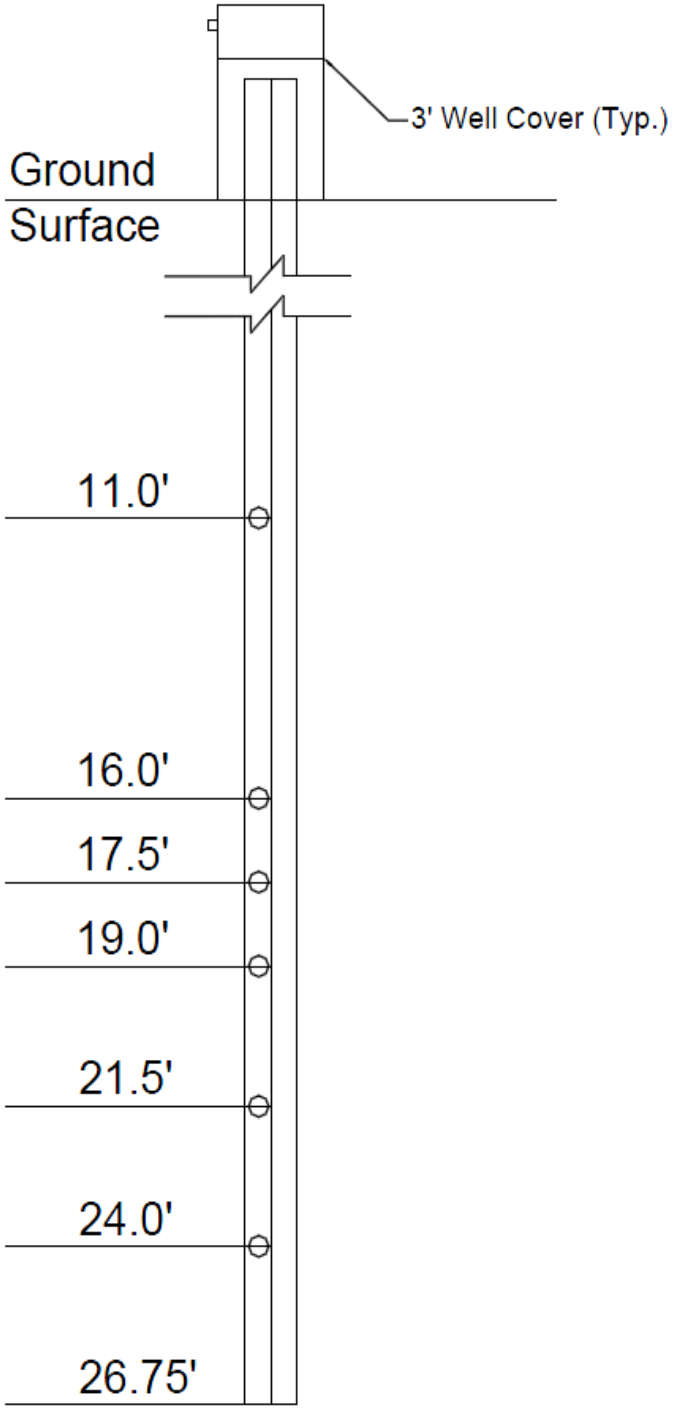

Figure 13. As-Built MLS hole distribution with depth from MW 38.

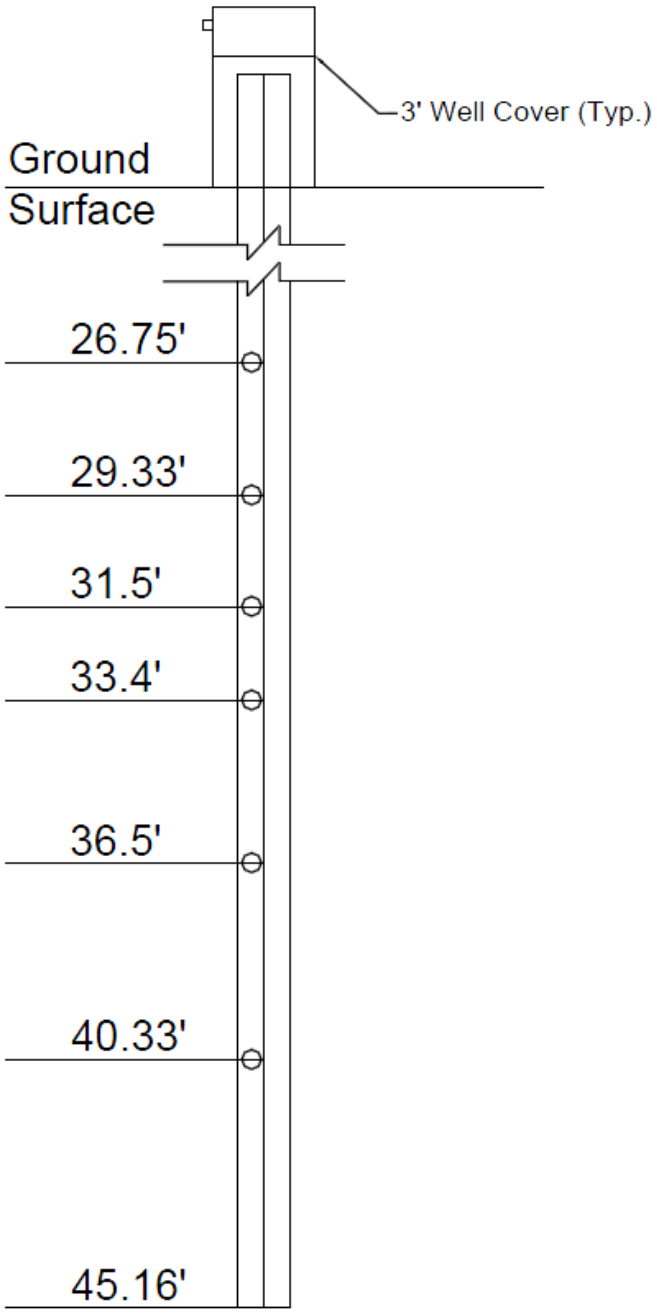

Figure 13. As-Built MLS hole distribution with depth from MW 173.

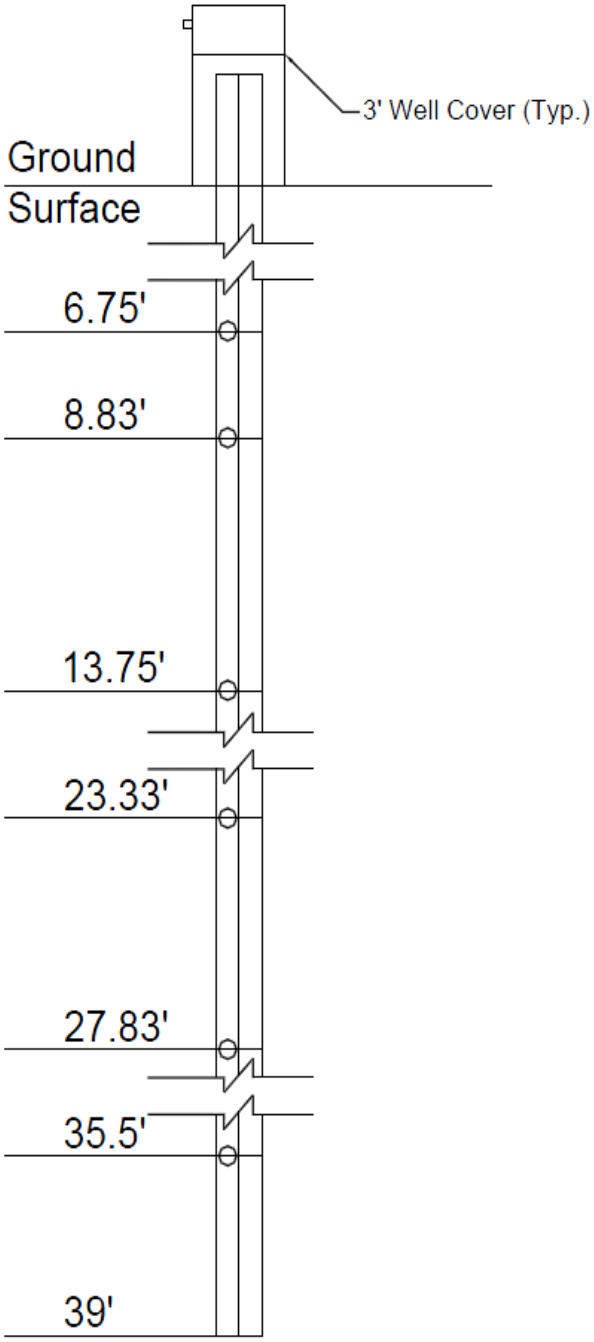

Figure 14. As-Built MLS hole distribution with depth from MW 700.

The main lesson learned from the installation of the multi-level systems is that they can be challenging to install in the field, as some problems were encountered during the placement of the tubes into the drilled holes. However, their ability to provide depth-discrete groundwater data for monitoring trends at a more appropriate scale means that installation is most likely worth the effort.

After the MLS were constructed, groundwater was purged multiple times and then sampled in order to determine the concentrations of TCE at each of the constructed depths. The following is a plot of TCE concentrations from a sampling that occurred on August 23, 2011:

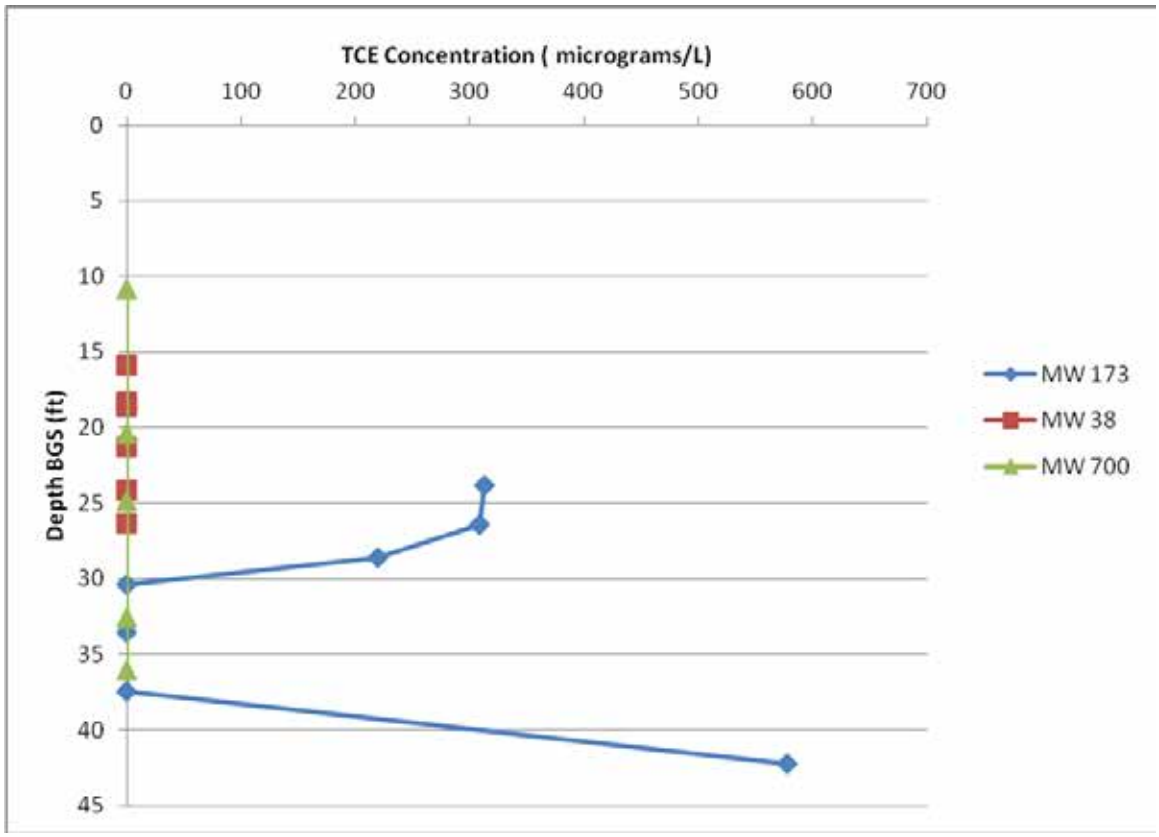

Figure 15. MLS TCE concentrations from MW's 38, 173 and 700.

D.7 ADMINISTRATIVE CONTACT

Any questions concerning anything contained within this report should be directed to:

Name	Kevin Saller
Phone	720-470-3384
FAX	970-491-8224
Email	Sallerk@gmail.com

APPENDIX B
SUPPORTING INFORMATION FOR SECTION 3: CHARACTERIZING LOW K ZONES: NAS JACKSONVILLE FIELD WORK

The material presented in this appendix is an expanded version of a manuscript being prepared for submission to a technical journal in October 2012. Partial funding for this work was supplied by ESTCP ER-201032.

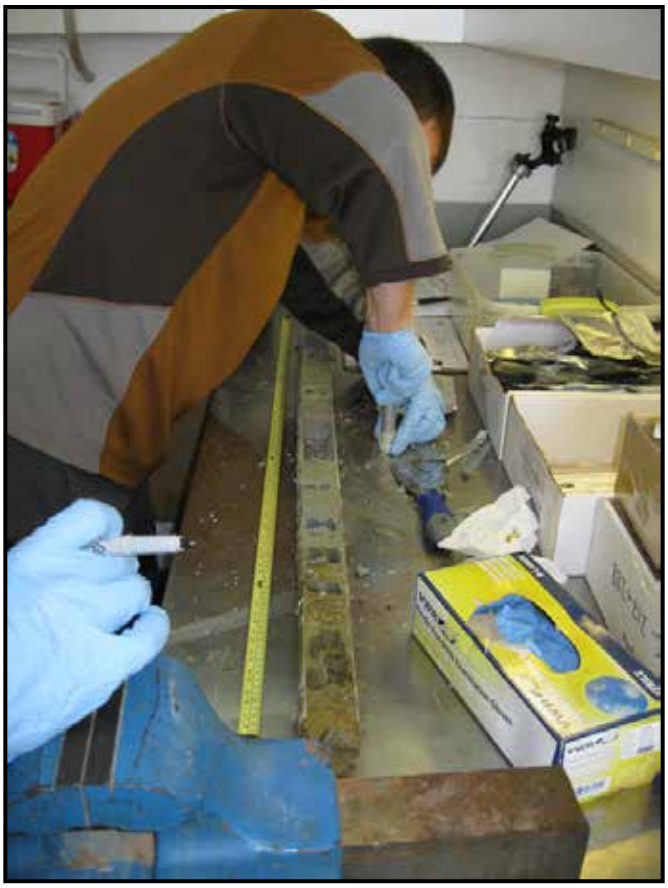

A.1 OBJECTIVES

The development of appropriate characterization methods for low permeability zones is a key overall objective of the SERDP ER-1740 project that is designed to enhance our technical understanding of the impact of contaminants stored and released from low permeability zones, A commercially-available technology that has been used extensively for environmental site characterization—Membrane Interface Probe (MIP) systems—can be used in low-permeability zones where direct-push drilling techniques are a practical option.

Our hypothesis is that an MIP operating protocol optimized for use in low permeability zones may provide a cost-effective alternative and/or compliment to collection and analysis of high resolution core data.

To test this hypothesis, the following specific objectives were addressed through a focused field study:

- Assess qualitative advantages and disadvantages of using MIP systems for characterizing low K zones by collecting MIP data from the same site and locations where other high-resolution characterization techniques will be employed.
- Determine the influence of modifying key MIP operating conditions (e.g., trunk line temperature, carrier gas flow rate, drive rate) on MIP data quality, with a particular focus on the impact within low K zones.
- Perform a quantitative statistical comparison of CVOC results obtained from soil cores with those obtained using standard and optimized MIP logging procedures. Determine the relative accuracy of the baseline MIP method (i.e., conventional continuous push) against MIP trials where key operational conditions have been varied. Supplement with supporting characterization data (e.g., CVOC in co-located groundwater samples, conductivity estimates) when available.
- Develop a Standard Operating Procedure (SOP) for MIP as an assessment tool for contaminant storage in low K zones, relying on results from MIP operational conditions testing and quantitative comparisons with soil data.

A.2 INTRODUCTION

The presence of heterogeneities in subsurface environments greatly contributes to the complexity of site characterization and remediation strategies. Chlorinated solvents released to the subsurface are preferentially transported within zones with the highest permeability, which may constitute only a small fraction of the total porosity (Payne et al., 2008). As high concentrations of aqueous-phase mass in transmissive zones come into contact with lower permeability zones, diffusion and slow advection can contribute to the storage of significant amounts of contaminant mass in these lower permeability zones, which may be enhanced by sorption given such zones typically contain appreciable organic carbon. These same processes contribute to relatively slow release of this mass and have the potential to sustain groundwater plumes for decades or longer (Parker et al., 2008; Sale et al., 2008; Seyeddabbasi et al., 2012). At sites where such permeability contrasts contribute to site complexity, it can be difficult to develop an appropriate conceptual site model (CSM) to guide decision-making (Sale and

Newell, 2010). One contributor to this uncertainty is a reliance on methods such as long-screened (e.g., 5 ft or more) groundwater monitoring wells during conventional site characterization efforts that can provide an incomplete picture of contaminant distribution because they are rarely designed to capture small-scale variations nor are they effective for assessing mass in lower permeability zones (Parker et al., 2006).

Collecting high-resolution characterization data, specifically data that identify contaminant and stratigraphic heterogeneity, can provide a more realistic understanding of how source zones and associated plumes will respond to remediation efforts (EPA, 2005; Parker et al., 2008; Payne et al., 2008; Mercer et al., 2010). This information is a critical step in developing a more accurate SCM that will contribute to informed and effective remedial decisions (Newell et al., 2011). This is of particular importance at sites where a significant portion of contaminant mass is present in lower permeability zones because treating the mass in these zones is often difficult using conventional technologies (Sale and Newell, 2010).

High resolution characterization approaches focus on increased data density, often by collecting large amounts of depth-discrete data across transects using one or more different methods in phases (Guilbeault et al., 2005; Chapman and Parker, 2005; Einarson et al., 2010; Mercer et al., 2010). Soil coring and analysis is considered a superior option during this type of effort in low permeability zones (Chapman and Parker, 2005) because: i) it quantifies mass in all compartments (e.g., dissolved, sorbed); ii) it allows for accurate soil type classification to identify zones of contrasting permeability; iii) depth-discrete sampling at tight intervals is possible, such that contaminant heterogeneity and associated permeability can be understood; and iv) core collection in low permeability zones is less impacted by several factors that make coring in higher permeability zones difficult. Because soil coring and analysis can be labor intensive and costly, there are a number of rapid data acquisition tools that can be used as an initial step to screen locations and depths for more focused (and cost-effective) characterization efforts using the more intensive methods.

One such screening tool is the Membrane Interface Probe (MIP) developed by Geoprobe (2005) to collect nearly continuous, depth-discrete characterization data in unconsolidated soils where it can be advanced using direct push equipment. The acceptance of MIP as a site characterization tool is illustrated by the publication of an ASTM standard for the technology (ASTM, 2007). The tool has a semi-permeable membrane fabricated from polytetrafluoroethene polymer on a stainless steel screen housed within a temperature-controlled heater block. As the tool is advanced, contaminants in adjacent soils and groundwater are volatilized and diffuse across the membrane, where the vapor is entrained in a carrier gas that transports the contaminants to the surface (via an internal trunk line) to a data acquisition system. This system typically consists of a set of detectors, including an electron capture detector (ECD), photoionization detector (PID), and flame ionization detector (FID), each of which can provide a gross response to the total contaminant load to which they are sensitive. Consequently, this setup allows collection of real-time data on CVOC distribution rapidly (up to 200 linear ft per day) and at a high density (generally every 0.05 ft). Because the MIP tool is also equipped with an electrical conductivity (EC) detector, it is also useful in many cases for rapidly providing stratigraphic characterization data that is relatively comparable yet much less costly than geophysical methods or geologic logging of soil cores (Schulmeister et al., 2003). Further, the MIP potentially generates more consistent stratigraphic data than geological logging since classification is less subject to human interpretation.

Previous applications have mostly focused on using the MIP to indirectly indicate the presence of DNAPL and as a semi-quantitative indicator of CVOC distribution because the detectors provide a bulk response that can be difficult to correlate to compound-specific concentrations. Further, the sensitivity to various compounds is not well-documented or necessarily reproducible across sites or MIP platforms, all of which complicate interpretation of MIP data (Bronders et al., 2009). There have been several attempts to develop more quantitative correlations between MIP data and CVOC concentrations (Costanza et al., 2002; Myers et al, 2002, McAndrews et al., 2003; Ravella et al., 2007; Bronders et al., 2009; Gee, 2010), which mostly provided mixed results and generally support MIP as a qualitative tool only. Regardless of whether the MIP data can be used to accurately predict concentration, comparisons to rigorous data collected using soil cores provides the most appropriate methodology for evaluating MIP results in heterogeneous media, and to date there has been no comprehensive evaluation of MIP performance focused on low permeability zones.

A.3 SITE OVERVIEW

All field work to support this phase of the project was conducted at NAS Jacksonville. This site was chosen after initial investigations at F.E. Warren AFB determined that the site was unlikely to generate adequate data to address project objectives (see **Appendix A** of this report). The following overview of NAS Jacksonville is largely based on information obtained from previous investigations and available site reports.

Site Location: NAS Jacksonville is a large site located within the city limits of Jacksonville, Florida with at least eight operable units (OUs) that are part of extensive investigation and cleanup efforts under Superfund. OU3 is a 134-acre area located in the eastern part of the facility near the eastern boundary (St. Johns River) and south of the flightline. Historically, OU3 has housed the Naval Aviation Depot where aircraft reworking activities and other support operations were centered. There are at least 50 buildings present at the site, and pavement covers most of the remaining area. Investigations to identify releases of hazardous materials to the environment were initiated in 1982. As a result of these earlier investigations, several potential sources of contamination have been identified within OU3. The primary area of focus for the current project is the former Building 106 source area (**Figure 1**), which is located in the north/northwest portion of OU3. (Note that the adjacent Building 780 source area is included in investigations for ESTCP ER-201032).

Site History: Building 106 served as the dry cleaner for the air station beginning in 1962 and was believed to have used approximately 150 gallons of PCE per month until 1990 when system improvements were implemented. It was identified as a potential source of contamination in 1993. Dry cleaning operations were halted in approximately 1990 and the building was demolished afterwards. The immediate area remains free of structures and is paved. It is surrounded by surface parking and there are several large buildings and access roads on all four sides. Air sparging and soil vapor extraction were implemented at the site in 1998 as part of the Record of Decision for OU3 but were discontinued following an optimization review completed in 2004-2005 (as part of the Five-Year Review). The need for additional remedies is currently being evaluated, but there are no on-going or planned operations that restrict the current project.

Site Geology and Hydrogeology: Soils underlying the site are part of Coastal Plain marine sediments, although surface soils have been extensively modified and there are extensive areas where fill was used, especially in previously low-lying areas. As a result, topography at the

surface is relatively flat. Below the surface fill, interbedded layers of sand, clayey sand, sandy clay, and clay are encountered to depths of approximately 150 ft bgs. Each of these layers is somewhat discontinuous and not encountered at all locations, but the upper soil intervals are generally dominated by sands. Laterally extensive clays have been encountered in the northern portion of the site in particular, and the extent of the clay layer near Building 106 (and Building 780) has been mapped more recently in this area as part of a comprehensive CPT survey in 2006. These investigations established that the clays were generally first encountered at depths of 10 to 20 ft bgs and ranged in thickness between 2 and 10 ft. In this portion of the site, the clay is often present as two smaller lenses, separated by thin sublayers of sandier soils. When present, the clayey sands are either interbedded in the clay or present in transitional zones between the upper sands and clay.

Figure 1. Project Site Map for NAS Jacksonville OU3.

The deposits at OU3 form a surficial aquifer unit that consists of two different layers within the northern portion of the site: 1) unconfined upper layer that extends from the surface to the depth of the clay (approximately 10 to 20 ft bgs); and 2) an intermediate layer that is confined by the clay. Because releases of hazardous materials occurred with the upper layer and came into contact with the low permeability clay, the upper layer of this surficial aquifer is the focus of the current investigation. Groundwater in the surficial aquifer generally flows in an easterly direction away from the Building 106 source area towards the eastern boundary of OU3 (at the St Johns River). Groundwater is first encountered at a depths 4 to 7 ft bgs, and water levels vary little throughout the year. The horizontal hydraulic conductivity for the upper sands based on pumping tests is approximately 20 ft/day. Horizontal conductivities in the clay layer has not been established, but it is described in site reports as having “a very low hydraulic conductivity” and USGS modeling efforts (1998, 2000) used a hydraulic conductivity of 0.001 ft/d for this

layer. Groundwater velocities within the surficial aquifer sands are 2 ft/yr on average. These data are summarized in **Table 1**.

Table 1. Summary of NAS Jacksonville OU3 Stratigraphy

Unit	Soil Type	Typical Thickness (ft)	Hydraulic Conductivity (ft/day) Maximum
Surficial	Sand	10-20	20
	Clay	2-10	0.001

Notes: (1) Units are described starting at the surface and then proceeding to deeper depths (surface fill not included); (2) Hydraulic conductivities represent field-based measurements when available; (3) Model values cited in site investigation reports used for units where field-based measurements were not performed.

Contaminant Distribution: The focus of this project is the unconfined portion of the aquifer, including both the upper sands and the underlying clay-rich layer. Constituents of concern at Building 106 include PCE, TCE, and associated degradation products (including 1,1-DCE, cis-1,2-DCE, trans-1,2-DCE, and VC). Note that the number of permanently-installed monitoring wells screened in the surficial aquifer is extremely limited (1 for Building 106, 1 for Building 780). At various times, investigations of groundwater conditions have been supplemented using i) groundwater samples collected from temporary piezometer points; and ii) depth-discrete groundwater samples collected during from direct-push borings. Both of these methods allow for one-time sample collection from the investigation point.

In the one permanently-installed monitoring well in the area (MW-28 located immediately east of Building 106), total CVOC concentrations in 1998 approached 30 mg/L with PCE as the major constituent. These concentrations have varied over time but remain well above regulatory screening limits for several chlorinated ethenes. A more comprehensive assessment of groundwater concentrations that was completed in 2006 as part of a direct push investigation encountered total CVOC concentrations that are generally highest in the area immediately under the former building and extending eastward (downgradient) for several hundred feet. There are several locations where the concentration of metabolites (particularly cis-1,2-DCE) exceed the concentration of parent compounds.

Limited soil concentration data have been collected at the site prior to the current demonstration. As part of a direct-push investigation in 2006, soil samples were collected at various locations near Building 106. Depths of these samples typically coincide with the start of the lower permeability clays identified across OU3. These data demonstrate that near the Building 106 source area, the VOC profile is generally dominated by PCE (maximum concentration of 77 mg/kg), with higher contributions from lesser chlorinated ethenes at downgradient locations. Note that these soil concentrations are much higher than what would be estimated based on groundwater samples in the area (which collect primarily from sandy intervals), reflecting the influence of mass storage within lower permeability zones in the surficial aquifer.

A.4 METHODS

Overview

Work completed at NAS Jacksonville was done in cooperation with the field program for ESTCP ER-201032 (*Determining Source Attenuation History to Support Closure by Natural Attenuation*)

at the same site. Personnel from GSI (Nick Mahler, David Adamson, Poonam Kulkarni) and University of Guelph (Steve Chapman, Adam Gilmore) implemented the field program with on-site technical and equipment support from Stone Environmental Inc (Seth Pitkin, Mike Rossi, David Crosby, Vincent DeLeone, Matthew Millard, Will Waterstrat). A local GeoProbe company (ProbeDomain) provided drilling services for all work phases (MIP, HPT, Waterloo profiling, soil coring, SP16 groundwater sampling) at NAS Jacksonville.

The following phases were completed to support SERDP ER-1740:

- ***MIP Data Collection:*** Baseline MIP logs at multiple locations, plus additional MIP logs at select locations after varying operational conditions.

- ***Soil Data Collection:*** Soil coring at same locations to generate high-resolution CVOC profile throughout the low K intervals (as well as overlying/underlying higher K intervals), plus groundwater sampling at several of the same depths to support data assessment (using the Waterloo^{APS} and/or Geoprobe SP16 sampling).

- ***Groundwater Data Collection:*** Groundwater sampling was completed at most locations sampling and at several of the same depths to support data assessment. Data were collected using a combination of the Waterloo^{APS}, Geoprobe SP16 sampling, and temporary piezometers. Only a subset of the groundwater data are included here; the full dataset will be part of the final report for ESTCP ER-201032 (expected to be available in early 2013).

- ***Stratigraphic Methods.*** Several different techniques for generating stratigraphic information were utilized at select locations, with the goal of obtaining side-by-side comparison of methods for identifying low permeability zones. This included the MIP system (electrical conductivity (EC) profile), Hydraulic Profiling Tool (HPT), the Waterloo^{APS} (index of hydraulic conductivity profile), and soil coring and classification. Only a subset of the data are included here; the full dataset will be part of the final report for ESTCP ER-201032 (expected to be available in early 2013).

Figure 2 shows the six sampling locations at the former Building 106 source area where data were collected.

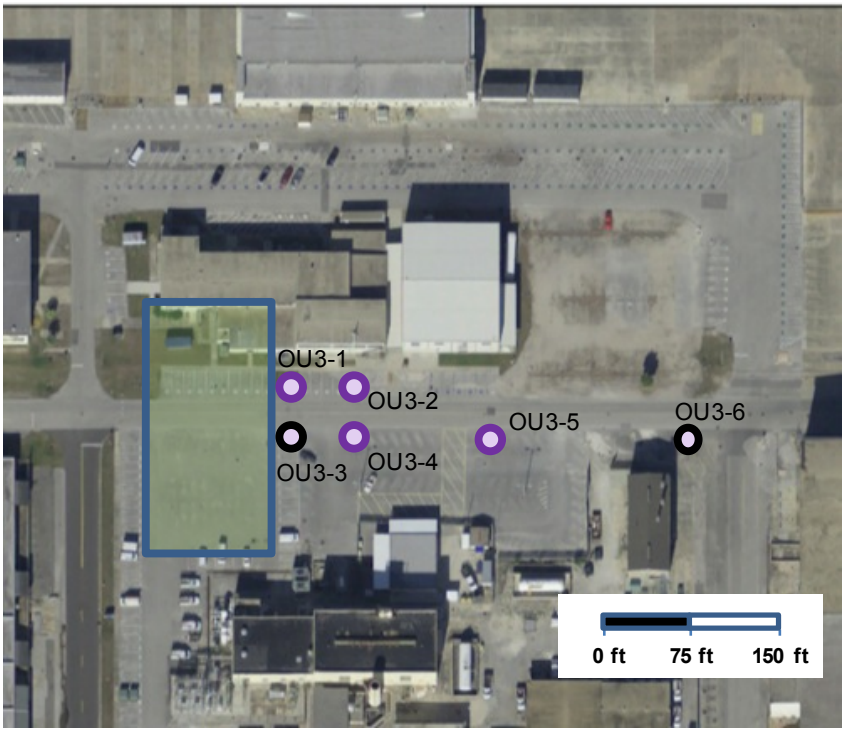

Figure 2. Sampling Locations at NAS Jacksonville OU3. Black symbols represent locations where more comprehensive characterization efforts were completed, including MIP operating condition testing.

MIP Data Collection Methods

Initial MIP data collection efforts focused on characterizing six locations within the former Building 106 source area using conventional techniques (**Figure 2**). **Table 2** lists the operating conditions for conventional MIP logs that served as baselines for further comparisons. These are based on recommendations from the manufacturer (Geoprobe, 2006) and the ASTM standard (D7352-07):

Table 2. Operating Conditions for Conventional MIP Logs

Parameter	Operating Condition during Conventional MIP
Trunk Line	Heated stainless steel (OU3-3 and OU3-6): PEEK (unheated) (remaining locations)
Drive Rate	1 ft/min
Carrier Gas Flow Rate	40 mL/min
Probe Temperature	120ºC
Direction of Data Collection	Data collected from surface to deepest point
Detector Types	ECD, PID, FID, EC

These efforts provided data to screen locations for further MIP testing, as well as to identify promising locations for subsequent soil coring. The project team identified the following operating parameters for testing (further information on MIP operating conditions and rationale is provided in **Table 3**):

- ***Trunk Line:*** Conventional MIP uses an unheated trunk line of PEEK (polyether ether ketone) material to carry subsurface vapors from the membrane to the above-ground data acquisition system. Heated (100ºC) trunk lines fabricated from stainless steel have been developed by Geoprobe in an effort to increase the transport rate and thereby minimize the potential for signal tailing as the MIP is advanced. As such, it would be expected to be particularly effective at improving signal resolution and reducing logging time for locations with high concentrations. This modification is expected to improve signal resolution for all soil types. Due to its widespread use, runs with the heated trunk line were used as the baseline at locations where operating parameter testing was completed (OU3-3 and OU3-6), and runs with the PEEK trunk line were used for comparison purposes.

- ***Drive Rate:*** Conventional MIP attempts to maintain a constant drive rate of 1 foot per minute while collecting data. Reducing the rate provides the opportunity for a higher mass of vapor to reach the detector(s) and would be expected to improve characterization within zones with low concentrations. Increasing the drive rate reduces the mass of vapor entering the system and may prevent overloading the detectors within high concentration zones.

- ***Carrier Gas Flow Rate:*** Conventional MIP uses a carrier gas flow rate of 40 mL per min to direct contaminant vapors through the tool to the detector. Decreasing the flow rate (to 20 mL/min) was hypothesized to increase detector sensitivity by increasing the pressure gradient between the formation and the tool and by decreasing the dilution of contaminant vapors in the carrier gas. Increasing the flow rate in higher concentration zones was hypothesized to reduce detector overload by decreasing pressure gradients and diluting higher concentration vapors.

- ***Probe Temperature:*** Conventional MIP uses a heater block to maintain a membrane probe temperature of approximately 120ºC. Higher temperatures (e.g., 140ºC) should increase desorption and volatilization of contaminant mass and thereby increase sensitivity within less contaminated zones. In high concentration zones, decreasing the temperature (80 - 100ºC) could improve resolution by reducing volatilization rates and thus the potential for overloading the detector***.***

- ***Direction of Data Collection.*** Conventional MIP collects data while the probe is being advanced to the bottom of the hole being characterized. For comparison purposes, the system was modified to collect data as the probe was retracted from the bottom of the hole. This “up-logging” method was used to identify the bottom of the contaminated interval because it eliminated potential carry-over of elevated MIP signals from the shallowest contaminated intervals.

Two of the six conventional MIP locations (OU3-3 and OU3-6) were chosen for further testing of the influence of varying operating conditions and to develop a standard operating protocol for MIP studies in low K intervals (**Table 2**). The following rationale was used for selecting these two locations:

- **OU3-3:** This location appeared to have the highest concentrations and was closest to the presumed location of the source zone (the former Building 106). As a high concentration location, it was appropriate for testing modifications to reduce sensitivity.

- **OU3-6:** This was the farthest downgradient location of those screened and appeared to have the lowest concentrations. As with the near-source location, the majority of mass at OU3-6 appeared to be present within the lowest permeability intervals. As a low concentration location, it was appropriate for testing modifications designed to increase MIP sensitivity.

Table 3 summaries how the MIP system was operated during testing at two locations within OU3. In general, operational conditions were tested systematically by varying a single parameter per MIP log (with the exception of the heated trunk line, which was used for each MIP runs listed in **Table 3**). For example, the drive rate was decreased at OU3-3 during one run (OU3-3-FD) while all other parameters were operated in the same manner as the baseline MIP. The gas flow rate was decreased during the subsequent MIP run (OU3-3-FR) while all other parameters (including the drive rate) were operated conventionally. This approach served to isolate the impact of any one parameter on the data obtained at the given location.

Table 3. Approach for Testing MIP Operating Conditions

Parameter	Operating Condition Tested at Location OU3-3 (Log ID)	Operating Condition Tested at Location OU3-6 (Log ID)
Trunk Line	Heated (OU3-3-HTL)	Heated (OU3-6-HTL)
Drive Rate	Fast – 2 ft/min (OU3-3-FD)	Slow – 0.5 ft/min (OU3-6-FD)
Gas Flow Rate	Fast – 80 mL/min (OU3-3-FR)	Slow – 20 mL/min (OU3-63-SR)
Probe Temperature	Low – 100ºC (OU3-3-LT)	High – 140ºC (OU3-6-HT)
Data Collection Direction	"Up-log" (OU3-3-UL)	"Up-log" (OU3-6-UL)

Notes: (1) Heated trunk line was used for all MIP tests in Table 3; (2) "Up-log" refers to collection of MIP data from the deepest point up to the surface. At each location, up-logging was completed in the same boreholes used to collect MIP data with the heated trunk line (i.e., OU3-3-HTL, OU3-6-HTL).

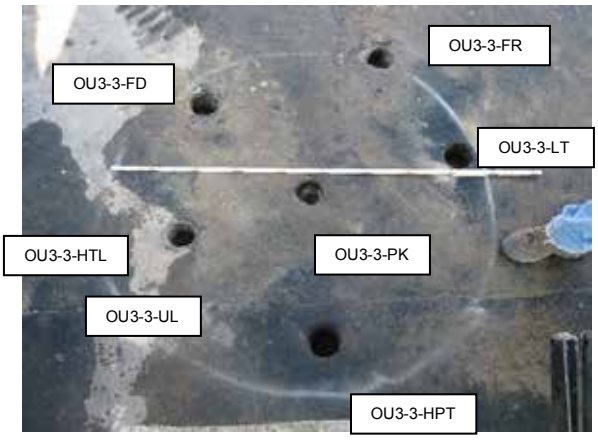

Figure 3. Example of Testing Approach: Location OU3-3.

Soil Data Collection Methods

Soil cores were collected from four locations within the former Building 106 source zone area (**Table 2**). Cores were collected in 4-ft lengths using the Geoprobe dual-tube sampling method. Recovery was generally 80% or higher, with nearly 100% recovery typical in the lower permeability clay-rich intervals. At each location, cores were collected to a total depth of up to 34 ft bgs.

Cored locations include both of those where comprehensive MIP testing was completed (OU3-3 and OU3-6) and two additional locations where conventional MIP logs were collected (OU3-4 and OU3-5). In addition, at location OU3-5, a duplicate core was collected within a 1-meter lateral distance of the first coring location. These four locations follow a downgradient transect from the presumed source zone and thus allow advective transport mechanisms to be considered during data evaluation.

A total of 209 soil samples were collected and analyzed for CVOCs from the Building 106 source area, including 95 at the two locations where comprehensive MIP testing was completed (not including duplicates). Samples were transferred in the field to vials containing pre-weighed amounts of methanol for shipment to the University of Guelph laboratory. At each location, additional samples were collected for physical property testing and other analyses (primary related to ESTCP ER-201032 project objectives). All soil CVOC analyses were performed at the University of Guelph.

To complement these evaluations, groundwater samples were also collected at all six of the MIP locations (**Figure 2**) using one or both of the following methods:

- ***Waterloo^{APS}:*** Stone's proprietary subsurface data acquisition system was used to collect both discrete-depth groundwater samples and an integrated set of companion data in a single, continuous direct push. Groundwater samples were collected by pumping water through screened ports located in the profiler tip; with stainless steel lines leading from the downhole tooling to 40-mL VOA vials for CVOC analysis using EPA Method 8260 at Stone's off-site analytical laboratory. Profiling was completed at all six locations where MIP screening was completed, and a total of 56 samples were collected from these locations. However, due to system limitations in collecting water from finer-grained soils, no samples were collected from the lower permeability clay intervals that are the focus of the current study.

- ***Groundwater Sampling using Geoprobe SP16 and Temporary Piezometers:*** At three locations where MIP screening was completed, groundwater was collected from at least 3 depths within the lower permeability zone at each location, along with at least 1 sample from both the higher permeability sands above and the below this interval. In higher permeability zones, Screenpoint (SP) groundwater sampling, consisting of the installation of protected screens within standard Geoprobe rods with an expendable drive point, was used. Once reaching the desired depth, the screen is held in place with extension rods while the drive rods are retracted. For this project, the SP16 system custom screens (1.0-in PVC, 2.5-ft long, 0.010-in slot size) was used. At intervals with lower permeability soils, temporary piezometers with similar screen characteristics were instead installed to provide more adequate time for well development. Using these two methods, groundwater was collected from a total of 6 to 7 different depths at each

location. Groundwater was collected from each of the points using a peristaltic pump after sufficient water was present. All CVOC analyses were completed at the University of Guelph.

Stratigraphic Data Collection Methods

A supplemental study was conducted within the former Building 106 source area to test different methods for characterizing stratigraphy. The specific objective was to examine each of the utility of each of these methods within low permeability zones using a side-by-side comparative approach.

The following methods were evaluated at one or more locations during the field program:

- ***MIP Electrical Conductivity (EC) Logs:*** The MIP system collects EC data throughout the characterized interval. Because higher EC values are typically associated with soils within higher clay content, this parameter can serve as an indicator of soil type. Semi-quantitative relationships have been developed such that the EC logs generated by MIP software packages typically designate the soil type associated with depth-discrete EC data. For this project, EC data was collected from the surface to the bottom of the characterized interval (typically at least 35 ft bgs) at all six of the locations where conventional MIP testing was completed.

- ***Waterloo^{APS}:*** Stone Environmental Inc.'s system provides continuous, real-time characterization of site stratigraphy with depth within the targeted portion of the saturated zone through the Index of Hydraulic Conductivity (I_k) data. These data are estimated by monitoring flow rates and pressure as the tool is advanced while injecting DI water, with lower permeability zones associated with higher pressures/lower flows and therefore lower I_k values. According to Stone, a one order-of-magnitude shift in I_k is generally equivalent to a one order-of-magnitude change in the hydraulic conductivity of the soil. I_k data were collected at all six of the same locations where MIP was completed.

- ***Soil Classification:*** Soil cores were collected from the four locations described previously. These cores were visually inspected and logged by site personnel, and subsamples were collected for physical property testing (e.g., grain size distribution and permeameter testing). Classification of soils based on these methods allowed for an estimate of relative hydraulic conductivity (either through direct measurement or based on typical literature values for similar soils). These data can then be compared to relative hydraulic conductivities generated at the same locations using the other field methods.

Data Evaluation Methods

To evaluate site data obtained as part of this project, qualitative, semi-quantitative, and statistical approaches were employed (**Table 5**). Qualitative and semi-quantitative methods focused on a visual inspection of the datasets to assess general trends and assign a ranking to each of the methods used to collect data. Statistical methods were employed as part of a quantitative exploratory data analysis of relevant datasets.

Table 5. Data Evaluation Methodology

Data to be Evaluated	Qualitative and/or Semi-Quantitative Methods	Statistical Methods
Comparison of Baseline MIP Characterization Data with Measured Soil Concentration Data	• Compare depth where max concentration is indicated • Compare depth intervals where elevated concentrations are indicated (bottom and top of contamination) • Identify false positives and/or false negatives	• Linear regression between MIP and concentration datasets (R^2 value) • Relative Percent Difference between normalized datasets (median RPD for all paired depth-discrete data)
Impact of Operating Conditions on Improving MIP Performance	• Compare depth where max concentration is indicated • Compare depth intervals where elevated concentrations are indicated (bottom and top of contamination) • Identify false positives and/or false negatives • Impact on detector sensitivity relative to baseline characterization • Assign rank based on comparisons to baseline and soil data	• Linear regression between MIP and concentration datasets (R^2 value) • Relative Percent Difference between normalized datasets (median RPD for all paired depth-discrete data)

For the semi-quantitative evaluation of MIP operating conditions on data quality, the criteria listed in the table above were used to assign a rank to each of the runs where one MIP operating parameter was varied:

- When comparing to the baseline MIP run (i.e., data collected the heated trunk line), the degree of carryover and sensitivity observed for each of the other runs were assigned a rank of 1 (worse), 2 (same), or 3 (better).
- When comparing the match of MIP data to the soil CVOC concentration data, the MIP runs were evaluated using the above criteria and assigned a rank of 1 (poor), 2 (fair), or 3 (good).

The statistical comparisons of MIP data to CVOC concentrations in soil required establishing a quantitative method for assessing the "accuracy" of the MIP contaminant distributions under the various operating conditions. Of the various statistical methods that could be appropriate for this type of evaluation, two relatively simple methods were chosen. The first was to calculate the ***relative percent difference*** (RPD) between soil concentrations and the MIP "concentrations" at corresponding depths. The following stepwise procedure was employed at each location were MIP data was collected:

1. At each depth, the concentrations of individual constituents were summed to obtain a total CVOC concentration from the soil data. The total CVOC concentration served as the "known" value (i.e., assumed to be the accurate benchmark).
2. The total CVOC concentration data was log transformed to be more consistent with its expected distribution.

3. At each depth, the MIP ECD and PID values were converted to the geomean of values obtained across the nearest 1-ft interval (e.g., the equivalent MIP signal at 20 ft bgs was calculated by taking the geomean of all MIP signals measured from 19.5 ft to 20.5 ft). This ensured a more representative dataset and minimized signal abnormalities that might have occurred at a single depth.
4. Each MIP dataset (ECD and PID) was log-transformed and then adjusted to account for the baseline signal (i.e., the minimum response for the detector over the interval being characterized).
5. The MIP datasets were then normalized using the maximum signal response at any depth at that location. This established a set range for each dataset between zero (no response) to one (maximum response) across the entire depth interval.
6. A similar normalization procedure was followed on the depth-discrete total CVOC concentrations obtained from the soil data.
7. The RPD between the normalized MIP data and the normalized soil CVOC concentration was then calculated at each depth. Values below zero indicated the MIP data generally underestimted the soil concentration, while values above zero indicated that the MIP data overestimated the soil concentration. The median RPD value across the entire depth interval was used as an overall indicator of accuracy.

The second method used as part of this evaluation was a more straightforward ***linear regression analysis*** to determine if predictive relationships between MIP signals could be established. In this approach, the log-transformed and baseline-adjusted MIP data were plotted on the y-axis versus the log-transformed soil CVOC concentration data on the x-axis. A standard linear regression model was then applied to obtain the corresponding regression equation and coefficient of determination (R^2 value), with the latter serving as the primary measure of the goodness of fit.

Note that each of the statistical evaluations was performed separately for the ECD response and the PID response. Both of these detectors are capable of detecting (with varying levels of response) all three of the primary constituents of concern at the site (PCE, TCE, and DCE isomers). FID data were not evaluated because an initial screening indicated that the FID response was poor and/or non-diagnostic at most locations for this set of contaminants. Additional evaluations were performed with DCE omitted from the total CVOC concentration datasets. Relative to PCE and TCE, the ECD detector is not particularly sensitive to cis-1,2-DCE, so the objective was to minimize the impact of this constituent (which is a major contributor to the measured soil concentration at some locations) on correlation efforts.

A.5 RESULTS

Comparison of Baseline MIP Characterization Data with Soil Concentration Data

Overview of Baseline Data: The results of the baseline MIP survey at the six locations suggested that the majority of contaminant mass (based on the ECD/PID data) was present within and immediately above a lower permeability layer first identified (using EC data) at a depth of 15 to 20 ft bgs. Data from the highest concentration (near source) location, OU3-3, is shown in **Figure 4A**, and the low concentration (farthest downgradient) location, OU3-6 is shown in **Figure 4B**. This shallow lower permeability layer was generally 8 to 12 ft thick, with downgradient locations characterized by thinner low permeability intervals and a higher degree of geologic heterogeneity. Contaminant concentrations appeared to be significantly higher near

the presumed source location (OU3-3) and typically exceeded the upper limit of the most sensitive MIP detector (ECD) for these contaminants. The PID was generally less responsive. The MIP signals decreased significantly in locations moving downgradient, particularly at OU3-6.

At all four locations where soil CVOC concentration data were collected (OU3-3, OU3-4, OU3-5 and OU3-6), the logging of the soil cores showed that the shallow permeable soils were sands (SP) with trace silt and clay and the underlying lower permeability soils were silty clays (CL). A gradual transition to increasingly finer-grained soils with depth was observed between the higher and lower permeability units. Soil CVOC concentration data confirmed the MIP results in that the majority of contaminant mass was detected within the lower permeability clays and in the overlying transition zone (**Figure 4**). At the near source location, OU3-3, the CVOC profile is dominated by PCE and TCE, with maximum total CVOC concentrations of approximately 30 mg/kg at 16 ft bgs. At least 80% of the total mass at this location occurred between 15 and 21 ft bgs, with little indication of penetration through the low permeability zone (**Figure 4A**). Downgradient at OU3-4 and OU3-5, the maximum total CVOC concentrations were similar to those at OU3-3 (approximately 20 to 40 mg/kg), but the relative contribution of cis-1,2-DCE was significantly higher, particularly in the higher permeability sands (see **Figure 4C and Figure 4D** section for plots). At these intermediate locations, the majority of the total CVOC mass (at least 80%) was encountered in these sand and transitional intervals above the low permeability clay. This overall trend continued at the farther downgradient location, OU3-6, where an even greater shift to cis-1,2-DCE was observed (approximately 90% of the observed mass) and the maximum CVOC concentration was approximately 5 mg/kg.

Groundwater data confirmed significant aqueous-phase mass is present within the low permeability intervals as well as the shallow permeable sands (see **Figure 5**). Total CVOC concentrations in samples collected from the near-source (OU3-3) location were generally between 10 and 100 mg/L throughout both the shallow sand and clay intervals, and concentrations dropped significantly within the underlying deeper sand unit. Similar patterns were observed at other locations, albeit with lower concentrations moving downgradient or cross-gradient. Based on comparisons of groundwater data to equivalent porewater concentrations estimated from soil data, there is some concern that the soil concentrations are artificially low in the permeable shallow sands due to loss or flushing of aqueous-phase mass during core collection and retrieval mostly at location OU3-3; more consistency between groundwater and soil-based concentration data was observed at the other locations. Collectively, the soil and groundwater data demonstrate that degradation of parent compounds has occurred at most locations, such that bulk correlations between actual soil concentrations and the various MIP signals will be influenced by the presence of multiple parent and daughter compounds.

The MIP EC data correlated well with stratigraphy observed through soil coring, demonstrating that the MIP can provide useful and relatively representative stratigraphic characterization data within lower permeability zones where clays are present. Elevated EC readings coincided with lower permeability clay units, and the EC data could be used to generally identify the upper and lower boundaries of these units. These results are consistent with those obtained by other high-resolution characterization studies that included direct-push electrical conductivity logging (e.g., Schulmeister et al., 2003; Wilson et al., 2005; Harrington and Hendry, 2006: Kober et al., 2009).

The primary disadvantage of MIP-based stratigraphic information (EC data) is that it is not able to capture small-scale heterogeneities as readily as some other methods (e.g., Waterloo^{APS},

Geoprobe's Hydraulic Profiling Tool). This is because the latter methods directly indicate the hydraulic response of the formation and thus provide information on relative permeability (Liu et al., 2012). The MIP EC sensor provides little information about apparent permeability contrasts in zones where clays (which are naturally electrically conductive) are absent. Note that the latest version of the MIP system incorporates the HPT to improve its overall utility.

Qualitative Comparison: At the high concentration location (OU3-3), the MIP ECD exceeded the upper detection limit throughout a large portion of the characterized interval, extending from approximately 14 to 31 ft bgs (**Figure 4A**). While this overlapped with the same interval where elevated soil CVOC concentrations were observed, it also indicated presence of contamination in deeper intervals that was not supported by the soil data, showing apparent carry-over or dragdown of the MIP ECD signal to deeper depths. Also a large ECD peak was present at approximately 8 to 10 ft bgs that was not consistent with the low soil CVOC concentrations at that depth. Soil concentrations could be biased low in the permeable shallow sands, potentially due to fluid loss or dilution during coring. At this location, there was not a particularly strong PID response, but an elevated PID signal was observed within a generally narrower interval (14 to 26 ft bgs) than the ECD, and the PID profile also suggested the presence of shallow contamination at 8 to 10 ft bgs. This discrepancy may have been due to loss or dilution of contaminant mass prior to analyses of core sub-samples or spatial variability.

At the low concentration location (OU3-6), the ECD did not reach its upper limit (**Figure 4B**). However, there was little overlap between the interval where an elevated ECD signal was observed (approximately 15 to >34 ft bgs) and the interval where the majority of soil CVOC mass was encountered (approximately 11 to 18 ft bgs), in part because the contaminant profile was dominated cis-1,2-DCE to which the ECD is not particularly sensitive. The PID was better at identifying the depth at which the maximum soil CVOC concentration was observed (approximately 15 ft), as well as the general interval with elevated soil CVOC concentrations. Both detectors appeared to show carry-over effects at this location.

At both of the intermediate locations (OU3-4, OU3-5), the MIP ECD signal again reached its upper limit, which impacted resolution of apparent concentration profiles (**Figure 4C and 4D).** At OU3-5 the intervals where the maximum ECD signal was observed did not overlap with the intervals where the highest soil CVOC concentrations were measured, however there was more consistency with the peak soil CVOC concentration interval at OU3-4. Carry-over effects were apparent at both locations with the ECD signal, particularly OU3-4. These data highlight that the heated trunk line, by itself, does not eliminate carry-over effects. The PID profiles at each location were generally similar to those observed with the ECD, although with less sensitivity and less evidence of carry-over.

Quantitative Comparison: Comparisons were made at the four locations where soil CVOC concentration data were collected, under "baseline" MIP operation, using both ECD and PID. Results are summarized in **Table 6** (linear regression) and **Table 7** (relative percent difference). The correlations of the PID and ECD responses with the soil CVOC concentration data varied widely, with R^2 values ranging between 0.03 and 0.62. **Figure 9** shows examples of the regression plots for locations OU3-3 and OU3-6. At three of the four locations, higher R^2 values were obtained using the PID than with the ECD, indicating that the PID had a better predictive capability. The ECD is not responsive to cis-1,2-DCE, such that including this compound is expected to negatively bias potential correlations between the ECD response and soil CVOC concentration data (see **Discussion** section). In some cases when cis-1,2-DCE was included, the slope of the regression line was negative, demonstrating that it is more appropriate to omit

DCE isomers from the correlations. In general, the R^2 values were higher for both ECD and PID response when DCE isomers were excluded from the soil CVOC concentration being evaluated. Correlations with the ECD profiles at the higher concentration locations were also hampered due to issues with exceeding the ECD detection range.

Table 6. Evaluation of Accuracy of MIP Data Relative to Soil CVOC Concentrations: Linear Regression of Normalized Datasets

Dataset	R^2 for Regression			
	ECD		PID	
	PCE+TCE	PCE+TCE+DCE	PCE+TCE	PCE+TCE+DCE
High Concentration Location (OU3-3)				
Heated Trunk Line (Baseline)	0.11	0.02	0.47	0.59
PEEK Trunk Line	0.25	0.004	0.43	0.21
Uplogged Data	0.25	0.48	0.006	0.14
Low Temperature	0.07	0.06	0.52	0.22
Fast Drive Rate	0.09	0.04	0.44	0.32
High Flow Rate	0.09	0.03	0.37	0.35
Combined Data from All Runs	0.09	0.00	0.23	0.23
Low Concentration Location (OU3-6)				
Heated Trunk Line (Baseline)	0.20	0.02	0.22	0.07
PEEK Trunk Line	0.23	0.04	0.17	0.22
Uplogged Data	0.15	0.32	0.06	0.20
Low Temperature	0.34	0.03	0.29	0.07
Fast Drive Rate	0.25	0.02	0.28	0.12
High Flow Rate	0.18	0.01	0.33	0.16
Combined Data from All Runs	0.13	0.01	0.12	0.09
Other Locations				
OU3-4-PK (Baseline)	0.28	0.04	0.62	0.41
OU3-5-PK (Baseline)	0.03	0.21	0.29	0.02

Following normalization, the median RPD value between MIP and soil CVOC datasets was also calculated at each location, using both the non-directional median RPD as an indicator of variability and the directional RPD as an indicator of bias (**Table 7**). During these comparisons, the inclusion of DCE isomers in the soil CVOC concentration generally decreased the median RPD values, but the difference was marginal and not clearly significant except for the ECD performance at OU3-6. The PID was more successful at matching data from the high concentration location than the ECD (largely due to much of the ECD response being over range), while the ECD performed similar or better at the other three locations.

Table 7. Evaluation of Accuracy of MIP Data Relative to Soil CVOC Concentrations: Relative Percent Difference Between Normalized Datasets

	Relative Percent Difference (%)							
	ECD				PID			
	PCE+TCE		PCE+TCE+DCE		PCE+TCE		PCE+TCE+DCE	
Dataset	Median (Non-Directional)	Median (Directional)	Median (Non-Directional)	Median (Directional)	Median (Non-Directional)	Median (Directional)	Median (Non-Directional)	Median (Directional)
High Concentration Location (OU3-3)								
Heated Trunk Line (Baseline)	61	47	62	41	39	-2	39	-14
PEEK Trunk Line	55	55	47	42	18	-11	18	-15
Uplogged Data	52	52	52	52	69	-67	67	-67
Low Temperature	56	40	56	30	47	-44	47	-46
Fast Drive Rate	57	50	60	41	56	-41	51	-48
High Flow Rate	56	36	56	26	129	-118	118	-118
Combined Data from All Runs	56	47	56	39	57	-39	53	-47
Low Concentration Location (OU3-6)								
Heated Trunk Line (Baseline)	109	57	42	13	160	-54	156	-149
PEEK Trunk Line	116	87	40	8	103	23	90	-90
Uplogged Data	121	-23	102	-90	200	-134	193	-185
Low Temperature	93	65	40	-37	99	19	95	-95
Fast Drive Rate	113	79	54	24	100	40	106	-57
High Flow Rate	145	82	38	5	112	37	110	-110
Combined Data from All Runs	121	65	48	-9	143	14	128	-113
Other Locations								
OU3-4-PK (Baseline)	44	17	36	13	50	-40	48	-48
OU3-5-PK (Baseline)	93	52	57	10	76	22	76	-76

An example of the RPD data vs. depth is shown in **Figure 6** for location OU3-3. Based on a visual inspection of the data at this and the other locations, there is reasonable consistency between results obtained using the PID and ECD. In general, the PID more frequently underestimated soil concentrations (as evident by several negative directional median RPD values (**Table 7**)), while the ECD appeared to overestimate the soil concentration at many intervals, particularly those intervals below where the peak MIP response is measured. This is likely attributable to slow flushing of high concentrations within the MIP system, resulting in carry-over in ECD readings as the probe is advanced to deeper intervals. Both the normalized soil data and the MIP signal tended to fluctuate at depths below the peak, demonstrating that that there is significant heterogeneity within these intervals. However, the frequently large differences between the MIP results and the measured soil concentration data indicate that predicting small-scale heterogeneities based solely on MIP response would be invalid.

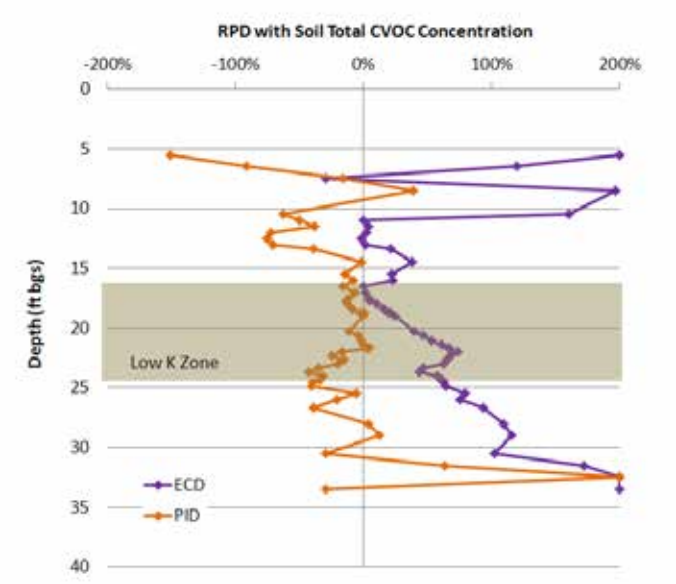

Figure 6. Relative Percent Difference between Baseline MIP Characterization Data and Soil CVOC Concentration Data at Location OU3-3. PID data are compared to sum of PCE, TCE, and cis-1,2-DCE soil concentrations. ECD data are compared to sum of PCE and TCE soil concentrations.

Variations of MIP Operating Conditions

Qualitative Comparison: MIP data obtained during runs when individual MIP operating parameters were varied were compared to the baseline MIP characterization data (heated trunk line; **Table 8**) and to the soil CVOC concentration data (**Table 9**). Composite plots of all MIP runs vs. depth-discrete soil CVOC concentration data at OU3-3 are included in **Figure 7A** (ECD) and **7B** (PID) and at OU3-6 in **Figure 8A** (ECD) and **8B** (PID). Note that these assessments are primarily based on a visual inspection of non-normalized data because most practitioners do not attempt any sort of transformation as part of their evaluation of MIP data.

- ***PEEK Trunk Line:*** The unheated PEEK trunk line, when compared to the baseline MIP, decreased the ECD/PID signal responses, which can serve to improve resolution at high concentration locations where detector overload is a concern. However, the profile obtained at the high concentration location (OU3-3) was strongly influenced by the "burn off" that was completed during the PEEK run. A "burn-off" event involves pausing the MIP for approximately five minutes to allow for contaminant mass, including mass entrained within the MIP and present on the outside of the tooling, to be flushed from the system through a combination of heat and carrier gas flow. This decreased ECD signal carry-over, such that the detector was maxed out for a shorter interval (14 to 25 ft bgs) than was observed with the heated trunk line (14 to 31 ft bgs). However this was the only run where the "burn off" procedure was employed. Using the PEEK trunk line, the ECD and PID failed to indicate the presence of elevated concentrations between 8 to 10 ft bgs that was observed in the heated trunk line run. The overall shape of the PID profile was

relatively similar to the soil CVOC profile using both types of trunk lines. At the lower concentration location (OU3-6), the unheated PEEK trunk line had a marginal effect, particularly on the PID data. The ECD signal response was slightly lower without maxing out the detector or modifying the general shape of the profile (relative to the baseline MIP characterization). However, there was little overlap between the interval where the maximum ECD response was obtained and the interval with the maximum soil CVOC concentrations. This same problem was encountered with both the PEEK and the heated trunk lines. A contributing factor may be the uncertainty in assigning depths to MIP and/or soil data. For the MIP system, travel time from the membrane to the detector is set by the software (on the basis of the times observed during the response test). Differing ratios of individual compounds (which travel at slightly different rates) encountered during tool advancement thus could influence the relative accuracy of this depth assignment. Furthermore, soil sample depth is subject to uncertainty when core recovery is lower.

- ***"Up-Logging":*** Operating the data collection mode in the opposite (i.e. upward) direction produced significantly different MIP profiles relative to baseline operation. At both locations, generally lower ECD signals were encountered at deeper intervals than were encountered during baseline operation, indicating that up-logging helped to eliminate the downward carry-over effects. At the lower concentration location (OU3-6), the interval where maximum ECD and PID signals were measured corresponded reasonably well with the interval with the highest soil CVOC concentrations, and the MIP data confirm that the majority of contaminant mass is confined to a relatively narrow interval. However, the MIP data at the higher concentration location (OU3-3) were less consistent. Once the ECD hit its maximum limit (at approximately 26 ft bgs), it remained at or near this limit until near the top of the hole (5 ft bgs). This indication of contaminant mass shallower than was observed in conventional downward MIP profiling suggests that carry-over is still a problem, but in the opposite direction. Based on the results at these two locations and the ranking system employed (**Tables 8 and 9**), the uplogging modification was the preferred option for collecting data at the low concentration location. Further, operating in this mode was shown to be useful in identifying the base of the contaminated interval, particularly in highly contaminated source areas. These data are consistent with a recent study by Bumberger et al. (2011) that showed that "backward" probing better matched the apparent bottom of contaminated intervals that was identified using an ultraviolet optical screening tool.
- ***Carrier Gas Flow Rate:*** Increasing the carrier gas flow rate generally improved ECD signal resolution at the higher concentration location (OU3-3) because it minimized (but did not eliminate) overload of the detector throughout the targeted interval. This operational change reduced carry-over of elevated contaminant detections across a deeper interval based on the ECD signal, while increasing PID response significantly without impacting the shape of the PID profile. Visual inspection of the PID data show reasonable agreement with the soil CVOC data at this high concentration location. Based on the ranking system (**Tables 8 and 9**), the high flow rate modification was the preferred option for collecting data at the high concentration location. The primary limitation was that the shallow contamination (above 15 ft bgs) was not detected as it was during the baseline run. At the lower concentration location (OU3-6), decreasing the flow rate did not have the same beneficial influence and only slightly increased the ECD signal response without significantly altering the shape of the profile relative to the baseline MIP run. The PID response at this lower flow rate was generally similar to or lower than the baseline run, with some evidence of signal carryover.

- ***Heater Block Temperature:*** Lowering the heater block temperature also improved ECD signal resolution at the higher concentration location (OU3-3) with less detector overload. However, while the shape of the ECD profile was relatively similar to the high flow rate ECD response, carry-over was more pronounced. The PID signal response was dampened significantly at the lower temperature at this location, but the general profile was relatively similar to the baseline profile. At the lower concentration location (OU3-6), little impact was observed (relative to the baseline) when the temperature of the heater block was increased. The interval where an elevated ECD signal was observed (approximately 15 to >30 ft bgs) was again not consistent with the interval where the majority of soil CVOC mass was encountered (approximately 11 to 18 ft bgs) showing carryover in the MIP data. Increasing the temperature did not improve the PID signal sensitivity, although the interval with maximum readings generally coincided with the interval with maximum soil CVOC concentrations. A previous lab-scale study examining the impact of the heater block temperature (Costanza et al., 2002) noted while flux across the membrane can increase at higher temperatures, the rates are not necessarily predictable due to the formation of water vapor that restricts transport. Normal heater block operation (120°C) exceeds the boiling point of most CVOCs, but also that of water. Consequently, higher temperatures may not provide an optimal balance between CVOC recovery and water vapor generation.
- ***Drive Rate:*** Advancing the MIP tool at a faster drive rate at the higher concentration location (OU3-3) resulted in an ECD signal profile that was relatively similar to the baseline run. Within the deeper sands (>30 ft bgs), the appearance of sharp, narrow peaks at approximately 4-ft intervals can be attributed to reaching the end of 4-ft rod sections and the pause in advancement while an additional rod was added (as opposed to elevated contaminant levels). Increasing the drive rate also resulted in the most significant carry-over of all of the operating parameters tested, with an elevated ECD signal to the base of the hole (46 ft bgs). The PID run at this drive rate provided a reasonable match with the narrow interval (14 to 16 ft bgs) where maximum contaminant levels were indicated by the soil CVOC data. At the lower concentration location (OU3-6), using a slower drive rate only marginally increased the ECD signal response within most intervals. Poor overlap with the intervals where maximum soil CVOC concentrations was again observed. The PID profile at this slower drive rate was not particularly well-resolved but matched the general location where peak soil CVOC concentrations were encountered, with some evidence of signal carryover.

Quantitative Comparison: At both locations and for both detectors, the R^2 values obtained after varying each of the operating conditions were generally similar to those obtained during the baseline characterization (**Table 6**). With a few exceptions, higher R^2 values were once again obtained with the PID datasets, indicating that the PID had a better predictive capability than the ECD. Similarly, R^2 values were typically higher when DCE isomers were excluded from the soil CVOC concentration being modeled, although this pattern was clearer for the ECD correlations (11 of 14 cases) than for the PID (10 of 14 cases), as expected based on the ECD's limited ability to detect cis-1,2-DCE. The maximum R^2 for any correlation was 0.62, indicating reasonable capability of the MIP to predict soil CVOC concentrations in some cases. The majority of R^2 values were much lower, suggesting little meaningful quantitative correlation. Additional linear regression analyses were performed on datasets developed using the optimized standard operating protocol for MIP, as well as the duplicate soil core dataset (see **Discussion** section).

The median non-directional and directional RPD between MIP and soil CVOC datasets was also calculated at each location to evaluate the impact of changes in operating conditions. The PID again performed better at the high concentration location than the ECD under most operating conditions, presumably because it did not suffer from detector overload. Significant improvements due to modified MIP operation were not observed at either location, with similar directional and non-directional median RPD values to the baseline characterization. In terms of variability, the median non-directional RPD value for the ECD datasets were nearly identical regardless of how the MIP was operated. For example, the median RPD at the high concentration location ranged between 47% and 61% for all 12 ECD datasets (including the soil CVOC concentrations in which DCE was included). The data provide little evidence that these biases can be reversed or diminished based on MIP operation, with the possible exception of the PID at the low concentration location.

Influence of Soil Type on Comparisons

Median (directional and non-directional) RPD and linear regression methods were again employed to evaluate whether soil type influenced potential correlations between MIP and soil data. Specifically, the median RPD and R^2 values for data from the low permeability zones at each location were compared to the median RPD and R^2 values for data from all zones. While individual values were determined for each run under the different operating conditions, the reduction in the number of data points limited the statistical power of the evaluation. Instead, data from all runs under all operating conditions at a single location were grouped, and the median RPD and R^2 values were calculated from the grouped data.

Table 10 displays the median non-directional RPD values calculated using this approach. For each detector at each location, there was a marked improvement in median RPD values when only the data from the low permeability zones are included. This provides evidence that there was less variability in the correlations within the lower permeability zones and that the MIP performance was not negatively impacted by soil type. Similar evidence of reduced bias within low permeability zones was obtained by calculating median directional RPD values (data not shown). The results of linear regression analysis did not clearly demonstrate that variability was reduced in low permeability zones (**Table 11**, **Figure 10**). At the high concentration location (OU3-3), the R^2 value was slightly higher when PID data from only the low permeability zone was included in the regression analysis. However, a decrease in the R^2 value was observed with the ECD data at this location, as well as both the ECD and PID datasets at the lower concentration location (OU3-6). Note that at both locations, the soil CVOC concentrations in the lower permeability zones fell within a narrower range than those present across the entire depth interval, and the dissimilar data distribution influences the comparison of regression line fits.

When evaluating individual MIP runs where operating conditions were modified, there was no clear decline in data quality when only the low permeability data were included. However, the slopes of the resulting regression lines were often close to zero or even negative, owing to detector overload (at the high concentration location) or limited detector response (at the low concentration location). Regardless, whenever possible, we recommend comparing MIP and soil data collected from similar soil types because variability in soil type may impact MIP performance.

A.6 DISCUSSION

Based on the results of the current study, a recommended SOP for using MIP as a characterization tool within low permeability zones is presented in **Table 12**. Because the benefits of various operating conditions varied slightly depending on the level of contamination present at locations being characterized, the MIP protocol implemented at a generic site should be consistent with the expected concentration (if known). In addition, the protocol includes a stepwise procedure for evaluating MIP data: 1) at each location, complete both baseline and up-logging MIP characterization, and use the latter for data correction purposes; ii) omit data from depth intervals where the detector limit is exceeded; and iii) compare data collected from the same soil type. The MIP profiles generated using this protocol (**Figure 11**) provide a relatively strong qualitative match with the soil concentration data, highlighting the usefulness of the tool in identifying contamination at sites with significant low permeability zones. **Figure 11** also shows the R^2 values for linear regression of data using the optimized MIP protocol for the high concentration location (R^2 = 0.32) and the low concentration location (R^2=0.49).

TABLE 12. Optimized Standard Operating Protocol for MIP in Low Permeability Zone Investigations

Option	Recommendation	
	Higher Concentration Areas	Lower Concentration Areas
Detector Utility	PID unless dominated by poorly-detected CVOCs (e.g., 1,1,1-TCA)	ECD if no DCE is present; PID if DCE is present
Heated Trunk Line	Utilize if available	Utilize if available
Drive Rate	Standard	Standard
Flow Rate	High	Standard
Temperature	Standard	Standard for ECD applications: High for PID applications
Uplogging	Use with baseline characterization to establish base of contaminated interval and for data correction	Use with baseline characterization to establish base of contaminated interval and for data correction

Notes: (1) Detector utility is based on detector likely to generate most useful data in chlorinated solvent source zones.FID may be more appropriate in petroleum hydrocarbon sites. Data from all available detectors should be reviewed as common practice. **(2)** "Standard" is based on standard protocol for MIP use detailed by ASTM (2007) and/or the baseline value used as part of this project (see Table 2 and Table 3).

Further discussion of key points used in developing the protocol is presented below, and a summary of the results of the various evaluation methods are presented in **Table 13** (high concentration location) and **Table 14** (low concentration location).

Detector Utility

Overall, the PID datasets provided more accurate representations of contaminant distributions for regions where contaminant levels are high (generally greater than 1 mg/kg). In areas where soil CVOC concentrations are lower (down to about 0.1 mg/kg), the ECD was more useful because of its greater sensitivity and lower detection limits. The detection limits found in this study are similar to those cited by Ravella et al. (2007) for the MIP ECD (200 μg/L PCE or TCE)

but lower than those cited by Bronders et al. (2009) for the MIP PID (10 mg/L TCE, 50 mg/L PCE).

The disparity in ECD response to compounds having two chlorine atoms (i.e., cis-1,2-DCE) versus compounds having three or more chlorine atoms (i.e. TCE and PCE) likely introduced variability and complicated data interpretation. The soil CVOC concentration data established that the contaminant profile in certain intervals is dominated by cis-1,2-DCE and in other areas more by TCE and PCE, causing a misrepresentation of CVOC levels by the ECD. Improved correlations were generally obtained when cis-1,2-DCE was removed from the total CVOC concentration, but the performance of the ECD was consistently poorer than the PID at locations with high concentrations. The PID is not nearly as sensitive to the amount of chlorine present and would be expected to be more representative of the contaminant distribution at OU3.

Supplemental MIP response test data for 1 mg/L solutions of c-DCE, TCE, and PCE were collected (see **Figure 12**) and demonstrated that the ECD response to cis-1,2-DCE is relatively strong (similar to that of the PID) and increases significantly between TCE and PCE runs. Conversely, PID responses for the same three compounds were all quite similar. Consequently, the PID is a more reliable detector when the contaminant profile and constituents present is not well established. The disadvantage to relying on the PID is that because its sensitivity is generally much lower than the ECD, it has less utility when working in lower concentration areas, and in general it is expected that both ECD and PID detectors would be utilized. In general it is recommended that both ECD and PID detectors should be utilized, given that MIP systems are generally equipped with multiple detectors. Operating procedures should be selected to avoid detector overload so that relative magnitudes of responses are maintained to the extent possible (e.g., splitting the ECD flow).

Influence of Soil Type

Evaluations conducted after sorting by soil type indicated that the MIP performed similarly or perhaps better within the lower permeability zones that were generally encountered between 15 and 25 ft bgs at most locations. This evaluation benefitted greatly from excluding the data from the higher permeability sands, where losses in soil contaminant mass due to core recovery, dilution with water (added to casing to minimize heaving sands) and volatility potentially contributed to variability. Based on the depth-discrete RPD data, the MIP characterization generally provided a more accurate representation of soil data within the lower permeability layers at all locations and for both detectors. More mixed results were seen using linear regression analyses.

The performance of MIP within lower permeability soils in this evaluation differs with a study conducted by Myers et al (2002) as part of a validation of the Site Characterization and Analysis Penetrometer System (SCAPS). This system uses a MIP platform in combination with a field portable direct sampling ion trap mass spectrometer (ITMS) to identify and quantify contaminants in unsaturated and saturated soils. During the SCAPS demonstration, the presence of finer grained soils was shown to negatively influence correlations between soil/groundwater TCE concentration data and ITMS-MIP data. A key difference in the Myers et al. (2002) dataset is that the TCE concentrations in the sand layers were generally higher than those in the current study, meaning that there was less emphasis on correlation near the lower detection limit of the tool. Further, while the ITMS-MIP performed best in sands, data from clay

soils were generally better than those from silts or sands mixed with silts/clays. The authors did not provide an explanation for why soil type influenced their results.

One potential limitation encountered during the current investigation was that the ECD baseline response (in the absence of elevated CVOC concentrations in the soil) was frequently higher within fine-grained intervals than in overlying permeable soils. This effect is most prevalent in the low concentration location (OU3-6) where the ECD response was highest in the interval of lowest permeability (between approximately 15 to 25 ft bgs) even though soil CVOC concentrations are relatively low in this interval. There are two primary factors that may cause the higher MIP detector response in lower permeability soils:

1. The lower permeability soils present a higher pressure gradient to the MIP system and the result is that more mass enters the MIP system. This is supported by a study conducted by Costanza et al. (2002) where it was demonstrated that the gas-phase pressure on the exterior of the probe was a significant driving force for contaminant mass. Data from the Costanza et al. (2002) study were consistent with pore-flow theory across a membrane, where diffusive flux is directly proportional to the difference in partial pressure across the membrane. A slightly different situation exists in the saturated zone, where diffusive flux is better quantified using Henry's law partitioning of aqueous-phase contaminants across the MIP membrane. However, Henry's law constants increase with pressure (Majer et al., 2008), such that contaminant flux would also be expected to increase when formation pressures increase. Pressure logs collected at OU3-3 using the Waterloo^{APS} confirm that pressures within the lower permeability unit were typically greater than 50 psi (after correcting for hydrostatic pressure). These levels are well over an order of magnitude higher than those in both the shallow sands and the deeper sands (generally less than 5 psi).
2. It is also possible that the entrainment of water vapor may have occurred in the lower permeability intervals, as the MIP has been known to entrain water when advancing through fine-grained soils. The presence of water vapor in the membrane is thought to influence flux by increasing sorption onto the membrane (Costanza et al., 2002). Note that the MIP system is equipped with a drier tube, which is normally able to reduce the water content to ensure that the ECD detector performs adequately. However, the location of this drier tube within the MIP system (above-ground, immediately before the detectors) means that it has little impact on water present in the membrane or trunk line.

In effect, the presence of lower permeability soils results in a higher background response throughout these intervals. This does not necessarily represent a limitation for the MIP tool in characterizing lower permeability soils, because increased pressure and heating within these zones would also improve sensitivity at lower concentration areas where signal response would already be expected to be low. It should be noted that there are several other variables associated with the soil type that can directly and indirectly influence MIP detector response, such as temperature and electrical conductivity.

Carry-Over Effects

As noted previously, carry-over of contaminant mass within the MIP system influenced data interpretation because it provided a misrepresentation of the intervals where mass was actually present. This was a particular concern at locations with higher concentrations, where the amount of time required to flush mass from the MIP trunk line appears to have been inadequate. It is also problematic in the context of low permeability zone investigations because mass

present within these zones may be confined to a relatively narrow depth interval near the interface with a higher permeability interval. In these cases, carry-over of an elevated MIP signal would falsely suggest deeper contamination as well as a higher contribution of total mass from the lower permeability soil layers. Further, DNAPL transport is highly influence by permeability interfaces, and the likely contribution of NAPL to MIP carry-over (Bumberger et al., 2011) would influence its utility within low permeability zones at sites where NAPL is present.

The observation of carry-over during MIP investigations is not new, and there are several methods that have been employed in an effort to minimize its influence. Bumberger et al. (2011) collected data with an unheated transfer line and showed that even when logging was periodically stopped at defined intervals (approximately every 1 ft) to allow for system "self-readjustment", it was difficult to interpret data due to time- and depth-dependent influences. They argued that coupling MIP with a mobile mass spectrometer was a successful approach for improving data interpretation, and also showed that collecting data in the upward direction could help identify the bottom of the contaminated interval. This latter conclusion was based on data obtained using an ultraviolet optical screening tool (UVOST) as opposed to soil data. Costanza et al. (2002) recommended using heater block temperatures of 120ºC to minimize carry-over in high concentration areas, even though they acknowledge that lower temperatures are generally preferable to ensure predictable diffusion rates across the membrane.

Most of the modifications tested as part of this study were designed to reduce carry-over, including the heated trunk line. The heated trunk line, by itself, was not found to reduce carryover. The only modification that resulted in a relatively clear benefit with respect to carryover during tool advancement was the use of a higher flow rate. This served to dilute contaminant mass that crossed the membrane and reached the detector, but also contributed to more rapid flushing through the entire MIP system. Periodic completion of a "burn-off" event is another option to minimize carry-over, as evidenced by the relatively strong correlation obtained using this procedure at OU3-3 with the PEEK trunk line. The burn-off approach is potentially cost-prohibitive to apply universally for conventional MIP investigations where rapid data acquisition is a major objective. It may be more appropriate at selected depth intervals (e.g., during changing of direct-push rods, or after 1 m of detector response continuously exceeding the maximum limit) or at sites where there are a few narrow intervals with high concentrations that can be targeted. Carryover will be more easily diagnosed if bi-directional logging is performed.

Possible Data Analysis and Adjustments

As noted above, several data correction methods are recommended as part of the MIP protocol for low permeability zone investigations. This includes combining conventional MIP with "up-logging" whenever possible. Up-logging provided good value in determining the bottom depth of contamination but was less indicative of soil concentrations at shallower depths. When correcting the baseline MIP run with the up-logging profile collected at the same location (i.e., taking the minimum value of two datasets at each depth), improved comparisons were obtained during the current study. As demonstrated in a "corrected" MIP profile in **Figure 11**, this step reduces the negative impact of carryover by providing a more accurate characterization of the zone below the peak concentration. Boundary effects may still be a concern even after data correction.

Further data corrections that are recommended to improve correlations include the removal of data from depths where the upper limit of the detector was exceeded (typically only applicable

to ECD data at chlorinated solvent sites) and segregating data by soil type such that low permeability soils can be compared directly. While these steps may have little impact on R^2 values obtained following linear regression, they can be helpful in proper visualizing and evaluating data from critical depth intervals.

Predictive Capabilities

The correlation data obtained during this study confirm that MIP is suitable as a qualitative screening tool and has limited ability to predict soil concentrations in most applications. During these analyses, values for MIP:Soil correlation R^2 using the optimized SOP were 0.32 for the low concentration location and 0.49 for the high concentration location for co-located points (within 1 meter) (**Figure 11**). These R^2 values are much lower than the R^2 value of 0.88 (0.95 with depth adjustments accounting for core recovery) obtained from a Soil:Soil comparison using concentration data from duplicate soil cores collected less than 1 meter apart at location OU3-5 (**Figure 11**). Depth shifting is justified based on incomplete core recovery in a key interval at OU3-5 from 3.0 to 4.5 m bgs (70%) with the 4.5 to 6.0 m bgs run apparently recovering some of the remnant material. The depth shifting aligns the position of the clay interface for the two locations.

The MIP:Soil results are consistent with an earlier study by Ravella et al. (2007) that obtained an R^2 value of 0.29 when comparing MIP ECD data to PCE concentrations from co-located soil samples and an R^2 value of 0.21 when comparing MIP ECD data to TCE concentrations from co-located groundwater samples. The SCAPS validation study (Myers et al., 2002) performed similar regression analyses and obtained several strong R^2 values when data was segregated by site and soil type, including a value of 0.95 for saturated soils at the NAS North Island site. However, the combined dataset from all 5 sites (including samples from both saturated and unsaturated soils) resulted in an R^2 value of only 0.34, which is more consistent with the results of this study. The SCAPS study also had the advantage that ITMS-MIP data could be accurately calibrated against a single constituent, such that the data could be reported directly in mg/L and influences from co-contaminants were minimized.

The high R^2 value obtained for the Soil:Soil comparison at one location (0.88, or 0.95 with depth adjustments) contrasts with the much lower R^2 values obtained from MIP:Soil comparisons even using the recommended SOP. Similarly, visual inspection of the profiles from the duplicate soil cores suggests strong agreement of depth and shape of the contaminated interval. This illustrates the difficulties in developing predictive relationships with MIP data. There are several factors that can negatively impact these types of correlations

- Spatial heterogeneity (both lateral and vertical directions) in soil type and contaminant distribution
- Challenges in accurately assigning MIP and soil concentration data to the correct depths; and
- Data that may not be normally distributed even after log normalization, lessening the impact of linear regression methods.

The primary goal of the statistical methods employed during this study was to evaluate the influence of various MIP operating parameters on data quality, not to predict soil concentration data. However, the authors recognize that, despite uncertainty in the accuracy in predicting soil concentrations using MIP data, some site managers will want develop site-specific correlations

between MIP and soil core data to provide an inexpensive way to estimate contaminant distribution on a fine vertical resolution. In these cases, the SOP described in this paper should ensure that higher quality MIP data are obtained.

A.7 CONCLUSIONS

Systematic field testing of the impact of MIP operating conditions on performance was used to develop a proposed Standard Operation Procedure (SOP) for MIP investigations in low permeability zones based on site-specific expectations on contaminant levels. Two measures were found to be particularly valuable: 1) using high carrier gas flow rate at high concentration locations to reduce carry-over via dilution of contaminant mass; 2) collecting MIP data in the opposite direction ("up-logging") to help establish the base of a contaminated interval; and 3) using a different detector based on concentration level.. These three and other related procedures resulted in MIP profiles that were more representative of contamination throughout the entire vertical extent of the interval being characterized.

The study results demonstrate the utility of the MIP in locating contamination in low permeability zones, determining the extent to which quantitative relationships can (or should) be established, and weighing the cost-benefit of the MIP data relative to other characterization methods. At a minimum, the MIP helps reveal the presence and relative distribution of contamination within lower permeability intervals that are too often ignored in conventional site characterization. The MIP is capable of resolving contamination in low permeability material as well as it does in high permeability material, and its overall efficacy is not limited to certain soil types. While the capability of the MIP to collect a large amount of depth-discrete data is valuable in demonstrating the general horizontal and vertical distribution of contamination at a site in both transmissive and low permeability compartments, the results of this study emphasize that the MIP data does not necessarily accurately reflect the actual small-scale, detailed contaminant heterogeneity. MIP data may provide a false sense of confidence that small-scale heterogeneities are well-understood, particularly when compared to soil core data.

The results of this study demonstrate that care should be taken when attempting to use MIP data to predict soil concentrations due to factors such as depth assignment, spatial heterogeneity, and limitations in commonly-used linear regression methods. Application of the SOP to a low and a high concentration location yielded a MIP:Soil correlation R^2 of 0.32 and 0.49, respectively (the MIP and soil sampling were conducted within one meter of each other). This compares to the control Soil:Soil correlation R^2 of 0.88 – 0.95 for co-located coring points (i.e., within 1 meter).

The economic benefit of using MIP as a characterization tool, particularly for sites with low permeability soils, is an important issue for the environmental remediation community. MIP is well-suited as a screening tool for rapid data acquisition, and the general goal of using MIP during high-resolution site characterization is to reduce the intensity of subsequent soil coring. The SOP developed as part of this study improves performance and represents a nominal incremental cost relative a conventional MIP investigation (approximately 10-20%, related to the time required to uplog the same hole where the system was advanced). These additional costs are likely to be recouped even if there is only a small reduction in high-resolution cores that are collected. An alternative high-resolution characterization strategy involves forgoing MIP altogether, and instead using a combination of soil coring and on-site analysis (via a mobile laboratory brought on-site) to provide near real-time data. The costs associated with this

approach depend highly on the scale of characterization required and the size of the site itself, but a planning-level economic analysis shows that a no-MIP high-resolution soil coring program is about 60% more expensive than a combination of MIP and limited soil sampling. If these approximate cost rules are correct, then a MIP program with the SOP from this study is only cost effective if it reduces the number of high resolution cores by more than 40% (for example, from 20 high resolution cores to 12). Ultimately, the choice to use MIP as part of a dynamic site characterization program likely depends on site-specific factors that balance data objectives and costs. Regardless, implementation of the protocol enhances the utility of MIP as a complementary investigative tool for identifying the location and magnitude of contamination within critical low permeability zones.

A.8 ACKNOWLEDGEMENTS

This study was completed to support two U.S. Department of Defense-funded projects, SERDP ER-1740 and ESTCP ER-201032. Additional laboratory and field work was completed by Poonam Kulkarni (GSI Environmental Inc.), Adam Gilmore (University of Guelph), Vincent DeLeone, Matthew Millard, Will Waterstrat, David Crosby (Stone Environmental Inc.) and James Laymon (ProbeDomain). Additional site support was provided by Tim Curtin and Bill Raspet (NAVFAC). Questions regarding this study should be directed to David Adamson (GSI Environmental Inc.; dtadamson@gsi-net.com)

A.9 REFERENCES

ASTM D7352, 2007. Standard Practice for Direct Push Technology for Volatile Contaminant Logging with the Membrane Interface Probe.

Bronders, J., I.V. Keer, K. Touchant, G. Vanerman, and D. Wilczek. 2009. Application of the membrane interface probe (MIP): An evaluation. *Journal of Soils and Sediments* 9, no. 1: 74–82.

Bumberger, J., D. Radney, A. Berndsen, T. Goblirsch, J. Flachowsky, and P. Dietrich. 2011. Carry-Over effects of the Membrane Interface Probe. *Ground Water*. 50, no. 4: 578-584..

Chapman, S.W., and B.L.Parker. 2004. Plume persistence due to aquitard back diffusion following dense nonaqueous phase liquid source removal or isolation. *Water Resources Research* 41: W12411.

Costanza, J., K.D. Pennell, J. Rossabi, B. Riha. 2002. Effect of temperature and pressure on the MIP sample collection process. *Remediation of Chlorinated and Recalcitrant Compounds - 2002*, Paper 1F-08.

Einarson, M.D., D.M. Mackay and P.J. Bennett. 2010. Sampling Transects for Affordable, High-Resolution Plume Characterization and Monitoring. *Ground Water* 48, no. 6: 805-808.

Guilbeault, M., B.L. Parker, and J.A. Cherry. 2005. Mass and flux distributions from DNAPL zones in sandy aquifers. *Ground Water* 43, no. 1: 70–86.

Gee, J.R.. 2010. Improving the accuracy and usefulness of the MIP using carbon-traps. *Remediation of Chlorinated and Recalcitrant Compounds - 2010*, Paper xxx.

Geoprobe, 2006. Geoprobe Membrane Interface Probe (MIP) Standard Operating Procedure. Technical Bulletin No. MK3010. Revised November 2006.

Harrington, G.A., and M.J. Henry. 2006. Using direct-push EC logging to delineate heterogeneity in a clay-rich aquitard. *Ground Water Monitoring & Remediation* 26, no. 1: 92-100.

Köber, R., G. Hornbruch, C. Leven, L. Tischer, J. Großmann, P. Dietrich, H. Weiß, and A. Dahmke. 2009. Evaluation of combined direct-push methods used for aquifer model generation. *Ground Water* 47, no. 4: 536-546.

Majer. V., J. Sedlbauer, and G. Bergin. 2008. Henry's law constant and related coefficients for aqueous hydrocarbons, CO2, and H2S over a wide range of temperature and pressure. *Fluid Phase Equilibria* 272, no. 1-2: 65-74.

McAndrews, B., K. Heinze, W. Diguiseppi. 2003. Defining TCE plume source areas using the membrane interface probe (MIP). *Soil and Sediment Contamination* 12, no. 6:799–813.

Mercer, J.W., R.M. Cohen, and M.R. Noel. 2010. DNAPL site characterization issues at chlorinated solvent sites. In Situ Remediation of Chlorinated Solvent Plumes, SERDP/ESTCP Environmental Remediation Technology 217-280, DOI: 10.1007/978-1-4419-1401-9_8.

Myers, K.F., J. Costanza, and W.M. Davis. 2002. Tri-service site characterization and analysis penetrometer system (SCAPS) validation of the membrane interface probe. Prepared for ESTCP and US Army Corps of Engineers Engineer Research and Development Center, Environmental Laboratory. Final Report, ERDC/EL TR-02-16.

Newell, C.J., S.K. Farhat, D.T. Adamson, and B.B. Looney. 2011. Contaminant plume classification system based on mass discharge. *Ground Water* 49, no. 6: 914-919.

Parker, B.L., J.A. Cherry, and B.J. Swanson. 2006. A multi-level system for high-resolution monitoring in rotosonic boreholes. *Ground Water Monitoring & Remediation* 26, no. 4: 57-73.

Parker, B.L., S.W. Chapman, and M.A. Guilbeault. 2008. Plume persistence caused by back diffusion from thin clay layers in a sand aquifer following TCE source-zone hydraulic isolation. *Journal of Contaminant Hydrology* 102, 86–104.

Pitkin, S.E., J.A. Cherry, R.A. Ingleton, and M. Broholm. 1999. Field demonstrations using the Waterloo Ground water Profiler. *Ground Water Monitoring and Remediation* 19, no. 2: 122–131.

Ravella, M., R.J. Fiacco, Jr., J. Frazier, D. Wanty, and L. Burkhardt. 2007. Application of the membrane interface probe (MIP) to delineate subsurface DNAPL contamination. *Environmental Engineer: Applied Research and Practice* 1, Winter 2007.

Sale, T.C., J.A. Zimbron, and D.S. Dandy. 2008. Effects of reduced contaminant loading on downgradient water quality in an idealized two-layer granular porous media. *Journal of Contaminant Hydrology* 102, no. 1-2: 72-85.

Sale, T., and C.J. Newell. 2010. Impacts of source management on chlorinated solvent plumes. In Situ Remediation of Chlorinated Solvent Plumes, SERDP/ESTCP Environmental Remediation Technology 185-216, DOI: 10.1007/978-1-4419-1401-9_7.

Schulmeister, M.K., J.J. Butler Jr., J.M. Healey, L. Zheng, D.A. Wysocki, and G.W. McCall. 2003. Direct-push electrical conductivity logging for high-resolution hydrostratigraphic characterization. *Ground Water Monitoring & Remediation* 23, no. 3: 52–62.

Seyedabbasi, M.A., C.J. Newell, D.T. Adamson, and T.C. Sale. 2012. Relative contribution of DNAPL dissolution and matrix diffusion to the long-term persistence of chlorinated solvent source zones. *Journal of Contaminant Hydrology* 134-135, no 1-2: 69-81.

Wilson, J.T., R.R. Ross, and S. Acree. 2005. Using direct-push tools to map hydrostratigraphy and predict MTBE plume diving. *Ground Water Monitoring & Remediation* 25, no. 3: 93-102.

Table 4. Matrix for MIP Operating Conditions and Rationale

High Concentration Area		
Run ID	**Operating Conditions**	**Rationale**
PEEK - Baseline	MIP Flow = 40 ml/min. Drive rate = 1 foot/min. Probe temperature set to 120 degrees C	
Heated Trunkline (HTL)	MIP Flow = 40 ml/min. Drive rate = 1 foot/min. Probe temperature set to 120 degrees C	HTL system deployed to determine if the heated and non-sorbing stainless steel carrier gas line would allow the MIP to be more effective at mapping the contaminant distribution and relative concentrations than that of the PEEK system.
HTL Up-Log. Probe pulled from bottom of hole to the top.	MIP Flow = 40 ml/min. Drive rate = 1 foot/min. Probe temperature set to 120 degrees C.	By conducting the MIP in reverse, from the bottom up, the true bottom of the contamination could be determined. MIP detector signals should be at or near basline conditions prior to starting uplogging procedure.
Fast Drive Rate	MIP Flow = 40 ml/min. **Drive rate = 2 foot/min.** Probe temperature set to 120 degrees C	By increasing drive rate through potentially heavily contaminated zones, there would be less time available for the system to become overloaded with contamination.
High Flow Rate	**MIP Flow = 80 ml/min.** Drive rate = 1 foot/min. Probe temperature set to 120 degrees C	By increasing the flow rate, via an increase in delivery pressure, it was hypothesized that 1) there would be less of a pressure gradient for driving contaminants into the tool and 2) the contaminants that did enter the tool would be more diluted than normal due to the higher volumetric flow rate.
Low Temperature	MIP Flow = 80 ml/min. Drive rate = 1 foot/min. **Probe temperature set to 100 degrees C**	By decreasing probe temperature, the amount of VOC volatilization would decrease and the zone of influence would also likely decrease. These two factors would likely result in less contaminant mass entering the gas phase and being available for migration across the membrane.
Low Concentration Area		
Run ID	**Operating Conditions**	**Rationale**
PEEK - Baseline	MIP Flow = 40 ml/min. Drive rate = 1 foot/min. Probe temperature set to 120 degrees C	
HTL	MIP Flow = 40 ml/min. Drive rate = 1 foot/min. Probe temperature set to 120 degrees C	HTL system deployed to determine if the heated and non-sorbing stainless steel carrier gas line would allow the MIP to be more effective at mapping the contaminant distribution and relative concentrations than that of the PEEK system.
HTL Up-Log. Probe pulled from bottom of hole to the top.	MIP Flow = 40 ml/min. Drive rate = 1 foot/min. Probe temperature set to 120 degrees C.	By conducting the MIP in reverse, from the bottom up, the true bottom of the contamination could be determined. MIP detector signals should be at or near basline conditions prior to starting uplogging procedure.
Slow Drive Rate	MIP Flow = 40 ml/min. **Drive rate = 0.5 foot/min.** Probe temperature set to 120 degrees C.	By decreasing the drive rate through the lesser contaminated zones, there would be more time available for the volatilization and hence more gas phase contamination available for migration into the tool.
Low Flow Rate	**MIP Flow = 20 ml/min.** Drive rate = 0.5 foot/min. Probe temperature set to 120 degrees C.	By decreasing the flow rate, via an decrease in delivery pressure, it was hypothesized that 1) there would be more of a pressure gradient for driving contaminants into the tool and 2) the contaminants that did enter the tool would be less diluted than normal due to the lower volumetric flow rate.
High Temperature	MIP Flow = 20 ml/min. Drive rate = 1 foot/min. **Probe temperature set to 140 degrees C.**	By increasing probe temperature, the amount of VOC volatilization would increase and the zone of influence would also likely increase. These two factors would likely result in more contaminant mass entering the gas phase and being available for migration across the membrane.

Table 8. Matrix for Evaluating MIP Operating Conditions Against Baseline MIP Characterization

Ranking Against MIP Baseline Run: 1 = Worse, 2 = Same; 3 = Better

	Degree of Carryover from Bottom of Contaminated Zone	
	ECD	PID
HIGH Concentration Location		
HTL - Baseline	NA	NA
PEEK	**3**	2
HTL Up-Log - Conducted after HTL Run	**3**	2
Fast Drive Rate	**3**	2
High Flow Rate	**3**	**3**
Low Temperature	2	1
Optimized SOP	***3***	***3***
	Degree of Sensitivity at Top of Contaminated Zone	
	ECD	PID
LOW Concentration Location		
HTL - Baseline	NA	NA
PEEK	1	2
HTL Up-Log - Conducted After HTL Run	**3**	1
Slow Drive Rate	2	2
Low Flow Rate	2	1
High Temperature	1	2
Optimized SOP	***3***	***3***

Notes: (1) HTL: heated trunk line; (2) PEEK: polyether ketone trunk line; (3) Uplog: MIP log with probe moving upward;: (3) Drive rate refers to rate of advancement of probe; (4) Flow rate refers to carrier gas flow rate; (5) Temperature refers to probe temperature.

APPENDIX B

Table 9. Matrix for Evaluating MIP Operating Conditions Against Soil CVOC Data

Ranking Against Soil CVOC Data: 1 = Poor, 2 = Fair; 3 = Good

			ECD Dectector					PID Dectector				
Run ID	Rationale	Top of Contam-ination	Bottom of Contam-ination	Location of Max	Overall Shape	**Rank** Worst = 0 Best = 12	Top of Contam-ination	Bottom of Contam-ination	Location of Max	Overall Shape	**Rank** Worst = 0 Best = 12
HIGH Concentration Location: OU3-3											
Heated Trunk Line (HTL) - Baseline	Use of heated inert material increases transport rate and minimize signal tailing (carry-over)	2	1	**3**	1	7	2	**3**	2	**3**	**10**
PEEK - unheated	Conventional trunk line material used extensively in early MIP systems	1	**3**	**3**	2	**9**	1	2	2	2	7
HTL Up-Log - Conducted after HTL Run	Collect data while retracting from hole to avoid carry-over and better identify base of contamination	1	**3**	**3**	1	8	2	2	1	1	6
Fast Drive Rate - 0.6 m/min	Reduces mass entering system to potentially minimize detector overload	2	1	**3**	1	7	2	1	**3**	3	9
High Flow Rate - 80 mL/min	Increases dilution to potentially minimize detector overload	1	2	**3**	**3**	**9**	1	**3**	**3**	**3**	**10**
Low Temperature - 100°C	Reduces volatilization rates to potentially minimize detector overload	1	1	2	1	5	1	2	3	2	8
Optimized SOP		***2***	***2***	***3***	***3***	***10***	***3***	***3***	***3***	***3***	***12***
LOW Concentration Location: OU3-6											
Heated Trunk Line (HTL) - Baseline	Use of heated inert material increases transport rate and improve signal resolution	1	1	1	1	4	1	1	**3**	2	7
PEEK - unheated	Conventional trunk line material used extensively in early MIP systems	1	1	1	1	4	1	1	2	2	6
HTL Up-Log -Conducted After HTL Run	Collect data while retracting from hole to avoid carry-over and better identify base of contamination	1	2	2	2	7	**3**	1	**3**	3	**10**
Slow Drive Rate - 1.2 m/min	Increases mass entering system to potentially improve sensitivity at top of contaminated interval	1	1	1	1	4	**3**	2	**3**	1	9
Low Flow Rate - 20 L/min	Decreases dilution to potentially improve sensitivity at top of contaminated interval	1	1	1	1	4	1	1	2	2	6
High Temperature - 140°C	Increases desorption and volatilization rates to improve potentially sensitivity at top of contaminated interval	1	1	1	1	4	2	2	**3**	2	9
Optimized SOP		***3***	***2***	***3***	***3***	***11***	***3***	***3***	***3***	***3***	***12***

Notes: (1) HTL: heated trunk line; (2) PEEK: polyether ketone trunk line; (3) Uplog: MIP log with probe moving upward;: (3) Drive rate refers to rate of advancement of probe; (4) Flow rate refers to carrier gas flow rate; (5) Temperature refers to probe temperature: (6) Top and Bottom of Contamination: ranked ability to detect extent of contamination in low permeability zone; (7) Location of Max: comparison of vertical location of maximum concentration (soil vs. MIP data); (8) Overall Shape: qualitative comparison of shape of MIP profile with soil concentration profile (vs. depth); (9) Overall Rank: sum of four categories (columns) across a row.

Table 10. Evaluation of Accuracy of MIP Data Relative to Soil CVOC Concentrations: Impact of Soil Type on Median Relative Percent Difference

Dataset	Relative Percent Difference (%) - Median (Non-Directional)			
	ECD		PID	
	All Soil Types	Low Permeability Soils Only	All Soil Types	Low Permeability Soils Only
High Concentration Location (OU3-3)				
All MIP Runs (All Operating Conditions)	56	43	53	41
Low Concentration Location (OU3-6)				
All MIP Runs (All Operating Conditions)	121	41	128	72

Notes: (1) Comparisons with PID data were made with soil concentrations that included cis-1,2-DCE, TCE, and PCE; (2) Comparisons with ECD data were made with soil concentrations that included TCE and PCE because the ECD is not response to cis-1,2-DCE.

Table 11. Evaluation of Accuracy of MIP Data Relative to Soil CVOC Concentrations: Impact of Data Corrections on Linear Regression

Dataset	Data Correction Applied	R^2 for Regression			
		ECD		PID	
		All Soil Types	Low Permeability Soils Only	All Soil Types	Low Permeability Soils Only
High Concentration Location (OU3-3)					
All MIP Runs	None	0.09	0.004	0.23	0.25
	Corrected with Uplogged Data	0.21	0.002	0.26	0.25
Low Concentration Location (OU3-6)					
All MIP Runs	None	0.13	0.001	0.09	0.03
	Corrected with Uplogged Data	0.20	0.09	0.12	0.16

Table 13. Summary of MIP Performance During Operating Condition Testing – High Concentration Location

MIP Operation	Semi-Quantitative Ranking	Correlations Using Linear Regression	Relative Percent Difference	Summary
Heated Trunk Line	Not Applicable (Baseline)			Better agreement between PID and soil CVOC data than with ECD due to carry-over
PEEK Trunk Line	ECD ↑	ECD ↑	ECD ↓	Benefit primarily attributable to burn off completed at this location
	PID ↓	PID ↓	PID ↓	
Uplogging	ECD ↑	ECD ↓	ECD ↓	Minimized carry-over effects in deeper intervals but carry-over was observed at shallower intervals
	PID ↓	PID ↓	PID ↓	
Heater Block Temperature	ECD ↓	ECD ↑	ECD ↓	No consistent improvement in data quality
	PID ↓	PID ↓	PID ↓	
Drive Rate	ECD ↑	ECD ↓	ECD ↓	No consistent improvement in data quality
	PID ↓	PID ↓	PID ↓	
Flow Rate	ECD ↑	ECD ↓	ECD ↓	Improved data quality only for ECD
	PID -	PID ↓	PID ↓	

Table 14. Summary of MIP Performance During Operating Condition Testing – Low Concentration Location

MIP Operation	Semi-Quantitative Ranking	Correlations Using Linear Regression	Relative Percent Difference	Summary
Heated Trunk Line	Not Applicable (Baseline)			Little agreement between soil CVOC data and data obtained with both detectors
PEEK Trunk Line	ECD -	ECD ↑	ECD ↓	No consistent improvement in data quality
	PID ↓	PID ↑	PID ↓	
Uplogging	ECD ↑	ECD ↑	ECD ↓	Minimized carry-over effects in deeper intervals but carry-over was observed at shallower intervals
	PID ↑	PID ↑	PID ↓	
Heater Block Temperature	ECD -	ECD ↑	ECD -	Slightly overall improvement in data quality (primarily PID)
	PID ↑	PID ↑	PID ↓	
Drive Rate	ECD -	ECD -	ECD ↓	No consistent improvement in data quality
	PID ↑	PID ↑	PID ↓	
Flow Rate	ECD -	ECD ↓	ECD ↑	No consistent improvement in data quality
	PID ↓	PID ↑	PID ↓	

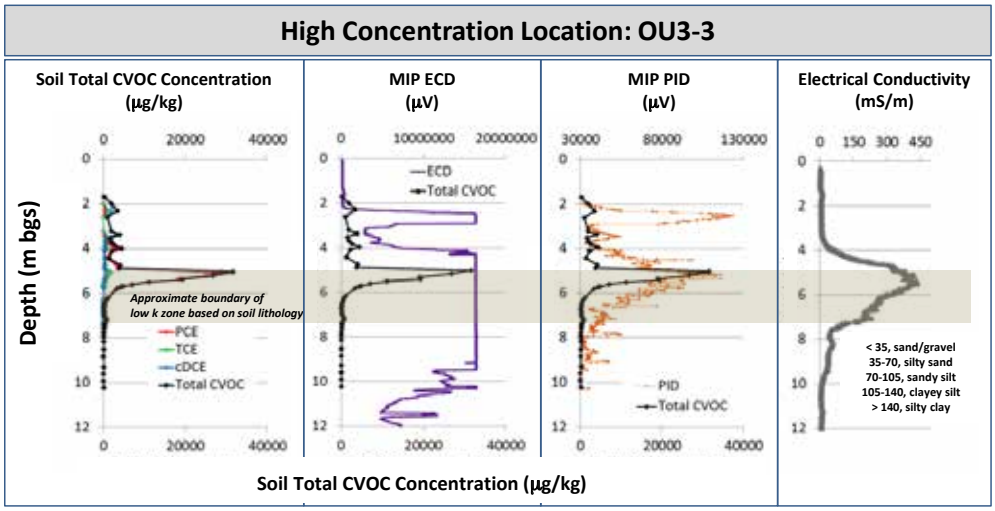

(A)

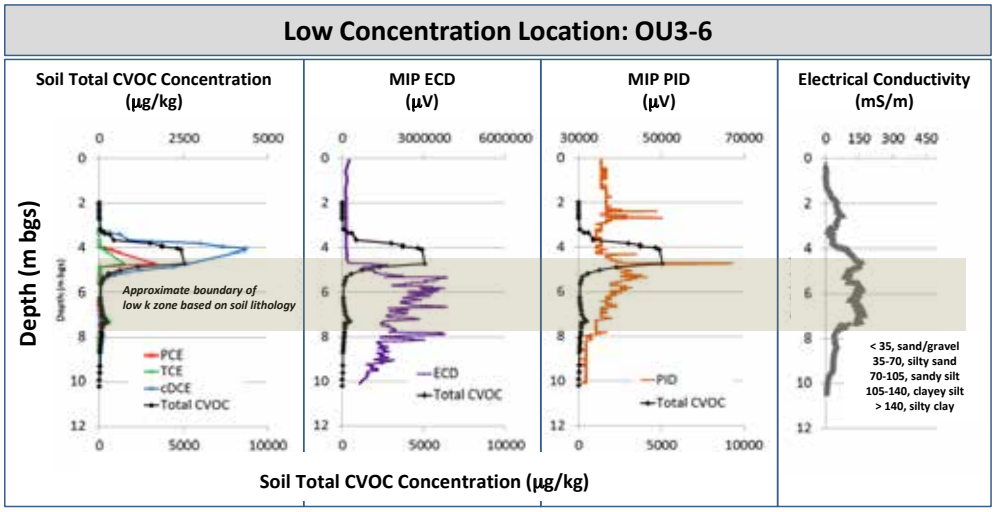

(B)

Figure 4. Baseline MIP Characterization Data vs. Soil CVOC Concentration Data at (A) Location OU3-3 (near source location); and (B) Location OU3-6 (downgradient location). Panels from left to right show CVOC Concentration Data (including by-products), ECD Data, PID Data, Electrical Conductivity Data, and Soil Lithology.

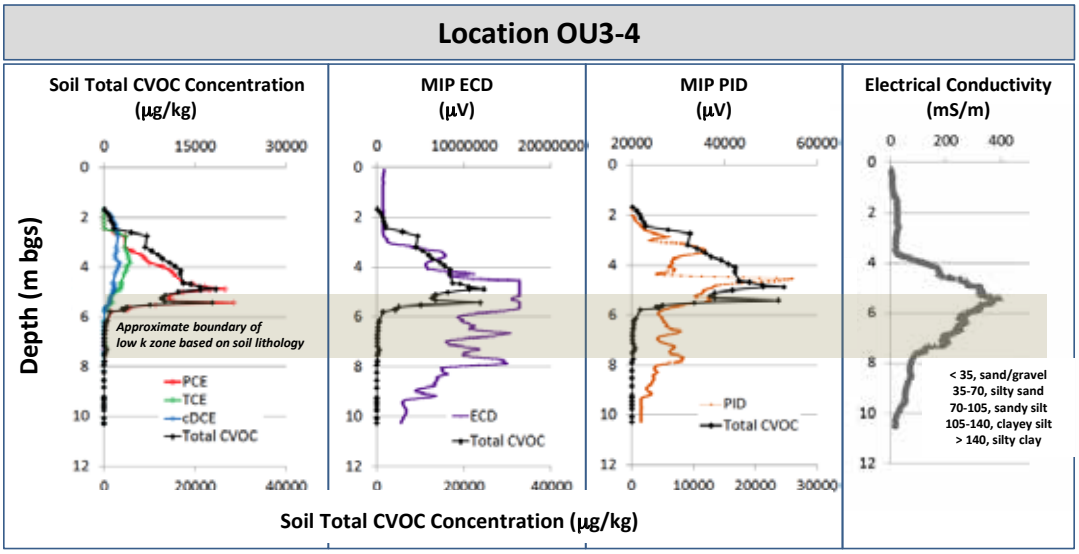

(C)

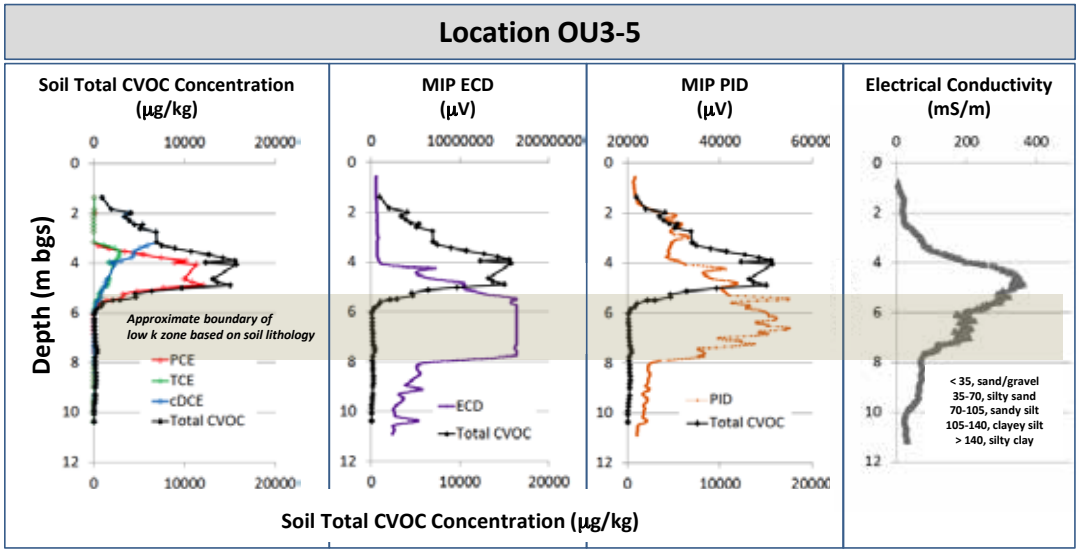

(D)

Figure 4. Baseline MIP Characterization Data vs. Soil CVOC Concentration Data at (C) Location OU3-4; and (B) Location OU3-5. Panels from left to right show CVOC Concentration Data (including by-products), ECD Data, PID Data, Electrical Conductivity Data, and Soil Lithology.

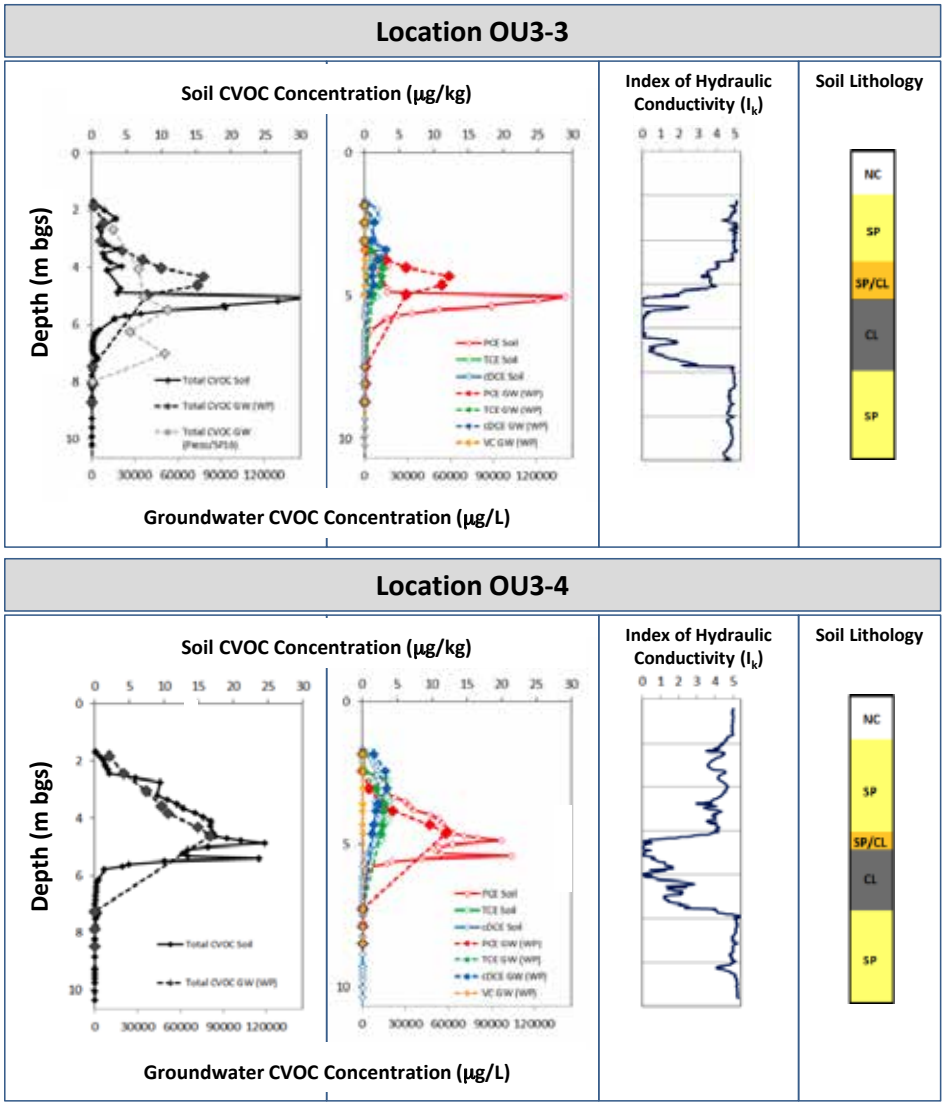

Figure 5. (Groundwater and Soil Data Collected at (A) Location OU3-3; and (B) Location OU3-4. First panel shows total CVOC concentration data collected using Geoprobe SP16 and Temporary Piezometers vs. Waterloo ^{APS} (WP) vs. Soil cores. Second panel shows soil and groundwater (WP) concentration data for individual CVOCs. Third panel shows index of hydraulic conductivity data collected in real-time by Waterloo ^{APS}. Fourth panel shows soil lithography based on United Soil Classification System (SP = sand (poorly graded); CL = clay (inorganic with low plasticity; SP/CL = sand/clay mix, SC = clayey sands; NC = not collected). Other groundwater analyses (field and geochemical parameters) collected but not shown. Geoprobe SP16/temporary piezometers not used to collect groundwater at location OU3-4.

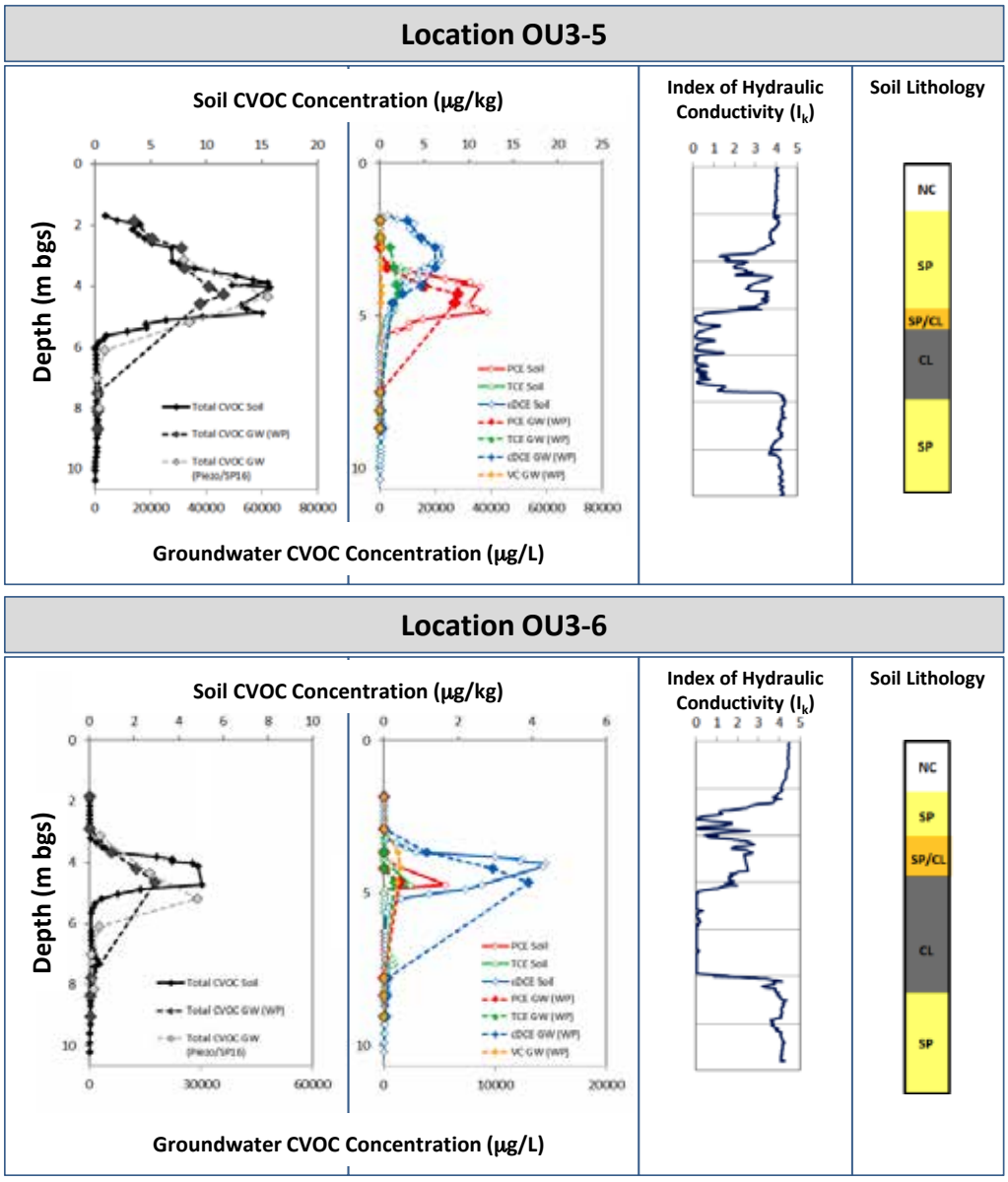

Figure 5. Groundwater and Soil Data Collected at (A) Location OU3-3; and (B) Location OU3-4. First panel shows total CVOC concentration data collected using Geoprobe SP16 and Temporary Piezometers vs. Waterloo ^{APS} (WP) vs. Soil cores. Second panel shows soil and groundwater (WP) concentration data for individual CVOCs. Third panel shows index of hydraulic conductivity data collected in real-time by Waterloo ^{APS}. Fourth panel shows soil lithography based on United Soil Classification System (SP = sand (poorly graded); CL = clay (inorganic with low plasticity; SP/CL = sand/clay mix, SC = clayey sands; NC = not collected). Other groundwater analyses (field and geochemical parameters) collected but not shown.

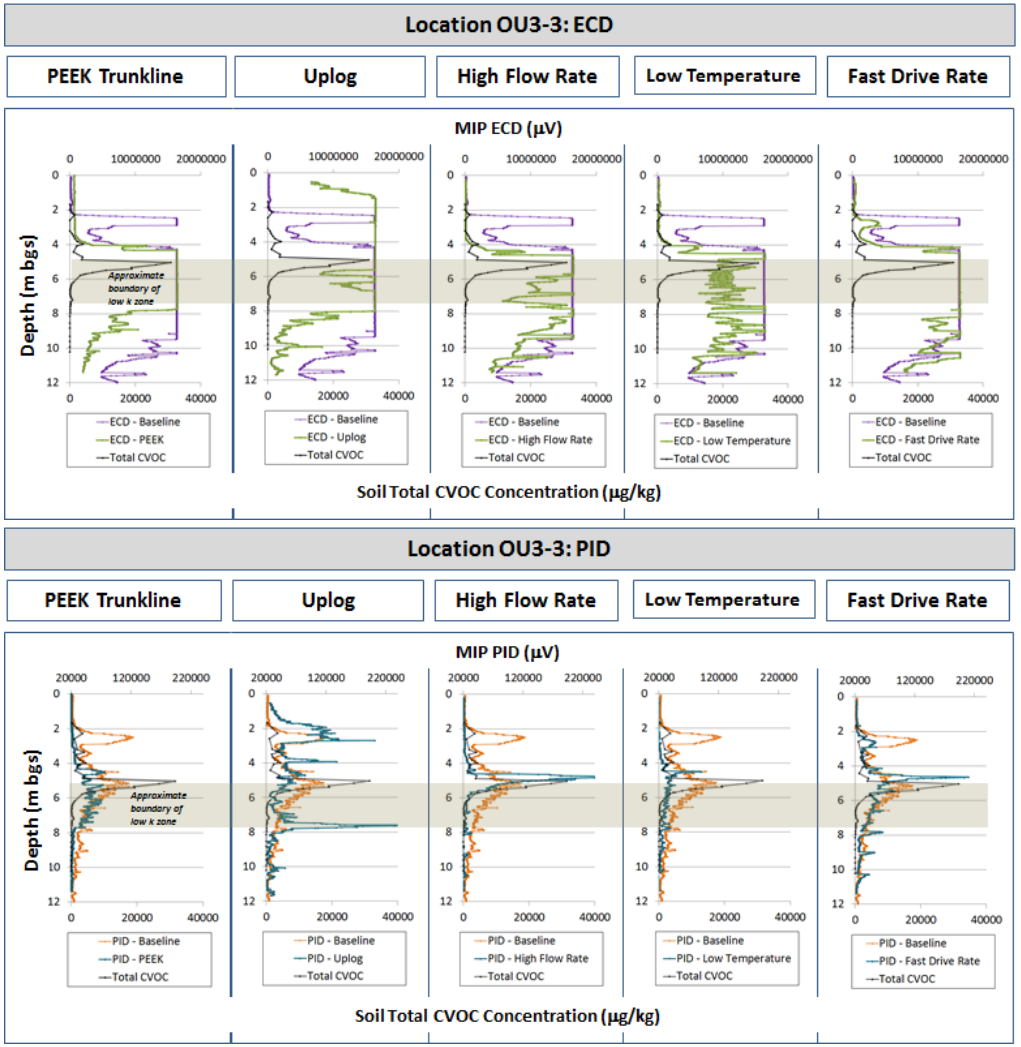

Figure 7. MIP Characterization Data for All Runs vs. Soil CVOC Concentration Data (linear scale) at Location OU3-3. (A) ECD Data; and (B) PID data. PID data are compared to sum of PCE, TCE, and cis-1,2-DCE soil concentrations. ECD data are compared to sum of PCE and TCE soil concentrations.

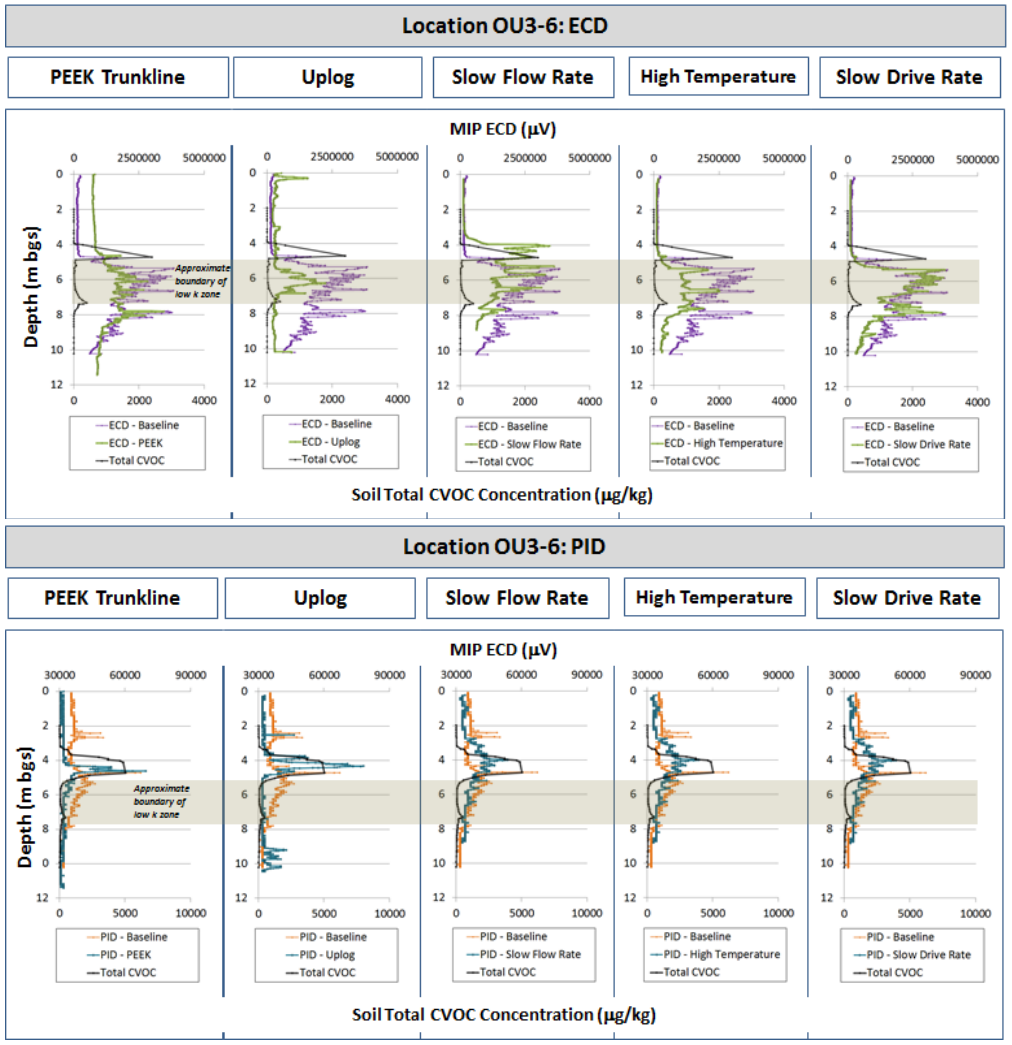

Figure 8. MIP Characterization Data for All Runs vs. Soil CVOC Concentration Data (linear scale) at Location OU3-6. (A) ECD Data; and (B) PID data. PID data are compared to sum of PCE, TCE, and cis-1,2-DCE soil concentrations. ECD data are compared to sum of PCE and TCE soil concentrations.

(A) Location OU3-3

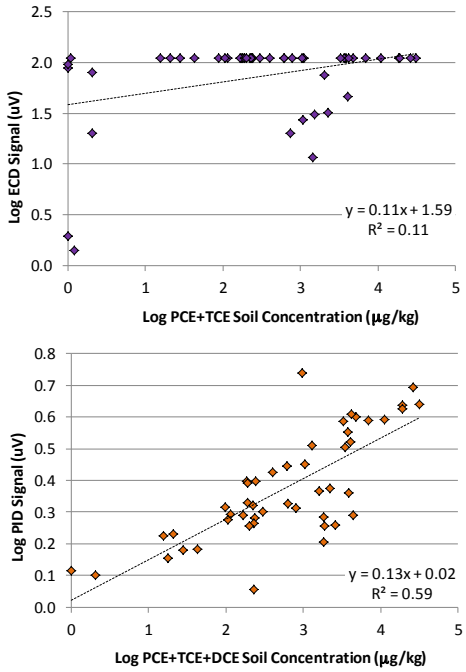

(B) Location OU3-6

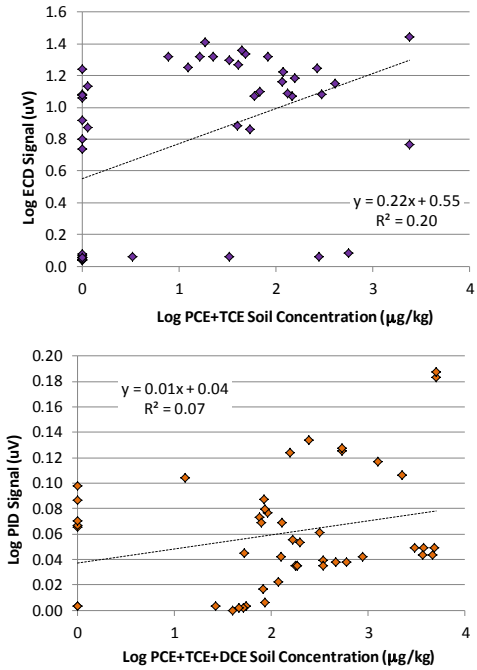

Figure 9. Linear Regression of Baseline MIP Characterization Data and Soil CVOC Concentration Data at (A) Location OU3-3; and (B) Location OU3-6. PID data are compared to sum of PCE, TCE, and cis-1,2-DCE soil concentrations. ECD data are compared to sum of PCE and TCE soil concentrations.

(A) Location OU3-3

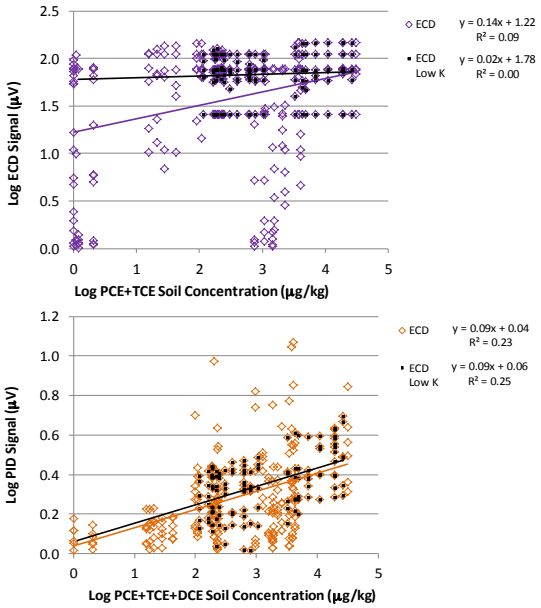

(B) Location OU3-6

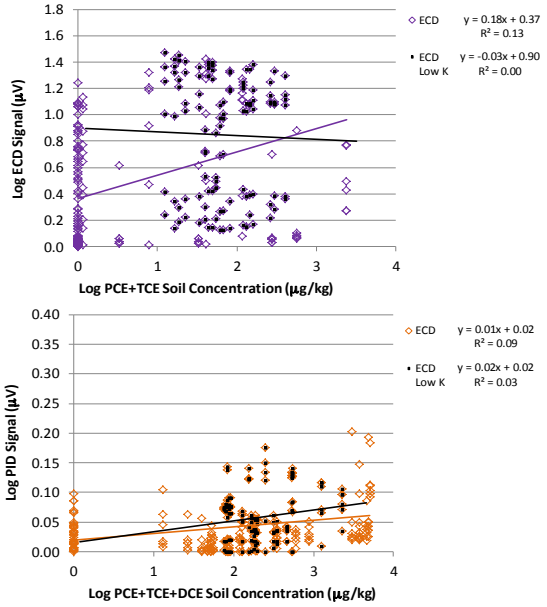

Figure 10. Linear Regression of All MIP Characterization Data and Soil CVOC Concentration Data at (A) Location OU3-3; and (B) Location OU3-6. Data from low permeability zones are highlighted to demonstrate impact of soil type on data quality. PID data are compared to sum of PCE, TCE, and cis-1,2-DCE soil concentrations. ECD data are compared to sum of PCE and TCE soil concentrations.

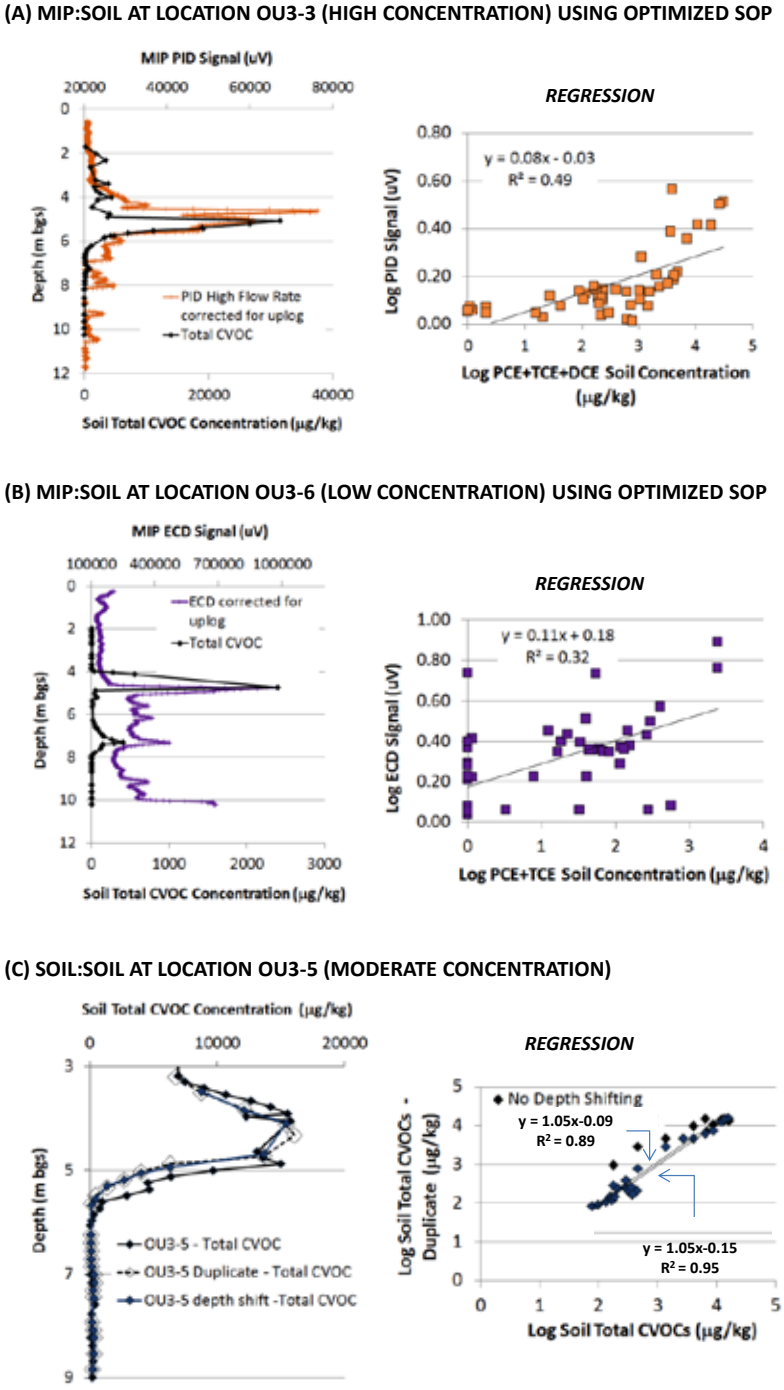

Figure 11. MIP Characterization Data Collected According to Optimized Standard Operating Protocol and Comparisons with Soil Data. (A) Location OU3-3 with PID Data Collected Using High Flow Rate and Uplogging-Corrected vs. Soil Total CVOC Concentration (PCE, TCE, and cis-1,2-DCE); (B) Location OU3-6 with ECD Data Uplogging-Corrected vs. Soil Total CVOC Concentration (PCE and TCE); (C) Comparison of Soil CVOC Concentrations Collected from Duplicate Boreholes at Location OU3-5.

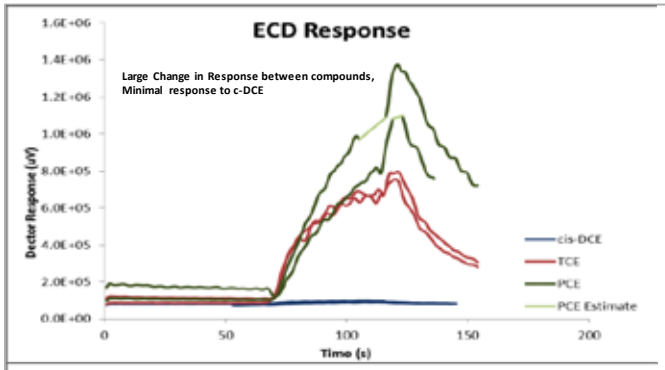

Response Test Summary Results

Compound	Response/as Rise in Baseline	
	PID	ECD
c-DCE	19	22
TCE	23	690
PCE	16	1300

Notes:
1. Response Test solutions comprised of 1 mg/L of study compound.

Figure 12. Sensitivity of MIP Detectors for CVOCs Present at NAS Jacksonville OU3.

APPENDIX C

SUPPORTING INFORMATION FOR SECTION 4: TRANSPORT IN HETEROGENEOUS MEDIA

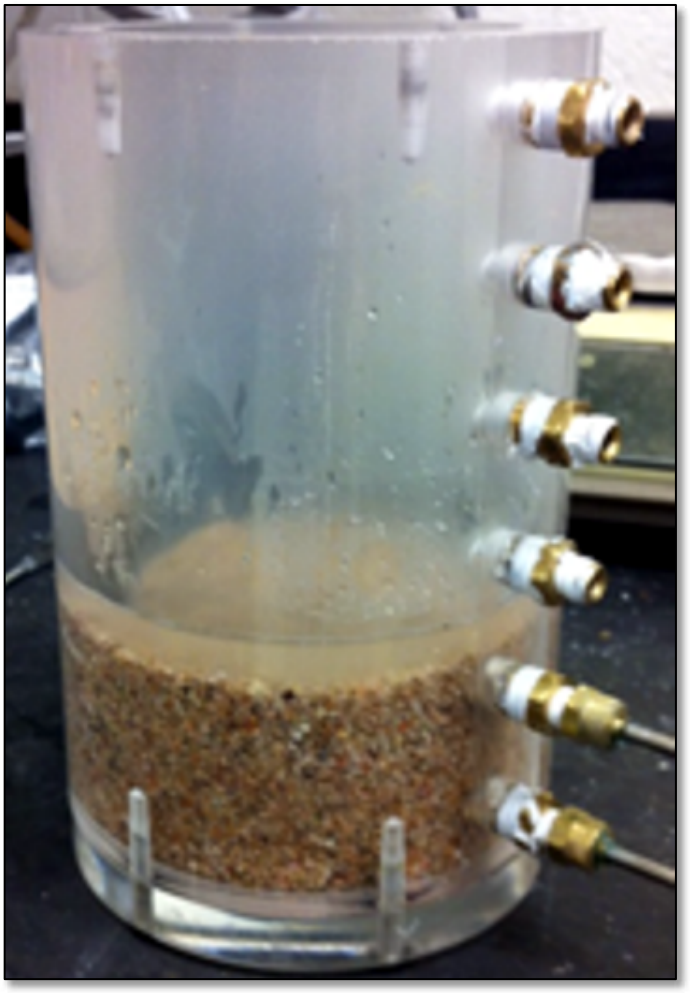

C.1: DERIVATION OF PRELIMINARY FINITE DIFFERENCE MODEL

Start with Fick's Second Law, allowing for the effective diffusion coefficient to vary in space,

$$\frac{\partial C}{\partial t} = \frac{\partial}{\partial x}\left(D^* \frac{\partial C}{\partial x}\right) \tag{1}$$

Converting to finite difference form,

$$\frac{C_{x,t} - C_{x,t-1}}{\Delta t} = D^{*\prime}_{x+1} \frac{C_{x+1,t} - C_{x,t}}{\Delta x^2} - D^{*\prime}_{x-1} \frac{C_{x,t} - C_{x-1,t}}{\Delta x^2} \tag{2}$$

Breaking out the terms,

$$\frac{C_{x,t}}{\Delta t} = \frac{C_{x,t-1}}{\Delta t} + D^{*\prime}_{x+1} \frac{C_{x+1,t}}{\Delta x^2} - D^{*\prime}_{x+1} \frac{C_{x,t}}{\Delta x^2} - D^{*\prime}_{x-1} \frac{C_{x,t}}{\Delta x^2} + D^{*\prime}_{x-1} \frac{C_{x-1,t}}{\Delta x^2} + \tag{3}$$

where the diffusion coefficients $D^{*'}_{x+i}$ refer to harmonic means of D^{*}_{x} and D^{*}_{x+i}. It is readily shown that eq. 3 can be solved for $C_{x,t}$ to yield the following equation,

$$C_{x,t} = \frac{\Delta t\left(D^{*\prime}_{x-1} C_{x-1,t} + D^{*\prime}_{x+1} C_{x+1,t}\right) + \Delta x^2 C_{x-1,t}}{\Delta x^2 + \Delta t(D^{*\prime}_{x-1} + D^{*\prime}_{x+1})} \tag{4}$$

Eq. 4 was solved in an Excel spreadsheet with the following boundary conditions:

$$\begin{gathered} at\ t = 0, C = 0\ outside\ the\ lens \\ at\ t = 0, C = 10\ inside\ the\ lens \\ for\ all\ t, C = 0\ at\ x = 0\ cm \\ for\ all\ t, C = 0\ at\ x = 27.5\ cm \end{gathered} \tag{5}$$

Fluxes across the lens boundaries were estimated from a finite difference approximation of Fick's First Law

$$J = -D^* \frac{\partial C}{\partial x} \tag{6}$$

Eq. 6 leads to the finite difference form for total flux across the upper and lower lens boundaries

$$J = -\frac{D^{*\prime}_{x-1}}{\Delta x}(C_{x-1} - C_x) - \frac{D^{*\prime}_{x+1}}{\Delta x}(C_{x+1} - C_x) \tag{7}$$

where C_x refers to the concentration immediately inside the lens boundary, and C_{x+i} refers to concentrations immediately outside the lens boundary.

C.2: CONVERSION OF DATALOGGER RELATIVE RESISTANCES TO RELATIVE CONDUCTIVITIES

Data recorded by the Campbell Scientific CR1000 are in units of millivolts (mV), proportional to the electrical resistance of the solution. As a salt tracer encounters a probe, the resistance is diminished and the recorded mV values decline (Figure C2-1).

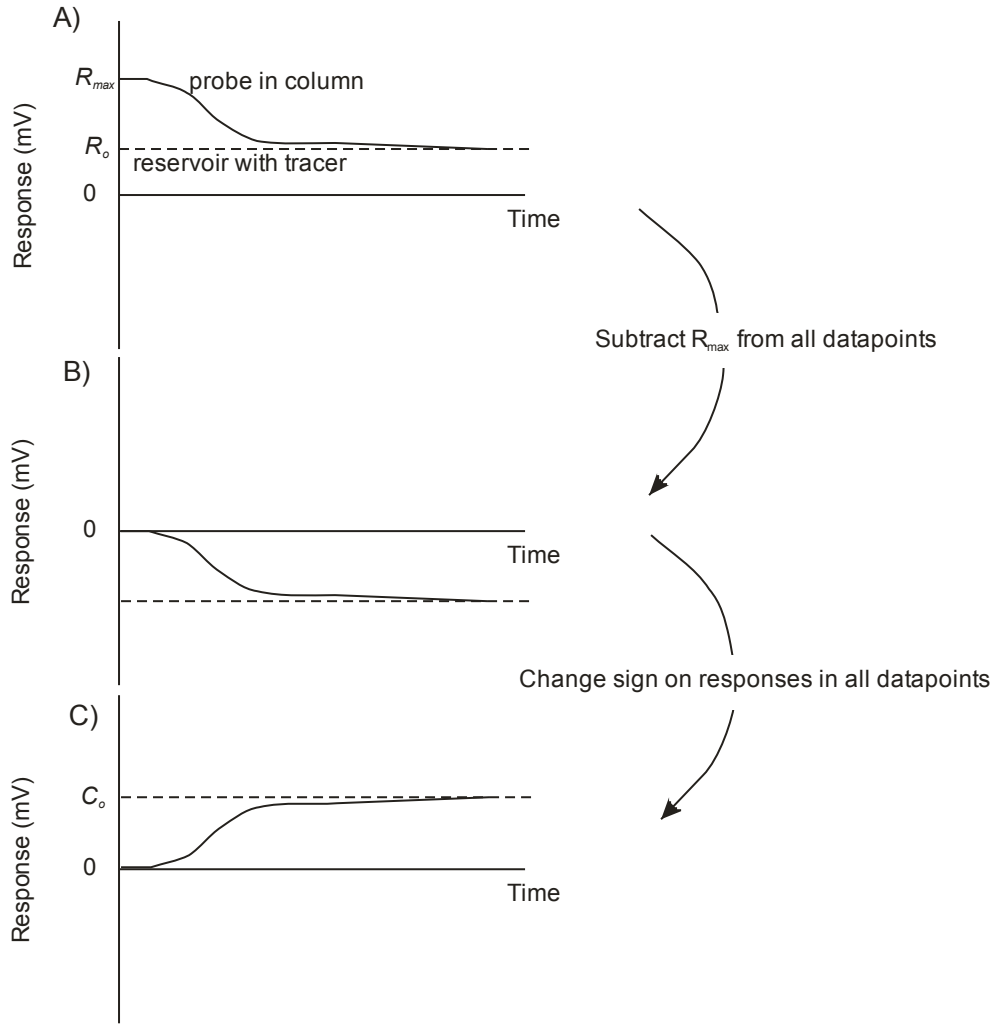

Figure C2-1: Schematic illustrating the corrections made to the datalogger data to express diffusion curves as conductances. Also shown is the conversion of the measured reservoir resistance, R_o, in mV to C_o for modeling purposes.

These resistance values can be converted to conductances through a 2-step process: 1) a background subtraction:

$$R_1 = R - R_{max} \quad (1)$$

Where R is a probe response either in the column or in the reservoir R_1 is a corrected probe response after the background subtraction, and R_{max} is the initial resistance of the

column probe not yet in contact with the saline tracer. After step 1, the initial response at the column probe should be zero, and all other responses should be negative. 2) a sign change on the responses to express them as positive values.

$$R_2 = -R_1 \quad (2)$$

From an examination of Figure 1, it can be seen that following these manipulations, the value of C_o needed to model diffusion at the probe in question is related to the initial reservoir resistance, R_o, through the relationship:

$$C_o = R_{max} - R_o \quad (3)$$

B.2.1: Justification of the Resistance to Conductance Conversion

The probes used in the DEC were calibrated to evaluate their relative responses and the linearity of their responses to salt concentration (Figure C2-2). The test showed that 6 probes responded nearly identically over the NaCl concentration range 0.0625 g/L to 1.0 g/L.

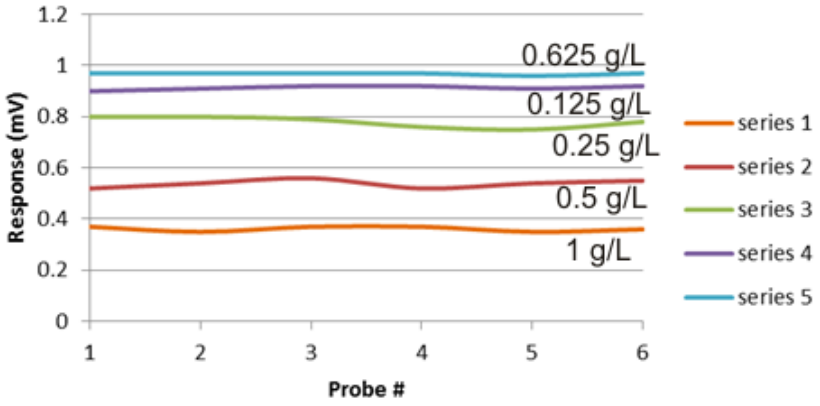

Figure C2-2: Responses of 6 probes to 5 solutions of NaCl.

A calibration curve was plotted to evaluate the linearity of the response. Responses taken directly from the data logger ranged from approximately 0.5 mV to 1 mV corresponding to the concentration range 0.0625 g/L to 0.5 g/L. This range was greater than that observed in the diffusion experiments, and exhibited a linear response with concentration (Figure C2-3A). These values were converted to conductances by subtraction from 1.0387 mV, which represented the resistance of deionized water (c_{NaCl} = 0 g/L). The conductances plotted similarly linearly (Figure C2-3B).

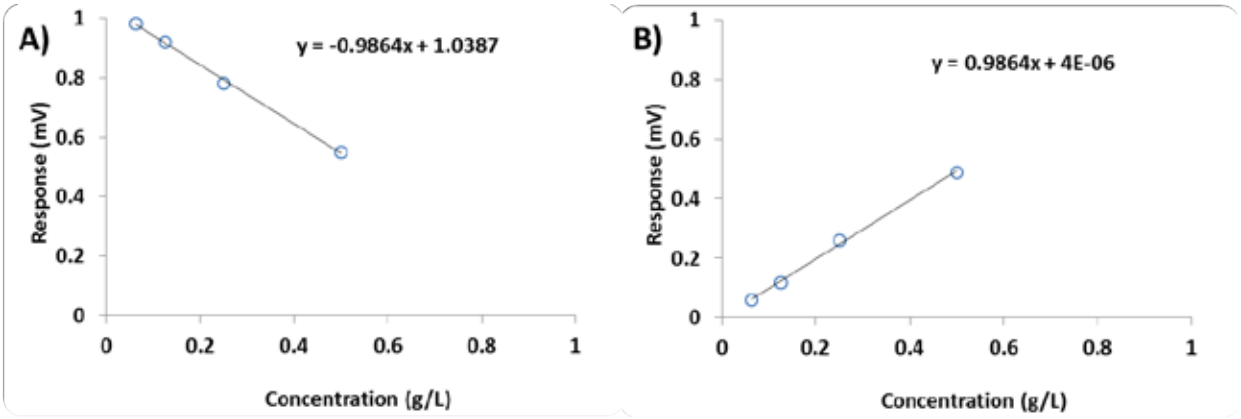

Figure C2-3: Calibration curves over the range of 0.5 g/L NaCl to 0.0625 g/L. A) in the form of resistance, B) in the form of conductance.

The linearity of these responses made it possible to perform the diffusion curve fitting directly on the conductance data rather than converting to concentration. The rationale for this is given below. A linear response-concentration curve has the form:

$$c = mR + B \tag{4}$$

where *c* is concentration, *m* is the slope of the response line, and *B* the intercept. Substituting into eq (1), and given that c_1 is the converted concentration (from a resistance-based response curve to a conductance-based curve):

$$R_1 = R - R_{max} \tag{5}$$

$$\frac{(c_1 - B)}{m} = \frac{(c - B)}{m} - \frac{(c_{max} - B)}{m}$$

$$c_1 = \frac{m(c - B)}{m} - m\frac{(c_{max} - B)}{m} + B$$

$$c_1 = c - c_{max} + B$$

For the case where $B << c_1$, which applies here, the conversions are seen to be equivalent.

C.3: MODFLOW ASSESSMENT OF THE EFFECT OF STIRRING ON FLOW IN A DEC

Experiments were performed with the DEC oriented vertically to prevent density-driven flow of the tracer solution into the column. When these experiments resulted in tracer invasion at a rate an order of magnitude greater than that expected from diffusion, it was hypothesized that the stirring of the source reservoir was causing advective flow in the column (Figure C3-1):

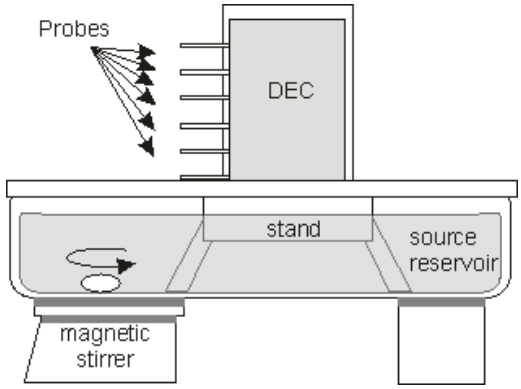

Figure C3-4: Schematic of the DEC experimental setup. Stirring of the reservoir was expected to cause primarily horizontal circulation of the water in the reservoir.

In order to test the hypothesis that stirring of the reservoir could drive flow in the column, an idealized version of the DEC was simulated in 2 dimensions using MODFLOW. The simulation was performed with a 20 (x) by 14 (y) grid representing a 25 cm long column in a reservoir 35 cm long. A 1 cm head drop was imposed across the reservoir to invoke flow that would simulate the effects of stirring (Figure C3-2).

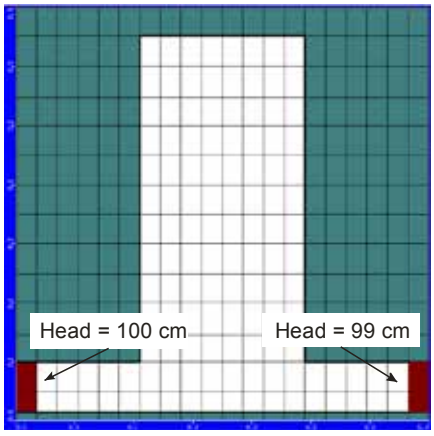

Figure C3-5: Grid and constant head boundaries to simulate a vertical column in a horizontal reservoir.

The hydraulic conductivity, *K*, of the porous medium in the column was set at 0.01 m/s, representative of well sorted coarse sands (Figure C3-3). The hydraulic conductivity of the reservoir was set 2 orders of magnitude higher to reflect the relatively high hydraulic

conductivity of the open water in the reservoir. Higher values of *K* did not change the outcome of the simulation meaningfully, but ran the risk of creating numerical problems associated with too sharp a *K* change across the interface.

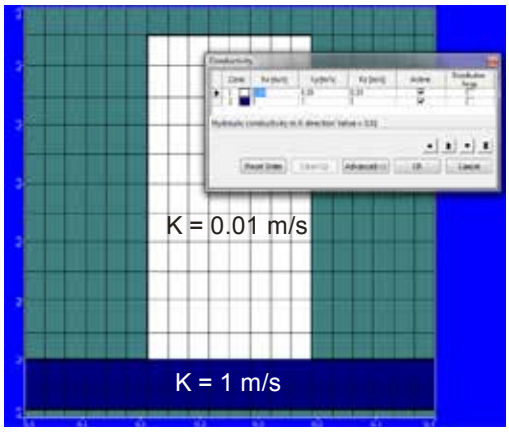

Figure C3-6: Hydraulic conductivity assignments in the model.

Particles were placed at the column inlet and their steady state pathlines calculated to illustrate the flow patterns in the DEC induced by water movement in the reservoir (Figure C3-4). Using the cell inspector feature in MODFLOW, velocities were determined at selected locations along the center of the column. These values were approximately constant across the column width. To gain an appreciation of the column flushing times these velocities represented, the times to move water the length of the column (25 cm) was determined for each of the reported velocities. The lowest velocity corresponded to a column flush time on the order of 24 hours (50 cm total travel distance), showing that the flow induced by stirring was of concern in the experiments.

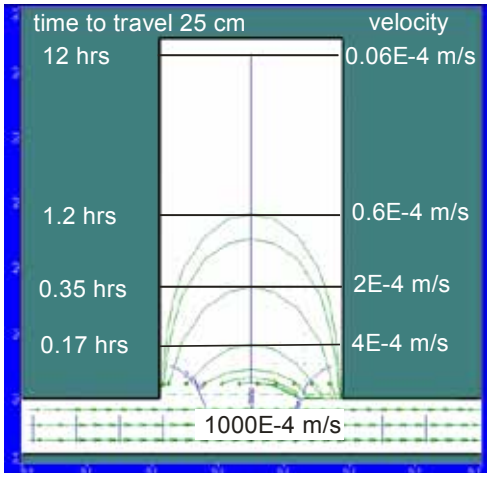

Figure C3-7: Particle tracks, velocities, and travel times for particles moving with induced flow in the DEC.

C.4: DIFFUSION IN A DEC WITH LAYERED SEDIMENTS

Based on the experimental results of diffusion in FEW sands and silts, effective diffusion coefficients were estimated to be 0.94 cm^2 day^{-1} and 0.04 cm^2 day^{-1}, respectively. Using these site-specific values, predictive modeling was carried out using a spreadsheet code for the case of a DEC packed with alternating layers of FEW sand and silt.

The sand and silt layers were packed in such a fashion that each of the probes was place in a different layer (Figure C4-1). The simulations were conducted assuming a C_o of 0.21 mV at the inlet of the column, and 0 everywhere else. The inlet end of the column was simulated with a Dirichlet type boundary ($C = C_o$, x=0, $t = t$), and the sealed end of the column was modeled as a constant flux boundary (J = 0). Responses at 51 days were simulated for the probes at 2.5 cm and 5.0 cm for 1) a homogeneous column case (sand only with D^* = 0.94 cm^2 day^{-1}) and 2) the heterogeneous case with alternating sand and silt layers (Figure C4-1). A time of 51 days was simulated to match the approximate times of the DEC experiments performed previously.

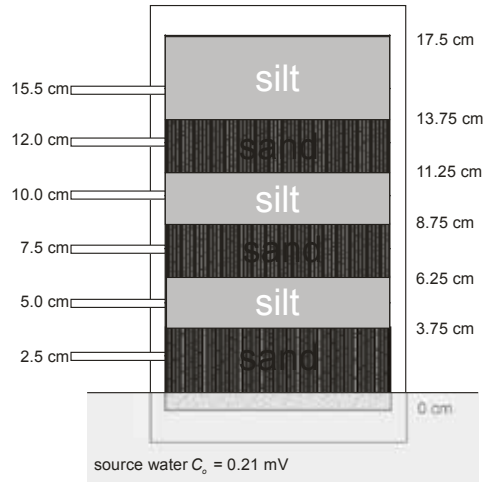

Figure C4-8: Schematic of the layered DEC simulated with the finite difference spreadsheet model.

The accuracy of the numerical solution was assessed by comparing it to an analytical solution of Fick's Second Law assuming a semi-infinite domain (no sealed end to the column) (Figure C4-2). A simulation time of 6 days was selected so the effects of the different boundaries on the sealed end of the column would not influence the solutions. The calculated profiles were found to be nearly identical, validating the numerical model.

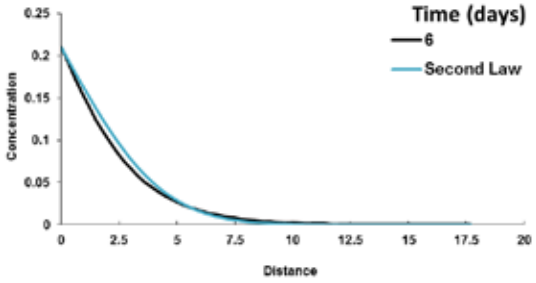

Figure C4- 9: Comparison of the numerical and analytical solutions verifying the accuracy of the numerical model.

The simulated homogeneous column produced a concentration profile that extended throughout the column by day 51 (Figure C4-3A). The numerical and analytical solutions coincide up to a distance of about 8 cm into the column after which the influence of the sealed end of the column causes the solutions to diverge. The responses at the two sampling ports (equivalent to the probes used in the DEC) showed good agreement between the analytical and numerical models because both were located within 8 cm of the inlet (Figure C4-3B and C4-3C).

The addition of layers to the simulation resulted in several changes to the solution (Figure C4-4A). First, after 51 days the profile that developed resembled steps, with the horizontally dominated portions corresponding to the sand layers and the vertically dominated portions corresponding to the silt layers. This pattern resembles a snapshot of one that could also develop from diffusion from several parallel sand layers in which the C_o in each was fixed by advection. Thus, care must be taken in the interpretation of profiles where heterogeneous sediments are present.

Second, the breakthrough at the 2.5 cm port occurred faster in the heterogeneous case than predicted by the semi-infinite solution of Fick's Second Law (Figure C4-4B). This appears to occur because the silt layers cannot conduct the tracer mass as quickly as sand. As a result, the tracer mass diffuses relatively quickly across the sand layers and then builds up against the silt layers. This phenomenon could lead to erroneously high estimates of D^* if curve fitting is the basis for such an assessment.

Third, the breakthrough at the 5.1 cm port occurred more slowly than what was predicted by the analytical solution (Figure C4-4C). This occurred because the port was located in a silt layer with a D^* less than that assumed in the analytical solution. Again, curve fitting in ignorance of the heterogeneous nature of the deposit would yield erroneous estimates of diffusion rates.

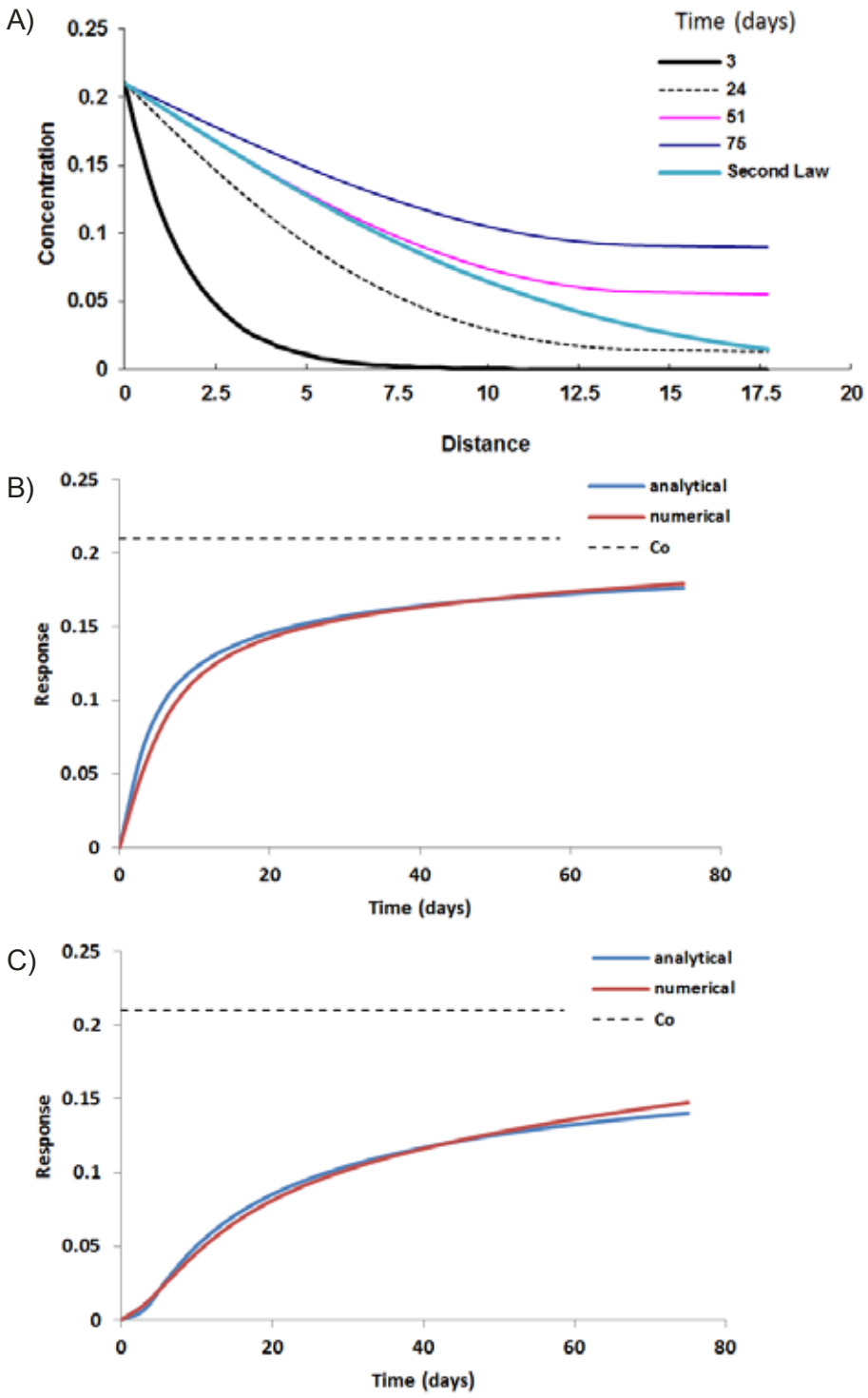

Figure C4-10: A) Profiles of tracer in a homogeneous sand column for 3, 24, 51, 75 days. B) Probe responses predicted over time for a sampling port located 2.4 cm from the inlet. C) Probe responses predicted over time for a sampling port located 5.1 cm from the inlet.

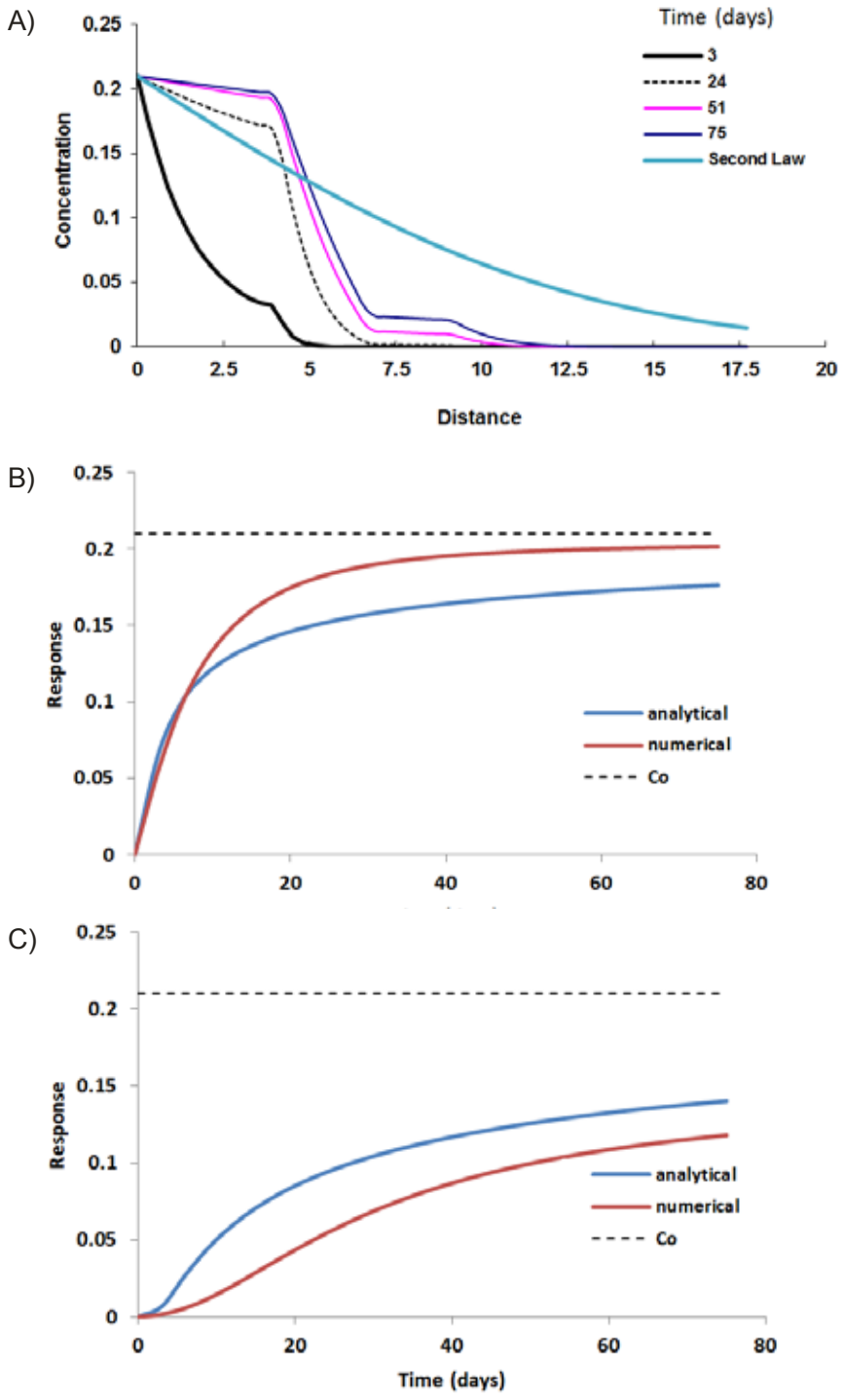

Figure C4-11: A) Profiles of tracer in a layered sand and silt column for 3, 24, 51, 75 days. B) Probe responses predicted over time for a sampling port located 2.4 cm from the inlet. C) Probe responses predicted over time for a sampling port located 5.1 cm from the inlet.

C.5: DATA USED IN HISTOGRAMS

Table C5-1: Effective diffusion coefficients for chloride species (Figure 4.1 in Report)

Tracer	D^* (cm^2/d)	Matrix	citation
Clayey sediments			
36Cl	2.9E-05	Clay	Van Loon, Lue R. et al., 2007
36Cl	1.0E-04	Clay	Van Loon, Lue R. et al., 2007
36Cl	2.1E-04	Clay	Van Loon, Lue R. et al., 2007
36Cl	3.4E-04	Clay	Van Loon, Lue R. et al., 2007
36Cl	4.3E-04	Clay	Van Loon, Lue R. et al., 2007
36Cl	7.5E-04	Clay	Garcia-Gutierrez, M. et al., 2006
36Cl	8.0E-04	Clay	Garcia-Gutierrez, M. et al., 2006
36Cl	9.5E-04	Clay	Van Loon, Lue R. et al., 2007
36Cl	1.0E-03	Clay	Van Loon, Lue R. et al., 2007
36Cl	2.0E-03	Clay	Van Loon, Lue R. et al., 2007
36Cl	2.0E-03	Clay	Garcia-Gutierrez, M. et al., 2006
36Cl	2.2E-03	Clay	Van Loon, Lue R. et al., 2007
36Cl	4.0E-03	Clay	Van Loon, Lue R. et al., 2007
36Cl	4.6E-03	Clay	Kim, Hong-Tae et al., 1993
36Cl	0.01	Clay	Kim, Hong-Tae et al., 1993
36Cl	0.01	Clay	Van Loon, Lue R. et al., 2007
36Cl	0.01	Clay	Van Loon, Lue R. et al., 2007
Cl-	0.01	Clay	De Soto, Isabel S. et al., 2012
36Cl	0.01	Clay	Van Loon, Lue R. et al., 2007
36Cl	0.02	Clay	Garcia-Gutierrez, M. et al., 2006
36Cl	0.02	Clay	Molera, Mireia et al., 2003
36Cl	0.02	Clay	Van Loon, Lue R. et al., 2007
36Cl	0.03	Clay	Garcia-Gutierrez, M. et al., 2006
36Cl	0.04	Clay	Van Loon, Lue R. et al., 2007
36Cl	0.05	Clay	Molera, Mireia et al., 2003
36Cl	0.07	Clay	Kim, Hong-Tae et al., 1993
Cl-	0.08	Clay	De Soto, Isabel S. et al., 2012
36Cl	0.09	Clay	Molera, Mireia et al., 2003
36Cl	0.12	Clay	Kim, Hong-Tae et al., 1993
36Cl	0.12	Clay	Molera, Mireia et al., 2003
Cl-	0.13	Clay	Shackelford, Charles. D. et al., 1991

Cl	0.15	Clay	Mazzieri, Francesco et al., 2010
Cl-	0.16	Clay	Shackelford, Charles. D. et al., 1991
36Cl	0.17	Clay	Kim, Hong-Tae et al., 1993
Cl	0.17	Clay	De Soto, Isabel S. et al., 2012
36Cl	0.19	Clay	Molera, Mireia et al., 2003
36Cl	0.31	Clay	Molera, Mireia et al., 2003
Cl-	0.38	Clay	Shackelford, Charles. D. et al., 1991
Cl-	0.41	Clay	Shackelford, Charles. D. et al., 1991
Cl-	0.43	Clay	Johnson, Richard.L. et al., 1989
Cl-	0.48	Clay	Shackelford, Charles. D. et al., 1991
Cl-	0.52	Clay	Shackelford, Charles. D. et al., 1991
Cl-	0.62	Clay	Shackelford, Charles. D. et al., 1991
36Cl	0.69	Clay	Molera, Mireia et al., 2003
36Cl	0.73	Clay	Molera, Mireia et al., 2003
Cl-	0.83	Clay	Shackelford, Charles. D. et al., 1991
Cl-	0.88	Clay	Shackelford, Charles. D. et al., 1991
Cl-	0.92	Clay	Shackelford, Charles. D. et al., 1991
NaCl	0.32	clay paste	Dutt, Gordon.R. et al., 1962
LiCl	0.35	clay paste	Dutt, Gordon.R. et al., 1962
Cl	0.51	clay till	Barone, F.S. et al., 1989
Cl	0.24	kaolinite	Shackelford, Charles D. et al., 1989
Cl	0.39	kaolinite	Shackelford, Charles D. et al., 1989
Cl	0.62	kaolinite	Shackelford, Charles D. et al., 1989
Cl	0.13	lufkin	Shackelford, Charles D. et al., 1989
Cl	0.14	lufkin	Shackelford, Charles D. et al., 1989
Cl	0.41	lufkin	Shackelford, Charles D. et al., 1989
Cl	0.51	Pacific red clay	Li, YH et al., 1974
Cl	0.91	Pacific red clay	Li, YH et al., 1974
Cl-	0.09	Silty clay	Crooks, Valerie.E. et al., 1984
Cl	0.49	Silty clay	Quigley, Robert M. et al., 1986
Cl-	0.49	Silty clay	Rowe, R.Kerry et al., 1988
Cl-	0.52	Silty clay	Rowe, R.Kerry et al., 1988
Cl-	0.55	Silty clay	Yanful, Ernest K. et al., 1990
Cl-	0.56	Silty clay	King, K.S. et al., 1993
Cl-	0.86	Silty clay	Crooks, Valerie.E. et al., 1984
Cl	0.48	soil-bentonite	Khandelwal, A. et al., 1998

Sandy sediments			
36Cl	0.60	Sand	Gillham, R.W. et al., 1984
36Cl	0.78	Sandy clay	Gillham, R.W. et al., 1984
36Cl	0.12	50/50 sand/clay	Robin, M.J.L. et al., 1987
36Cl	0.19	50/50 sand/clay	Robin, M.J.L. et al., 1987
36Cl	0.19	50/50 sand/clay	Robin, M.J.L. et al., 1987
36Cl	0.25	50/50 sand/clay	Robin, M.J.L. et al., 1987
36Cl	0.38	50/50 sand/clay	Robin, M.J.L. et al., 1987
36Cl	0.41	50/50 sand/clay	Robin, M.J.L. et al., 1987
36Cl	0.47	50/50 sand/clay	Robin, M.J.L. et al., 1987
36Cl	0.55	50/50 sand/clay	Robin, M.J.L. et al., 1987
36Cl	0.61	50/50 sand/clay	Robin, M.J.L. et al., 1987

Table C5-2: Effective diffusion coefficients for sodium species (Figure 4.1 in report).

Tracer	**D^* (cm^2/d)**	**Matrix**	**citation**
Clayey sediments			
Na	0.29	bentonite paste	Gast, R. et al., 1962
Na	0.64	bentonite paste	Gast, R. et al., 1962
22Na	0.01	Clay	Kozaki, Tamotsu et al., 2005
22Na	0.01	Clay	Kozaki, Tamotsu et al., 2005
22Na	0.01	Clay	Kozaki, Tamotsu et al., 2005
22Na	0.01	Clay	Kozaki, Tamotsu et al., 2005
22Na	0.01	Clay	Kozaki, Tamotsu et al., 2005
22Na	0.01	Clay	Glaus, Martin et al., 2007
22Na	0.02	Clay	Glaus, Martin et al., 2007
22Na	0.02	Clay	Kozaki, Tamotsu et al., 2005
22Na	0.02	Clay	Kozaki, Tamotsu et al., 2005
22Na	0.02	Clay	Kozaki, Tamotsu et al., 2005
22Na	0.02	Clay	Glaus, Martin et al., 2007
22Na	0.02	Clay	Glaus, Martin et al., 2007
22Na	0.02	Clay	Kozaki, Tamotsu et al., 2005
22Na	0.02	Clay	Kozaki, Tamotsu et al., 2005
22Na	0.02	Clay	Glaus, Martin et al., 2007
22Na	0.02	Clay	Kozaki, Tamotsu et al., 2005
22Na	0.02	Clay	Kozaki, Tamotsu et al., 2005
22Na	0.02	Clay	Kozaki, Tamotsu et al., 2005
22Na	0.03	Clay	Kozaki, Tamotsu et al., 2005

22Na	0.03	Clay	Kozaki, Tamotsu et al., 2005
22Na	0.03	Clay	Kozaki, Tamotsu et al., 2005
22Na	0.03	Clay	Kozaki, Tamotsu et al., 2005
22Na	0.03	Clay	Kozaki, Tamotsu et al., 2005
22Na	0.03	Clay	Kozaki, Tamotsu et al., 2005
22Na	0.03	Clay	Kozaki, Tamotsu et al., 2005
22Na	0.03	Clay	Kozaki, Tamotsu et al., 2005
22Na	0.03	Clay	Kozaki, Tamotsu et al., 2005
22Na	0.04	Clay	Kozaki, Tamotsu et al., 2005
22Na	0.04	Clay	Kozaki, Tamotsu et al., 2005
22Na	0.04	Clay	Kozaki, Tamotsu et al., 2005
22Na	0.04	Clay	Kozaki, Tamotsu et al., 2005
22Na	0.04	Clay	Kozaki, Tamotsu et al., 2005
22Na	0.04	Clay	Oscarson, Dennis.W. et al., 1994
22Na	0.04	Clay	Kozaki, Tamotsu et al., 2005
22Na	0.04	Clay	Kozaki, Tamotsu et al., 2005
22Na	0.05	Clay	Kozaki, Tamotsu et al., 2005
22Na	0.05	Clay	Kozaki, Tamotsu et al., 2005
22Na	0.05	Clay	Kozaki, Tamotsu et al., 2005
22Na	0.05	Clay	Kozaki, Tamotsu et al., 2005
22Na	0.05	Clay	Kozaki, Tamotsu et al., 2005
22Na	0.05	Clay	Kozaki, Tamotsu et al., 2005
22Na	0.05	Clay	Kozaki, Tamotsu et al., 2005
22Na	0.06	Clay	Kozaki, Tamotsu et al., 2005
22Na	0.06	Clay	Kozaki, Tamotsu et al., 2005
22Na	0.06	Clay	Oscarson, Dennis.W. et al., 1994
22Na	0.06	Clay	Kozaki, Tamotsu et al., 2005
22Na	0.06	Clay	Kozaki, Tamotsu et al., 2005
22Na	0.06	Clay	Kozaki, Tamotsu et al., 2005
22Na	0.06	Clay	Kozaki, Tamotsu et al., 2005
22Na	0.06	Clay	Kozaki, Tamotsu et al., 2005
22Na	0.06	Clay	Kozaki, Tamotsu et al., 2005
22Na	0.07	Clay	Kozaki, Tamotsu et al., 2005
22Na	0.07	Clay	Kozaki, Tamotsu et al., 2005
22Na	0.07	Clay	Kozaki, Tamotsu et al., 2005
22Na	0.07	Clay	Kozaki, Tamotsu et al., 2005
22Na	0.08	Clay	Kozaki, Tamotsu et al., 2005
22Na	0.08	Clay	Kozaki, Tamotsu et al., 2005
22Na	0.09	Clay	Kozaki, Tamotsu et al., 2005
22Na	0.10	Clay	Kozaki, Tamotsu et al., 2005

22Na	0.10	Clay	Oscarson, Dennis.W. et al., 1994
22Na	0.10	Clay	Kozaki, Tamotsu et al., 2005
22Na	0.10	Clay	Kozaki, Tamotsu et al., 2005
22Na	0.11	Clay	Kozaki, Tamotsu et al., 2005
22Na	0.11	Clay	Kozaki, Tamotsu et al., 2005
22Na	0.12	Clay	Kozaki, Tamotsu et al., 2005
22Na	0.13	Clay	Kozaki, Tamotsu et al., 2005
22Na	0.17	Clay	Kozaki, Tamotsu et al., 2005
22Na	0.17	Clay	Kozaki, Tamotsu et al., 2005
22Na	0.19	Clay	Kozaki, Tamotsu et al., 2005
22Na	0.21	Clay	Kozaki, Tamotsu et al., 2005
NaCl	0.32	clay paste	Dutt, Gordon.R. et al., 1962
Na	0.40	clay till	Barone, F.S. et al., 1989
Na	0.48	clay till	Barone, F.S. et al., 1989
Na	0.30	Pacific red clay	Li, YH et al., 1974
Na	0.50	Pacific red clay	Li, YH et al., 1974
Silty clay sediments			
Na	0.17	Silty clay	Yanful, Ernest K. et al., 1990
Na+	0.22	Silty clay	Crooks, Valerie.E. et al., 1984
Na+	0.30	Silty clay	Crooks, Valerie.E. et al., 1984
Na+	0.52	Silty clay	Crooks, Valerie.E. et al., 1984

Table C5-3: Effective diffusion coefficients for tritiated water (HTO) (Figure 4.2 in report).

Tracer	**D^* (cm^2/d)**	**Matrix**	**citation**
Clayey sediments			
HTO	0.01	Clay	Garcia-Gutierrez, M. et al., 2006
HTO	0.04	Clay	Garcia-Gutierrez, M. et al., 2006
H2O	0.05	Clay	Berry, J.A. et al., 1992
HTO	0.05	Clay	Garcia-Gutierrez, M. et al., 2006
H2O	0.07	Clay	Berry, J.A. et al., 1992
HTO	0.08	Clay	Garcia-Gutierrez, M. et al., 2006
HTO	0.10	Clay	Berry, J.A. et al., 1992
HTO	0.11	Clay	Oscarson, Dennis.W. et al., 1994
HTO	0.13	Clay	Garcia-Gutierrez, M. et al., 2006
HTO	0.13	Clay	Berry, J.A. et al., 1992
HTO	0.13	Clay	Oscarson, Dennis.W. et al., 1994
HTO	0.13	Clay	Berry, J.A. et al., 1992

HTO	0.16	Clay	Oscarson, Dennis.W. et al., 1994
HTO	0.17	Clay	Berry, J.A. et al., 1992
HTO	0.17	Clay	Garcia-Gutierrez, M. et al., 2006
HTO	0.18	Clay	Oscarson, Dennis.W. et al., 1994
HTO	0.20	Clay	Berry, J.A. et al., 1992
HTO	0.22	Clay	Garcia-Gutierrez, M. et al., 2006
HTO	0.27	Clay	Garcia-Gutierrez, M. et al., 2006
HTO	0.29	Clay	Garcia-Gutierrez, M. et al., 2006
HTO	1.04	Clay	Gillham, R.W. et al., 1984
HTO	0.86	Clayey sand	Gillham, R.W. et al., 1984
HTO	0.46	kaolinite	Phillips, R.E. et al., 1968
HTO	0.58	kaolinite	Phillips, R.E. et al., 1968
HTO	0.85	kaolinite	Phillips, R.E. et al., 1968
HTO	0.94	kaolinite	Phillips, R.E. et al., 1968
HTO	0.39	montmorillonite	Phillips, R.E. et al., 1968
HTO	0.55	montmorillonite	Phillips, R.E. et al., 1968
HTO	0.62	montmorillonite	Phillips, R.E. et al., 1968
HTO	0.78	montmorillonite	Phillips, R.E. et al., 1968
HTO	0.69	Sand	Gillham, R.W. et al., 1984
HTO	0.08	sodium bentonite	Miyahara, K. et al., 1991
HTO	0.16	sodium bentonite	Miyahara, K. et al., 1991
HTO	0.33	sodium bentonite	Miyahara, K. et al., 1991
HTO	0.71	sodium bentonite	Miyahara, K. et al., 1991
HTO	1.21	sodium bentonite	Miyahara, K. et al., 1991
H2O	0.08	Till	Hendry, M.Jim. et al., 2009
H20	0.12	Till	Hendry, M.Jim. et al., 2009
Silty clay sediments			
HTO	0.28	Silty clay	Young, Dirk F. et al., 1998
HTO	0.33	Silty clay	Young, Dirk F. et al., 1998
HTO	0.37	Silty clay	Young, Dirk F. et al., 1998
HTO	0.41	Silty clay	Young, Dirk F. et al., 1998
HTO	0.44	Silty clay	Young, Dirk F. et al., 1998
HTO	0.46	Silty clay	Young, Dirk F. et al., 1998
HTO	0.48	Silty clay	Young, Dirk F. et al., 1998
HTO	0.51	Silty clay	Young, Dirk F. et al., 1998
HTO	0.73	Silty clay	Yanful, Ernest K. et al., 1990
Sandy sediments			
HTO	1.47	Sand	Gillham, R.W. et al., 1984

HTO	0.95	sandy clay	Gillham, R.W. et al., 1984
HTO	0.92	Silty sand	Van Rees, Kenneth C.J. et al., 1991
HTO	1.02	Silty sand	Van Rees, Kenneth C.J. et al., 1991
HTO	1.10	Silty sand	Van Rees, Kenneth C.J. et al., 1991
HTO	1.14	Silty sand	Van Rees, Kenneth C.J. et al., 1991
HTO	1.23	Silty sand	Van Rees, Kenneth C.J. et al., 1991
HTO	1.30	Silty sand	Van Rees, Kenneth C.J. et al., 1991
HTO	1.36	Silty sand	Van Rees, Kenneth C.J. et al., 1991
HTO	1.54	Silty sand	Van Rees, Kenneth C.J. et al., 1991
HTO	1.55	Silty sand	Van Rees, Kenneth C.J. et al., 1991
HTO	1.59	Silty sand	Van Rees, Kenneth C.J. et al., 1991
HTO	1.60	Silty sand	Van Rees, Kenneth C.J. et al., 1991
HTO	1.63	Silty sand	Van Rees, Kenneth C.J. et al., 1991
HTO	1.68	Silty sand	Van Rees, Kenneth C.J. et al., 1991
HTO	1.83	Silty sand	Van Rees, Kenneth C.J. et al., 1991

C.6: METHODS

Preliminary testing of a custom build apparatus referred to as the dead-end-column (DEC) was completed using a porous medium consisting of a commercial sand, obtained from a local hardware store. The sand was predominantly medium grained, and moderately well sorted based on visual inspection (Figure C6-1). Once the methodology was established, sieved samples of sand from F.E. Warren (FEW) Air Force Base, provided by Colorado State University and processed to remove organics, were subjected to diffusion testing in the DEC.

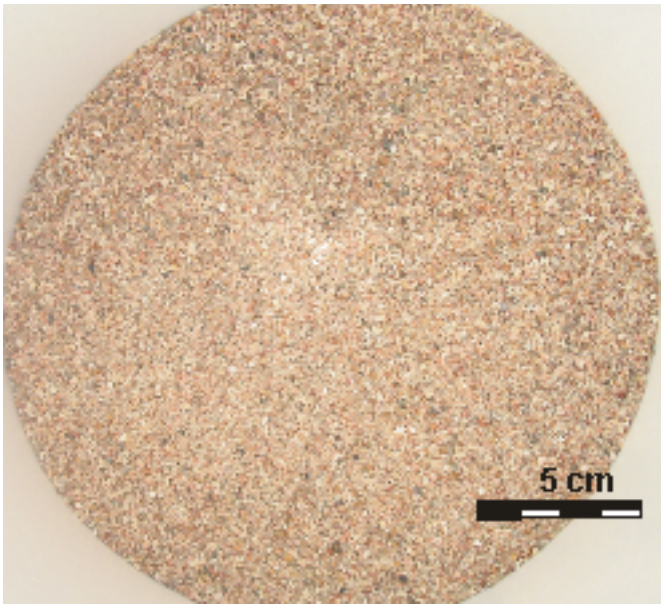

Figure C6-1: Commercial sand used in preliminary testing of the DEC.

The DECs (Figure C6-2) were constructed of 7.6 cm long by 15.2 centimeter diameter Plexiglass pipe. Six ports, containing brass compression tube fittings, were spaced 2.5 cm apart along the column to house electrical conductivity probes. The probes were constructed from 5.08 cm long, 0.37 cm inner diameter, insulated stainless steel needles inserted into 15 gauge 0.146 cm outer diameter needles and fixed in place with silicone to prevent short-circuiting and leakage of water (Figure C6-3). The inner needles protruded from the outer needles at both ends. One of the ends was designated the sensor and was inserted half way into the DECs during packing. The other ends were connected to Campbell Scientific CR1000 dataloggers using 16 gauge speaker wire and attached to the DEC probes by 1 3/8”alligator clips (Figure C6-4). The datalogger was programed to collect data at fifteen minute intervals.

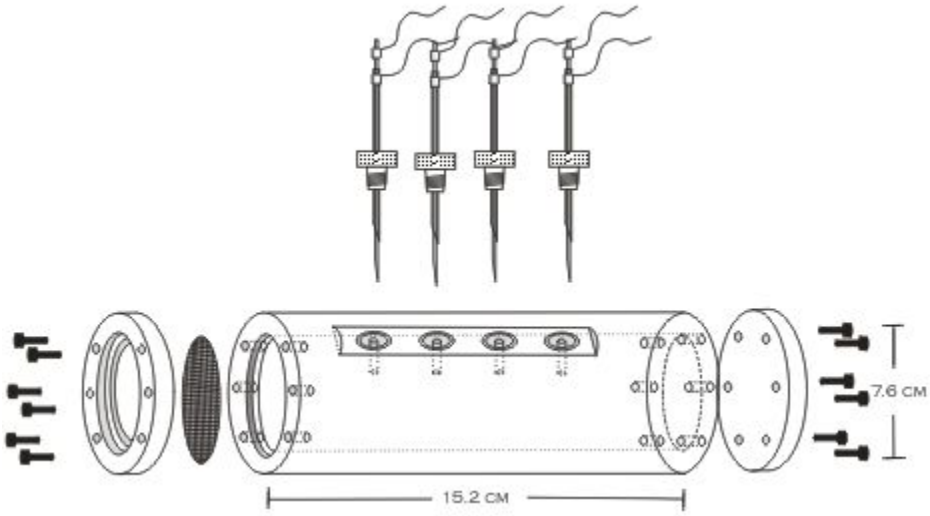

Figure C6-12: Schematic of diffusion cell tube. Ports on cell tube allow needles attached to conductivity probes to be inserted into sediment sample.

Figure C6-13: (A) Electrical conductivity probes (B) plastic tubing separates outer stainless steel needle from inner needle.

In each diffusion experiment, one end of the DEC was sealed with a water-tight Plexiglas ® lid while the opposite end was terminated with a screen mesh that allowed diffusive transport of tracer while preventing the porous medium from leaving the DEC. With only one end of the column in contact with the tracer reservoir, the possibility of advective flow in the column was greatly reduced.

The porous media tested were wet packed (using deionized water) to minimize entrapment of air during flooding. In the case of sand-packed columns, about a centimeter of water was maintained above the sediment level throughout the packing procedure (Figure C6-5). Sand was added to the column in 1 cm lifts, and tamped. The probes were inserted into the column as the sand bed reached their respective levels. After packing, at least 3 days were allowed for the media and the interstitial water to equilibrate before any diffusion testing was begun.

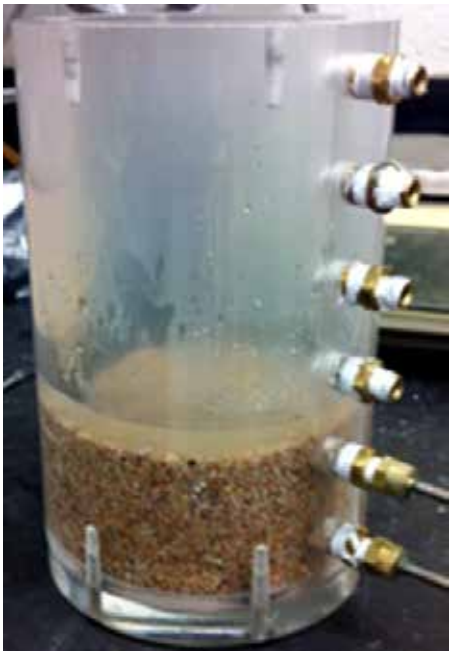

Figure C6-14: Wet packing FEW sand into DEC and maintaining a 1 cm layer of water over the sediment bed.

The silt used in the experiment did not settle quickly enough for the procedure above to be applied. Instead, the silt was placed into a beaker and mixed with deionized water until it became a thick, saturated slurry (Figure C6-6). The slurry was placed into the DEC with water to maintain fully saturated conditions. The slurried silt was tamped regularly to further ensure no air was entrapped and to minimize stratification. Probes were installed as described previously.

The columns were seated vertically in stands and placed into reservoirs consisting of 62 L Rubbermaid containers filled with 16 L of deionized water (Figure C6-6). Subsequently, the reservoir waters were spiked with NaCl to a concentration of between 0.5 g/L and 1g/L, which was found to be easily detected by the conductivity probes. Tracer amendments were prepared by dissolving sodium chloride reagent-grade crystals, used as received from Fisher Scientific, into 1 L of water in a graduated cylinder. The NaCl solution was poured into the reservoir while a magnetic stirrer rotated to evenly distribute the tracer throughout the reservoir. After 2-3 minutes of stirring, the stirring was stopped in order to prevent the circulation of water from causing advective flow in the DECs.

The probes were connected to a Campbell Scientific CR1000 datalogger as described previously (Figure C6-7). The experiments began with the first contact of the column with the reservoir tracer solution, and diffusion was tracked for periods up to about 80 days.

Figure C6-15: (A) FEW silt sample placed in beaker (B) water added to make saturated slurry (C) wet packing silt slurry into DEC.

Figure C6-16: DEC in reservoir containing tracer-spiked water.

Figure C6-17: DEC in reservoir and attached to datalogger.

Over the durations of the experiments evaporative losses of water from the reservoirs was a potential problem, leading to both depleted water levels and altered salt tracer concentrations. To prevent these changes, a Mariotte bottle was used to fix the level of water in the reservoir, continuously replacing any water lost due to evaporation (Figure C6-8).

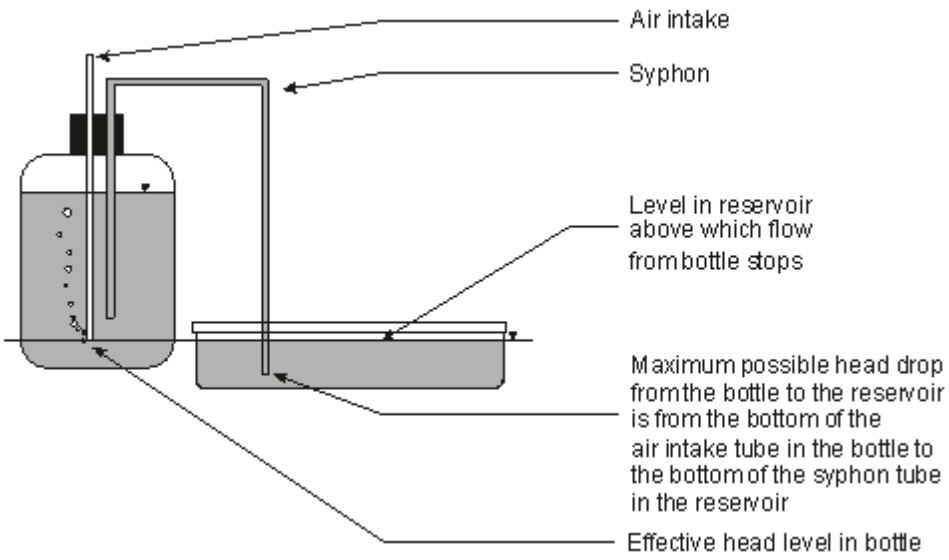

Figure C6-18: Schematic of the Mariotte bottle system used to maintain a constant level of water in the tracer reservoir.

Figure C6-19: Layered column with alternating sand and silt layers.

Figure C6-10: Open column experiment where only water is placed into column.

APPENDIX D

SCREENING METHOD TO ESTIMATE IF A CHLORINATED SOLVENT SITE IS IN ITS *EARLY, MIDDLE OR LATE STAGE*

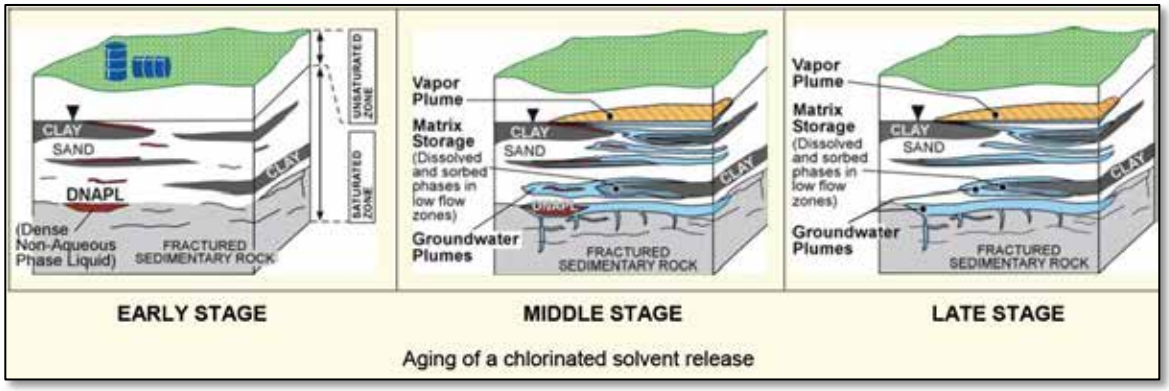

Aging of a chlorinated solvent release

Screening Method To Estimate if a Chlorinated Solvent Site is in its *Early, Middle or Late Stage*

(C. Newell, T. Sale, D. Adamson)

In the "Chlorinated Solvent FAQ", the idea that chlorinated solvent sites went through various stages during the site's life cycle was presented (Sale et al., 2008):

> *With time, subsurface chlorinated solvent releases age. Early in their lives, they are dominated by DNAPL, but slowly DNAPLs dissolve, plumes develop, and contaminants accumulate in permeable zones. Eventually, little to no DNAPL remains, and plumes are sustained by the release of contaminants from low permeability zones via diffusion (Chapman and Parker, 2005). Although recoverable DNAPL can still be found within some source zones, it is notoriously difficult to find DNAPLs at the heads of many persistent plumes. At some sites (see late stage below), it simply may not be there any longer, even though the source zone (see FAQ 4) is still active. Key factors controlling the rate at which chlorinated solvent releases age include the amount of DNAPL released, the solubility of the constituent in the DNAPL, the rate of groundwater flow, and the architecture of transmissive and low permeability zones*.

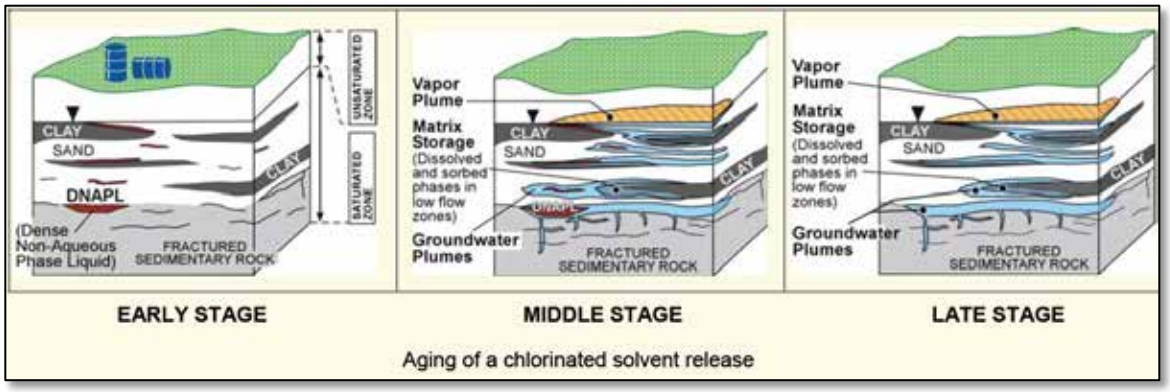

Aging of a chlorinated solvent release

The following is a methodology we developed to help site managers, consultants, remediation specialists, and regulators try to understand if they are working on an early, middle, or late stage site. The method is based on experience working in chlorinated solvent source zones with some assistance from recently developed matrix diffusion models developed by the authors that form the basis of the ESTCP Matrix Diffusion Toolkit (Farhat et al., 2013). The method is our first attempt at this classification system, and the approach may change as we all learn more about how chlorinated solvent sites age.

Some key considerations about the Screening Method are:

- It is designed for chlorinated solvent sites, although it may be possible to adapt it for other contaminants.
- It is mainly derived from our experience at trichoroethene (TCE) sites. Although it has provisions for applying it for other DNAPL constituents, the body of site experience is fro DNAPL sites.
- It is relatively general and relies on several interpretations when compiling the data required to apply the Screening Method. Therefore it is possible two different users may generate two different answers.
- It may take some time to go through this; it requires some careful thinking about your site and the data required to use the method.

Screening Method To Estimate if a Chlorinated Solvent Site is in its *Early, Middle or Late Stage (EML)*

(C. Newell, T. Sale, D. Adamson)

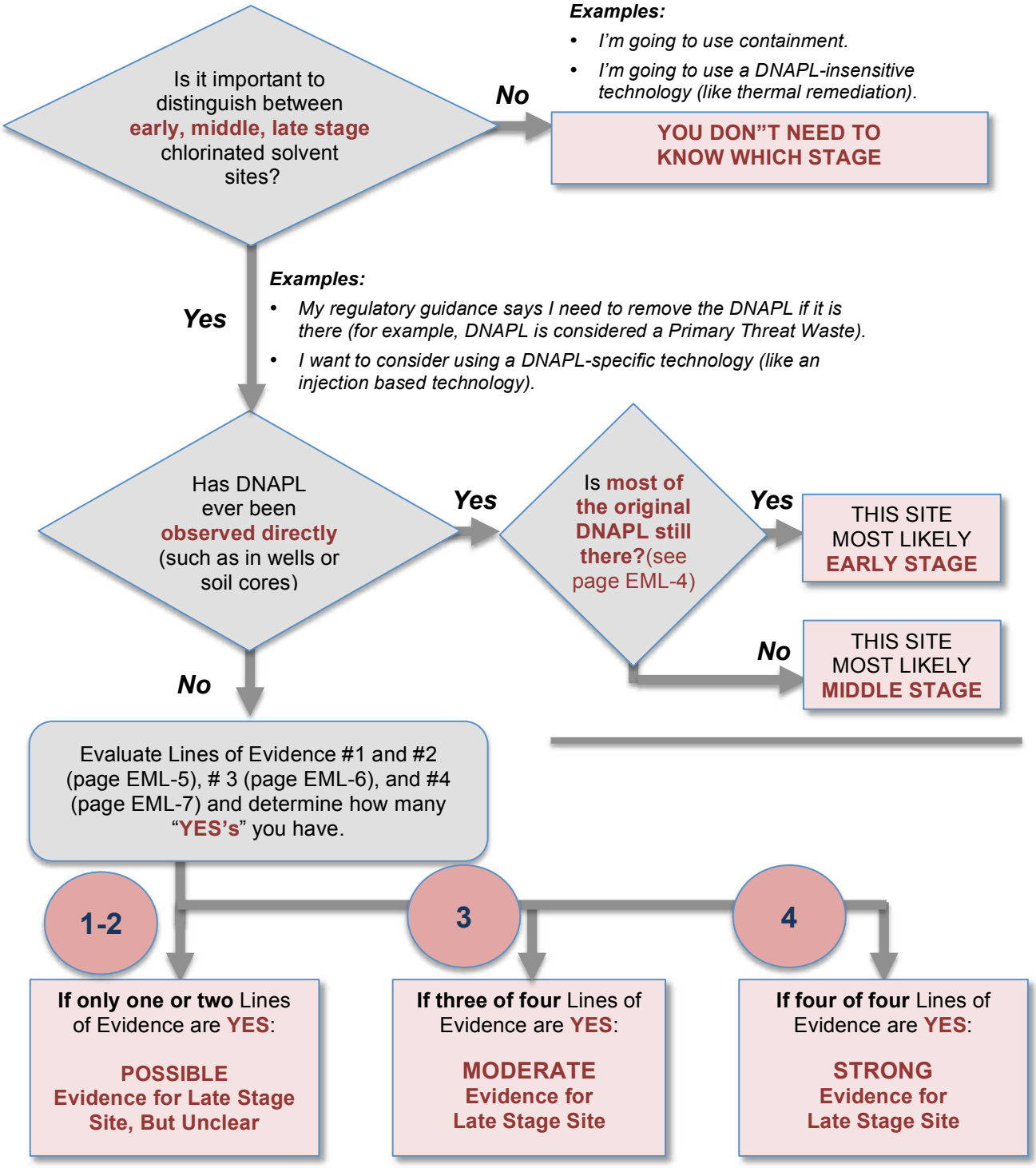

Has Most of the Original DNAPL Still There?

This can be a difficult and controversial question to answer. The following are some thoughts, observations, speculations from the authors. These may change over time as better methods to understand DNAPL source zones are developed.

In this application, when we refer to "DNAPL" we mean "DNAPL chemicals" rather than an insoluble oils or other chemicals in the original release.

The answer depends on several variables that can be very difficult to determine, such as the amount of the release, the composition of the DNAPL, the source architecture; as well as more commonly measured geochemical and hydrogeologic variables.

There are simple dissolution models that can be used to provide some guidance. But generally if on assumes the DNAPL is mostly in the ganglia or blob form, the resulting dissolution times are often just a few years. DNAPL pools, particularly long ones (10s of meters), can last many many decades.

In general, the answer is more likely to be a "**No**" if the site has more of these characteristics than not:

- There are only a few indicators of DNAPL presence (e.g., a couple of stains on just a few cores);
- No significant DNAPL accumulation in groundwater monitoring wells has been observed;
- The source release is small (a few hundred or few thousand kilograms or less);
- The source release mechanism and the geology will spread the DNAPL into a large volume in the subsurface;
- Groundwater seepage velocities are moderate to high (tens of meters per year or more);
- There has been successful removal of much of the DNAPL mass from the transmissive zone with an in-situ remediation technology;
- The key constituents are more soluble (several hundred or thousand mg/L or more);
- It has been several decades since most of the DNAPL was released.

In general, the answer is more likely to be a "**Yes**" if the site has more of these characteristics than not:

- There are only a multiple indicators of DNAPL presence (e.g., many cores with positive dye test tests; several monitoring wells with DNAPL accumulations);
- No significant DNAPL accumulation in monitoring wells has been observed;
- The release was very large (hundreds of thousands or millions of kilograms);
- The release point and subsurface geology result in the formation of large DNAPL pools;
- Groundwater seepage velocities are low (meters per year or less);
- No remediation or DNAPL removal has occurred;
- The key constituents have relatively low solubility (tens or a few hundreds of mg/L);
- It has been just a few years since most of the DNAPL was released.

At most sites, DNAPL is never observed so this is not needed to go through this flowchart.

LINE OF EVIDENCE 1: Adequate DNAPL Search?

Was a *thorough* direct DNAPL investigation was conducted, where one or more of the following were performed:

- Interfaces above low perm zones were sampled.

  OR
- A vertical transect was used to identify high flux zones that were then sampled for DNAPL.

  OR
- Soil samples were investigated using enhanced techniques like hydrophobic dye.

  OR
- Other DNAPL-specific characterization technologies were used.

If ANY of these were done, Line of Evidence 1 is "YES"

If NONE were done, Line of Evidence 1 is "NO"

(*VERY IMPORTANT: the "1% rule" should not used to indicate the presence of DNAPL)*

LINE OF EVIDENCE 2: Old Plume + Heterogeneity?

Does your site meet *both* of these qualitative conditions?

- Site has identified low–k zones (such as silts, clays, sandstone, limestone) with hydraulic conductivity of at least 100 times lower than fastest transmissive zones that is or was in contact with the plume.

  AND

- The original release likely occurred more than 30 years ago.

If BOTH of these are TRUE, Line of Evidence 2 is "YES"

If EITHER IS FALSE, Line of Evidence 2 is "NO"

LINE OF EVIDENCE 3: Can the Low-k Zone Hold Enough Mass? *(see EML-8 for basis)*

1. Calculate TCE Mass per cubic meter of low-k material with Graph A.
2. Estimate the volume of low-k material at your site using Graph B.
3. Multiple the two values together to get an estimated mass in low–k unit in kilograms .
4. This particular chart is designed for TCE and for a source zone. You can apply this to other chlorinated solvents by multiplying by the pure-phase solubility of your DNAPL chemical in mg/L and dividing by 1000 mg/L (value we used for TCE).
5. You can do this for different parts of the site, such as the original source zone, a high concentration part of the plume, and a low concentration area, each with a different concentration, year since low-k diffusion started, and areas, and add the numbers.

If the Mass is > 100 kilograms, Line of Evidence 3 is "YES"

If the Mass is < 100 kilograms, Line of Evidence 3 is "NO"

Graph A - Mass TCE Per Cubic Meter of Low-k Material

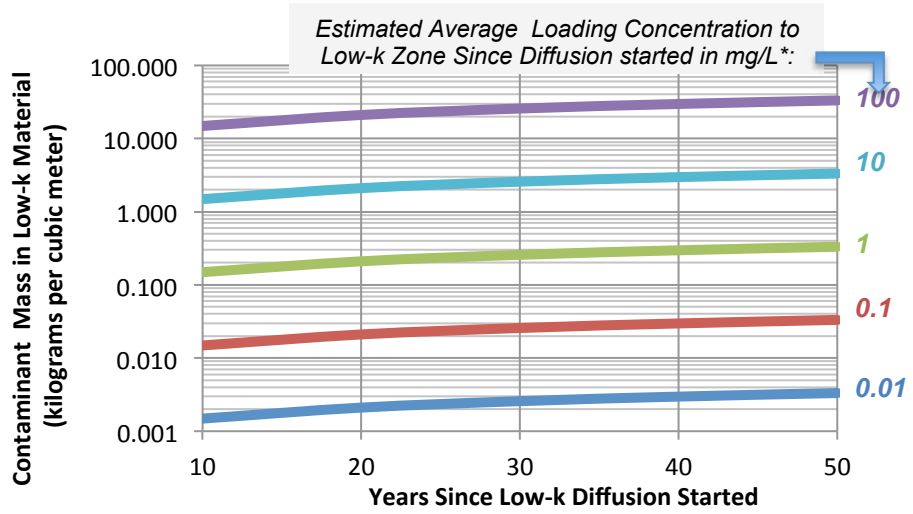

** If unknown, just use maximum historcal concentration for this area.*

Multiply these two values to get mass of TCE in low-k zone >100 kg:"YES" <100 kg:"NO"

Graph B - Potential Volume of Low-k Material for Matrix Diffusion

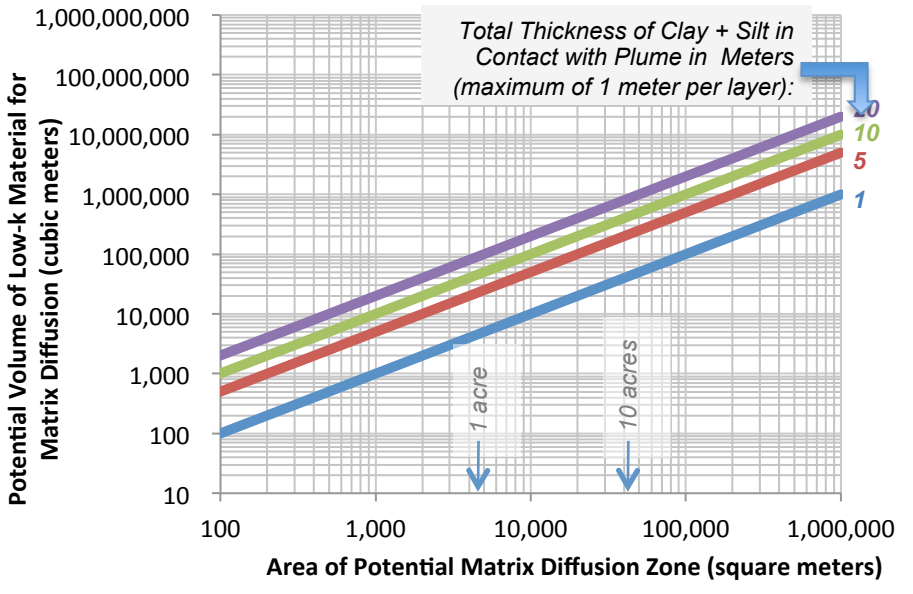

LINE OF EVIDENCE 4: Can Low-k Zones Create High Enough Concentrations?

Instructions for Line of Evidence 4 *(see page EML-8 for the technical basis)*

1. Estimate the length of the low-k zone parallel to groundwater flow that might have been in contact with a high-strength plume in the past.

2. Enter the graph and select the line for the contaminant you are interested in evaluating. If you have a different contaminant, find the line for the chemical with the solubility that is closest to your contaminant (for this graph the solubility of 1,2-DCA, cis-DCE, TCE, and PCE were assumed to be 8690, 1000, 800, and 143 mg/L, respectively. Alternatively you can run the *Matrix Diffusion Toolkit* to evaluate potential monitoring well concentrations from low-k zones.

3. Go to the Y-Axis and find the potential maximum concentration in groundwater in a monitoring well with a 10-foot screen in mg/L (note it is a log scale)

If the potential maximum concentration in Step 3 is greater than the maximum historical concentration for that contaminant at your site, ***Line of Evidence 4 is "YES"***

If the potential maximum concentration in Step 3 is less than the maximum historical concentration for that contaminant at your site, ***Line of Evidence 4 is "NO"***

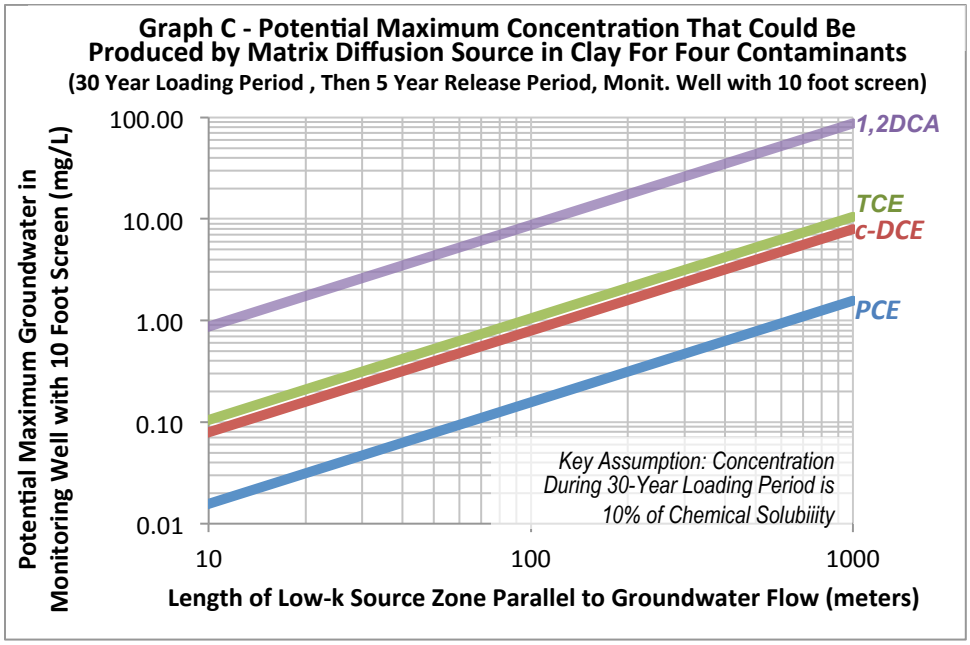

TECHNICAL BASIS: How Does This Work?

Overall Basis: Assume Simple Geometry, One Low-k Unit, One Transmissive Unit

This methodology is designed for sites with unconsolidated hydrogeologic settings (sand, silt, clay), with a single low-k unit in contact with a plume in a transmissive zone. The methodology can be adapted to other configurations such as multi-layered systems and fractured rock sites by those familiar with matrix diffusion modeling by multiplying the results in Line of Evidence 3 and 4 by the number of contacts between transmissive and low-k units.

Line of Evidence 1: Adequate DNAPL Search?

A strong, but not conclusive line of evidence of a late stage site is that a thorough search for DNAPL using current DNAPL-specific DNAPL techniques did not find any evidence of DNAPL in the source zone. Determining if a particular field program rates a "YES" or "NO" is somewhat subjective, but the main criteria is that a DNAPL-specific field program to find direct evidence of DNAPL is wells, soil cores, etc. was performed. Use of the 1% should not be used for Line of Evidence 1 because matrix diffusion modeling indicates that strong matrix diffusion sources can create concentrations greater than 1% of the effective solubility of DNAPL.

Line of Evidence 2: Old Plume + Heterogeneity?

These are two key ingredients for a strong, long lived matrix diffusion source: heterogeneity using the rule of thumb that a 100-fold difference in hydraulic conductivity will lead to matrix diffusion processes (B. Parker, U. of Guelph); and the fact that old sites can load more mass in low-k zones.

Line of Evidence 3: Can the Low-k Zone Hold Enough Mass?

The Square Root model in the Matrix Diffusion Toolkit (Farhat et al.,2013) was used to estimate the contaminant mass that could diffuse into a single low-k layer that was at least 1 meter thick. The total thickness of the clay and silt in contact with a plume is then applied to the calculated potential mass per cubic meter. Note you can break a site up into different zones and use this method to estimate the mass separately in high, medium, and low concentration zones and the add the masses together.

Why 100 kilograms? This is the amount that can sustain an average plume (Mag 5 plume in the Plume Magnitude System) for 50 years. (Newell et al., 2011).

Line of Evidence 4: Can Low-k Zones Create High Enough Concentrations?

This line of evidence assumes that a plume with concentrations at 10% of the pure-phase solubility of the contaminant e was in contact with a low-k zone for 30 years. If unknown, assume the length of the low-k zone is the length of the source zone at the site parallel to groundwater flow. The low-k zone was assumed to be clay with a fraction organic carbon of 0.002 grams per gram, giving retardation factors for DCA, DCE, TCE, and PCE of 1.4, 1.7, 1.2, and 2.1 in the clay, respectively. The Matrix Diffusion Toolkit's Square Root Model (Farhat et al., 2013) was used to generate the concentrations as a function of the length of the low-k zone.

You can evaluate different contaminants by picking which one of the four lines has the solubility closest to your contaminant. If you have process knowledge that the concentration during the loading period is different than the 10% solubility assumed above, then just adjust the final result by the ratio of your solubility to 10% (i.e., if you think the loading concentration was equal to 50% of TCE pure-phase solubility, multiply the concentrations on the Y-Axis by 5.

REFERENCES

Chapman, S.W. and B.L. Parker. 2005. Plume Persistence Due to Aquitard Back Diffusion Following Dense Nonaqueous Phase Liquid Removal or Isolation, Water Resource Research, Vol. 41, No. 12, W12411.

Farhat, S.K., C.J. Newell, T.C. Sale, D.S. Dandy, J.J. Wahlberg, M.A. Seyedabbasi, J.M. McDade, and N.T. Mahler, 2012. Matrix Diffusion Toolkit, developed for the Environmental Security Technology Certification Program (ESTCP) by GSI Environmental Inc., Houston, Texas. Download at http://www.gsi-net.com/software.html

Newell, C. J., Farhat, S. K., Adamson, D. T. and Looney, B. B. (2011), Contaminant Plume Classification System Based on Mass Discharge. Ground Water, 49: 914–919. doi: 10.1111/j.1745-6584.2010.00793.x Nov/Dec 2011.

Sale, T., C. Newell, H. Stroo, R. Hinchee, and P. Johnson, 2008. Frequently Asked Questions Regarding Management of Chlorinated Solvent in Soils and Groundwater, Developed for the Environmental Security Testing and Certification Program (ER-0530). http://www.gsi-net.com/Publications/papers2.asp

Sale, T. and C. J. Newell, 2011. A Guide for Selecting Remedies for Subsurface Releases of Chlorinated Solvent Sites. ESTCP Project ER-05 30. Environmental Security Technology Certification Program, Washington DC.